

Synthetic, Mechanistic and Theoretical  
Studies Related to the Kinamycin  
Antibiotics

by

Glenn Lee Abbott

A thesis  
presented to the University of Waterloo  
in fulfillment of the  
thesis requirement for the degree of  
Doctor of Philosophy  
in  
Chemistry

Waterloo, Ontario, Canada, 2011

©Glenn Lee Abbott 2011

## **AUTHOR'S DECLARATION**

I hereby declare that I am the sole author of this thesis. This is a true copy of the thesis, including any required final revisions, as accepted by my examiners.

I understand that my thesis may be made electronically available to the public.

Glenn Lee Abbott

## Abstract

The synthesis of an isosteric-isoelectronic analogue of prekinamycin, an *N*-cyanobenzo[*b*]carbazoloquinone **2.1**, is described. The key steps include a Vilsmeier-Haack formylation, a regioselective bromination, a Buchwald-Hartwig cross-coupling, a palladium mediated oxidative cyclization and *N*-cyanation to furnish the target in fifteen steps in an overall yield of 1.6%. Subsequent bioactivity studies were conducted in which the cytotoxicity of various compounds on K562 cells, a human erythroleukemic cell line, revealed that the analogue had a similar bioactivity profile to prekinamycin. These results suggest that the diazo functionality may not be an absolute requirement for bioactivity.

A study of the reactivity of nitric oxide with diphenyldiazomethane, kinamycin A and isoprekinamycin diacetate was undertaken. Three products were isolated from the reaction with diphenyldiazomethane: a nitrimine **3.7**, benzophenone and, for the first time, dinitrodiphenylmethane **3.9**. The source of the two nitrogens in the nitrimine and dinitrodiphenylmethane was elucidated through isotopic labeling experiments with <sup>15</sup>N-labeled diphenyldiazomethane. Results suggest that two separate 1,3-dipolar cycloadditions generating two different 5-membered intermediates via two separate [3+2] cycloadditions, furnishing the nitrimine and benzophenone, are occurring. Subsequent theoretical studies reveal that the [3+2] cycloadditions are in accord with experimental results. Further calculations show that the proposed intermediates and transition state structures are in good agreement with the product distribution and isotopic labeling studies. The kinamycins were found to be unresponsive to NO exposure in which theoretical calculations reveal that the

free energy of activation for the 1,3 dipolar cycloadditions is significantly higher for the natural products than for diphenyldiazomethane.

A comprehensive theoretical study on the chemistry of the *N*-acetyl indole-2,3-quinodimethanes (*N*-Ac IQDM **5.1**) at the DFT B3LYP 6-31 G(d) level is described. Investigation of amide conformations of *N*-Ac IQDM in which good agreement between experimental and theoretical results is shown. Subsequent studies addressing regioselectivity and stereoselectivity of Diels-Alder (DA) reactions are described. FMO theory does not provide a rationalization for the regioselectivity observed in DA reactions of *N*-Ac IQDM. Transition state calculations were carried out to probe the regioselectivity of DA reactions of this system. For acrolein,  $\Delta^\ddagger G$  was found not to be predictive of regiochemistry as observed experimentally. However, the calculated barriers,  $\Delta^\ddagger E$  and  $\Delta^\ddagger H$ , are in qualitative agreement with experimental trends in which the major regioisomer is predicted to be C-2 DA adduct. Methacrolein and crotonaldehyde were also examined. On comparison to acrolein,  $\Delta^\ddagger G$  predicts that both  $\alpha$ -substitution (i.e. methacrolein) and  $\beta$ -substitution (i.e. crotonaldehyde) increases regioselectivity for the C-2 regioisomer. Furthermore, the  $\Delta^\ddagger E$  and  $\Delta^\ddagger H$  data sets for methacrolein predicts increased regioselectivity for the C-2 adduct; the  $\Delta^\ddagger E$  and  $\Delta^\ddagger H$  data sets for crotonaldehyde predicts decreased C-2 regioselectivity.

Efforts towards the synthesis of tetrahydrofluorenes via DA reactions of ethyl 2,3-dimethylene-2,3-dihydro-1*H*-indene-1-carboxylate (**6.20**) and diethyl 2,3-dimethylene-2,3-dihydro-1*H*-indene-1,1-dicarboxylate (**6.36**) are described and were generated from the corresponding ethyl 2-(2-(1-acetoxybuta-2,3-dien-2-yl)phenyl)acetate (**6.18**) and the diethyl 2-(2-(1-acetoxybuta-2,3-dien-2-yl)phenyl)malonate (**6.35**), respectively. Employing various

solvents and bases, the carboxylate **6.20** failed to provide the desired DA adduct with methyl acrylate. The malonate **6.35** was synthesized by carboxyalkylation followed by a Stille cross coupling reaction. DA reactions with methyl acrylate were carried out in which evidence of a DA adduct was observed in the  $^1\text{H}$  NMR spectrum but attempts of its purification proved futile. DA reactions with *N*-phenylmaleimide provided the corresponding DA adduct in 77% yield. Quantum chemical calculations reveal that the two dienes **6.20** and **6.36** have termini that are significantly different and would suggest that FMO interactions would be a determining factor in the regioselectivity of Diels-Alder cycloadditions. In the case of acrolein, inspection of the MO coefficients predicts that the C-2 cycloadducts would be the major regioisomer. TS calculations agree with the qualitative interpretation that FMO arguments provide.

## Acknowledgements

My gratitude goes to my adviser, Dr. Gary I. Dmitrienko, who provided myself with a great opportunity to conduct research studies in his laboratory. From the very beginning, Gary gave me carte blanche on my projects and allowed me to flesh out my own ideas. I couldn't begin to imagine all that I have learned through my research projects. What I have realized is I have learned much about organic synthesis, medicinal chemistry, biochemistry, physical organic chemistry and theoretical/computational chemistry.

I thank my committee members, Dr. William Tam, Dr. Eric Fillion, and Dr. J. Michael Chong for their help and constructive advice throughout the course of my research.

Past and present members of the Dmitrienko lab are acknowledged for their help and discussions about chemistry. Mr. Darryl Evanoff, Dr. Muhong Shang, Dr. Oedayo Adidayo, Dr. Nan Chen, Dr. Anthony Krismanich, Dr. Ahmad Ghavami, Mr. Timothy Rasmusson, Mr. Timothy Ramadhar, Mrs. Miriam Heynen, Mrs. Valerie Goodfellow, Dr. Laura Marrone, Dr. Thammaiah Viswanatha and Mr. Taras Rybak. In particular, a special acknowledgement goes towards Dr. Nan Chen and Dr. Ahmad Ghavami. I have known Nan or "Coke" since my early days at Waterloo and he has never ceased to entertain me. Nan is quite unconventional, especially the manner in which he has demonstrated his use of the English language. His innate ability to coin phrases from the far reaches of the English lexicon will remain a mystery to me. There is not a soul on this planet that has described beer as "portable AC"...what a lovely thought. Nan and I share a love of wine as well and this has fuelled many conversations. In February 2007, Dr. Ahmad Ghavami came to us as a postdoctoral fellow and immediately the lab became a better place to work. Ahmad's enthusiasm and love

for life are beyond words. There is not a kinder, more sincere and genuine person on this earth. An office mate for the last three years, my life has been enriched tremendously of which I'm lost for words to describe. A friend whose friendship has been unwavering. Together, Nan, Ahmad and I have had many dinners and BBQ's over the years. Our discussions on topics not just of chemistry but of art, music, literature, religion, cooking and cuisine, culture and pop culture...the list is never ending. It is these things that bind us. Their cultural influences on various topics were evident and refreshing and have given me insight and perspective that I would of otherwise never acquired. These experiences have provided an informal education far beyond what any text book could offer. Taras, an undergraduate student who worked on the naphthoquinone project, gave me everything he had and more. Taras' work ethic was outstanding and by the end of that year, I believe he taught me more about chemistry than I taught him. I wish him well. The girls down the hall, Val and Laura, are another part of the family for which the lab could not be functional. Laura's baking and other delights she has brought to the office have been great. Val was one of the very first people I met at UW and she has also entertained us with BBQs at her place in the summer.

During the course of my research, it is with great sadness that Dr. Thammaiah Viswanatha or "TV" as we affectionately called him, left us. TV was on my PhD oral comprehensive committee. I will never forget his reaction to my answers. With his head bowed, he listened to me intensely and nodded at each answer I made about enzyme kinetics and particularly, my derivation of the Michaelis-Menton equation. He left with me some very powerful words which I will never forget. He told me not to be discouraged if one has read something several

times before you understand it. And then he said to me the most poetic words "...Repetition is the mother of learning..." Indeed, this has always been a metaphor for my life. Thank you.

Dr Nicholas Taylor, the departments X-ray crystallographer, left us as well. Nick procured the very first single crystal X-ray structure for me, that of the nitrimine, presented in this thesis. I remember with great fondness, discussions with him about his art at his favorite smoking post. In a moment of intellectual discourse, he and I returned to his office, to retrieve a rather old book on the subject and upon returning to his post, he communicated to me various aspects of his art. His passion was evident and profound.

As well I acknowledge the help and support of many of the support staff within the department and include the following. From Chemistry Stores; Ms. Lena Zepf, Ms. Maya Bernier, Mrs. Suhair Ammouri, Mrs. Slavica Bogdanovic, Mr. Ken Gosselink, Mr. Matt Sternbauer and Mr. Luke Bott. From the Chemistry office, Mrs. Cathy van Esch. Cathy has always been a tremendous help throughout my years at UW. Technical staff including Mrs. Janet Venne, Mr. Mike Ditty, Dr. Jalil Assoud and Dr. Richard W. Smith are acknowledged. Jan, Mike, Jalil and Richard always gave me their best on solving my problems. Their professionalism cannot be overstated.

Dr. Leonardo and Mrs. Josephine Simon have extended their hospitality to me through the many dinners and BBQ's at their place and is acknowledged here. Thanks to Mr. Ryan Bonfield who has gifted me with fine scotch and cigars...Montreal here I come...full house: aces over kings!

My world outside the chemistry department could largely be affiliated with the Graduate House on campus. The "Grad House" has become a second home to me. Who to thank and



acknowledge? Staff, coworkers and patrons many of which became good friends all too numerous to mention. Special mention goes to Rose Vogt. Rose, a tireless, enthusiastic, professional and engaging individual...(need I say more?) whose name and face is synonymous with the GH. Rose's dedication and passion for the GH is evident and I share that passion with her. We have shared dialogue through the years over many topics and she has become a great friend grown out of our mutual respect and admiration for one another. My promotion to a supervisory role this past fall (September 2010) would seem to be the high point for my years of service at the GH. Thank you Rose! As well, my passion for athletics soon found me on the soccer team (GHFC) and before I knew it, I was running the practices and training hard. Reluctant to accept titles, my teammates soon cast the title of coach upon me. But if their declaration is an acknowledgement for my enthusiasm, passion and dedication, than I am a willing acceptor. This past fall (November 2010), for the first time, the GHFC won the intermediate level of the intramural soccer league on campus and finally, one my dreams came to fruition...champions! Some of my best friends come from the football team. Miroslav Koprnicky, Elodie Fourquet, Jeff Dicker, Matt Houlahan, Ryan Sim, Eric Camm, Vlad Ciubo, Jamil Absoula, Jay Murray and Patrick Roh. Thanks to Miro, Jay, Lori and Pat for the lodging when I needed it most. Jeff has furnished me many a cigar, fine beers and scotch...thanks. Special thanks to Miro and Elodie...you have become two of my best friends. We are three explorers on a discovery mission about life. I will not forget our road trip to Boston (April 2010) to see Jeff and it is nice to see that we have already made a quick few road trips to London to see him again. Rock n' roll babies.....let the good times roll...Go GHFC!!!

## Dedication

*For my family.*

*For my mother and father whose endless love and support came by unspoken words.*

*For my grandmother whose words provided the inspiration.*

*"Repetition is the mother of learning"*

- Russian proverb

## Table of Contents

AUTHOR'S DECLARATION.....	ii
Abstract.....	iii
Acknowledgements.....	vi
Dedication.....	x
Table of Contents.....	xii
List of Figures.....	xvi
List of Schemes.....	xix
List of Tables.....	xxiv
Abbreviations.....	xxvii
Chapter 1 Introduction.....	1
1.1 Natural Products.....	1
1.1.1 Overview.....	1
1.1.2 Diazo containing Natural Products.....	2
1.2 The Kinamycins and related compounds.....	4
1.2.1 Historical Background.....	4
1.2.2 Overview of the Kinamycins and related Benzofluorenes.....	6
1.2.3 Reassessment of Kinamycin nomenclature.....	10
1.2.4 Structural reassignment of the Kinamycins.....	11
1.3 Biosynthesis.....	17
1.3.1 Initial studies: derivation of the carbon skeleton and oxidative elaboration of the D-ring.....	17
1.3.2 Advanced studies: dehydrorabelomycin from a decaketide intermediate.....	19
1.3.3 New metabolites, gene cloning, enzymes and the implications with respect to biogenesis.....	22
1.3.4 Proposal for the source of the terminal nitrogen of the diazo group.....	25
1.4 Synthesis.....	26
1.4.1 Benzo[ <i>b</i> ]carbazoloquinones syntheses and related chemistry.....	26
1.4.2 Diazobenzo[ <i>b</i> ]fluorenequinone syntheses.....	37
1.5 Mechanism of Action Studies.....	52
1.5.1 Moore's proposed mechanism for the <i>N</i> -cyanobenzo[ <i>b</i> ]carbazoles.....	52
1.5.2 Model diazo compounds.....	54
1.5.3 Mechanism studies using Kinamycins and closely associated models.....	56

1.5.4 Advanced studies: Dmitrienko's efforts towards understanding the mechanism of the cytotoxicity of the Kinamycins .....	67
1.6 Concluding remarks.....	70
Chapter 2 Synthesis of an Isosteric-Isoelectronic Analogue of Prekinamycin and Evaluation of its Bioactivity .....	72
2.1 Introduction .....	72
2.2 An Isosteric-Isoelectronic Analogue of Prekinamycin.....	73
2.3 Synthesis.....	74
2.3.1 Introduction .....	74
2.3.2 Attempts towards Buchwald-Hartwig couplings of cyanamide to aryl halides.....	77
2.3.3 Synthesis of the <i>N</i> -cyanobenzo[ <i>b</i> ]carbazoloquinone analogue of Prekinamycin.....	80
2.4 Other reported syntheses of Benzo[ <i>b</i> ]carbazoloquinones .....	93
2.5 Bioactivity .....	97
2.5.1 Introduction and Background .....	97
2.5.2 Bioactivity of Pyrido[4,3- <i>b</i> ]carbazoles and Indolo[2,3- <i>a</i> ]pyrrolo[3,4- <i>c</i> ]carbazoles .....	98
2.5.3 Bioactivity of Benzo[ <i>b</i> ]carbazoles .....	101
2.6 Conclusion.....	116
Chapter 3 The Reactivity of Nitric Oxide with Diazo compounds: Structure and Mechanism .....	117
3.1 Introduction .....	117
3.2 Results and Discussion.....	122
3.2.1 Exposure of Diphenyldiazomethane to Nitric Oxide and characterization of its products	122
3.2.2 Mechanistic proposal.....	126
3.2.3 <sup>15</sup> N-labeling and NO exposure: Insight into Mechanism.....	129
3.2.4 Quantum chemical calculations.....	136
3.2.5 Kinamycin A and Isoprekinamycin diacetate.....	158
3.2.6 A Proposal for the source of the terminal nitrogen of the Diazo group.....	160
3.3 Conclusion.....	162
Chapter 4 Diels-Alder Reactions of Indole-2,3-quinodimethanes and Related Chemistry .....	163
4.1 Introduction .....	163
4.2 Background and Overview .....	163
4.2.1 <i>o</i> -QDM .....	163
4.2.2 IQDM .....	166

4.3 Previous work in this laboratory .....	172
4.3.1 Early studies.....	172
4.3.2 Advanced Studies.....	182
4.4 Efforts towards optimizing Diels-Alder reactions of <i>N</i> -acetyl Indole-2,3-Quinodimethanes and its Application in Total Synthesis of Kinamycin Analogues .....	188
4.4.1 Oxygenated IQDMs .....	188
4.4.2 Synthetic efforts towards oxygenated <i>N</i> -acetyl Indole-2,3-Quinodimethanes.....	190
4.4.3 Efforts towards increasing product yields of Lewis-acid catalyzed Diels-Alder reactions of <i>N</i> -acetyl Indole-2,3-Quinodimethanes .....	193
4.4.4 Studies employing Mukai's method to generate <i>N</i> -substituted Indole-2,3-Quinodimethanes .....	196
4.5 Future efforts: Towards stereoselective induction using Yamamoto's BLA catalyst and/or Corey's oxazaborolidine catalyst.....	204
Chapter 5 A Theoretical Investigation into the Chemistry of the <i>N</i> -acetyl Indole-2,3-Quinodimethanes: A Quantum Chemical Study .....	205
5.1 Introduction.....	205
5.2 Theoretical investigation of IQDM by others .....	205
5.3 Quantum Chemical Calculations of the <i>N</i> -acetylindole-2,3-quinodimethanes at the DFT B3LYP 6-31G(d) level.....	212
5.3.1 Background.....	212
5.3.2 Quantum Chemical Calculations: Ab Initio and Density Functional Theory .....	214
5.3.3 Theoretical Investigation of the Conformational Mobility of the <i>N</i> -Acetyl-Indole-2,3-Quinodimethanes .....	215
5.3.4 Theoretical Investigation of Diels-Alder Reactions of the <i>N</i> -Acetyl-Indole-2,3-Quinodimethanes. ....	220
5.3.5 Theoretical Investigation of Lewis acid catalyzed Diels-Alder Reactions of the <i>N</i> -Acetyl-Indole-2,3-Quinodimethanes.....	268
5.4 Conclusion .....	303
Chapter 6 Efforts towards the Synthesis of Substituted Tetrahydrofluorenes through Diels-Alder Reactions of 2,3-Dimethylene Indene Carboxylates and Malonates .....	305
6.1 Introduction.....	305
6.2 Synthesis .....	306

6.2.1 Ethyl 2-(2-(1-acetoxybuta-2,3-dien-2-yl)phenyl)acetate.....	306
6.2.2 Diethyl 2-(2-(1-acetoxybuta-2,3-dien-2-yl)phenyl)malonate.....	312
6.2.3 Future synthetic efforts.....	321
6.3 Quantum chemical calculations.....	323
6.4 Conclusion.....	338
Chapter 7 Experimental.....	339
7.1 General Procedures.....	339
7.2 Experimental Procedures.....	341
Appendices.....	445
Appendix A Nitric oxide gas generating apparatus.....	445
Appendix B X-ray crystallographic data for <i>N</i> -(diphenylmethylene)nitramide <b>3.7</b> .....	446
Appendix C X-ray crystallographic data for Dinitrodiphenylmethane <b>3.9</b> .....	451
Appendix D X-ray crystallographic data for 1,1'-(2'-methylene-3,4-dihydrospiro[carbazole-2,3'-indolin]-1',9(1 <i>H</i> )-diyl)diethanone <b>4.55</b> .....	455
References.....	460

## List of Figures

<b>Figure 1.1:</b> Some diazo-containing natural products.....	3
<b>Figure 1.2:</b> The (a) originally proposed and (b) revised structures of the kinamycins A-D.....	5
<b>Figure 1.3:</b> Naturally occurring benzofluorenes.....	9
<b>Figure 1.4:</b> <sup>13</sup> C NMR spectroscopic assignments of selected cyanamides.....	12
<b>Figure 1.5:</b> (+)- $\alpha$ -methylbutyrate derivative of kinamycin D <b>1.49</b> and 9-diazofluorene <b>1.50</b> .....	14
<b>Figure 1.6:</b> Possible structures obtained from the deazotization of isoprekinamycin.....	16
<b>Figure 1.7:</b> Resonance depicted in IPK confers diazonium character to the diazo group.....	58
<b>Figure 2.1:</b> <b>2.1</b> as an isosteric-isoelectronic analogue of prekinamycin <b>2.2</b> .....	74
<b>Figure 2.2:</b> Clinically relevant bioactive carbazoles.....	98
<b>Figure 2.3:</b> Bioactive benzo[ <i>b</i> ]carbazoles.....	102
<b>Figure 2.4:</b> The HOMO and LUMO of <b>2.1</b> and <b>2.2</b> and their corresponding energy levels (eigenvalues) generated at the DFT B3LYP 6-31 G(d) level.....	106
<b>Figure 2.5:</b> Frontier molecular orbital energies (a.u.) of cyanamide <b>2.1</b> , prekinamycin <b>2.2</b> and GS <sup>-</sup> <b>2.109b</b> obtained at the DFT B3LYP 6-31 G(d) level.....	107
<b>Figure 2.6:</b> The HOMO of <b>2.109b</b> calculated at the DFT B3LYP 6-31 G(d) level of theory.....	108
<b>Figure 2.7:</b> The LUMO of <b>2.110</b> and <b>2.108</b> and their corresponding energy levels (eigenvalues) generated at the DFT B3LYP 6-31 G(d) level.....	110
<b>Figure 2.8:</b> The electrostatic potential (ESP) surfaces of <b>2.1</b> and <b>2.2</b> generated at the DFT B3LYP 6-31 G(d) level.....	112
<b>Figure 2.9:</b> Bond lengths (Å) as observed in the minimized structures of <b>2.1</b> and <b>2.2</b> obtained at the DFT B3LYP 6-31 G(d) level.....	113
<b>Figure 2.10:</b> The LUMO of <b>2.61</b> and <b>2.111</b> and their corresponding energy levels (eigenvalues) generated at the DFT B3LYP 6-31 G(d) level.....	115
<b>Figure 3.1:</b> Representative members of the kinamycin family.....	117
<b>Figure 3.2:</b> Single crystal X-ray structures of nitrimine <b>3.7</b> and dinitrodiphenylmethane <b>3.9</b> .....	124
<b>Figure 3.3:</b> Frontier molecular orbital energies (a.u) for the 1,3-dipolar cycloaddition of diphenyldiazomethane <b>3.5a</b> with N <sub>2</sub> O <sub>2</sub> <b>3.21</b> obtained at the DFT B3LYP 6-31 G(d) level.....	137
<b>Figure 3.4:</b> The free energy of activation ( $\Delta^\ddagger G$ ) of the two regio-[3+2] cycloadditions of <b>3.5a</b> with <b>3.21</b> furnishing adducts <b>3.25</b> and <b>3.27</b> calculated at the DFT B3LYP 6-31(G)d level of theory.....	141



<b>Figure 3.5:</b> Transition state structures of TS3 and TS6 obtained at the DFT B3LYP 6-31 G(d) level.....	146
<b>Figure 3.6:</b> The FES of the reactants <b>3.5a</b> and <b>3.21</b> generating products <b>3.7</b> and <b>3.8</b> calculated at the DFT B3LYP 6-31-G(d) level.....	153
<b>Figure 3.7:</b> The FES of the reactants <b>3.5a</b> and <b>3.21</b> generating products <b>3.7</b> and <b>3.8</b> calculated at the DFT B3LYP 6-31-G(d) level.....	154
<b>Figure 4.1:</b> The structures of <i>o</i> -QDM <b>4.1</b> and IQDM <b>4.2</b> .....	163
<b>Figure 4.2:</b> Natural products accessible through IQDM chemistry.....	168
<b>Figure 4.3:</b> The proposed structure of the homodimer assigned to be <b>4.44</b> first reported by Marinelli.....	172
<b>Figure 4.4:</b> Four possible isomers of the homodimer and the corresponding single crystal X-ray structure of <b>4.55</b> obtained by S.F. Vice.....	175
<b>Figure 4.5a:</b> IQDM rotamers <b>4.58</b> and their associated spectroscopic assignments obtained by S.R. White.....	178
<b>Figure 4.5b:</b> VT <sup>1</sup> H NMR spectra (500 MHz, acetone- <i>d</i> <sub>6</sub> , 180-213 K; S.R. White).....	179
<b>Figure 4.5c:</b> VT <sup>1</sup> H NMR spectra (500 MHz, acetone- <i>d</i> <sub>6</sub> , 223-273 K; S.R. White).....	180
<b>Figure 4.6:</b> Racemic alkylchloroborane <b>4.76</b> and chiral imidazolidinone <b>4.77</b> .....	186
<b>Figure 4.7:</b> Proton/Iodine scavenging reagents.....	194
<b>Figure 4.8:</b> The initial X-ray structure of <b>4.55</b> .....	202
<b>Figure 4.9:</b> Chiral catalysts <b>4.122</b> and <b>4.123</b> used in enantioselective Diels-Alder cycloadditions.....	204
<b>Figure 5.1:</b> <i>N</i> -acetylidole-2,3-quinodimethane.....	205
<b>Figure 5.2:</b> The HOMO of IQDMs <b>5.1</b> , <b>5.2</b> , <b>5.3</b> as calculated by Pindur.....	206
<b>Figure 5.3:</b> Energy and selected MO coefficients of the HOMO of <b>5.2</b> calculated with the MNDO, MINDO/3, PM3 and AM1 Hamiltonian as reported by S.R. White.....	208
<b>Figure 5.4:</b> The HOMO-1 of <b>5.2</b> calculated at the MNDO level by S.R. White.....	209
<b>Figure 5.5:</b> Energies and selected MO coefficients of the HOMO and the HOMO-1 for <b>5.1a</b> and <b>5.1b</b> calculated at the AM1 level by S.R. White.....	210
<b>Figure 5.6:</b> Computed activation energy ( $\Delta^\ddagger E$ ), enthalpy of activation ( $\Delta^\ddagger H$ ) and free energy of activation ( $\Delta^\ddagger G$ ) and the experimental free energy of activation ( $\Delta^\ddagger G$ ) for the rotation of the amide moiety of <b>5.1</b> (DFT B3LYP 6-31G(d) level).....	219
<b>Figure 5.7:</b> Considerations of computational efforts towards Diels-Alder reactions of <b>5.1</b> .....	221

<b>Figure 5.8:</b> Frontier molecular orbital energies (a.u) for the $[4\pi_s+2\pi_s]$ cycloaddition of <b>5.1</b> with <b>5.7</b> calculated at the DFT B3LYP 6-31G(d) level.....	226
<b>Figure 5.9:</b> The transition state structures of TS11 and TS15.....	245
<b>Figure 5.10:</b> Frontier molecular orbital energies (a.u) for the $[4\pi_s+2\pi_s]$ cycloaddition of <b>5.1</b> with <b>5.15</b> calculated at the DFT B3LYP 6-31G(d) level.....	249
<b>Figure 5.11:</b> Frontier molecular orbital energies (a.u) for the $[4\pi_s+2\pi_s]$ cycloaddition of <b>5.1</b> with <b>5.16</b> calculated at the DFT B3LYP 6-31G(d) level.....	250
<b>Figure 5.12:</b> The transition state structures of a) TS27 and TS31; b) TS43 and TS48.....	266
<b>Figure 5.13:</b> Frontier molecular orbital energies (a.u.) for the $[4\pi_s-2\pi_s]$ cycloaddition of <b>5.1</b> with <b>5.7c</b> , <b>5.7d</b> , <b>5.7e</b> , and <b>5.7f</b> calculated at the DFT B3LYP 6-31G(d) level.....	273
<b>Figure 5.14:</b> The transition state structures of TS56 and TS77.....	288
<b>Figure 5.15:</b> Achiral aluminum and titanium oxazolidinones.....	290
<b>Figure 5.16:</b> Frontier molecular orbital energies (a.u.) for the $[4\pi_s + 2\pi_s]$ cycloaddition of <b>5.1</b> with <b>5.27</b> calculated at the DFT B3LYP 6-31 G(d) level.....	295
<b>Figure 5.17:</b> Frontier molecular orbital energies (a.u.) for the $[4\pi_s + 2\pi_s]$ cycloaddition of <b>5.1</b> with <b>5.28</b> calculated at the DFT B3LYP 6-31 G(d) level.....	296
<b>Figure 5.18:</b> The transition state structures of TS81 and TS82.....	302
<b>Figure 6.1:</b> Selected 2D NMR correlations of <b>6.28</b> and <b>6.29</b> .....	317
<b>Figure 6.2</b> .....	320
<b>Figure 6.3:</b> Frontier molecular orbital energies (a.u.) for the $[4\pi_s + 2\pi_s]$ cycloaddition of <b>6.20</b> and <b>6.36</b> with acrolein obtained the DFT B3LYP 6-31 G(d) level.....	326
<b>Figure 6.4:</b> The transition state structures of a) TS85 and TS90; b) TS102 and TS106.....	338

## List of Schemes

<b>Scheme 1.1:</b> Mithani and Dmitrienko's synthesis of <b>1.48</b> .....	13
<b>Scheme 1.2:</b> Proposed mechanism for the interconversion between PK and IPK.....	16
<b>Scheme 1.3:</b> Gould's biosynthetic studies of kinamycins C and D.....	18
<b>Scheme 1.4:</b> Gould's early proposal for the biosynthesis of the kinamycins.....	19
<b>Scheme 1.5:</b> Gould's revised biosynthesis of the kinamycins.....	21
<b>Scheme 1.6:</b> Gould's proposal for the origin of the "cyanamide" carbon.....	22
<b>Scheme 1.7:</b> Gould's current biosynthetic proposal for the kinamycins.....	24
<b>Scheme 1.8:</b> Possible enzyme participation in kinamycin biosynthesis.....	25
<b>Scheme 1.9:</b> Dmitrienko's synthesis of <i>N</i> -cyanoindoles and <i>N</i> -cyanoindoloquinones.....	27
<b>Scheme 1.10:</b> Dmitrienko's synthesis of benzoannulated indoloquinones.....	28
<b>Scheme 1.11:</b> Murphy's synthesis of <b>1.109</b> .....	29
<b>Scheme 1.12:</b> Echavarren's reported synthesis of <b>1.36</b> , <b>1.119</b> and <b>1.121</b> .....	30
<b>Scheme 1.13:</b> Interpretation of Echavarren's product distribution.....	31
<b>Scheme 1.14:</b> Reinterpretation of Echavarren's results.....	33
<b>Scheme 1.15:</b> Analysis and reinterpretation of the <i>N</i> -cyanation events of Echavarren's synthesis.....	35
<b>Scheme 1.16:</b> Castedo's synthesis.....	36
<b>Scheme 1.17:</b> Knolker and O'Sullivan's synthesis of 7-deoxyprekinamycin.....	37
<b>Scheme 1.18:</b> Hauser and Zhou's synthesis of prekinamycin.....	38
<b>Scheme 1.19:</b> Birman's synthesis of prekinamycin.....	39
<b>Scheme 1.20:</b> Porco's enantioselective synthesis of kinamycin C.....	41
<b>Scheme 1.21:</b> Porco's enantioselective synthesis of kinamycin C (continued).....	42
<b>Scheme 1.22:</b> Ishikawa's synthesis of ( $\pm$ ) <i>O</i> -methyl-kinamycin C.....	43
<b>Scheme 1.23:</b> Ishikawa's synthesis of ( $\pm$ ) <i>O</i> -methyl-kinamycin C (continued).....	44
<b>Scheme 1.24:</b> Nicolaou's enantioselective syntheses of kinamycins C, F and J.....	45
<b>Scheme 1.25:</b> Nicolaou's enantioselective syntheses of kinamycins C, F and J (continued).....	46
<b>Scheme 1.26:</b> Dmitrienko's biomimetic approach to the synthesis of the D-ring.....	48
<b>Scheme 1.27:</b> Dmitrienko's total synthesis of isoprekinamycin.....	49
<b>Scheme 1.28:</b> Dmitrienko's total synthesis of isoprekinamycin (continued).....	49
<b>Scheme 1.29:</b> Dmitrienko's total synthesis of isoprekinamycin (continued).....	50
<b>Scheme 1.30:</b> Herzon's enantioselective synthesis of kinamycin F.....	51

<b>Scheme 1.31:</b> Moore's proposal for the bioreductive alkylation of kinamycin C.....	53
<b>Scheme 1.32:</b> Early mechanistic studies with simple aryl diazo compounds.....	55
<b>Scheme 1.33:</b> Dmitrienko's synthesis of IPK model <b>1.262</b> .....	56
<b>Scheme 1.34:</b> Nucleophilic attack on an aryl diazonium species to elicit aryl radicals.....	57
<b>Scheme 1.35:</b> Experimental conditions to test relative electrophilicities of IPK and <b>1.262</b> .....	60
<b>Scheme 1.36:</b> Feldman and Eastman's MOA studies of dimethyl prekinamycin.....	61
<b>Scheme 1.37:</b> Melander's experiment in which DTT activation of kinamycin D was observed.....	62
<b>Scheme 1.38:</b> Melander's MOA studies using kinamycin D.....	63
<b>Scheme 1.39:</b> Skibo's postulate of protonated <i>o</i> -quinone methide intermediates as DNA alkylating reagents.....	65
<b>Scheme 1.40</b> .....	66
<b>Scheme 2.1:</b> Mithani's target <i>N</i> -cyanobenzo[ <i>b</i> ]carbazoloquinone <b>2.4</b> obtained from <b>2.3</b> .....	76
<b>Scheme 2.2:</b> Retrosynthetic analyses of <b>2.1</b> .....	77
<b>Scheme 2.3:</b> Potential synthetic routes to access <b>2.7</b> via Buchwald-Hartwig couplings.....	78
<b>Scheme 2.4:</b> Buchwald-Hartwig coupling of <i>o</i> -bromoanisole and benzamide.....	79
<b>Scheme 2.5:</b> Synthesis of <b>2.25</b> .....	81
<b>Scheme 2.6:</b> Possible synthetic routes for the amination of bromo-naphthoquinones.....	82
<b>Scheme 2.7:</b> Production of <b>2.29</b> and attempts of its regioselective dehydrohalogenation.....	83
<b>Scheme 2.8:</b> CAN oxidation of <b>2.25</b> .....	84
<b>Scheme 2.9:</b> Copper and palladium catalyzed cross-couplings of bromoanisoles.....	86
<b>Scheme 2.10:</b> Various amination attempts towards the synthesis of <b>2.38</b> .....	87
<b>Scheme 2.11:</b> Attempted copper catalyzed cross-couplings of aryl bromides <b>2.14</b> and <b>2.25</b> .....	88
<b>Scheme 2.12:</b> Palladium catalyzed cross-couplings of aryl bromides.....	89
<b>Scheme 2.13:</b> Synthesis of <b>2.47</b> and subsequent use in Buchwald-Hartwig couplings.....	90
<b>Scheme 2.14:</b> Synthesis of <b>2.57</b> .....	91
<b>Scheme 2.15:</b> The remaining steps of the synthesis towards <b>2.1</b> .....	93
<b>Scheme 2.16:</b> Estevez's efforts towards the synthesis of <b>2.69</b> using Heck chemistry.....	94
<b>Scheme 2.17:</b> Estevez's synthesis of the benzo[ <i>b</i> ]tetrahydrocarbazoloquinone <b>2.79</b> .....	95
<b>Scheme 2.18:</b> Diastereoselectivity of the Henry reaction producing <b>2.75</b> .....	96
<b>Scheme 2.19:</b> Estevez's synthesis of the benzo[ <i>b</i> ]tetrahydrocarbazoloquinone <b>2.90</b> .....	97
<b>Scheme 2.20:</b> The acid dissociation of glutathione <b>2.109a</b> to yield the corresponding thiolate <b>2.109b</b> .....	108

<b>Scheme 2.21:</b> Possible interaction of GSH with kinamycin F.....	109
<b>Scheme 3.1:</b> Synthesis of diphenyldiazomethane <b>3.5</b> .....	122
<b>Scheme 3.2:</b> Exposure of diphenyldiazomethane to NO furnishing the corresponding products.....	123
<b>Scheme 3.3:</b> Ionic-type mechanism for attack of diazo species <b>3.13</b> on NO.....	127
<b>Scheme 3.4:</b> [4+1] cycloadditions of N <sub>2</sub> O <sub>2</sub> with phosphine <b>3.20</b> and diphenyldiazomethane <b>3.5a</b> .....	128
<b>Scheme 3.5:</b> Two possible regio-[3+2] cycloaddition pathways of N <sub>2</sub> O <sub>2</sub> with diphenyldiazomethane to furnish nitrimine <b>3.7</b> , benzophenone <b>3.8</b> and dinitrodiphenylmethane <b>3.9</b> calculated at the DFT B3LYP 6-31 G(d) level of theory.....	129
<b>Scheme 3.6:</b> Synthesis of <sup>15</sup> N-labeled <b>3.4b</b> and its oxidation to <b>3.5b</b> .....	130
<b>Scheme 3.7:</b> Mechanistic manifold illustrating three possible pathways that generate <b>3.7</b> , <b>3.8</b> and <b>3.9</b> calculated at the DFT B3LYP 6-31 G(d) level of theory.....	134
<b>Scheme 3.8:</b> Radical addition of NO with <b>3.5b</b> producing <b>3.31</b> .....	135
<b>Scheme 3.9:</b> Ionic pathway for the generation of <b>3.37</b> from <b>3.5a</b> and <b>3.21</b> .....	138
<b>Scheme 3.10:</b> Possible reaction channels that may generate <b>3.7</b> and <b>3.8</b> .....	158
<b>Scheme 3.11:</b> TS obtained for 1,3 dipolar cycloaddition of N <sub>2</sub> O <sub>2</sub> with kinamycin A and IPK diacetate.....	160
<b>Scheme 3.12:</b> Possible <i>N</i> -nitrosation events in the biosynthesis of the diazo group.....	161
<b>Scheme 4.1:</b> The early experiments of Finkelstein and Cava.....	164
<b>Scheme 4.2:</b> Methods of generating <i>o</i> -QDM <b>4.1</b> .....	165
<b>Scheme 4.3:</b> Kitagaki's method for <i>o</i> -QDM generation and use in IMDA.....	166
<b>Scheme 4.4:</b> Plieninger's generation of IQDM and use in Diels-Alder reactions.....	167
<b>Scheme 4.5:</b> The key step of Magnus' total synthesis of <i>dl</i> -aspidospermidine.....	168
<b>Scheme 4.6:</b> Methods of generating IQDM <b>4.2</b> .....	169
<b>Scheme 4.7:</b> Mukai's generation of IQDM <b>4.41</b> and its Diels-Alder trapping.....	170
<b>Scheme 4.8:</b> Fuwa and Sasaki's generation of <b>4.41</b> and its Diels-Alder trapping.....	171
<b>Scheme 4.9:</b> S.F. Vice's initial conditions generating IQDM and trapping in DA reactions.....	174
<b>Scheme 4.10:</b> The probable mechanism furnishing <b>4.58</b> interpreted from NMR studies performed by Vice and White.....	177
<b>Scheme 4.11:</b> Wu's initial experiments defining conditions for LA-catalyzed reactions.....	183
<b>Scheme 4.12:</b> Wu's stereoselective Diels-Alder reactions of <i>N</i> -Ac-IQDM using <b>4.73</b> .....	185

<b>Scheme 4.13:</b> Wu's stereoselective Diels-Alder reactions of <i>N</i> -Ac-IQDM using <b>4.78</b> .....	187
<b>Scheme 4.14:</b> Proposed synthesis of carbazoles and kinamycin analogues.....	188
<b>Scheme 4.15:</b> Jakiwczyk's synthetic plan for lactones <b>4.88</b> and <b>4.91</b> .....	189
<b>Scheme 4.16:</b> The potential generation of oxygen substituted IQDM <b>4.94</b> from <b>4.93</b> .....	190
<b>Scheme 4.17:</b> a) Attempted bromination of <b>4.95</b> ; b) Possible compounds generated via the thermal process of the GCMS experiment.....	192
<b>Scheme 4.18:</b> Attempts at iodination and acetoxylation of <b>4.95</b> .....	193
<b>Scheme 4.19:</b> Proposed degradation pathways of IQDM <b>4.58</b> .....	194
<b>Scheme 4.20:</b> a) Mukai's method to generate tetrahydrocarbazoles b) potential extension to carbocyclic systems to furnish benzo-annulated tetrahydrofluorenes.....	197
<b>Scheme 4.21:</b> Synthesis of allenylaniline <b>4.40</b> .....	198
<b>Scheme 4.22:</b> Repeat of Mukai's experiment under new conditions.....	200
<b>Scheme 4.23:</b> Production of <b>4.102</b> and <b>4.55</b> and the corresponding the X-ray of <b>4.55</b> .....	203
<b>Scheme 5.1:</b> TS calculations of the Diels-Alder cycloaddition of <i>s</i> -trans acrolein and <i>N</i> -formyl-IQDM calculated at the DFT B3LYP 6-31G(d) level by R. Laufer.....	211
<b>Scheme 5.2:</b> Tsoleridis's study of 1,3 dipolar cycloadditions of <i>N</i> -substituted IQDMs and nitrile oxides.....	212
<b>Scheme 5.3:</b> Secondary orbital interactions as a determining factor in the regioselectivity of Diels-Alder cycloadditions of 1-methylbutadiene with methyl acrylate.....	227
<b>Scheme 5.4:</b> Possible BF <sub>3</sub> complexes of <i>N</i> -Ac IQDM and subsequent cycloadditions.....	287
<b>Scheme 5.5:</b> Wu's stereoselective Diels-Alder reactions of <i>N</i> -Ac-IQDM using <b>5.23</b> .....	289
<b>Scheme 6.1:</b> Access to a) carbazoloquinones <b>6.4</b> and b) fluorenequinones <b>6.7</b> .....	305
<b>Scheme 6.2:</b> Generation of bis-methylene indene <b>6.11</b> and its use in Diels-Alder cycloadditions.....	306
<b>Scheme 6.3:</b> Synthesis of <b>6.18</b> .....	307
<b>Scheme 6.4:</b> Attempted Diels-Alder reactions of allenyl phenyl acetate <b>6.18</b> .....	309
<b>Scheme 6.5:</b> a) Possible decomposition of <b>6.18</b> via oligomerization b) Attempted cycloadditions using pivalate <b>6.25</b> .....	311
<b>Scheme 6.6:</b> Attempts at carboxyalkylation of <b>6.16</b> .....	313
<b>Scheme 6.7:</b> Possible mechanistic pathways furnishing <b>6.28</b> , <b>6.29</b> and <b>6.26</b> .....	315
<b>Scheme 6.8:</b> Synthesis of malonate <b>6.35</b> .....	318
<b>Scheme 6.9:</b> Cycloaddition reaction of <b>6.35</b> with <b>6.40</b> to furnish <b>6.41</b> .....	321

<b>Scheme 6.10:</b> Diels-Alder cycloadditions using alternative strategies.....	322
--	-----

## List of Tables

<b>Table 1.1:</b> Original and revised structures of the kinamycins and related natural products.....	8
<b>Table 1.2:</b> Calculated IR frequencies and bond lengths of the diazo group of selected compounds.....	59
<b>Table 2.1:</b> Attempted Buchwald-Hartwig couplings of cyanamide with <i>o</i> -bromoanisole.....	80
<b>Table 2.2:</b> The growth inhibition of K562 cells (IC <sub>50</sub> μM) for selected compounds.....	104
<b>Table 3.1:</b> Product distribution of nitrimine <b>3.7</b> and benzophenone <b>3.8</b> under different solvent conditions.....	123
<b>Table 3.2a:</b> Selected bond lengths for nitrimines <b>3.11</b> , <b>3.12</b> and <b>3.7</b> in angstroms (Å).....	125
<b>Table 3.2b:</b> Selected bond angles (in degrees) for nitrimines <b>3.11</b> , <b>3.12</b> and <b>3.7</b> .....	125
<b>Table 3.3:</b> <sup>15</sup> N NMR chemical shifts and couplings for <b>3.4b</b> , <b>3.29</b> and <b>3.5b</b> .....	133
<b>Table 3.4:</b> The relative ground state energies ( <i>E</i> , <i>H</i> , <i>G</i> ) of <b>3.24</b> , <b>3.25</b> and <b>3.27</b> and the corresponding free energies of activation ( $\Delta^\ddagger G$ ) for the indicated pericyclic reaction obtained at the DFT B3LYP 6-31 G(d) level.....	139
<b>Table 3.5:</b> FMO energies (a.u.) and orbital coefficients of <b>3.5a</b> and <b>3.21</b> obtained at the DFT B3LYP 6-31 G(d) level.....	143
<b>Table 3.6:</b> Energies of all reactants, cycloadducts and intermediates in Pathways A, A', B and B' calculated at the DFT B3LYP 6-31-G(d) level.....	147
<b>Table 3.7:</b> Energies and energy barriers for reaction channels calculated at the DFT B3LYP 6-31 G(d) level.....	150
<b>Table 4.1:</b> The observed regioselectivity of DA reactions of IQDMs generated from <b>4.57</b> .....	182
<b>Table 4.2:</b> Wu's experimental conditions of Lewis acid catalyzed DA reactions of β-unsubstituted-α,β-unsaturated enals and <i>N</i> -Ac-IQDM <b>4.58</b> .....	184
<b>Table 4.3:</b> Diels-Alder SnCl <sub>4</sub> catalyzed reactions of <b>4.58</b> with additives.....	195
<b>Table 5.1:</b> Summary of Pindur's studies of Diels-Alder reactions with IQDM <b>5.3</b> .....	207
<b>Table 5.2:</b> Experimental and calculated rotamer populations and ground-state energies of <i>N</i> -Ac-IQDM rotamers <b>5.1a</b> and <b>5.1b</b> (DFT B3LYP 6-31G(d) level).....	217
<b>Table 5.3:</b> The energies (a.u.) and relative energies (kcal·mol <sup>-1</sup> ) of <i>N</i> -Ac-IQDM and acrolein and their corresponding Diels-Alder adducts obtained at the DFT B3LYP 6-31G(d) level.....	224
<b>Table 5.4:</b> FMO energy (a.u.) and orbital coefficients of the HOMO of <i>N</i> -Ac-IQDM <b>5.1a</b> and <b>5.1b</b> obtained at the DFT B3LYP 6-31G(d) level.....	229



<b>Table 5.5:</b> FMO energy (a.u.) and orbital coefficients of the LUMO of acrolein <b>5.7a</b> and <b>5.7b</b> obtained at the DFT B3LYP 6-31G(d) level.....	231
<b>Table 5.6:</b> Selected structural data and energies of TS structures of Diels-Alder reactions of <i>N</i> -Ac-IQDM and acrolein obtained at the DFT B3LYP 6-31G(d) level.....	235
<b>Table 5.7:</b> The energies (a.u.) and relative energies (kcal·mol <sup>-1</sup> ) of methacrolein and crotonaldehyde and their corresponding Diels-Alder adducts obtained at the DFT B3LYP 6-31G(d) level.....	247
<b>Table 5.8:</b> FMO energy (a.u.) and orbital coefficients of the LUMO of methacrolein <b>5.15a</b> and <b>5.15b</b> obtained at the DFT B3LYP 6-31G(d) level.....	251
<b>Table 5.9:</b> FMO energy (a.u.) and orbital coefficients of the LUMO of crotonaldehyde <b>5.16a</b> and <b>5.16b</b> obtained at the DFT B3LYP 6-31G(d) level.....	253
<b>Table 5.10:</b> Selected structural data and energies for TS structures of Diels-Alder reactions of <i>N</i> -Ac-IQDM and methacrolein obtained at the DFT B3LYP 6-31G(d) level.....	258
<b>Table 5.11:</b> Selected structural data and energies for TS structures of Diels-Alder reactions of <i>N</i> -Ac-IQDM and crotonaldehyde obtained at the DFT B3LYP 6-31G(d) level.....	262
<b>Table 5.12:</b> The energies (a.u.) and relative energies (kcal·mol <sup>-1</sup> ) of BF <sub>3</sub> -complexed acrolein, methacrolein and crotonaldehyde and their corresponding Diels-Alder adducts obtained at the DFT B3LYP 6-31G(d) level.....	269
<b>Table 5.13:</b> FMO energies (a.u.) and orbital coefficients of the LUMO of BF <sub>3</sub> -complexed acrolein <b>5.7c</b> , <b>5.7d</b> , <b>5.7e</b> and <b>5.7f</b> obtained at the DFT B3LYP 6-31G(d) level.....	274
<b>Table 5.14:</b> Selected structural data and energies of TS structures of Diels-Alder reactions of <i>N</i> -Ac-IQDM and BF <sub>3</sub> -complexed acrolein obtained at the DFT B3LYP 6-31G(d) level.....	279
<b>Table 5.15:</b> The energies (a.u.) and relative energies (kcal·mol <sup>-1</sup> ) of aluminum and titanium <i>N</i> -acyloxazolidinones and their corresponding Diels-Alder adducts obtained at the DFT B3LYP 6-31G(d) level.....	291
<b>Table 5.16:</b> FMO energy (a.u.) and orbital coefficients of the LUMO of <b>5.27a</b> and <b>5.27b</b> obtained at the DFT B3LYP 6-31G(d) level.....	297
<b>Table 5.17:</b> FMO energy (a.u.) and orbital coefficients of the LUMO of <b>5.28a</b> and <b>5.28b</b> obtained at the DFT B3LYP 6-31G(d) level.....	298
<b>Table 5.18:</b> Selected structural data and energies of TS structures of Diels-Alder reactions of <i>N</i> -Ac-IQDM <b>5.1</b> and <b>5.27</b> and <b>5.28</b> obtained at the DFT B3LYP 6-31G(d) level.....	299
<b>Table 6.1:</b> Attempted optimization of Diels-Alder reactions of <b>6.18</b> with <b>6.19</b> .....	308
<b>Table 6.2:</b> Attempts at carboxyalkylation of <b>6.16</b> .....	314

<b>Table 6.3:</b> Diels-Alder cycloadditions of <b>6.35</b> with <b>6.19</b> .....	319
<b>Table 6.4:</b> The energies (a.u.) and relative energies (kcal·mol <sup>-1</sup> ) of carboxylate <b>6.20</b> , malonate <b>6.36</b> and acrolein and their corresponding Diels-Alder adducts calculated at the DFT B3LYP 6-31 G(d) level.....	323
<b>Table 6.5:</b> FMO energy (a.u.) and orbital coefficients of the HOMO of <b>6.20</b> calculated at the DFT B3LYP 6-31 G(d) level.....	328
<b>Table 6.6:</b> FMO energy (a.u.) and orbital coefficients of the HOMO of <b>6.36</b> calculated at the DFT B3LYP 6-31 G(d) level.....	329
<b>Table 6.7:</b> Selected structural data and energies of TS structures of Diels-Alder reactions of <b>6.20</b> and acrolein obtained at the DFT B3LYP 6-31 G(d) level.....	331
<b>Table 6.8:</b> Selected structural data and energies of TS structures of Diels-Alder reactions of <b>6.36</b> and acrolein obtained at the DFT B3LYP 6-31 G(d) level.....	335

## Abbreviations

$\Delta$	difference, heat
Å	angstrom
°	degrees
Ac	acetyl
acac	acetylacetone
AcCl	acetyl chloride
ACN	acetonitrile
AIBN	2,2'-azobisisobutyronitrile
Ar	aryl
ATCC	American Type Culture Collection
atm	atmosphere
a.u.	atomic unit
ax.	axial
BINAP	2,2'-bis(diphenylphosphino)-1,1'-binaphthyl
bn	benzyl
boc	<i>tert</i> -butoxycarbonyl
br	broad
BSO	buthionine sulfoximine
<i>t</i> -bu	<i>tert</i> -butyl
bz	benzoyl
°C	degrees Celsius

CAN	ceric ammonium nitrate
CI	chemical ionization (mass spectrometry)
CHO	Chinese hamster ovary (cell)
COSY	correlation spectroscopy
<i>m</i> -CPBA	<i>meta</i> -chloroperbenzoic acid
Cpd	compound
CSA	camphor sulfonic acid
$\Delta d$	difference in bond length, distance
d	doublet
DA	Diels-Alder cycloaddition
dba	dibenzylideneacetone
DBU	1,8-diazabicyclo[5.4.0]undec-7-ene
DCE	dichloroethane
dd	doublet of doublets
DDQ	2,3-dichloro-5,6-dicyano-1,4-benzoquinone
DFT	density functional theory
DIEA	diisopropylethylamine
DIPEA	diisopropylethylamine
D-DIPT	D(-)-diisopropyl tartrate
DMAP	4- <i>N,N</i> -dimethylaminopyridine
DMDO	dimethyl dioxirane
DME	1,2-dimethoxyethane

DMF	<i>N,N</i> -dimethylformamide
DMSO	dimethylsulfoxide
DNA	deoxyribonucleic acid
DON	6-diazo-5-oxo- <i>L</i> -norleucine
DTT	dithiothreitol
<i>E</i>	electronic energy
$\Delta^\ddagger E$	electronic activation energy
ee	enantiomeric excess
EA	electron affinity
EI	electron impact (mass spectrometry)
eq.	equatorial
ESI	electrospray ionization (mass spectrometry)
ESR	electron spin resonance
Et	ethyl
Et <sub>3</sub> N	triethylamine
EtOH	ethanol
FES	free energy surface
FMO	frontier molecular orbital
FT	Fourier transform
g	gram
<i>G</i>	free energy
$\Delta^\ddagger G$	free energy of activation

GCMS	gas chromatography mass spectrometry
GSH	<i>L</i> -glutathione
GST	<i>L</i> -glutathione- <i>S</i> -transferase
h	hour
[H]	reduction
<i>H</i>	enthalpy
$\Delta^\ddagger H$	enthalpy of activation
HF	Hartree Fock
HMBC	heteronuclear multiple bond coherence
HMDS	hexamethyldisilazane
HMPA	hexamethylphosphoramide
HMQC	heteronuclear multiple quantum coherence
HOAc	acetic acid
HOMO	highest occupied molecular orbital
HPLC	high pressure/performance liquid chromatography
HRMS	high resolution mass spectroscopy/spectrum
Hz	hertz
IC <sub>50</sub>	concentration needed to inhibit a given biological process by 50%
IF	imaginary frequency
imid	imidazole
IPK	isoprekinamycin
IQDM	indole quinodimethane

IR	infrared
JMOD	<i>J</i> -modulated
K	degrees Kelvin
KAT	kinamycin acetyl transferase
kDa	kilodalton
$K_M$	the Michaelis constant
kin	kinamycin
L	liter, ligand
LDA	lithium diisopropylamide
LiHMDS	lithium bis(trimethylsilyl)amide
LTMP	lithium 2,2,6,6-tetramethylpiperidide
LUMO	lowest unoccupied molecular orbital
m	multiplet
M	metal, molarity (concentration)
$M^+$	molecular ion
Me	methyl
MeCN	acetonitrile
MeOH	methanol
MEP	minimum energy pathway
$\mu\text{M}$	micromolar
mg	milligram
MHz	megahertz

min	minute
mL	milliliter
mm	millimeter
MO	molecular orbital
MOA	mechanism of action
MOM	methoxymethyl
mp	melting point
<i>Mr</i>	relative molecular mass
Ms	methanesulfonyl, mesyl
MS	mass spectrum, molecular sieves
MSA	methanesulfonic acid
NADP	nicotinamide adenine dinucleotide phosphate
NADPH	reduced form of nicotinamide adenine dinucleotide phosphate
NBS	<i>N</i> -bromosuccinimide
nm	nanometer
NMR	nuclear magnetic resonance
NO	nitric oxide
nOe	nuclear Overhauser effect
Nu	nucleophile
[O]	oxidation
OAc	acetate
<i>Oi</i> -Pr	isopropoxide



OTC	(-)-2-oxo-4-thiazolidinecarboxylic acid
OTf	triflate
<i>P</i>	pressure
PES	potential energy surface
pH	negative log of proton activity/concentration
Ph	phenyl
PhMe	toluene
PhOCN	phenyl cyanate
pKa	negative log of the acid equilibrium constant
PK	prekinamycin
ppm	parts per million
<i>i</i> -Pr	<i>iso</i> -propyl
Py	pyridine
Pyr	pyridine
QDM	quinodimethane
<i>R</i>	conventional R-factor (X-ray)
<i>R<sub>w</sub></i>	Hamiltonian weighted R-factor
<i>R<sub>f</sub></i>	retention factor
R1	rotamer 1
R2	rotamer 2
<i>rac</i>	racemic
ROS	reactive oxygen species

rt	room temperature
s	singlet
sec	seconds
SET	single electron transfer
t	triplet
<i>T</i>	temperature
TBAF	tetra- <i>n</i> -butylammonium fluoride
TBAI	tetra- <i>n</i> -butylammonium iodide
TBDMS	<i>tert</i> -butyldimethylsilyl
TBS	<i>tert</i> -butyldimethylsilyl
Tf	trifluoromethanesulfonyl, triflyl
TFA	trifluoroacetic acid
TFAA	trifluoroacetic anhydride
THF	tetrahydrofuran
TLC	thin layer chromatography
TMEDA	tetramethylethylenediamine
TMS	trimethylsilyl
TPAP	tetrapropylammonium perruthenate
<i>p</i> -TSA	<i>para</i> -toluenesulfonic acid
TS	transition state
TSs	transition state structure
TsOH	( <i>para</i> -) toluenesulfonic acid

UV	ultraviolet
ZPE	zero point (vibrational) energy
ZPVE	zero point vibrational energy



# Chapter 1

## Introduction

### 1.1 Natural Products

#### 1.1.1 Overview

A natural product, by the broadest definition of the term, may be classified as any material that can be isolated from any living organism.<sup>1-3</sup> Natural products may be further classified as products of primary metabolism or secondary metabolism although this classification is arbitrary.<sup>1</sup> Generally speaking, primary metabolites would include simple sugars and carbohydrates, fatty acids and lipids, amino acids and proteins, nucleotides and nucleic acids and thus appear to be ubiquitous and essential. On the other hand, secondary metabolites were initially considered non-essential; however, they may have pharmacological, toxicological and ecological importance and thus may offer some type of advantage to the organism in which it is found. Most literature sources consider natural products as secondary metabolites only. Secondary metabolites are generally classified according to their structure and biosynthetic origin.

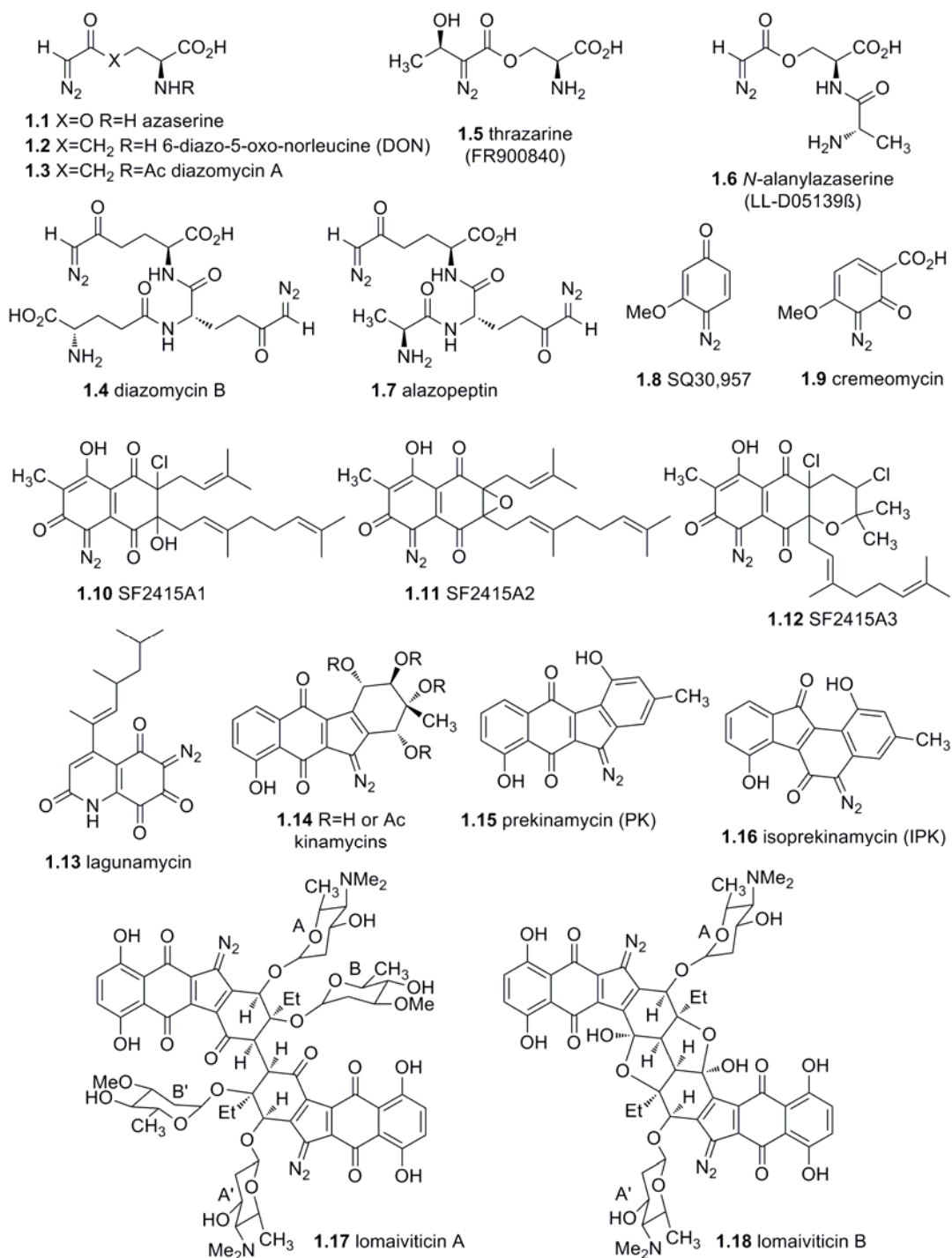
The sheer number of reports published in the literature yearly on natural products would seem to reflect their immense importance to mankind. Indeed, many of these compounds possess potent antibiotic or anticancer activity and thus have provided the scientific community a strong motivation to find suitable pharmacological candidates in the ongoing battle against disease and infection. Almost two thirds of the known antibiotics of natural origin are produced by members of the genus *Streptomyces*<sup>4,5</sup> with relevant examples given in the following discussion.

### 1.1.2 Diazo containing Natural Products

Of the many known natural products, only a handful contain a diazo group within their structure, most of which are shown in Figure 1.1. Some of these are derivatives of  $\alpha$ -amino acids including azaserine (**1.1**),<sup>6-8</sup> 6-diazo-5-oxo-norleucine (DON **1.2**),<sup>9</sup> diazomycins A and B (**1.3** and **1.4**, respectively),<sup>10</sup> thazarine (**1.5**),<sup>11-14</sup> *N*-alanylazaserine (**1.6**)<sup>15</sup> and alazopeptin (**1.7**).<sup>16,17</sup> Two simpler, six-membered cyclic species are represented by SQ30,957 (**1.8**)<sup>18</sup> and cremeomycin (**1.9**).<sup>19,20</sup> Fused bicyclics are represented by four members, SF2415A1 and its two congeners (**1.10**, **1.11** and **1.12**)<sup>21,22</sup> as well as lagunamycin (**1.13**).<sup>23,24</sup> The tetracyclic kinamycins (**1.14**, **1.15** and **1.16**)<sup>25-33</sup> and the related lomaiviticins (**1.17** and **1.18**),<sup>34</sup> a dimeric form of the kinamycins, have been also been reported. With the exception of **1.6**, **1.8**, **1.17** and **1.18**, all of these diazo-containing natural products were isolated from *Streptomyces* *sp.*

Recently, the lomaiviticins **1.17** and **1.18** were shown to possess profound cytotoxicity for a number of cancer cell lines.<sup>34</sup> This demonstration of such potent toxicity has re-stimulated interest in the kinamycin group of natural products. The group of natural products encompassing the kinamycins and related structures are discussed in the following sections.

**Figure 1.1:** Some diazo-containing natural products.



## 1.2 The Kinamycins and related compounds

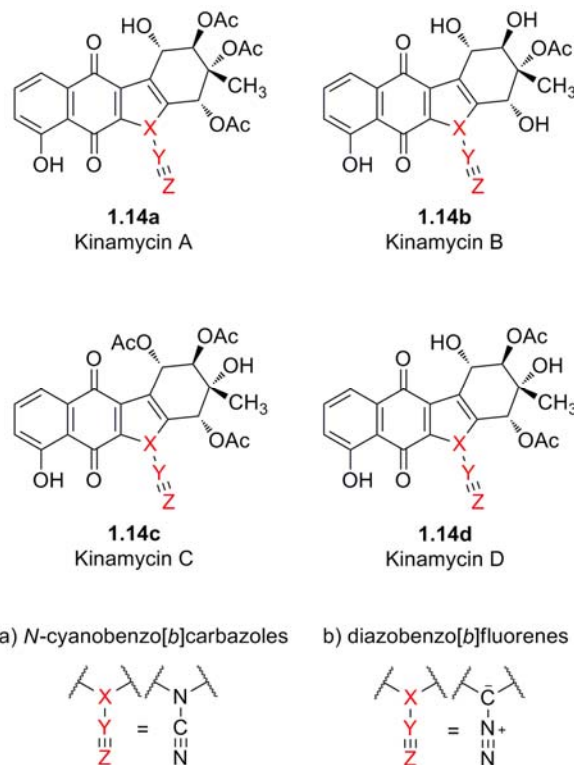
### 1.2.1 Historical Background

The kinamycins are a family of natural products that have a long and storied history. The first public disclosure of their existence was presented by Omura and co-workers on September 19<sup>th</sup>, 1969 at the 169<sup>th</sup> Scientific Meeting of the Japan Antibiotics Research Association, Tokyo, Japan. Subsequently, the same group provided the first literature account of the kinamycins in 1970, in which four active components, namely kinamycin A, B, C and D were described (Figure 1.2), isolated from the soil bacterium *Streptomyces murayamaensis* sp. nov. Hata *et* Ohtani as an orange crystalline substance.<sup>25</sup> They possessed anti-bacterial activity, largely against Gram-positive bacteria and less so against Gram-negative bacteria. Initial spectroscopic studies provided evidence of a quinone and a nitrile or isonitrile functional group. A subsequent report described kinamycin A and C as yellow needles and kinamycin B and D as orange needles and through various chemical and spectroscopic studies, the Omura group was able to confirm the presence of both ester and phenolic functional groups as well as to verify the quinone and the apparent nitrile/isonitrile moieties.<sup>26</sup> Furthermore, kinamycins A and C demonstrated lower activity against Gram-positive bacteria than kinamycins B and D. An anticancer activity profile was provided in which kinamycin C afforded some increase in survival against Ehrlich ascites carcinoma and sarcoma-180 in mice, whereas kinamycin D did not.

Further reports by Omura's group provided a structure for kinamycin C consistent with data provided by chemical modification studies<sup>27</sup> and together with a single crystal X-ray structure of the *p*-bromobenzoate derivative,<sup>28</sup> permitted these workers to establish the



**Figure 1.2:** The (a) originally proposed and (b) revised structures of the kinamycins A-D.



stereochemistry of the D ring. The authors proposed “... a structure with a nitrile or isonitrile group attached to N atom on pyrrole [*sic*] ring was presumed...” and upon liberation of ammonia but not formic acid with the treatment with 30% KOH the “...kinamycins were confirmed to have a nitrile group...”<sup>27</sup> and support their findings that “...a cyano group is bonded to the N atom of the pyrrole ring, which is rather unusual in an antibiotic...”<sup>28</sup> The likelihood of the diazo functionality was not considered presumably owing to its perceived inherent instability and that few natural products containing the diazo group were known at the time. The other kinamycins, A, B, and D “...were assumed to have difference in the

number and position of functional groups in the D ring from NMR, IR and mass spectra...”<sup>27</sup>

The fifth report from the Omura group described more extensive chemical modification studies and the UV, IR, NMR and mass spectrometric data<sup>29</sup> and corroborated those authors' findings from their earlier investigations. From these five seminal reports by the Omura group, those workers concluded that these compounds contained the cyanamide functionality and thus the kinamycins were assigned as *N*-cyanobenzo[*b*]tetrahydrocarbazoloquinones. Later, the application of long range heteronuclear COSY experiments by the Gould group provided the fully assigned proton and carbon spectra for kinamycin D and appeared to confirm the structures assigned to the kinamycins.<sup>35</sup>

The significance of these proposed structures is that they provided the spark that ignited the efforts towards elucidating the biosynthesis of these compounds and consequently their syntheses from which arose some speculation that the kinamycins were not *N*-cyanocarbazoles as originally described. It would be some 24 years after Omura's initial report that the kinamycins would be assigned their true identity as diazobenzo[*b*]fluorenes<sup>30,31</sup> thus again reigniting investigative efforts towards their synthesis as well as their mechanism of action. The following discussion will give a brief account of this journey that provides a unique and interesting story of the kinamycin group of natural products.

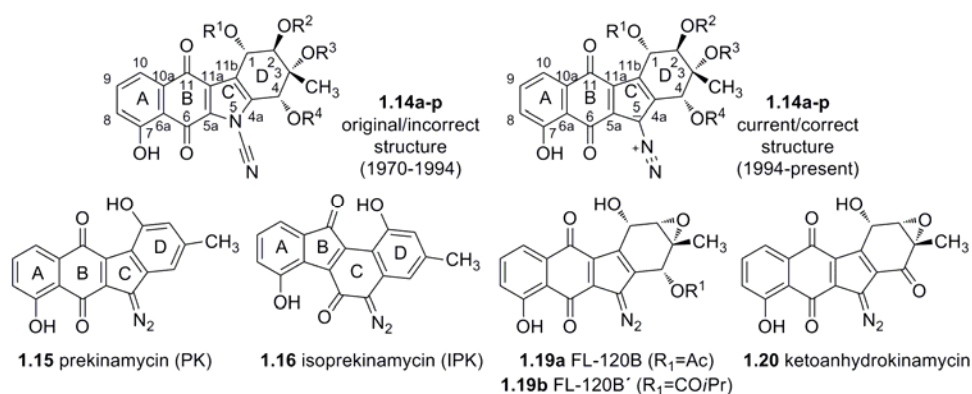
### **1.2.2 Overview of the Kinamycins and related Benzofluorenes**

All kinamycins contain a diazo group which is not acid sensitive, an anomalous feature as the diazo group is typically unstable towards acidic conditions.<sup>36</sup> This behavior has been justified in previous studies by our group here at Waterloo, which have revealed the

diazonium ion character of isoprekinamycin (IPK).<sup>37,38</sup> Kinamycins are diazobenzo[*b*]fluorenes with the exception of IPK, which is a diazobenzo[*a*]fluorene. The benzo[*b*]fluorenes and the benzo[*a*]fluorenes structures are rarely found in nature.<sup>32</sup> In the kinamycins first isolated by the Omura group, the A-ring is a phenol, the B-ring is a *p*-benzoquinone and the C-ring is diazo-cyclopentadiene, features common to all kinamycins. Kinamycins A-D are distinguished by the substitution pattern of the D-ring. There are now sixteen known members of this class of secondary metabolites that possess a cyclohexene D ring with four contiguous stereocenters that are hydroxyl substituents and/or acyloxy substituents and combinations thereof. Three other members possess an epoxide within the saturated D ring and both PK and IPK possess aromatic D rings. The numbering of atoms of all derivatives of benzo[*b*]fluorene metabolites is consistent with the standard numbering of the benz[*a*]anthraquinone biosynthetic precursors<sup>39</sup> at the recommendation made by Gould<sup>30</sup> and by the conventions of *Chemical Abstracts* and applies to the benzo[*a*]fluorenes as well.<sup>33</sup> Table 1.1 provides the structures of the kinamycins and related members.

Kinamycins possess strong activity against Gram-positive bacteria and less against Gram-negative bacteria and moderate to significant antitumor activity. Protein, DNA and cellular inhibition studies have also been reported on various cell lines. Naturally produced kinamycins originate from either *Streptomyces sp.* or *Actinomycetes sp.* and in some cases semi-synthetic kinamycins have been prepared from these isolates.

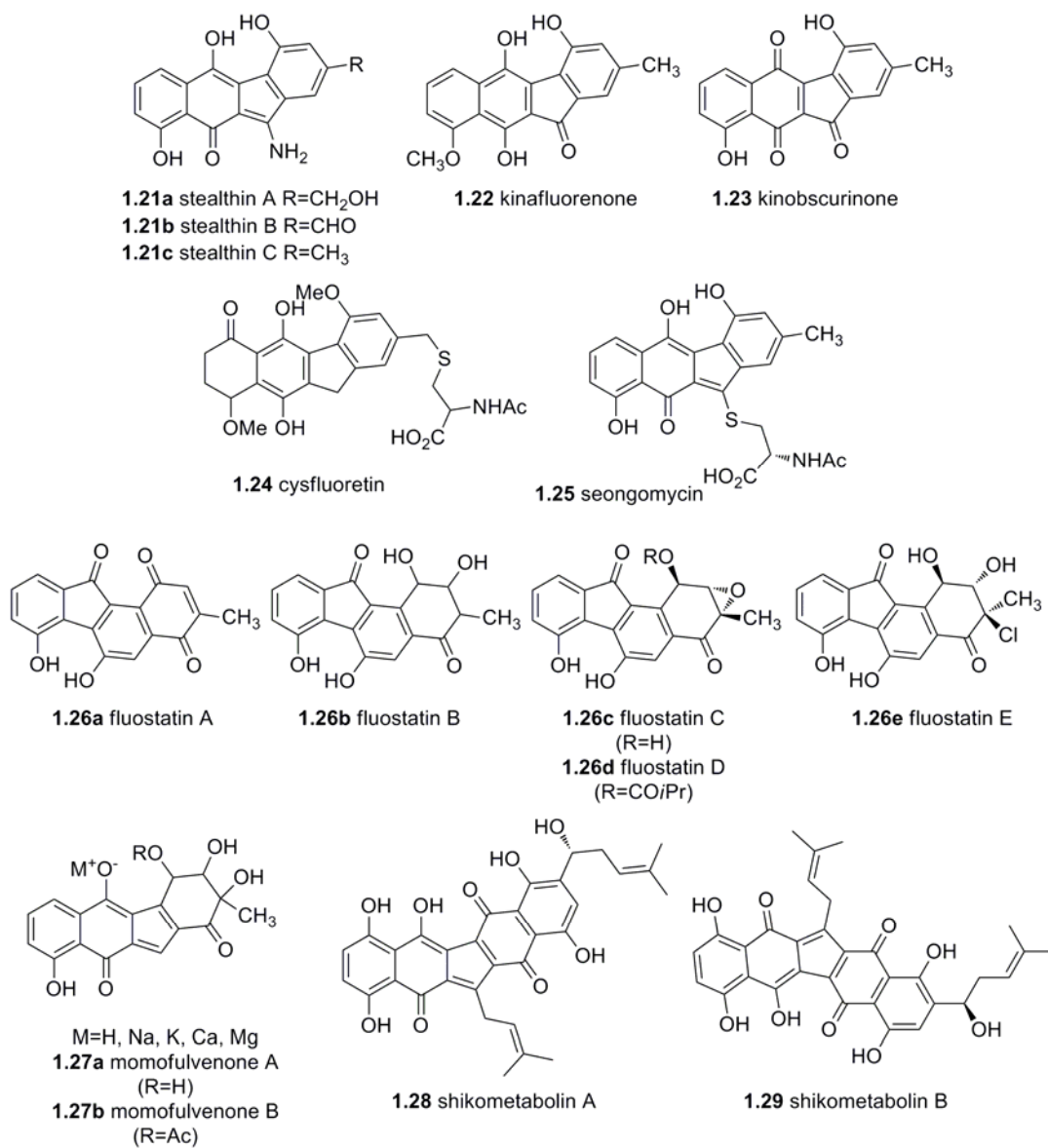
**Table 1.1:** Original and revised structures of the kinamycins and related natural products.



Name (year first reported)	R <sup>1</sup>	R <sup>2</sup>	R <sup>3</sup>	R <sup>4</sup>	Source
kinamycin A <b>1.14a</b> (1970)	H	Ac	Ac	Ac	a
kinamycin B <b>1.14b</b> (1970)	H	H	Ac	H	a
kinamycin C <b>1.14c</b> (1970)	Ac	Ac	H	Ac	a
kinamycin D <b>1.14d</b> (1970)	H	Ac	H	Ac	a,b
kinamycin E <b>1.14e</b> (1989)	H	H	H	Ac	a
kinamycin F <b>1.14f</b> (1989)	H	H	H	H	a
kinamycin G <b>1.14g</b> (1989)	Ac	Ac	CO <i>i</i> -Pr	Ac	c,d
kinamycin H <b>1.14h</b> (1989)	Ac	Ac	H	CO <i>i</i> -Pr	c,d
kinamycin I <b>1.14i</b> (1992)	Ac	CO <i>i</i> -Pr	H	CO <i>i</i> -Pr	d
kinamycin J <b>1.14j</b> (1973)	Ac	Ac	Ac	Ac	semi-synthetic
kinamycin K <b>1.14k</b> (1992)	Ac	Ac	CO <i>i</i> -Pr	CO <i>i</i> -Pr	d
kinamycin L <b>1.14l</b> (1989)	H	Ac	H	H	a
FL-120A <b>1.14m</b> (1994)	H	Ac	CO <i>i</i> -Pr	Ac	b
FL-120C <b>1.14n</b> (1994)	H	Ac	H	CO <i>i</i> -Pr	b
FL-120C' <b>1.14o</b> (1994)	H	Ac	H	COEt	b
FL-120D' <b>1.14p</b> (1994)	H	H	H	CO <i>i</i> -Pr	b
prekinamycin <b>1.15</b> (1994)	-	-	-	-	a,e
isoprekinamycin <b>1.16</b> (1989)	-	-	-	-	a
FL-120B <b>1.19a</b> (1994)	Ac	-	-	-	b
FL-120B' <b>1.19b</b> (1994)	CO <i>i</i> -Pr	-	-	-	b
ketoanhydrokinamycin <b>1.20</b> (1989)	-	-	-	-	a

- a. *Streptomyces murayamaensis* sp. nov. Hata et Ohtani (ATCC 21414)  
 b. *S. chattanoogaensis* subsp. *taitungensis* (strain IY2-13/CCRC 15124)  
 c. *S. saccharothrix* (strain M1293-N4)  
 d. unidentified *Actinomycete* sp. (strain A83016)  
 e. *S. murayamaensis* mutant MC2.

**Figure 1.3:** Naturally occurring benzofluorenes.



Despite the fact that benzofluorenes are infrequently found in nature,<sup>32</sup> examples other than the kinamycins have been reported and are shown in Figure 1.3. These include the stealthins (1.21),<sup>40,41</sup> kinafluorenone (1.22),<sup>42</sup> kinobscurinone (1.23),<sup>43</sup> cysfluoretin (1.24),<sup>44</sup> seongomycin (1.25),<sup>45</sup> the fluostatins A (1.26a), B (1.26b),<sup>46,47</sup> C (1.26c), D (1.26d), E(1.26e),<sup>48,49</sup> the momfulvenones (1.27)<sup>50</sup> and shikometabolins A (1.28) and B (1.29).<sup>51</sup> Some of these structures such as stealthin C 1.21c and kinobscurinone 1.23 are significant as they are implicated as intermediates in kinamycin biosynthesis.<sup>4</sup>

### 1.2.3 Reassessment of Kinamycin nomenclature

Presently, there is some confusion in the literature regarding kinamycin nomenclature. Their corresponding structural assignment(s) as well as their origin has been recognized. In particular, the 1997 review by Gould<sup>32</sup> reports structures that have been incorrectly named, most notably with kinamycins G, H and I, perhaps owing to clerical errors during transcription. These corrected structures are shown in Table 1.1. A brief review of the pertinent primary literature to correct the assumed errors is given below.

In 1989, Isshiki and coworkers isolated 3-*O*-isobutyrylkinamycin C and 4-*O*-deacetyl-4-*O*-isobutyrylkinamycin C,<sup>52</sup> designated as kinamycins G and H, respectively, in Gould's 1997 review. Shortly thereafter in 1992, Smitka and coworkers also isolated 3-*O*-isobutyrylkinamycin C and 4-*O*-deacetyl-4-*O*-isobutyrylkinamycin C, as well a new kinamycin, A83016A<sup>53</sup> designated kinamycin I by Gould. However the structure of 3-*O*-isobutyrylkinamycin C reported by Smitka *et al.* did not match the structure by the same name described by Isshiki *et al.* and this apparently new compound is assigned the name kinamycin K (1.14k) for the purposes of this thesis. This error made by Smitka regrettably

was reproduced by Gould in his review. Gould had assigned kinamycin J (**1.14j**) as a natural kinamycin, whereas in fact it has never been isolated from microbial fermentation broths and has only been generated from semi-synthetic<sup>29</sup> or synthetic preparations.<sup>54</sup> In 1989, Seaton and Gould isolated a kinamycin corresponding to structure **1.14l** but identified it only as “PY1” in that report.<sup>55</sup> For the purposes of this thesis, structure **1.14l** is named kinamycin L. The structure reported for kinamycin A by Gould as well as by others, is also in error and is corrected in Table 1.1. These observations along with the ensuing corrections have also been reported by N. Chen from this laboratory.<sup>56</sup>

#### 1.2.4 Structural reassignment of the Kinamycins

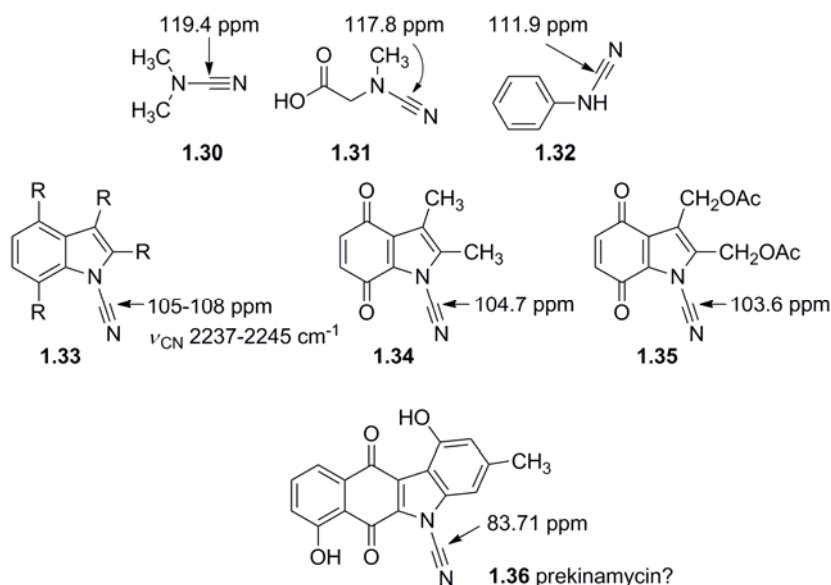
##### 1.2.4.1 The Kinamycins are diazobenzo[*b*]fluorenes and not *N*-cyanobenzo[*b*]carbazoles

The early work by the Omura group had proposed the kinamycins as *N*-cyanobenzo[*b*]carbazoles.<sup>25-29</sup> However, investigations by several laboratories, including our own, would call into question the validity of the cyanamide functionality. The uncertainty regarding the cyanamide moiety was supported by several studies detailed below.

In 1988, Gould and coworkers observed the <sup>13</sup>C NMR resonance at 78.5 ppm for the “cyanamide carbon” of a <sup>15</sup>N-enriched sample of kinamycin D.<sup>57</sup> The anomalously large upfield shift of ~30 ppm for the cyanamide functionality could not be explained by the authors but was attributed to possible electronic effects of the indoloquinone.<sup>30,32</sup> Earlier studies by Omura and coworkers found the corresponding <sup>13</sup>C NMR resonances for **1.30** and **1.31** to be 119.4 and 117.8 ppm, respectively (Figure 1.4).<sup>58</sup> In 1990, the synthesis of various *N*-cyanoindoles **1.33** in this laboratory provided <sup>13</sup>C NMR chemical shifts between 105-108 ppm and IR data for  $\nu_{\text{CN}}$  in the range 2237-2245 cm<sup>-1</sup>. As well, *N*-cyanoindoloquinones **1.34**

and **1.35** gave  $^{13}\text{C}$  NMR shifts of 104.7 ppm and 103.6 ppm, respectively.<sup>59</sup> Then in 1993, Echavarren's total synthesis of what was thought to be prekinamycin **1.36**<sup>60</sup> gave spectroscopic data that did not correspond to what Gould claimed was prekinamycin (later found to be isoprekinamycin<sup>33,61,62</sup>) isolated from fermentation broths of *S. murayamaensis*.<sup>55</sup> Although the structures and corresponding spectroscopic data provided by Echavarren in that report have been drawn into question<sup>31</sup> (see section 1.4.1) it nonetheless fueled speculation about the validity of the kinamycin structure originally proposed by the Japanese group.

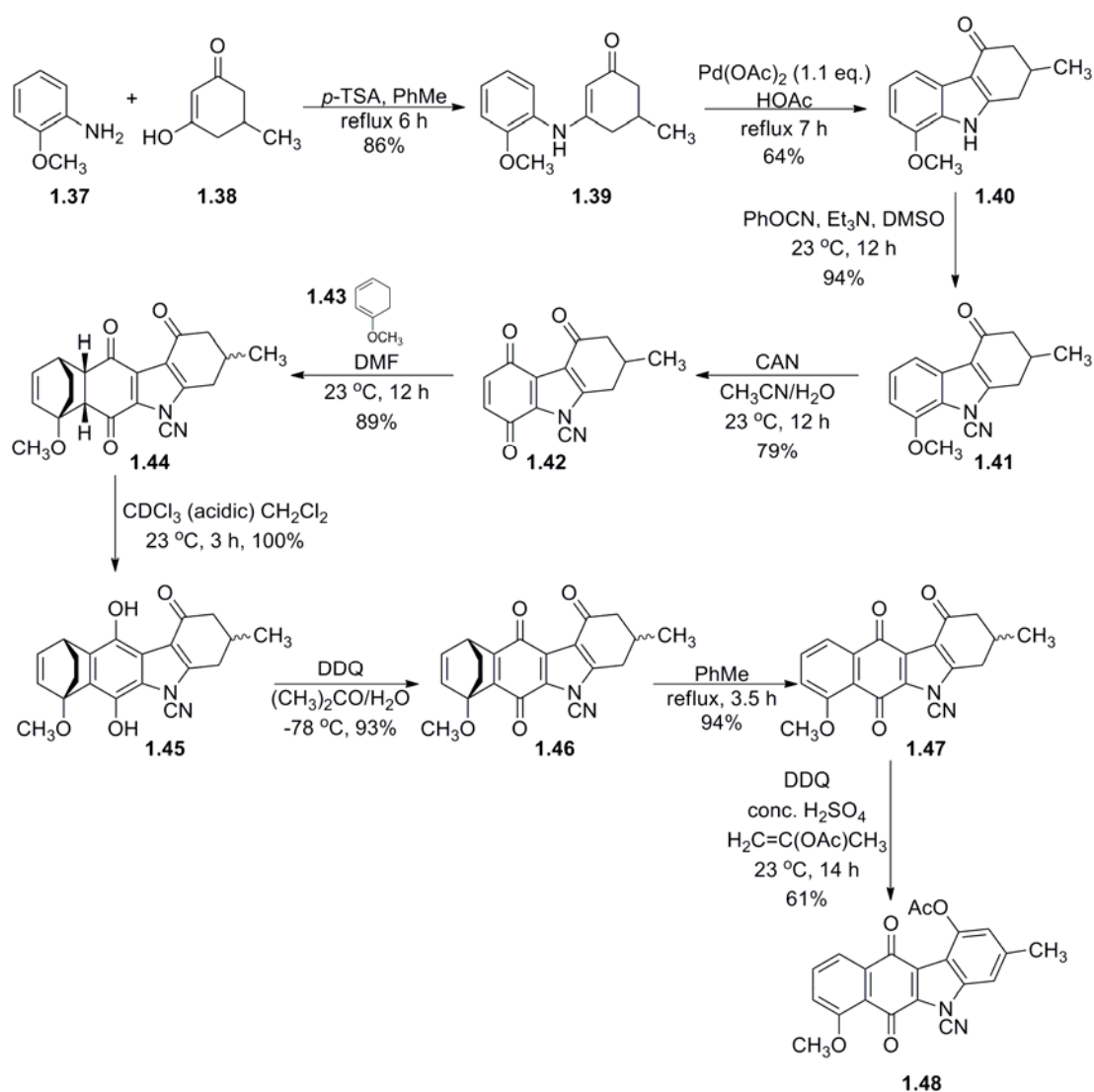
**Figure 1.4:**  $^{13}\text{C}$  NMR spectroscopic assignments of selected cyanamides.



The efforts by our group here at Waterloo, as well as Gould and Echavarren, hastened speculation that the cyanamide functionality should be reconsidered. This culminated in the simultaneous disclosure by our group here at Waterloo and Gould's group at Oregon, that the kinamycins are diazobenzo[*b*]fluorenes and not *N*-cyanobenzo[*b*]carbazoles.<sup>30,31</sup>



**Scheme 1.1:** Mithani and Dmitrienko's synthesis of **1.48**.



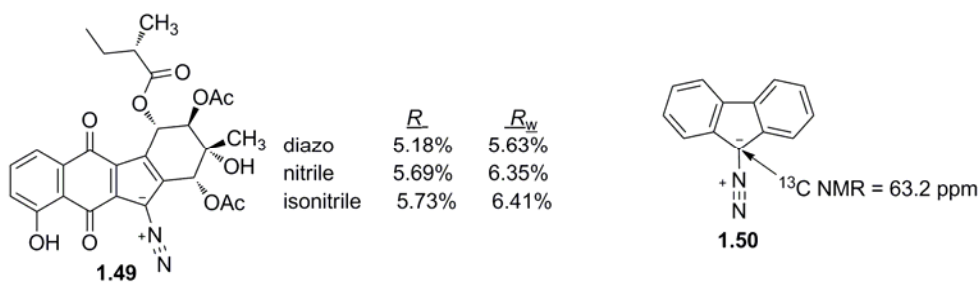
S. Mithani in this laboratory accomplished a regioselective synthesis of the *N*-cyanobenzo[*b*]carbazoloquinone **1.48** via a regioselective Diels-Alder reaction and a Pd-induced cyclization as the key steps (Scheme 1.1).<sup>31</sup> The cyano carbon gave rise to <sup>13</sup>C NMR resonance at 105 ppm and an IR band at 2253 cm<sup>-1</sup>, consistent with the *N*-cyanoindoles mentioned earlier. This was in contrast to the observations by Gould for kinamycin D (78.5

ppm)<sup>57</sup> and prekinamycin diacetate (83.71 ppm)<sup>55</sup> (later shown to be isoprekinamycin diacetate<sup>33,61,62</sup>). Thus the spectroscopic characteristics of the target of Mithani's syntheses showed that the kinamycin(s) could not be *N*-cyanocarbazoloquinones and that clearly, other alternatives must be considered.

In the second report, Gould and coworkers were able to crystallize the (+)- $\alpha$ -methylbutyrate derivative of kinamycin D **1.49** and subsequent X-ray diffraction studies demonstrated that the diazo group had a significantly better statistical fit to the data set than the cyanamide group (Figure 1.5).<sup>30</sup> Furthermore, it was pointed out by the Waterloo group<sup>31</sup> that the <sup>13</sup>C NMR resonances of a number of known diazo compounds<sup>63</sup> exhibited chemical shifts in the 60-80 ppm region. For example, the diazo carbon signal for 9-diazafluorene **1.50** is observed at 63.2 ppm which compares favorably with kinamycin D at 78.5 ppm.

These milestone achievements by the group here at Waterloo and that of Gould at Oregon clearly designated the kinamycins as diazobenzo[*b*]fluorenes. This in turn provided a new motivation for the synthesis of kinamycins as well as simpler diazo containing compounds, which in turn would generate new efforts towards determining their biological basis of action.

**Figure 1.5:** (+)- $\alpha$ -methylbutyrate derivative of kinamycin D **1.49** and 9-diazafluorene **1.50**.



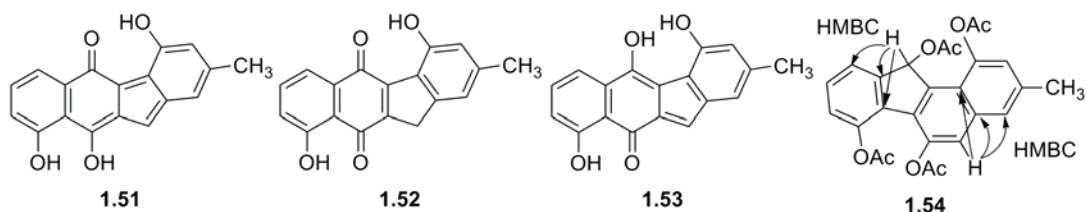
#### 1.2.4.2 Isoprekinamycin is a diazobenzo[*a*]fluorene

In 1996, the first reported total synthesis of prekinamycin **1.15** was achieved by Hauser and Zhou.<sup>61</sup> Unexpectedly, it was found that the spectral properties of Hauser's synthetic target were not identical to those reported by Seaton and Gould in 1989, a compound named P1,<sup>55,64</sup> that Gould had arbitrarily designated "Cpd A".<sup>62</sup> During this time, spectroscopic studies undertaken by the Gould lab<sup>62</sup> found there were small differences in the IR, <sup>1</sup>H NMR and HPLC-PDA data between Cpd A and the synthetic prekinamycin provided by Hauser and Zhou. Furthermore, that same study found that the synthetic sample matched yet another metabolite (named "Cpd B") from extracts of *S. murayamaensis* mutant MC2 and upon isolation of Cpd B from fermentation broths, produced identical UV-Vis spectra with synthetic prekinamycin. Ensuing HPLC-coinjection produced a single peak and subsequent purification established Cpd B as prekinamycin, leaving the identity of Cpd A unclear.

The issue was finally resolved by a collaborative effort by this group here at Waterloo and P. Proteau at Oregon State.<sup>33</sup> Using extensive 2D NMR techniques (HSQC, HMBC) and ab initio M.O. calculations, compound A was recognized as a diazobenzo[*a*]fluorene **1.16**, a 6,5,6,6 tetracyclic species isomeric with prekinamycin and Cpd A was given the name isoprekinamycin (IPK). The ring system in IPK is related to that in the fluostatins A **1.26a** and B **1.26b**.<sup>47</sup> Treatment of IPK with Rh<sub>2</sub>(OAc)<sub>4</sub> produced a deazotized product compatible with any of the structures **1.51**, **1.52** or **1.53** (Figure 1.6) but all were incongruous with nOe and HMBC NMR results. Ab initio calculations showed **1.51** was particularly unfavorable and it was concluded that IPK was not a diazobenzo[*b*]fluorene. The definitive evidence was provided by sodium borohydride treatment, deazotization and acetylation of IPK furnishing

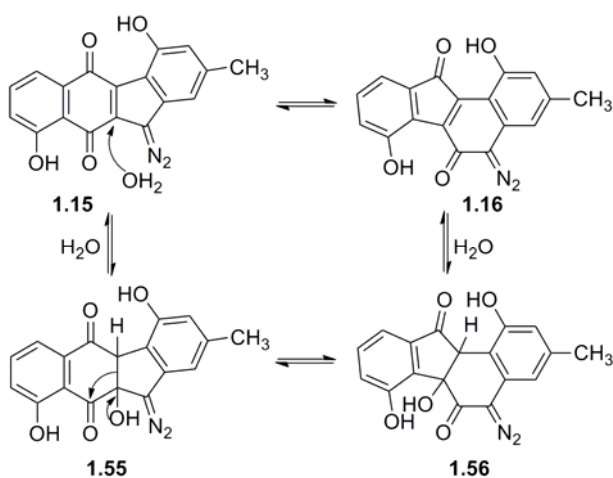
the tetraacetate derivative **1.54** which was now amenable to conventional NMR techniques. Thus, the identity of Cpd A was revealed as the benzo[*a*]fluorene isoprekinamycin **1.16** and is in fact, the corrected structure of the compound first described by Gould in 1989 (named P1 in that report), which had been inadvertently assigned the prekinamycin structure.<sup>55</sup>

**Figure 1.6:** Possible structures obtained from the deazotization of isoprekinamycin.



The co-occurrence of both **1.15** and **1.16** within the same bacterial cell suggest the possibility an enzyme catalyzed rearrangement such that a reversible hydration, 1,2-C shift and dehydration sequence occurs (Scheme 1.2).<sup>33</sup> This group has suggested further that **1.15** and **1.16** are variants of the same pharmacophore.<sup>38</sup>

**Scheme 1.2:** Proposed mechanism for the interconversion between PK and IPK.



## 1.3 Biosynthesis

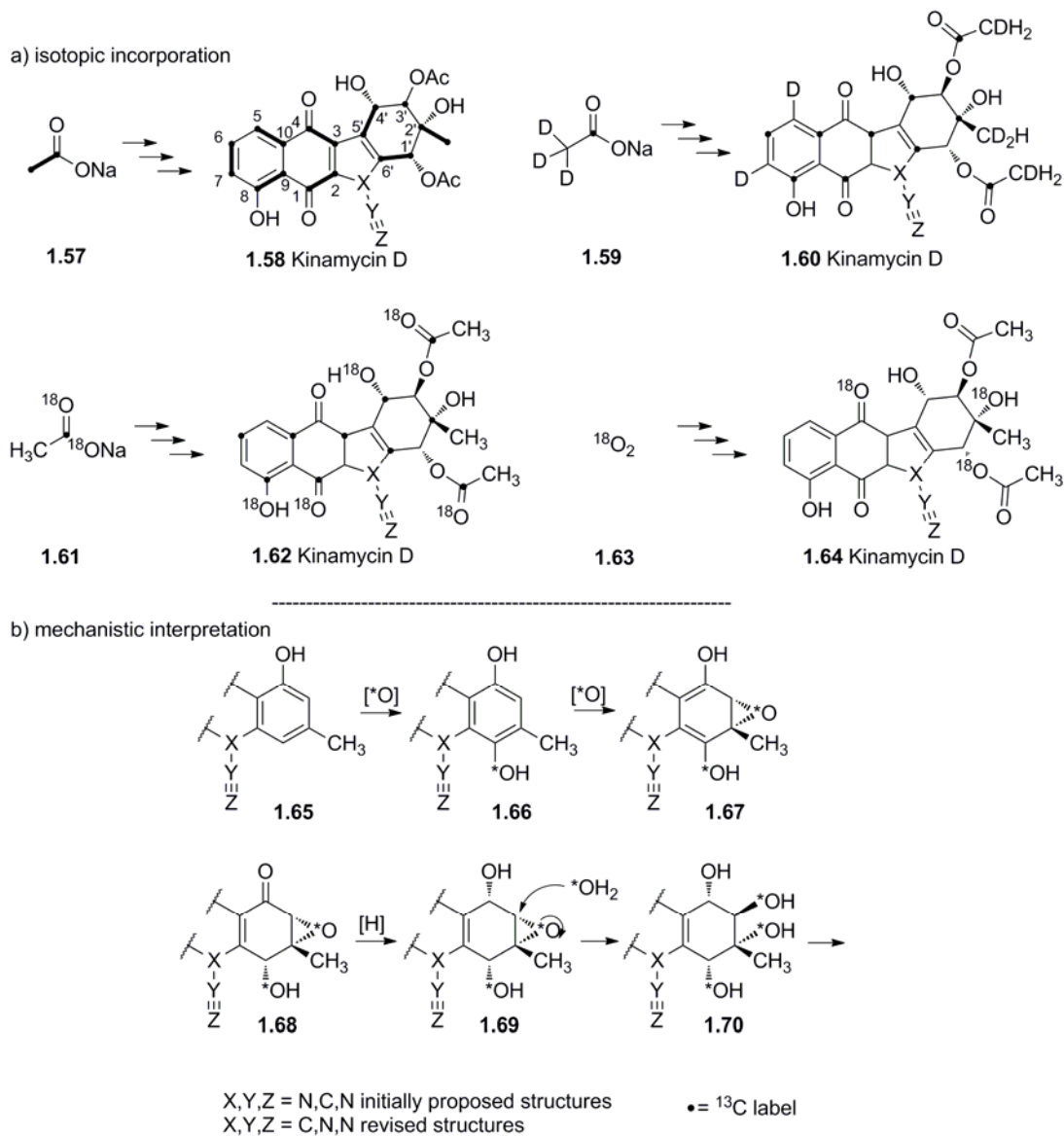
### 1.3.1 Initial studies: derivation of the carbon skeleton and oxidative elaboration of the D-ring

The elucidation of the biosynthesis of the kinamycins was largely accomplished by Gould and co-workers and has been reviewed in 1997.<sup>32</sup> In 1976, the first report on the biosynthesis of the kinamycins was described by Omura and coworkers in which those workers fed both sodium [1-<sup>13</sup>C] and [2-<sup>13</sup>C]acetate to separate cultures of *S. murayamensis* and isolated kinamycin D.<sup>58</sup> From cultures supplied with sodium [1-<sup>13</sup>C]acetate exclusively and using IR methods, they observed a shift from 2155 cm<sup>-1</sup> to 2139 cm<sup>-1</sup> of kinamycin D apparently due to <sup>13</sup>C enrichment of the apparent “cyanamide carbon” [*sic*] (diazo group) from the C-1 of acetate.

In 1985 and 1986, Sato and Gould published two separate reports establishing the skeleton of the kinamycins was derived entirely from acetate and that the D-ring was functionalized via acetate and molecular oxygen.<sup>65,66</sup> This was accomplished, in part, by feeding sodium [1, 2-<sup>13</sup>C<sub>2</sub>]acetate **1.57** to the fermentation broths of *S. murayamaensis* yielding a mixture of kinamycins C and D (Scheme 1.3, top panel). Further purification afforded kinamycin D **1.58** enriched at all carbons by an average of 3.1% and with the exception of C-3' (2.5% enrichment), all showing coupling to at least one carbon. Subsequently, the orientation of each acetate in kinamycin C and D was revealed by assimilation of [2-<sup>2</sup>H<sub>3</sub>, 1-<sup>13</sup>C]acetate **1.59**. The source of the oxygens and thus the oxidative elaboration of the D-ring was shown by assimilation of [1-<sup>13</sup>C, 1,1-<sup>18</sup>O<sub>2</sub>]acetate **1.61** and <sup>18</sup>O<sub>2</sub> **1.63** in separate experiments. These two <sup>18</sup>O experiments led the authors to suggest the sequence of events that is consistent with

the observed stereochemistry and isotopic labeling as described in the bottom panel of Scheme 1.3.

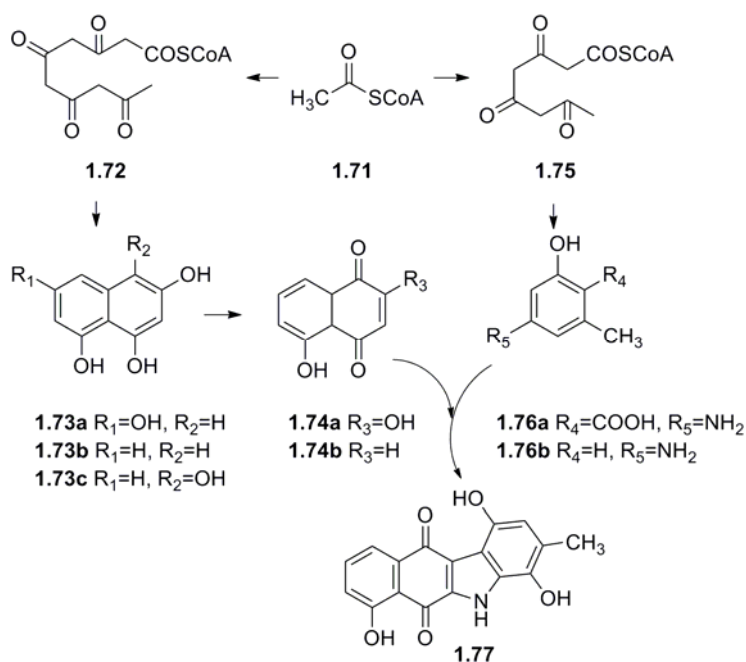
**Scheme 1.3:** Gould's biosynthetic studies of kinamycins C and D.



Furthermore, Sato and Gould suggested two intermediates; a substituted 2,4,5-trihydroynaphthalene **1.73** (to afford a juglone species **1.74**) and a substituted toluic acid

**1.76**, derived from two different polyketide intermediates **1.72** and **1.75**, respectively, furnishing the kinamycins (Scheme 1.4). In both of those reports, the authors did not observe the  $^{13}\text{C}$  NMR resonance of the “cyanamide carbon”, contradicting the earlier report by Omura. The absence of the "cyanamide carbon" signal was attributed to quadrupolar relaxation by the two nitrogens directly attached to the "cyanamide carbon". Thus the origin(s) of the “cyanamide carbon” remained unknown.

**Scheme 1.4:** Gould’s early proposal for the biosynthesis of the kinamycins.



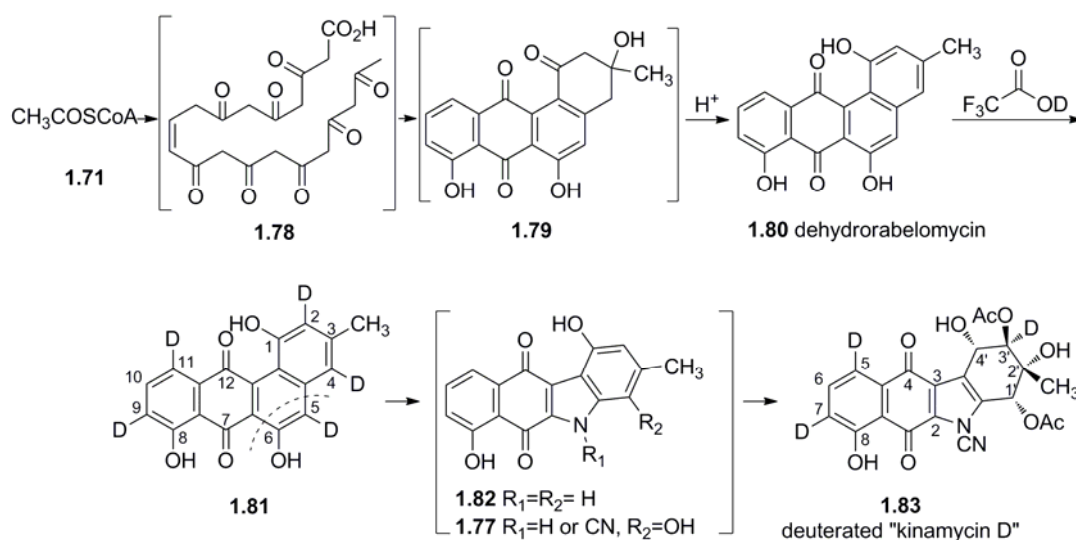
### 1.3.2 Advanced studies: dehydrabelomycin from a decaketide intermediate

In 1987, Seaton and Gould reported their unsuccessful attempts to support their hypothesis shown in Scheme 1.4<sup>39</sup> the suggestion of which came from two notable observations, the first of which was the failure to isolate labeled kinamycin D from bacterial cultures fed various

deuterated hydroxynaphthalenes (**1.73**) and hydroxynaphthoquinones (**1.74**). Secondly, isolation of other metabolites, one of which was dehydrorabelomycin **1.80** (a benz[*a*]anthraquinone) as dark green needles, previously obtained from the acid-catalyzed dehydration of rabelomycin **1.79** in a separate study.<sup>67</sup> The *in vivo* generation of **1.80** suggested an alternative biosynthesis (Scheme 1.5) to that shown in Scheme 1.4. To this end, **1.80** was heated in the presence of deuteriotrifluoroacetic acid in a sealed tube in the absence of oxygen to produce [2,4,5,9,11-<sup>2</sup>H<sub>5</sub>] dehydrorabelomycin **1.81** and was subsequently fed to fermentation broths of *S. murayamaensis*. Compound **1.81** was recovered with no change in deuterium content and kinamycin D **1.83** enriched at C-7, C-5, and C-3' was also isolated, thus establishing dehydrorabelomycin **1.80** as a key intermediate in the biosynthesis of kinamycin D. It was proposed that subsequent oxidative cleavage of the C-ring, excision of C-5 and C-6, and insertion of nitrogen yield the tetracycle **1.82**, a benzo[*b*]carbazole (proof of which Gould claims was obtained as the cyanamide derivative of **1.82**, albeit in small quantities with incomplete characterization). The observation of deuterium retention at C-3' but not at C-1' of **1.83** was fully consistent with the intermediacy of the hydroquinone **1.77**. Thus, the kinamycin skeleton was proposed to be derived from **1.80** via a novel decaketide **1.78**.



**Scheme 1.5:** Gould's revised biosynthesis of the kinamycins.

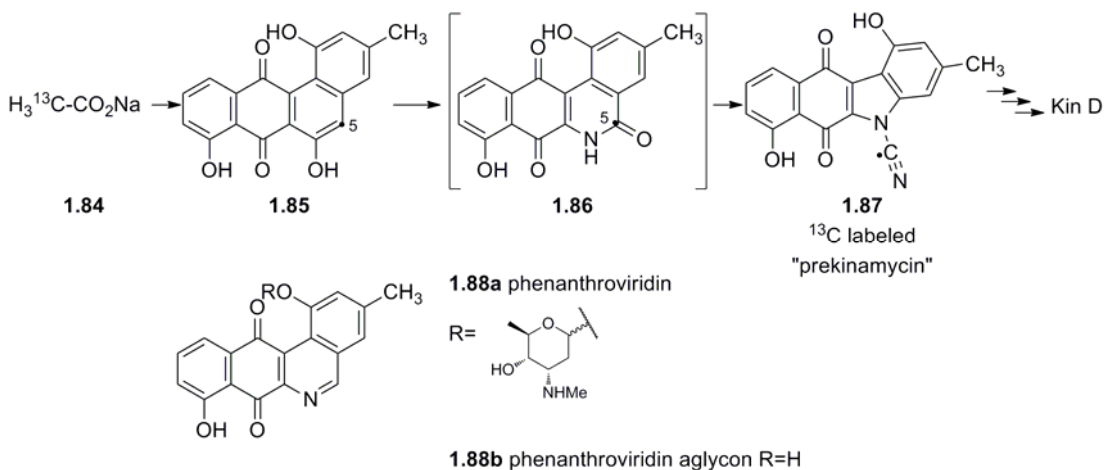


Further research towards determining the origin of the “cyanamide carbon” was pursued by feeding *S. murayamensis* with  $(^{15}\text{NH}_4)_2\text{SO}_4$ .<sup>57</sup> Surprisingly, the  $^{13}\text{C}$  NMR spectrum displayed a doublet of doublets at 78.5 ppm ( $J = 5.4, 21.2$  Hz), which permitted the determination of the biosynthetic origin of the “cyanamide carbon”. A review of  $^{13}\text{C}$  NMR spectra of non-isotopically labeled kinamycin samples showed a small singlet at this chemical shift, almost overlapped by the  $\text{CDCl}_3$  resonance that had previously been assumed to arise from a minor impurity. Subsequently, separate feedings with  $[1-^{13}\text{C}]$ acetate and  $[2-^{13}\text{C}]$ acetate, showed a 2.7% enrichment of the “cyanamide carbon” of **1.85** obtained from the  $[2-^{13}\text{C}]$  acetate feeding (Scheme 1.6). The isolation and characterization of **1.36** from other parallel studies<sup>55</sup> allowed Gould to propose that the cyanamide carbon originated from C-5 of **1.85** by way of oxidative ring cleavage and nitrogen insertion to give the pyridinone **1.86** (a

benzo[*b*]phenanthridine). Ring contraction/rearrangement was suggested to generate what was thought to be  $^{13}\text{C}$ -labeled prekinamycin **1.87**.

The synthesis of **1.88b** and the corresponding pyridinone **1.86** were reported in 1992<sup>68</sup> and two years later Gould reported the detection of **1.88b** in a UV-mutant of *S. murayamaensis* MC2.<sup>69</sup> The first naturally occurring benzo[*b*]phenanthridine to be isolated was phenanthroviridin **1.88a** and its aglycon **1.88b** from *Streptomyces viridochromogenes* DSM 3972.<sup>70</sup>

**Scheme 1.6:** Gould's proposal for the origin of the "cyanamide" carbon.

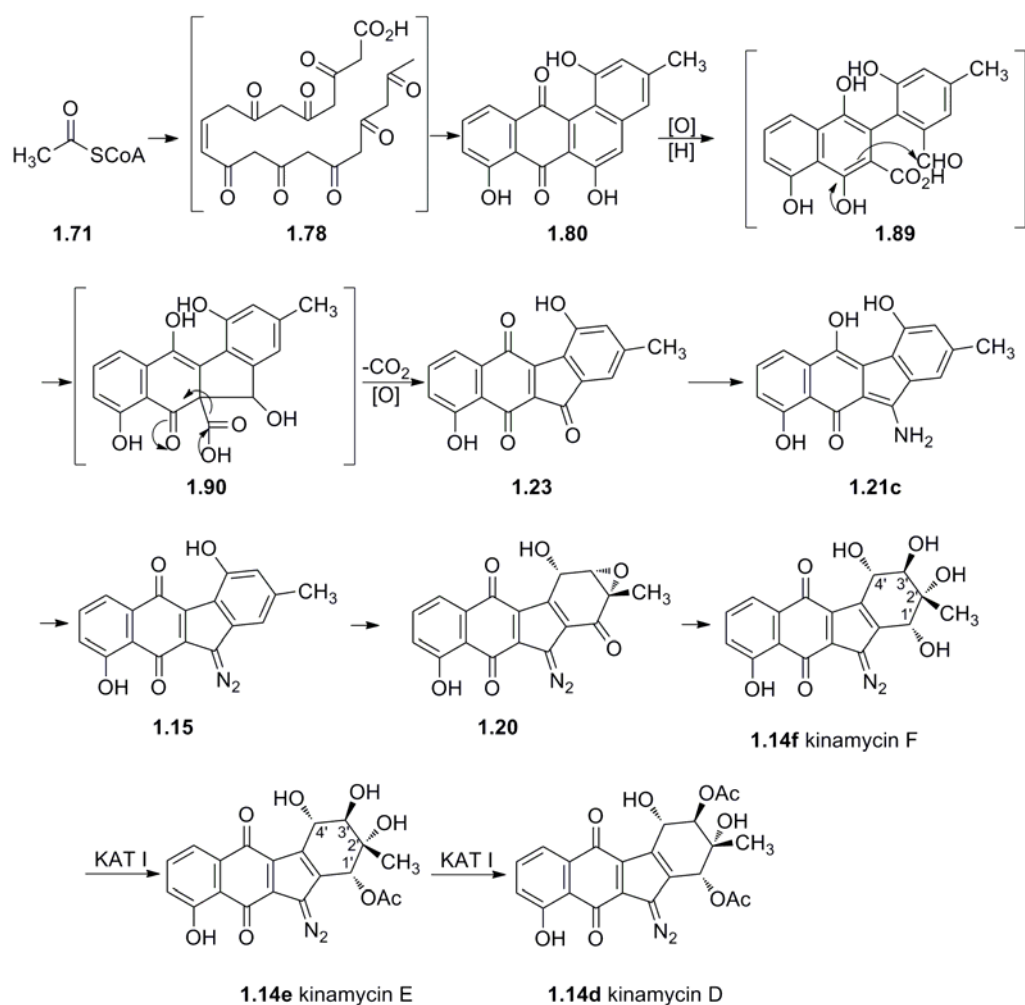


### 1.3.3 New metabolites, gene cloning, enzymes and the implications with respect to biogenesis

The 1989 report that had identified the alleged prekinamycin (see Section 1.2.4) also identified a number of potential key intermediates including keto-anhydrokinamycin **1.20**, and kinamycins F **1.14f** and E **1.14e**.<sup>55</sup> Other metabolites such as kinobscurinone **1.23**<sup>43</sup> and stealthin C **1.21c**<sup>41</sup> were isolated and were shown to be intermediates in kinamycin

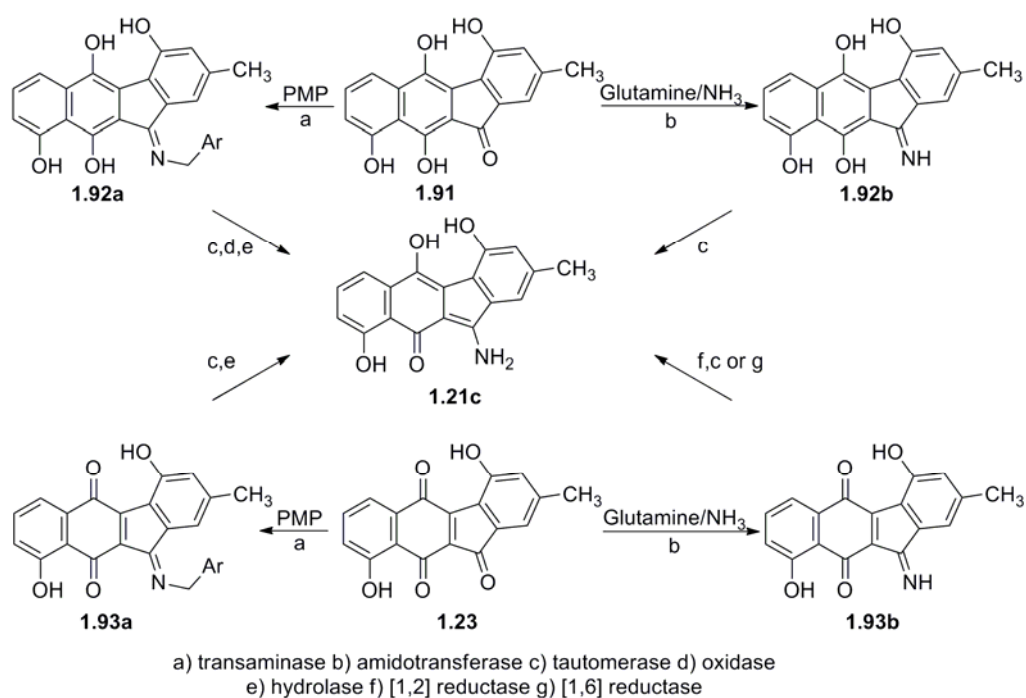
biosynthesis. The then recent structural revision of the kinamycins as diazo compounds required a new biosynthetic proposal as shown in Scheme 1.7. Subsequently the cloning and heterologous expression of genes from the kinamycin biosynthetic pathway of *S. murayamaensis* was reported to provide stealthin C but not the full kinamycin system that incorporated the diazo group.<sup>4</sup> This report also identified kinafluorenone **1.22** and seongomycin **1.25** as shunt metabolites. A kinamycin acetyltransferase (KAT I,  $M_R > 669$  kDa), a membrane-associated multifunctional enzyme was identified and was shown to catalyze the sequential acetylations of **1.14f** to **1.14e** and **1.14e** to **1.14d**.<sup>71</sup>

**Scheme 1.7:** Gould's current biosynthetic proposal for the kinamycins.



Other genes identified were the gene for cleaving the C-ring as well as the gene(s) for introducing the first (internal) nitrogen of the diazo group; although **1.23** had been detected in cultures of *S. murayamaensis*, the precise target of the amination had yet to be identified. Should **1.23** be the amination substrate, then the glutamine or ammonia dependent amidotransferases are worthy of consideration whereas **1.91** would invoke the pyridoxamine phosphate-dependent transaminases (Scheme 1.8).<sup>4</sup>

**Scheme 1.8:** Possible enzyme participation in kinamycin biosynthesis.



### 1.3.4 Proposal for the source of the terminal nitrogen of the diazo group

Although the introduction of the first nitrogen seems likely from the possibilities presented in Scheme 1.8, experimental evidence is still lacking. As well, the source of the terminal nitrogen in the diazo group has yet to be identified. Two avenues exist for the incorporation of the diazo function, one of them being the involvement of a hydrazine intermediate.<sup>72</sup> The occurrence of enzymes believed to oxidize aryl hydrazines to aryl diazonium salts have been reported,<sup>73</sup> but the existence of a hydrazine species in the kinamycin biosynthesis has yet to be reported. Another possibility that has been raised in the Waterloo group but not as yet published is the involvement of nitric oxide in some capacity. Speculation in this regard is fueled by the well known behavior of soil bacteria to convert nitrate to ammonia in a series

of redox reactions with the production of nitric oxide (NO).<sup>74</sup> These observations have led this laboratory to speculate that the possibility of *N*-nitrosation events that may occur with NO and stealthin C as the likely target. This notion bodes well with the known behavior of stealthins as potent radical trapping agents<sup>40</sup> and with the lack of biochemical and genetic evidence, presents a viable alternative which is discussed further in Chapter 3.

## 1.4 Synthesis

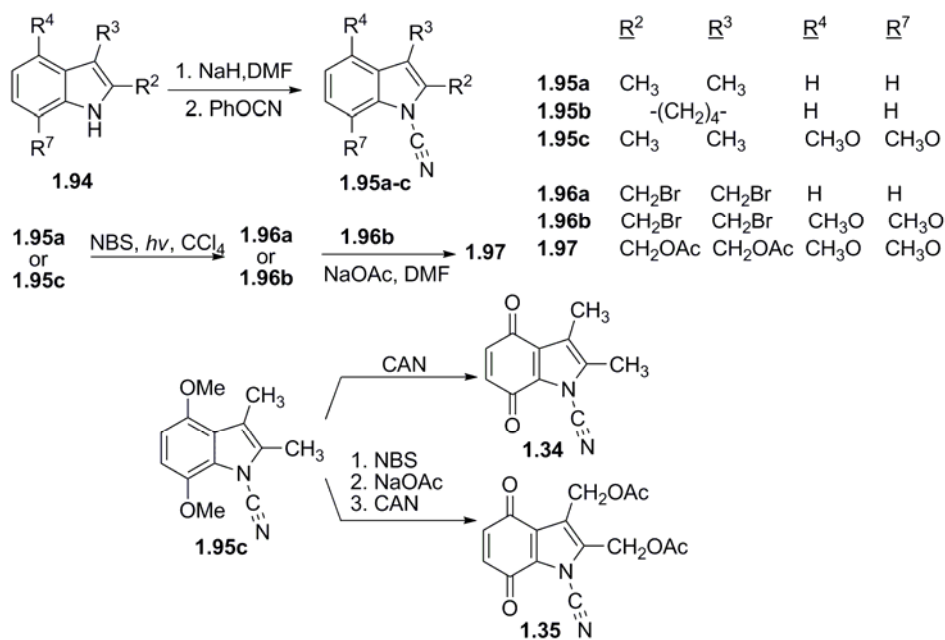
### 1.4.1 Benzo[*b*]carbazoloquinones syntheses and related chemistry

Much of the biosynthesis discussed in the preceding section provided the impetus to synthesize the natural products, intermediates and/or analogues. This eventually led to the major structural revision that the kinamycins are noted for, from *N*-cyanobenzo[*b*]carbazoloquinones to diazobenzo[*b*]fluorenequinones. This period carries several reports on efforts towards synthesizing the kinamycins as benzo[*b*]carbazoles and related chemistry.<sup>59,60,68,75-83</sup> The discussion of the synthetic approaches directed towards the kinamycins will only include those synthetic efforts up until 1994, when the kinamycins were still considered carbazoles. Discussion on more recent advances in carbazole synthesis will be presented in Chapter 2. The number of reports in the literature describing syntheses of carbazoles and their derivatives is extensive and it is beyond the scope of this thesis to describe them in detail. For this purpose, one can consult the extensive and comprehensive reviews written by Knolker<sup>84-87</sup> and Gallagher.<sup>88</sup>

Efforts from this laboratory towards the syntheses of various *N*-cyanoindoles<sup>59</sup> (Scheme 1.9) were an important step towards the structural reassignments of the kinamycins (Section

1.2.4). The indoloquinones **1.34** and **1.35** were envisioned as BC ring synthons in Diels-Alder reactions.

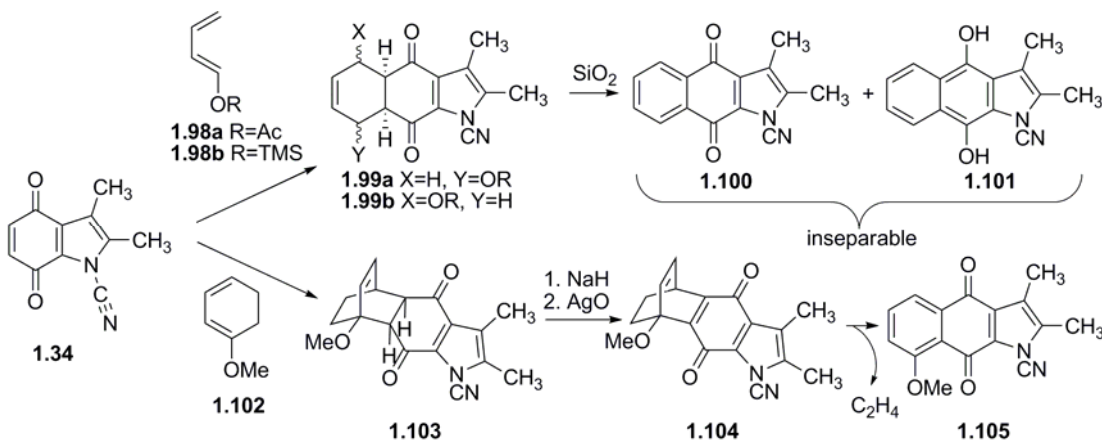
**Scheme 1.9:** Dmitrienko's synthesis of *N*-cyanoindoles and *N*-cyanoindoloquinones.



Using the *N*-cyanoindoles-4,7-diones provided in the aforementioned report allowed this laboratory to pursue the construction of the ABC rings of the kinamycins via Diels-Alder reactions (Scheme 1.10).<sup>75</sup> These studies were initiated based on an understanding of the regioselectivity of Diels-Alder reactions provided by FMO analysis<sup>89,90</sup> with the knowledge that C-1'-alkoxy or acyloxy dienes should provide the requisite regioisomer. In practice it was found that 1-acetoxybutadiene **1.98a** or 1-trimethylsilyloxybutadiene **1.98b** led to a ~2:1 mixture of adducts that were unstable, decomposing to **1.100** and **1.101** as an inseparable mixture, precluding structural characterization that would allow confirmation of the regioselectivity predicted by FMO analysis. Using 1-methoxy-1,3-cyclohexadiene **1.102** as

the diene, afforded adduct **1.103** in 76% yield as the endo product, which upon enolization and oxidation followed by a thermal retro Diels-Alder, furnished **1.105** in 19% yield over three steps.

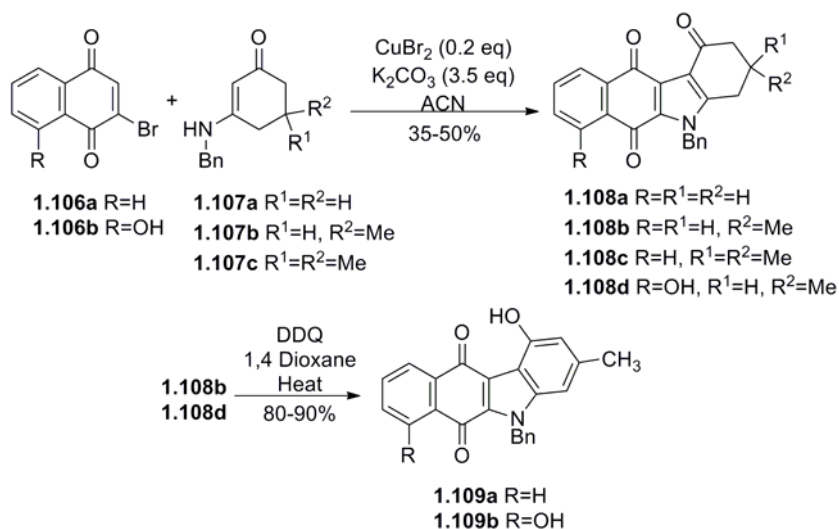
**Scheme 1.10:** Dmitrienko's synthesis of benzoannulated indoloquinones.



The first regioselective synthesis of the kinamycins as tetrahydrocarbazoles was accomplished by Murphy and coworkers<sup>78</sup> using their bromoquinone enamine annulation methodology.<sup>91</sup> Using naphthoquinones **1.106** and *N*-benzyl enamino ketones **1.107**, they obtained the desired regioselective annulation, furnishing tetrahydrobenzo[*b*]carbazole-1,6,11 triones **1.108** in modest yields (Scheme 1.11). Aromatization afforded the benzo[*b*]carbazoloquinones **1.109**. There were neither efforts towards the synthesis of the *N*-cyano compounds nor any mention of their biological testing in this report. This may be attributed to the fact that *N*-benzylindoles are resistant to standard *N*-debenzylation methods which may have precluded any follow-up reports by these workers.

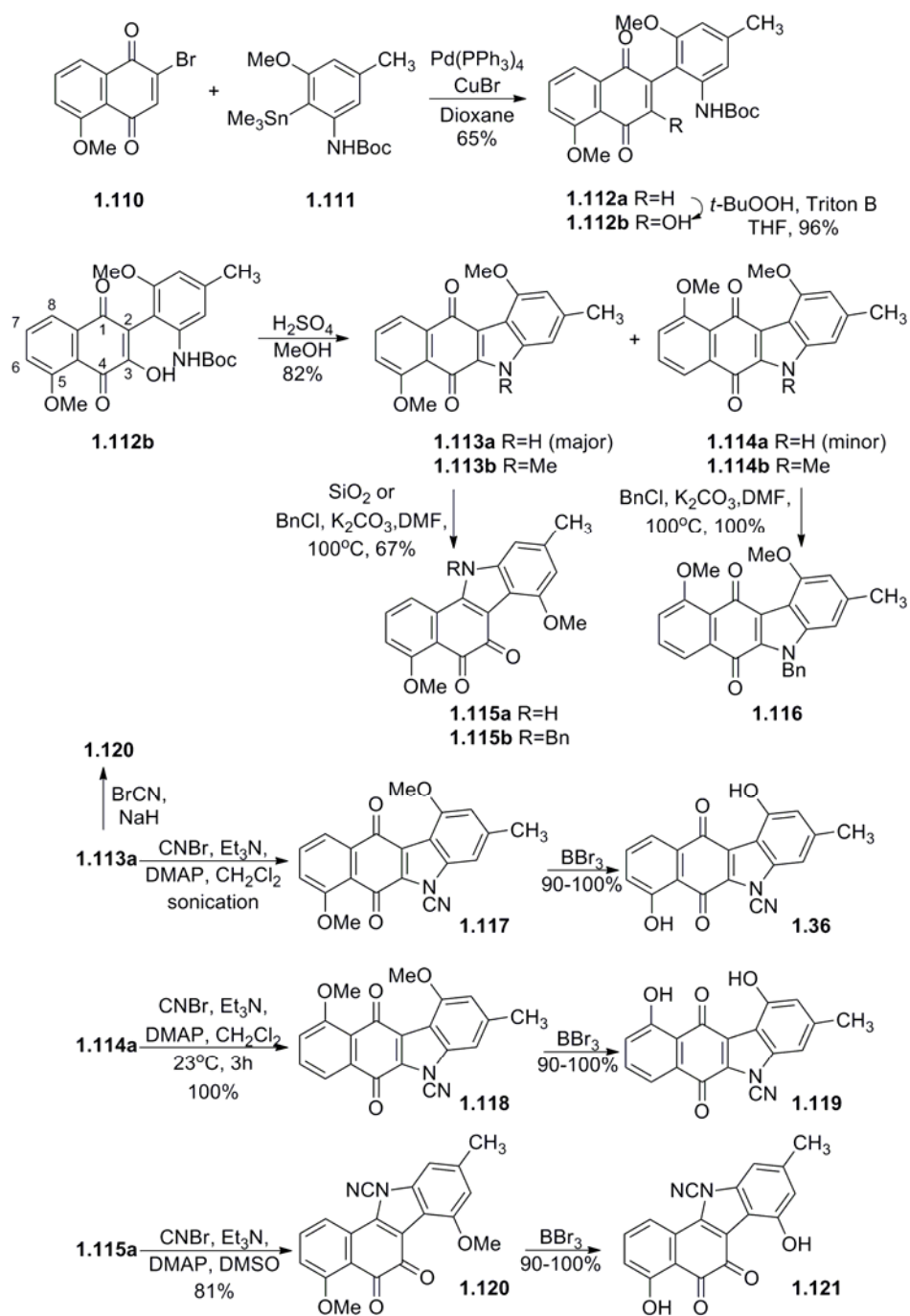


**Scheme 1.11:** Murphy's synthesis of **1.109**.

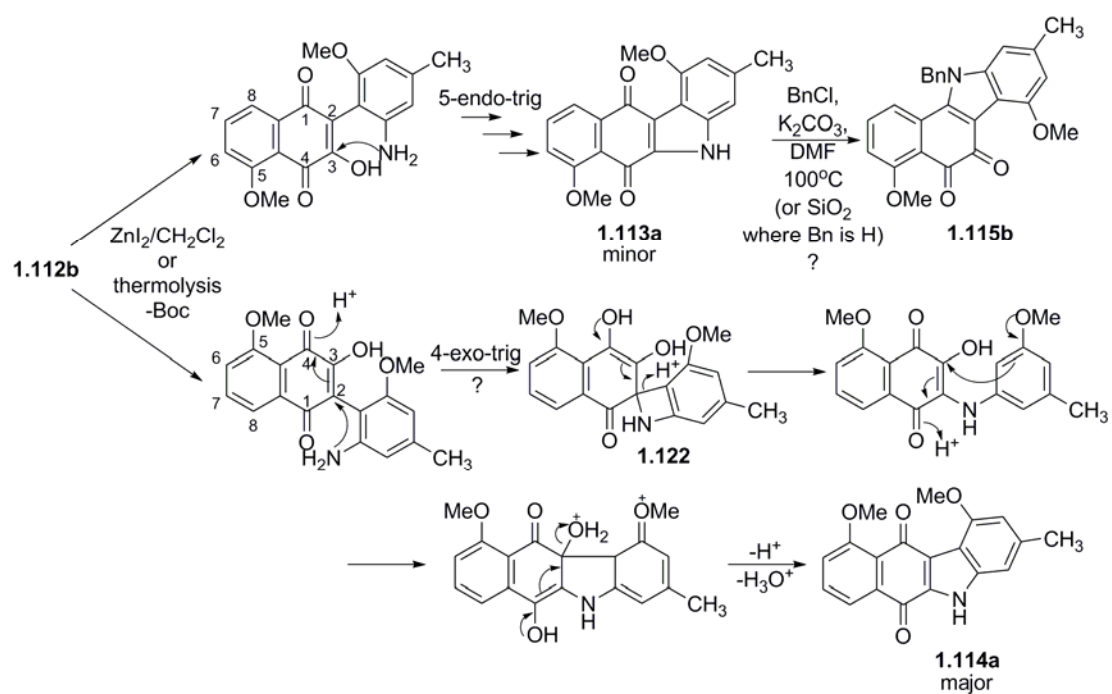


Using a Stille cross-coupling of the 5-methoxy-2-bromojuglone (**1.110**) with the aryl stannane **1.111**, Echavarren and coworkers reported the total synthesis of the *N*-cyanobenzo[*b*]carbazole **1.36**, the assumed structure of prekinamycin (Scheme 1.12).<sup>60</sup> However, the proposed structures and their corresponding assignments in that report must be viewed with caution. We have observed a disagreement of the assignments reported by Echavarren with our own assignments<sup>31</sup> and with those of others.<sup>55</sup> As this was the first reported total synthesis of what was thought to be prekinamycin **1.36**, it merits an in depth look beginning with a summary of the Echavarren synthesis as it appeared in that report, shown in Scheme 1.12.

**Scheme 1.12:** Echavarren's reported synthesis of **1.36**, **1.119** and **1.121**.



**Scheme 1.13:** Interpretation of Echavarren's product distribution.



Scheme 1.13 offers, in part, an interpretation of Echavarren's analyses of their results. Treatment of **1.112b** under catalytic conditions of  $\text{H}_2\text{SO}_4$  in methanol provided the regioisomers **1.113a**:**1.114a** in 1.4:1 ratio. However, thermolysis of **1.112b** or treatment with  $\text{ZnI}_2$  in  $\text{CH}_2\text{Cl}_2$  and cyclization in  $\text{DMSO}-d_6$  led to ratios of 1:3 and 1:6, respectively, in which they suggest that **1.114a** is formed via the azetidinium intermediate **1.122** by way of attack of the amino group at C-2 of the quinone and subsequent migration of the aryl moiety to C-3. Although those authors admit other mechanistic interpretations could be conceived, the structures as well as the regioisomeric yields are questionable. *N*-Benzylation of **1.114a** was reported to produce **1.116** in quantitative yield. However, *N*-benzylation of **1.113a**

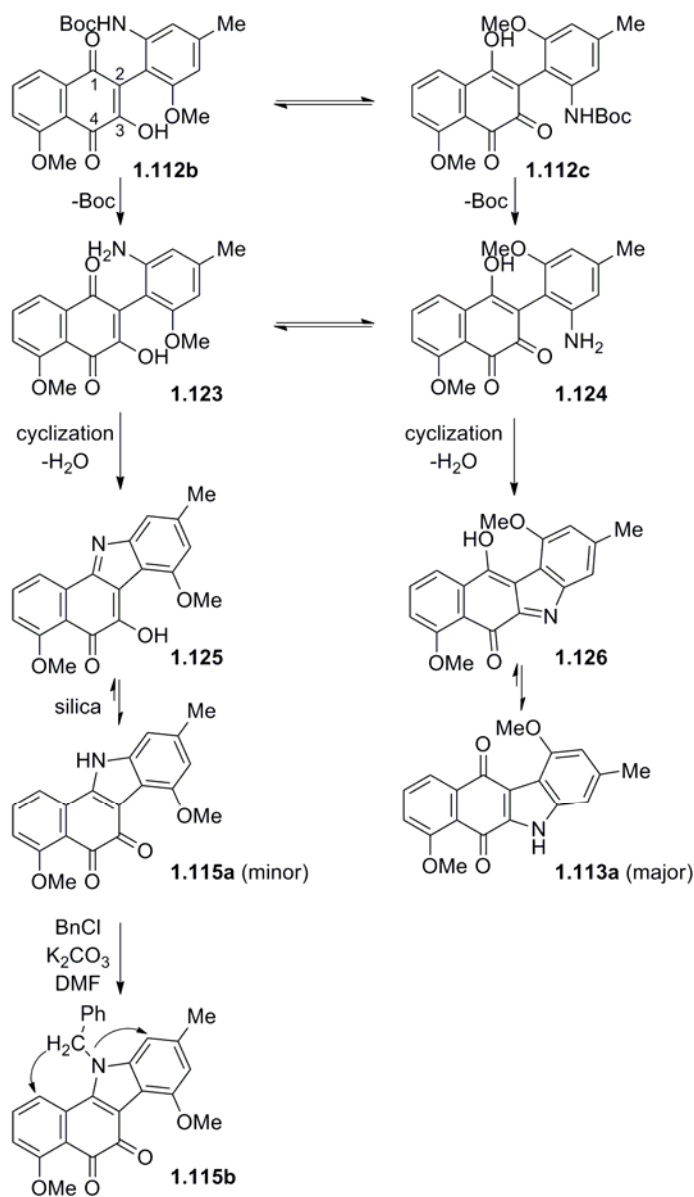
produced **1.115b** apparently through a novel rearrangement which also occurred upon standing on SiO<sub>2</sub> affording **1.115a**.

Cyanation of **1.114a** was reported to furnish **1.118** in quantitative yield, but cyanation of **1.113a** to give **1.117** proceeded sluggishly apparently owing to its insolubility. Cyanation of **1.115a** required a change of solvent to DMSO to afford **1.120** in 81% yield. Deprotection proceeded uneventfully to furnish “prekinamycin” and its two regioisomers in 90-100% yield. The assignments reported for **1.36** were markedly different from those reported by Gould and consequently Echavarren felt that the structure described by Gould<sup>55</sup> is a different structure from that of Echvarren’s synthetic target. More perplexing was the fact that the <sup>13</sup>C NMR resonances assignable to the cyanamide carbon were reported to be in the range of 115-123 ppm, whereas those observed for the *N*-cyanoindoles prepared in this laboratory were in the range 105-108 ppm. This led us to re-evaluate<sup>92</sup> Echavarren's report and, through some thought, to reinterpret the experiments which then allowed a chemically reasonable proposal, avoiding unusual arrangements, which would explain the apparent spectroscopic discrepancies.

Our interpretation of the likely product distribution involves two separate cyclizations of **1.112b** at C-3 and C-1 to give **1.113a** and **1.115a**, respectively, as the corresponding major and minor products as shown in Scheme 1.14, contrary to Echavarren's analysis (Schemes 1.12 and 1.13). The likelihood that **1.114a** exists at all is questionable and those workers qualify its formation from the mechanism offered in Scheme 1.13. Accordingly, the most likely events to occur are that **1.112b** exists as two tautomers **1.112b** and **1.112c** in equilibrium, which upon pyrolysis, yield the corresponding tautomers **1.123** and **1.124**, also

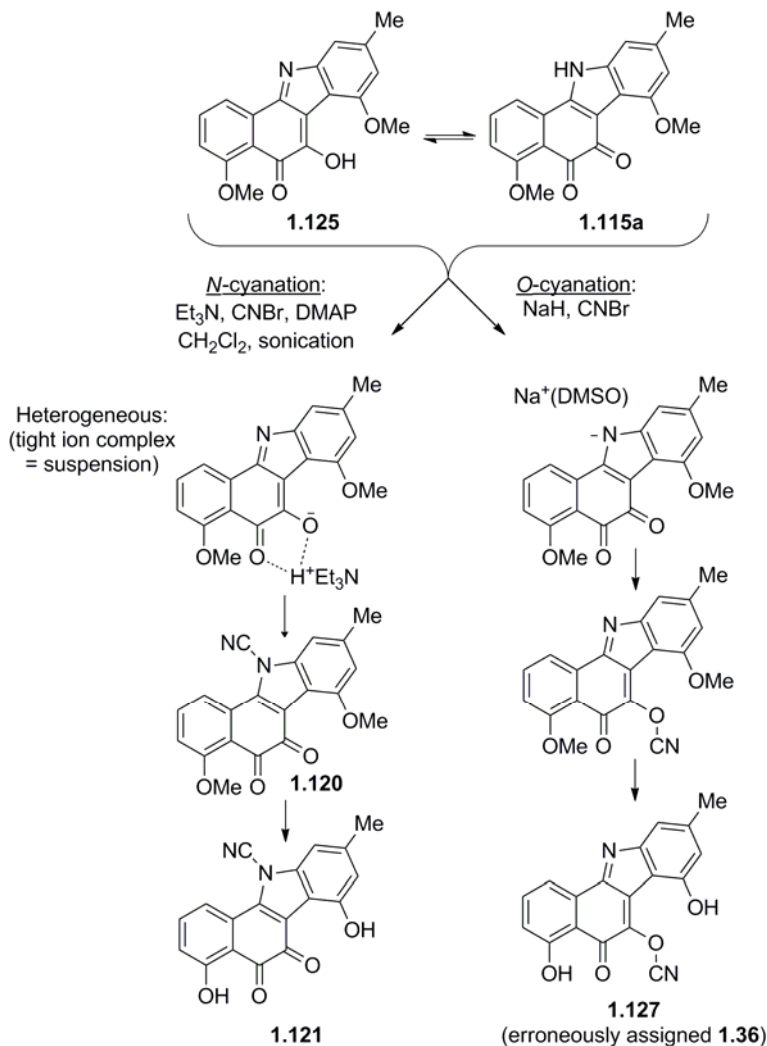
in equilibrium which undergo separate cyclizations to furnish **1.125** and **1.126**, respectively. Tautomerization then gives the respective products observed, **1.115a** and **1.113a**. The unusual rearrangement of **1.113a** to **1.115a** upon exposure to silica is thus avoided and the reaction can be simply rationalized as a tautomerization between **1.125** and **1.115a**.

**Scheme 1.14:** Reinterpretation of Echavarren's results.



Cyanation of the “major product” thought by Echavarren to be **1.114a** (but that is actually **1.113a**) proceeds without incident to give **1.117** (and not **1.118**) quantitatively and appears reasonable. However, cyanation of the “minor product” **1.113a** (which is actually **1.115a**) to give **1.120** can be explained in terms of competing *O*-cyanation versus *N*-cyanation as shown in Scheme 1.15. In all likelihood, it is the *O*-cyano product **1.127** that arises from these transformations in which Echavarren has erroneously assigned the structure prekinamycin **1.36**. A later publication by Echavarren and coworkers corrected these misassignments.<sup>93</sup>

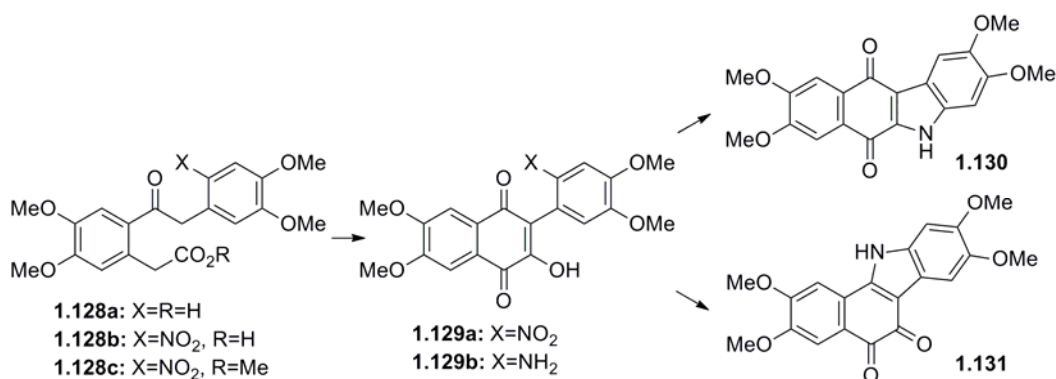
**Scheme 1.15:** Analysis and reinterpretation of the *N*-cyanation events of Echavarren's synthesis.



Using nitroquinone **1.129a**, Castedo and coworkers obtained **1.130** in 98% yield (Scheme 1.16).<sup>80</sup> Nitroketoester **1.128c** was prepared from the nitration of the ketoacid **1.128a**<sup>94</sup> affording **1.128b** which was subsequently esterified to give **1.128c**. Treatment of **1.128c** in refluxing aqueous methanolic sodium hydroxide produced nitro-quinone **1.129a** in which the

authors propose a mixed Claisen condensation followed by oxidation of the cyclized product. Reduction of the nitro moiety was carried out with NaBH<sub>4</sub> in isopropanol which underwent cyclization to afford a red-coloured compound **1.130**. The other possibility **1.131** was ruled out as the *N*-methyl derivative of the red product did not undergo a benzilic acid rearrangement as observed for pontevodrine,<sup>95</sup> a natural product containing an ortho quinone functionality.

**Scheme 1.16:** Castedo's synthesis.

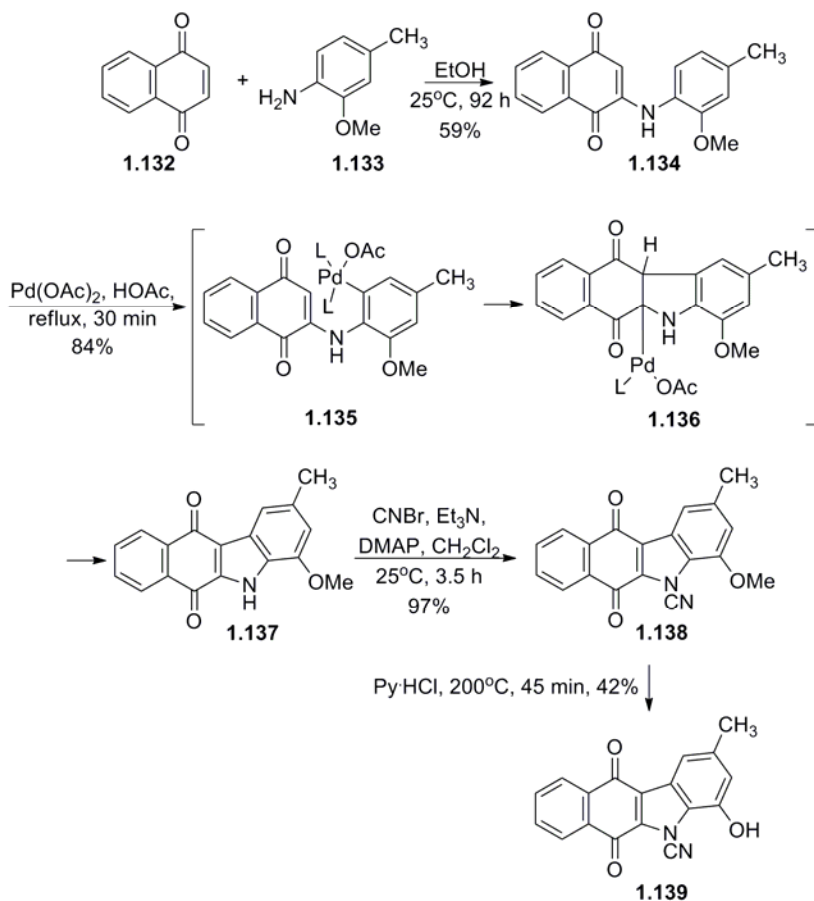


Knölker and O'Sullivan reported a four step synthesis of a 7-deoxyprekinamycin **1.139**, incorporating a Pd-promoted oxidative coupling as the key step (Scheme 1.17).<sup>81</sup> This isomeric analogue of prekinamycin represented a possible alternative to the proposed structure of prekinamycin. The IR band for the cyano group was found at 2252 cm<sup>-1</sup> and is in good agreement with spectroscopic data reported by the Dmitrienko group.<sup>59</sup> The mechanism proposed is electrophilic attack on the Pd (II) species by the aromatic ring to give an  $\sigma$ -arylpalladium (II) complex **1.135**. Insertion of the quinone double bond generated the  $\sigma$ -



alkylpalladium complex **1.136**, which after  $\beta$ -elimination provides **1.137**. Although at the time **1.139** presented an appropriate analogue, no ensuing biological studies were reported.

**Scheme 1.17:** Knölker and O'Sullivan's synthesis of 7-deoxyprekinamycin.



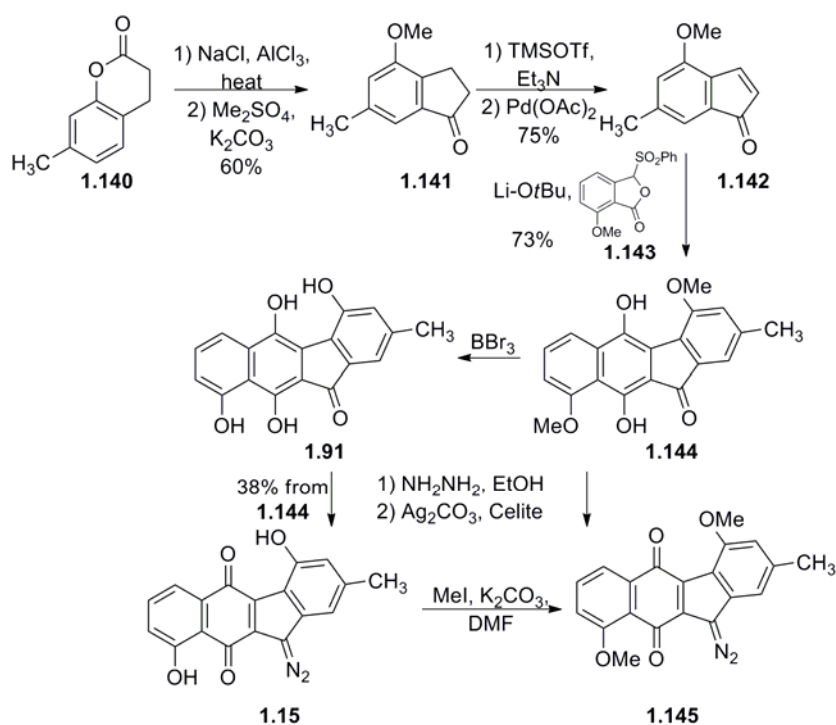
## 1.4.2 Diazobenzo[*b*]fluorenequinone syntheses

### 1.4.2.1 Hauser and Zhou's synthesis of Prekinamycin

The first reported synthesis of the kinamycins as diazobenzo[*b*]fluorenes was by Hauser and Zhou in 1996,<sup>61</sup> using their phthalide annelation methodology<sup>96</sup> as the key step, furnishing prekinamycin **1.15** in nine steps as shown in Scheme 1.18. The highlight of the

synthesis was the condensation of the anion of the phthalide sulfone **1.143** with indenone **1.142** to afford the benzo[*b*]fluorenone **1.144** regioselectively. As discussed in Section 1.2.4, this report led to the realization that the compound (Cpd A) to which the structure **1.15** had been assigned must have a different structure, eventually shown to be **1.16** by the Waterloo and Oregon State groups.

**Scheme 1.18:** Hauser and Zhou's synthesis of prekinamycin.

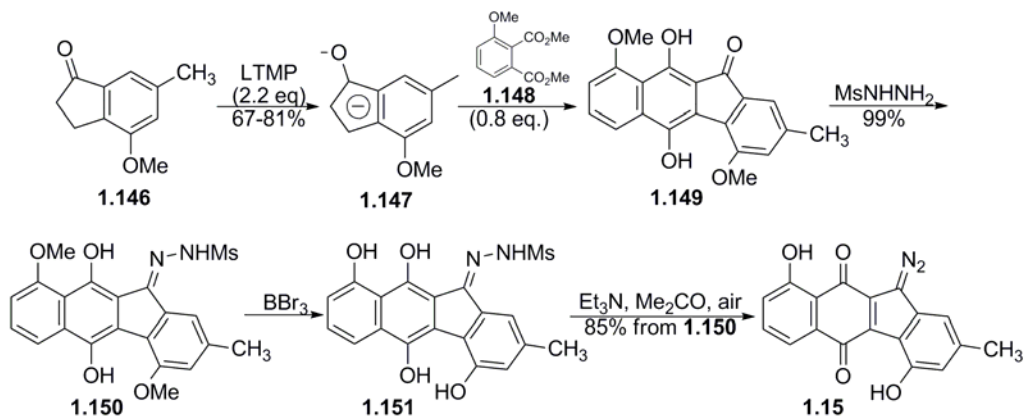


#### 1.4.2.2 Birman's synthesis of Prekinamycin

More recently, Birman and coworkers accomplished a total synthesis of prekinamycin in 2007, shown in Scheme 1.19.<sup>97</sup> This relied on the dianion **1.147** attacking the biselectrophile **1.148** regioselectively, furnishing the fluorenone **1.149** in modest to good yields.

Condensation of the fluorenone with mesyl-hydrazine produced the hydrazone **1.150** in high yield. Global deprotection and oxidation provided the target prekinamycin in five steps.

**Scheme 1.19:** Birman's synthesis of prekinamycin.



#### 1.4.2.3 Porco's synthesis of Kinamycin C

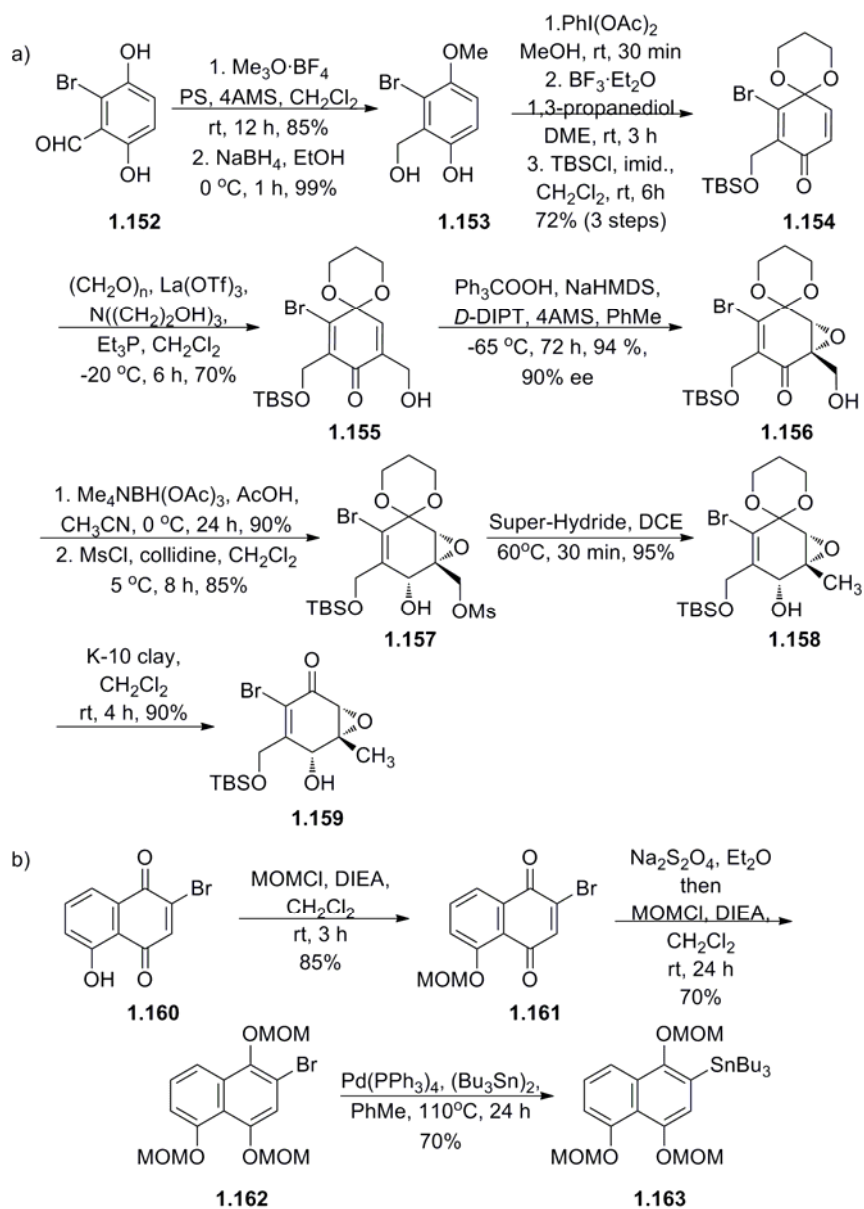
The first enantioselective synthesis of any kinamycin was accomplished by Porco and coworkers when they reported the total synthesis of kinamycin C in 2006.<sup>98</sup> Porco's synthesis is shown in Scheme 1.20 with the synthesis of two fragments **1.159** and **1.163** and the subsequent Stille coupling of these fragments illustrated in Scheme 1.21.

Synthesis of **1.159** begins with regioselective methylation of **1.152** followed by reduction to provide **1.153** (Scheme 1.20a). Subsequent oxidation, transketalization and silyl protection gave quinone monoketal **1.154**. Modified Baylis-Hillman conditions provided access to **1.155**, which provided the necessary handle for the impending hydroxyl directed asymmetric nucleophilic epoxidation, which furnished **1.156** in 94% yield and 90% ee. Diastereoselective reduction followed by selective mesylation of the primary alcohol afforded **1.157**, which

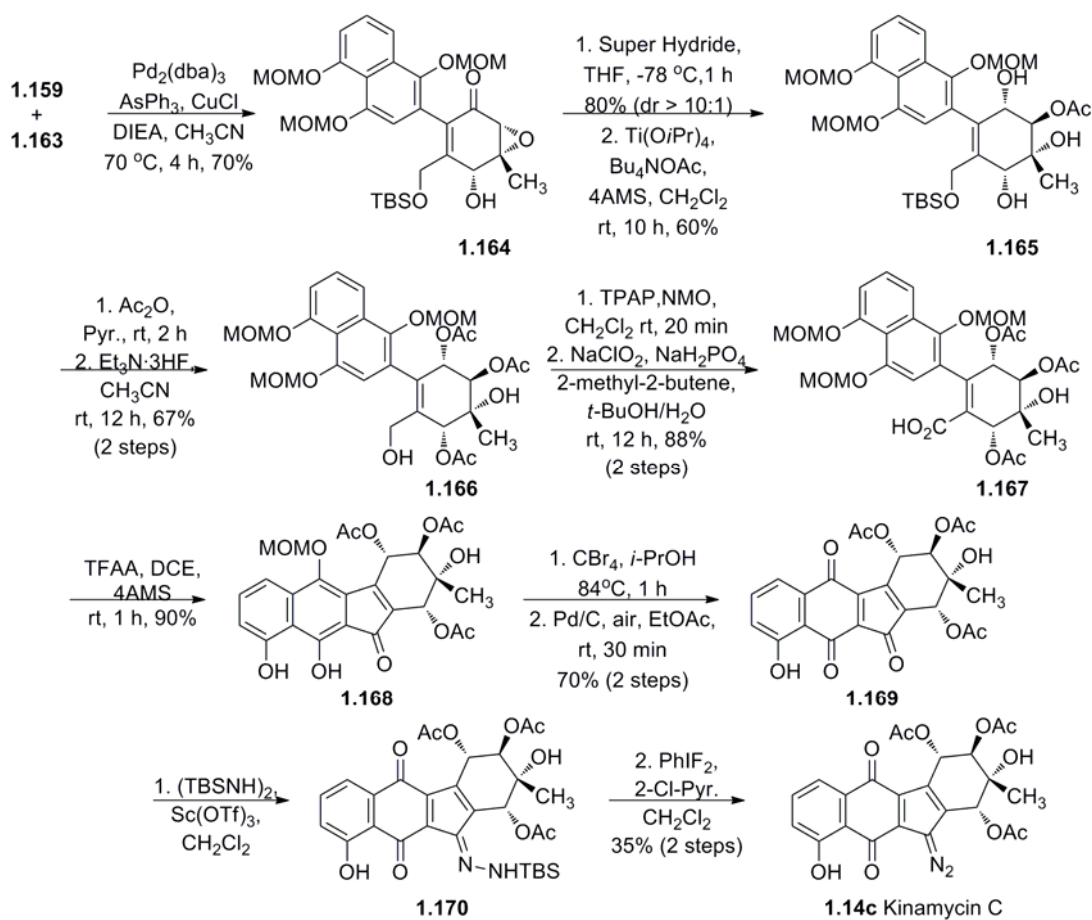
underwent reductive demesylation to give **1.158**. Removal of the cyclic ketal using K-10 clay gave the requisite epoxy enone **1.159**. Access to naphthylstannane **1.163** was provided by *O*-alkylation of **1.160**, reduction and *O*-alkylation of **1.161** to give naphthylbromide **1.162** which underwent stannylation producing the requisite arylstannane **1.163** (Scheme 1.20b).

The Stille coupling of **1.159** and **1.163** proceeded at a modest 70% yield producing **1.164**, which underwent diastereoselective reduction and epoxide opening to give **1.165** (Scheme 1.21). Acylation and deprotection of the TBDMS silyl ether furnished **1.166**, which underwent subsequent oxidations using TPAP and then sodium chlorite affording the carboxylic acid **1.167**. Ring closure was executed by employing TFAA, furnishing the tetracycle **1.168** with the serendipitous regioselective cleavage of two MOM groups. Cleavage of the remaining MOM group and oxidation in air using Pd/C gave ketoquinone **1.169**, which was condensed with bis-TBS-hydrazine and then oxidized with PhIF<sub>2</sub> to give kinamycin C.

**Scheme 1.20:** Porco's enantioselective synthesis of kinamycin C.



**Scheme 1.21:** Porco's enantioselective synthesis of kinamycin C (continued).

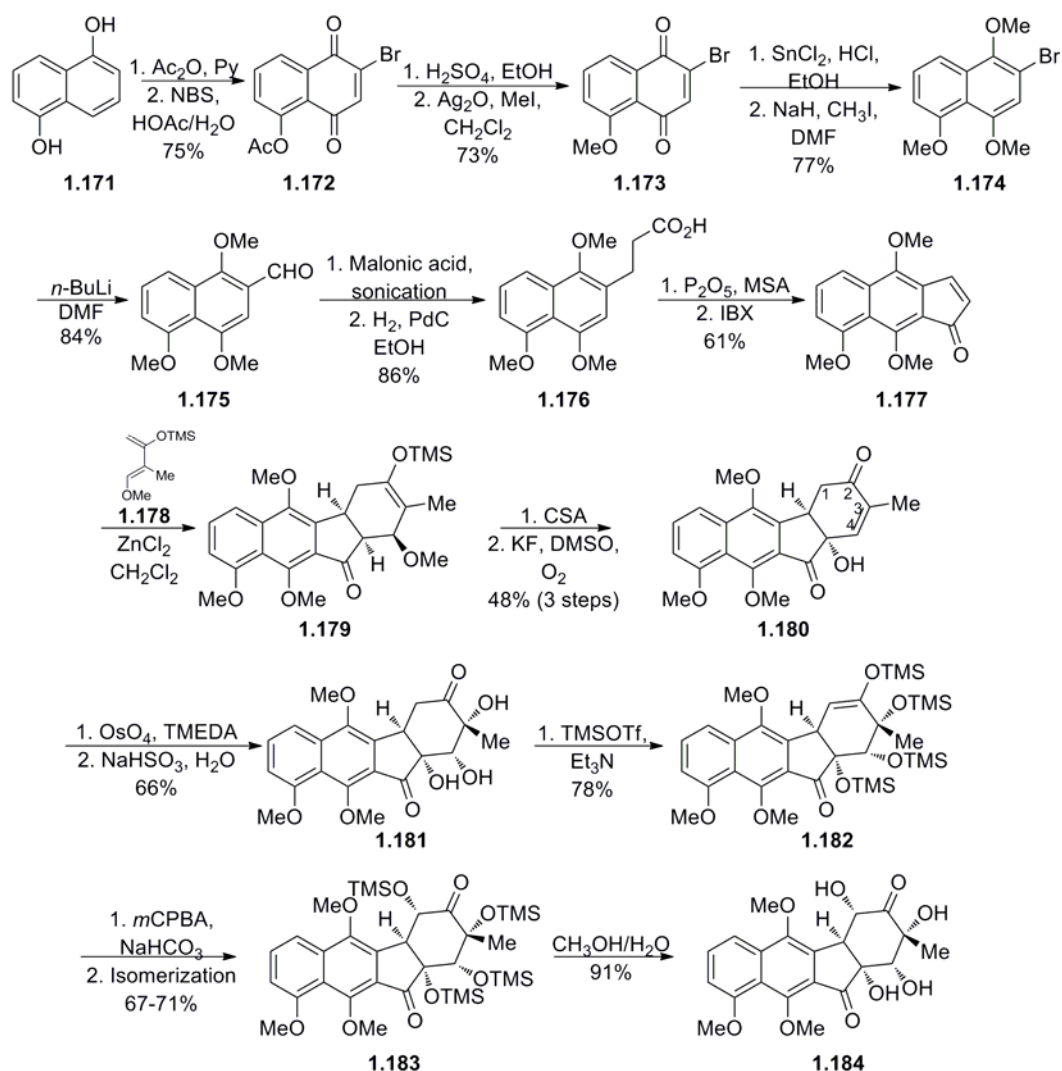


1.4.2.4 Ishikawa's synthesis of ( $\pm$ )-*O*-methyl Kinamycin C

In 2007 Ishikawa's group reported the synthesis of racemic *O*-methyl-kinamycin C.<sup>99,100</sup> Acetylation and oxidative bromination of **1.171** afforded quinone **1.172**, which was deacetylated and *O*-methylated to give **1.173** (Scheme 1.22). Reduction and *O*-methylation gave the trimethoxy bromonaphthalene **1.174**, which upon treatment with *n*-BuLi and DMF produced naphthaldehyde **1.175**. Knoevenagel reaction of **1.175** with malonic acid under sonication followed by catalytic hydrogenation gave naphthalenepropanoic acid **1.176**. Ring

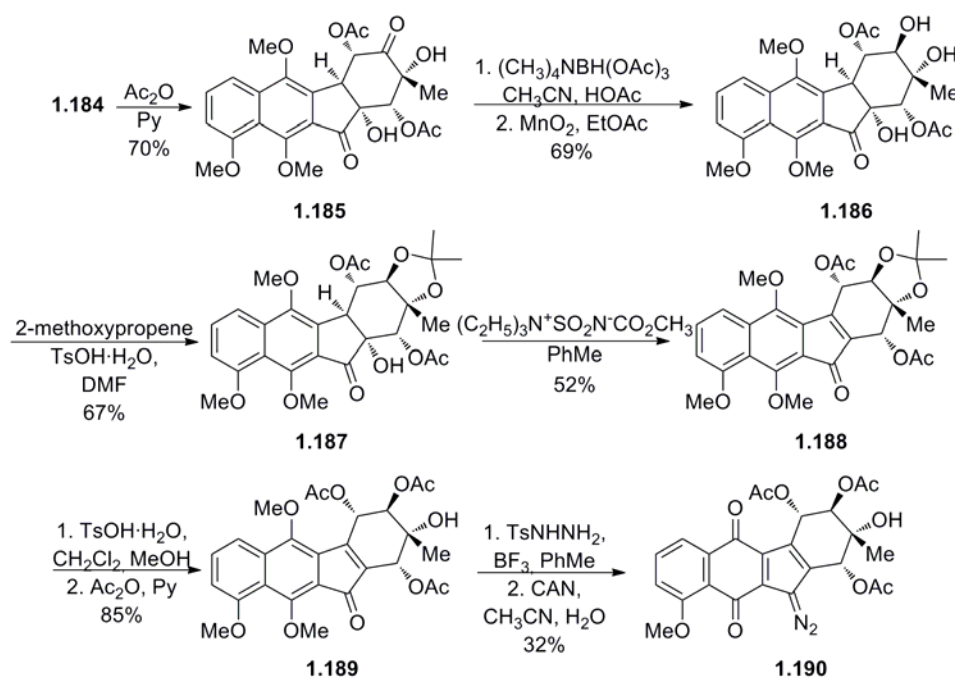
closure by an intramolecular Friedel-Crafts reaction provided the benzoindanone which was oxidized to the indenone **1.177** using IBX, providing the dienophile for the impending Diels-Alder reaction. The cycloaddition with the Danishefsky-type diene **1.178** gave adduct **1.179**, which, when treated with CSA followed by air oxidation in the presence of KF, provided enone **1.180** in three steps at 48% yield.

**Scheme 1.22:** Ishikawa's synthesis of ( $\pm$ ) *O*-methyl-kinamycin C.



The hydroxyl group at C-4a provided the necessary handle for the diastereoselective syn-dihydroxylation using OsO<sub>4</sub>-TMEDA, giving the *cis*, *cis*-triol **1.181**. Global silylation afforded **1.182** which underwent a Rubottom oxidation using *m*CPBA and allowed to isomerize to the desired 1 $\alpha$ -siloxyketone **1.183**. Global deprotection was executed using methanol-water, furnishing **1.184**.

**Scheme 1.23:** Ishikawa's synthesis of ( $\pm$ ) *O*-methyl-kinamycin C (continued).



Acetylation of **1.184** gave **1.185** which underwent a diastereoselective reduction with tetramethylammonium triacetoxyborohydride to give the *trans*-diol **1.186** (Scheme 1.23). Manganese dioxide converted any over-reduced product back to **1.186**. Ketalization gave **1.187** and subsequent dehydration using Burgess's reagent furnished **1.188**. Deprotection, and subsequent oxidation of the enone system, furnished **1.190**.

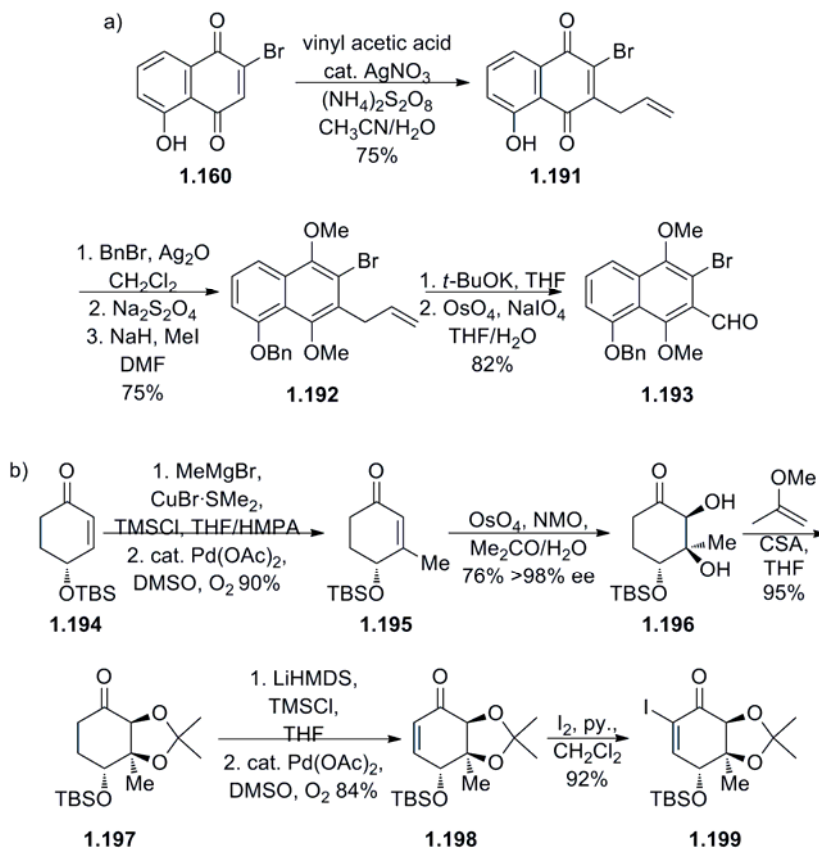


acetylation and installation of the diazo functionality produced ( $\pm$ )-*O*-methyl-kinamycin C **1.190**.

#### 1.4.2.5 Nicolaou's synthesis of Kinamycins C, F and J

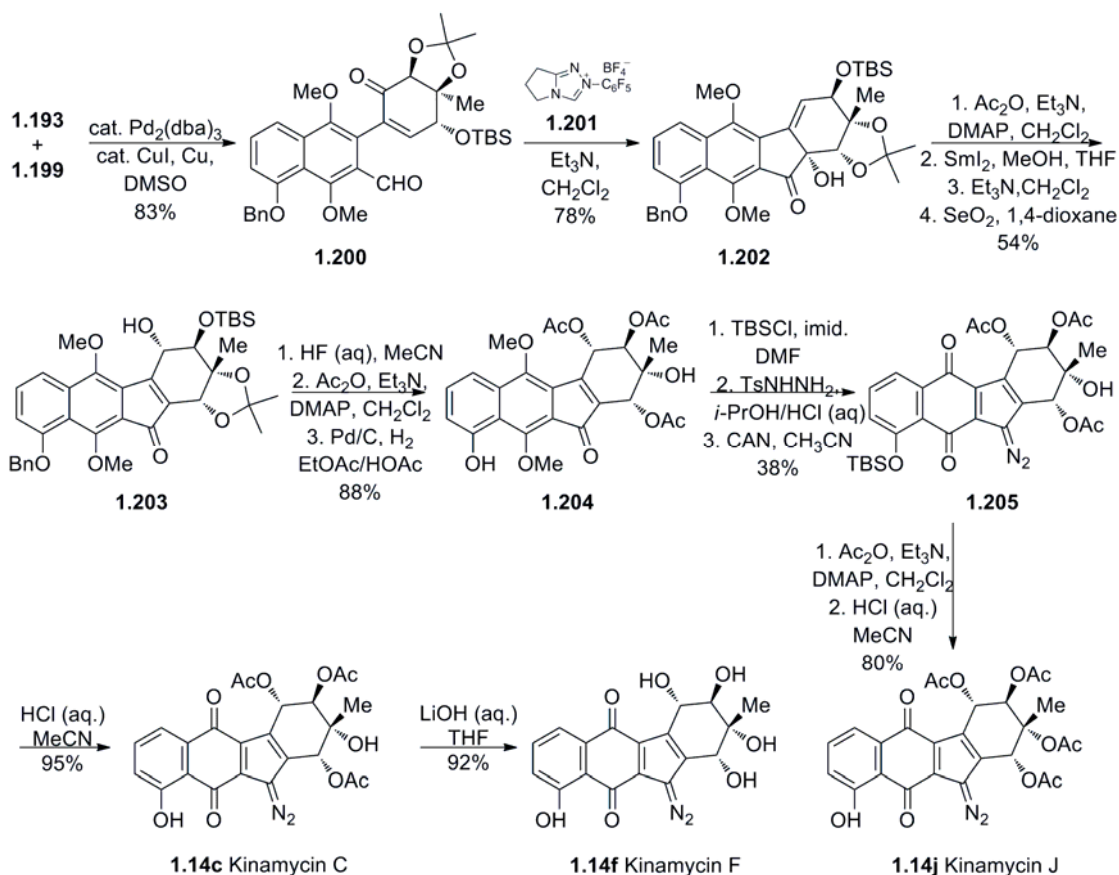
In 2007, Nicolaou's group reported the enantioselective syntheses of kinamycins C, F and J.<sup>54</sup> The synthesis begins, as shown in Scheme 1.24, with the allylation of 2-bromojuglone **1.160** under radical conditions to provide **1.191**. This compound underwent *O*-benzylation, reduction, and *O*-methylation to afford **1.192**. Isomerization under basic conditions and oxidative cleavage gave the bromonaphthaldehyde **1.193**.

**Scheme 1.24:** Nicolaou's enantioselective syntheses of kinamycins C, F and J.



The chiral enone **1.194** underwent conjugate addition of a methyl group and trapped as the silyl-enol ether. The subsequent Saegusa oxidation furnished **1.195**. The diastereoselective oxidation of the olefin with  $\text{OsO}_4$  and protection as the acetonide gave **1.197**. The Saegusa oxidation sequence was re-iterated and a regioselective iodination afforded the iodo-enone **1.199**.

**Scheme 1.25:** Nicolaou's enantioselective syntheses of kinamycins C, F and J (continued).



Fragments **1.193** and **1.199** were coupled under modified Ullman conditions to give **1.200**. Using the Rovis catalyst **1.201** in a benzoin-like reaction, the benzo[*b*]fluorenone **1.202** was obtained. The alcohol was acetylated and the acetoxy group was reductively cleaved using

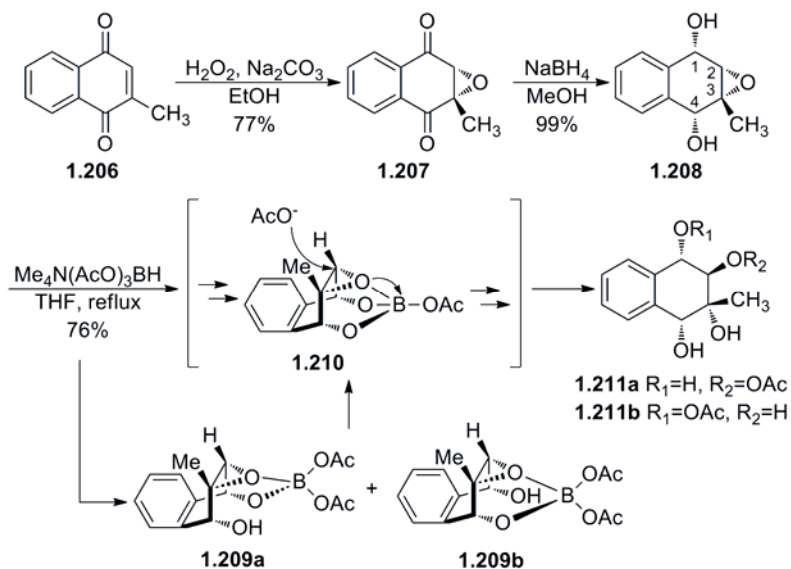
samarium iodide in the presence of methanol and then Et<sub>3</sub>N, migrating the double bond into conjugation. Allylic oxidation with selenium dioxide provided the allylic alcohol **1.203**. Deprotection of the TBS and acetonide groups, acetylation and debenylation gave fluorenone **1.204**, in which the phenolic hydroxyl was TBS protected, installation of the hydrazone moiety and subsequent CAN oxidation furnished the TBS-protected kinamycin C **1.205**. A series of deprotections and acetylations provided the natural products kinamycins C, F and J.

#### 1.4.2.6 Dmitrienko's biomimetic approach to construction of the D-ring

Porco's, Ishikawa's and Nicolaou's syntheses illustrated different approaches to the construction of the highly oxygenated D-ring. Using a simple model system, N. Chen in this laboratory has successfully demonstrated a three-step diastereoselective elaboration of the D-ring using a biomimetic approach (Scheme 1.26).<sup>101</sup> Epoxidation of 2-methyl-1,4-naphthoquinone **1.206** with hydrogen peroxide under basic conditions gave epoxy-diketone **1.207**. This epoxy-diketone was reduced with NaBH<sub>4</sub> with high diastereoselectivity, owing to steric shielding by the protic solvent via H-bonding with the epoxide, consequently promoting hydride approach trans to the epoxide oxygen, producing **1.208**. Ring-opening of the epoxide was achieved with Me<sub>4</sub>NBH(OAc)<sub>3</sub> with high regio- and diastereoselectivity. The mechanism is thought to be analogous to that reported by Caron and Sharpless for ring opening of epoxy alcohols with Ti(OiPr)<sub>4</sub>.<sup>102</sup> It is thought that the Lewis acid reacts initially with the alcohol to provide a tethered Lewis acid that then facilitates epoxide ring opening. In the case of **1.208**, two complexes form, **1.209a** and **1.209b**, which react further to form the cyclic complex **1.210**. The selectivity is attributed to the cyclic complex **1.210** in which the

boron serves as an intramolecular Lewis acid to assist with epoxide ring opening by the nucleophile via backside attack at the less crowded C-2 to provide **1.211**.

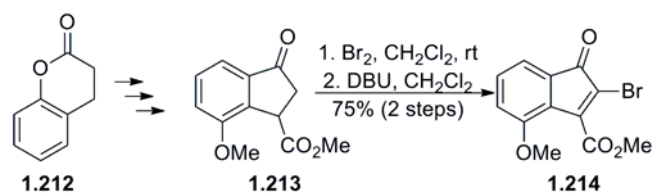
**Scheme 1.26:** Dmitrienko's biomimetic approach to the synthesis of the D-ring.



#### 1.4.2.7 Dmitrienko's total synthesis of Isoprekinamycin

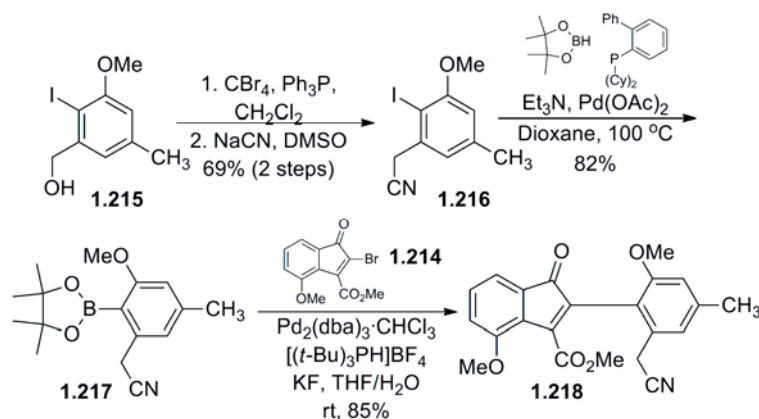
W. Liu in this laboratory accomplished the first total synthesis of isoprekinamycin employing a Suzuki coupling as a key step.<sup>38</sup> Synthesis of the AB ring synthon is shown in Scheme 1.27. The substituted indanone **1.213** was synthesized from the commercially available dihydrocoumarin **1.212**. Dibromination and then DBU-induced dehydrobromination furnished **1.214**.

**Scheme 1.27:** Dmitrienko's total synthesis of isoprekinamycin.



The D-ring synthon was prepared from the *o*-iodoarylbenzyl alcohol **1.215** which was converted to the nitrile **1.216** and then to the boronate **1.217** using a Pd coupling with pinacol borane (Scheme 1.28). The Suzuki coupling proceeded uneventfully to give **1.218** in 85% yield.

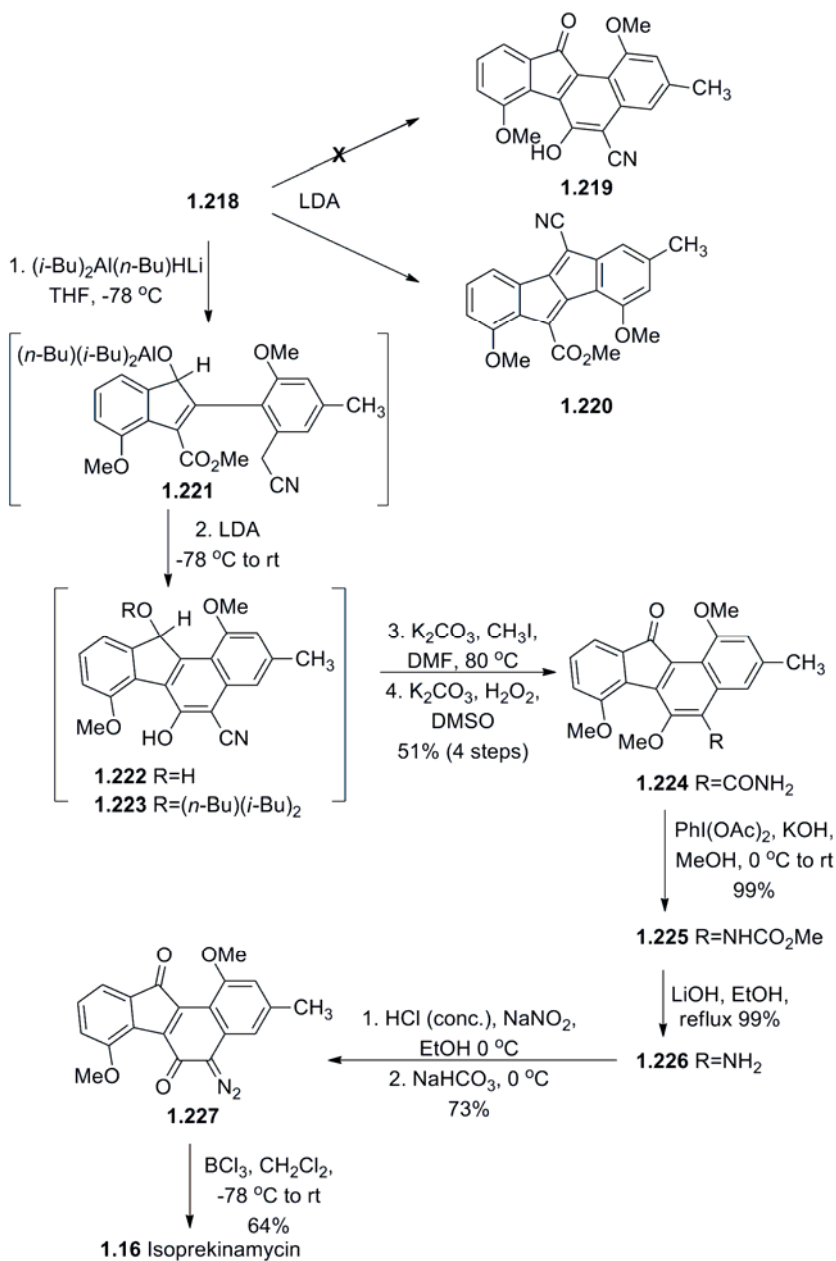
**Scheme 1.28:** Dmitrienko's total synthesis of isoprekinamycin (continued).



Cyclization of **1.218** required modified conditions, reducing the ketone first by using a combination of *n*-BuLi and DIBAL affording **1.221** which was then treated with LDA and upon aqueous workup gave a mixture of **1.222** and **1.219** formed from partial air oxidation. The mixture was *O*-alkylated and the nitrile hydrolyzed to the amide **1.224** with concomitant oxidation to the ketone using  $\text{K}_2\text{CO}_3/\text{H}_2\text{O}_2$ . Using modified Hofmann conditions the amide

was transformed to the carbamate **1.225** which was hydrolyzed to the aniline **1.226** and diazotized to afford **1.227**. Deprotection with  $\text{BCl}_3$  provided the target **1.16** in 64% yield.

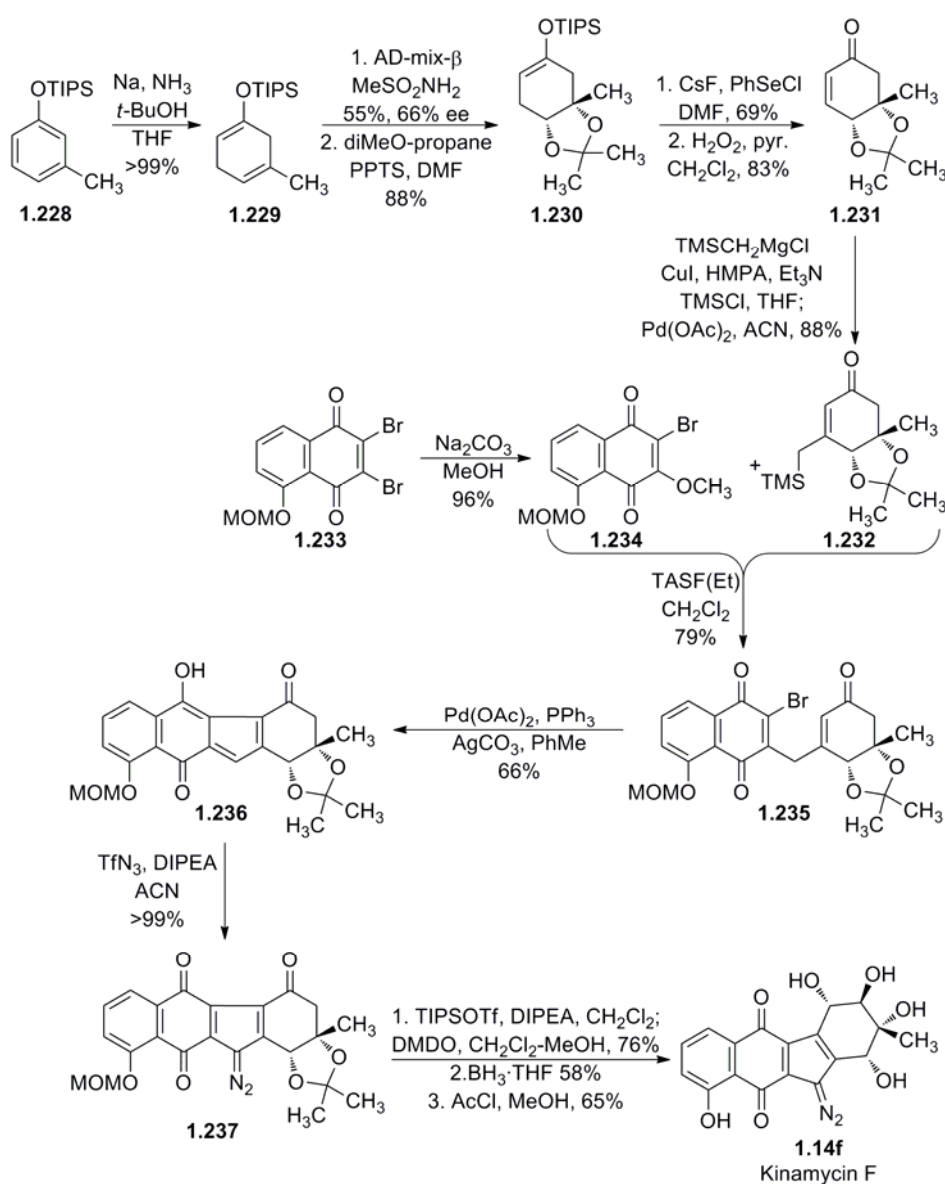
**Scheme 1.29:** Dmitrienko's total synthesis of isoprekinamycin (continued).



#### 1.4.2.8 Herzon's enantioselective synthesis of Kinamycin F

Most recently, Herzon and coworkers have described an enantioselective synthesis of kinamycin F in twelve steps (Scheme 1.30).<sup>103</sup> Employing a Birch reduction and a subsequent Sharpless asymmetric dihydroxylation followed by protection as the ketal (three steps in 48%) provided the key chiral building block **1.230** to produce kinamycin F.

**Scheme 1.30:** Herzon's enantioselective synthesis of kinamycin F.



## 1.5 Mechanism of Action Studies

### 1.5.1 Moore's proposed mechanism for the *N*-cyanobenzo[*b*]carbazoles

Prior to 1994, kinamycins were thought to be cyanamides and appropriately it was felt that the mechanism of action (MOA) was analogous to that of the mitomycins, the well-known DNA bis-alkylating agents, as suggested by Moore in 1977.<sup>104</sup> Both the mitomycin and kinamycin structures contain an indoloquinone incorporating appropriately positioned leaving groups and consequently Moore speculated that kinamycin C could be a reductively activated alkylating reagent.

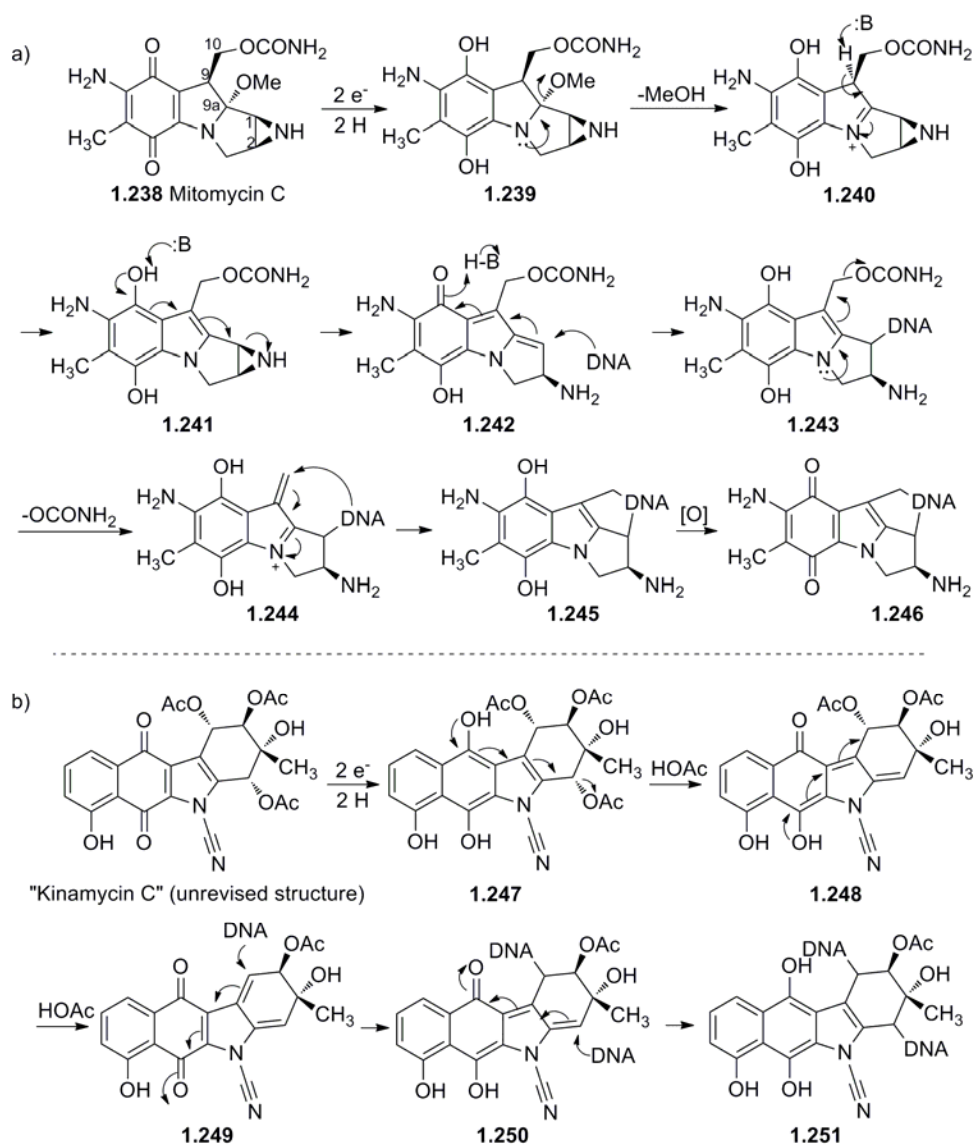
Mitomycin C, a clinical chemotherapy agent, is a known DNA cross-linking agent under reducing conditions in which the generally accepted mechanism is shown in Scheme 1.31a.<sup>105,106</sup> Thus, reduction of the quinone **1.238** to the dihydroquinone **1.239** and expulsion of the angular methoxy group provides **1.240** and tautomerization gives **1.241**. The aziridine ring is now induced to open and consequently provides the vinylogous quinone methide **1.242**, the incipient electrophile for a nucleophilic species such as N-2 of the deoxyguanosine nucleoside.<sup>107-111</sup> Next, the expulsion of the carbamate moiety generates vinylogous iminium ion **1.244**, another electrophilic site for nucleophilic attack. Oxidation back to the quinone species may be an obligatory step to prohibit the release of DNA.

It was reasonable to suggest that kinamycin C (unrevised structure) might undergo similar chemistry, wherein reduction and the loss of two acetates gives **1.249**, a double Michael acceptor and is a potential bis-alkylating agent (Scheme 1.31b). Moore's original hypothesis did not implicate the cyanamide group in the mechanism. In this context, it is worth pointing out that the bioreductive activation of the kinamycins cannot be overlooked as either



cyanamides or as diazo compounds as the diazo group is isosteric and isoelectronic with the cyanamide group. The speculation that the diazo group is implicated in the mechanism has been borne out by studies of kinfluorenone **1.20**, lacking the diazo group, displays no detectable antibiotic activity against *B. subtilis* ATCC 6633, an organism very sensitive to the kinamycins.<sup>42</sup>

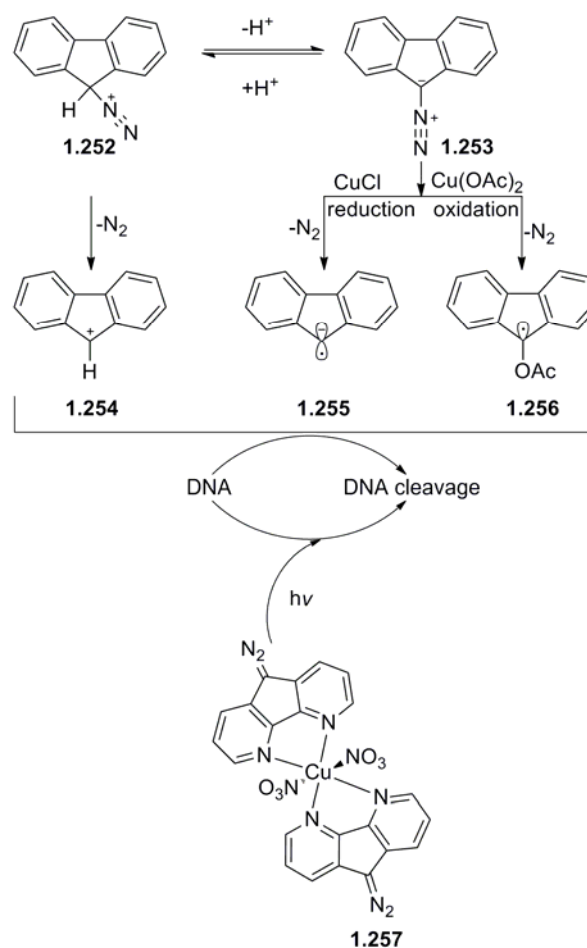
**Scheme 1.31:** Moore's proposal for the bioreductive alkylation of kinamycin C.



### 1.5.2 Model diazo compounds

Studies using simple aryl diazo compounds were the first reports to appear related to the mechanism of action of the kinamycins. Jebaratnam and Arya proposed potential reactive intermediates that may arise from 9-diazofluorene **1.253** which may go on to cleave DNA via three potential pathways: (a) the loss of N<sub>2</sub> to generate a carbocation (b) the reduction and loss of N<sub>2</sub> to generate a radical anion (c) the oxidation and loss of N<sub>2</sub> to generate a radical cation (Scheme 1.32).<sup>112</sup> The cleavage of pBR322 DNA in the presence of cupric acetate led those workers to speculate that DNA cleavage may result from the acetoxy radical **1.256**. Carbenes as mediators of DNA cleavage were ruled out as all reactions were performed in the dark, but authors did not preclude the possible intervention of copper-carbenoid species. The nature of the mechanism responsible for DNA cleavage remains speculative and may involve more reactive oxygen-centered radicals generated from carbon-centered radicals and molecular oxygen. The other possibility is that the cuprous ions generated from the oxidation of **1.253** with cupric acetate generates reactive-oxygen species (ROS) such as Cu(I)-oxygen or Cu(I)-hydroxyl radical, which then are able to effect H-atom abstraction and to eventually cleave DNA.<sup>113</sup> Maiya and coworkers have reported the generation of carbenes by photoirradiation of **1.253**;<sup>114</sup> however there are no reports which suggest kinamycins are activated by light.

**Scheme 1.32:** Early mechanistic studies with simple aryl diazo compounds.



Zaleski and coworkers demonstrated **1.257** is an effective DNA photocleaving agent in the absence of oxygen using visible light (Scheme 1.32).<sup>115</sup> Electrophoretic studies showed DNA cleavage at concentrations ranging from 12.5 to 200  $\mu M$ . Subsequent spectrophotometric experiments suggest that metal-ligand redox chemistry may play an active role in the activation of the diazo group, possibly generating a diazonium cation prior to  $N_2$  release and electrochemical studies were invoked to support their hypothesis. The suggestion that the quinone moiety of kinamycin C serves as an internal redox switch to facilitate release of  $N_2$

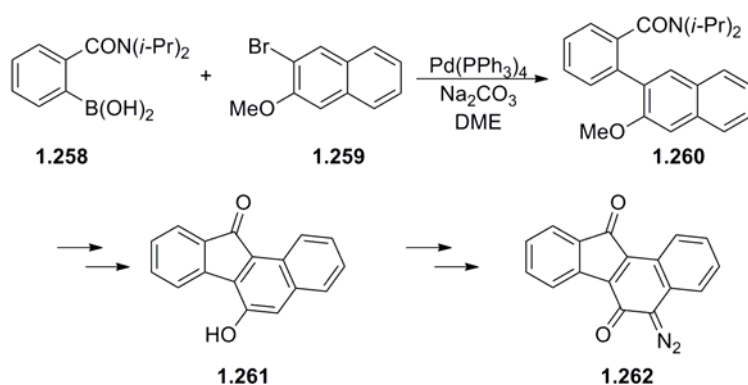
is intriguing; however, reports on parallel studies using kinamycin C by these workers have yet to appear. These studies are difficult to extrapolate to the kinamycins, in which reports describing their photo-activation are lacking. Indeed, no requirement for light has been noted in any subsequent DNA cleavage studies with the kinamycins. Both of these reports by Zaleski *et al.* and Jebaratnam and Arya implicate  $\text{Cu}^{+2}$  as a species involved in DNA cleavage; however, a biological surrogate has yet to be identified.

### 1.5.3 Mechanism studies using Kinamycins and closely associated models

1.5.3.1 Dmitrienko: increased diazonium character correlates with increased electrophilicity and biological activity

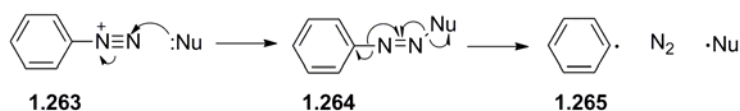
R. Laufer from this laboratory has pursued studies aimed at gaining insight into potential mechanistic pathways in which the kinamycins exert their biological activity.<sup>37</sup> This was accomplished in part by the synthesis of the IPK model **1.262** employing a Suzuki coupling (Scheme 1.33).

**Scheme 1.33:** Dmitrienko's synthesis of IPK model **1.262**.



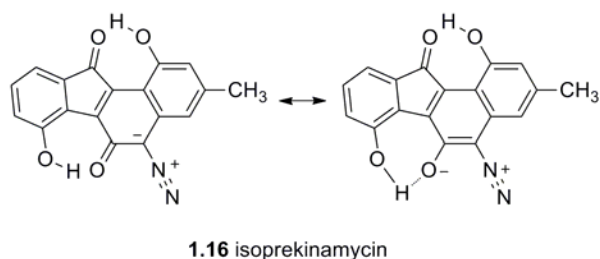
Previous reports in other laboratories on *o*- and *p*-quinodiazides<sup>116</sup> and aryl diazonium ions<sup>117,118</sup> suggest that their biological activity is elicited via aryl radicals that are able to chemically modify nucleic acid residues. More specifically, aryl diazonium ions **1.263** have been shown to undergo nucleophilic attack at the terminal nitrogen, generating the aryl radical **1.265** upon the subsequent release of N<sub>2</sub> via homolytic cleavage reactions (Scheme 1.34).<sup>119</sup> Nucleophilic attack by the C-6 amino group and/or the C-2 amino group of adenine or guanine, respectively, on aryl diazonium ions precedes aryl radical formation, furnishing labelled triazenes which then, upon release of N<sub>2</sub>, provide radicals which can then react with nucleic acid residues in a number of established pathways. Thus, the kinamycins may elicit some of their biological effects via sp<sup>2</sup> radicals that can chemically modify nucleic acid residues in a similar manner.

**Scheme 1.34:** Nucleophilic attack on an aryl diazonium species to elicit aryl radicals.



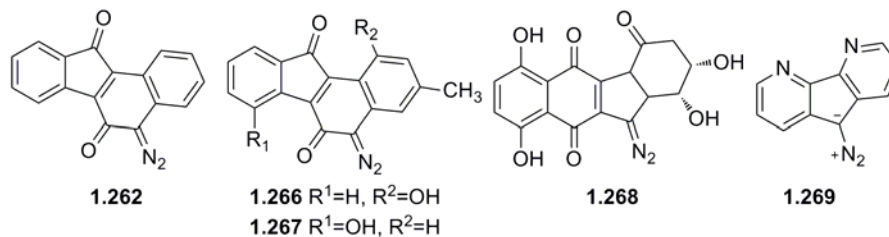
Data from this laboratory showed that the IR stretching frequency of the diazo group in compound **1.262** was 57 cm<sup>-1</sup> lower than in IPK **1.16** which was reproduced well by ab initio calculations (52 cm<sup>-1</sup>) and also revealed a shorter N-N bond length in IPK compared to **1.262**. This suggests IPK possesses an enhanced diazonium ion character that is thought to be a consequence of the intramolecular hydrogen bonding network, shown as the resonance contributor illustrated in Figure 1.7. This would render the terminal nitrogen of the diazo group more electrophilic and consequently more susceptible to nucleophilic attack.

**Figure 1.7:** Resonance depicted in IPK confers diazonium character to the diazo group.



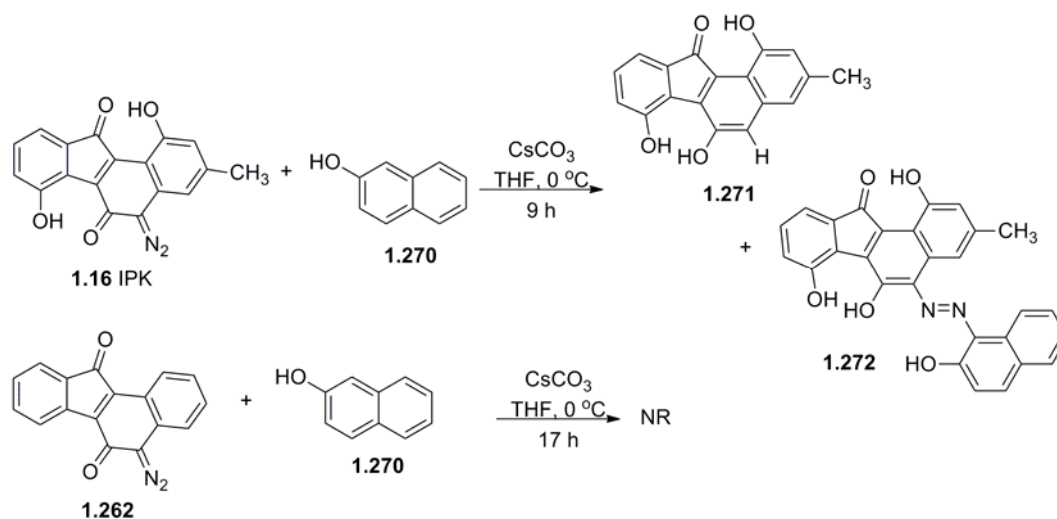
This trend was reproduced well for a number of model compounds in a series of calculations whose results are shown in Table 1.2. These calculations revealed an even higher diazonium ion character in the N-N bond of the kinamycins as well as in the simplified model of lomaiviticin A **1.268**. To this end, IPK and **1.262** were subjected to conditions that would test their relative electrophilicities (Scheme 1.35), the results of which indicated the higher degree of electrophilicity of IPK, consistent with IR studies and ab initio calculations. Complete conversion of IPK to **1.271** and **1.272** within 9 hours at 0 °C was observed, whereas a negligible reaction of **1.262** was observed after 17 hours. Thus the kinamycins and the closely related lomaiviticins may be activated towards nucleophilic attack at the terminal nitrogen of the diazo group which may play a role in antibacterial and antitumor activity.

**Table 1.2:** Calculated IR frequencies and bond lengths of the diazo group of selected compounds.<sup>37</sup>



Compound	Calculated $\nu$ ( $\text{cm}^{-1}$ )	Calculated N-N ( $\text{\AA}$ )
9-diazofluorene <b>1.253</b>	1906	1.133
2,1-naphthoquinodiazide <b>1.269</b>	2056	1.111
<b>1.262</b>	2087	1.108
<b>1.266</b>	2101	1.107
<b>1.267</b>	2125	1.105
IPK <b>1.16</b>	2139	1.103
Kinamycin B <b>1.14b</b>	2188	1.099
<b>1.268</b>	2212	1.097
Ph-N $\equiv$ N <sup>+</sup> Cl <sup>-</sup> <b>2.263</b>	2212	1.100

**Scheme 1.35:** Experimental conditions to test relative electrophilicities of IPK and **1.262**.<sup>37</sup>

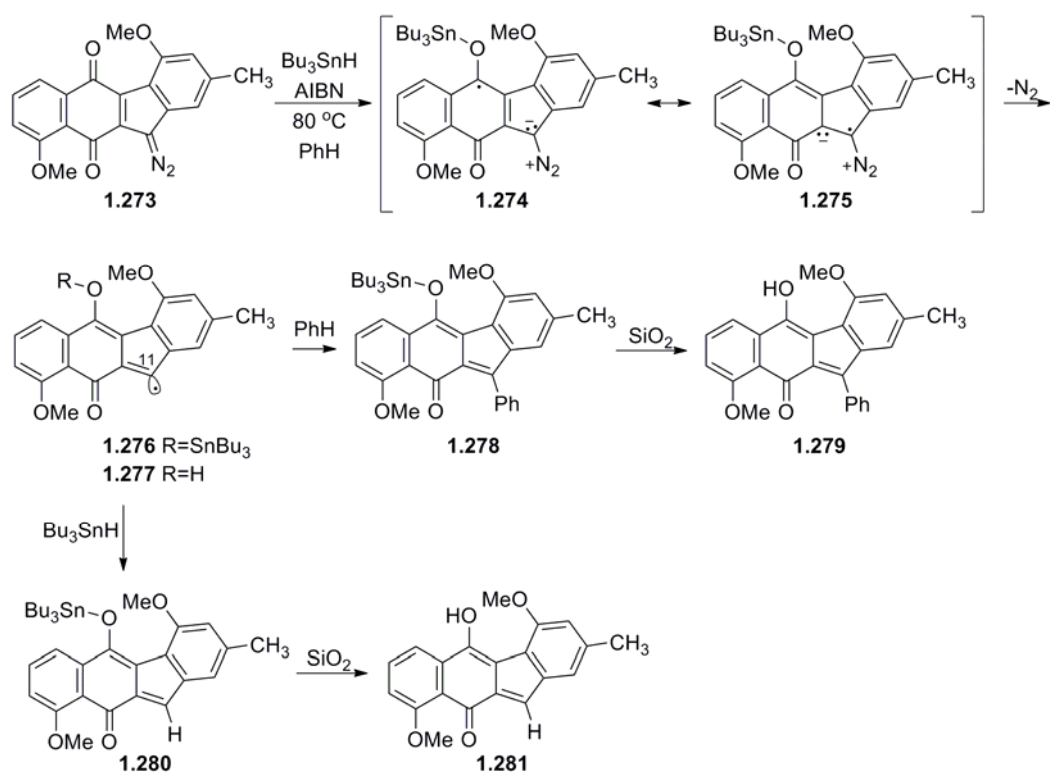


### 1.5.3.2 Feldman: a one electron reduction to afford an aryl radical

Feldman and Eastman have used prekinamycin derivatives in studies aimed at elucidating other pathways that may furnish DNA damaging reactive species.<sup>120-123</sup> They propose a one electron reduction that generates an aryl radical **1.277** capable of causing DNA lesions.<sup>124,125</sup> Under standard radical generating conditions using  $\text{Bu}_3\text{SnH}$  as a one electron donor in the presence of AIBN and heated in benzene at  $80^\circ\text{C}$  they were able to isolate the phenyl adduct **1.279** from dimethyl prekinamycin **1.273** (Scheme 1.36). The authors suggest that this chemistry serves as a model for a single electron reduction for the activation of the kinamycins as DNA cleaving agents *in vivo*.



**Scheme 1.36:** Feldman and Eastman's MOA studies of dimethyl prekinamycin.



The exact nature of the reactive intermediate that preceded the formation of adduct **1.279** was addressed through a suite of experiments using 1:1 molar mixtures of benzene and a series of electron-rich and electron-deficient aromatic solvents. The increased relative rates of aromatic solvent addition with **1.273** (an accelerating effect of most substituents relative to H) as well as *o*:*m*:*p* ratios (additions that place radical density on the substituent-bearing carbon) suggested a radical aromatic substitution mechanism, ruling out electrophilic aromatic substitution processes.

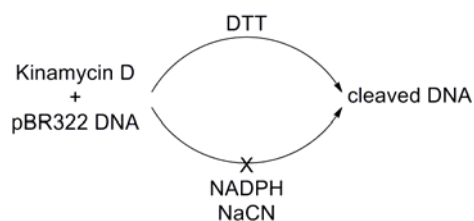
In separate experiments using increasing concentrations of Bu<sub>3</sub>SnH, they isolated the reduced product with no change observed in the ratio of aromatic trapping products

consistent with the apparent radical addition mechanism. Although this study provides convincing evidence of a C-11 radical as well as insight into the intrinsic reactivity of prekinamycin under abiological radical-inducing conditions, it is difficult to extrapolate those findings to the biological environment in which the kinamycins are inherently associated with and to draw any relevant conclusions.

#### 1.5.3.3 Melander: a two electron activation by thiols

Melander and coworkers have also explored kinamycin activity through DNA cleavage assays.<sup>126,127</sup> Initial studies under conditions using DTT, NADPH, or NaCN revealed that plasmid DNA was cleaved by kinamycin D only in the presence of DTT, albeit at high concentrations of 1 M (Scheme 1.37).<sup>126</sup> This study also identified a small number of substituted 9-diazofluorene derivatives that also recapitulated the activity of kinamycin D.

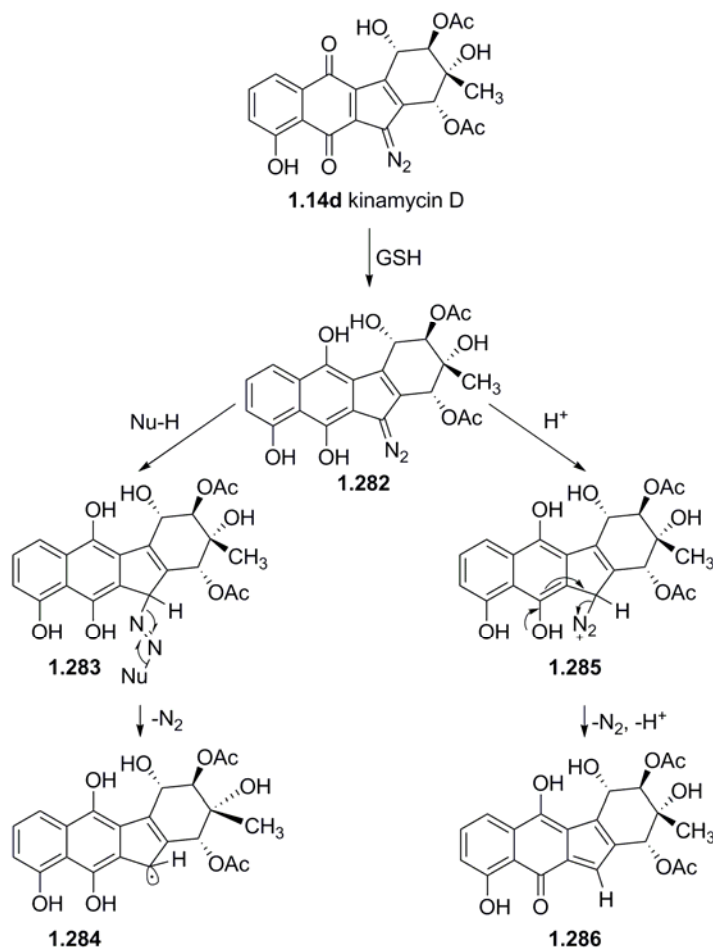
**Scheme 1.37:** Melander's experiment in which DTT activation of kinamycin D was observed.



A follow-up study addressed the abnormally high concentrations of DTT, employing glutathione (GSH) at more biologically relevant concentrations, and DNA cleavage was observed in a time, temperature and concentration dependent manner.<sup>127</sup> Sulfides are recognized sources of  $2e^-$  equivalents and thus it is unlikely that a  $1e^-$  reduction is occurring. Calculations revealed that the LUMO resides within the quinone moiety and appropriately,

reduction to the hydroquinone would ensue upon exposure to GSH. Consequently, there are two mechanistic pathways that may furnish species capable of DNA scission (Scheme 1.38). Nucleophilic attack on the distal nitrogen of the diazo group would lead to an aryl radical that may go on to cleave DNA in a number pathways previously mentioned (*vide supra*). The other would invoke protonation at the diazo carbon and the subsequent expulsion of  $N_2$  provides the ortho quinone methide, a good electrophile, although alkylating events in themselves do not necessarily lead to DNA cleavage.<sup>128,129</sup>

**Scheme 1.38:** Melander's MOA studies using kinamycin D.

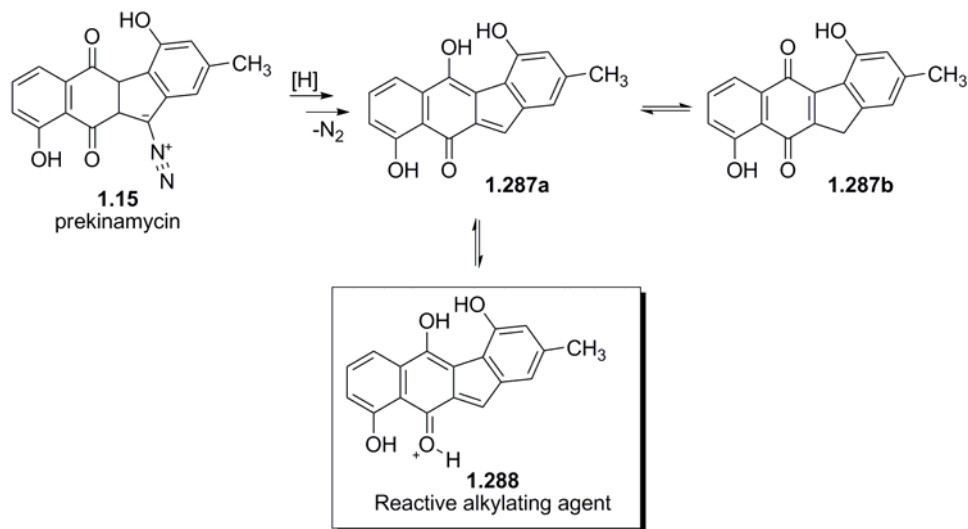


The most recent efforts from Melander suggest that, in the presence of a reducing agent at low pH, kinamycin D is capable of generating reactive oxygen species, which are then able to damage DNA.<sup>130</sup>

#### 1.5.3.4 Skibo: Quinone Methide of Prekinamycin

Recently, Skibo and coworkers have carried out physical organic chemistry experiments aimed at identifying a possible mode of action of prekinamycin.<sup>131</sup> In particular, this group has prepared prekinamycin and a number of analogues with the diazo carbon atom enriched with <sup>13</sup>C and have subjected these to catalytic hydrogenation to mimic a two electron reduction that might occur in vivo. This has allowed them to detect certain intermediates that are reactive and possibly electrophilic. This group suggests that their observations are consistent with the formation of an *ortho*-quinone methide intermediate **1.287a** upon reductive dediazonation of prekinamycin **1.15** which can exist in equilibrium with a deazotized quinone **1.287b** (Scheme 1.39). It is postulated further that those prekinamycin analogues that favour the *ortho*-quinone methide tautomer over the quinone tautomer are more likely to act as electrophiles with DNA bases as nucleophilic partners in conjugate addition reactions. Such alkylated DNA is then suggested to be unstable with respect to elimination reactions that ultimately effect cleavage of the DNA-backbone, thus rationalizing anticancer and antimicrobial activity on the basis of bioreductive activation of the prekinamycin system in vivo to create electrophilic species that can alkylate DNA leading eventually to sufficient damage to induce cell death.

**Scheme 1.39:** Skibo's postulate of protonated *ortho*-quinone methide intermediates as DNA alkylating reagents.

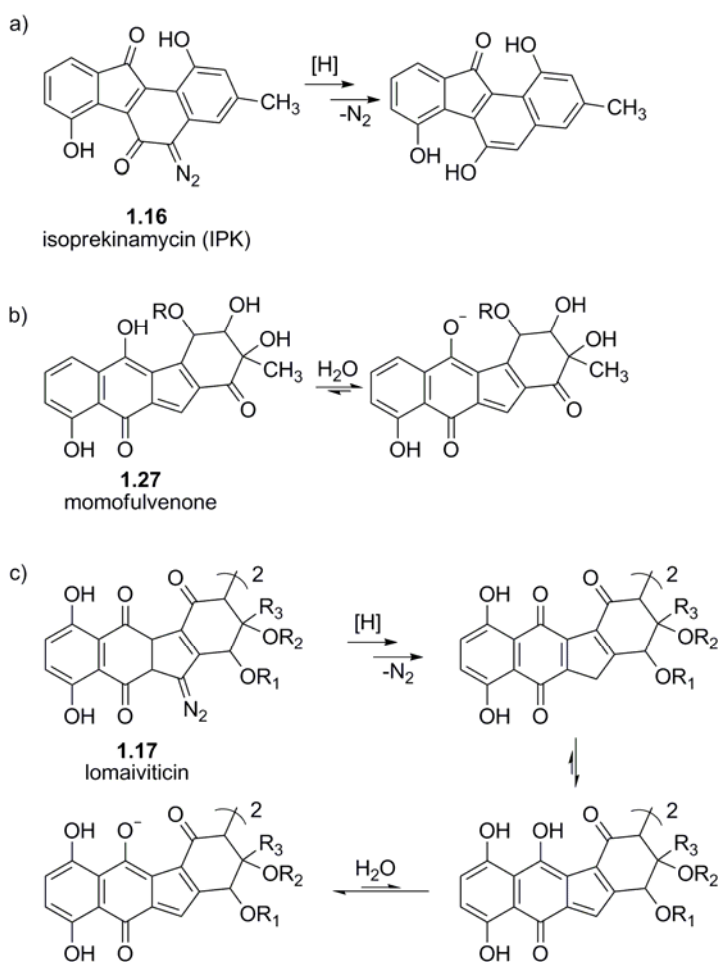


There are a number of interesting, but somewhat troubling aspects to the proposals by the Skibo group in regard to the mechanism of action of prekinamycin and, by implication, of the kinamycins, the lomaiviticins and IPK. In the case of IPK **1.16**, hydrodediazonation yields an aromatic system rather than an *ortho*-quinone methide so that the Skibo mechanism cannot be operative in that case (Scheme 1.40a). Thus, to accept the Skibo mechanism for biological activity one needs to assume that, despite their structural similarity, IPK and prekinamycins must act by different mechanisms. The Skibo mechanism also invokes an unusually high basicity for the ketone carbonyl group oxygen atom ( $pK_a \sim 7$ ) wherein the non-protonated *ortho*-quinone methide is argued to be unreactive as an electrophile and must first be *O*-protonated. Why such a carbonyl group would be so basic is not clear.

In the case of the momofulvenones **1.27**, which incorporate an *ortho*-quinone methide system of the type invoked by the Skibo group, the enolic OH is very acidic and such

systems exist in their conjugate base form at physiological pH (Scheme 1.40b). Likewise, the presence of the keto group in ring D of the lomaiviticins **1.17** is likely to cause the corresponding *ortho*-quinone methide to exist in its deprotonated form at pH 7 which would make the system unable to function as an electrophile (Scheme 1.40c). Thus, the Skibo mechanism for mode-of-action of prekinamycin is unlikely to be the mode of action of the lomaiviticins which are very potent anticancer agents.

### Scheme 1.40



#### **1.5.4 Advanced studies: Dmitrienko's efforts towards understanding the mechanism of the cytotoxicity of the Kinamycins**

In recent years, our group here at Waterloo has established a collaboration with Dr. Brian Hasinoff in the Faculty of Pharmacy at the University of Manitoba, aimed at more in depth kinamycin MOA studies through various cell culture and enzyme assay techniques.<sup>38,132-134</sup>

The first study,<sup>132</sup> in a effort to determine the mechanism by which the kinamycins exert their cytotoxicity towards cancer cells, revealed that both kinamycins A and C possessed potent cell growth inhibitory growth effects on both Chinese hamster ovary (CHO) and human K562 leukemia cells, with kinamycin A observed to be the more potent of the two. Cell cycle analysis revealed that kinamycin A induced a G<sub>1</sub>/S cell cycle block on CHO cells, but, unusually, after the cells had passed through one full cell cycle and was attributed to using non-synchronized cells. Appropriately, studies using synchronized cells indicated that kinamycin A does not directly act on cell components necessary for exiting G<sub>0</sub>/G<sub>1</sub> or entering S phase. Parallel studies using unsynchronized K562 cells showed no G<sub>1</sub>/S block for both kinamycin A and C although cell cycle comparisons were difficult to assess, either as a consequence of synchronization in CHO cells and/or inherent differences between CHO and K562 cells. Kinamycins A and C also induced apoptosis (programmed cell death) in K562 cells, with the latter exhibiting higher potency. Both kinamycin A and C inhibited the decatenation activity (i.e. nicking and separating strands of DNA) of human topoisomerase II $\alpha$ , but were found not to be poisons of this enzyme, as is etoposide. However, kinamycin A and C inhibition of topo II-catalytic activity did not correlate with cell growth inhibitory effects. Topoisomerase II $\alpha$  is an enzyme intimately involved in DNA replication and transcription in which it alters DNA topology by the catalyzing the passing of intact ds-DNA

through a transient double-stranded fracture made in the other ds-DNA helix. This relieves torsional stress caused by native supercoiled DNA, thus allowing the normal processes of replication to ensue. Etoposide, an in-use clinical anticancer agent, is believed to exert its cytotoxicity by stabilizing the covalent topoisomerase II-DNA adduct. Lastly, both of these drugs were observed not to cross-link DNA nor produce damaging DNA double-stranded breaks. It was speculated that the kinamycins may be targeting sulfhydryl residues of topoisomerase-II $\alpha$  as a mode of their inhibitory action and this is supported by two observations. Firstly, the inhibitory activity of the kinamycins rested upon the fact whether they were pre-incubated with DTT. Pretreatment of kinamycins with DTT protected topoisomerase II $\alpha$  activity. Secondly, topoisomerase-II $\alpha$  has been shown to be sensitive to sulfhydryl-reactive drugs such as cisplatin and quinones. The NCI antitumor SOM cluster analysis database was used to identify potential kinamycin C target(s) and projected a region that has not been assigned a function as of yet. This suggests that kinamycin C exercises its cell growth inhibitory activity on a cellular target unlike other known anticancer compounds.

A follow-up study<sup>133</sup> with kinamycin F showed that this drug weakly bound to calf thymus DNA and induced a small amount of nicking of pBR322 DNA by itself. However, in the presence of GSH, substantial increases of nicked DNA were seen with an increase in time but were attenuated when DMSO, catalase or deferoxamine was added. In K562 cell studies, kinamycin F promoted ss-DNA breaks but chemical reagents that were added to the cell culture media to either increase or decrease GSH levels did not seem to have an effect upon kinamycin F induced DNA strand breaks. However, kinamycin F inhibited the decatenation ability of topoisomerase II $\alpha$  and was more potent than both kinamycins A and C by roughly



an order of magnitude but did not act as a poison similar to kinamycins A and C. Reducing or increasing levels of GSH increased or decreased kinamycin cytotoxicity respectively, an observation contrary to the cell-free study. The  $IC_{50}$  value of 0.33  $\mu$ M over a 72 h window is similar to kinamycins A and C at 0.31 and 0.37  $\mu$ M, respectively and suggests that metabolic deacetylation by intracellular esterases might be obligatory and may play a role in the delayed entry into a  $G_1/S$  block observed with kinamycins A and C.

This study showed that kinamycin F bound to DNA weakly and that DNA damage was greatly enhanced in the presence of GSH and that GSH promoted nicking of DNA occurred in an iron-, hydrogen-peroxide- and hydroxyl radical-dependent manner. Kinamycin F reacted with GSH in a complex manner suggesting that its cytotoxicity may be modulated by GSH. Treatment of K562 cells that either increased or decreased intracellular GSH levels resulted in decreased and increased kinamycin F cytotoxicity, respectively; however, DNA damage in K562 cells as elicited by kinamycin F was independent of GSH levels. EPR spectroscopy revealed the presence of semiquinone and phenoxy free radicals that may go on to produce protein and DNA damaging species. Most recently, kinamycin F was observed to selectively downregulate cyclin D3 in K562 leukemia cells at the transcription level. This is the first indication that the kinamycins may not function simply by damaging DNA but might have a specific biological target associated with the induction of apoptosis.<sup>134</sup>

Lastly, the bioactivity of isoprekinamycin was recently reported in which the growth inhibition of CHO and K562 cell lines was observed and that isoprekinamycin diacetate was also found to inhibit topoisomerase II $\alpha$  catalyzed decatenation.<sup>38</sup>

## 1.6 Concluding remarks

The kinamycins, first reported as *N*-cyanobenzo[*b*]carbazoloquinones but then reassigned as diazobenzo[*b*]fluorenequinones, have been the subject of intensive work with recent studies emerging on the total synthesis and the mechanism of action of these natural products.

The following work described in this thesis is primarily aimed at those aspects that focus on the mechanism of action and particularly the diazo group's role in the bioactivity. This is addressed by the total synthesis of a prekinamycin analogue, an *N*-cyanobenzo[*b*]carbazoloquinone and the subsequent bioactivity studies, presented in Chapter 2. Chapter 3 addresses the notion of the possible protective/scavenging role the kinamycins may play upon exposure of the host bacteria to nitric oxide (NO). Structural elucidation studies together with theoretical work provide a distinction between diazo groups found in the kinamycins to that of simpler diaryl diazo compounds. Chapter 4 reports on the synthetic efforts aimed at improving Diels-Alder cycloadditions of the indole-2,3-quinodimethanes (IQDM) which would permit access to tetrahydrocarbazoles, the BCD ring of potential kinamycin analogues. The corresponding theoretical descriptions of these Diels-Alder reactions of the IQDM are presented in Chapter 5. In Chapter 6, synthetic efforts towards tetrahydrofluorenes are presented which would permit access to the BCD ring system of the kinamycins.

The intent of this work was to provide some insight into the identity of the pharmacophore(s) required for the kinamycins to elicit their bioactivity. As well, it is hoped that future studies of kinamycin analogues synthesized from methods developed and

presented in this thesis, may contribute towards identifying the cellular target(s) necessary for the observed biological activity.

## Chapter 2

# Synthesis of an Isosteric-Isoelectronic Analogue of Prekinamycin and Evaluation of its Bioactivity

### 2.1 Introduction

The previous chapter provided a detailed historical account of the kinamycins in which the structural revisions reported by our group and others established the kinamycins as diazobenzo[*b*]fluorenes. Benzo-annulated fluorenes are structures rarely found in nature<sup>32</sup> and only a small number of reports on their biological activity exist. A recent literature search uncovered 128 references regarding biological studies associated with benzofluorenes, of which 108 references focused on the benzo[*b*]fluorenes (August 2009 Scifinder Scholar). The majority of these reports focused on tobacco, petroleum, soil, foodstuffs, wastewater, waste incinerators and so forth and addressed toxicological, carcinogenic, mutagenic, and ecological/environmental issues. Only a handful of these studies reported on antibacterial and/or anticancer activity and this reflects the paucity of information on this class of compounds as potential therapeutic agents. The kinamycins and lomaivitcins are the only known diazobenzo[*b*]fluorenes with the latter possessing very potent DNA damaging activity and cytotoxicity.<sup>34</sup> The biological evaluation of the kinamycins with a focus on the mechanism and mode of action is an ongoing endeavor in this laboratory.<sup>37,38,132-134</sup>

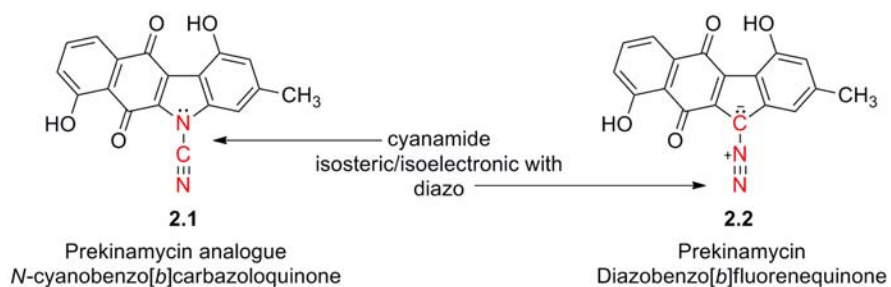
Benzo[*b*]carbazoles represent only a small subset of the carbazole family.<sup>84,87</sup> The carbazoles constitute a large family of alkaloids in which many compounds have demonstrated biological activity.<sup>84-87</sup> To date, very few reports have appeared on the activity of the benzo[*b*]carbazoles, none of which have focused on the cyanamide analogues of the

kinamycins, despite previous synthetic efforts towards these compounds.<sup>60,81,83,93</sup> Historically, owing to the confusion surrounding the kinamycins, the principal interest early on was firmly establishing the structure of the kinamycins and consequently efforts towards structural revision were of paramount interest whereas detailed bioactivity studies appeared to be of lesser significance.

## **2.2 An Isosteric-Isoelectronic Analogue of Prekinamycin**

Most studies have focused on the chemical reactivity of the diazo group in relation to the bioactivity of the kinamycins.<sup>37,38,112,115,124-127</sup> An idea that has not been addressed is the notion that the mode of action (i.e. inhibition) may be a consequence of a complementary fit to a biological receptor rather than the intrinsic chemical reactivity of the diazo moiety. This could conceivably be tested by abrogating the potential chemical reactivity of the diazo group while still keeping the overall size and electronic distribution intact. An isosteric-isoelectronic replacement that would also afford the vinylogous resonance of the lone pair at C-11 with the quinone moiety would be the ideal candidate. All of these attributes are conveniently found within the *N*-cyano functionality as an isosteric-isoelectronic replacement of the diazo group (Figure 2.1) and that bioactivity of the kinamycins may be approached from this yet to-be-addressed perspective.

**Figure 2.1:** **2.1** as an isosteric-isoelectronic analogue of prekinamycin **2.2**.



In light of the many studies that propose a role of the diazo group, parallel studies have yet to appear for the cyanamide analogues of the kinamycins. Replacing the diazo group with a cyanamide would seem obvious and thus would permit insight into the diazo group's role, if any, in the biological activity of the kinamycins. Thus, the primary motivation for the synthesis of **2.1** was to initiate biological studies not only to assess the importance of the diazo group, but also to evaluate benzo[*b*]carbazoloquinones in general which may be helpful in identifying the pharmacophore(s) responsible for the biological properties of the kinamycins and lomaiviticins. Ultimately, this novel information might facilitate drug design towards potential therapeutic agents.

## 2.3 Synthesis

### 2.3.1 Introduction

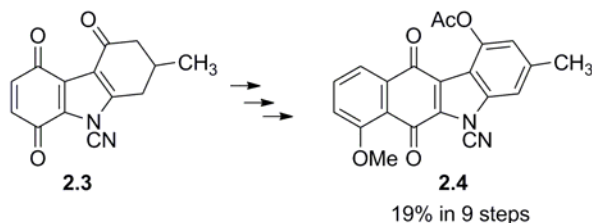
Benzo-annulated carbazole ring systems are found very rarely in nature.<sup>84,87</sup> Benzo[*b*]carbazoles and their quinoid counterparts have been synthesized by several groups: Grinev,<sup>135</sup> Kametani,<sup>136</sup> Thomson,<sup>137</sup> Snieckus,<sup>138</sup> Kano,<sup>139</sup> Gribble,<sup>140-145</sup> Moody,<sup>146,147</sup> Liebeskind,<sup>148</sup> Sha,<sup>149</sup> Ley,<sup>150</sup> Kreher and Dyker,<sup>151</sup> Bergman,<sup>152</sup> Pindur,<sup>153-155</sup> Bittner,<sup>156</sup> Suginome,<sup>76,157</sup> Hoornaert,<sup>158</sup> Murphy,<sup>78</sup> Molina,<sup>159</sup> Brown,<sup>160</sup> Echavarren,<sup>60,93</sup> Castedo,<sup>80</sup>

Srinivasan,<sup>82</sup> Vollhardt,<sup>161</sup> Knölker,<sup>81,83</sup> Dmitrienko,<sup>31</sup> Kucklander,<sup>162,163</sup> Koomen,<sup>164</sup> Åkermark,<sup>165,166</sup> Markgraf,<sup>167</sup> Cheng,<sup>168</sup> Kirsch,<sup>169</sup> Shi and Wang,<sup>170</sup> Kobayashi,<sup>171</sup> Black,<sup>172</sup> Schmittel,<sup>173</sup> Estevez,<sup>174-179</sup> Miki,<sup>180</sup> Mal,<sup>181,182</sup> Bowman,<sup>183</sup> Mohammed,<sup>184</sup> Xu<sup>185</sup> and Fagnou<sup>186</sup> and have been reviewed elsewhere.<sup>84-88</sup> Only four of these studies have reported bioactivity data<sup>162-164,168</sup> with molecular modeling studies<sup>155,187,188</sup> also described. Reports of biological studies on **2.1** or its derivatives have yet to appear in the literature.

Previous synthetic efforts from this laboratory towards the *N*-cyanobenzo[*b*]carbazoloquinones were described in Chapter 1 (Sections 1.2.4 and 1.4.1).<sup>31,59,75</sup> The methods developed in this laboratory towards the synthesis of indoloquinones were subsequently employed in Diels-Alder reactions. Using this strategy, a total synthesis of **2.4** was accomplished by S. Mithani in nine steps with an overall yield of 19% (Scheme 2.1).<sup>31</sup> Although this synthesis adequately provided material that was vital in that structural elucidation study, future synthetic efforts towards this natural product analogue would require a revision of the synthesis. When this project began, the only reports pertaining to the synthesis of benzo[*b*]carbazoloquinones were studies in which the syntheses were plagued by low yields, nitrogen substituent issues and targets that lacked the appropriate A and D ring substitution pattern owing to either simplified or symmetrical precursors used in the early stages of the synthesis. Potentially any biological data obtained from these compounds would be better understood in light of parallel data provided by **2.1**. There are only two studies that have reported the synthesis of **2.1**;<sup>60,93</sup> however, the earlier study by Echavarren provided incorrect assignments for the proposed structure of **2.1** that subsequently were corrected in their later report as discussed in Section 1.4.1. A drawback of

the studies by the Echavarren group is that they suffered from regioselectivity issues during cyclization.

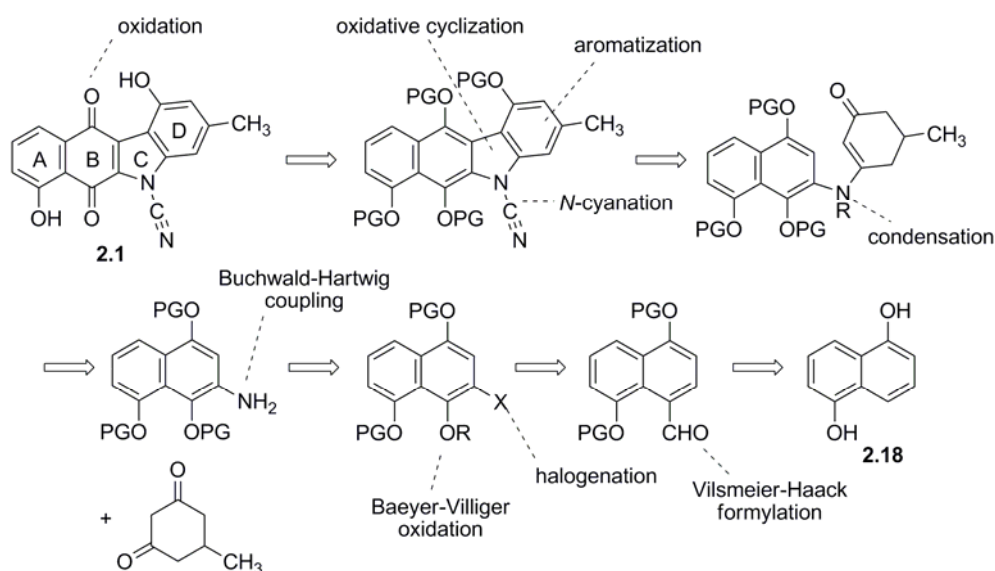
**Scheme 2.1:** Mithani's target *N*-cyanobenzo[*b*]carbazoloquinone **2.4** obtained from **2.3**.



With respect to Mithani's carbazole synthesis of **2.4**, two issues of concern were to be addressed. First, was to shorten the lengthy linear sequence and secondly to avoid stoichiometric amounts of metals used (i.e. palladium) in the oxidative ring closure, with the hopes of implementing a catalytic step at this point. Retrosynthetic considerations indicate that **2.1** could be generated from a functionalized naphthylamine which in turn comes from readily available 1,5-dihydroxynaphthalene **2.18** (Scheme 2.2). The key disconnections suggest that an oxidative cyclization, a condensation, a Buchwald-Hartwig cross-coupling and acylation with appropriate functional group transformations might be appropriate to obtain the target. In Scheme 2.2, the cyanamide moiety is introduced in the later stages of the synthesis. However, introduction of the cyanamide at an earlier stage might expedite the synthesis and appropriate exploratory efforts towards the cross-coupling of cyanamide to aryl electrophiles were pursued and are discussed in the following section.



## Scheme 2.2: Retrosynthetic analyses of 2.1.



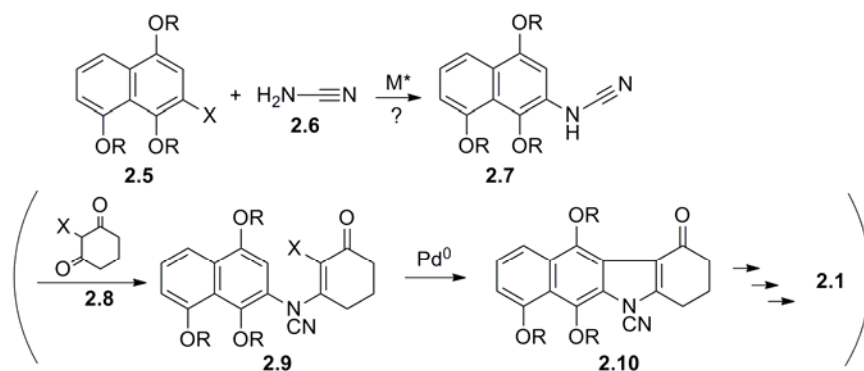
### 2.3.2 Attempts towards Buchwald-Hartwig couplings of cyanamide to aryl halides

Reports employing carbon-carbon and carbon-heteroatom bond forming methods have undergone a surge in recent years owing to the many advances in transition metal-mediated cross-coupling reactions.<sup>189-193</sup> It was envisioned that cyanamide might be coupled to an aryl halide directly providing expedient access to the desired functionality thus abrogating the necessary steps of coupling with an ammonia surrogate, hydrogenolysis and *N*-cyanation (Scheme 2.3). Discussion of this chemistry with Professor Buchwald revealed that the Buchwald group had never attempted such a coupling of an aryl halide with a cyanamide. This represented several obstacles, of which one was a lack of a literature precedent for coupling cyanamide as carbon-nitrogen bond forming methods are generally restricted to amines and amides. The ortho substitution pattern represented another challenge inherent to the synthesis, with some literature accounts reporting sensitivity to ortho substituents.<sup>194</sup>

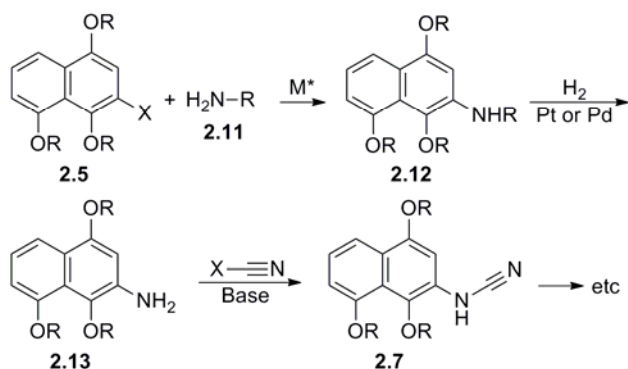
Lastly, the use of relatively inexpensive copper catalysts compared to palladium catalysts was also a consideration and consequently studies using simple model systems were initiated employing copper reagents.

**Scheme 2.3:** Potential synthetic routes to access **2.7** via Buchwald-Hartwig couplings.

a) Proposed Buchwald-Hartwig coupling of cyanamide:



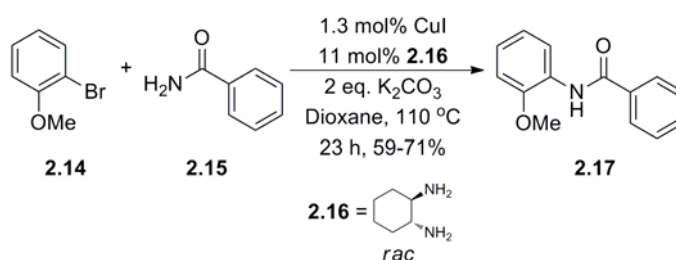
b) Conventional Buchwald-Hartwig coupling, hydrogenolysis and *N*-cyanation:



\* where M= Ni, Pd, Cu, etc

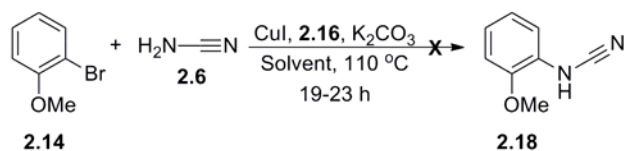
2-Bromoanisole (**2.14**) represents an appropriate model for the naphthyl halide **2.5** shown in Scheme 2.3. The Buchwald group reported the coupling of 2-bromoanisole with benzamide in 84% yield.<sup>195</sup> This experiment was repeated under the same conditions, and a 59-71% isolated yield was obtained (Scheme 2.4). A small increase in the yield was observed when using copper iodide that had been purified.<sup>196</sup>

**Scheme 2.4:** Buchwald-Hartwig coupling of *o*-bromoanisole and benzamide.



Encouraged by this result, those conditions were then extrapolated to the coupling of cyanamide in which some of the experimental parameters were varied (Table 2.1). The spectroscopic assignments of **2.18** were established by an independent synthesis employing *o*-anisidine and cyanogen bromide. In all cases, inspection of the <sup>1</sup>H NMR spectrum of the crude material revealed no trace of **2.18**. and in some of these cases, a complex mixture resulted (entries 3, 5-7). In the end, it was found that these conditions were of little synthetic value. To this date, studies on metal catalyzed cross-coupling reactions employing cyanamide remains an unexplored area.<sup>197</sup> The failure of the cyanamide couplings meant that the more conventional approach to the synthesis of the AB synthon would be required using an ammonia equivalent as shown in Scheme 2.3b.

**Table 2.1:** Attempted Buchwald-Hartwig couplings of cyanamide with *o*-bromoanisole.



Entry	CuI (eq.)	Ligand (eq.)	$\text{K}_2\text{CO}_3$ (eq.)	Solvent	Additives	Results
1	0.01	0.11	2.1	Dioxane	nil	a
2	0.01	0.11	2.1	Dioxane	nil	a
3	0.1	1.1	2.1	Dioxane	nil	b
4	0.1	1.1	2.0	Dioxane	0.2 KI	a
5	0.1	1.1	2.0	Toluene	0.2 KI	b
6	0.5	5.5	2.1	Dioxane	nil	b
7	0.1	1.1	5.1	Toluene	nil	b

a. starting materials recovered.

b. complex mixture.

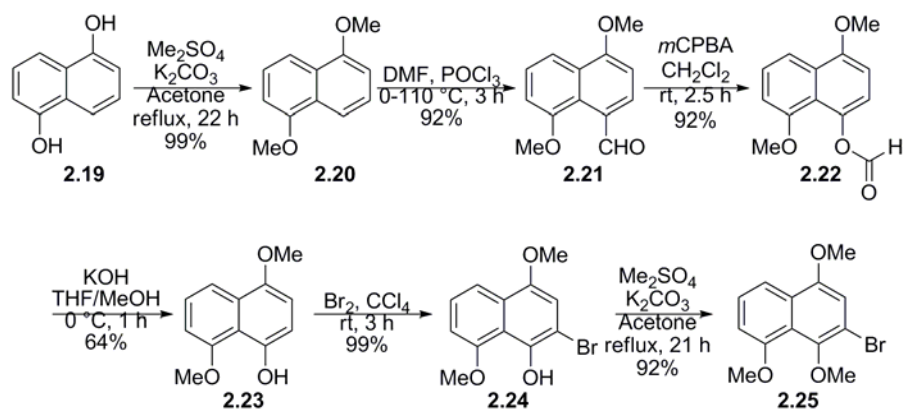
### 2.3.3 Synthesis of the *N*-cyanobenzo[*b*]carbazoloquinone analogue of Prekinamycin

The synthesis of **2.1** relies on the condensation of an AB ring synthon with 5-methylcyclohexane-1,3-dione as the D ring, and subsequent carbon-carbon bond formation between the B and D rings producing the C ring pyrrole, thereby furnishing the tetracycle (Scheme 2.2).

Efforts towards the synthesis of **2.1** began with **2.19** which was *O*-methylated affording **2.20** in nearly quantitative yield (Scheme 2.5).<sup>198,199</sup> Using procedures reported by Rapoport,<sup>200</sup> installation of the C-1 hydroxyl was accomplished under Vilsmeier-Haack conditions producing aldehyde **2.21** and a subsequent Baeyer-Villiger oxidation to afford the formate **2.22** which, after methanolysis, yielded naphthol **2.23** in 54% yield over three steps. The formate **2.22** obtained from the Baeyer-Villiger oxidation invariably contained a

persistent impurity even after extensive washing and chromatography and was thought to be *m*-chlorobenzoic acid. Alternative procedures using potassium fluoride<sup>201</sup> showed modest increases in purity of the crude product after aqueous workup but gave a lower yield of 83%. Another procedure in which dichloromethane was replaced by ethyl acetate<sup>202</sup> did not resolve any of these issues, producing a yield of 59%. A small portion that had been extensively washed was loaded onto a column of silica which afforded a few fractions that were of sufficient purity to permit full characterization. Regioselective bromination of **2.23** produced **2.24** and subsequently *O*-methylated to afford the trimethoxy-bromonaphthalene **2.25** in 49% yield over six steps and provided the key intermediate for the impending Buchwald-Hartwig cross-coupling.

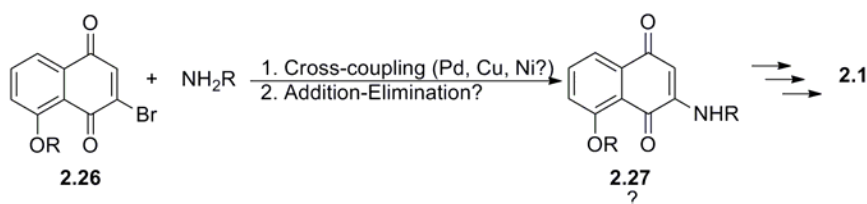
**Scheme 2.5:** Synthesis of **2.25**.



Although this route provided sufficient amount of the requisite material, a shorter route to **2.25** or analogue thereof was recognized. Reports on the rapid and easy access to halogenated naphthoquinones<sup>200,203-207</sup> are known as are reports of Stille,<sup>60,77,93,208</sup> Suzuki-Miyaura,<sup>209,210</sup> and Castro-Stephens/Sonogashira<sup>211,212</sup> cross-couplings using bromo-naphthoquinones that

potentially could be translated into Buchwald-Hartwig couplings, thus significantly reducing the overall number of steps to access the quinoid analogue of **2.25**, making this an attractive route. To this end, exploratory efforts in this lab were pursued by an undergraduate student T. Rybak to test the feasibility of Buchwald-Hartwig couplings of bromo-naphthoquinones as well as other strategies (Scheme 2.6).

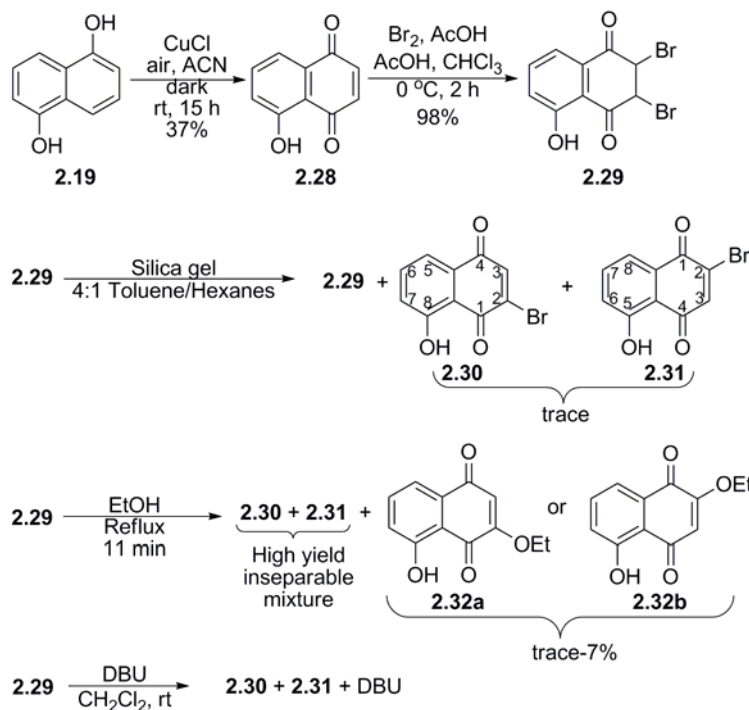
**Scheme 2.6:** Possible synthetic routes for the amination of bromo-naphthoquinones.



Juglone (**2.28**)<sup>213</sup> was obtained in 37% yield from **2.19** (Scheme 2.7) which was then brominated to afford dibromo-dihydrojuglone **2.29**<sup>214</sup> which was stable and did not aromatize to the hydroquinone. Efforts towards regioselective dehydrodehalogenation of **2.29** included exposure to silica gel<sup>214</sup> and refluxing in ethanol,<sup>203,207,215</sup> as described in the literature and DBU-induced elimination. Exposure of **2.29** to silica gel chromatography returned mostly starting material with small amounts **2.30** and **2.31**. Alternatively, conditions of refluxing ethanol provided a quantitative yield of the two regioisomers **2.30** and **2.31** as an inseparable mixture even after repeated attempts at chromatography, as well as a small quantity of the ethoxy-juglone **2.32**, isolated in 7% yield in a separate experiment under identical conditions. Others have also reported the generation of **2.30** and **2.31** obtained from refluxing **2.29** in ethanol.<sup>200</sup> Efforts at fractional crystallization<sup>207</sup> also proved futile. Attempts at dehydrohalogenation using DBU produced a complex mixture in which large amounts of DBU were observed even after extensive washings with a saturated solution of ammonium

chloride. Efforts towards **2.30** will be pursued as a future endeavor as it is an important intermediate that has potential use within the synthetic program for the kinamycins in this laboratory.

**Scheme 2.7:** Production of **2.29** and attempts of its regioselective dehydrohalogenation.

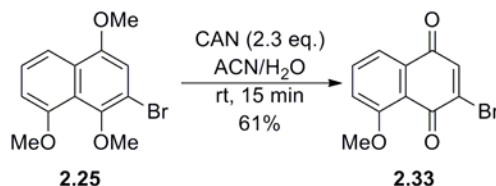


Assignment of the two regioisomers, 3-bromojuglone (**2.30**) and 2-bromojuglone (**2.31**), was based on previous work in other laboratories. The synthesis of the acetate of **2.30** (m.p. 148 °C) was accomplished by Wheeler and Scott<sup>216</sup> (initially mistaken to be acetate of **2.31**). The unambiguous synthesis of the acetate of **2.31** (m.p. 158 °C) by chromic acid oxidation of 2,4-dibromo-5-acetoxy-1-naphthol was accomplished by Carter *et al.* In the present study, examination of a pure mixture of **2.30** and **2.31** did not indicate which regioisomer was produced in excess. However, Brimble *et al.*<sup>214</sup> and Tietze *et al.*<sup>215</sup> have both indicated that

**2.30** is produced in excess of **2.31** when conditions of refluxing ethanol were employed. Thus, the observations of both Brimble and Tietze were used in the present study to facilitate assigning the signals in the  $^1\text{H}$  NMR and  $^{13}\text{C}$  NMR spectra of a pure mixture of the regioisomers to the respective compound.

During this investigation, it was also observed that the  $^{13}\text{C}$  NMR assignments reported for C-2 (142.40 ppm) of **2.30** by Brimble<sup>214</sup> did not match ours and initially, albeit erroneously, we had assigned this resonance to C-2 of **2.31** (assigned as 140.90 ppm by Brimble). Further structural elucidation studies of a pure mixture of the two regioisomers was accomplished by comparison to reports made by others (vide supra) in conjunction with extensive NMR studies including JMOD, COSY, HMQC and HMBC NMR experiments which permitted the assignment of C-2 of **2.30** to 139.26 ppm, corresponding to Tobinaga's assignment at 139.29 ppm.<sup>207</sup> Despite the unsuccessful attempts of producing **2.30** in adequate amounts, access to material readily available in this laboratory by other methods provided **2.33** (Scheme 2.8) and subsequently permitted exploratory efforts into different amination strategies. The oxidation of **2.25** using ceric ammonium nitrate (CAN) furnished **2.33** in 61% yield as shown in Scheme 2.8.

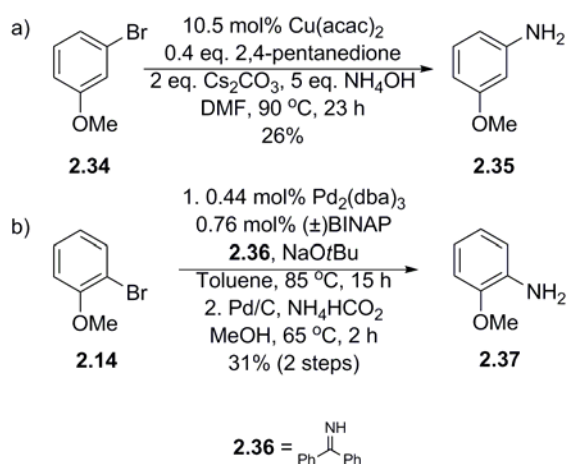
**Scheme 2.8:** CAN oxidation of **2.25**.





Reports on the direct coupling of ammonia to aryl halides<sup>217-221</sup> have appeared in recent years and in particular the study by Xia and Taillefer<sup>220</sup> was compelling owing to the readily available and inexpensive catalyst system used in that report. That system performed well for either electron rich or electron poor aryl iodides and bromides, but the observation that electron poor aryl bromide systems worked well provided the motivation to pursue this strategy with the bromo-naphthoquinone system **2.33**. Those authors reported an 85% yield of *m*-methoxyaniline **2.35** from *m*-bromoanisole **2.34**. In our hands, we obtained a 26% yield (Scheme 2.9a) but felt that the low yield may be offset by the fewer number of steps taken in the synthesis of aminonaphthoquinones **2.27**. As well, traditional palladium cross-couplings using ammonia surrogates would also be explored. Under conditions reported by Buchwald using benzophenone imine as the ammonia equivalent,<sup>222</sup> a 31% isolated yield (two steps) of **2.37** was obtained (Scheme 2.9b) where those authors reported an 87% isolated yield. Having achieved modest yields using these couplings on model systems, attention was then turned to 8-methoxy-2-bromojuglone **2.33** (Scheme 2.10) with the hopes of using the chemistry outlined in Scheme 2.9, towards the synthesis of **2.1**.

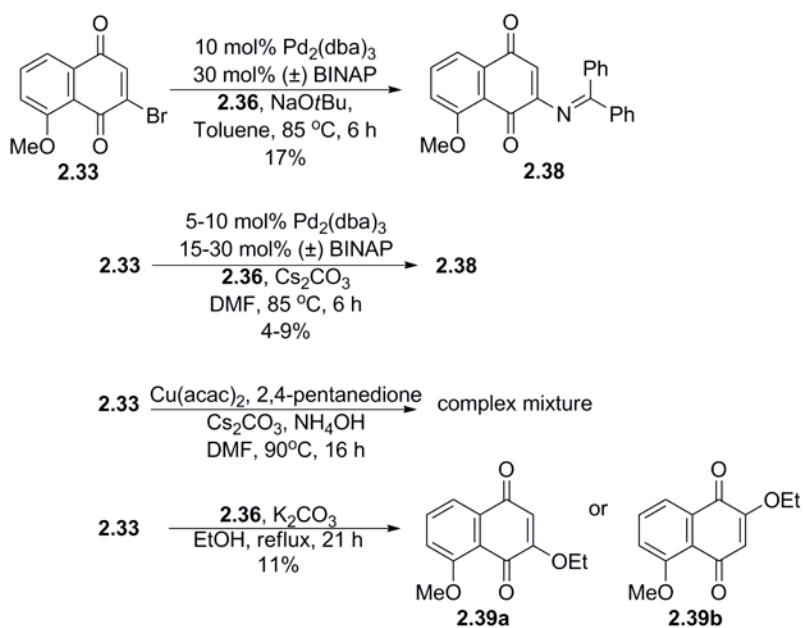
**Scheme 2.9:** Copper and palladium catalyzed cross-couplings of bromoanisoles.



Initial studies under conventional Buchwald-Hartwig conditions (0.68% Pd<sub>2</sub>(dba)<sub>3</sub>, 1.87% BINAP, 1.3 eq. NaOtBu, toluene, 85 °C) provided a small amount of product as observed in the <sup>1</sup>H NMR spectrum of the crude residue. Increasing the loadings of the catalyst and ligand to 10 mol% and 30 mol%, respectively, afforded **2.38** in 17% isolated yield (Scheme 2.10). Under modified conditions, changing the base to cesium carbonate and the solvent to DMF, the isolated yield dropped to 9%. For this system employing cesium carbonate and DMF, the isolated yields doubled from 4% to 9% when the catalyst (2.7 mol% to 5 mol%) and ligand (15 mol% to 30 mol%) loadings were doubled. Disappointingly, the copper system produced a complex mixture. With the desired target produced in low yields, these cross-coupling conditions were of little synthetic value, thus our focus turned to other strategies. Recognizing that **2.33** is amenable to addition-elimination conditions<sup>223-227</sup> attempts using **2.36** failed to provide **2.38**, instead isolating the vinyl ether **2.39** in 11% yield, analogous to the earlier result that gave **2.32**. Despite these low yields, we were able to demonstrate that

these cross-couplings using these substrates are indeed feasible. To the best of our knowledge, there are no reports on couplings of imines with halogenated naphthoquinones and thus this is the first demonstration of a Buchwald-Hartwig cross-coupling employing these types of systems.

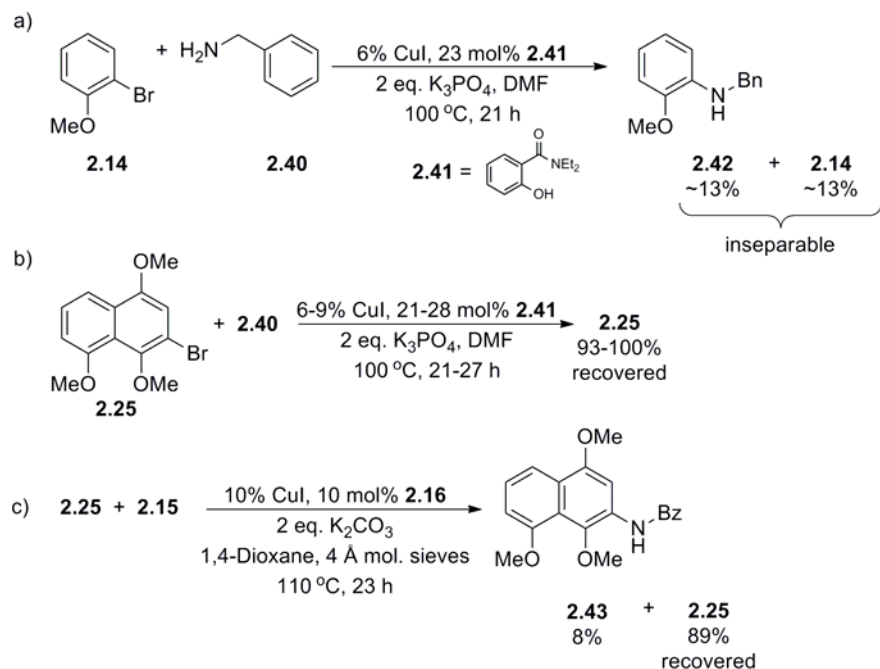
**Scheme 2.10:** Various amination attempts towards the synthesis of **2.38**.



Based on the realization that **2.33** is a poor substrate under various cross-coupling conditions, it was decided that further attempts at installing the amino group would be explored using the aromatic system **2.25** with copper reagents. Kwong and Buchwald have reported the coupling of primary amines to aryl bromides in high yields using copper iodide and *N,N*-diethylsalicylamide **2.41** as the ligand.<sup>228</sup> In this study low yields and recovery of starting material were observed (Scheme 2.11). Unsure of whether the catalyst-ligand combination or the substrate was the cause of the low yields, the experiment was repeated as shown in Scheme 2.4 replacing **2.14** with **2.25**. A yield of 8% of **2.43** (Scheme 2.11c)

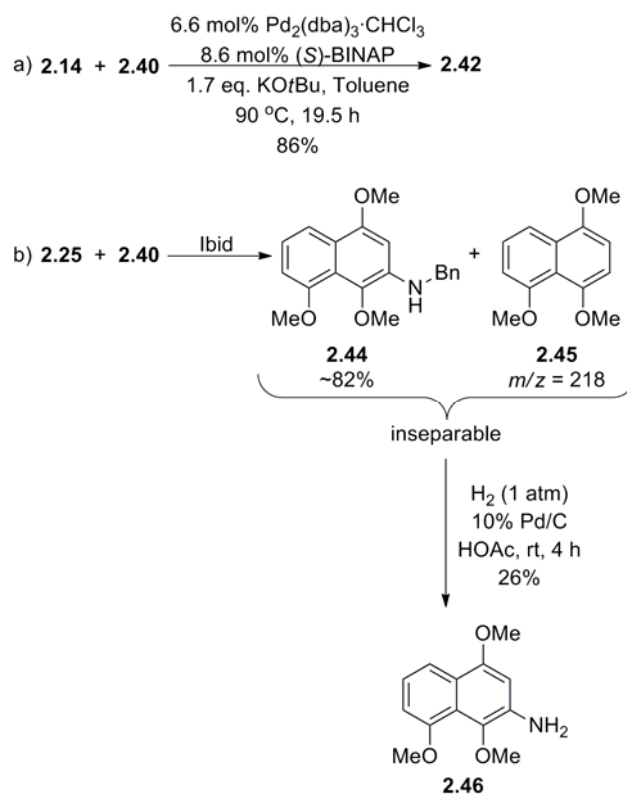
suggested that the substrate **2.25** was intrinsically unsuitable with these copper reagents for reasons unknown and this approach was abandoned in favor of the use of palladium reagents.

**Scheme 2.11:** Attempted copper catalyzed cross-couplings of aryl bromides **2.14** and **2.25**.



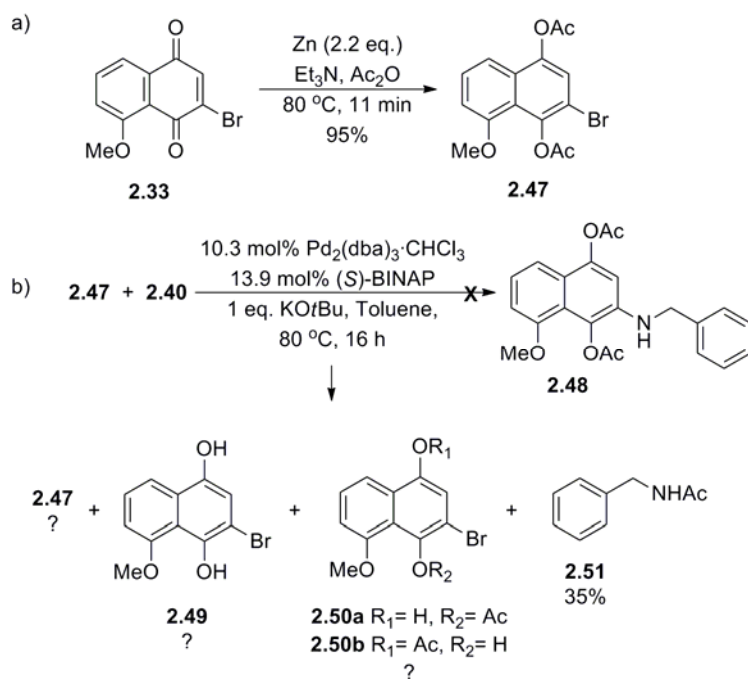
The palladium catalyzed coupling produced a yield of 86% with the model system **2.14** (Scheme 2.12a) but when **2.25** was employed under similar conditions, small amounts of the reduced arene **2.45**, identified by GC-MS analysis ( $m/z = 218, M^+$ ), was observed along with the desired coupled product **2.44** as an inseparable mixture even after repeated chromatography (Scheme 2.12b). Hydrogenolysis of this mixture provided **2.46** in 26% yield.

**Scheme 2.12:** Palladium catalyzed cross-couplings of aryl bromides.



Other phenol protection strategies were investigated with the hopes of resolving the reduced arene from the coupled product and to increase the yield of **2.46**. A one pot reduction-acetylation<sup>92</sup> of **2.33** gave **2.47** in 95% yield (Scheme 2.13a). The cross-coupling of **2.47** under similar conditions as described in Scheme 2.12a, failed to provide the desired target **2.48** (Scheme 2.13b). Analysis of the <sup>1</sup>H NMR spectrum of a chromatographic fraction revealed it to be a mixture of what was thought to be **2.50** as the major component with a small amounts of **2.47** and **2.49** as well as **2.51** obtained in a separate fraction indicating deacetylation had occurred. The results of these studies hastened efforts towards other routes that would provide **2.46** in an efficient manner.

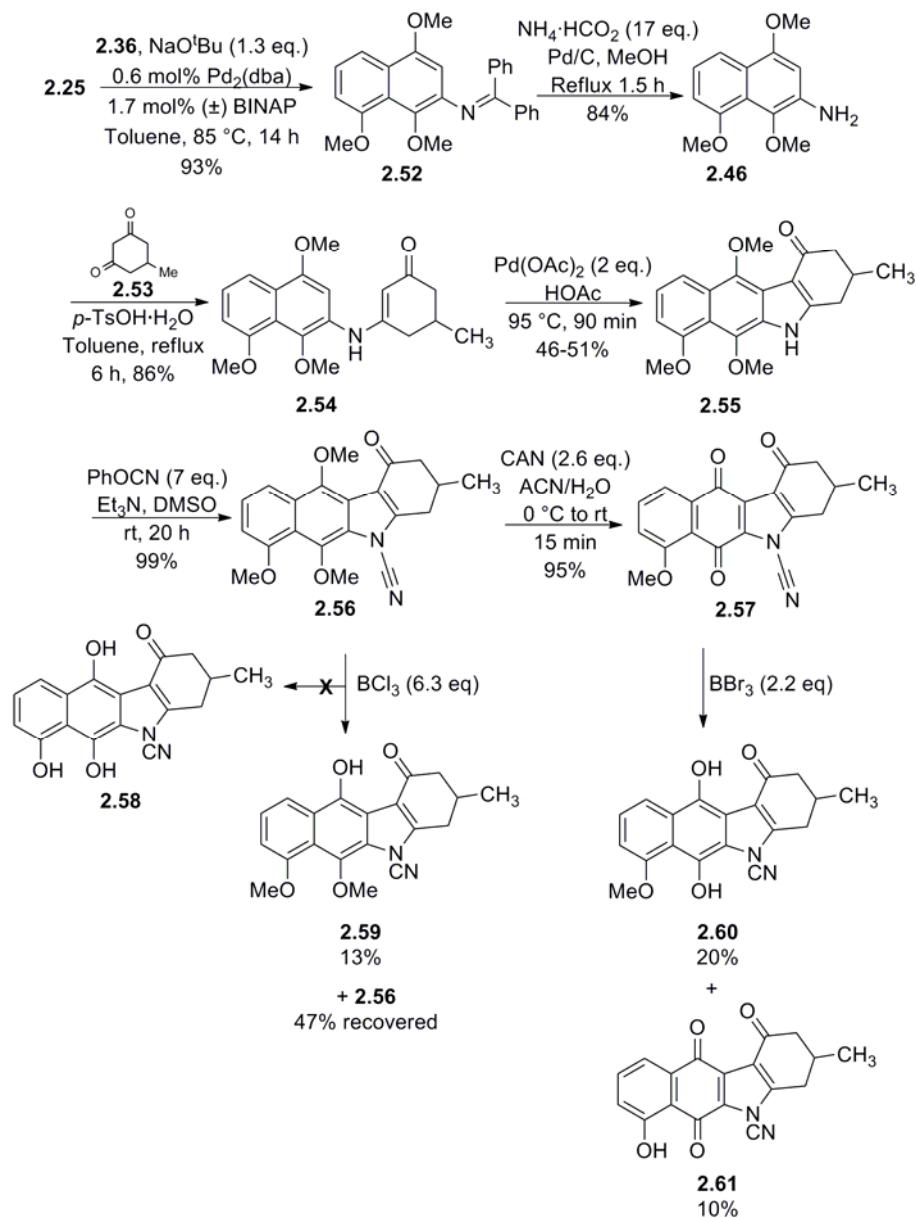
**Scheme 2.13:** Synthesis of **2.47** and subsequent use in Buchwald-Hartwig couplings.



The strategy of using benzophenone imine (**2.36**) as the ammonia surrogate was revisited as shown in Scheme 2.14. Coupling of **2.25** with **2.36** proceeded uneventfully producing **2.52** which, after hydrogenolysis, gave the requisite naphthylamine **2.46** in a gratifying 78% yield over two steps. Condensation of **2.46** with **2.53** afforded anilinoketone **2.54** and subsequent oxidative ring closure<sup>84,229</sup> produced the tetracycle, the benzo[*b*]tetrahydrocarbazole **2.55**. Annulation typically gave yields of 27-36%. Several attempts were made to increase the yields by varying the time, temperature and the amount of oxidant. Substituting trifluoroacetic acid (TFA)<sup>229</sup> for acetic acid resulted in recovered starting material. In the end it was found that two equivalents of palladium acetate provided the best yields at 46-51%. *N*-

Cyanation using phenyl cyanate<sup>230</sup> proceeded smoothly to give **2.56** and subsequent oxidation to the quinone **2.57** occurred in 95% yield.

**Scheme 2.14: Synthesis of 2.57.**

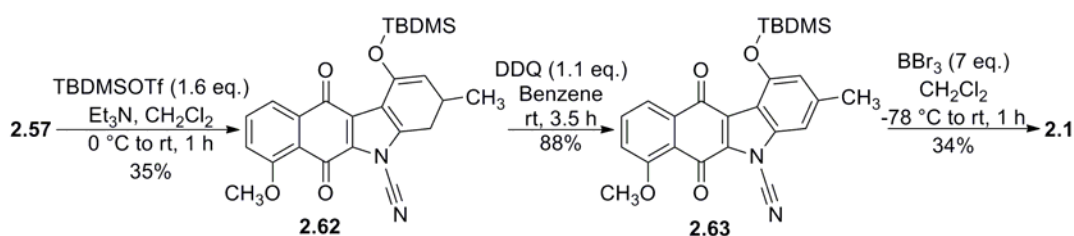


Access to **2.58** and **2.61** (obtained from **2.56** and **2.57**, respectively) was desired as there was interest in the implications that the cyclohexenone moiety (D-ring) may have on the bioactivity in comparison to that of the target **2.1** and the natural product **2.2**. Attempts at global deprotection of **2.56** using  $\text{BCl}_3$  resulted in recovery of starting material (47%) as well as a mono-deprotected species, presumably **2.59** (13% yield) owing to the possible directing effect afforded by the D-ring carbonyl. Owing to this fact, it was felt that the 1,4-quinone moiety of **2.57** should facilitate deprotection and since the plan was to obtain **2.57** in any event, various demethylation conditions were attempted on **2.57**. The use of five equivalents of  $\text{BBr}_3$  led to a complex mixture, but when the Lewis acid was scaled back to two equivalents, **2.60** and **2.61** were observed, although in low yields. The appearance of **2.60** led us to believe a disproportionation reaction was occurring in which **2.57**, acting as a hydride source, furnished the hydroquinone **2.60**. Alternative strategies using  $\text{BBr}_3$  with DDQ,  $\text{BCl}_3$  and pyridinium·HCl gave complex mixtures.

The remaining steps of silylation, aromatization and deprotection are shown in Scheme 2.15. Enolization of the keto-D-ring was achieved by silylation of **2.57** to give the silyl enol ether **2.62** and subsequent aromatization with DDQ afforded **2.63**. Global deprotection with  $\text{BBr}_3$  furnished the target compound **2.1** in a 35% yield with an overall yield of 1.6% over fifteen steps.



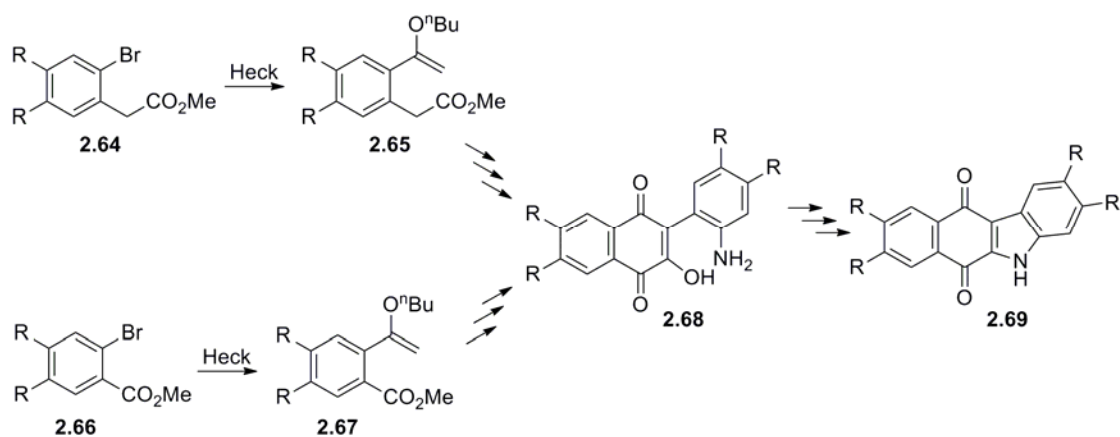
**Scheme 2.15:** The remaining steps of the synthesis towards **2.1**.



## 2.4 Other reported syntheses of Benzo[*b*]carbazoloquinones

During the time in which the synthesis of **2.1** was undertaken, a number of reports illustrating different approaches towards benzo[*b*]carbazoloquinones (also known as indolonaphthoquinones) have appeared. Most notably are the recent efforts by Estevez and coworkers.<sup>178,179</sup> Their early strategy relied on a Heck coupling of *n*-butyl vinyl ether with either *o*-bromophenylacetic acid **2.64**<sup>174,176</sup> or *o*-bromobenzoic acid **2.66**<sup>175</sup> that displayed novel regioselectivity under either modified (TIOAc added) or classical Heck conditions, affording the  $\alpha$ -arylation product **2.65** and **2.67**, respectively (Scheme 2.16). They attributed the high  $\alpha$ -regioselectivity to the chelating effect of the carboxymethyl group<sup>231</sup> which differs from the mechanism proposed by Cabri.<sup>232</sup> The goal of these early efforts was accessing the 3-hydroxy-2-aminophenyl-1,4-naphthoquinones **2.68**, the requisite synthetic intermediate also used by others<sup>60,80,93</sup> in the construction of benzo[*b*]carbazoloquinones. Depending on experimental conditions access to the benzo[*a*]carbazoles was also possible, providing a divergent synthetic strategy.<sup>177</sup> Admittedly, Estevez has acknowledged experimental difficulties owing to the early preparation of naphthoquinone subunit,<sup>177</sup> and may be due to purification issues, a problem also encountered in this laboratory (vide supra).

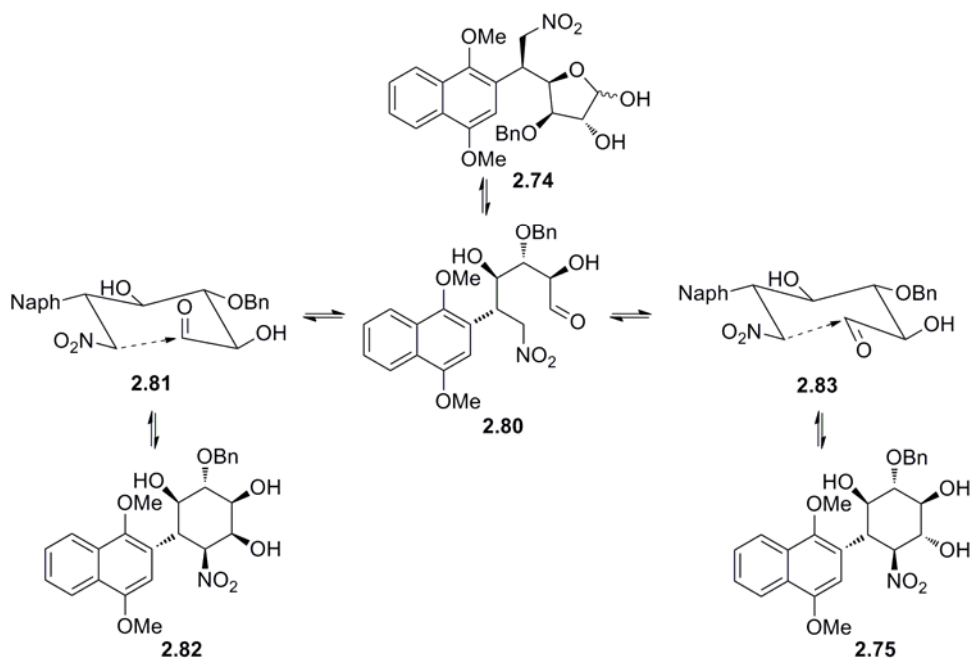
**Scheme 2.16:** Estevez's efforts towards the synthesis of **2.69** using Heck chemistry.



Recognizing the lack of available methods for preparing functionalized tetrahydrocarbazoles, Estevez employed a Michael addition of naphthalene **2.70** to nitrosugar **2.71** followed by an intramolecular Henry reaction of **2.74** providing **2.75** as the key step towards the synthesis of **2.79** (Scheme 2.17). The conjugate addition of the lithionaphthalene derived from **2.70** to both faces of the nitroethylene moiety of **2.71** produced a mixture of epimers **2.72** and **2.73** in a 4.7:1 ratio in which stereoselectivity was due to preferential attack at the *si* face of the double bond and was confirmed by X-ray studies. Removal of the acetonide protecting group produced the furanose **2.74**, which under basic conditions (i.e. Henry reaction), cyclized to **2.75** in 95% yield.



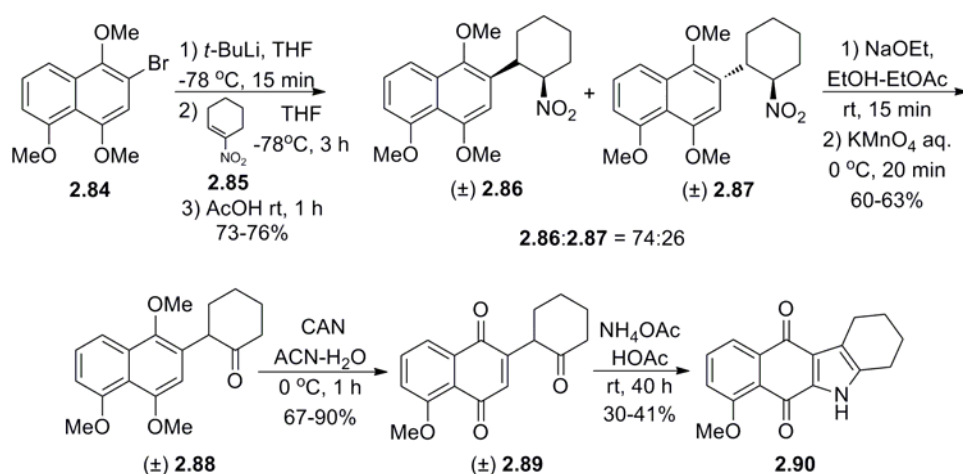
**Scheme 2.18:** Diastereoselectivity of the Henry reaction producing **2.75**.



A subsequent study by Estevez using nitrocyclohexene **2.85** illustrates another method by which 1,2,3,4-tetrahydro-5*H*-benzo[*b*]carbazole-6,11-dione **2.90** could be accessed (Scheme 2.19). The diastereomeric pair **2.86** and **2.87** was subjected to Nef reaction conditions producing **2.88** which was oxidized to the quinone **2.89** and treated with ammonium acetate in glacial acetic acid to give the heteroannulated target **2.90**.

These methods by Estevez illustrate two different approaches at introducing a cyclohexene D-ring providing tetrahydrobenzo[*b*]carbazoles which, in the former case, can be highly functionalized. The interest of these authors in producing compounds such as **2.79** and **2.90** is ultimately to access the corresponding *N*-cyano derivatives for the purpose of biological and chemical studies of which reports on their future endeavors are highly anticipated by this laboratory.

**Scheme 2.19:** Estevez's synthesis of the benzo[*b*]tetrahydrocarbazoloquinone **2.90**.



## 2.5 Bioactivity

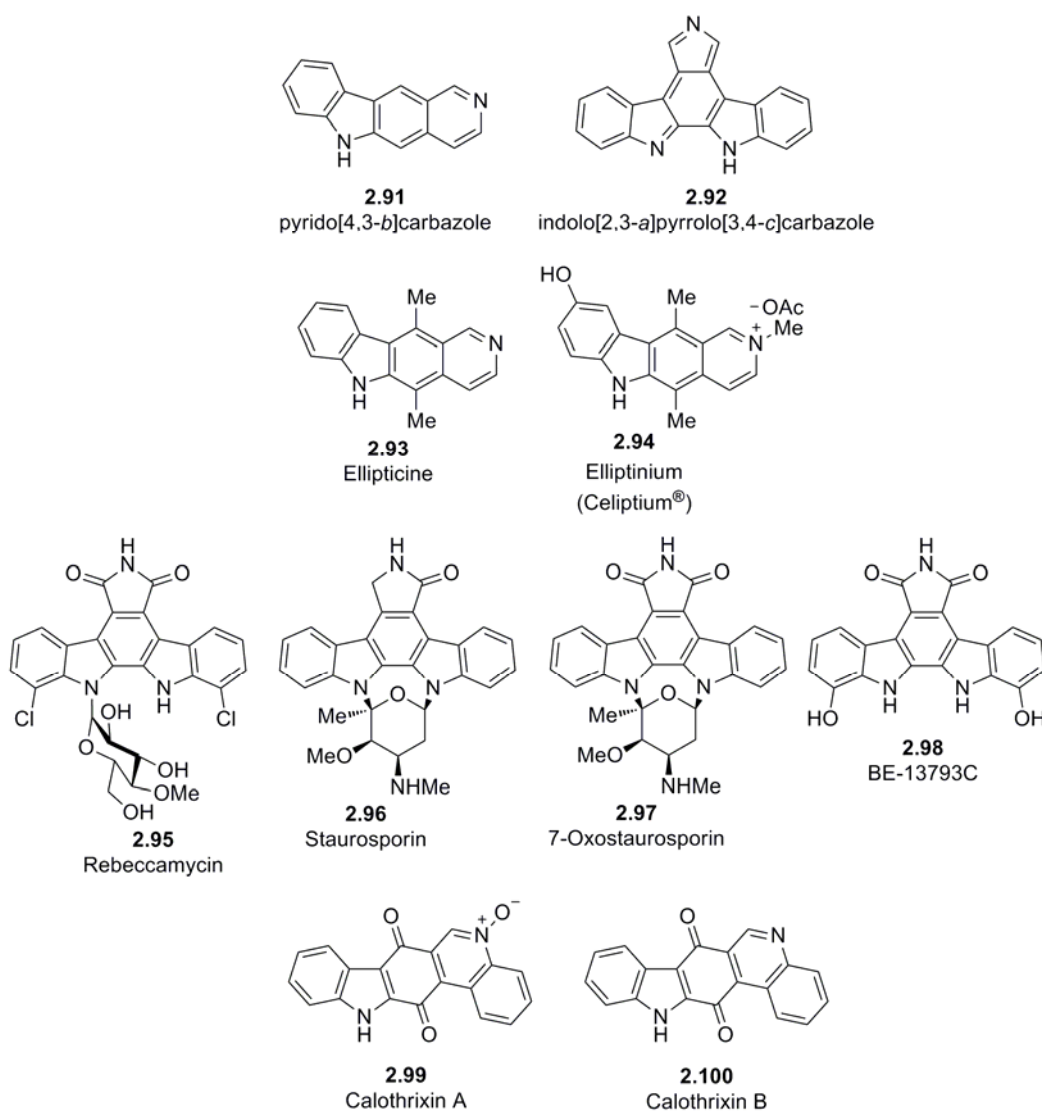
### 2.5.1 Introduction and Background

The occurrence, isolation and structure elucidation of natural carbazoles has created great interest as potential therapeutic agents owing to their vast display of pharmacological activity which in some cases, has been observed to be extremely high.<sup>87</sup> This in turn has provided the motivation to synthesize various analogues of these natural products with the goal of attaining more desirable biological properties than the parent compound. Many of the carbazoles isolated from Nature range from the simpler tricycles to more elaborate systems in which there is extensive structural variation around the carbazole nucleus. The large body of reports focused on the activity of carbazoles precludes the presentation of a comprehensive overview here; however, there is some merit in discussing a select few representative members of the carbazole family and comparing structure-activity relationships (SAR) to the target **2.1**.

## 2.5.2 Bioactivity of Pyrido[4,3-*b*]carbazoles and Indolo[2,3-*a*]pyrrolo[3,4-*c*]carbazoles

Of the carbazoles, members of the pyrido[4,3-*b*]carbazole **2.91** and indolo[2,3-*a*]pyrrolo[3,4-*c*]carbazole **2.92** families encompass a large group of therapeutically useful antitumour agents and are either currently employed in the clinical environment or are in various stages of clinical development (Figure 2.2).<sup>87</sup>

**Figure 2.2:** Clinically relevant bioactive carbazoles.



A representative member of the family **2.91**, ellipticine **2.93** is one of the most well known carbazoles.<sup>233</sup> Displaying potent cytotoxicity against a number of tumours and leukemias, ellipticine is too toxic to be of therapeutic use. However elliptinium **2.94** (celiptium<sup>®</sup>, NSC 264-137) an ellipticine analogue, has been used in cancer chemotherapy since its introduction in 1977.<sup>234-238</sup> In the 1980's, second generation ellipticine-derived anti-tumour reagents were developed, some of which demonstrate better activity than **2.94**.<sup>239,240</sup> The mechanism of action of ellipticine and its derivatives is not well understood, but it is believed that more than one mechanism is operative in vivo.<sup>241</sup> Ellipticine as well as its derivatives, intercalate DNA with cytotoxicity observed as a consequence of DNA strand cleavage associated with the enzyme DNA topoisomerase II.<sup>87</sup> Human DNA topoisomerase II is an enzyme intimately involved in DNA replication in which catenation (interlinking two circular DNA strands) and decatenation (separation of two circular DNA strands), supercoiling and relaxation, knotting and unknotting take place.<sup>242</sup> Thus, topoisomerase II cleaves and rejoins DNA strands. Eukaryotic topoisomerases II only relax supercoils and do not generate them and are able to hydrolyze ATP. The corresponding complements in prokaryotes, also known as DNA gyrases, have been studied extensively. The DNA gyrases catalyze the stepwise negative supercoiling of DNA with concomitant hydrolysis of ATP. This manifests as double-stranded breaks in the DNA, an important step in DNA replication and occurs with all topoisomerase II enzymes, regardless of origin. Topoisomerase II bonds to the 5-phosphate on adjacent DNA strands via tyrosine, four base pairs apart forming the DNA-enzyme complex. The stabilization of this complex owing to its interaction with certain drugs such as **2.93**, form the cleavable complex which then lead to the cleavage of double-stranded DNA. Thus, inhibiting

this enzyme selectively kills proliferating cells and consequently topoisomerase II is the target of widely used cancer drugs.

The second group, the indolo[2,3-*a*]pyrrolo[3,4-*c*]carbazole **2.92**, possess anti-tumour properties which may be due to DNA intercalation, topoisomerase inhibition, and inhibition of protein kinases of which several representatives of this group are in clinical trials.<sup>87</sup> They have been classified broadly into two groups based on their structure and mechanism of anti-tumour activity. The first group are inhibitors of DNA topoisomerase I and do not possess kinase inhibitory activity. Rebeccamycin **2.95** and its derivatives are found here.<sup>243,244</sup> The other group includes the protein kinase C inhibitors such as staurosporine **2.96**<sup>245,246</sup> and its derivatives. 7-Oxostaurosporine **2.97** showed activity against K562 cells, a human erythroleukemia cell line.<sup>247</sup> Another isolate, BE-13793C **2.98** displayed strong activity against human topoisomerase I and II.<sup>248</sup> These observations are significant in the context of the activities reported for the kinamycins presented in Chapter 1, Section 1.5.4. Examples of the quinolino[4,3-*b*]carbazole-1,4-quinone (indolophenanthridine) family are represented by calothrixin A **2.99** and calothrixin B **2.100** and deserve mention on the basis of structural features that extend the ellipticine skeleton and incorporate the 1,4-quinone moiety as well as their unique activity profile in which the growth inhibition of chloroquin-resistant strain of the malaria parasite *Plasmodium falciparum* has been reported.<sup>249</sup>

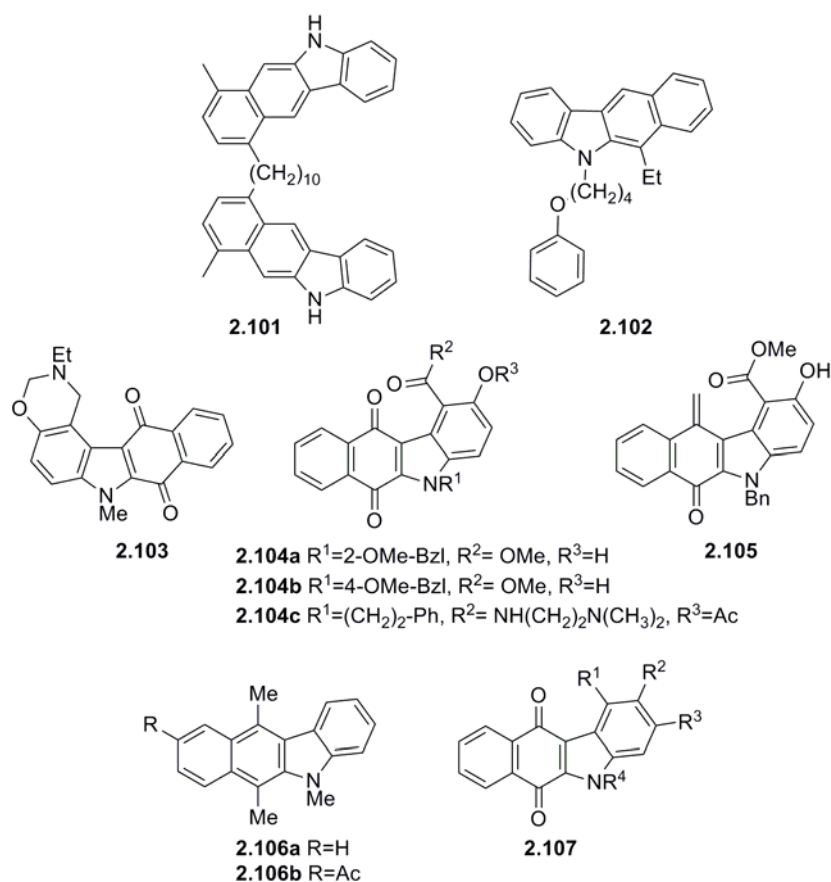


### 2.5.3 Bioactivity of Benzo[*b*]carbazoles

#### 2.5.3.1 Early reports

Gribble reported the potential bifunctional DNA intercalating agent **2.101** (Figure 2.3).<sup>141</sup> Pindur has performed extensive molecular modeling studies on benzo[*b*]carbazoles intercalating with DNA<sup>155,187,188</sup> and found that **2.102** possessed cytostatic activity against L1210 leukemia cells. Kucklander's earlier efforts found **2.103** was active against a variety of colon and lung cancers.<sup>162</sup> Later studies revealed that **2.104** and **2.105** possessed marked potency against specific melanoma and leukemia cell lines.<sup>163</sup> Strikingly, **2.105** bearing a quinone methide, displayed activity that was comparable to clinically established anticancer agents such as amsacrine or mitomycin C. Those authors attribute the potent anticancer activity of **2.105** to its ability to intercalate DNA, a phenomenon not observed with compounds **2.104**. Koomen observed **2.106** to have low cytostatic activity which suggested the presence of the pyridine nitrogen found in ellipticine **2.93** was essential for antitumour activity.<sup>164</sup> Cheng synthesized **2.107** with varying substitution patterns but in all cases only low growth inhibitory action against the human promyelocytic leukemia cell line HL-60 was observed.<sup>168</sup>

**Figure 2.3:** Bioactive benzo[*b*]carbazoles.

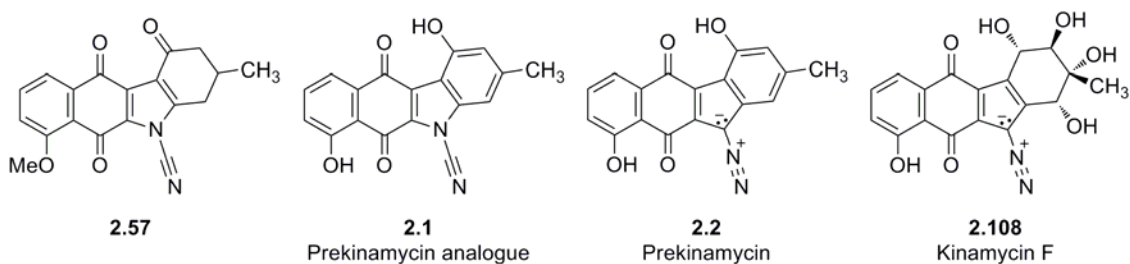


### 2.5.3.2 Bioactivity studies from this laboratory

The results from the testing of the growth inhibition of K562 cells by two cyanamide analogues prepared in the present study as well as by prekinamycin and kinamycin F are shown in Table 2.2. The details of the cellular inhibition assay are given elsewhere.<sup>133</sup> The  $\text{IC}_{50}$  value is a measure of how much of a particular substance is needed to inhibit a given biological process by 50% compared to that of a control group. Stated otherwise, the  $\text{IC}_{50}$  is

the measure of the effectiveness of a compound at inhibiting a biological/biochemical function by 50%.

Inspection of Table 2.2 reveals that kinamycin F is the most active compound with an  $IC_{50}$  range  $\sim 0.3$ - $0.7$   $\mu$ M. The cyanamide compound **2.57**, an earlier synthetic precursor of **2.1**, is the least bioactive with an  $IC_{50}$  range of  $\sim 21$ - $49$   $\mu$ M. Further inspection of Table 2.2 reveals that entries 1 and 2 indicate that prekinamycin is slightly more active than the cyanamide, whereas entry 3 indicates the opposite scenario with the cyanamide demonstrating slightly higher activity than prekinamycin. Taken together, entries 1-3 would suggest **2.1** and **2.2** possess comparable biological activity owing to the tight range of data (i.e. within the same order of magnitude) but does not imply that activity is necessarily elicited by the same mechanism. This observation raises the question of what role the diazo function has with respect to mechanism of action (MOA) and what the putative intracellular target or targets might be. These results have obvious implications in regard to the design of kinamycin analogues as well. We have suggested that the cytotoxicity of kinamycin F is due in part to the unique conformation of the polyhydroxylated D-ring, which has been shown to increase the diazonium ion character of the diazo group.<sup>101</sup> In this context, the results presented in Table 2.2 raise the issue of whether kinamycin F is a more potent inhibitor than its cyanamide congener. Future synthetic efforts from this laboratory will be addressing these issues.

**Table 2.2:** The growth inhibition of K562 cells ( $IC_{50}$   $\mu$ M) for selected compounds.

		$IC_{50}$ ( $\mu$ M)				
Entry	Trial	<b>2.57</b>	<b>2.1</b>	<b>2.2</b>	<b>2.108</b>	
1	Control	1	$46.7 \pm 4.8$	$13.9 \pm 1.0$	$10.7 \pm 1.1$	$0.728 \pm 0.063$
2	"	2	$49.2 \pm 8.9$	$11.9 \pm 2.7$	$8.46 \pm 1.5$	$0.429 \pm 0.071$
3	"	3	$44.0 \pm 12.4$	$14.6 \pm 1.9$	$22.2 \pm 2.1$	$0.536 \pm 0.112$
4	"	4	21.3	10.9	na	0.356
5	"	5	na	na	na	$0.333 \pm 0.02^a$
6	OTC	1	na	$5.23 \pm 1.56$	$4.30 \pm 1.92$	$0.36 \pm 0.08$
7	BSO	1	$9.48 \pm 3.85$	$4.60 \pm 0.92$	$5.88 \pm 2.47$	$0.37 \pm 0.06$

n.a.: not available; a. previous literature value (Ref. 133); OTC: (-)-2-oxo-4-thiazolidinecarboxylic acid (OTC); BSO: buthionine sulfoximine.

Data shown in entries 6 and 7 were collected from conditions in which cultures were exposed to (-)-2-oxo-4-thiazolidinecarboxylic acid (OTC) and buthionine sulfoximine (BSO) before exposure to any of the compounds listed in Table 2.2. OTC and BSO increase and decrease, respectively, the intracellular concentrations of glutathione (GSH), an endogenously produced antioxidant containing a thiol functional group. Previous work by our laboratory has shown that kinamycin F, when incubated with GSH, is reductively activated to cleave DNA in vitro. In cell culture studies, however, raising intracellular GSH levels by exposure to OTC or lowering GSH levels with BSO did not affect the cytotoxicity of kinamycin F,<sup>133</sup> although the standard errors in such measurements are relatively large.

If direct, bimolecular reaction of GSH and  $\text{GS}^-$  were to be involved in either the activation or deactivation of these compounds in whole cells, one might have expected a significant influence of intracellular GSH levels on  $\text{IC}_{50}$  measurements. It is possible, however, that GSH/ $\text{GS}^-$  are involved but in an enzyme catalyzed process involving glutathione-S-transferase (GST). GST catalyzes the reaction of GSH with exogenous electrophilic species and thus serves to detoxify such compounds, although with certain compounds the "detoxification" process leads to actual activation of compounds into cytotoxic forms (e.g. certain enediynes). It is possible that the  $[\text{GSH}]$  remains substantially in excess of the  $K_M$  for GSH such that the GST-catalyzed reaction remains saturated with respect to GSH over the entire range that  $[\text{GSH}]$  is varied in the whole cell experiments using OTC or BSO.

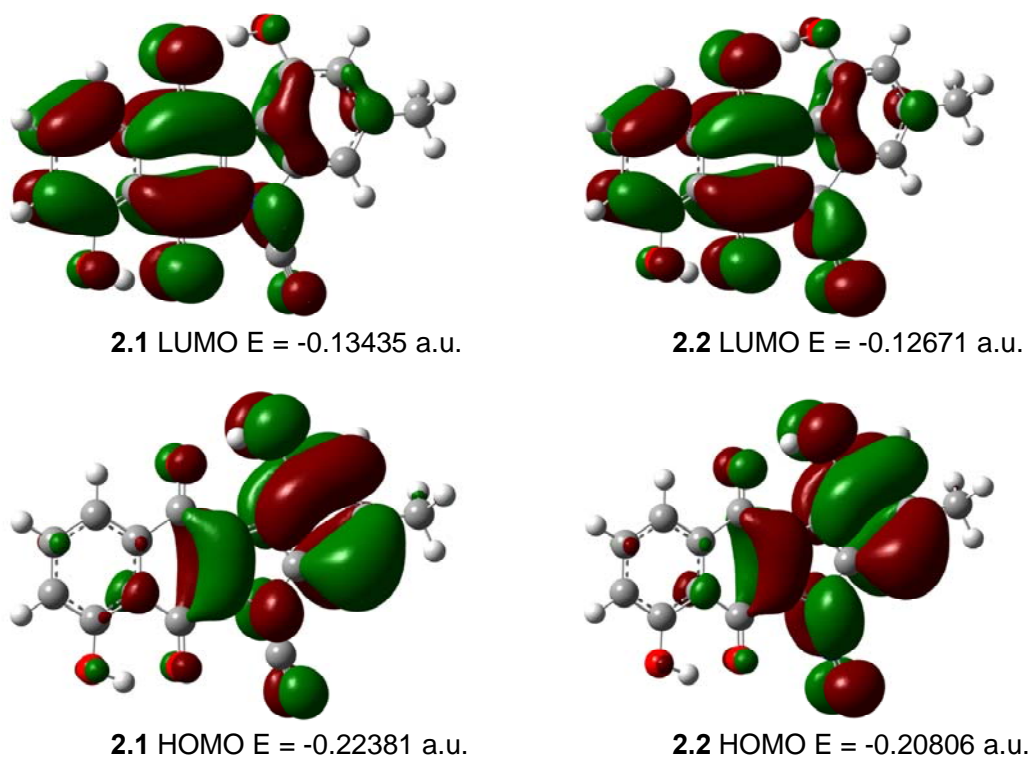
$$\text{rate} = \frac{k_{\text{cat}}[\text{E}]_0[\text{S}]}{K_M + [\text{S}]}$$

If  $[\text{S}] \gg K_M$   
then  $\text{rate} = k_{\text{cat}}[\text{E}]_0$  ← independent of  $[\text{S}]$

The results presented in Table 2.2 also invite theoretical studies that may lend insight into the reactivity of these compounds. Quantum chemical calculations were undertaken on **2.1**, **2.2** and  $\text{GS}^-$  **2.109b** at the DFT B3LYP 6-31 G(d) level of theory. Figure 2.4 illustrates the respective HOMOs and LUMOs of **2.1** and **2.2** and their corresponding energy levels. These data are partially reiterated in Figure 2.5 in which the frontier molecular orbital energies of **2.1**, **2.2** and **2.109b** are shown. Inspection of the HOMO energies reveals that the HOMO of cyanamide **2.1** is  $9.9 \text{ kcal}\cdot\text{mol}^{-1}$  lower in energy than that of prekinamycin **2.2**. As well, inspection of the LUMOs reveals that the LUMO of **2.1** is  $4.8 \text{ kcal}\cdot\text{mol}^{-1}$  lower in energy than that of **2.2**. The Gibbs free energy ( $G$ ) was retrieved for **2.1** ( $-1102.150580 \text{ a.u.}$ ) and for

**2.2** (-1102.130649 a.u.), indicating that the cyanamide analogue is thermodynamically more stable than prekinamycin by 12.5 kcal·mol<sup>-1</sup>.

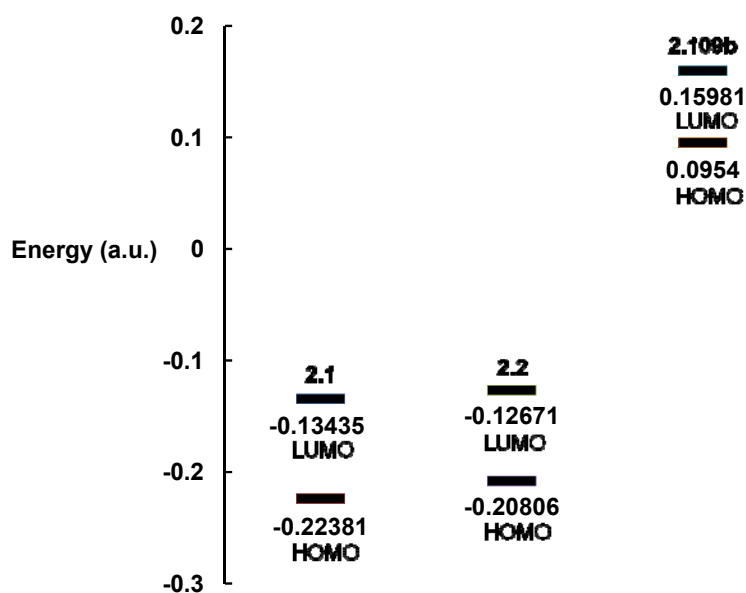
**Figure 2.4:** The HOMO and LUMO of **2.1** and **2.2** and their corresponding energy levels (eigenvalues) generated at the DFT B3LYP 6-31 G(d) level (1 a.u. = 627.5095 kcal·mol<sup>-1</sup>).



Intracellular concentrations of GSH **2.109a** can be as high as 10 mM.<sup>250</sup> The pKa of the thiol moiety of GSH is 8.66<sup>251</sup> and at physiological pH (6.8 to 7.4), ~1-5% would exist ionized as the thiolate, GS<sup>-</sup> **2.109b** (Scheme 2.20). In general, it is the thiolate form of GSH that is the predominant nucleophilic species rather than the thiol (Figure 2.6). Unpublished data obtained from studies conducted by N. Chen from this laboratory, in which kinamycin F

was allowed to react with GSH, suggest that kinamycin F, possessing an electrophilic diazo moiety, is attacked by GSH at the terminal nitrogen, furnishing an azo adduct. Subsequently, it may be envisioned that in the biological milieu, the azo adduct, upon homolysis, produces molecular nitrogen and an aryl radical, presumably leading to cell death via a number of potential pathways (Scheme 2.21) and is discussed in the context of Figure 2.7 (vide infra).

**Figure 2.5:** Frontier molecular orbital energies (a.u.) of cyanamide **2.1**, prekinamycin **2.2** and  $\text{GS}^-$  **2.109b** obtained at the DFT B3LYP 6-31 G(d) level (1 a.u. = 627.5095 kcal·mol<sup>-1</sup>).



**Scheme 2.20:** The acid dissociation of glutathione **2.109a** to yield the corresponding thiolate **2.109b**.

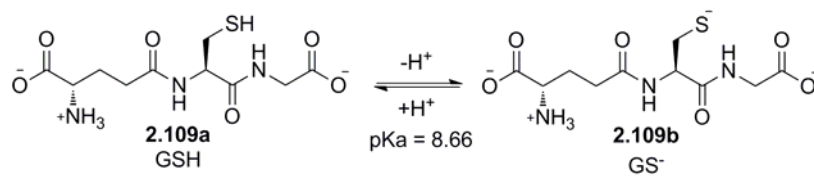
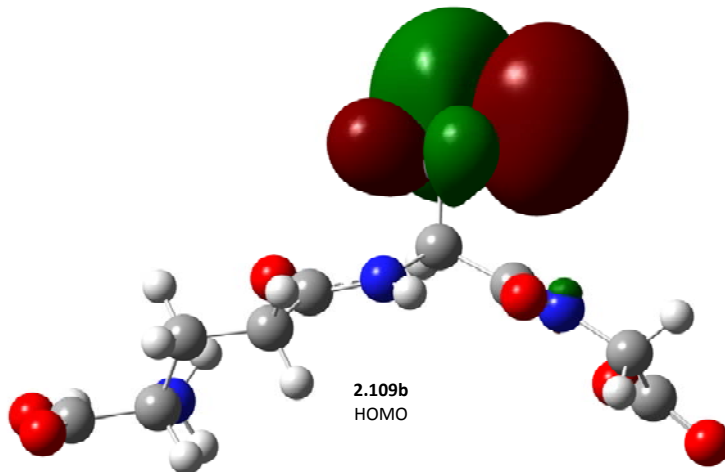
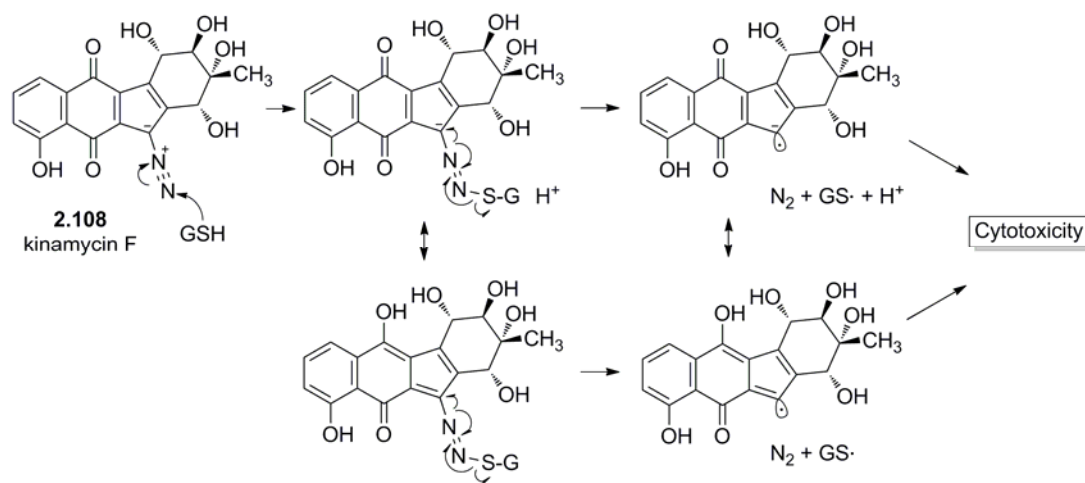


**Figure 2.6:** The HOMO of **2.109b** calculated at the DFT B3LYP 6-31 G(d) level of theory.





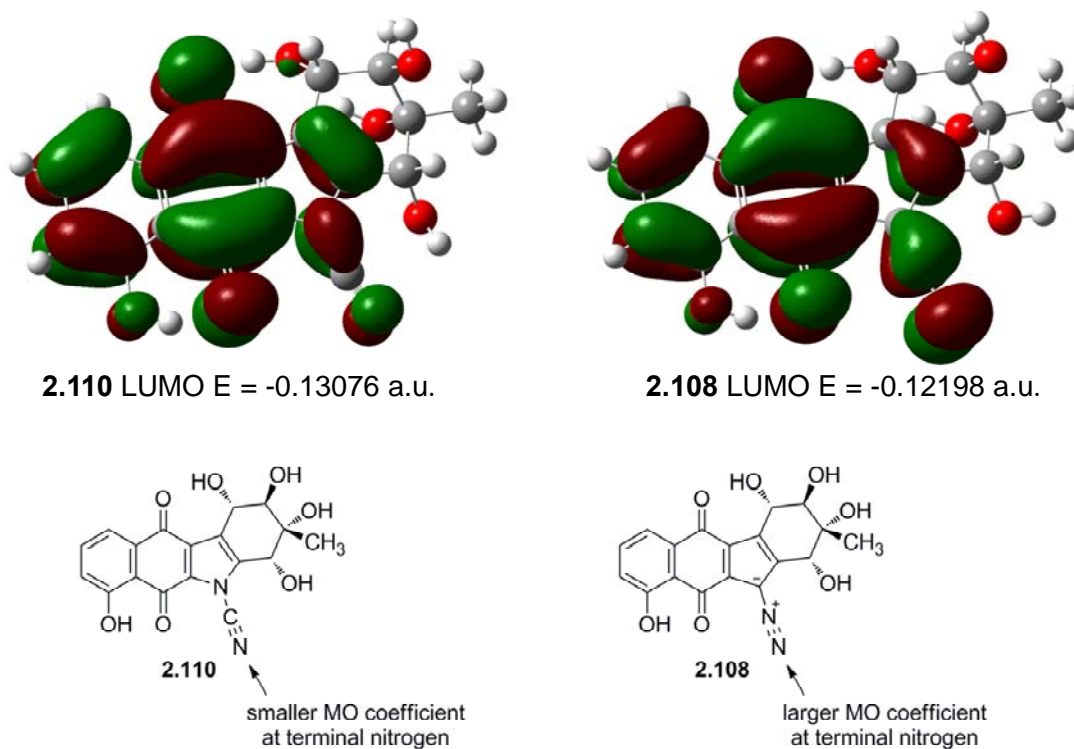
**Scheme 2.21:** Possible interaction of GSH with kinamycin F.



If frontier orbital interactions are important in the nucleophilic addition of GS<sup>-</sup> to these systems, then **2.2** is expected to be more reactive since the GS<sup>-</sup><sub>HOMO</sub>-**2.2**<sub>LUMO</sub> gap is smaller than the GS<sup>-</sup><sub>HOMO</sub>-**2.1**<sub>LUMO</sub> energy gap (Figure 2.5). On the other hand, if electron transfer is important, the lower LUMO for **2.1** would suggest a higher electron affinity (EA) and a greater tendency of **2.1** to accept an electron in a single electron transfer (SET). That is, **2.2** is more electrophilic but **2.1** has a higher electron affinity. This may suggest that compounds of the *N*-cyanocarbazole series may be more prone to the formation of free radicals including oxygen free radicals (i.e. S + <sup>3</sup>O<sub>2</sub> → S<sup>+</sup> + <sup>3</sup>O<sub>2</sub><sup>-</sup> →→→ ·OH, ·OOH, etc.) than are the kinamycins. Further ground state quantum chemical calculations on kinamycin F **2.108** and its hypothetical cyanamide analogue **2.110** were pursued to investigate this query (Figure 2.7). Indeed, **2.110** has lower LUMO (5.5 kcal·mol<sup>-1</sup>), while **2.108** possesses a significantly larger coefficient at the terminal nitrogen than **2.110**. The difference in free energies (Δ*G*) predicts that the **2.110** should be more stable than **2.108** by 11.6 kcal·mol<sup>-1</sup>. Taken together,

these data parallel the same trend as found for comparisons of the electronic properties of **2.1** and **2.2**.

**Figure 2.7:** The LUMO of **2.110** and **2.108** and their corresponding energy levels (eigenvalues) generated at the DFT B3LYP 6-31 G(d) level (1 a.u. = 627.5095 kcal·mol<sup>-1</sup>).



In order to probe the electronic differences between **2.1** and **2.2** further, an electrostatic potential energy (ESP) surface for both **2.1** and **2.2** was generated. Figure 2.8 displays the ESP surface of **2.1** and **2.2**, inspection of which reveals some notable observations. For the most part, the gross molecular electron distribution is relatively similar with a few key differences. Firstly, the terminal nitrogen of the cyano moiety of **2.1** possesses more electron

density than that of the terminal nitrogen of the diazo group of **2.2** and intuitively, of course, one would not expect the terminal nitrogen of the cyanamide group to be electrophilic. In general, it is assumed that the EA is approximated by the negative reciprocal of a molecule's LUMO energy.<sup>252,253</sup> From this perspective, **2.1** would be a better electron acceptor owing to its lower energy LUMO and hence higher EA. The low electron density found at the terminal nitrogen of the diazo group of **2.2** fits well with the previous observations made by others from this laboratory of the electrophilic character of the diazo group of the kinamycins.<sup>38,199</sup> Secondly, the phenolic oxygens of prekinamycin display more electron density and, hence, more partial negative charge than that of the cyanamide. This may be a consequence of the increase in hydrogen bonding to the quinoid oxygens of the B-ring. If this is indeed the case, the difference in the O-H bond length of **2.1** and **2.2** would indicate this quality. Indeed, inspection of the bond lengths reveals stronger H-bonding to the quinoid oxygens in **2.2** than that in **2.1** as shown in Figure 2.9.

**Figure 2.8:** The electrostatic potential (ESP) surfaces of **2.1** and **2.2** generated at the DFT B3LYP 6-31 G(d) level (isoval 0.0004) and range from  $\pm 30.8$  kcal·mol<sup>-1</sup> for **2.1** and  $\pm 26.3$  kcal·mol<sup>-1</sup> for **2.2**. Regions coloured red indicate negative values of the ESP and regions coloured blue indicate positive values of the ESP with green being zero ESP.

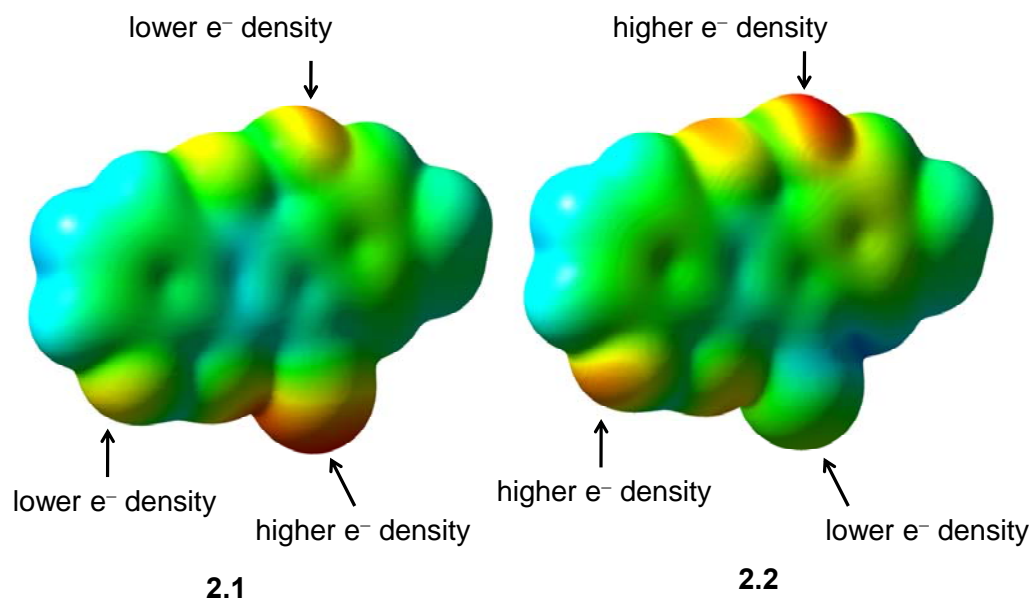
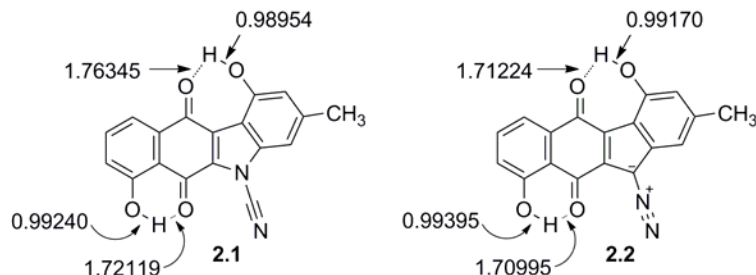
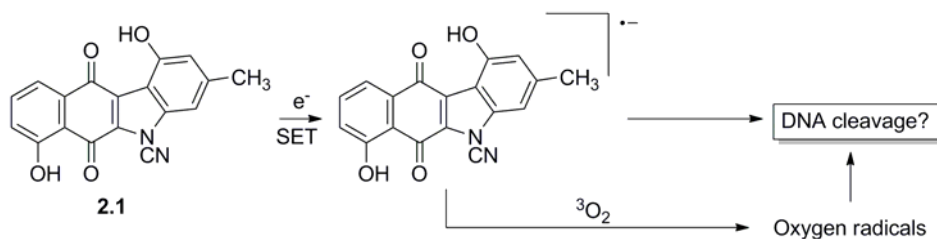


**Figure 2.9:** Bond lengths (Å) as observed in the minimized structures of **2.1** and **2.2** obtained at the DFT B3LYP 6-31 G(d) level.

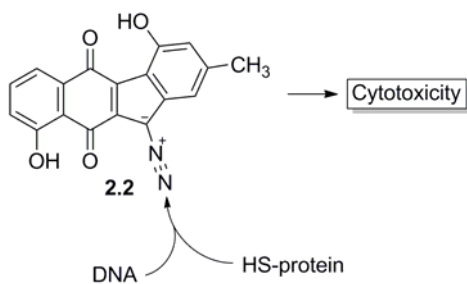


It is possible that multiple interactions with various targets contribute to the activity of prekinamycin **2.2** and the cyanamide analogue **2.1**. These include:

1. Electron transfer to generate a radical anion which might then interact directly with DNA or first  $^3\text{O}_2$  leading to oxygen radicals which then go and cleave DNA. This is possible for **2.1** and **2.2** but is more likely for **2.1** owing to its lower LUMO.



2. Reaction with biological nucleophiles such as DNA bases or thiol groups on protein targets. This applies for **2.2**.

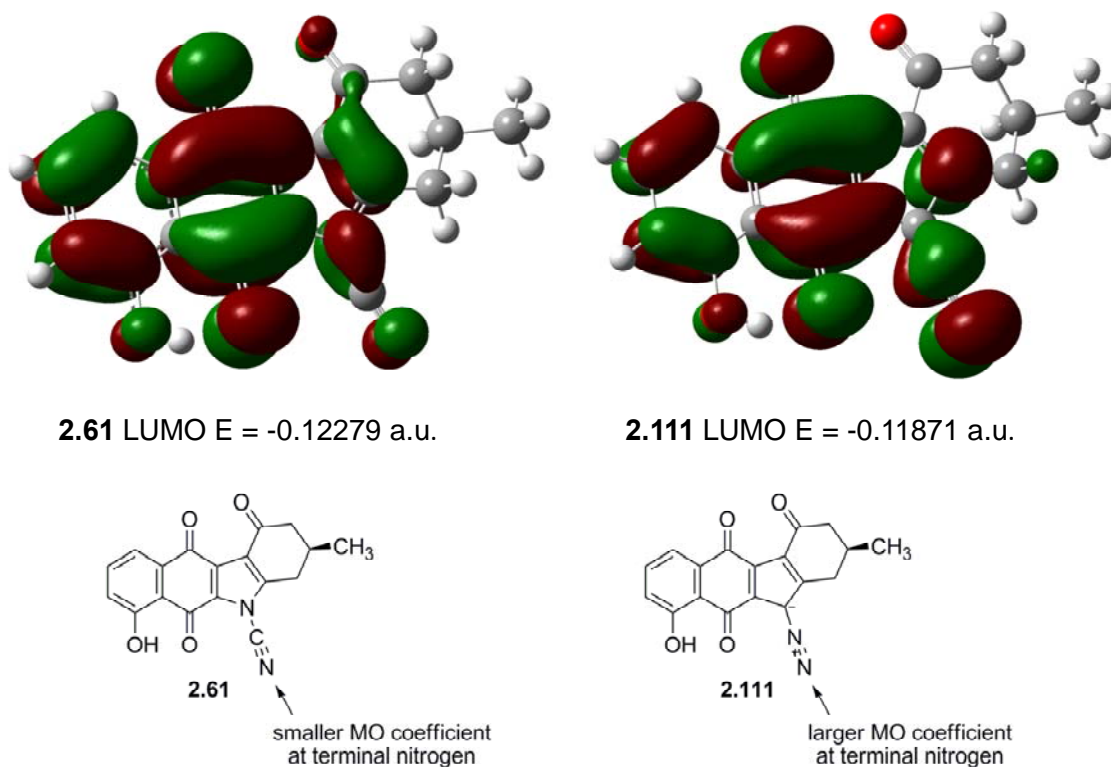


3. Non-covalent binding to a biological receptor which is possible for both **2.1** and **2.2**. However, as indicated from the ESP data, both **2.1** and **2.2** have somewhat different electronic character that might lead to significantly different affinity for the target. In the case of kinamycin F, a recent study involving this laboratory has revealed that kinamycin F may be specifically targeting a protein involved in transcription of cyclin D3, one of a group of proteins involved in the cell cycle. The contribution of such an interaction to the overall MOA of kinamycin F is unlikely to be the consequence of a non-selective DNA cleavage event.<sup>134</sup> A non-covalent or possibly a covalent binding to such a protein target by kinamycin F or one of its metabolites might explain the cytotoxicity since the diminution of cyclin D3 levels is known to induce apoptosis (programmed cell death). It is not yet known if similar effects on cyclin D3 levels are induced by prekinamycin, isoprekinamycin or the lomaiviticins.

One interpretation of the comparable cytotoxicity of **2.1** and **2.2** is that for **2.1**, the electron transfer MOA makes a better contribution to the cytotoxicity effect, whereas for **2.2** the reaction with biological nucleophiles may be more important. Another interesting observation is the very low activity of the ketone **2.57**. In the kinamycin series, the dimeric analogues called the lomaiviticins possess such a keto group and are very active in DNA cleavage experiments under reducing conditions and are highly cytotoxic to cancer cells; more so than the monomeric kinamycins that lack the keto group. It is not clear, however, if the *O*-methyl group might play a role in the low activity of **2.57**. A more direct assessment of the influence of the keto group is the comparison of both the diazo and the cyanamide version of the phenols **2.61** and **2.111**. Compound **2.61** is potentially available from our

synthetic efforts and compounds such as **2.111** may be accessible via the excellent total synthesis approach reported recently from the Herzon group.<sup>103</sup> Ground state chemical calculations indicate that the LUMO of **2.61** is 2.6 kcal·mol<sup>-1</sup> lower than that of **2.111**, while **2.111** possesses a significantly larger coefficient at the terminal nitrogen than **2.61**. The difference in free energies ( $\Delta G$ ) predicts that the **2.61** should be more stable than **2.111** by 15.5 kcal·mol<sup>-1</sup>. These data parallel, in similar fashion, the two other data sets; the **2.1/2.2** series and **2.110/2.108** series.

**Figure 2.10:** The LUMO of **2.61** and **2.111** and their corresponding energy levels (eigenvalues) generated at the DFT B3LYP 6-31 G(d) level (1 a.u. = 627.5095 kcal·mol<sup>-1</sup>).



## 2.6 Conclusion

This study has afforded some insights into the behavior of the kinamycins group of antibiotics through the synthesis and subsequent biological studies of its *N*-cyanocarbazole analogues. The data presented here has cast some light on the role of the diazo group of the kinamycins with respect to its bioactivity profile and draws questions about its relevance where so many others have implicated its importance. Synthetic studies of kinamycin analogues from this laboratory are ongoing and will address these queries in due course.



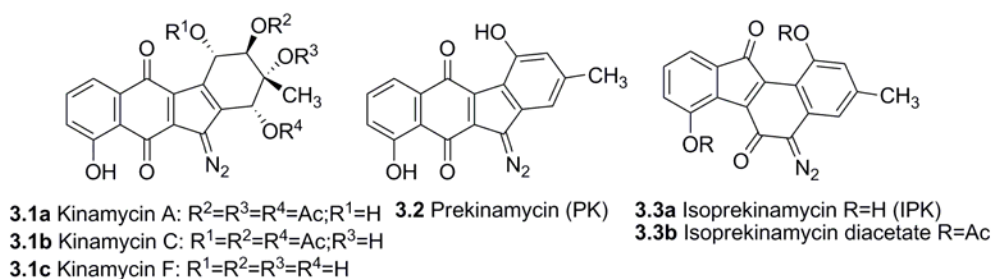
## Chapter 3

### The Reactivity of Nitric Oxide with Diazo compounds: Structure and Mechanism

#### 3.1 Introduction

Nitric oxide (NO) is a small stable radical whose biological importance is reflected by its role in a number of physiological and pathophysiological states.<sup>74,254,255</sup> Owing to the intrinsic importance of NO to biological systems, the generation, use and clearance of NO is tightly regulated. Indeed, the mechanisms by which NO is generated and regulated in vivo by mammalian systems has been well established.<sup>74,254,255</sup> Regulatory mechanisms in prokaryotic systems have also been well studied and the means by which bacteria and related organisms deal with NO are becoming clearer.<sup>256-258</sup>

**Figure 3.1:** Representative members of the kinamycin family.



Our laboratory has a long standing interest in the kinamycin group of natural products (Figure 3.1), particularly the synthesis of,<sup>31,37,38,101</sup> as well as the biological evaluation and mechanism of action of the parent compounds and their analogues.<sup>37,38,101,132-134</sup> The

kinamycins, originally designated as *N*-cyanobenzo[*b*]carbazoles but later found to be diazobenzo[*b*]fluorenes,<sup>30,31</sup> are among only a handful of natural products known to contain the diazo functionality.<sup>6-9,19,25-34,259-272</sup>

Several studies have attempted to elucidate the reactivity of the diazo moiety in the context of biological activity. Jeberatnam and Arya demonstrated the DNA cleaving ability of the model compound 9-diazofluorene under oxidizing conditions with Cu(OAc)<sub>2</sub>.<sup>112</sup> In another model study, Eppley *et al.* were able to show that bis(9-diaza-4,5-diazafluorene)copper(II)nitrate photocleaved DNA under anaerobic conditions in the presence of light<sup>115</sup> although there is no evidence to indicate the light is involved in the biological activity of the kinamycins. Studies by Feldman and Eastman, under non-biological conditions, suggested that the one electron reduction to the semiquinone affords, after nitrogen expulsion, an sp<sup>2</sup> radical at C-11 that is implicated in DNA damage via a number of potential mechanistic pathways.<sup>124,125</sup> In that study, prekinamycin was exposed to Bu<sub>3</sub>SnH/AIBN in toluene at 80 °C, where Bu<sub>3</sub>SnH served as the one electron surrogate, generating the sp<sup>2</sup> radical species, which subsequently undergoes radical aromatic substitution with the aromatic solvent. Electrophilic aromatic substitution was ruled out when they examined 1:1 mixtures of either electron poor or electron rich aromatic solvents and benzene and measured the relative rates of incorporation as well as the *o,m,p* ratios. Melander's group has shown that under reducing conditions using a high concentration of DTT, simple analogues as well as kinamycin D cleave DNA.<sup>126</sup> In a later report using glutathione at biologically relevant concentrations, they were able to show a time, temperature and concentration dependence on DNA cleavage.<sup>127</sup> Melander suggested a two

electron reduction of the quinone to the quinol from which arise two potential pathways for DNA cleavage. The first pathway describes a nucleophilic attack at the terminal nitrogen of the diazo moiety, furnishing a radical species which then can damage DNA. The second pathway involves protonation and subsequent loss of N<sub>2</sub>, providing the orthoquinone methide which may serve as a DNA alkylating agent, although DNA cleavage by this pathway has yet to be reported as alkylation itself does not lead to DNA cleavage.<sup>128,129</sup>

Our laboratory has shown previously that the diazo group of isoprekinamycin is diazonium-like and thus possesses electrophilic character and hence should be activated toward attack by nucleophiles at the terminal nitrogen of the diazo group.<sup>37</sup> More recently, we have demonstrated that kinamycins A and C (**3.1a**, **3.1b**) are inhibitors, but not poisons, of topoisomerase II $\alpha$  and are potent cell growth inhibitors.<sup>132</sup> Furthermore, we have also shown that kinamycin F **3.1c**, the deacetylated form of the kinamycins, is able to cleave some DNA on its own with increased cleavage in the presence of glutathione, albeit slowly under either condition.<sup>133</sup> The total synthesis of isoprekinamycin **3.3a** was recently accomplished in our laboratory and was shown to cause significant growth inhibitory effects on CHO and K562 cells.<sup>38</sup> The discovery of the lomaiviticins by the Wyeth group,<sup>34</sup> a dimeric form of the kinamycins that displayed very potent cytotoxicity against several cancer cell lines and consequently has intensified interest surrounding the mode of action of the kinamycins.

The efforts described above have largely centered on (i) elucidating the reactivity of the diazo group in simple aryl diazo compounds as well as the kinamycins themselves requiring (ii) some type of redox dependent activation to (iii) generate as of yet, an unidentified intermediate(s) that is directly or indirectly involved in DNA cleavage. The more recent

enzyme inhibition and cytotoxicity studies by our own laboratories have added to the kinamycin bioactivity database, but the mechanistic interpretation of the exact events that lead to these observations remain speculative and await further studies. DNA cleavage is just one of the many possible modes in which the kinamycins may elicit their cytotoxicity. Most recently, kinamycin F was observed to selectively downregulate cyclin D3 in K562 leukemia cells at the transcription level and suggests that the kinamycins may not function simply by damaging DNA but might have a specific biological target associated with the induction of apoptosis.<sup>134</sup> Despite these intensive efforts, the focus of kinamycin research for the most part has been directed towards DNA cleavage and thus other biochemical events in which the kinamycins are intimately involved with may have been overlooked. These biological processes include but are not limited to immunity and protection; regulation, sequestering and chaperoning; signaling, trafficking, communication and so forth and may involve some well known biological participants.

One obvious candidate is nitric oxide, which is known to mediate a host of physiological processes.<sup>74,254,255</sup> Reports on the reactivity of the kinamycins with NO are nonexistent; however, studies focusing on the reactivity of NO with diazo compounds are known although no experimental evidence addressing mechanism has been offered. Appropriately, mechanistic studies of NO with simple diazo compounds and the parallel experiments using the kinamycins would be justified. The data obtained from these studies would lend insight into the diverse reactivity of the diazo moiety, thus providing a fundamental understanding of NO reactivity with simple and more complex diazo compounds.

The first known studies on the reactivity of diazo compounds with NO was reported by Kirmse and coworkers in which diphenyldiazomethane was exposed to NO.<sup>273,274</sup> The products, identified only by IR spectroscopy and elemental analysis, were a diphenylnitrimine, benzophenone and nitrous oxide (N<sub>2</sub>O) with no other data supplied. Chapman and Heckert repeated the same studies undertaken by Kirmse in an effort to identify the nature of any intermediates.<sup>275</sup> Their observation of an alkylideneaminoxyl radical (also known as an iminoxyl radical and incorrectly assigned as a nitroxyl radical by the authors) by ESR studies support Kirmse's earlier suggestion of the involvement of the radical species, but offered little in evidence and few experimental details. In this context, it occurred to us that the kinamycins may be NO scavengers and thus the kinamycins might exist as a possible protective mechanism employed by *Streptomyces murayamensis*. More recently, it has been shown through extensive calculations by the Houk group, that the reactivity of NO is dramatically increased upon dimerization in the presence of an aromatic scaffold<sup>276</sup> and in some part, this may reflect events at the cellular level. These studies encouraged us to begin our own investigations into the reactivity of kinamycins as well as simpler diaryl diazo compounds with NO.

A discussion pertaining to the reactivity of NO with diphenyldiazomethane is given below in which the formation of three products, namely *N*-(diphenylmethylene)nitramide, benzophenone and for the first time a minor component, namely dinitrodiphenylmethane, are observed. A mechanistic model is given that is supported by both isotopic labeling studies as well as quantum chemical calculations. As well, the intrinsic lack of reactivity of kinamycin

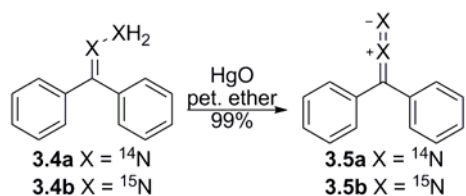
A and isoprekinamycin diacetate towards NO is shown and a rationale is offered based on molecular modeling studies interpreted through the framework of the mechanistic model.

## 3.2 Results and Discussion.

### 3.2.1 Exposure of Diphenyldiazomethane to Nitric Oxide and characterization of its products

Our initial objective was to reproduce the chemistry under the conditions reported earlier<sup>274</sup> with diphenyldiazomethane exposed to NO and to firmly establish the identity of all products from that reaction. Diphenyldiazomethane **3.5a** was synthesized according to standard literature procedures in near quantitative yield (Scheme 3.1).<sup>277</sup>

**Scheme 3.1:** Synthesis of diphenyldiazomethane **3.5**.



A NO generating apparatus (see Experimental) was employed to expose **3.5a** to NO,<sup>278</sup> typically over 16 to 20 hour period. The production of NO was confirmed by a positive test result in the Griess assay.<sup>279-281</sup> The crude reaction mixture was concentrated under reduced pressure and purified by flash silica gel column chromatography to afford three products, nitrimine **3.7**, benzophenone **3.8** and a previously unidentified product, dinitrodiphenylmethane **3.9**, shown in Scheme 3.2. As well, a small solvent effect was

observed (Table 3.1). Initially we failed to isolate **3.9** owing to the small quantity produced and that analytical TLC (similar  $R_f$  values) and  $^1\text{H}$  NMR (overlapping spectra) data were not diagnostic. Earlier reports provide no mention of **3.9**, in all likelihood for the same reason.

**Scheme 3.2:** Exposure of diphenyldiazomethane to NO furnishing the corresponding products.

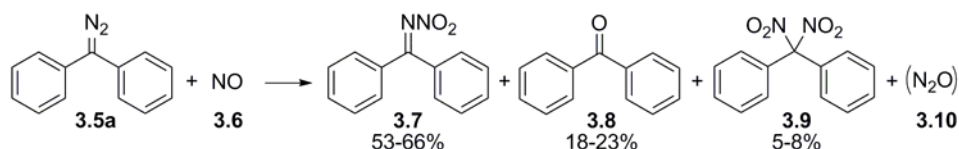


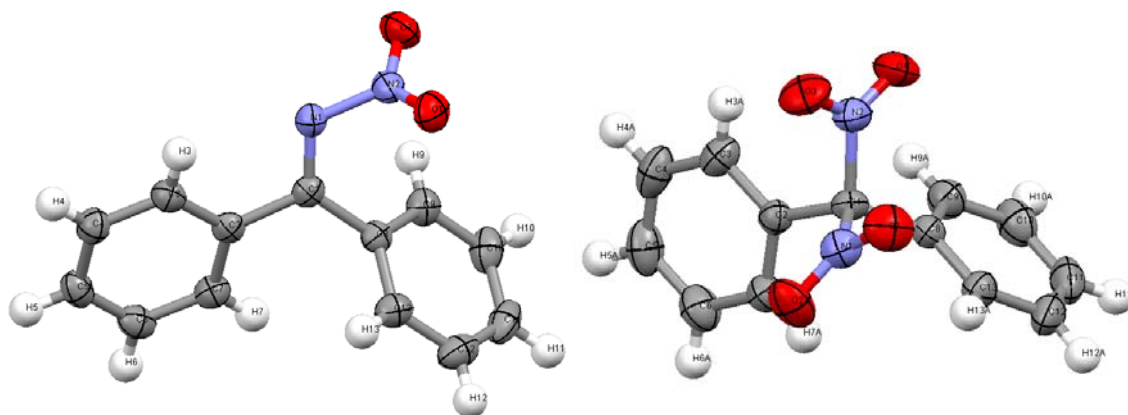
**Table 3.1:** Product distribution of nitrimine **3.7** and benzophenone **3.8** under different solvent conditions.

Solvent	Equivalents of Nitrimine (% yield)	Equivalents of Benzophenone (% yield)
Benzene	2.3 (53)	1 (23)
50/50 Benzene/Cyclohexane	3.1 (58)	1 (19)
Cyclohexane	3.6 (66)	1 (18)

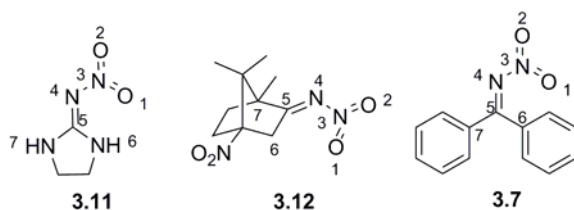
**X-ray structures.** Single crystal X-ray structures were obtained for **3.7** and **3.9** and are shown in Figure 3.2. X-ray structures of other nitrimines have been determined<sup>282-295</sup> including derivatives of guanidines,<sup>282,283,292</sup> imidazolidines,<sup>288,291,295</sup> thiazoles,<sup>290</sup> triazines<sup>289,293</sup> and pyridyl<sup>284-287</sup> systems. A selected summary of bond lengths and bond angles appear in Tables 3.2a and 3.2b, respectively of imidazolidine **3.11**<sup>295</sup> and camphorimine **3.12**<sup>294</sup> derivatives and **3.7**. The 2-nitriminoimidazolidine **3.11** shows a planar

nitroguanidine moiety and a slightly bent imidazolidine ring. This is in contrast to the "bent orthogonal" shape observed in both *N*-dinitrocamphorimine **3.12** and nitrimine **3.7**, in which both species have the nitro moiety orthogonal to the imine moiety.

**Figure 3.2.** Single crystal X-ray structures of nitrimine **3.7** (left) and dinitrodiphenylmethane **3.9** (right). Structures were generated using Mercury 2.2 (carbon = grey; hydrogen = white; nitrogen = blue; oxygen = red).





**Table 3.2a:** Selected bond lengths for nitrimines **3.11**, **3.12** and **3.7** in angstroms (Å).

Bond	<b>3.11</b>	<b>3.12</b>	<b>3.7</b>
N(3)-O(1)	1.237(1)	1.24(2)	1.232(3)
N(3)-O(2)	1.238(1)	1.20(2)	1.234(2)
N(3)-N(4)	1.339(1)	1.461(9)	1.447(2)
N(4)-C(5)	1.353(1)	1.273(7)	1.309(3)
C(5)-C/N(6)	1.326(1)	1.511(8)	1.503(3)
C(5)-C/N(7)	1.324(1)	1.498(8)	1.506(3)

**Table 3.2b:** Selected bond angles (in degrees) for nitrimines **3.11**, **3.12** and **3.7**.

Bond Angle	<b>3.11</b>	<b>3.12</b>	<b>3.7</b>
O(1)-N(3)-O(2)	121.5(1)	128(1)	125.9(2)
O(1)-N(3)-N(4)	115.0(1)	115(1)	115.6(2)
O(2)-N(3)-N(4)	123.5(1)	117(1)	118(2)
N(3)-N(4)-C(5)	117.9(1)	113.8(5)	115.4(2)
N(4)-N(5)-C/N(6)	117.1(1)	130.4(5)	125.4(2)
N(4)-N(5)-C/N(7)	132.3(1)	120.7(5)	114.8(2)

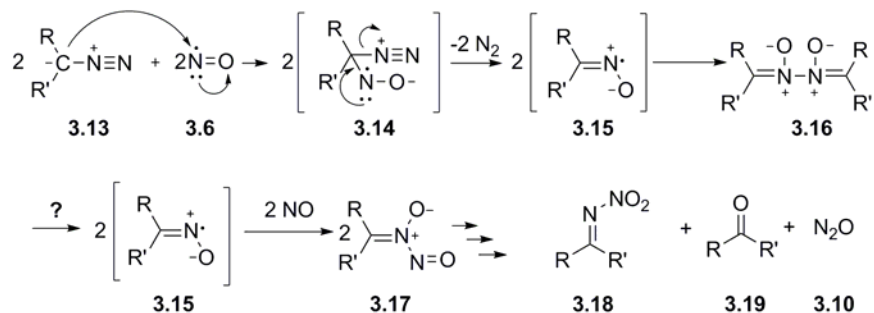
The identity of **3.9** initially proved to be elusive as standard spectroscopic techniques could not unequivocally identify it and was established only through X-ray studies. Initial inspection of the  $^{13}\text{C}$  NMR spectrum revealed four well resolved resonances with a fifth barely visible signal that was initially attributed to an impurity in the deuterated chloroform

solvent. We repeated the NMR experiment using deuterated dichloromethane and increased the relaxation delay (2 to 10 sec) over a 36 hour acquisition window and observed a small signal at 127.5 ppm. This resonance observed by us matches that reported by others<sup>296</sup> but with no mention of the low intensity of this signal. Levy *et al.* have noted that <sup>13</sup>C nuclei attached to <sup>14</sup>N nuclei often exhibit broad resonances in the <sup>13</sup>C NMR spectrum.<sup>297</sup>

### 3.2.2 Mechanistic proposal

Once the identity of all products was firmly established, the focus then turned towards elucidating the mechanistic pathway(s) that produce the observed products. A reasonable mechanistic proposal has been offered in which nucleophilic attack by the diazo compound **3.13** on NO occurs which, after expulsion of N<sub>2</sub>, furnishes an iminoxyl radical **3.15** which then can combine with NO to afford the *N*-nitrosanitron **3.17** from which the nitrimine **3.18**, ketone **3.19** and nitrous oxide **3.10** are generated (Scheme 3.3).<sup>274</sup> During the time that we undertook our investigation, a significant report was published by Houk and coworkers on the theoretical basis for NO reactivity with diazo compounds in the presence of aromatic solvents.<sup>276</sup>

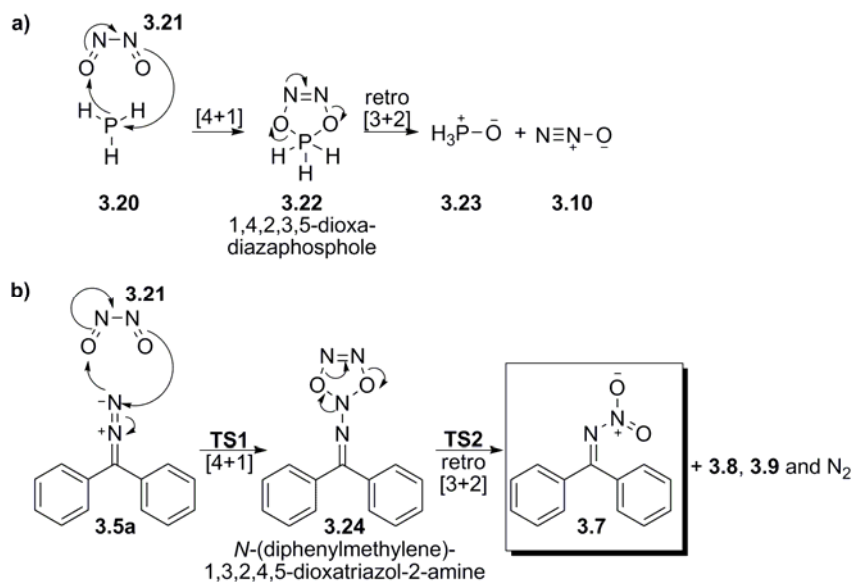
**Scheme 3.3:** Ionic-type mechanism for attack of diazo species **3.13** on NO. Reproduced from reference 274 with modifications.



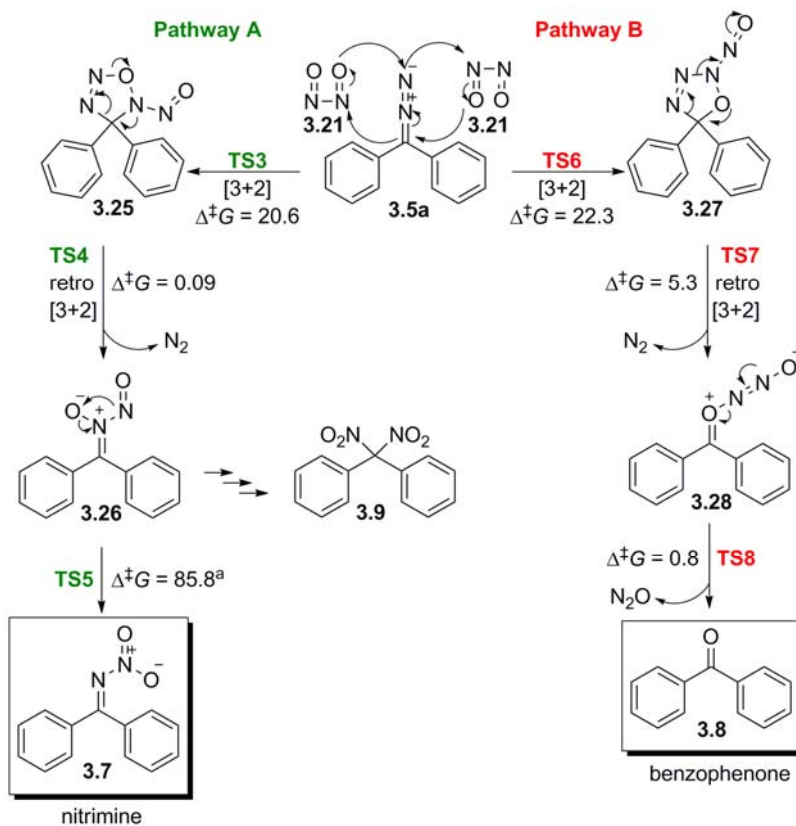
From that report, several key findings emerged one of which was that the equilibrium constant for dimerization of  $2\text{NO} \rightarrow \text{N}_2\text{O}_2$  increases by a factor of 150 in the presence of aromatic solvents. It was also found that  $\text{N}_2\text{O}_2$  possesses a lower lying LUMO than NO and that it is  $\text{N}_2\text{O}_2$ , rather than NO, that is the reactive electrophile in reactions. This carries mechanistic implications and in the context of this report, we felt we could offer other mechanistic possibilities other than that originally proposed by Kirmse and coworkers. In Houk's report, a [4+1] cycloaddition (chelotropic trapping) of phosphine **3.20** with  $\text{N}_2\text{O}_2$  generated the dioxadiazaphosphole **3.22** and subsequently undergoes a [3+2] cycloreversion producing phosphine oxide and nitrous oxide as shown Scheme 3.4a. By analogy to this reaction of **3.20** with  $\text{N}_2\text{O}_2$ , **3.5a** may react with  $\text{N}_2\text{O}_2$  in a similar fashion as shown in Scheme 3.4b, although it is not immediately clear how benzophenone **3.8** or dinitrodiphenylmethane **3.9** are generated by this pathway. On the other hand, it is well known that diazo compounds, acting as 1,3 dipoles, can participate in [3+2] cycloadditions (Scheme 3.5).<sup>298</sup> Depending on the regioselectivity of the [3+2] cycloaddition of  $\text{N}_2\text{O}_2$  with

**3.5a**, either **3.7** or **3.8** may be produced via pathway A or pathway B, respectively. It is also conceivable that **3.9** is produced at a point where pathway A bifurcates at **3.26**. Here, **3.26** may proceed on to generate **3.7** or undergo homolytic cleavage to furnish NO and the corresponding iminoxyl radical, which upon recombination, produces a dinitroso compound which can be oxidized further to furnish **3.9**. Thus, these different pathways are able produce the observed products via [4+1] or [3+2] cycloadditions.

**Scheme 3.4:** [4+1] cycloadditions of  $N_2O_2$  with a) phosphine (**3.20**)<sup>276</sup> b) diphenyldiazomethane (**3.5a**).



**Scheme 3.5:** Two possible regio-[3+2] cycloaddition pathways of  $N_2O_2$  with diphenyldiazomethane to furnish nitrimine **3.7**, benzophenone **3.8** and dinitrodiphenylmethane **3.9**. The free energies of activation ( $\Delta^\ddagger G$ ) are given in kcal·mol<sup>-1</sup> and were calculated at the DFT B3LYP 6-31 G(d) level of theory.



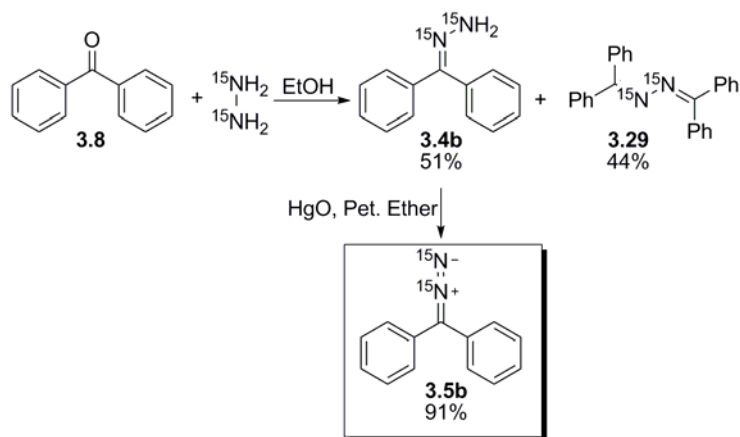
a. see discussion in section 3.2.4.

### 3.2.3 <sup>15</sup>N-labeling and NO exposure: Insight into Mechanism

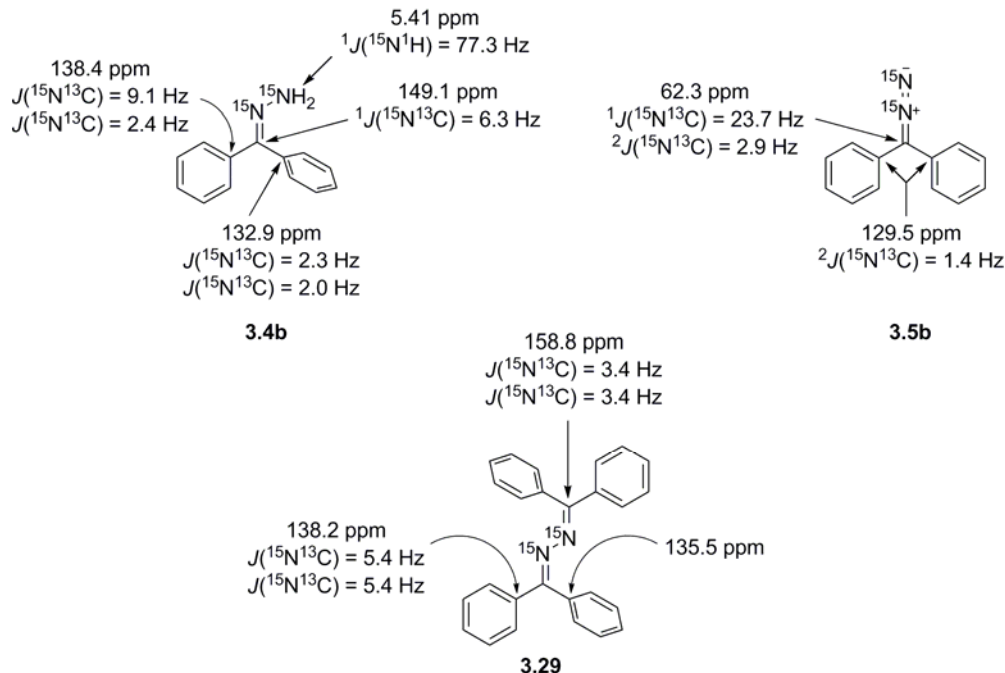
Hence experiments were conceived that might lend support to or refute either of the mechanistic possibilities shown in Schemes 3.4 and 3.5. One of the simplest means to investigate both the mechanism and thus the origin of the nitrogens in both the nitrimine **3.7** and the dinitrodiphenylmethane **3.9** would be best approached by using doubly-labeled <sup>15</sup>N-diphenyldiazomethane **3.5b**. Retrosynthetically, the <sup>15</sup>N,<sup>15</sup>N-labeled diazo compound would

be obtained from the  $^{15}\text{N},^{15}\text{N}$ -labeled hydrazone, which in turn would be obtained from the parent ketone and  $^{15}\text{N},^{15}\text{N}$ -labeled hydrazine. Owing to the expense of  $^{15}\text{N},^{15}\text{N}$ -labeled hydrazine, optimization of the conditions to obtain the labeled hydrazone was required. Using unlabeled hydrazine, the number of equivalents of hydrazine was reduced to 1.25 relative to benzophenone in refluxing ethanol ( $\text{Mg}/\text{I}_2$ ) over 72 hours to obtain the hydrazone in almost quantitative yield. It is imperative that the ethanol solvent used be rigorously dried under refluxing conditions of magnesium and iodine. Having established optimum conditions for the hydrazone synthesis, condensation of the  $^{15}\text{N},^{15}\text{N}$ -labeled hydrazine with benzophenone generated the  $^{15}\text{N},^{15}\text{N}$ -labeled hydrazone **3.4b** in 51% yield which was subsequently oxidized to the  $^{15}\text{N},^{15}\text{N}$ -labeled diphenyldiazomethane **3.5b** in 91% yield as described earlier (Scheme 3.6). The azine **3.29** was easily resolved from **3.4b** chromatographically and was recovered in 44% yield.

**Scheme 3.6:** Synthesis of  $^{15}\text{N}$ -labeled **3.4b** and its oxidation to **3.5b**.



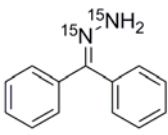
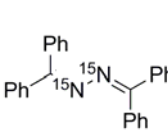
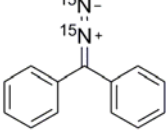
The  $^1\text{H}$  NMR spectra of **3.4a** and **3.4b**, the unlabeled and  $^{15}\text{N}$ -labeled hydrazone, respectively, appear identical in the aromatic region of the spectrum indicating that there is no coupling between either one of the two nitrogens and an aromatic proton (i.e.  $^4J(^{15}\text{N}^1\text{H})$  or  $^5J(^{15}\text{N}^1\text{H})$  are not observed). However, in the  $^1\text{H}$  NMR spectrum of **3.4b**, the amino protons show coupling to the terminal nitrogen to give a doublet ( $^1J(^{15}\text{N}^1\text{H}) = 77.3$  Hz and is typical for  $\text{sp}^3$  nitrogen<sup>299</sup>) but not a doublet of doublets as coupling to the imino nitrogen is not evident (i.e.  $^2J(^{15}\text{N}^1\text{H})$  is not observed). The observation of matching  $^1\text{H}$  NMR spectra in the aromatic region is also observed for **3.5a** and **3.5b** indicating no coupling between either of the two nitrogens to an aromatic proton. A direct comparison of the  $^1\text{H}$  NMR spectra of **3.29** with the unlabeled azine was not possible as the unlabeled material was not prepared.



Inspection of the  $^{13}\text{C}$  NMR spectra of the  $^{15}\text{N}$ -labeled compounds provides useful data on the structural and conformational heterogeneity of these compounds. In the  $^{13}\text{C}$  NMR spectrum of **3.4b**, the two quaternary phenyl carbons display different chemical shifts and couplings indicative of hindered rotation as well as different orientation relative to the lone pair on the  $\text{sp}^2$  imino nitrogen. A dd at 138.4 ppm with couplings of 9.1 and 2.4 Hz and a dd at 132.9 ppm with couplings of 2.3 and 2.0 Hz were observed. The configuration of these two carbons at the  $\text{C}=\text{N}$  double bond can be determined from the magnitude of the coupling constants,<sup>300</sup> where couplings of 7-13 Hz are assigned to carbons syn the lone pair (and thus the carbon at 138.4 ppm) and couplings of 1-3 Hz are assigned to carbons anti to the lone pair (and thus the carbon at 132.9 ppm).<sup>301</sup> Furthermore, it has been shown that C-N couplings are attenuated when the aromatic ring is twisted out of coplanarity with the  $\text{C}=\text{N}$  bond.<sup>302,303</sup> The chemical shift of the imino carbon (149.1 ppm) is typical for phenyl hydrazone<sup>304</sup> and the coupling of 6.3 Hz is in reasonable agreement with 7.2 Hz reported for benzaldehyde phenylhydrazone.<sup>305</sup> This analyses can also be applied to **3.29**, although one of the quaternary carbons fails to show any couplings at all. The  $^{13}\text{C}$  NMR spectrum of **3.5b** appears straightforward with no conformational issues where the chemical shifts and couplings are consistent with those previously reported.<sup>300,306</sup>



**Table 3.3:**  $^{15}\text{N}$  NMR chemical shifts and couplings for **3.4b**, **3.29** and **3.5b**.

	Observed $^{15}\text{N}$ chemical shift (ppm) <sup>a</sup>	Couplings (Hz)
 <b>3.4b</b>	320.37, 106.16	$J_{\text{NN}} = 12.4$ Hz
 <b>3.29</b>	353.05	na
 <b>3.5b</b>	439.96, 304.86 <sup>b</sup>	$J_{\text{NN}} = 9.6$ Hz

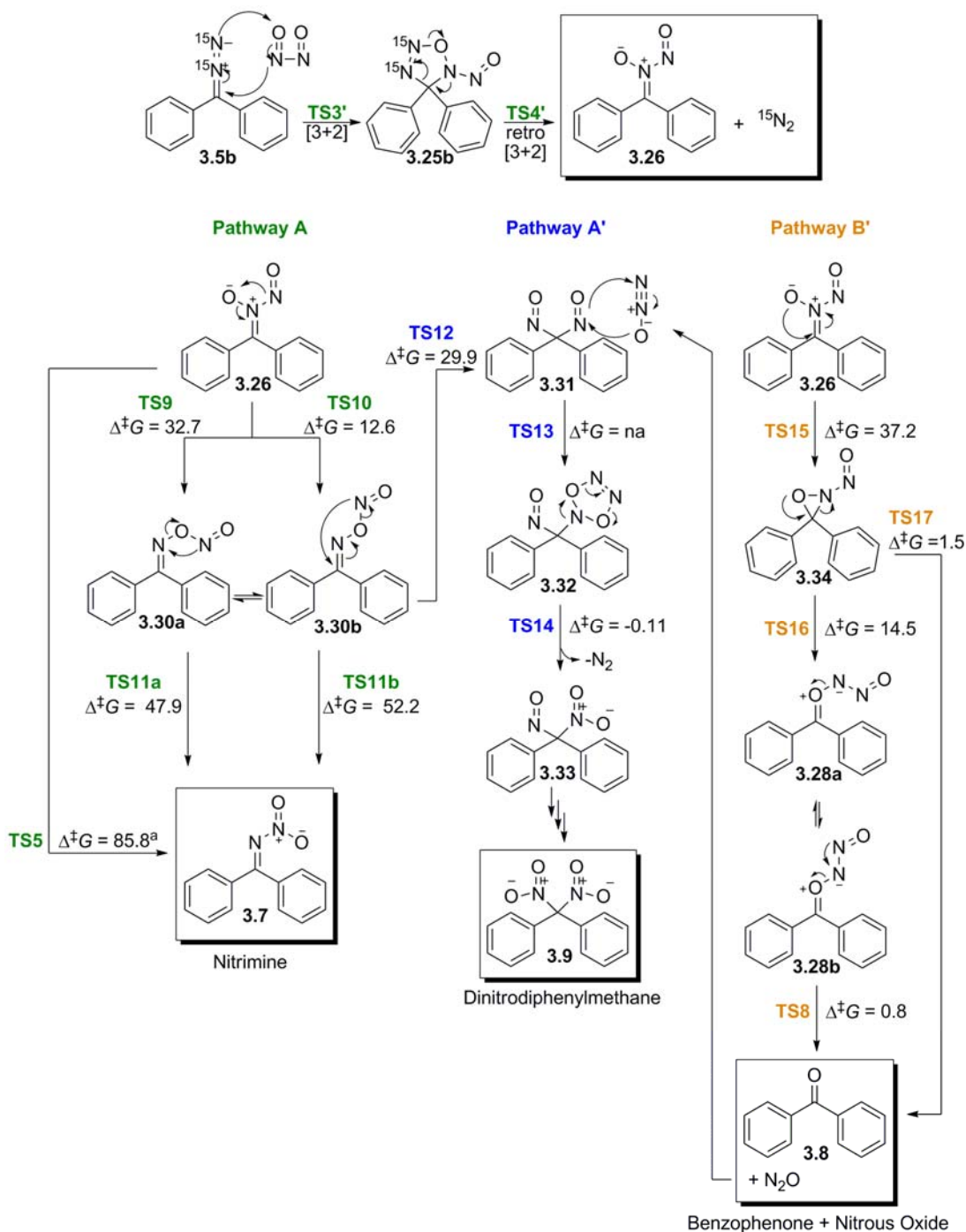
a. Referenced to  $^{15}\text{N}$ -formamide at 112.82 ppm in DMSO  $d_6$  (equivalent to ammonia at 0 ppm)

b. Literature value = 438.8, 302.7 ppm (see reference 306,307).

Table 3.3 shows the  $^{15}\text{N}$  NMR chemical shifts and couplings of the  $^{15}\text{N}$ -labeled materials and are representative for compounds of their class.<sup>308</sup> The  $^{15}\text{N}$  NMR spectrum of **3.5b** has the internal nitrogen assigned to the upfield resonance and the terminal nitrogen is assigned the more deshielded resonance as reported by others.<sup>306,307</sup>

With the labeled material in hand it was then exposed to NO as described earlier, affording the same three products as described previously. The nitrimine and dinitrodiphenylmethane were observed to lack any  $^{15}\text{N}$  enrichment as shown by  $^{15}\text{N}$  NMR,  $^{13}\text{C}$  NMR, IR and HRMS-EI, indicating that the [4+1] mechanism shown in Scheme 3.4 is not occurring and that the [3+2] cycloaddition may be appropriate (Scheme 3.5).

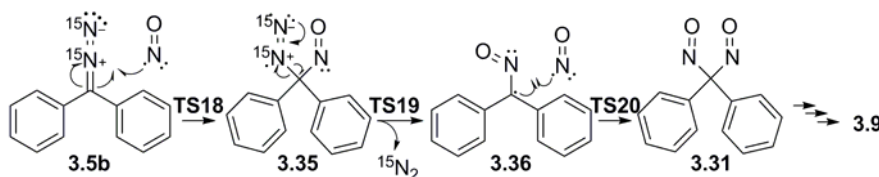
**Scheme 3.7:** Mechanistic manifold illustrating three possible pathways that generate **3.7**, **3.8** and **3.9**. The free energies of activation ( $\Delta^\ddagger G$ ) are given in kcal·mol<sup>-1</sup> and were calculated at the DFT B3LYP 6-31 G(d) level of theory.



a. see discussion in section 3.2.4.

With this new evidence in hand, a novel mechanistic proposal could be envisioned. Scheme 3.7 illustrates a comprehensive mechanistic manifold that shows the reaction of **3.5b** with  $\text{N}_2\text{O}_2$  in a [3+2] cycloaddition to afford the cycloadduct **3.25b** which then undergoes a [3+2] cycloreversion furnishing the *N*-nitrosnitron **3.26**, a common intermediate from which the nitrimine **3.7** (Pathway A), benzophenone **3.8** (Pathway B') and dinitrodiphenylmethane **3.9** (Pathway A') might be produced. The proposed manifold also accounts for the lack of  $^{15}\text{N}$ -labeling in **3.7** and **3.9**, consistent with our observations from the  $^{15}\text{N}$ -labeling experiments. Nitrous oxide ( $\text{N}_2\text{O}$ ), produced in Pathway B' is most likely consumed as an oxidant, furnishing **3.9** from dinitrosodiphenylmethane **3.31**, either in a separate [3+2] cycloaddition or ionic type of mechanism. To the best of our knowledge, there are no known examples of 1,3 dipolar cycloadditions of  $\text{N}_2\text{O}$  with a nitroso species. As well, nitric oxide may react with **3.5b** in a radical fashion generating dinitrosodiphenylmethane **3.31** (Scheme 3.8) which would then go on to furnish dinitrodiphenylmethane **3.9**. However, in light of Houk's report and in conjunction with the well-known behavior of diazo compounds in cycloadditions as well as our own observations, we suggest that the mechanisms shown in Schemes 3.5 and 3.7 are more appropriate.

**Scheme 3.8:** Radical addition of NO with **3.5b** producing **3.31**.



Insight into these mechanistic possibilities was addressed by theoretical methods. The reaction channels shown in Schemes 3.4, 3.5, 3.7 and 3.8 are the subject of quantum chemical calculations and is the focus of the following discussion.

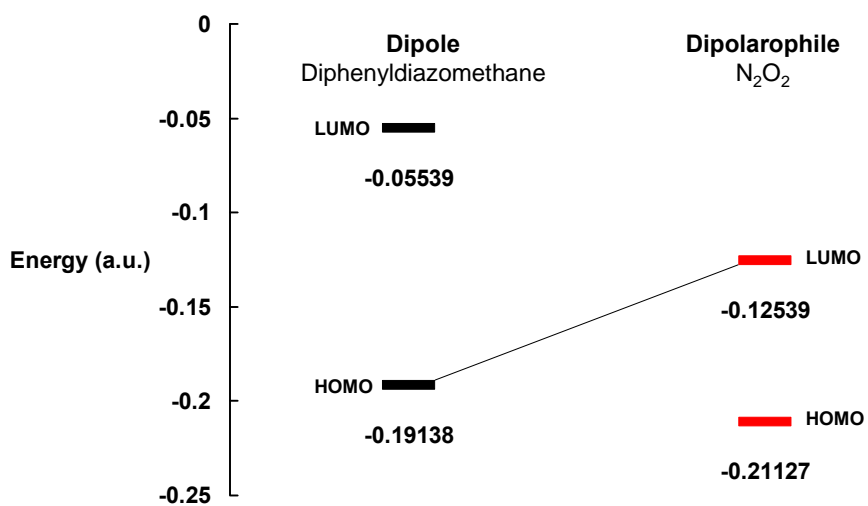
### 3.2.4 Quantum chemical calculations

The periselectivity of the [4+1] chelotropic process versus the competing [3+2] cycloaddition manifold as well the regioselectivity of the two [3+2] cycloadditions can be addressed through theoretical calculations. Quantum chemical calculations of structures and energies were accomplished using the Gaussian 03 suite of software programs.<sup>309</sup> The geometry of the reactants, intermediates, products as well as the transition state structures (TSs) for the various processes in Scheme 3.7 were fully optimized at the hybrid density functional B3LYP level of theory<sup>310,311</sup> employing the 6-31G(d) basis set.<sup>312</sup> All calculations were carried out in the gas phase at  $T = 298.15$  K and  $P = 1$  atm. Vibrational analysis confirmed that the TSs manifested as a single imaginary frequency (i.e. vibrational mode). The intrinsic reaction coordinate procedure (IRC)<sup>313,314</sup> was followed upon acquisition of the TSs to connect the TSs with the two closest minima and to confirm that this saddle point was a representative TSs for the indicated reaction. The corresponding zero point energy corrections were calculated using the same theoretical platform for all optimized structures but were not scaled.<sup>315</sup> Chapter 5 provides detailed information on the theoretical platform used in this study.

**FMO interactions.** The frontier molecular orbital (FMO) energies of the two reactants **3.5a** and **3.21** are shown in Figure 3.3. There are two possible interactions shown: HOMO<sub>dipole</sub>-LUMO<sub>dipolarophile</sub> and HOMO<sub>dipolarophile</sub>-LUMO<sub>dipole</sub>. From this illustration, the

HOMO<sub>dipole</sub>-LUMO<sub>dipolarophile</sub> would indicate the reactivity of this cycloaddition is governed by this interaction owing to the smaller energy gap, should this reaction be FMO controlled. According to Sustmann's classification of 1,3-dipoles, the reaction of the HOMO<sub>dipole</sub> of diphenyldiazomethane with the LUMO<sub>dipolarophile</sub> of N<sub>2</sub>O<sub>2</sub> is a Type 1.<sup>316</sup>

**Figure 3.3:** Frontier molecular orbital energies (a.u) for the 1,3-dipolar cycloaddition of diphenyldiazomethane **3.5a** (dipole, black) with N<sub>2</sub>O<sub>2</sub> **3.21** (dipolarophile, red) obtained at the DFT B3LYP 6-31 G(d) level.



One atomic unit (a.u.) = 627.5095 kcal/mol.

**Periselectivity: [4+1] versus [3+2].** The periselectivity of the two cycloaddition processes can be addressed through FMO theory and the free energy surfaces (FES) constructed from the reactants and their corresponding cycloadducts and their associated energy barriers.

The ground state energies of the first intermediate in each of the three individual pathways, namely cycloadducts **3.24**, **3.25** and **3.27** and the corresponding free energy of activation,  $\Delta^\ddagger G$ , (TS1, TS3, and TS6, respectively) are shown in Table 3.4. Barriers were obtained for **3.5a**+**3.21**→**3.25** (TS3,  $\Delta^\ddagger G = 20.61 \text{ kcal}\cdot\text{mol}^{-1}$ ) and **3.5a**+**3.21**→**3.27** (TS6,  $\Delta^\ddagger G = 22.29 \text{ kcal}\cdot\text{mol}^{-1}$ ). Despite many repeated attempts, a transition state structure (TSs) could not be located for **3.5a**+**3.21**→**3.24** (TS1). The notion that **3.24** may not be generated by a pericyclic process, but rather through an ionic-type mechanism producing a zwitterionic intermediate is shown in Scheme 3.9. Although the energy minimum structure for **3.37** was successfully obtained from our calculations, location of the corresponding TSs for this reaction channel was denied despite repeated attempts.

**Scheme 3.9:** Ionic pathway for the generation of **3.37** from **3.5a** and **3.21**.

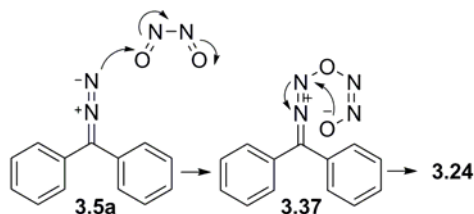
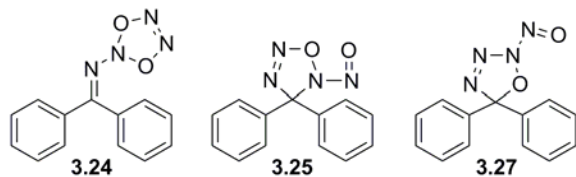


**Table 3.4:** The relative ground state energies ( $E$ ,  $H$ ,  $G$ ) of **3.24**, **3.25** and **3.27** and the corresponding free energies of activation ( $\Delta^\ddagger G$ ) for the indicated pericyclic reaction obtained at the DFT B3LYP 6-31 G(d) level.



Adduct	Energy $E$ , <sup>a</sup> $H$ , <sup>b</sup> $G$ <sup>c</sup> (a.u.) <sup>d</sup>	Relative Energy (kcal·mol <sup>-1</sup> )	Reaction channel <sup>e</sup>	Energy $E$ <sup>f</sup> , $H$ <sup>g</sup> , $G$ <sup>h</sup> (a.u.) <sup>d</sup>	Energy barriers $\Delta^\ddagger E$ , <sup>i</sup> $\Delta^\ddagger H$ , <sup>j</sup> $\Delta^\ddagger G$ <sup>k</sup> (kcal·mol <sup>-1</sup> )
<b>3.24</b>	-870.406529 <sup>a</sup>	20.627	<b>3.5a+3.21→3.24</b> (TS1)	na	na
	-870.390410 <sup>b</sup>	20.693			
	-870.451396 <sup>c</sup>	20.348			
<b>3.25</b>	-870.424840	9.137	<b>3.5a+3.21→3.25</b> (TS3)	-870.409891 <sup>f</sup>	<b>7.576</b> <sup>i</sup>
	-870.408709	9.211		-870.392874 <sup>g</sup>	<b>7.031</b> <sup>j</sup>
	-870.468458	9.642		-870.454640 <sup>h</sup>	<b>20.611</b> <sup>k</sup>
<b>3.27</b>	-870.439401	0	<b>3.5a+3.21→3.27</b> (TS6)	-870.406591	<b>9.647</b>
	-870.423387	0		-870.389594	<b>9.089</b>
	-870.483823	0		-870.451964	<b>22.289</b>

a., b., c. Energies are taken from minimized structures and are a) the electronic and zero point energies (i.e.  $E = E_{elec} + ZPE = E0$ ), b) the electronic, zero point and thermal enthalpies (i.e.  $H = E0 + H_{corr}$ ), c) the electronic, zero point and thermal free energies (i.e.  $G = E0 + G_{corr}$ ).

d. One atomic unit (a.u.) = 627.5095 kcal/mol.

e. Each TS calculation was carried out using the Synchronous Transit-Guided Quasi-Newton Method (QST2 or QST3, Ref. 317,318) using Gaussian 03 rev. B.04 or C.02 implemented on a desktop computer running Linux OS (Redhat). TS calculations times were typically 12-36 hours in duration. All structures reported here as TSs exhibit only one imaginary frequency. The imaginary vibrations were animated with Gaussview 3.09 or 4.1 to determine if they were in qualitative agreement with the bond-making/bond-breaking processes associated with the reaction of interest. In each case, intrinsic reaction coordinate (IRC, Ref. 313,314) calculations were performed to determine that the observed TS could be linked reasonably to the assumed reactant and product geometries.

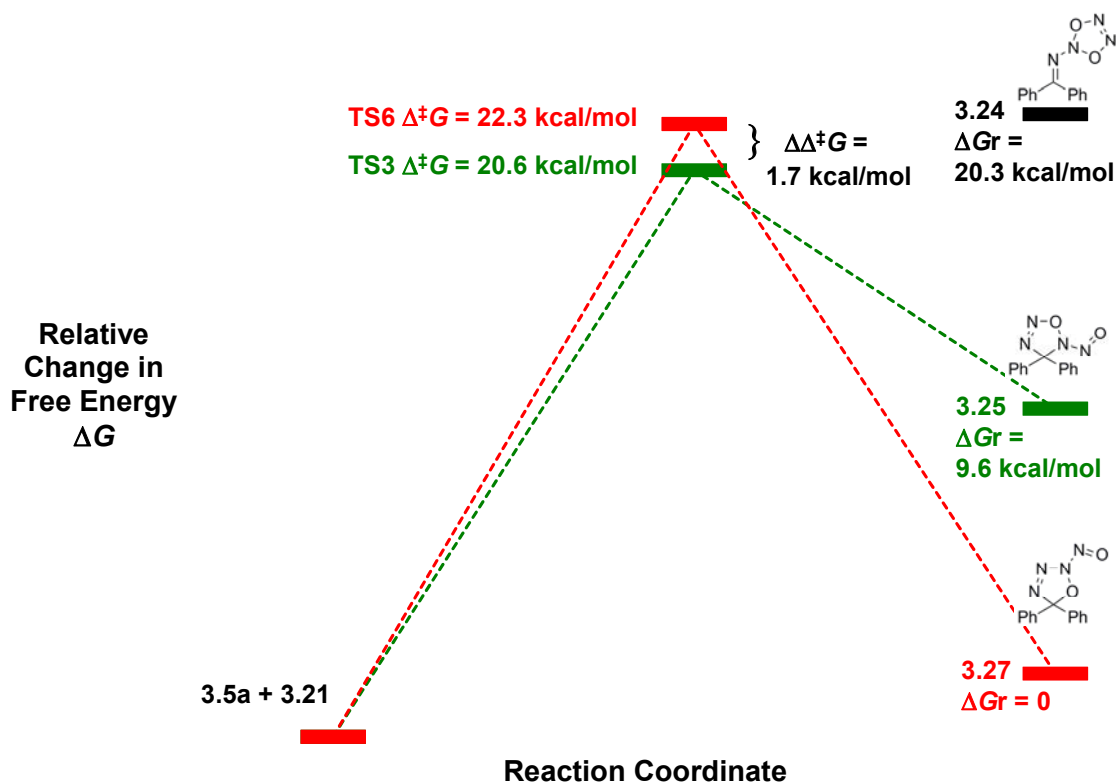
f., g., h. Energies are taken from transition state structures and are f) the electronic and zero point energies (i.e.  $E = E_{elec} + ZPE = E0$ ), g) the electronic, zero point and thermal enthalpies (i.e.  $H = E0 + H_{corr}$ ), h) the electronic, zero point and thermal free energies (i.e.  $G = E0 + G_{corr}$ ).

i.  $\Delta^\ddagger E$  (=  $\Delta^\ddagger E0$ ), j.  $\Delta^\ddagger H$ , k.  $\Delta^\ddagger G$  in kcal/mol.

Table 3.4 also reveals another important aspect regarding the two pericyclic processes. The ground state energy of cycloadduct **3.24** is 10.71 and 20.35 kcal·mol<sup>-1</sup> higher in energy than cycloadducts **3.25** and **3.27**, respectively (See Figure 3.3). Perhaps more importantly, the *ground state energy* of **3.24** is slightly higher than the *free energy of activation* observed with TS3 and TS6 by 2.04 and 0.36 kcal·mol<sup>-1</sup>, respectively. Thus, the relatively high energy of **3.24** compared to that **3.25** and **3.27** may suggest that its corresponding TS may not be accessible and that the genesis of the chelotropic product **3.24** may not be feasible on kinetic grounds. An alternative explanation is that TS1 exists as a low lying barrier with respect to **3.24** such that the reverse reaction, (i.e. the chelotropic extrusion: **3.24**→**3.5a**+**3.21**) occurs instantaneously only to refurbish the reactants which then proceed on to the other reaction channels. This data alone would suggest that the two [3+2] cycloadditions are the dominant possible pericyclic reaction channels (Pathways A and B of Scheme 3.5) and is corroborated by the isotopic labeling experiments.



**Figure 3.4:** The free energy of activation ( $\Delta^\ddagger G$ ) of the two regio-[3+2] cycloadditions of **3.5a** with **3.21** furnishing adducts **3.25** (highlighted in green) and **3.27** (highlighted in red). The relative free energy ( $\Delta Gr$ ) is given for **3.24**, **3.25** and **3.27**. All calculations are at the DFT B3LYP 6-31(G)d level of theory.

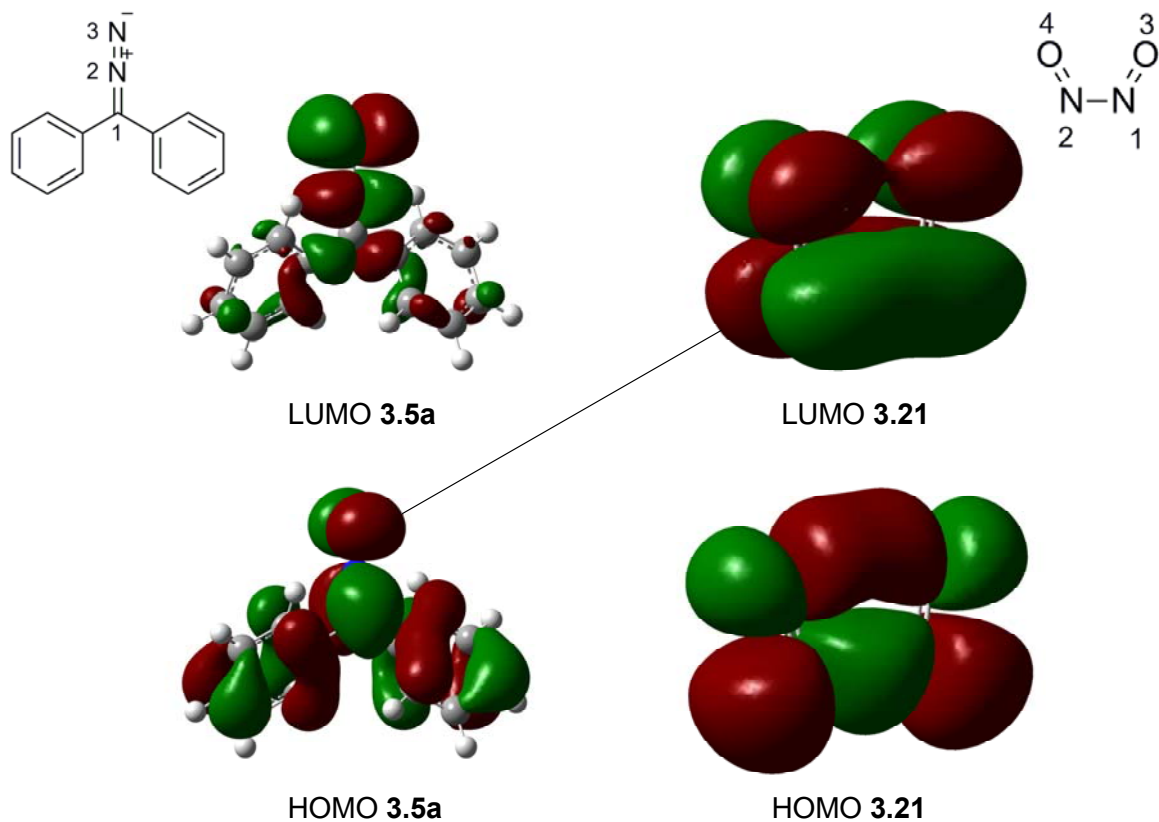


**Regioselectivity of [3+2].** The energy barrier of these two regio-[3+2] cycloadditions is shown in Figure 3.4. The  $\Delta\Delta^\ddagger G$  of the two [3+2] cycloadditions is  $1.69$  kcal·mol<sup>-1</sup> (TS3 and TS6) and provides a good indication of the relative yield of **3.7** to **3.8** (Table 3.1). From the  $\Delta^\ddagger G$  given in Table 3.4, the regioselectivity can be estimated by the Eyring relationship (see Chapter 5), which indicates a  $\sim 17:1$  ratio for **3.25:3.27**. Although this result is in qualitative

agreement with the product distribution given in Table 3.1, it is clearly at odds with the experimental result of 2.3-3.6:1 (**3.7:3.8**) and may suggest that the other reaction channels have implications on the relative yields of the three products. It is also conceivable that a cycloreversion is occurring (i.e. **3.25**  $\rightarrow$  **3.5a** + **3.21**) which refurbishes the reactants which then proceed onto the other reaction channel, TS6, generating the cycloadduct **3.27** (pathway B) which goes on to provide benzophenone.

Table 3.5 shows the FMO coefficients and energies of both reactants **3.5a** and **3.21** calculated at the DFT B3LYP 6-31 G(d) level. Reactions in which the orbitals are closest in energy and maximal bond overlap in the transition state will occur with a concomitant lowering of the energy barrier.<sup>319-323</sup> Inspection of Table 3.5 shows that for the HOMO of diphenyldiazomethane, the largest coefficients reside on the termini of the dipole (C-1 and N-3) with the N-3 coefficient possessing a marginally higher magnitude over the C-1 coefficient. In the LUMO of **3.21**, the coefficients of nitrogen and oxygen are also of comparable magnitude with the nitrogen (N-1 and N-2) slightly larger than those of oxygen (O-3 and O-4). Thus FMO theory would predict that the orbital(s) N-3 of diphenyldiazomethane and the orbital(s) N-1 (or N-2) of NO would afford the greatest orbital overlap in the transition state, generating **3.27** in the process (and hence **3.8**) as the major product as shown in Scheme 3.5, although the regioselectivity would be predicted to be very slight. As mentioned above, the relative differences in the magnitudes of the C-1 and N-3 coefficients within the HOMO of **3.5a** are so small it could be argued that both cycloadducts **3.25** and **3.27** would be produced in relatively equal amounts if the reaction were FMO controlled. Thus other means were sought to rationalize the regioselectivity.

**Table 3.5:** FMO energies (a.u.) and orbital coefficients of **3.5a** and **3.21** obtained at the DFT B3LYP 6-31 G(d) level.



Diphenyldiazomethane <b>3.5a</b>			
	Energy (a.u.)	Orbital	Coefficient
<b>HOMO</b>	-0.19138	C1 2p <sub>z</sub>	-0.33530
		C1 3p <sub>z</sub>	-0.25995
		N2 2p <sub>z</sub>	-0.14499
		N2 3p <sub>z</sub>	-0.12382
		N3 2p <sub>z</sub>	0.34587
		N3 3p <sub>z</sub>	0.28723

N <sub>2</sub> O <sub>2</sub> 3.21			
	Energy (a.u.)	Orbital	Coefficient
<b>LUMO</b>	-0.12539	N1 2p <sub>z</sub>	0.36885
		N1 3p <sub>z</sub>	0.34232
		N2 2p <sub>z</sub>	0.36894
		N2 3p <sub>z</sub>	0.34238
		O3 2p <sub>z</sub>	-0.33762
		O3 3p <sub>z</sub>	-0.30675
		O4 2p <sub>z</sub>	-0.33771
		O4 3p <sub>z</sub>	-0.30680

Inspection of TSs may offer insight into these regioselectivity issues. Early reports have indicated that significant bending of the dipole must occur to facilitate the cycloaddition.<sup>324-326</sup> Early work by Houk and coworkers suggested that dipole bending may be implicated in the regioselectivity of 1,3 dipolar cycloadditions.<sup>327</sup> The MOs in the bent dipole may differ significantly from those of the linear dipole this could conceivably have an outright influence on regioselectivity.<sup>328</sup> However calculations by the Houk group on diazomethane revealed only small changes in the relative magnitudes of the coefficients and energies of the  $\pi$  MOs of linear and bent dipoles.

The notion that the activation barrier ( $\Delta^\ddagger E$ ) is the sum of distortion ( $\Delta^\ddagger E_d$ ) and interaction energies ( $\Delta^\ddagger E_i$ ) has been used to rationalize 1,3-dipolar cycloadditions<sup>329-331</sup> and has also been applied in rationalizing endo vs. exo selectivity of Diels-Alder reactions.<sup>332-335</sup> Furthermore, other studies have indicated that distortion energies influence barrier

heights.<sup>336,337</sup> More recently, high level ab initio calculations have led to the proposal of the distortion/interaction reactivity model by Houk.<sup>329,330</sup> Those reports show that there was a direct correlation between the activation energy and the energy required to distort the dipole and dipolarophile into the TS geometries but devoid of any interaction between the dipole and dipolarophile. This observation has also been reported by others.<sup>338</sup> Indeed, examination the transition state structures TS3 and TS6 is completely consistent with these observations. The C-1---N-2---N-3 bond angles of **3.5a** were retrieved and were found to be 143.49° (TS3,  $\Delta^\ddagger G = 20.6 \text{ kcal}\cdot\text{mol}^{-1}$ ) and 135.85° (TS6,  $\Delta^\ddagger G = 22.3 \text{ kcal}\cdot\text{mol}^{-1}$ ) indicating that there is more distortion in the dipole of TS6 compared to TS3 and is in qualitative agreement with Houks observations (Figure 3.5).

Inspection of the TSs of TS3 reveals an asynchronous cycloaddition. Examination of the vibrational mode corresponding to the imaginary frequency (IF =  $-337.7 \text{ cm}^{-1}$ ) indicates this motion is principally between the diazo carbon (C-1) of **3.5a** and the nitrogen (N-1) of the NO dimer **3.21**. Asynchronicity may also be measured by calculating the difference in bond lengths between the two developing bonds ( $\Delta d$ ). Thus N-3---O-3 (2.3329 Å) subtract C-1---N-1 (1.9317 Å) gives a  $\Delta d = 0.4012 \text{ Å}$ . Examination of the TSs of TS6 also reveals an asynchronous cycloaddition in which the vibrational mode corresponding to the imaginary frequency (IF =  $-320.3 \text{ cm}^{-1}$ ) indicates the principal motion is between N-3 of **3.5a** and N-1 of **3.21**. The  $\Delta d = 0.4576 \text{ Å}$ , indicating advanced bond formation between N-3 and N-1 (1.7099 Å) over that of N-3 and O-3 (2.1675 Å). The IRC reveals minima closely resembling the reactants and products. Figure 3.5 shows the TS complexes for TS3 and TS6 with the relevant geometrical data.

**Figure 3.5:** Transition state structures of TS3 and TS6 obtained at the DFT B3LYP 6-31 G(d) level. The hydrogens have been omitted for clarity. Bond lengths are in angstroms (Å).

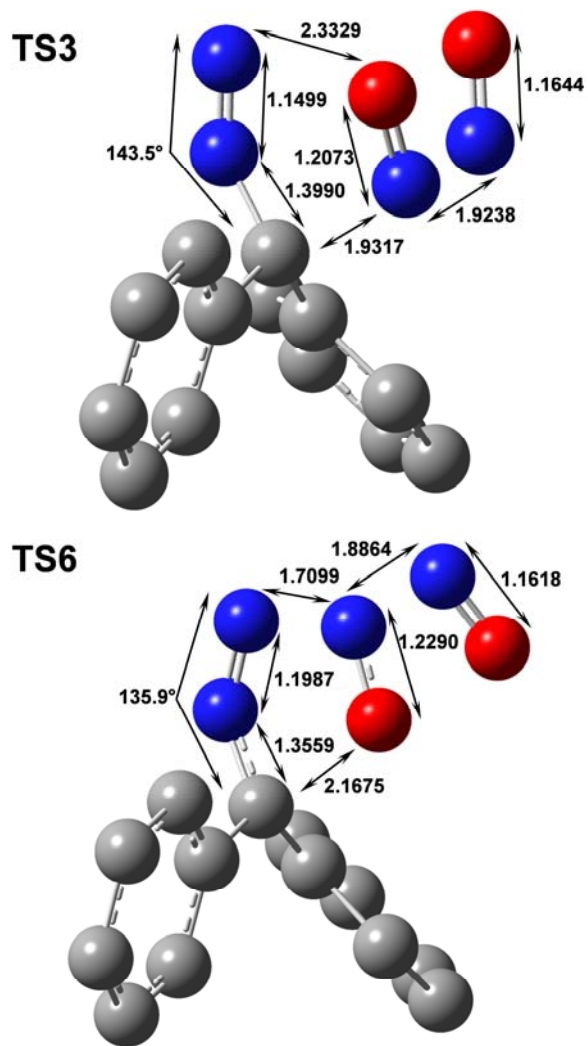


**Table 3.6:** Energies of all reactants, cycloadducts and intermediates in Pathways A, A', B and B' calculated at the DFT B3LYP 6-31-G(d) level.

Structure	Energy		Structure	Energy	
	$E,^a H,^b G^c$	(a.u.) <sup>d</sup>		$E,^a H,^b G^c$	(a.u.) <sup>d</sup>
<b>N<sub>2</sub></b>	-109.518530 <sup>a</sup>		<b>3.25</b>	-870.424840 <sup>a</sup>	
	-109.515225 <sup>b</sup>			-870.408709 <sup>b</sup>	
	-109.536980 <sup>c</sup>			-870.468458 <sup>c</sup>	
<b>3.1a</b>	-1787.902266		<b>3.26</b>	-760.998085 <sup>e</sup>	
	-1787.868405			-760.983073 <sup>e</sup>	
	-1787.968590			-761.040207 <sup>e</sup>	
<b>3.3b</b>	-1407.276601		<b>3.27</b>	-870.439401	
	-1407.249223			-870.423387	
	-1407.335709			-870.483823	
<b>3.5a</b>	-610.659980		<b>3.28a</b>	-760.969190 <sup>e</sup>	
	-610.647183			-760.954494 <sup>e</sup>	
	-610.699291			-761.011248 <sup>e</sup>	
<b>3.6</b>	-129.883620		<b>3.28b</b>	-760.973796 <sup>e</sup>	
	-129.880315			-760.958948 <sup>e</sup>	
	-129.903626			-761.015822 <sup>e</sup>	
<b>3.7</b>	-761.021965 <sup>e</sup>		<b>3.30a</b>	-760.999410	
	-761.007486 <sup>e</sup>			-760.984304	
	-761.064037 <sup>e</sup>			-761.042166	
<b>3.8</b>	-576.440229 <sup>e</sup>		<b>3.30b</b>	-761.006082	
	-576.428571 <sup>e</sup>			-760.991010	
	-576.477770 <sup>e</sup>			-761.048880	
<b>3.9</b>	-911.370683		<b>3.31</b>	-760.963250	
	-911.354297			-760.947797	

	-911.415020		-761.006167
<b>3.10</b>	-184.649054	<b>3.32</b>	945.553622
	-184.645425		-945.536250
	-184.670373		-945.598425
<b>3.21</b>	-259.761984	<b>3.33</b>	-836.169720
<i>s</i> -cis	-259.756895		-836.153745
	-259.788193		-836.213466
<b>3.21</b>	-259.746158	<b>3.34</b>	-760.975289 <sup>c</sup>
<i>s</i> -trans	-259.741216		-760.960732 <sup>c</sup>
	-259.771225		-761.016970 <sup>c</sup>
<b>3.24</b>	-870.406529	<b>3.38</b>	-2165.509844
	-870.390410		-2165.468409
	-870.451396		-2165.586092
		<b>3.39</b>	-1745.586152
			-1745.552641
			-1745.653472

a., b., c. Energies are taken from minimized structures and are a) the electronic and zero point energies (i.e.  $E = E_{\text{elec}} + \text{ZPE} = E0$ ), b) the electronic, zero point and thermal enthalpies (i.e.  $H = E0 + H_{\text{corr}}$ ), c) the electronic, zero point and thermal free energies (i.e.  $G = E0 + G_{\text{corr}}$ ).

d. One atomic unit (a.u.) = 627.5095 kcal/mol.

e. These values are added to the appropriate energies of nitrogen such that the FES is scaled as shown in Figures 3.6 and 3.7.



**Free Energy Surface.** The 1,3 dipolar cycloadditions serve as a gateway to the four reaction channels A, A', B and B' which together comprise a mechanistic manifold that furnishes the three products **3.7**, **3.8** and **3.9**. A theoretical investigation into these pathways (shown in Schemes 3.5 and 3.7) would provide detailed information on structure, mechanism and energetics.

Table 3.6 provides the ground state electronic energy ( $E$ ), enthalpy ( $H$ ) and free energy ( $G$ ) for all reactants, intermediates and products of the four reaction channels, pathways A, A', B and B'. From those structures the appropriate transition state calculations were accomplished to acquire the corresponding energy barriers (activation energy  $\Delta^\ddagger E$ , enthalpy of activation  $\Delta^\ddagger H$ , free energy of activation  $\Delta^\ddagger G$ ) shown in Table 3.7. The free energy of activation ( $\Delta^\ddagger G$ ) was then used to construct the free energy surfaces (FES) for pathways A, B and B' and are shown schematically in Figures 3.6 and 3.7. The FES for pathway A' is not schematically represented but is discussed later on. The reaction channels described in Scheme 3.8 were not obtained in spite of many repeated attempts and will not be discussed any further. The following discussion excludes comment on TS3 and TS6.

**Table 3.7:** Energies and energy barriers for reaction channels calculated at the DFT B3LYP 6-31 G(d) level.

Reaction Channel	TSs <sup>a</sup>	IF <sup>b</sup>	Energy $E^c, H^d, G^e$ (a.u.) <sup>f</sup>	Energy barrier $\Delta^\ddagger E, \Delta^\ddagger H, \Delta^\ddagger G^i$ (kcal·mol <sup>-1</sup> )	
<b>3.5a + 3.21 → 3.24</b>	TS1	na	na	na	
<b>3.24 → 3.7</b>	TS2	na	na	na	
<b>3.5a + 3.21 → 3.25</b>	TS3	-337.7	-870.409891	<b>7.576</b>	
			-870.392874	<b>7.031</b>	
			-870.454640	<b>20.611</b>	
<b>3.25 → 3.26 + N<sub>2</sub></b>	TS4	-233.5	-870.425241	<b>-0.252</b>	
			-870.409315	<b>-0.380</b>	
			-870.468311	<b>0.092</b>	
<b>3.26 → 3.7</b>	TS5	-473.2	-760.944410 <sup>j</sup>	<b>33.682</b>	
			-760.928894 <sup>j</sup>	<b>33.998</b>	
			-760.988158 <sup>j</sup>	<b>32.661</b>	
			-928.7	-760.861769 <sup>j</sup>	<b>85.539</b>
			-760.847163 <sup>j</sup>	<b>85.285</b>	
			-760.903516 <sup>j</sup>	<b>85.775</b>	
<b>3.5a + 3.21 → 3.27</b>	TS6	-320.3	-870.406591	<b>9.647</b>	
			-870.389594	<b>9.089</b>	
			-870.451964	<b>22.289</b>	
<b>3.27 → 3.28 + N<sub>2</sub></b>	TS7	-352.6	-870.431637	<b>4.872</b>	
			-870.415717	<b>4.813</b>	
			-870.475326	<b>5.332</b>	
<b>3.28 → 3.8 + N<sub>2</sub>O</b>	TS8	-405.4	-760.971919 <sup>j</sup>	<b>1.178</b>	
			-760.957031 <sup>j</sup>	<b>1.203</b>	
			-761.014550 <sup>j</sup>	<b>0.798</b>	

<b>3.26 → 3.30a</b>	TS9	-473.0	-760.944412	<b>33.680</b>
			-760.928895	<b>33.997</b>
			-760.988157	<b>32.662</b>
<b>3.26 → 3.30b</b>	TS10	-89.3	-760.978333	<b>12.395</b>
			-760.963806	<b>12.090</b>
			-761.020082	<b>12.629</b>
<b>3.30a → 3.7</b>	TS11a	-607.8	-760.921280	<b>49.027</b>
			-760.905826	<b>49.246</b>
			-760.965742	<b>47.957</b>
<b>3.30b → 3.7</b>	TS11b	-607.9	-760.921280	<b>53.214</b>
			-760.905827	<b>53.453</b>
			-760.965742	<b>52.169</b>
<b>3.30b → 3.31</b>	TS12	-117.3	-760.960560	<b>28.565</b>
			-760.946078	<b>28.195</b>
			-761.001271	<b>29.875</b>
<b>3.31 → 3.32</b>	TS13	na	na	na
<b>3.32 → 3.33</b>	TS14	-342.7	-945.554201	<b>-0.363</b>
			-945.537163	<b>-0.573</b>
			-945.598605	<b>-0.113</b>
<b>3.26 → 3.34</b>	TS15	-329.9	-760.939724 <sup>j</sup>	<b>36.622</b>
			-760.925482 <sup>j</sup>	<b>36.139</b>
			-760.980870 <sup>j</sup>	<b>37.235</b>
<b>3.34 → 3.28a</b>	TS16	-248.3	-760.952421 <sup>j</sup>	<b>14.349</b>
			-760.937808 <sup>j</sup>	<b>14.385</b>
			-760.993862 <sup>j</sup>	<b>14.500</b>
<b>3.34 → 3.8</b>	TS17	-404.8	-760.971919	<b>2.115</b>
			-760.957030	<b>2.323</b>
			-761.014560	<b>1.512</b>
<b>3.1a + 3.21 → 3.38</b>	TS21	-217.5	-2047.625036	<b>24.607</b>

			-2047.587087	<b>23.979</b>	
			-2047.696795	<b>37.643</b>	
<b>3.3b + 3.21</b>	<b>→ 3.39</b>	TS22	-428.5	-1667.009000	<b>18.565</b>
				-1666.977252	<b>18.114</b>
				-1667.073112	<b>31.871</b>

a. Each TS calculation was carried out using the Synchronous Transit-Guided Quasi-Newton Method (QST2 or QST3, Ref. 317,318) using Gaussian 03 rev. B.04 or C.02 implemented on a desktop computer running Linux OS (Redhat). TS calculations times were typically 12-48 hours in duration. All structures reported here as TSs exhibit only one imaginary frequency. The imaginary vibrations were animated with Gaussview 3.09 or 4.1 to determine if they were in qualitative agreement with the bond-making/bond-breaking processes associated with the reaction of interest. In each case, intrinsic reaction coordinate (IRC, Ref. 313,314) calculations were performed to determine that the observed TS could be linked reasonably to the assumed reactant and product geometries.

b. IF = imaginary frequency in reciprocal centimeters and are not scaled (Ref. 315).

c., d., e. Energies are taken from transition state structures and are c) the electronic and zero point energies (i.e.  $E = E_{elec} + ZPE = E0$ ), d) the electronic, zero point and thermal enthalpies (i.e.  $H = E0 + H_{corr}$ ), e) the electronic, zero point and thermal free energies (i.e.  $G = E0 + G_{corr}$ ).

f. One atomic unit (a.u.) = 627.5095 kcal/mol.

g.  $\Delta^\ddagger E (= \Delta^\ddagger E0)$ , h.  $\Delta^\ddagger H$ , i.  $\Delta^\ddagger G$  in kcal/mol.

j. These values are added to the appropriate energies of nitrogen such that the FES is scaled as shown in Figures 3.6 and 3.7.

**Figure 3.6:** The FES of the reactants **3.5a** and **3.21** generating products **3.7** and **3.8** (Pathways A in green, Pathway B in red) calculated at the DFT B3LYP 6-31-G(d) level.

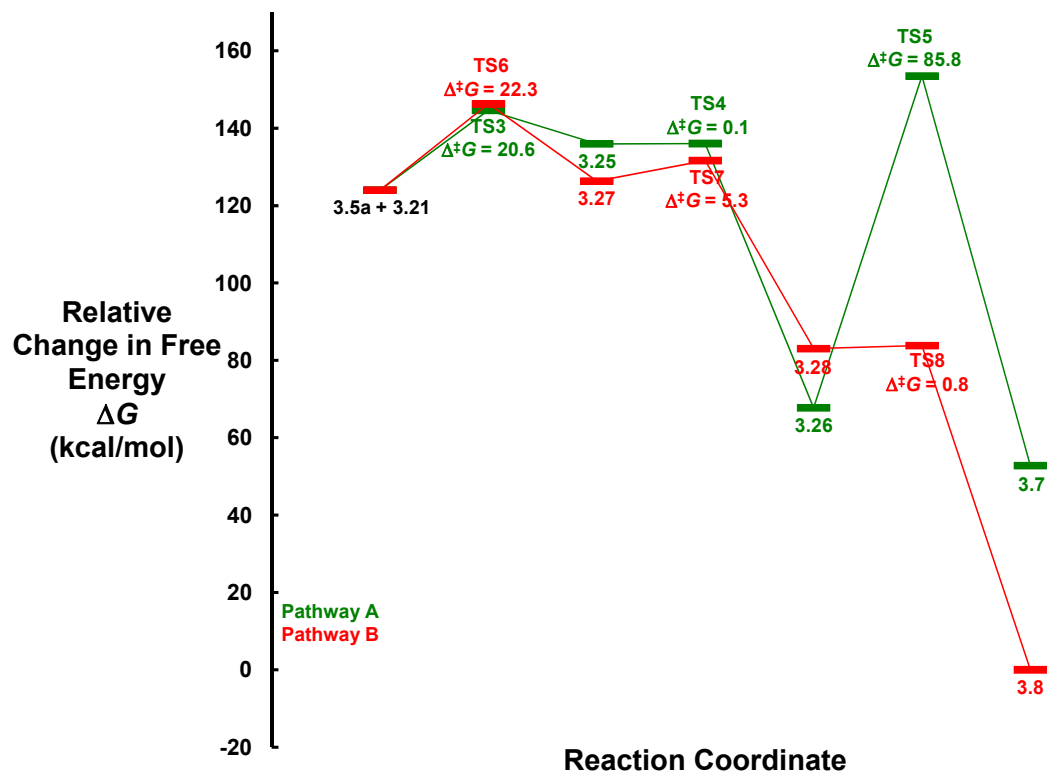
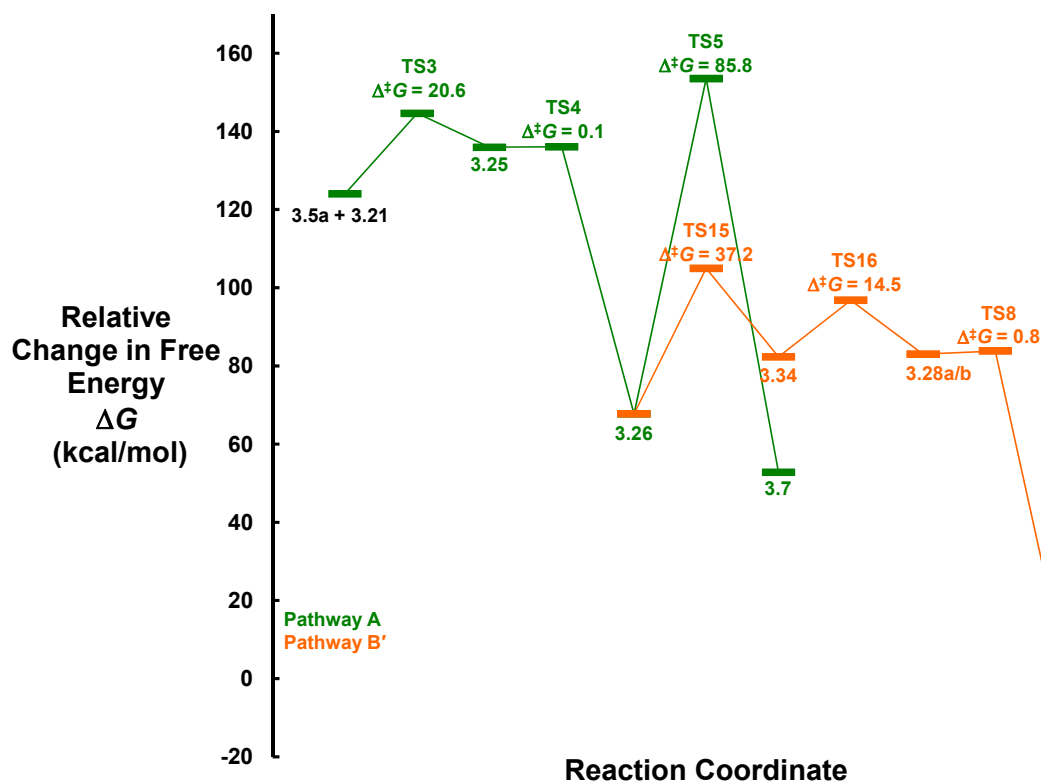


**Figure 3.7:** The FES of the reactants **3.5a** and **3.21** generating products **3.7** and **3.8** (Pathways A in green, Pathway B' in orange) calculated at the DFT B3LYP 6-31-G(d) level.



**Pathway A: Nitrimine.** The cycloadduct **3.25** generates the *N*-nitrosanitronne **3.26** and N<sub>2</sub> (TS4 Δ<sup>‡</sup>G = 0.09 kcal·mol<sup>-1</sup>) and appears to be thermodynamically driven (see Scheme 3.5 and Figure 3.6). The one step transformation of **3.26** to nitrimine **3.7** (TS5 Δ<sup>‡</sup>G = 32.7 kcal·mol<sup>-1</sup>) provided a TSs that appeared to be consistent with the product. Examination of the vibrational mode appeared to correspond with the bond making/breaking process. However, the intrinsic reaction coordinate (IRC) for this calculation did not converge and appeared ambiguous. Incidentally, this TSs appeared to be identical to that obtained for the

conversion of **3.26** to the *O*-nitrosooxime **3.30a** (TS9  $\Delta^\ddagger G = 32.7 \text{ kcal}\cdot\text{mol}^{-1}$ ) described in pathway A and is corroborated by the energy values found in Table 3.7. These results provided the impetus to locate new TSs and accordingly the computational parameters were changed to a tighter grid search to provide a second TSs and an IRC profile that was consistent with the calculation of interest. However, the barrier  $\Delta^\ddagger G$  ( $85.8 \text{ kcal}\cdot\text{mol}^{-1}$ ) is not consistent for reactions carried out at ambient conditions. Thus other reaction channels were considered. The nitrone **3.26** provided the *O*-nitrosooxime **3.30a/3.30b** (TS9, TS10 respectively) which in turn furnish **3.7** (TS11a, TS11b respectively) and represents another route by which the nitrimine **3.7** may be accessed. The pathway of TS9 to TS11 would be considered to make a very small contribution to the overall pathway owing to the higher energy barriers. It is conceivable that other reaction channels exist (such as an intermolecular oxidative process) some of which are shown in Scheme 3.10 but were not explored owing to time constraints in the present thesis. Efforts towards identifying other reaction channels in pathway A that are consistent with experimental results are the focus of ongoing studies.

**Pathway A': Dinitrodiphenylmethane.** Generation of the *N*-nitrosonitron **3.26** provides access to four different reaction channels (TS5, TS9, TS10 and TS15). Three of these have been discussed already TS5, TS9 and TS10 with TS15 found in pathway B'. An equilibrium is most likely established between **3.30a** and **3.30b** but it is **3.30b** that furnishes **3.31** (TS12  $\Delta^\ddagger G = 29.9 \text{ kcal}\cdot\text{mol}^{-1}$ ). Attempts at using **3.30a** to access the reaction channel that would furnish **3.31** were denied. The reaction channel TS13 did not converge and consequently the entire FES for pathway A' could not be completed and hence is not shown. Of special interest, the cycloreversion of **3.32** to **3.33** (TS14  $\Delta^\ddagger G = -0.11 \text{ kcal}\cdot\text{mol}^{-1}$ ) is the only reaction

channel found in this study that is barrierless. These types of reactions are typical of carbene and/or radical reactions. The extrusion of molecular nitrogen and the formation of the nitro moiety are thermodynamically driven but the negative energy barrier may be describing other effects that are not immediately apparent. Descriptions of barrierless reactions are found throughout the literature the majority of which focus on carbenes and radicals with very few reports on closed shell molecules. An alternative explanation is that an intermediate exists that has not been identified and possesses a lower energy than that for the TSs. This possibility has been described by others.<sup>339</sup> This would then provide a positive value for the energy barrier. Furthermore, Wang and Weitz also note that a negative  $\Delta^\ddagger G$  is likely due to errors in the DFT calculation. The assumption of harmonic vibrational modes can also introduce errors in the calculation of the enthalpy, entropy and zero point energy corrections and thus the most suitable interpretation is that  $\Delta^\ddagger G$  is small. The idea of hidden intermediates and hidden transition states has been reported by others.<sup>340</sup> Efforts focused on resolving this issue is the subject of further studies.

**Pathway B: Benzophenone.** This pathway constitutes the major pathway by which benzophenone is produced. The acquired TSs were unremarkable. The TSs of TS7 and TS8 ( $\Delta^\ddagger G = 5.3$  and  $0.8$  kcal·mol<sup>-1</sup>, respectively) provide barriers consistent with room temperature reactions.

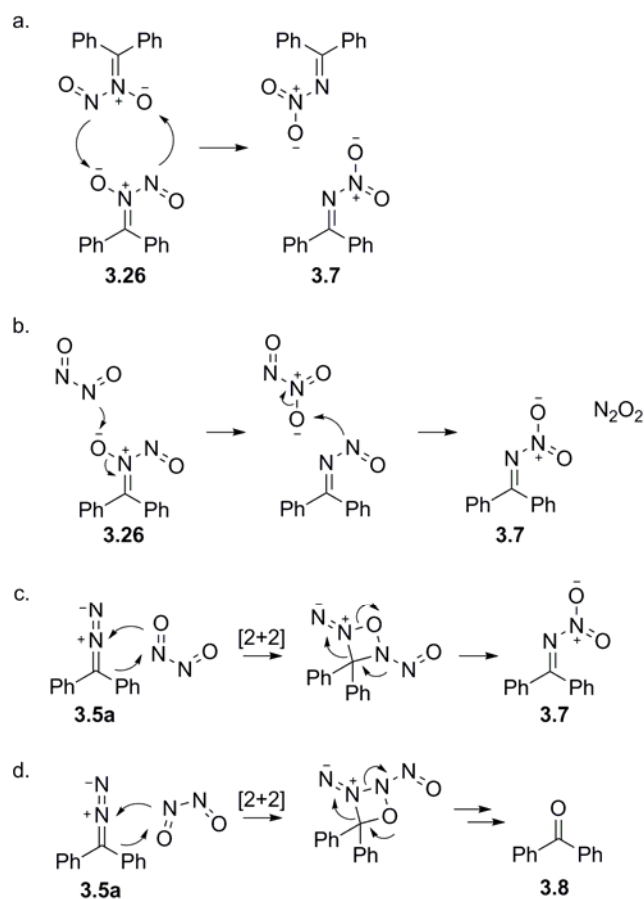
**Pathway B': Benzophenone.** This may be considered the minor pathway that produces benzophenone. TS15 ( $\Delta^\ddagger G = 37.2$  kcal·mol<sup>-1</sup>) is the kinetic bottleneck in this pathway. The nitrene **3.26** is presumably able to generate all three products but it is the only intermediate identified in this study that produces the nitrimine **3.7**. However, production of the nitrene



**3.26** also contributes to the production of benzophenone **3.8** and hence a small amount of **3.26** may be available to contribute to pathway B' that would otherwise be available for pathways A and A'. The generation of the *N*-nitrosooxaziridine **3.34** furnishes **3.28a** (TS16  $\Delta^\ddagger G = 14.5 \text{ kcal}\cdot\text{mol}^{-1}$ ) which presumably undergoes a conformational change to give **3.28b** which then produces benzophenone (TS8  $\Delta^\ddagger G = 0.8 \text{ kcal}\cdot\text{mol}^{-1}$ ) in the same manner already described for pathway B. Benzophenone could not be accessed employing **3.28a**. The TSs obtained for the reaction channel TS17 ( $\Delta^\ddagger G = 1.5 \text{ kcal}\cdot\text{mol}^{-1}$ ) appeared identical to the TSs for TS8 as shown by their respective energies and thus TS17 may represent a variation of the reaction channel TS8. Efforts are ongoing to address these issues.

Other intermediates were considered in the manifold but were not obtained owing to non-convergence in the calculation. Some of these are shown in Scheme 3.10.

**Scheme 3.10:** Possible reaction channels that may generate **3.7** and **3.8**.

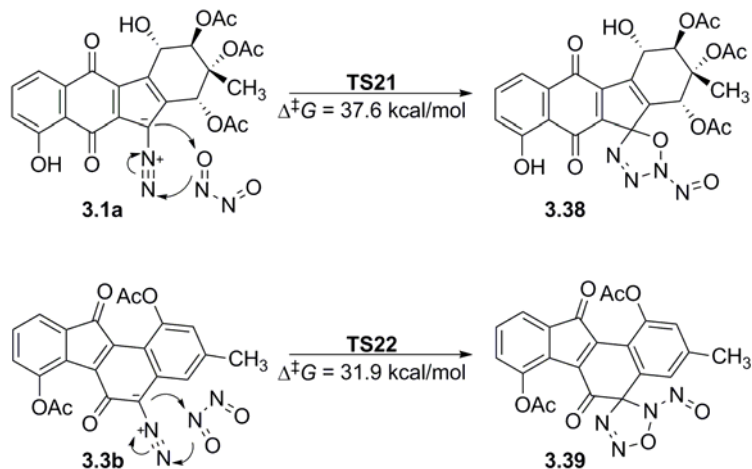


### 3.2.5 Kinamycin A and Isoprekinamycin diacetate

Having satisfied our query about the nature of the nitric oxide reactivity with diphenyldiazomethane, we then eagerly turned our attention towards the kinamycin group of natural products. Under the same conditions employed in the diphenyldiazomethane experiments, kinamycin A and isoprekinamycin diacetate were exposed to nitric oxide. We recovered both species from the reaction quantitatively without any indication of chemical modification as observed by <sup>1</sup>H and <sup>13</sup>C NMR spectroscopy. This led us to undertake some

calculations which may explain the lack of reactivity of kinamycins towards NO whilst simpler model diaryl diazo compounds react. The ground state energies of the natural products and simple diazo compounds were examined. Although we have established that the regioselectivity of  $N_2O_2$  with diphenyldiazomethane is not FMO controlled, FMO interactions will contribute to the activation energy. The HOMO of both kinamycin A (-0.24573 a.u.) and isoprekinamycin diacetate (-0.22680 a.u.) were examined and found to be significantly lower than that of diphenyldiazomethane by 33.8 and 21.4 kcal·mol<sup>-1</sup>, respectively. As well, the free energy of activation ( $\Delta^\ddagger G$ ) for the corresponding [3+2] cycloadditions were found to be significantly larger and that acquisition of the 5-membered intermediates **3.38** and **3.39** would appear to be inaccessible on kinetic grounds (Scheme 3.11). Furthermore, the other scenario in which the interaction of the HOMO of  $N_2O_2$  (-0.21127 a.u.) with the LUMO of either kinamycin A (-0.13487 a.u.) or IPK diacetate (-0.12084 a.u.) indicate that these interactions would be of lesser importance owing to the larger energy gaps than that of the HOMO of diphenyldiazomethane with the LUMO of  $N_2O_2$  as described in Figure 3.3. These observations would appear to justify the lack of reactivity of the natural products in comparison to simple diaryl diazomethanes.

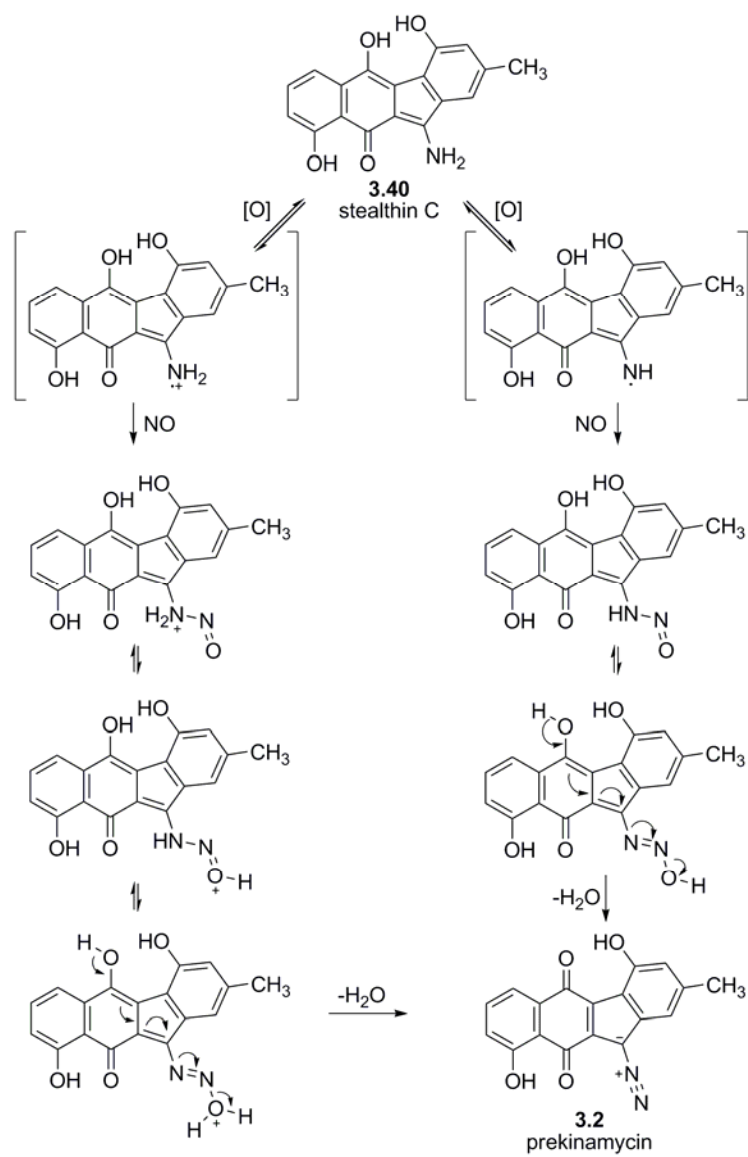
**Scheme 3.11:** TS obtained for 1,3 dipolar cycloaddition of  $N_2O_2$  with kinamycin A and IPK diacetate.



### 3.2.6 A Proposal for the source of the terminal nitrogen of the Diazo group

Certain species of bacteria found in the soil are known to convert nitrate to ammonia with the production of nitric oxide via a sequence of redox reactions.<sup>74</sup> The group of natural products known as the stealthins have been shown to be potent radical trapping agents.<sup>40,41</sup> One member, stealthin C, has been isolated from fermentation broths of *S. murayamaensis* which has led the Waterloo group to speculate that *N*-nitrosation events may occur within the organism that, through a series of chemical reactions, generate the diazo group furnishing prekinamycin (Scheme 3.12).

**Scheme 3.12:** Possible *N*-nitrosation events in the biosynthesis of the diazo group.



### 3.3 Conclusion

Diphenyldiazomethane reacts with nitric oxide to produce three products nitrimine **3.7**, benzophenone **3.8** and a previously unidentified product, dinitrodiphenylmethane **3.9** via two separate [3+2] cycloadditions, supported by isotopic labeling experiments and theoretical studies. As well we observed that the natural products kinamycin A and isoprekinamycin diacetate were found to be unresponsive to nitric oxide exposure. This lack of reactivity was supported by theoretical studies. This suggests that the kinamycins are not NO scavengers and that their biological role interpreted through the context of the diazo group remains speculative. Other ongoing studies that are addressing the mode of activity of the kinamycins will be disclosed in due course.

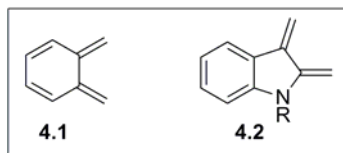
## Chapter 4

# Diels-Alder Reactions of Indole-2,3-quinodimethanes and Related Chemistry

### 4.1 Introduction

The highly reactive *cis*-diene *o*-quinodimethane **4.1** (*o*-QDM) also known as *o*-xylylene or *o*-quinododimethide and 2,3-dimethylene-2,3-dihydro-1*H*-indole, the so-called indole-2,3-quinodimethane (IQDM) **4.2** have been the focus of extensive research over many years owing to their synthetic value due in part to the variety of methods available to generate them.

**Figure 4.1:** The structures of *o*-QDM **4.1** and IQDM **4.2**.

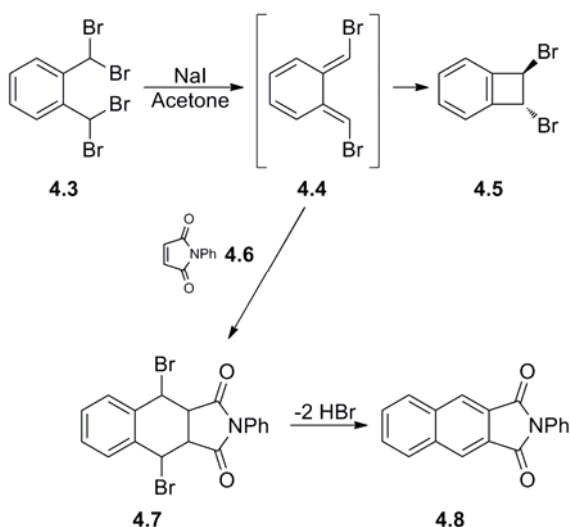


### 4.2 Background and Overview

#### 4.2.1 *o*-QDM

In 1910, Finkelstein reported the isolation of 1,2-dibromobenzocyclobutene **4.5** upon treating  $\alpha,\alpha,\alpha',\alpha'$ -tetrabromo-*o*-xylene **4.3** with sodium iodide (Scheme 4.1).<sup>341</sup> It was assumed that the *o*-QDM **4.4** was generated and this was subsequently confirmed by Cava *et al.* who reported the trapping of **4.4** in a Diels-Alder reaction with *N*-phenylmaleimide, establishing *o*-quinodimethane **4.4** as the obligatory intermediate.<sup>342,343</sup>

**Scheme 4.1:** The early experiments of Finkelstein and Cava.



Owing to the synthetic potential of **4.1**, others have reported alternative methods for generating *o*-QDM, some of which are shown in Scheme 4.2. There are six major classifications based on the precursor and method employed to generate *o*-QDM and these have been reviewed elsewhere:<sup>344-346</sup>

- 1,4-elimination of  $\alpha,\alpha'$ -substituted *o*-xylenes **4.9** induced by:
  - a. thermal eliminations.
  - b. reductive eliminations.
  - c. base-catalyzed eliminations.
  - d. ion-induced catalyzed eliminations.
2. Diels-Alder-cycloreversions of **4.10** and are typically lactones or azo compounds, where  $X-Y = (-OC=O)$  and  $(-N=N-)$ , respectively.



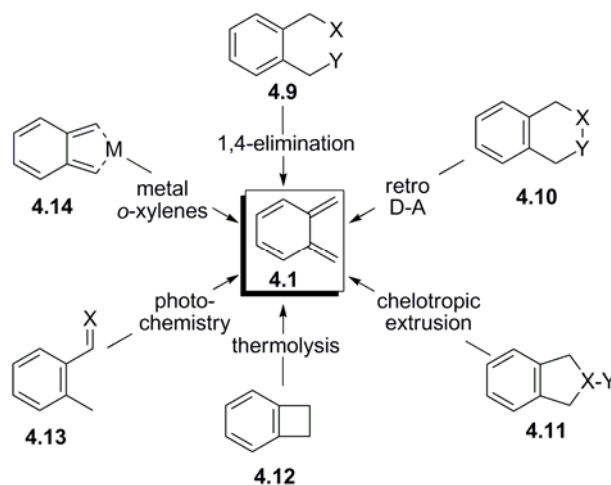
3. Chelotropic extrusion from **4.11** and are typically sulfones or ketones, where X-Y = (SO<sub>2</sub>) and (C=O), respectively.

4. Thermolysis of benzocyclobutenes **4.12**.

5. Photo-enolization of *o*-methylbenzaldehydes **4.13** (X = O) and/or photo-rearrangement of *o*-methylstyrenes **4.13** (X = CH<sub>2</sub>).

6. From *o*-xylylene-metal complexes **4.14**.

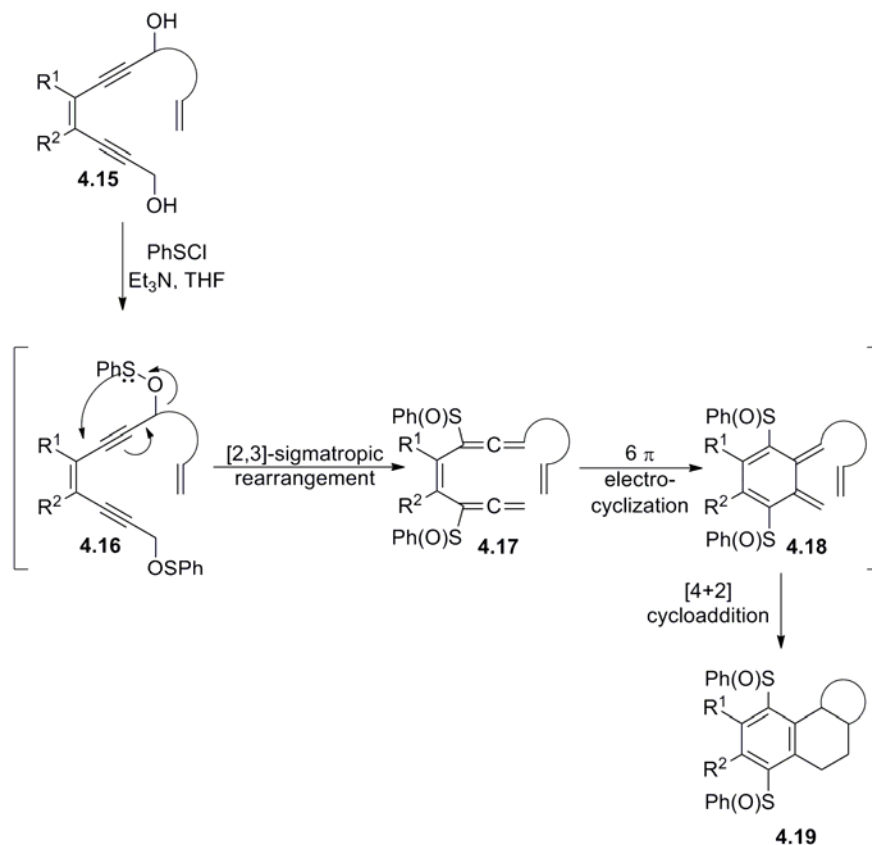
**Scheme 4.2:** Methods of generating *o*-QDM **4.1**.



More recently, Kitagaki<sup>347</sup> has reported the generation of *o*-QDM **4.18** and its use in Diels-Alder (DA) reactions, prepared in situ from ene-bis(propargyl alcohols) **4.15** and benzenesulfonyl chloride to produce the ene-bis(propargyl sulfenate) **4.16** which undergoes a [2,3]-sigmatropic rearrangement to afford the ene-bis(sulfinylallene) **4.17** (Scheme 4.3). Subsequently, a 6 $\pi$  electrocyclization of **4.17** furnishes the *o*-QDM **4.18** for the ensuing intramolecular Diels-Alder (IMDA) cycloaddition to give a one-pot construction of the polycyclic adduct **4.19**. In addition to the obvious benefit of a single pot preparation of the

polycycle, this method also possesses the intrinsic advantage of avoiding high temperatures required by the many of the methods illustrated in Scheme 4.2. Kitagaki has also demonstrated the use of this method in intermolecular cycloadditions.<sup>348</sup>

**Scheme 4.3:** Kitagaki's method for *o*-QDM generation and use in IMDA.

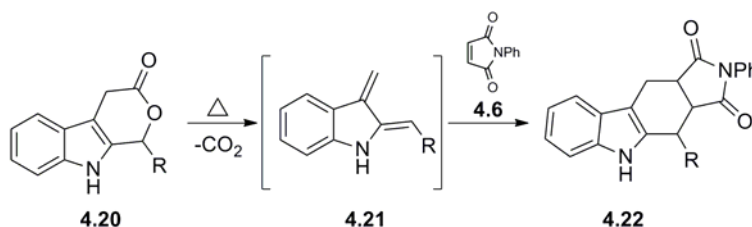


#### 4.2.2 IQDM

In 1964, Plieninger *et al.*, extending the ideas put forth by Finkelstein and Cava *et al.*, reported the generation of indole-2,3-quinodimethane **4.21** in situ from pyranoidole **4.20** and demonstrated its reactivity in [4 + 2] cycloadditions as shown in Scheme 4.4.<sup>349</sup> The

adduct **4.22** was characterized only by elemental analysis and no further reports were issued by the Plieninger group on this chemistry.

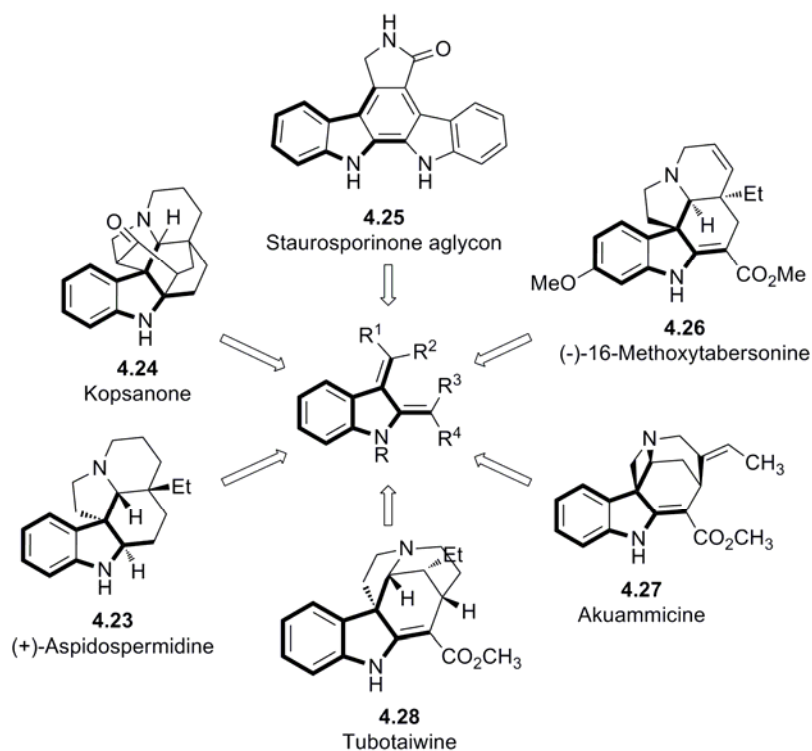
**Scheme 4.4:** Plieninger's generation of IQDM and use in Diels-Alder reactions.



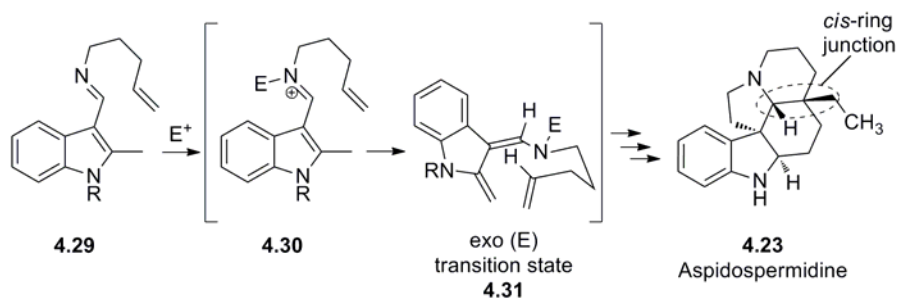
The access to various heterocycles using IQDM chemistry has been demonstrated in the syntheses of several natural products such as aspidospermidine **4.23**,<sup>350,351</sup> kopsanone **4.24**,<sup>352,353</sup> staurosporinone **4.25**,<sup>354,355</sup> and 16-methoxytabersonine **4.26**<sup>356</sup> (Figure 4.2). IQDM chemistry could be potentially applied to the syntheses of akuammicine **4.27**<sup>357-365</sup> and tubotaiwine **4.28**<sup>366-368</sup> as well as the vinca alkaloids, vindoline<sup>356,369</sup> and vinblastine<sup>370,371</sup> (not shown).

Magnus and coworkers have made extensive use of intramolecular Diels-Alder reactions employing IQDMs in the synthesis of complex indole alkaloids.<sup>350-356,370,372</sup> In particular, the general applicability of this method towards the syntheses of the *Aspidosperma* alkaloids was first demonstrated by Magnus<sup>350,372</sup> who reported the total synthesis of the natural product *dl*-aspidospermidine **4.23**,<sup>351</sup> by generating an IQDM in situ which undergoes an intramolecular Diels-Alder reaction as the key step (Scheme 4.5). The desired *cis*-fused geometry of the ring-junction between the piperidine and cyclohexane rings was attributed to the exo (E) transition state **4.31**.

**Figure 4.2:** Natural products accessible through IQDM chemistry.



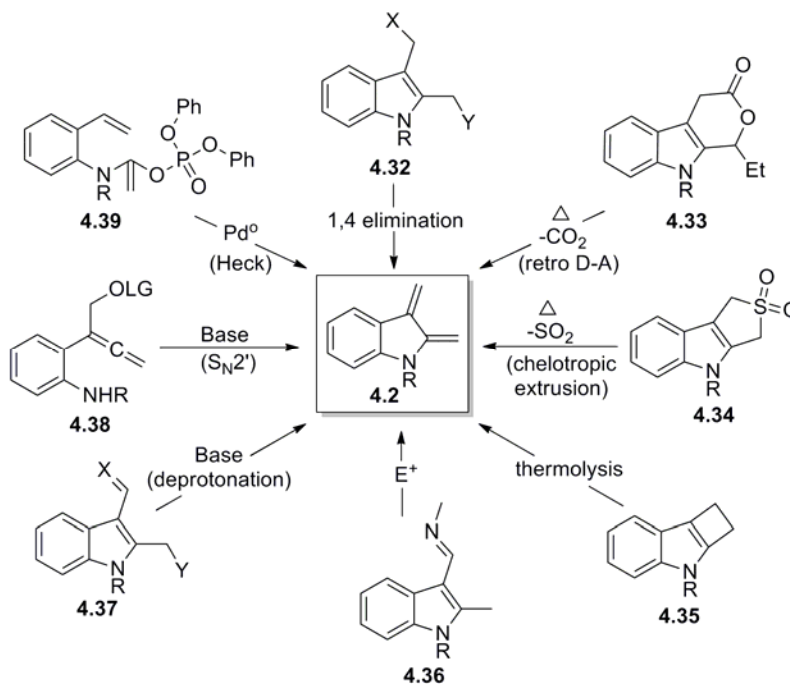
**Scheme 4.5:** The key step of Magnus' total synthesis of *dl*-aspidospermidine.



Methods for generating **4.2** are shown in Scheme 4.6 and have been reviewed elsewhere.<sup>346,373-375</sup> Recent reports employing **4.38** and **4.39** by Mukai and coworkers<sup>376,377</sup>

and Fuwa and Sasaki,<sup>378,379</sup> respectively, as IQDM progenitors have extended the synthetic scope of IQDM chemistry.

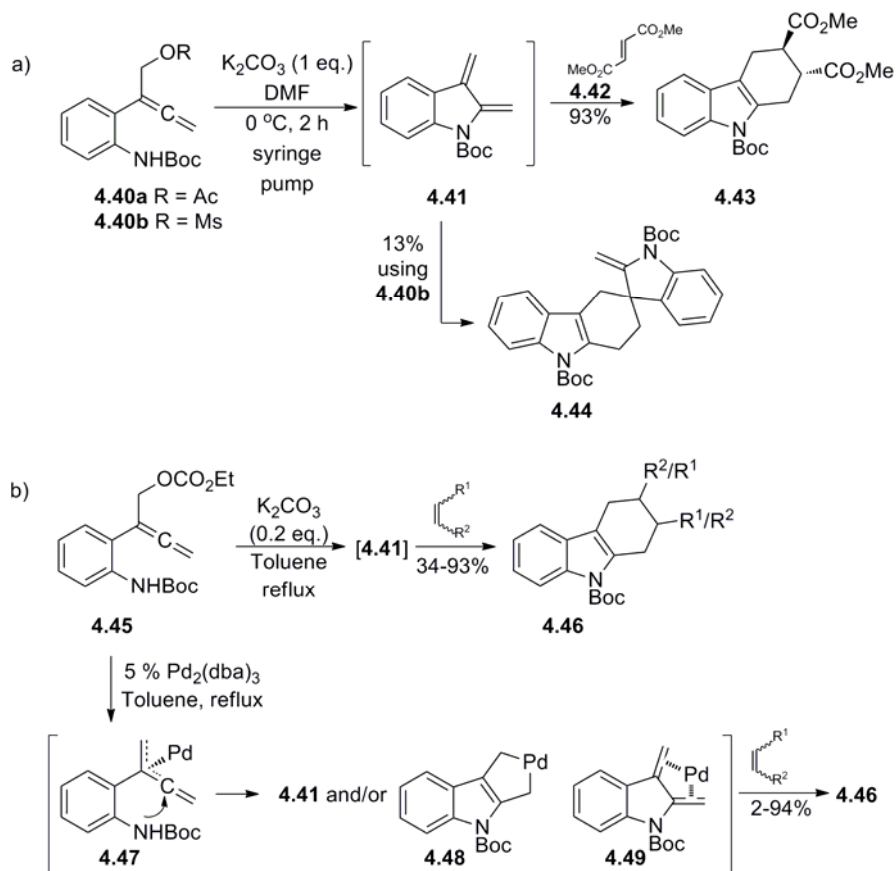
**Scheme 4.6:** Methods of generating IQDM **4.2**.



Recently, Mukai *et al.* have developed a novel approach to access IQDMs under mild conditions (Scheme 4.7a).<sup>376</sup> The 2-allylaniline **4.40a** produces IQDM **4.41** in situ under basic conditions, which can then be trapped with dienophiles already present in the reaction vessel. When **4.40a** was added slowly via syringe to solution of **4.42** in DMF and potassium carbonate, the adduct **4.43** was provided in 93% yield. Premixing a solution of **4.40b** and **4.42** was less efficient, providing **4.43** in 76% yield in addition to a small amount (13%) of the homodimer **4.44**. When dimethyl maleate (not shown) was substituted for dimethyl

fumarate **4.42**, the adduct was produced in 7% yield with an 85% recovery of **4.44**, a significant decrease compared to the reaction with dimethyl fumarate.

**Scheme 4.7:** Mukai's generation of IQDM **4.41** and its Diels-Alder trapping.

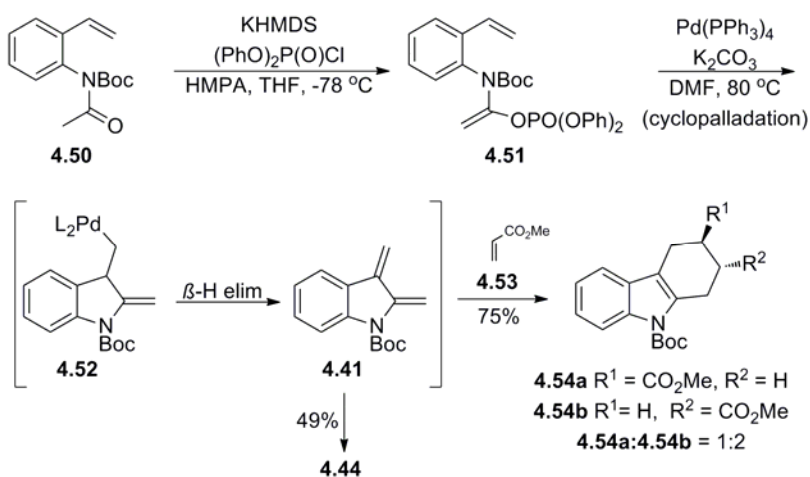


A subsequent report<sup>377</sup> by those authors addressed these issues using alternative methods which included substituting the acetoxy group with an ethyl carbonate group (as in **4.45** in Scheme 4.7b). When **4.45** was refluxed with dimethyl maleate in toluene and a catalytic amount of potassium carbonate, the yield increased markedly to 82% with 13% of **4.44** produced. This method worked well for a number of dienophiles, but not so for quinones. Realizing that allylic carbonates can produce the corresponding ( $\pi$ -allyl)-palladium complex

**4.47** (or the related palladium complexes **4.48** and **4.49**) when treated with Pd<sup>0</sup> catalysts, those workers treated **4.45** with 5% Pd<sub>2</sub>(dba)<sub>3</sub> in refluxing toluene to produce good to excellent yields of Diels-Alder adducts not accessible under basic conditions. Thus **4.45** was able to provide access to various targets under divergent conditions.

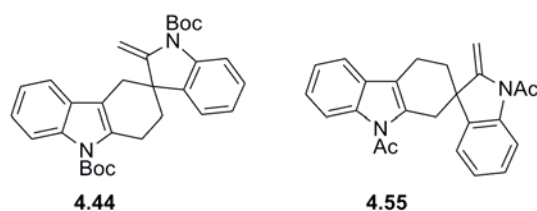
Fuwa and Sasaki have also implemented Pd<sup>0</sup> catalysis in a novel tandem intramolecular Heck/Diels-Alder reaction (Scheme 4.8).<sup>378</sup> IQDM **4.41** was generated from the acyclic  $\alpha$ -phosphono enecarbamate **4.51** and trapped with **4.53** to provide a 1:2 ratio of **4.54a**:**4.54b** in 75% yield. This procedure could be modified by changing the solvent to either THF, toluene or acetonitrile to accommodate various dienophiles which afforded yields of 32-93%. The dimer **4.44** was recovered in 49% yield in the absence of a dienophile. A follow up report by these workers employed allenamides in place of **4.51** to generate IQDM which were then trapped with various dienophiles in yields of 53-93%.<sup>379</sup>

**Scheme 4.8:** Fuwa and Sasaki's generation of **4.41** and its Diels-Alder trapping.



The observation of **4.44** has provided evidence of the intermediacy of IQDM **4.41** that was first reported by Marinelli in 1982.<sup>380</sup> Marinelli's report was significant as it was the first to describe Diels-Alder reactions of IQDMs with unsymmetrical dienophiles. Although the reports mentioned here have provided a structure for the homodimer and have suggested it to be **4.44**, there is a lack of evidence, spectroscopic or otherwise, to support this structural assignment. Work performed from this laboratory has revealed that the homodimer possesses structure **4.55** (Figure 4.3). This structure was deduced from extensive NMR studies as well as a single crystal X-ray study.<sup>381,382</sup> Efforts from this laboratory towards the structural elucidation of the homodimer are discussed in the following sections.

**Figure 4.3:** The proposed structure of the homodimer assigned to be **4.44** first reported by Marinelli. The structural reassignment of the homodimer to **4.55** as reported by S.F. Vice.<sup>381</sup>



## 4.3 Previous work in this laboratory

### 4.3.1 Early studies

This laboratory has extensive experience with the chemistry of IQDMs.<sup>381-388</sup> S.F. Vice developed the initial conditions to generate *N*-acetyl-indole-2,3-quinodimethane (*N*-Ac-IQDM) **4.58** (Scheme 4.9).<sup>381</sup> Heating *N*-acetyl-2,3-dimethyl indole **4.56** with two equivalents of *N*-bromosuccinimide in carbon tetrachloride with a 250W Brooder lamp



afforded **4.57** at 80% yield and in gram quantities. These conditions were later modified by J.Y.J. Wu in this group, changing the solvent from carbon tetrachloride to dichloromethane.<sup>386</sup> Initial experiments using zinc, DMF and maleic anhydride failed to produce the desired adduct **4.60**, instead returning **4.56** and **4.55**, indicating the dimerization had occurred faster than the cycloaddition. It was also found that dimerization was highly regioselective producing a single diastereomer **4.55**. Since the dimer could exist as four possible isomers, its structure was elucidated through extensive NMR studies on selectively deuterated analogues as well as by a single crystal X-ray crystallographic analysis. The structure of the homodimer was determined to be **4.55** (Figure 4.4).

**Scheme 4.9:** S.F. Vice's initial conditions generating IQDM and trapping in DA reactions.<sup>381</sup>

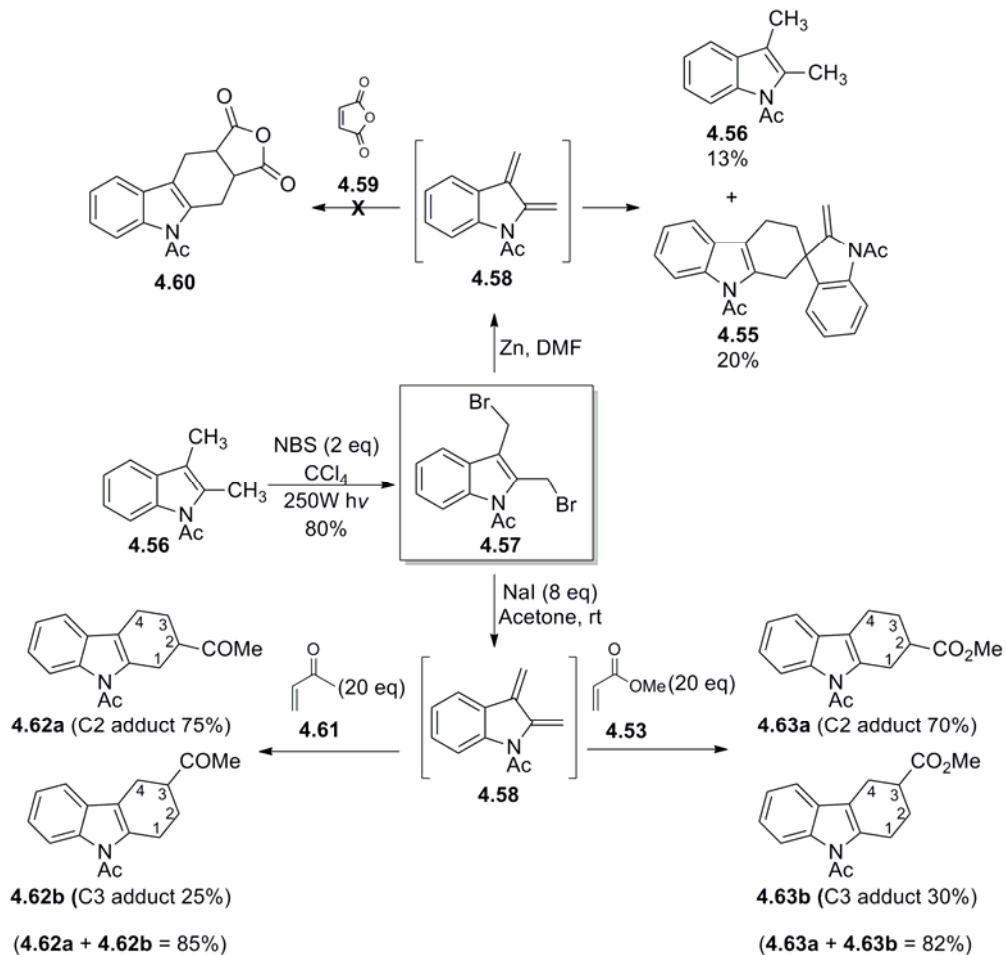
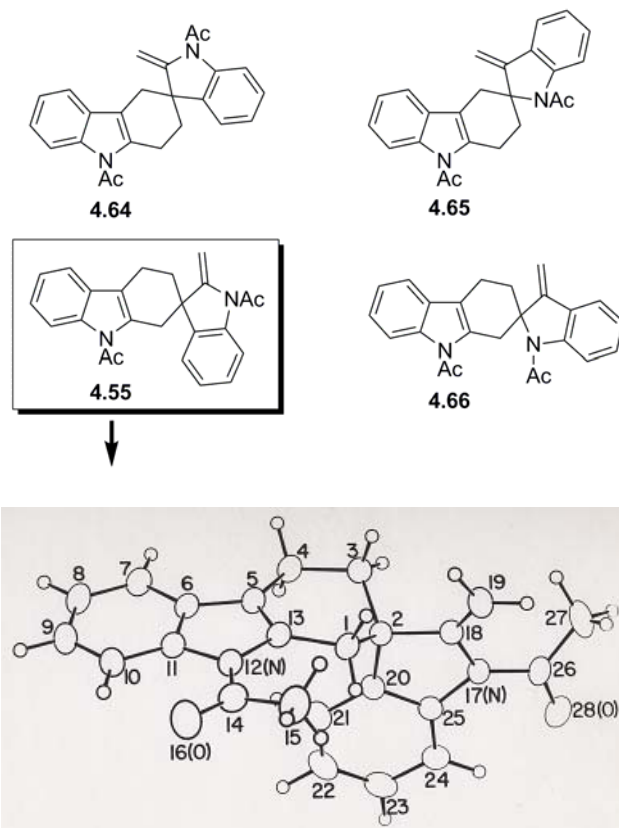


**Figure 4.4:** Four possible isomers of the homodimer and the corresponding single crystal X-ray structure of **4.55** obtained by S.F. Vice.



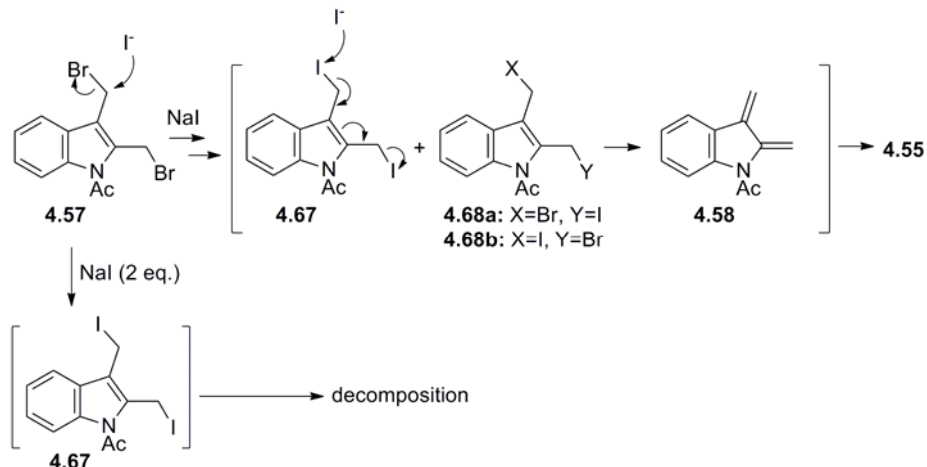
Through some experimentation it was found that the generation of **4.58** from **4.57** could be accomplished by addition of eight equivalents of sodium iodide in acetone at room temperature (Scheme 4.9). However, these cycloaddition reactions suffered from poor regioselectivity ( $\sim 3:1$  for C-2 adduct:C-3 adduct) and required a large excess of dienophile to overcome the competing dimerization of **4.58**. Theoretical investigations pertaining to the observed regioselectivity are discussed in Chapter 5 through quantum chemical calculations.

In the absence of a dienophile, only **4.55** was obtained. An independent and unambiguous synthesis<sup>389</sup> of **4.62b** permitted the identification of the regioisomers that are shown in Scheme 4.9. The rapid generation of *N*-Ac-IQDM **4.58** under those mild conditions suggested the possibility that its genesis may be observed spectroscopically at lower temperatures.

The initial suite of experiments was executed by adding a solution of NaI in acetone-*d*<sub>6</sub> to a pre-cooled (-23 °C) solution the dibromide **4.57** in a 5 mm NMR tube and observing the <sup>1</sup>H and <sup>13</sup>C NMR spectra obtained on an 80 MHz spectrometer. A brown colour was generated upon addition of NaI, indicative of iodine formation. Poorly resolved signals in the δ 5.5 to 5.8 region in the <sup>1</sup>H NMR were taken to be preliminary evidence for the formation of the *N*-Ac-IQDM **4.58**. Later, more detailed studies at 400 MHz provided evidence for the intermediacy of the diiodide **4.67** and/or monoiodomonobromides **4.68**. In particular, recording the spectrum at -23 °C, immediately after mixing, yielded signals assignable to the *N*-Ac-IQDM vinyl hydrogens (δ 5.50, 5.55, 5.70, 5.76) as well as singlets at δ 4.82 and 5.10 ppm that disappeared with time to be replaced by signals resulting from the dimer **4.55** as well as those from the *N*-Ac-IQDM.

Owing to the availability of NMR instrumentation and pulse sequences that were more advanced than those available to S.F. Vice, these spectroscopic studies were further extended by S.R. White in this group using variable temperature NMR (VT <sup>1</sup>H NMR, 500 MHz) techniques.<sup>385</sup> Taken together, additional insights into mechanistic as well as structural/conformational queries could be addressed as illustrated in Scheme 4.10 and Figure 4.5.

**Scheme 4.10:** The probable mechanism furnishing **4.58** interpreted from NMR studies performed by Vice<sup>381</sup> and White.<sup>385</sup>



The VT <sup>1</sup>H NMR data provided valuable insight into the conformational mobility of the amide moiety of **4.58** initially observed by Vice and confirmed by White and is illustrated in the top panel of Figure 4.5a. The -60 °C panel in Figure 4.5b shows substantial broadening of the H-7 and H-2 $\alpha$  protons indicative of a hindered conformational rotation. Thus, the NMR probe was cooled to -93 °C to observe the slow exchange extreme for the two rotamers **4.58a** and **4.58b** in a ratio of 2.6:1. This prevalence of rotamer 1 over rotamer 2 is addressed by quantum chemical calculations discussed in Chapter 5. Warming **4.58** induces dimerization spontaneously to provide **4.55** (Figure 4.5c, 0 °C panel) in accord with Vice's earlier observations.

**Figure 4.5a:** IQDM rotamers **4.58** and their associated spectroscopic assignments obtained by S.R. White.<sup>385</sup>

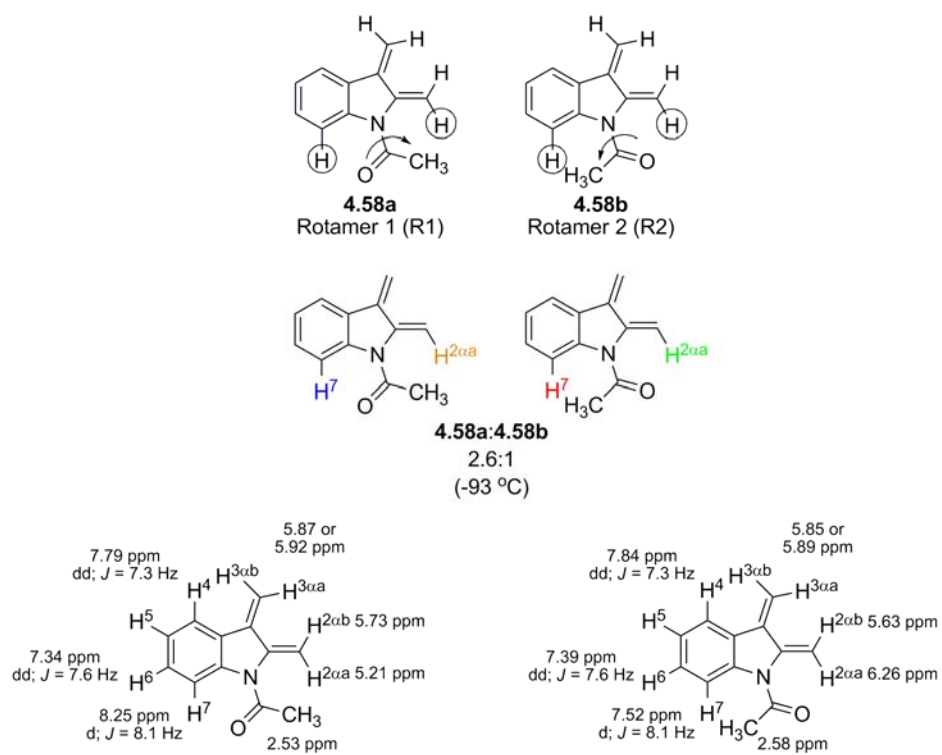


**Figure 4.5b:** VT  $^1\text{H}$  NMR spectra (500 MHz, acetone- $d_6$ , 180-213 K; S.R. White).

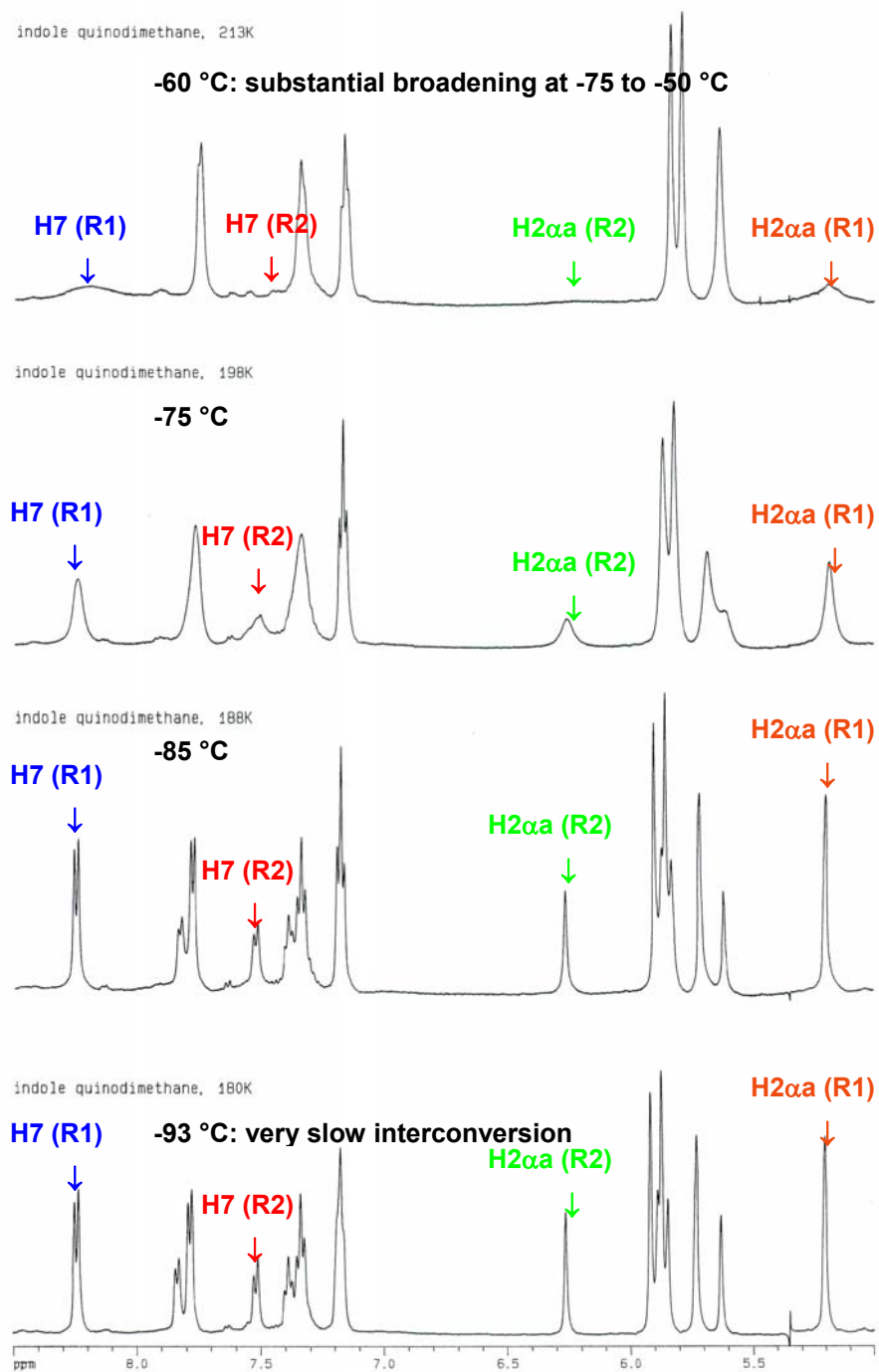
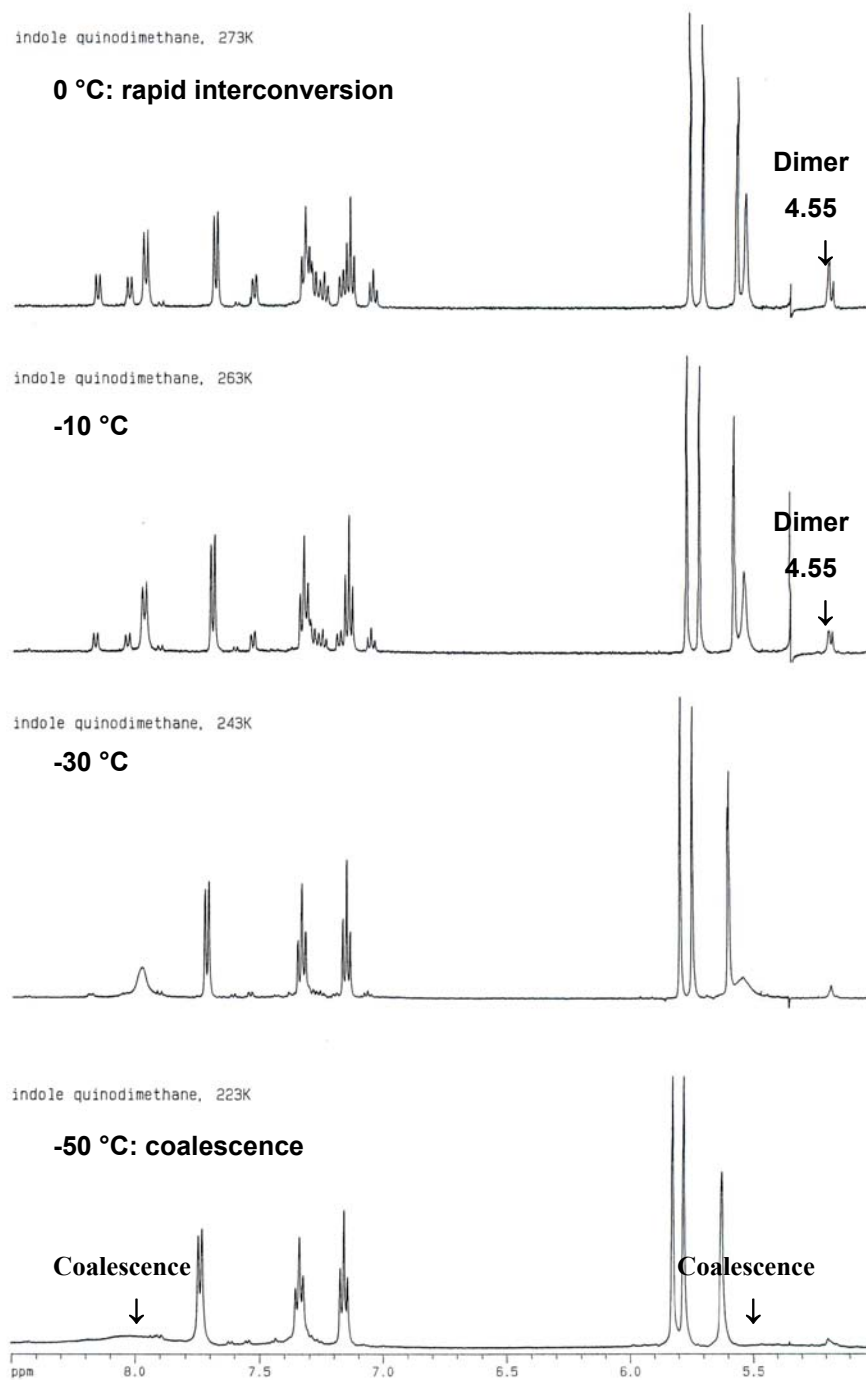


**Figure 4.5c:** VT  $^1\text{H}$  NMR spectra (500 MHz, acetone- $d_6$ , 223-273 K; S.R. White).



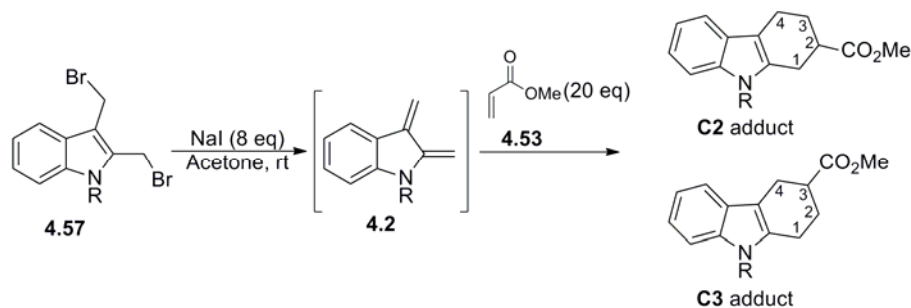


On the basis of chemical shift arguments, the major and minor rotamers could be assigned as conformers **4.58a** and **4.58b**, respectively. The proton H-7 of the major component (**4.58a**, rotamer 1) was assigned 8.25 ppm (d;  $J = 8.1$  Hz) while in the minor component (**4.58b**, rotamer 2) H-7 was assigned 7.52 ppm. These assignments can be justified as H-7 is found within the deshielding region of the amide carbonyl of **4.58a** thus shifting the resonance further downfield on comparison to **4.58b**. The same argument can also be applied to the assignment for H-2 $\alpha$  of **4.58b** to 6.26 ppm which is shifted downfield compared to that of **4.58a** at 5.21 ppm. These studies permitted the  $^1\text{H}$  NMR assignments for both rotamers as shown in the bottom panel of Figure 4.5a.

Initial attempts at increasing the regioselectivity of intermolecular Diels-Alder reactions of **4.58** were investigated by varying the indolic nitrogen substituents. The purposes of these studies were twofold. Purification issues had plagued the synthetic utility of this method; the crude product was often an inseparable mixture of the two regioisomers. Secondly, it was felt that the molecular orbital coefficients of the diene would be sufficiently altered by the *N*-substituent such that it would invoke a high degree of regioselectivity for either the 2- or 3-substituted tetrahydrocarbazole. Alternatives to replace the acetyl moiety were trifluoroacetyl ( $\text{CF}_3\text{CO-}$ ), *tert*-butoxycarbonyl (*t*-Boc), trifluoromethanesulfonyl (Tf),<sup>381</sup> and cyano ( $-\text{CN}$ )<sup>384</sup> (Table 4.1). Experiments were carried out using methyl acrylate as the dienophile under those conditions described in Scheme 4.9. Disappointingly, only a marginal improvement was observed even for the highly electron withdrawing substituents, trifluoroacetyl and triflyl. The cyanamide system was found to dimerize more readily than the *N*-acetyl system, making Diels-Alder trapping with dienophiles difficult. Owing to these observations **4.57**

would be used in all successive studies due to its ease of preparation and handling as well as its stability.

**Table 4.1:** The observed regioselectivity of DA reactions of IQDMs generated from **4.57**.



Entry	R	C2:C3 (%)
1	COCH <sub>3</sub> (Ac)	70:30
2	COCF <sub>3</sub>	75:25
3	SO <sub>2</sub> CF <sub>3</sub> (Tf)	71:29
4	CO <sub>2</sub> <i>t</i> Bu ( <i>t</i> -Boc)	66:34
5 <sup>a</sup>	CN	70:30

a. Conditions: TEAL in CH<sub>2</sub>Cl<sub>2</sub>.

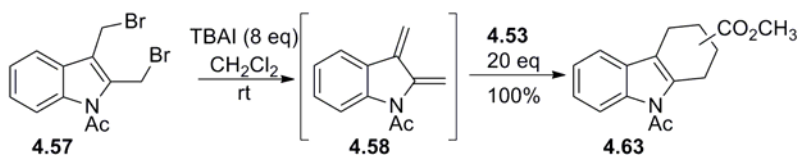
### 4.3.2 Advanced Studies

Hence attention was turned to other avenues at increasing the regioselectivity, one of which was to employ Lewis acids. The theoretical descriptions pertaining to the observed regio- and stereochemistry of Diels-Alder reactions and have been summarized in several key reports.<sup>90,320,390-393</sup> The effect of Lewis acids on the acceleration,<sup>394</sup> and enhancement of regio- and stereo-control<sup>395</sup> is well documented. The early synthetic efforts of Vice employed DMF as the solvent and the VT NMR studies by White indicated that **4.58** was stable between 30-35 °C in acetone. However, many Lewis acids owing to their oxophilic character

are not compatible with these solvents. Vice had initially screened Lewis acid compatible solvents and the corresponding source of soluble iodide and found tetra-butylammonium iodide (TBAI) in dichloromethane worked well.

Accordingly, new and improved conditions were later defined by J.Y.J. Wu<sup>386</sup> and are shown in Scheme 4.11. Generation of **4.58** from **4.57** was accomplished upon adding **4.57** via syringe to a solution of eight equivalents of TBAI in CH<sub>2</sub>Cl<sub>2</sub> at room temperature and trapping **4.58** with an excess of **4.53** affording a quantitative yield of **4.63**.

**Scheme 4.11:** Wu's initial experiments defining conditions for LA-catalyzed reactions.<sup>386</sup>

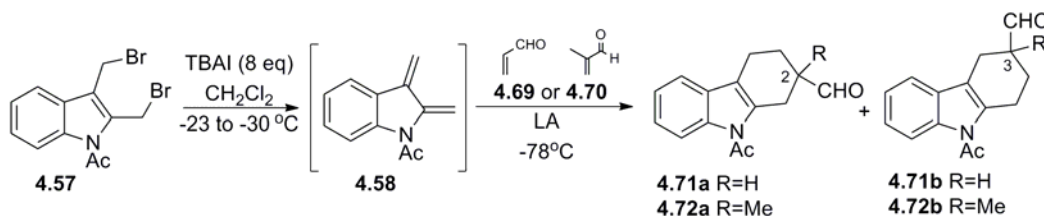


This demonstrated that Lewis acid catalysis was indeed feasible and the next suite of experiments was executed under these newly defined conditions. The IQDM was generated as before but in the range of -23 to -30 °C and was stable at this temperature, abrogating dimerization which in turn permitted a significant decrease in the amount of dienophile required. The temperature was then dropped to -78 °C and two equivalents of either **4.69** or **4.70** and one equivalent of Lewis acid were added. A significant increase in the regioselectivity was observed, especially in the reaction using SnCl<sub>4</sub> at -94 °C (13.5:1 for **4.72a**:**4.72b**) as shown in entry 6 of Table 4.2.

Several other key observations also came from this work. In the absence of Lewis acids no Diels-Alder adducts were observed and consequently only dimer was generated. Lower

temperatures led to higher regioselectivity and the amount of dienophile required was decreased by an order of magnitude. In a later study, using  $\beta$ -substituted- $\alpha,\beta$ -unsaturated enals (e.g. *trans*-pentenal **4.74**), an absolute requirement for strong Lewis acids such as  $\text{BF}_3 \cdot \text{OEt}_2$  and low temperatures ( $-94^\circ\text{C}$ ) provided satisfactory regiocontrol at 9:1 (C-2:C-3) but the yields were moderate at 44%. Non-aldehyde type dienophiles such as ketones and esters provided regioselectivities lower than observed for the enals.

**Table 4.2:** Wu's experimental conditions of Lewis acid catalyzed DA reactions of  $\beta$ -unsubstituted- $\alpha,\beta$ -unsaturated enals and *N*-Ac-IQDM **4.58**.



Entry	Dienophile	Dienophile: Diene	Dienophile: LA	Temp ( $^\circ\text{C}$ )	LA	Ratio (C2:C3)	Isolated Yield
1	<b>4.69</b>	4:1	2:1	-30	$\text{SnCl}_4$	4:1	nd
2	"	2:1	"	-78	"	9:1	57-68
3	"	4:1	"	-30	$\text{ZnCl}_2$	4:1	nd
4	"	4:1	"	-30	$\text{BF}_3$	3.5:1	nd
5	<b>4.70</b>	2:1	"	-78	$\text{SnCl}_4$	11:1	68
6	"	2:1	"	-94	"	13.5:1	47

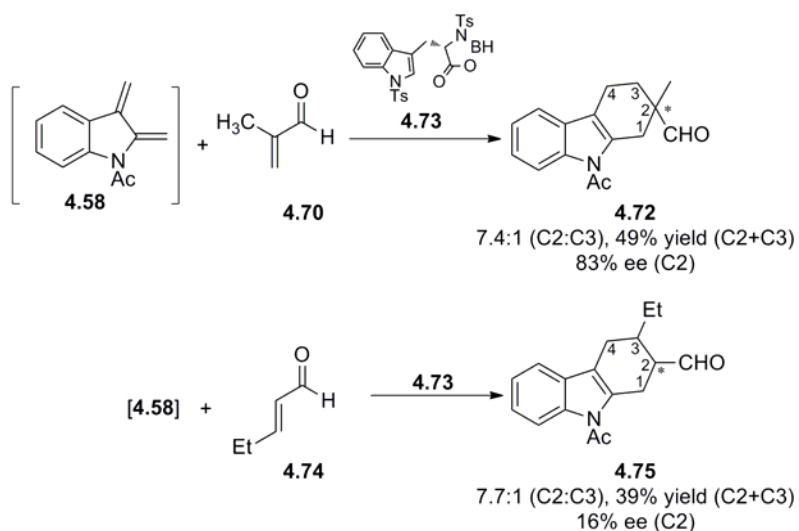
nd: not determined

These seminal studies indicated that further explorations using Lewis acids would be appropriate to widen the synthetic scope. Having established methods that could potentially provide the C-2-substituted tetrahydrocarbazole in excess of the C-3 regioisomer (13.5:1),

issues regarding stereoselectivity could now be addressed. Accordingly, both chiral catalysts and chiral auxiliaries were investigated.

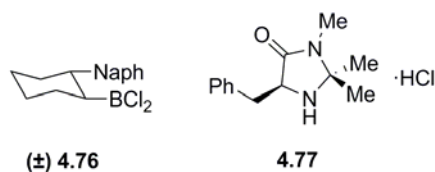
Corey's tryptophan-derived oxazaborolidine chiral Lewis acid catalyst **4.73**<sup>396</sup> provided ee's up to 82% when using **4.70**. However, poor enantioselectivity (16% ee) was achieved when using **4.74**.

**Scheme 4.12:** Wu's stereoselective Diels-Alder reactions of *N*-Ac-IQDM using **4.73**.



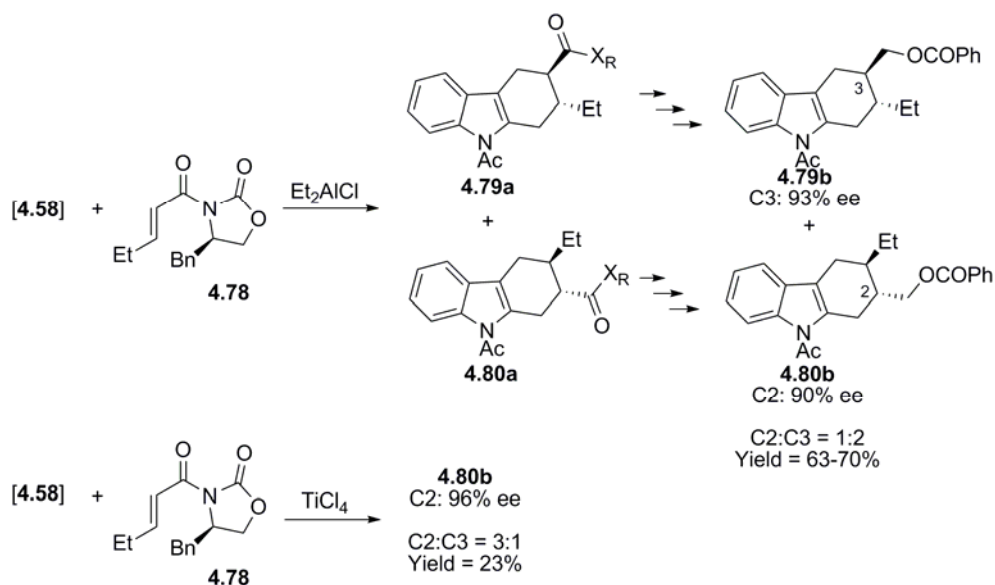
It was anticipated that other chiral catalysts such as Hawkins' aromatic alkylidichloroborane **4.76**<sup>397,398</sup> and/or MacMillan's chiral imidazolidinones **4.77**<sup>399</sup> (Figure 4.6) would provide adduct **4.75** with high ee's. Efforts using enantiopure **4.76** were not pursued as racemic **4.76** was used in the initial studies to probe whether it could efficiently catalyze Diels-Alder reactions using IQDM. However, both of these catalysts failed to provide the desired Diels-Alder adduct.

**Figure 4.6:** Racemic alkyldichloroborane **4.76** and chiral imidazolidinone **4.77**.



Thus attention was turned to Evan's chiral oxazolidinones.<sup>400</sup> The  $\beta$ -substituted- $\alpha,\beta$ -unsaturated acyl chiral oxazolidinones **4.78** provided high diastereoselectivity. After removal of the chiral auxiliary, up to 96% ee was observed (Scheme 4.13). Crystals were obtained for **4.79a** and **4.80a** and the ensuing X-ray diffraction studies permitted assignment of the two chiral centres (C-2 and C-3) to the R configuration. Of paramount importance was that the regioselectivity could be controlled, affording either the C-2 or C-3 regioisomer in excess of the other by using either  $\text{TiCl}_4$  or  $\text{Et}_2\text{AlCl}$ , respectively. It was felt that reactions which used the titanium reagents were FMO controlled whereas the reactions using aluminum reagents were charge controlled. This suggestion is one of the issues that are addressed in Chapter 5 in which theoretical calculations are invoked to provide insight into the processes governing regioselectivity. The auxiliary employed in these studies was the only method used that was compatible with  $\beta$ -substituted enals.

**Scheme 4.13:** Wu's stereoselective Diels-Alder reactions of *N*-Ac-IQDM using **4.78**.



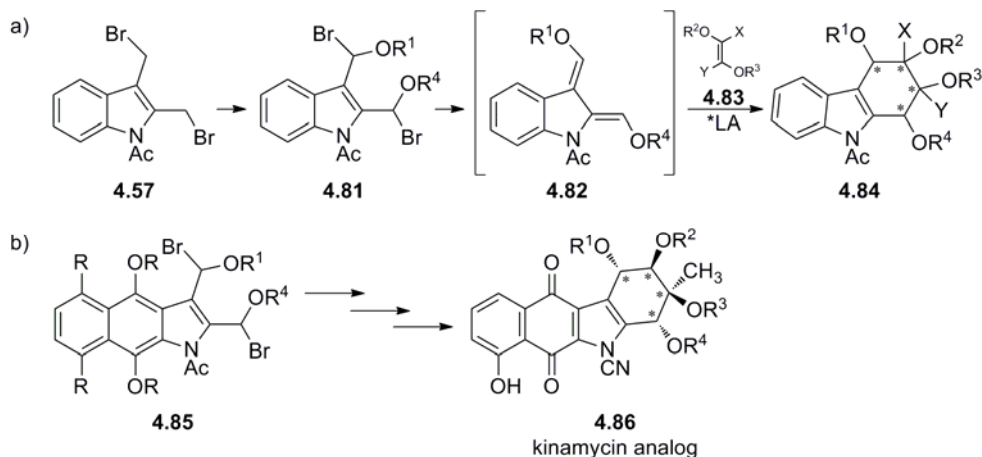
A drawback with the  $\text{TiCl}_4$  mediated reactions were the low isolated yields (23%). One assumption was that the iodine generated in the reaction was reacting with *N*-Ac-IQDM **4.58** producing **4.67**. Thus 1,3-propanedithiol was added to the reaction mixture to quench the iodine and the yields were observed to increase to 68% as well as the regioisomeric ratio increased to 4.4:1 (C-2:C-3). Although this was a substantial increase in the yield, there were no further attempts employing other sequestering reagents. Recent efforts towards alternative synthetic approaches and quenching strategies in IQDM chemistry are discussed in the following section.

## 4.4 Efforts towards optimizing Diels-Alder reactions of *N*-acetyl Indole-2,3-Quinodimethanes and its Application in Total Synthesis of Kinamycin Analogues

### 4.4.1 Oxygenated IQDMs

One of the very early strategies employing IQDMs in synthesis was to access and implement substituted IQDMs in natural product synthesis. Of particular interest was the oxygen substituted IQDM **4.82** and in the presence of the appropriately substituted dienophile **4.83** and chiral Lewis acid (vide supra) could in principle provide carbazole **4.84** with four contiguous stereocentres (Scheme 4.14a). This in turn could be applied to the multistep synthesis of kinamycin analogues (Scheme 4.14b). This strategy would allow the introduction of the oxygen substituents at an earlier stage rather than later. Thus one of the early goals of this laboratory was to develop methods using oxygenated IQDMs<sup>384</sup> that would permit easy access towards the multistep synthesis of these analogues.

**Scheme 4.14:** Proposed synthesis of carbazoles and kinamycin analogues.

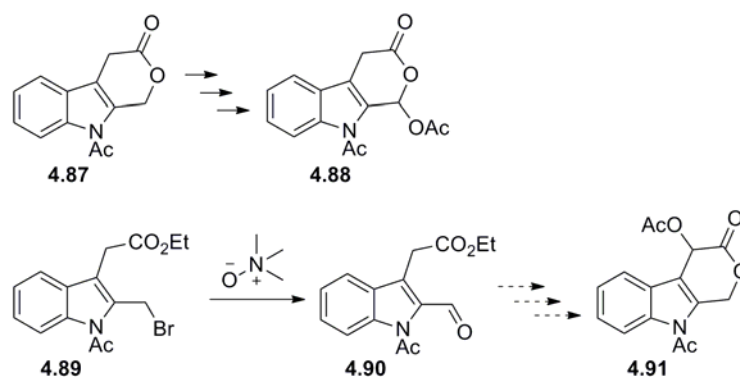


Early exploratory efforts were initiated by O.M. Jakiwyzk using lactone **4.87**<sup>384</sup> (Scheme 4.15) with the belief that the access to **4.87** would be straightforward owing to previous work



in this laboratory preparing pyranoindoles.<sup>383</sup> At the time these studies were performed there were no reports on the synthesis of the kinamycins which were still thought to be benzoannulated carbazoles. In practice it was found that preparation of **4.88** was plagued by substantial quantities of unanticipated side products, tedious purification and recovery of significant amounts of starting material which, taken together, provided low yields of the desired target. Strategies for synthesizing the regioisomer **4.91** had advanced as far as **4.90** but never fully materialized beyond this stage. The inherent disadvantage to using **4.88** or **4.91** was the requirement of elevated temperatures to generate IQDMs for their use in Diels-Alder reactions. These conditions would preclude the use of Lewis acids and low temperatures described in section 4.2.2 and therefore this route was not pursued for the purposes of this thesis.

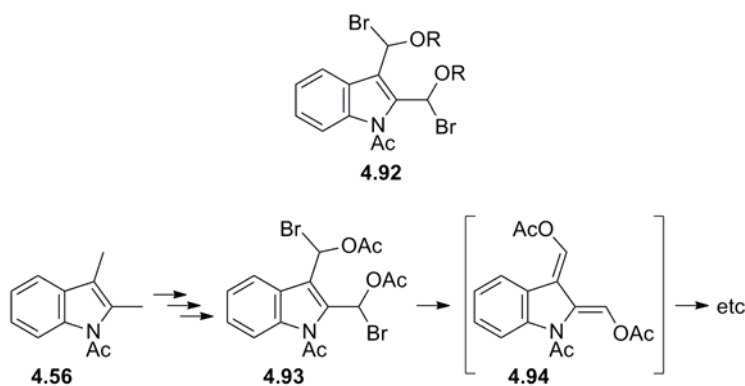
**Scheme 4.15:** Jakiwczyk's synthetic plan for lactones **4.88** and **4.91**.



#### 4.4.2 Synthetic efforts towards oxygenated *N*-acetyl Indole-2,3-Quinodimethanes

Owing to the limitations described above, new strategies toward oxygen substituted IQDMs were attempted in the present study. It was realized early on that  $\alpha$ -bromoether **4.92** would be unstable and difficult to handle (Scheme 4.16). However the corresponding  $\alpha$ -bromoacetate **4.93** may be stable owing to the stabilizing electron withdrawing effect of the carbonyl moiety. Hence efforts towards **4.93** were developed with **4.56**.

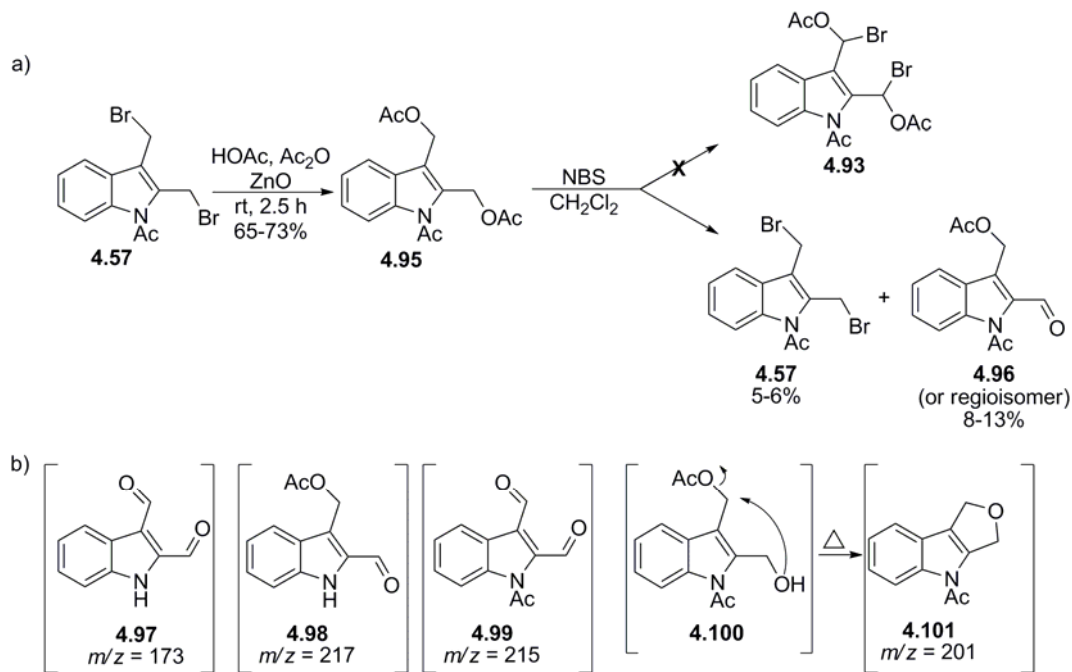
**Scheme 4.16:** The potential generation of oxygen substituted IQDM **4.94** from **4.93**.



The diacetoxy indole **4.95** was synthesized from **4.57** in 65-73% yield (Scheme 4.17a).<sup>401</sup> Attempts at bromination of **4.95** produced a complex mixture in which a number of products were evident as indicated by analytical TLC. This was corroborated by the <sup>1</sup>H NMR spectrum of the crude residue which revealed novel peaks at 10.41 and 10.21 ppm as well as a number of peaks in the 3.86-6.61 ppm range with the diminution and/or absence of peaks in various capacities assigned to the methylene, acetoxy and acetamide groups of **4.95**. The crude material was dissolved in a small amount of CH<sub>2</sub>Cl<sub>2</sub> for the purposes of purification via chromatography in which the evolution of gaseous fumes of acetic acid occurred. A number of fractions were procured which permitted the identification of two compounds; **4.57**

isolated in 5-6% yield and **4.96** (or its regioisomer) in 8-13% yield as shown in Scheme 4.17a. On several occasions, a separate fraction was routinely found to contain an inseparable mixture of what was thought to be **4.98** and **4.100**. Inspection of the  $^1\text{H}$  NMR spectrum of this fraction provided chemical shifts of 10.22, 6.61, 5.57, 2.10 ppm and is consistent with **4.98**. In the same spectrum, peaks were also observed at 5.54, 4.77, 2.80, 2.07 ppm and are consistent with **4.100**. The signal at 6.61 ppm was assigned to either the hydroxyl proton or indolic nitrogen proton. An aliquot of this sample was then subjected to GCMS analysis providing mass to charge ratios for the molecular ions 217 and 201, consistent with structures **4.98** and **4.101**, respectively (Scheme 4.17b). It was assumed that under the thermal conditions provided by the GCMS instrumentation, **4.100** furnishes **4.101** by intramolecular displacement of acetate. As well, ions at  $m/z$  of 173 and 215, consistent with **4.97** and **4.99**, respectively, were also observed routinely and can be justified by the same thermal processes of the GCMS experiment. In the end this sequence was repeated several times to firmly establish the identity of as many compounds as possible. Since access to oxygenated IQDMs by this route did not seem to be feasible, other avenues to obtain **4.93** or an analogue thereof were explored.

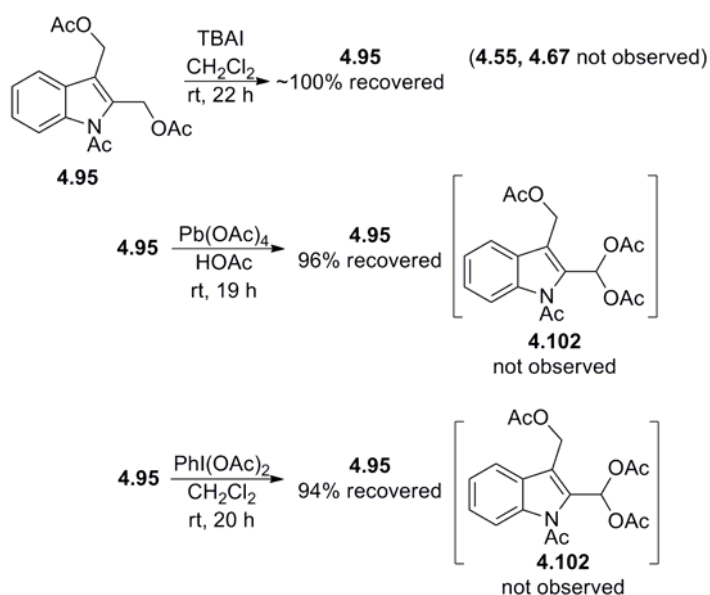
**Scheme 4.17:** a) Attempted bromination of **4.95**; b) Possible compounds generated via the thermal process of the GCMS experiment.



Structures are an educated guess based on *m/z* data obtained from GCMS analyses

Compound **4.93** was not isolated and its generation could not be satisfactorily determined. Thus it was anticipated that the tri-acetoxy system **4.102** might better serve our purposes to obtain oxygenated IQDMs and thus efforts towards obtaining **4.102** were pursued (Scheme 4.18). It was felt that the generation of the diiodide **4.67** may in turn produce **4.58** in situ (which would dimerize to **4.55**) but in the end this resulted in quantitative recovery of starting material. Attempts at acetoxylation using lead tetra-acetate or diacetoxy iodobenzene also resulted in recovery of large amounts of starting material. These exploratory studies provided some insight into the synthesis of substituted IQDMs and other routes of obtaining materials able to generate **4.94** or its analogues will be pursued in the future.

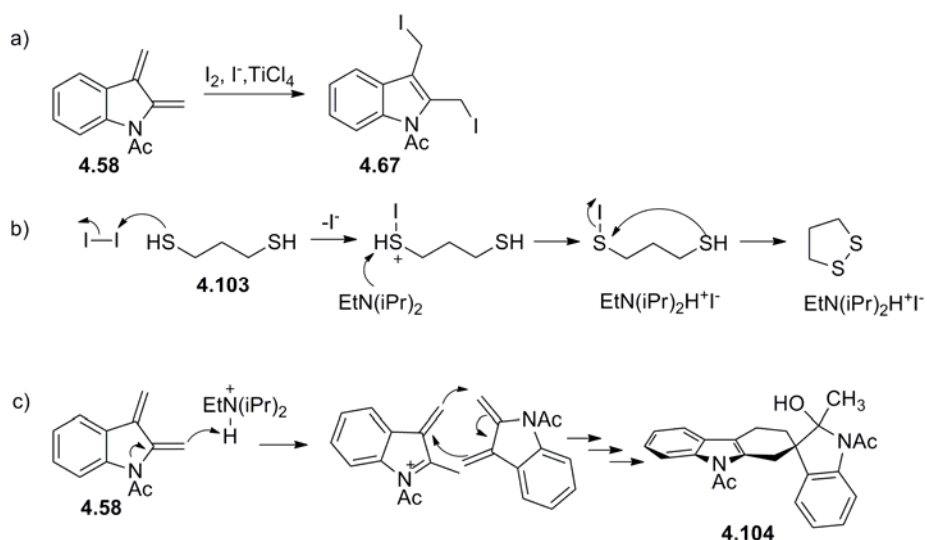
**Scheme 4.18:** Attempts at iodination and acetoxylation of **4.95**.



#### 4.4.3 Efforts towards increasing product yields of Lewis-acid catalyzed Diels-Alder reactions of *N*-acetyl Indole-2,3-Quinodimethanes

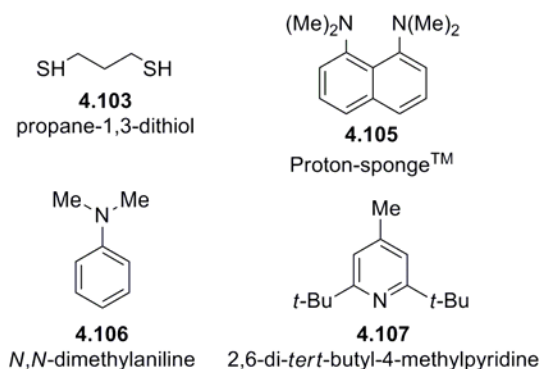
Wu had demonstrated several advances of using Lewis acid catalyzed Diels-Alder reactions of IQDMs to access substituted tetrahydrocarbazoles in a highly regioselective and stereoselective manner (Section 4.2.2). In the case with  $\text{TiCl}_4$  catalyzed reactions using chiral  $\beta$ -substituted- $\alpha,\beta$ -unsaturated *N*-acyl oxazolidinones, the product yield increased dramatically upon the addition of 1,3-propanedithiol. The excess iodine in the reaction may have reacted with **4.58** catalyzed by  $\text{TiCl}_4$  as shown in Scheme 4.19a. As well, any acid produced by the dithiol reagent was scavenged by the tertiary amine (Scheme 4.19b). The amine salt may, in turn, act as a Brønsted acid which is deprotonated by **4.58** furnishing **4.104**,<sup>386</sup> a known compound (Scheme 4.19c).

**Scheme 4.19:** Proposed degradation pathways of IQDM **4.58**.



Thus a small number of iodine and acid scavenging reagents (Figure 4.7) were investigated with the aim to increase the yields in the presence of any Lewis acid with the additive. These included 1,8-bis(dimethylamino)naphthalene (Proton-sponge™) **4.105**,<sup>402</sup> *N,N*-dimethylaniline (**4.106**),<sup>403</sup> the substituted pyridine **4.107**<sup>404</sup> and the dithiol **4.103**.

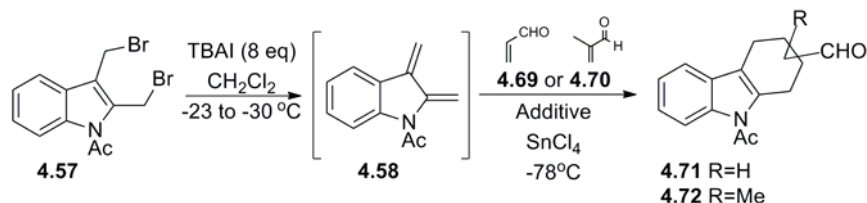
**Figure 4.7:** Proton/Iodine scavenging reagents.



The yields of the SnCl<sub>4</sub> catalyzed reactions were moderate (47-68%) but gave high regioselectivities (Table 4.2) and accordingly efforts towards increasing these yields began

with these tin catalyzed reactions (Table 4.3). The first attempts using acrolein **4.69** with the dithiol **4.103** and the substituted pyridine **4.107** produced only the dimer **4.55** and it was assumed that the thiol reagent was attacking acrolein leaving **4.58** in solution, furnishing the known dimer **4.55** upon workup. Thus attention was turned towards methacrolein **4.70** and the experiment repeated under the same conditions which afforded 49% yield of the desired adducts. The use of **4.105** produced the highest regioisomeric ratio (entry 3) whereas employing **4.106** provided the highest yield at 61% (entry 4).

**Table 4.3:** Diels-Alder  $\text{SnCl}_4$  catalyzed reactions of **4.58** with additives.



Entry	Dienophile	Dienophile: Diene	Dienophile: $\text{SnCl}_4$	Dienophile: Additive	Isolated Yield (%) (C2:C3) <sup>a</sup>	Dimer <b>4.55</b> (%) <sup>b</sup>
1	<b>4.69</b>	2:1	2:1	2:1 ( <b>4.103</b> ) + 1:1 ( <b>4.107</b> )	0 <sup>b</sup>	100
2	<b>4.70</b>	2:1	2:1	2:1 ( <b>4.103</b> ) + 1:1 ( <b>4.107</b> )	49 (11.3:1)	16 22 <sup>c</sup>
3	<b>4.70</b>	2:1	2:1	2:1 ( <b>4.105</b> )	57 (21:1)	27
4	<b>4.70</b>	2:1	2:1	1:1 ( <b>4.106</b> )	61 (17:1)	27
5	<b>4.70</b>	4:1	2:1	2:1 ( <b>4.105</b> )	39 (16:1)	30

a. regioisomeric ratios were obtained by integrating the aldehydic protons from the chromatographically pure sample containing both **4.72a** and **4.72b** as an inseparable mixture.

b. as estimated by inspection of the proton NMR spectrum of the crude product.

c. isolated yield.

From these studies it was clear that the use of these additives did not provide the desired adducts in high yields. The factors contributing towards these low yields may not be those that were initially anticipated. Further studies towards resolving these issues will need to be addressed in the future.

Synthetic efforts towards optimizing Lewis acid catalyzed Diels-Alder reactions of *N*-acetyl-indole-2,3-quinodimethanes remains an ongoing interest in this laboratory and may be supported by studies at the theoretical level. Indeed, high level quantum chemical calculations may provide insight into many of these observations and from this, issues regarding regioselectivity, stereoselectivity and reactivity may be better understood. The following chapter provides an in-depth discussion of quantum chemical calculations performed on the chemistry of *N*-acetyl-indole-2,3-quinodimethanes which in almost all cases, has shown good agreement for many of the experimental observations discussed in this chapter.

#### **4.4.4 Studies employing Mukai's method to generate *N*-substituted Indole-2,3-Quinodimethanes**

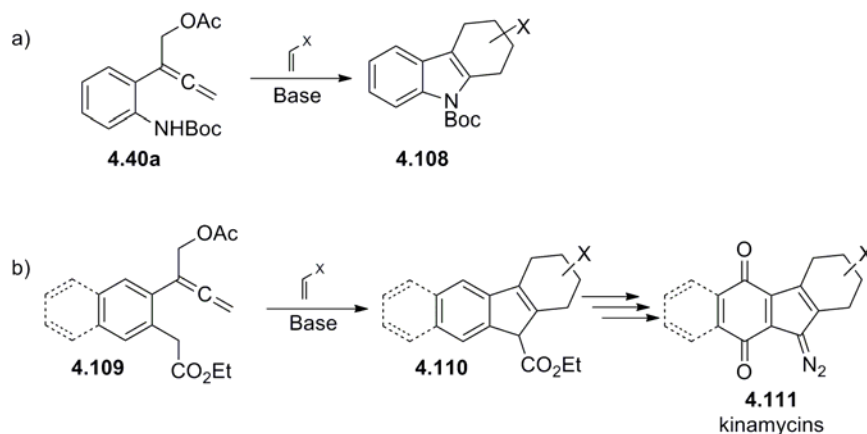
As outlined in the overview, one of the inherent advantages of Mukai's method is the mild conditions used to generate IQDMs and thus we were compelled to reproduce this chemistry with the goal in mind that this chemistry may be extended to carbocyclic systems and ultimately the kinamycins (Scheme 4.20). This chemistry is described in Chapter 6 and will not be discussed any further here.

In the spirit of reproducibility, this chemistry was re-iterated with three goals in mind. The first goal was to reproduce Mukai's results before any attempts of the carbocyclic system



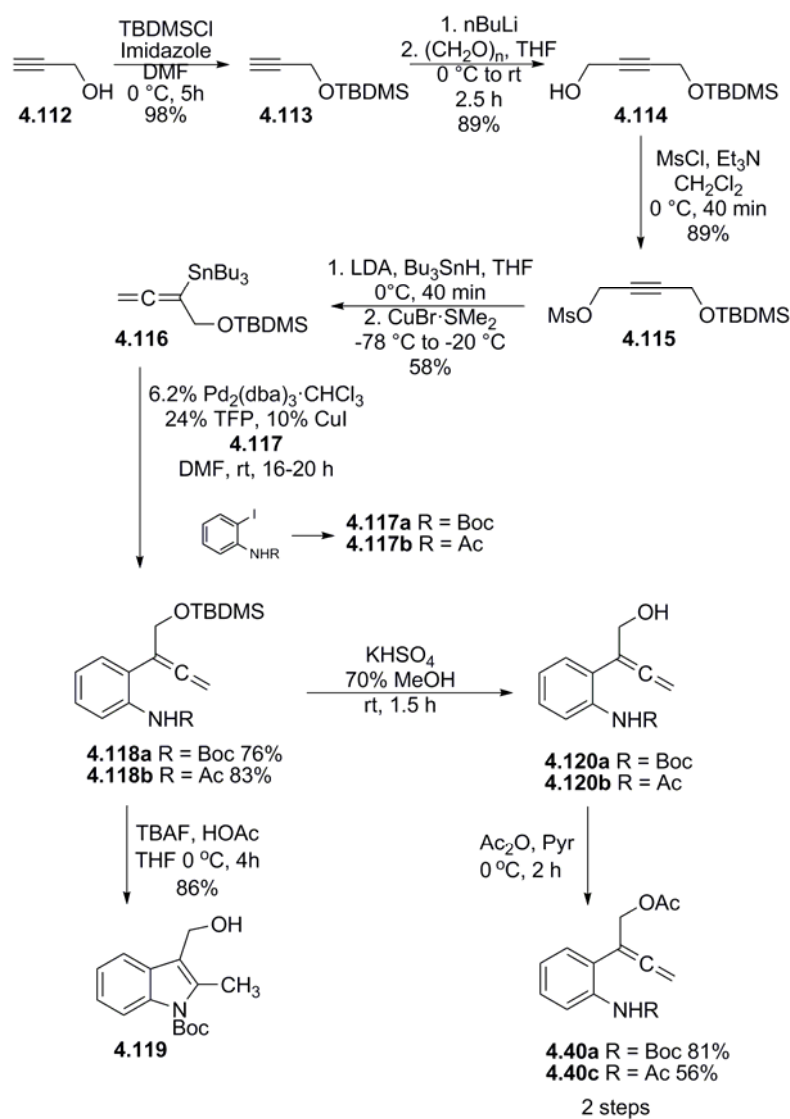
**4.109** would be investigated. Secondly, if this chemistry could be repeated without difficulty then interest in substituting the Boc group with acetyl as the *N*-substituent and then probing Diels-Alder reactions under Lewis-acid friendly conditions just described would be appropriate. Thirdly, owing to significant advances in NMR and X-ray technology within the last 25 years, a suite of in depth spectroscopic studies as well as a higher resolution single crystal X-ray structure of **4.55** were in order.

**Scheme 4.20:** a) Mukai's method to generate tetrahydrocarbazoles b) potential extension to carbocyclic systems to furnish benzo-annulated tetrahydrofluorenes.



Efforts towards **4.40** began with procedures described by Marshall and Palovich<sup>405</sup> to furnish **4.114** as shown in Scheme 4.21. Propargyl alcohol **4.112** was silylated to afford **4.113** in 98% yield which underwent hydroxymethylation under strongly basic conditions. Quenching with paraformaldehyde provided **4.114** in 89% yield. Activation of the alcohol **4.114** proceeded uneventfully to furnish the mesylate **4.115** in 89% yield.<sup>406</sup> The allenylstannane **4.116** was furnished by S<sub>N</sub>2' displacement of **4.115** by a tin-copper reagent produced in situ, in a moderate yield of 58%.

**Scheme 4.21: Synthesis of allenylaniline 4.40.**



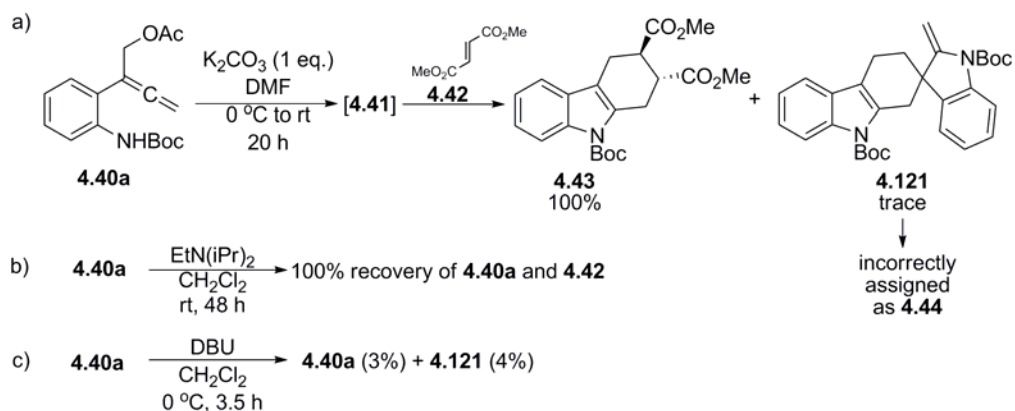
With a good quantity of **4.116** in hand it was decided to utilize some of this material in two separate Stille cross-coupling reactions. The first cross-coupling reaction employed the Boc-protected aniline **4.117a** (obtained from 2-iodoaniline in 78% yield<sup>407</sup>) and the second coupling reaction used the acetanilide **4.117b** (obtained from 2-iodoaniline in 91% yield<sup>408</sup>)

which provided the allenylanilines **4.118a** and **4.118b** in 76% and 83% yield, respectively. Deprotection of **4.118a** using TBAF as described by Mukai<sup>376</sup> did not provide the requisite alcohol, instead cyclization to **4.119** occurred in 86% yield. It appears that the fluoride ion, acting as a base, deprotonated the aniline furnishing **4.119**. The experiment was repeated with strict adherence to literature protocol only to find cyclization had repeated itself. The material **4.118a** was identical to that used as reported by Mukai, yet it was puzzling that there was no mention of cyclization reported by those workers. Ironically, an earlier publication by Mukai explicitly illustrates the use of TBAF to access indoles from the corresponding 2-allenylanilines.<sup>406</sup> Thus other methods of deprotection were sought, preferably under mild acidic conditions with the hopes of abrogating any deprotonation. Reports of desilylation of TBS ethers under very mild conditions have been reported by Perumal using KHSO<sub>4</sub> in aqueous methanol.<sup>409</sup> When this method was employed using **4.118a**, the alcohol was furnished in high yield which in turn was acetylated to give **4.40a** in a gratifying 81% yield over two steps. The same procedure was then applied to **4.118b** to produce **4.40c** in 56% yield over two steps. Both **4.40a** and **4.40c** were produced in eight steps with an overall yield of 22% and 19%, respectively.

The next objective was to repeat the Diels-Alder reaction employing **4.40a** with dimethyl fumarate as described by Mukai.<sup>376</sup> In that report, **4.40a** was added via syringe over a two hour period, to a solution of **4.42** and potassium carbonate in DMF at 0 °C, furnishing the adduct **4.43** in 93% yield with no trace of **4.44** (which is actually **4.121**) (Scheme 4.7). In practice, this experiment was repeated only to find small amounts of product with large amounts of starting material recovered. It was decided to allow the reaction mixture to warm

to room temperature and to use a longer reaction time. Under these conditions **4.43** was obtained in 71% isolated yield. No traces of **4.121** were observed in the  $^1\text{H}$  NMR spectrum of the crude material. Having satisfied ourselves that the reaction was indeed feasible, concerns now turned towards increasing the yields. Thus, the experiment was repeated with the modification that **4.40a** and **4.42** were dissolved in DMF, cooled to 0 °C and then  $\text{K}_2\text{CO}_3$  was added and stirred overnight, warming to ambient temperature. We were pleased to recover a quantitative yield of **4.43** with a very small amount of the dimer **4.121** (Scheme 4.22a).

**Scheme 4.22:** Repeat of Mukai's experiment under new conditions.

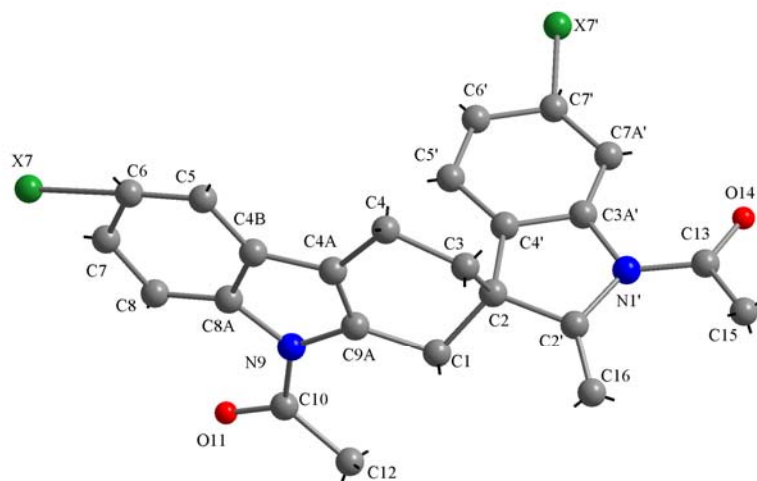


The next step was to probe if these reaction conditions were conducive to Lewis acid catalysis. Dichloromethane was the solvent of choice owing to the precedent already established and the bases DBU and Hünig's base (diisopropylethylamine) were used for these initial explorations. A quantitative recovery of starting material was observed for the reaction employing Hünig's base (Scheme 4.22b). Conditions using DBU resulted in 3% recovery of **4.40a** and 4% of **4.121** as well as a small amount of unidentified material was produced but its identity was not pursued (Scheme 4.22c). These efforts described above have provided

some insight into the feasibility of using **4.40a** to generate IQDM under Lewis acid friendly conditions.

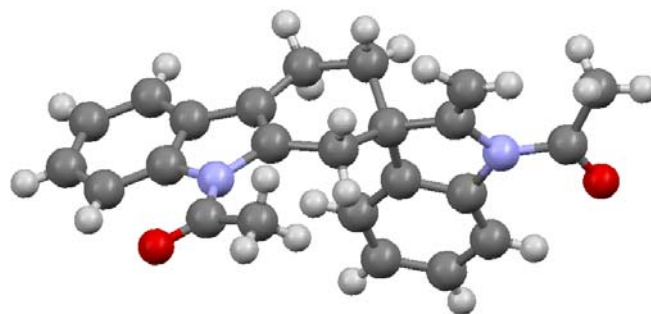
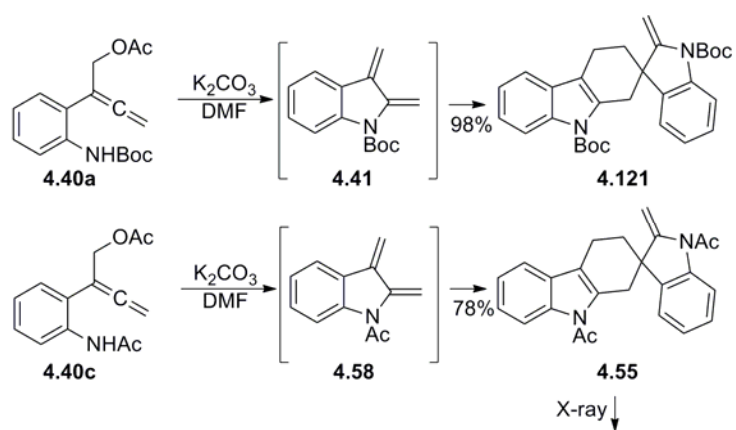
Efforts towards obtaining the dimer **4.55** using methods outlined in Schemes 4.9 and 4.11 failed to provide material suitable to grow crystals for the purpose of X-ray diffraction studies. In practice, using TBAI in  $\text{CH}_2\text{Cl}_2$  to generate **4.55** provided material that appeared to be sensitive to deuterated solvents required for NMR studies. It was found that **4.55** obtained under those conditions appeared colorless as an ethereal solution but appeared as a pale yellow solution in  $\text{CDCl}_3$  or  $\text{CD}_2\text{Cl}_2$ , suggesting decomposition of the product upon standing. It is possible that this material contained traces of TBAI and air oxidation of  $\text{I}^-$  might lead to formation of  $\text{I}_2$  and reaction of  $\text{I}_2$  with the dimer might be the cause of the apparent instability. Upon standing in deuterated solvents, the dimer slowly decomposed over time and it was felt that the iodine reacted with the dimer promoting its decomposition via deacetylation. All attempts to purify **4.55** from iodine were ineffective. Despite the fact that preparations of **4.55** were insufficiently pure, in one instance, crystals were obtained from these efforts from which the ensuing single crystal X-ray study revealed an anomalously high density around C6/C7 and C7' suggestive of a small amount (~1%) of iodinated dimer, shown as X7 and X7', respectively, in Figure 4.8.

**Figure 4.8:** The initial X-ray structure of **4.55**.



Later on, another analysis of the crystal structure data revealed that the iodine occupancy at these coordinates was less than the statistical standard deviation. The original suggestion of iodine could be conceivably attributed to artifacts such as twinning. In any event, all methods involving iodine and metals were abandoned in favor of using **4.40a** and **4.40c** which provided yields of 98% and 78% for **4.121** and **4.55**, respectively. From this, crystals of **4.55** were obtained from diethyl ether and were suitable for a single crystal X-ray study shown in the bottom panel of Scheme 4.23 (Appendix D). The very close spectroscopic similarity of **4.121** and **4.55** suggests that the structure **4.121** is analogous to **4.55**.

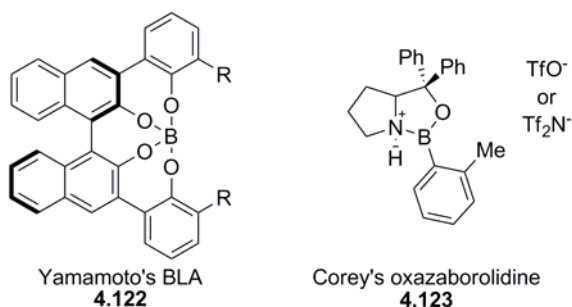
**Scheme 4.23:** Production of **4.102** and **4.55** and the corresponding the X-ray of **4.55**.



#### 4.5 Future efforts: Towards stereoselective induction using Yamamoto's BLA catalyst and/or Corey's oxazaborolidine catalyst

One of the early goals of the work intended to be in this thesis was to initiate new methods that would allow stereoselective induction in Diels-Alder reactions employing **4.58**. The  $\beta$ -substituted  $\alpha,\beta$ -unsaturated enals used in attempted cycloadditions with **4.58** were found to be unreactive. A solution to this problem was provided by the Evan's auxiliary which gave good diastereoselectivities; however, efforts at installing and removing the oxazolidinone were laborious and time consuming. Consequently, the result of these efforts provided the motivation to pursue other catalyst systems. There are a number of appropriate catalysts available,<sup>410,411</sup> but future studies would employ either Yamamoto's BLA **4.122**<sup>412</sup> or Corey's oxazaborolidine **4.123**<sup>413-416</sup> (Figure 4.8) in efforts towards enantioselective Diels-Alder reactions of **4.58**.

**Figure 4.9:** Chiral catalysts **4.122** and **4.123** used in enantioselective Diels-Alder cycloadditions.





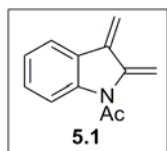
## Chapter 5

# A Theoretical Investigation into the Chemistry of the *N*-acetyl Indole-2,3-Quinodimethanes: A Quantum Chemical Study

### 5.1 Introduction

The preceding chapter provided experimental observations of the chemistry of *N*-acetylindole-2,3-quinodimethane (*N*-Ac-IQDM) **5.1**, in which amide rotamer conformations as well as regioselectivity and stereoselectivity studies of Diels-Alder reactions with **5.1** were described. This chapter provides the corresponding quantum chemical calculations as an extension of those studies as a continuation of our long-standing interest in IQDM chemistry. A brief review of the computational methods employed and previous computational studies on IQDMs is given in the discussion below.

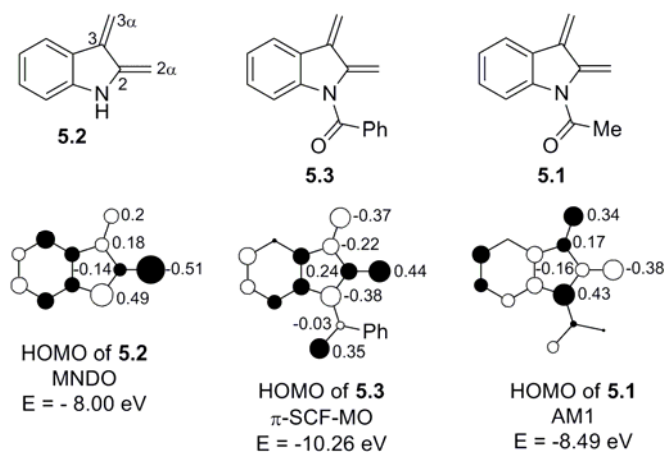
**Figure 5.1:** *N*-acetylindole-2,3-quinodimethane.



### 5.2 Theoretical investigation of IQDM by others

Pindur and coworkers were the first to describe the chemistry of IQDMs by computational methods using MNDO,<sup>375</sup>  $\pi$ -SCF<sup>417</sup> and AM1<sup>418</sup> calculations. The HOMO of **5.1**, **5.2** and **5.3** and the corresponding molecular orbital (MO) coefficients as reported by Pindur are shown in Figure 5.2.

**Figure 5.2:** The HOMO of IQDMs **5.1**, **5.2**, **5.3** as calculated by Pindur.

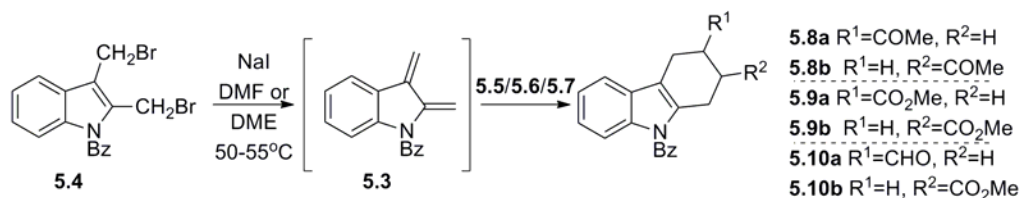


Experimentally, Pindur employed **5.4** to generate the benzoyl IQDM **5.3** which was trapped with dienophiles methyl vinyl ketone (MVK) **5.5**, methyl acrylate **5.6** and acrolein **5.7** (Table 5.1). The results of the cycloaddition reactions using methyl acrylate and acrolein<sup>418</sup> were consistent with Vice's and Jakiwczyk's results;<sup>381,382,384</sup> however, the reaction with MVK was perplexing and contradicted the results from this laboratory. Where Vice had obtained a 1:3 ratio of **5.8a** to **5.8b**, Pindur's laboratory reported a 4:1 ratio.<sup>417,419</sup> Pindur has rationalized the regioselectivity through the use of Frontier Molecular Orbital theory:<sup>90</sup>

“...The heterocyclic diene reactivity of **5.2** is primarily determined by the 2-aminobutadiene structural unit. Our MNDO calculations on the parent compound **5.2** have shown that the  $[4\pi_s + 2\pi_s]$ -cycloaddition reactions with electron-poor dienophiles are HOMO<sub>diene</sub>-LUMO<sub>dienophile</sub> controlled processes and that the peri- and regioselectivities found

in the numerous experimental syntheses can be predicted satisfactorily from the HOMO topologies of **5.1**...<sup>375</sup>

**Table 5.1:** Summary of Pindur's studies of Diels-Alder reactions with IQDM **5.3**.



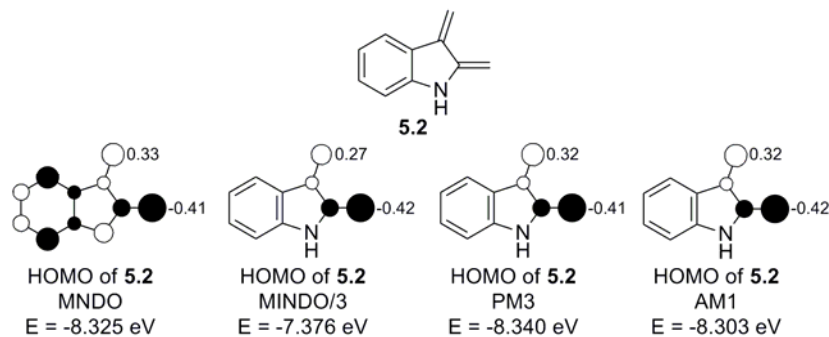
Entry	Dienophile	Adduct ratio	Yield (%)
		a:b	
1	Methyl vinyl ketone <b>5.5</b>	<b>5.8a:5.8b</b> = 4:1	59
2	Methyl acrylate <b>5.6</b>	<b>5.9a:5.9b</b> = 1:3	22
3	Acrolein <b>5.7</b>	<b>5.10a:5.10b</b> = 1:3	8

Pindur's MNDO studies predict, albeit erroneously, the 3-substituted-1,2,3,4-tetrahydrocarbazoles to be the major product and are clearly at odds with results from our laboratory and others<sup>380</sup> in which the 2-substituted-1,2,3,4-tetrahydrocarbazole were found to be the major product. S.R. White from this laboratory repeated these calculations employing the MNDO Hamiltonian as per Pindur's study, as well as the AM1, PM3 and MINDO/3 methods and obtained energies and MO coefficients markedly different from those reported by Pindur. White's results are shown in Figure 5.3.<sup>385</sup>

The discrepancy between White's MNDO results and those of Pindur is surprising. It is possible that the data set reported by Pindur was obtained from structure(s) in which a full geometry optimization was not performed. The possibility also exists that the MINDO/3 Hamiltonian was inadvertently used for this study and seems plausible when one compares

Pindur's results with White's results from the MINDO/3 calculations. In practice it was found that the MINDO/3 method was unsuitable to describe the structure and chemistry of **5.2** and hence was abandoned. The results of the MNDO, AM1 and PM3 calculations provide MO coefficients at the termini that are closer together in magnitude than those reported by Pindur and indicate a modest preference for the C-3-substituted carbazole, if the reaction is assumed to be FMO controlled. A later study by Pindur<sup>417</sup> attributed the low degree of regioselectivity to small differences in the HOMO coefficients of the terminal carbon atoms of the 2-aminobutadiene unit.

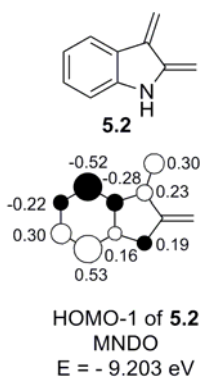
**Figure 5.3:** Energy and selected MO coefficients of the HOMO of **5.2** calculated with the MNDO, MINDO/3, PM3 and AM1 Hamiltonian as reported by S.R. White.



The HOMO-1 was calculated for **5.2** at the MNDO level and is shown in Figure 5.4. The coefficients at C-3 and C-3 $\alpha$  are 0.23 and 0.30, respectively, whereas C-2 and C-2 $\alpha$  do not contribute to this molecular orbital. Hence the HOMO-1 is governed by a styrene-like contribution of the IQDM. Interaction of the HOMO-1<sub>diene</sub> with the LUMO<sub>dienophile</sub> would favor the C-2-substituted carbazole generated from the Diels Alder trapping of **5.2** with dienophiles. However, this interaction is less important than that between the HOMO<sub>diene</sub>

with  $\text{LUMO}_{\text{dienophile}}$  as the strength of orbital interactions is inversely proportional to the difference in energy between the orbitals (i.e. -8.325 eV for the HOMO gives a stronger interaction than the HOMO-1 at -9.203 eV).

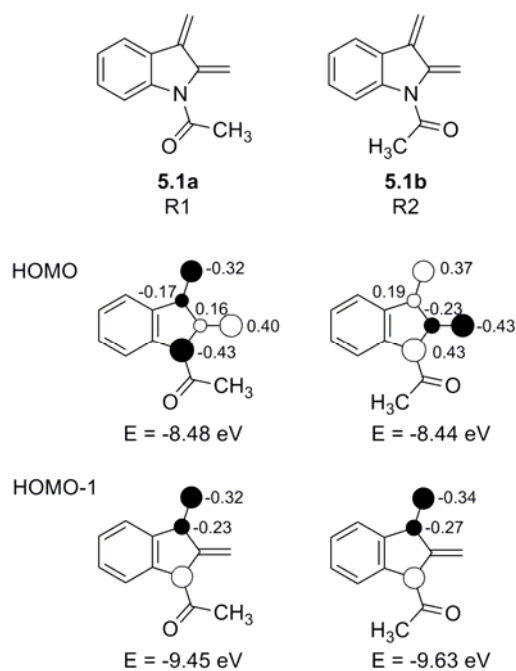
**Figure 5.4:** The HOMO-1 of **5.2** calculated at the MNDO level by S.R. White.



Intrigued by these results, these computational studies were then extended to the *N*-Ac-IQDM **5.1**. Figure 5.5 shows the HOMO and HOMO-1 energies and coefficients for both rotamers of **5.1**. Again, the HOMO indicates a slight preference for the C-3-substituted carbazole with the larger eigenvectors manifesting at the C-2 $\alpha$  terminus. Much like the HOMO-1 of the parent system **5.2**, the HOMO-1 of **5.1a** and **5.1b** shows a similar topology with negligible coefficients at C-2 and C-2 $\alpha$  and substantial coefficients at C-3 and C-3 $\alpha$  giving the familiar styrene-like MO. The energetically favorable interaction with the  $\text{LUMO}_{\text{dienophile}}$  (i.e. p-orbitals at centres with coefficients that are relatively large preferably interact with another) predicts the C-2-substituted-1,2,3,4-tetrahydrocarbazoles as the major product. However, these interactions would be considered to be much less important than the

HOMO<sub>diene</sub>-LUMO<sub>dienophile</sub> interaction. As it has already been shown, the eigenvalues and eigenvectors are heavily dependent on the theoretical platform used to describe these systems.

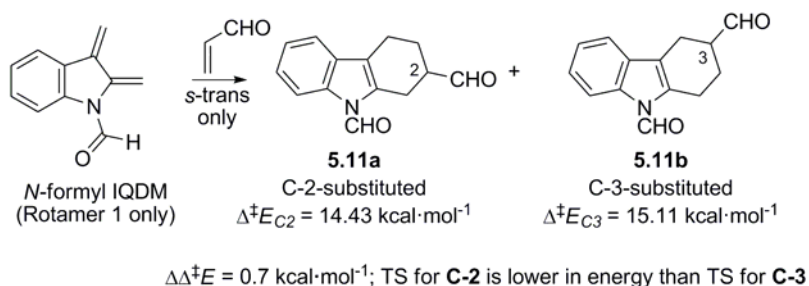
**Figure 5.5:** Energies and selected MO coefficients of the HOMO and the HOMO-1 for **5.1a** and **5.1b** calculated at the AM1 level by S.R. White.



Owing to this confusion, R. Laufer from this laboratory initiated higher level ab initio studies, abandoning the oft-used semi-empirical approaches. High level calculations with lower basis sets such as the 3-21 G basis set gave results similar to those obtained with the semi-empirical methods. However, use of the 6-31G(d) basis set generated coefficients at the termini that were essentially equal and hence could not be used to explain the regioselectivity through FMO theory. The HOMO-1 calculated at this level revealed topologies similar to S.R. White's studies and might contribute a modest influence towards the regioselectivity.

Additionally, transition state (TS) calculations were undertaken and found to be predictive of the observed regioselectivity (Scheme 5.1). Accordingly, this approach was also used in computational studies described later in this chapter. In the studies by R. Laufer from this laboratory, only the *N*-formyl IQDM was employed for the TS calculations and not the *N*-acetyl IQDM **5.1**. Furthermore, conformations were restricted to *s*-trans acrolein and a single rotamer of the diene (i.e. R1).

**Scheme 5.1:** TS calculations of the Diels-Alder cycloaddition of *s*-trans acrolein and *N*-formyl-IQDM calculated at the DFT B3LYP 6-31G(d) level by R. Laufer.



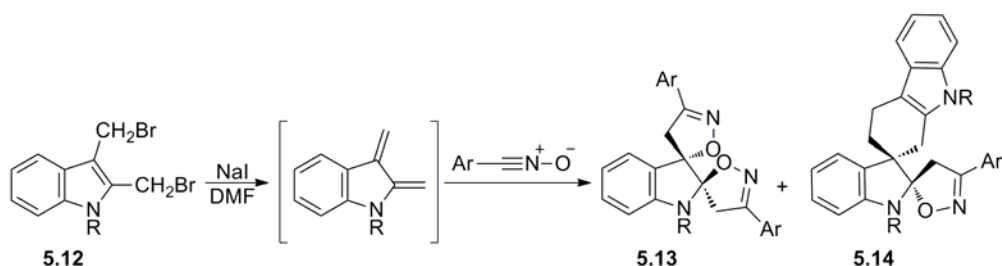
Thorough and extensive theoretical investigations of cycloadditions employing **5.1** describing the influence of IQDM amide conformation, dienophile conformation and facial approach have yet to be reported. Additionally, the Lewis acid catalyzed versions of these cycloaddition reactions have not been extensively pursued. A major goal of the work presented in this chapter is to evaluate a computational method(s) that effectively describes the chemistry of the IQDMs from experiment and then to implement those method(s) for successive studies in an effort to describe issues of regioselectivity and stereoselectivity. This might be accomplished by a thorough comprehensive treatment using high level quantum chemical calculations.

### 5.3 Quantum Chemical Calculations of the *N*-acetylindole-2,3-quinodimethanes at the DFT B3LYP 6-31G(d) level

#### 5.3.1 Background

The discrepancies found between the results reported by Pindur and our own laboratory provided the impetus to initiate a thorough in-depth theoretical study to address some of these ambiguities and to establish an appropriate computational method that effectively describes the behavior and reactivity of the IQDMs. This would be accomplished in part by reiterating calculations previously accomplished by others from this laboratory as well as those already reported in the literature. The subject of these quantum chemical calculations presented in this chapter is based on the experimental work reported in Chapter 4.

**Scheme 5.2:** Tsoleridis's study of 1,3 dipolar cycloadditions of *N*-substituted IQDMs and nitrile oxides.



Theoretical descriptions of Diels-Alder reactions are found throughout the literature. Additionally, there have been considerably more computational studies of *o*-QDMs compared to IQDMs of which only a handful have utilized quantum chemical calculations.<sup>420-423</sup> The only computational studies of IQDMs have been reported by Pindur and more recently by Tsoleridis.<sup>424</sup> The studies by Tsoleridis and coworkers focused on 1,3-



dipolar cycloadditions of aryl nitrile oxides to both of the exocyclic double bonds of IQDMs, generating dispiroisoxazolines **5.13** (Scheme 5.2). These experimental results were then followed up by computational studies at the AM1 level in which those authors' proposed mechanism was supported by FMO arguments and transition state calculations. Interestingly, one of the products isolated in that study (**5.14**) was "...a remarkable indole quinodimethane dimerization and cycloaddition product..." generated from two different cycloaddition processes: the [4+2] cycloaddition of one IQDM with the C-3/C-3 $\alpha$  exocyclic bond of another IQDM; the other, a [3+2] cycloaddition of the nitrile oxide with the other exocyclic double bond (C-2/C-2 $\alpha$ ). This product **5.14** is another example of which dimerization has occurred with complete regioselectivity. Furthermore, this product appears to have been generated by the same regioselective processes that govern the genesis of the homodimer of **5.1** as reported by Vice, discussed in Chapter 4.

To date, high-level quantum chemical calculations on the IQDMs have yet to appear. Studies employing the hybrid density functional B3LYP and the 6-31G(d) basis set have given excellent descriptions of Diels-Alder reactivity and selectivity despite its limitations.<sup>334,425-435</sup> More recently, Houk and coworkers have reported on the Diels-Alder reactions of butadiene with a series of dienophiles using Corey's cationic oxazaborolidine catalyst<sup>411,413-416</sup> in which the computational results showed excellent agreement with the experimental results with respect to stereoinduction and enantiomeric ratio.<sup>436</sup> In this context, it was anticipated that calculations using this theoretical platform would be appropriate with respect to the work described in Chapter 4 of this thesis.

### 5.3.2 Quantum Chemical Calculations: Ab Initio and Density Functional Theory

All quantum mechanical methods depend on solving the Schrödinger equation. Ab initio literally translated means “from the beginning” and these types of calculations use purely theoretical approaches to compute chemical structures, their properties, and reactivity. There are different levels of theory of which one of the most frequently used is Hartree-Fock (HF) which calculates the wavefunction to determine structure, properties and reactivity. Other ab initio approaches include Moller-Plesset perturbation theory (MP2, MP3, MP4), Configuration Interaction (CIS, CISD), Multi-Configuration SCF (MCSCF, CASSCF) and Coupled Cluster Theory (CCSD, CCSD(T)). These are called post-SCF methods that are typically applied after a standard ab initio method to correct for deficiencies in the HF method.

On the other hand, Density Functional Theory (DFT) uses a functional (a function of a function) to relate the electron density to the quantum mechanical description of the system (i.e. that there is a one-to-one mapping from the ground state electron density to the ground state electronic wavefunction). This is based on the Hohenberg-Kohn theorem,<sup>437</sup> which states that all the ground-state properties of a system are functions of the charge density and thus enables one to write the total electronic energy as a function of the electron density. In other words, the properties, structure and reactivity of a system are related to its electron density rather than the wavefunction (i.e. HF methods). In practice the DFT method often reduces computational cost considerably while giving results that are as good, and in some cases better, than those obtained using HF methods.

Computational methods are generally stated by the level of theory followed by the basis set used (e.g. HF 6-311+G\*, MP2 aug-cc-pVTZ, CBS-QB3, etc). A basis set is the set of functions that are used in linear combinations to create the molecular orbitals. In a very qualitative way, these basis functions can be thought of as approximating the atomic orbitals centered on the atoms.

All computational studies presented in this thesis were performed at the DFT level of theory employing the hybrid density functional B3LYP<sup>310,311</sup> (Becke three-parameter Lee-Yang-Parr exchange-correlation functional) and the 6-31G(d) basis set<sup>438</sup> (a valence double-zeta polarized basis set) using the suite of programs accessible in the commercially available software package Gaussian 03 by Gaussian Inc. (Copyright © 1994-2003, Gaussian, Inc)<sup>309</sup> installed on a desktop computer running the Linux operating system. Unless otherwise stated, all calculations were carried out in the gas phase at  $T = 298.15$  K and  $P = 1$  atm.

### **5.3.3 Theoretical Investigation of the Conformational Mobility of the *N*-Acetyl-Indole-2,3-Quinodimethanes**

Calculations were initiated with the aim of using the variable temperature NMR (VT NMR) work performed by S.R. White as the first model study to assess the predictability at the DFT B3LYP 6-31 G(d) level of theory. The observation of a 2.6:1 ratio of **5.1a**:**5.1b** at -93 °C (Chapter 4 Section 4.3.1) indicated a hindered conformational change that manifested as the deshielding of the H-7 proton and H-2 $\alpha$  protons in the <sup>1</sup>H NMR spectrum. Using this data one can calculate an experimental value for the corresponding energies of the two rotamer populations (Table 5.2). According to Gibbs free-energy relationship (equation 5.1), the difference in the ground state energy between these two rotamers is:

$$(5.1) \quad \Delta^\circ G_{R1R2} = -RT \ln K_{eq}$$

$$\Delta^\circ G_{R1R2} = -(1.98588 \text{ e}^{-3} \text{ kcal} \cdot \text{K}^{-1} \cdot \text{mol}^{-1}) (180\text{K}) \cdot \ln(2.6)$$

$$\Delta^\circ G_{R1R2} = -0.34 \text{ kcal} \cdot \text{mol}^{-1}$$

Next, the ground state energy minimum structures of both rotamers were computed. These calculations are called minimizations as the computation locates a geometry that is consistent with the corresponding energy value to be a minimum based on several criteria of the algorithm employed by the software program. Thus a minimized structure may be thought of as a structure possessing the most relaxed geometry. These calculations revealed that **5.1a** was 0.75 ( $\Delta E$ ), 0.75 ( $\Delta H$ ) and 0.67 ( $\Delta G$ ) kcal·mol<sup>-1</sup> lower in energy than **5.1b** and is in reasonable agreement with the experimental value of 0.34 kcal·mol<sup>-1</sup>. The modest difference between these two values may possibly be attributed to the experimental conditions employing deuterated acetone whereas the computations are carried out in the gas phase. Using the value -0.67 kcal·mol<sup>-1</sup> and substituting into equation 5.1:

$$(5.1) \quad \Delta^\circ G_{R1R2} = -RT \ln K_{eq}$$

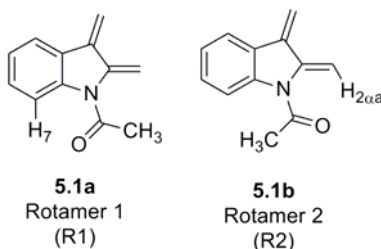
$$-0.67 \text{ kcal} \cdot \text{mol}^{-1} = -(1.98588 \text{ e}^{-3} \text{ kcal} \cdot \text{K}^{-1} \cdot \text{mol}^{-1}) (180\text{K}) \cdot \ln K_{eq}$$

$$\ln K_{eq} = 1.874$$

$$K_{eq} = 6.52$$

This value is in reasonable agreement with the value of 2.6 obtained from VT NMR study. These values, both experimental and theoretical, are presented in Table 5.2.

**Table 5.2:** Experimental and calculated rotamer populations and ground-state energies of *N*-Ac-IQDM rotamers **5.1a** and **5.1b**. Computations were accomplished at the DFT B3LYP 6-31G(d) level at -93 °C (180K).



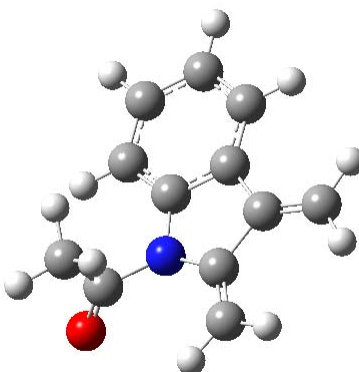
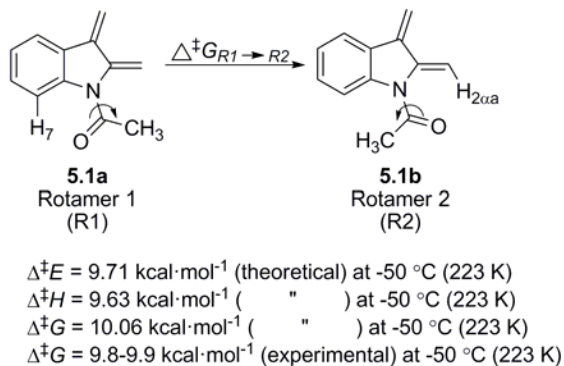
Rotamer population	R1	R2
experimental	2.6	1
theoretical	6.5	1
Relative energy $\Delta G$ (kcal·mol <sup>-1</sup> )	R1	R2
experimental	0	0.34
theoretical	0	0.67

These computational results correspond with the VT NMR study and thus provide assurance on the predictability of this method to pursue transition state (TS) studies. Accordingly, the free energy of activation ( $\Delta^\ddagger G$ ) for rotation of the amide moiety was calculated. From the VT NMR studies, a ratio of 2.6:1 at -93°C with peak coalescence occurring at -50°C was observed. From equation 5.2,<sup>439</sup> the activation barrier for R1→R2 could be calculated. Two different values are given for  $\Delta\nu$  depending on whether one uses H-7 (365 Hz) or H-2 $\alpha\alpha$  (525 Hz) and thus calculations using both values are shown:

$$\begin{aligned}
(5.2) \quad \Delta^\ddagger G_c &= 2.3 RT_c [10.32 + \log(T_c/k_c)]; \text{ where } k_c = \pi\Delta v/\sqrt{2} \\
&= 2.3(8.314472 \text{ J}\cdot\text{K}^{-1}\cdot\text{mol}^{-1})(223\text{K}) [10.32 + \log(223\text{K}/\pi(365 \text{ or } 525)/\sqrt{2})] \\
&= 4264.492689 [10.32 + \log(223\text{K}/810.826 \text{ or } 1166.256 \text{ Hz})] \\
&= 4264.492689 [10.32 + \log(0.275 \text{ or } 0.1912)] \\
&= 4264.492689 [10.32 + (-0.5606 \text{ or } -0.7185)] \\
&= 4264.492689 [9.759 \text{ or } 9.6015] \\
&= 41618.79 \text{ or } 40945.57 \text{ J}\cdot\text{mol}^{-1} \\
&= 41.61879 \text{ or } 40.94557 \text{ kJ}\cdot\text{mol}^{-1} \\
&= 9.94 \text{ or } 9.78 \text{ kcal}\cdot\text{mol}^{-1}
\end{aligned}$$

Next, the corresponding computation for the transition state structure (TSS) of the rotation of the amide moiety was accomplished. The free energy of activation provided  $\Delta^\ddagger G_{R1 \rightarrow R2}$  of 10.06 kcal·mol<sup>-1</sup> and is in excellent agreement with the experimental value of 9.78-9.94 kcal·mol<sup>-1</sup> calculated from the VT NMR studies (Figure 5.6).

**Figure 5.6:** Computed activation energy ( $\Delta^\ddagger E$ ), enthalpy of activation ( $\Delta^\ddagger H$ ) and free energy of activation ( $\Delta^\ddagger G$ ) and the experimental free energy of activation ( $\Delta^\ddagger G$ ) for the rotation of the amide moiety of **5.1**. The bottom panel shows the respective TSs (DFT B3LYP 6-31G(d) level).



By providing reasonably accurate quantitative data on both structure and energies, these two model studies provided a good assessment of the computational method employed such that examination of Diels-Alder reactions of **5.1** could now be pursued and this is the focus of the following discussion.

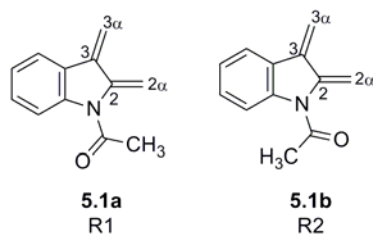
#### **5.3.4 Theoretical Investigation of Diels-Alder Reactions of the *N*-Acetyl-Indole-2,3-Quinodimethanes.**

In their analyses of the outcomes of Diels-Alder reactions of **5.3**, Pindur and coworkers had rationalized the regioselectivity in terms of FMO theory using semi-empirical calculations. The use of FMO theory as a predictive tool for such phenomena is well established amongst the organic chemistry community. However, other approaches may be used to rationalize chemo-, regio- and stereoselectivity should FMO theory fail to adequately predict the outcome of such reactions. Particularly, the use of transition state theory (TST), wherein the free energy of activation ( $\Delta^\ddagger G$ ) may be calculated which then may be applied to the analyses of Diels-Alder reactions as an alternative means to predict selectivity.

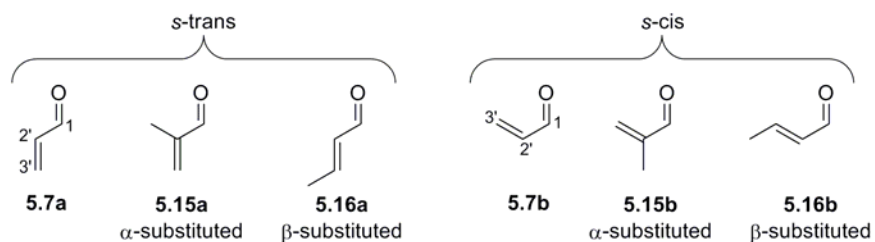


**Figure 5.7:** Considerations of computational efforts towards Diels-Alder reactions of **5.1**.

**1. Diene:**

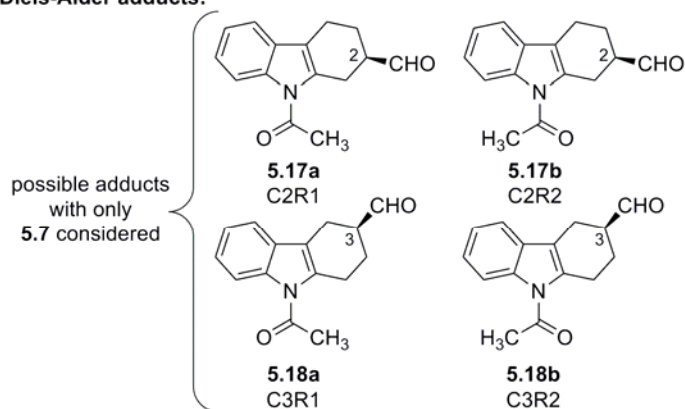


**2. Dienophile:**



**3. Dienophile approach:** endo vs. exo approach of dienophile (diastereoselectivity)

**4. Diels-Alder adducts:**



**5. Summary:** one dienophile can react with **5.1** to produce four DA adducts through sixteen possible reaction channels.

A number of criteria were established for both the diene and dienophile and are summarized in Figure 5.7. Both rotamers would be invoked in these studies to investigate if the two different conformations have implications on selectivity and is one issue that has not been explicitly addressed before. This is particularly important for reactions carried out under low temperature conditions. The choice of dienophiles would begin with the simple unsubstituted, unsymmetrical system, acrolein **5.7**. The effect of dienophile conformation (*s-trans* vs. *s-cis*) on selectivity would also be evaluated. Should these calculations parallel experimental results, then evaluation with the  $\alpha$ -substituted species methacrolein **5.15** and the  $\beta$ -substituted series *trans*-2-butenal (crotonaldehyde) **5.16**, both in their *s-cis* and *s-trans* conformations would be pursued. These dienophiles are chosen to probe the sensitivity of **5.1** to structural and conformational differences of the dienophile. Diastereoselectivity issues would be addressed by endo versus exo docking of the dienophile in TS calculations. Taken together, this data can provide useful information on feasibility of using various dienophiles in Diels-Alder reactions with **5.1** to construct substituted carbazoles as well kinamycin analogues.

#### 5.3.4.1 Acrolein

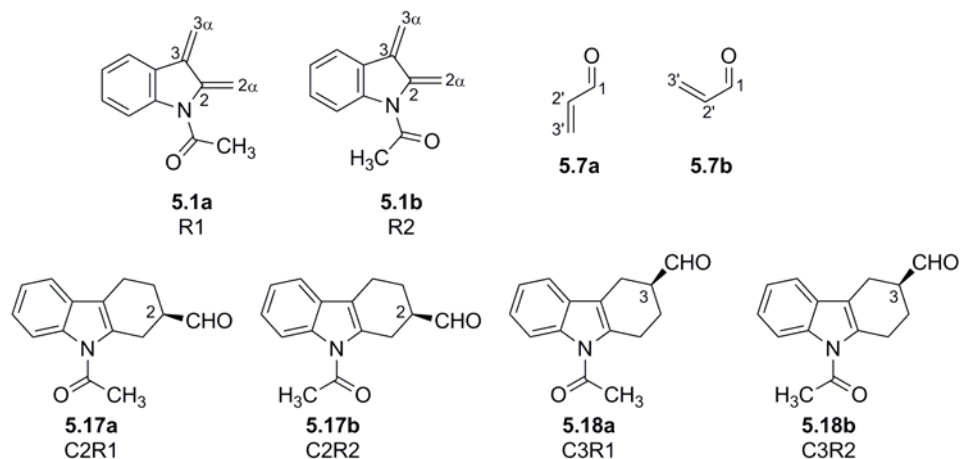
Appropriately, minimizations of **5.1**, **5.7** and the corresponding Diels-Alder adducts **5.17** and **5.18** were performed and from these calculations, the ground state electronic energy, enthalpy and free energy (*E*, *H*, *G* respectively) were retrieved and are given in Table 5.3. Only one enantiomer of each adduct was minimized due to the fact that the diene **5.1** is achiral and hence facial selectivity issues are non-existent in TS calculations. Separate adducts were calculated with respect to amide rotations (e.g. C2R1 and C2R2) even though

they represent the same product (in this case the C-2 regioisomer). This was accomplished so that TS calculations are focused on the appropriate reaction channel, the Diels-Alder reaction, and not bond rotation. If this were not so, then these conditions could compromise the calculation as the mathematical algorithms implemented in the software will in effect be looking for two transitions states in a single calculation. Thus it becomes a mandatory stipulation that the reactants have the same conformation as the products with the only differences being the loci at which bond formation (or cleavage) takes place. Obviously, this condition does not apply if the conformational change is the desired reaction path of investigation. The success of these calculations requires that close attention be paid to issues of conformation from bond rotation, sterics, Van der Waals contacts and so forth.

Focusing on the free energy values,  $G$ , examination of Table 5.3 reveals several observations:

1. Rotamer 1 (**5.1a**) is more stable than rotamer 2 (**5.1b**) by  $0.62 \text{ kcal}\cdot\text{mol}^{-1}$  as described in the preceding discussion (*vide supra*).
2. Acrolein is more stable in its *s*-trans conformation (**5.7a**) than its *s*-cis conformation (**5.7b**) by  $\sim 1.6 \text{ kcal}\cdot\text{mol}^{-1}$ .
3. Rotamer 2 adducts (**5.17b**, **5.18b**) are more stable than the corresponding rotamer 1 adducts (**5.17a**, **5.18a**) by  $\sim 0.3\text{-}1.6 \text{ kcal}\cdot\text{mol}^{-1}$ .
4. The adducts are more stable when the CHO group is in the axial conformation compared to the corresponding equatorial conformation by  $\sim 0.1\text{-}0.5 \text{ kcal}\cdot\text{mol}^{-1}$ .

**Table 5.3:** The energies (a.u.) and relative energies ( $\text{kcal}\cdot\text{mol}^{-1}$ ) of *N*-Ac-IQDM and acrolein and their corresponding Diels-Alder adducts obtained at the DFT B3LYP 6-31G(d) level at 25 °C (298 K).



Entry	Structure	Energy $E, {}^a H, {}^b G^c$ (a.u.) <sup>d</sup>	Relative Energy ( $\text{kcal}\cdot\text{mol}^{-1}$ )	Structure	Energy $E, {}^a H, {}^b G^c$ (a.u.) <sup>d</sup>	Relative Energy ( $\text{kcal}\cdot\text{mol}^{-1}$ )
1	<b>5.1a</b>	-593.656665 <sup>a</sup>	0	<b>5.1b</b>	-593.655457 <sup>a</sup>	0.76
		-593.644035 <sup>b</sup>	0		-593.642853 <sup>b</sup>	0.74
		-593.694444 <sup>c</sup>	0		-593.693453 <sup>c</sup>	0.62
2	<b>5.7a</b>	-191.850315	0	<b>5.7b</b>	-191.847638	1.68
		-191.845018	0		-191.842339	1.68
		-191.876592	0		-191.874058	1.59
3	<b>5.17a</b>	-785.569609 (eq.) <sup>e</sup>	1.85	<b>5.17b</b>	-785.571655 (eq.) <sup>e</sup>	0.57
		-785.553280 (eq.)	2.04		-785.555405 (eq.)	0.70
		-785.613216 (eq.)	1.31		-785.615164 (eq.)	0.09

		-785.570004 (ax.) <sup>f</sup>	1.61		-785.572562 (ax.) <sup>f</sup>	0
		-785.553922 (ax.)	1.64		-785.556528 (ax.)	0
		-785.612740 (ax.)	1.61		-785.615308 (ax.)	0
4	<b>5.18a</b>	-785.570122 (eq.)	1.53	<b>5.18b</b>	-785.571824 (eq.)	0.46
		-785.553830 (eq.)	1.69		-785.555593 (eq.)	0.59
		-785.613601 (eq.)	1.07		-785.615191 (eq.)	0.07
		-785.571626 (ax.)	0.59		-785.572032 (ax.)	0.33
		-785.555553 (ax.)	0.61		-785.555982 (ax.)	0.34
		-785.614391 (ax.)	0.58		-785.614909 (ax.)	0.25

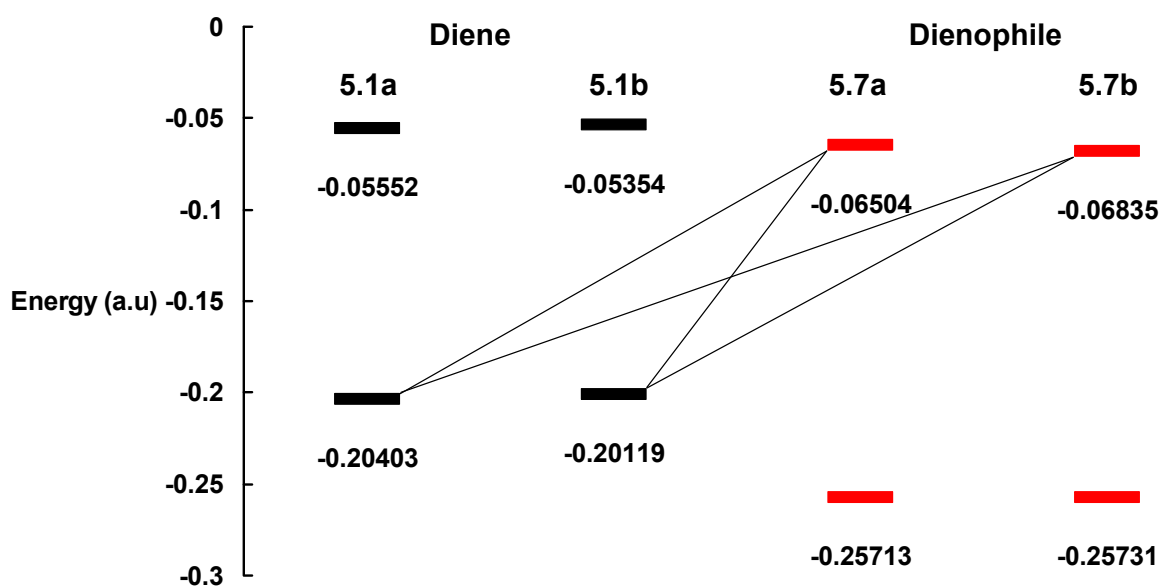
a., b., c. Energies are taken from minimized structures and are a) the electronic and zero point energies (i.e.  $E = E_{elec} + ZPE = E0$ ), b) the electronic, zero point and thermal enthalpies (i.e.  $H = E0 + H_{corr}$ ), c) the electronic, zero point and thermal free energies (i.e.  $G = E0 + G_{corr}$ ).

d. One atomic unit (a.u.) = 627.5095 kcal/mol.

e, f. The abbreviations eq. and ax. refer to the cyclohexene ring conformation in which the CHO group is in an equatorial and axial orientation, respectively.

The frontier molecular orbital (FMO) energies of the two reactants *N*-Ac-IQDM **5.1** and acrolein **5.7** are shown in Figure 5.8. There are two possible interactions: HOMO<sub>diene</sub>-LUMO<sub>dienophile</sub> and HOMO<sub>dienophile</sub>-LUMO<sub>diene</sub>. From this illustration, the HOMO<sub>diene</sub>-LUMO<sub>dienophile</sub> would indicate the reactivity of this cycloaddition would be governed by this interaction owing to the smaller energy gap, if the reaction is indeed FMO controlled.

**Figure 5.8:** Frontier molecular orbital energies (a.u) for the  $[4\pi_s+2\pi_s]$  cycloaddition of **5.1** with **5.7** calculated at the DFT B3LYP 6-31G(d) level. The four black solid lines indicate the four possible lowest energy HOMO-LUMO interactions of the HOMO of *N*-Ac-IQDM **5.1** (diene, black) with the LUMO of acrolein **5.7** (dienophile, red).

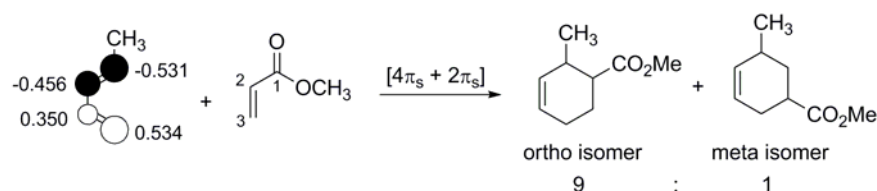


One atomic unit (a.u.) = 627.5095 kcal/mol.

Table 5.4 and Table 5.5 show the FMO energies and corresponding MO coefficients of **5.1** and **5.7**, respectively. The MO coefficients of both **5.1a** and **5.1b** are very similar at the termini; -0.25/0.25 (**5.1a**) and 0.28/-0.27 (**5.1b**) for C-2 $\alpha$ /C-3 $\alpha$  as shown in Table 5.4 ( $2p_z$  orbital only). This is in contrast to those reported by Pindur in which AM1 calculations gave

-0.38 for C-2 $\alpha$  and 0.34 for C-3 $\alpha$ . As previously stated, it would appear that Pindur's calculations do not provide the correct HOMO topology of **5.1** as initially reported, leading to erroneous conclusions on regioselectivity provided by FMO arguments derived from those calculations. Inspection of Table 5.5 reveals the largest MO coefficients are on C-3' of acrolein. It has been argued that, in some instances of dienes where the 2p orbital coefficients are too close in magnitude to determine regioselectivity of Diels-Alder reactions, the so called "secondary orbital" interactions may be the determining factor. For example, in the DA reaction of 1-methylbutadiene with methyl acrylate, the 2p orbital coefficients at C-1 (-0.531) and C-4 (0.534) are very similar, but the coefficient at C-2 (-0.456) is significantly greater than that at C-3 (0.350) (Scheme 5.3).<sup>440</sup>

**Scheme 5.3:** Secondary orbital interactions as a determining factor in the regioselectivity of Diels-Alder cycloadditions of 1-methylbutadiene with methyl acrylate.

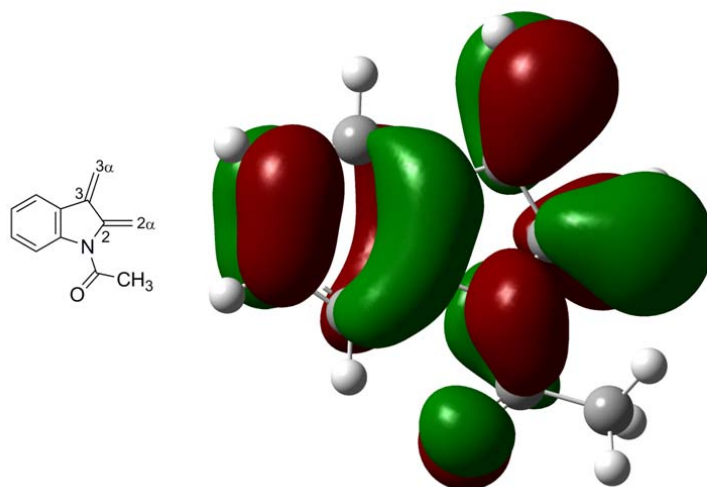


In this case it has been argued that the reaction is still FMO controlled with a preferential stabilizing interaction in an endo-transition state between the C-2 2p orbital and that of the 2p orbital on the activating group carbon of the dienophile (i.e. C-1). That secondary FMO interactions cannot explain the regioselectivity in the case of the DA reactions of the *N*-acetyl IQDM's is indicated by a comparison of the HOMO coefficients at C-2 (-0.11178) and at C-3

(0.11187) of rotamer 1. Thus, FMO theory does not provide a rationalization for the regioselectivity observed in DA reactions of IQDMs. Taken together, this suggests that there would be negligible differences in the regioselectivity of these DA reactions. Thus other means were sought to rationalize the regioselectivity. To this end, TS calculations were accomplished from which the energy barriers were obtained.



**Table 5.4:** FMO energy (a.u.) and orbital coefficients of the HOMO of *N*-Ac-IQDM **5.1a** and **5.1b** obtained at the DFT B3LYP 6-31G(d) level.<sup>a</sup>



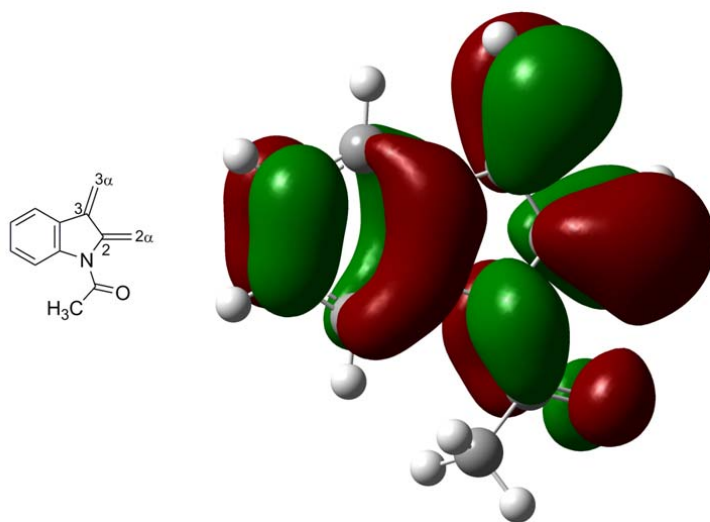
**5.1a (R1)**

	Energy (a.u.)	Orbital	Coefficient
<b>HOMO</b>	-0.20403	C2α 2p <sub>z</sub>	-0.25128
		C2α 3p <sub>z</sub>	-0.21190
		C2 2p <sub>z</sub>	-0.11178
		C3 2p <sub>z</sub>	0.11187
		C3α 2p <sub>z</sub>	0.25534
		C3α 3p <sub>z</sub>	0.21680

a. The 6-31 G(d) basis set is a polarized basis set in which d functions have been added to heavy atoms (atoms other than H and He). 6-31 G(d) is a split valence (double zeta) basis set that uses six Gaussians for the core orbitals (6 Cartesian d functions) and a 31G split valence shell. In the 6-31 G(d) basis set, the "6" is the number of primitive Gaussian type orbitals representing the core orbitals, whereas the "31" indicates how many functions the valence orbitals are split into and how many primitive Gaussian type orbitals are used for their representation. In other words, the numbers before the G indicate the s and p functions in the basis (i.e. 6-31), whereas the polarization function is placed after the G (i.e. d). In molecular modeling language, 6-31 G(d) is simply known as a valence double-zeta polarized basis

set. The purpose of the extra functions is to increase flexibility of the basis set and thus produce more realistic wavefunctions (Ref. 441-444).

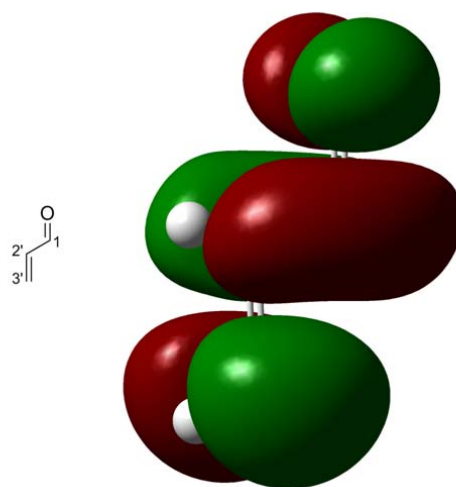
**Table 5.4** (continued)



**5.1b (R2)**

	Energy (a.u.)	Orbital	Coefficient
<b>HOMO</b>	-0.20119	C2 $\alpha$ 2p <sub>z</sub>	0.28030
		C2 $\alpha$ 3p <sub>z</sub>	0.23003
		C2 2p <sub>z</sub>	0.14873
		C2 3p <sub>z</sub>	0.10694
		C3 2p <sub>z</sub>	-0.12729
		C3 $\alpha$ 2p <sub>z</sub>	-0.27298
		C3 $\alpha$ 3p <sub>z</sub>	-0.22703

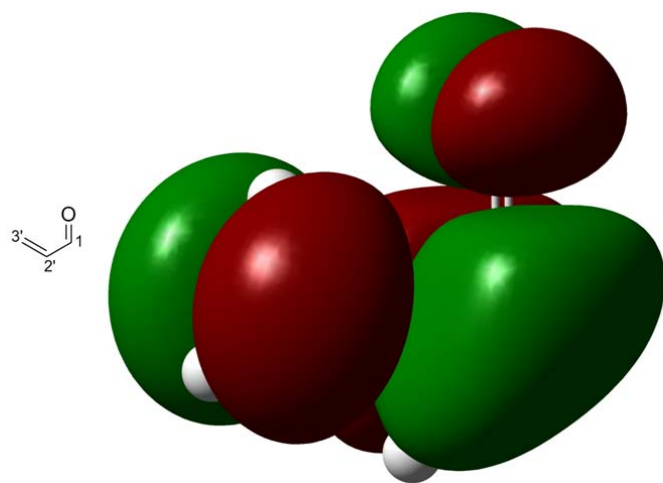
**Table 5.5:** FMO energy (a.u.) and orbital coefficients of the LUMO of acrolein **5.7a** and **5.7b** obtained at the DFT B3LYP 6-31G(d) level.



**5.7a**

	Energy (a.u.)	Orbital	Coefficient
<b>LUMO</b>	-0.06504	C1 2p <sub>z</sub>	-0.33525
		C1 3p <sub>z</sub>	-0.30754
		C2' 2p <sub>z</sub>	-0.21578
		C2' 3p <sub>z</sub>	-0.27339
		C3' 2p <sub>z</sub>	0.37601
		C3' 3p <sub>z</sub>	0.44245

**Table 5.5** (continued)



**5.7b**

	Energy (a.u.)	Orbital	Coefficient
<b>LUMO</b>	-0.06835	C1 2p <sub>z</sub>	-0.34179
		C1 3p <sub>z</sub>	-0.32196
		C2' 2p <sub>z</sub>	-0.19995
		C2' 3p <sub>z</sub>	-0.26879
		C3' 2p <sub>z</sub>	0.36256
		C3' 3p <sub>z</sub>	0.44785

Transition state calculations were pursued to obtain the energy barriers (electronic activation energy  $\Delta^\ddagger E$ , enthalpy of activation  $\Delta^\ddagger H$ , free energy of activation  $\Delta^\ddagger G$ ) for these cycloadditions and to acquire structural information (Table 5.6). Some general remarks can be made upon examination of the TS structures and their corresponding free energies of activation ( $\Delta^\ddagger G$ ). Both geometrical and energetic issues are considered:

1. Inspection of all TS structures (TSs) reveals an asynchronous cycloaddition owing to differences in bond lengths of the two incipient bonds.

2. The *s*-cis TSs are more asynchronous than the corresponding *s*-trans TSs as revealed by a larger difference in bond length between the two developing bonds (e.g. TS2 vs. TS4). As a measure of asynchronicity, one can calculate the difference in the length of the two developing bonds,  $\Delta d$ :  $(C-3\alpha-C-3')-(C2\alpha-C2') = \Delta d$  (or alternatively,  $(C-3\alpha-C2')-(C2\alpha-C-3') = \Delta d$ ). This is accomplished for the *s*-trans TSs and for the *s*-cis TSs (data not shown). Thus  $\Delta d$  is larger in the *s*-cis TSs than in the *s*-trans TSs, hence, more asynchronicity is observed in the *s*-cis TSs.

3. In all cases, a lower energy barrier (i.e. the most stable TS) is achieved by *s*-cis acrolein, the higher energy conformation of acrolein, as shown in Table 5.3, an example of which is TS2 compared to TS4. Others have described that, for unsymmetrical dienophiles, the more asynchronous the TS, the lower the energy barrier.<sup>445,446</sup>

4. All *s*-trans TSs are endoselective (e.g. TS1 vs. TS2) and this observation has also been reported by others.<sup>334,447-449</sup> Endoselectivity has been justified in several reports, including the "maximum accumulation of unsaturation" by Alder,<sup>450</sup> secondary orbital

interactions,<sup>322,390,440,451,452</sup> dipole-dipole,<sup>453</sup> charge-transfer,<sup>454</sup> electrostatic<sup>455</sup> and steric interactions<sup>392</sup> as influencing factors.

5. Rotamer 1 furnishes C-2 adducts with lower barriers than that for the corresponding C-3 adduct (e.g. TS1 vs. TS5). However, rotamer 2 and *s*-trans acrolein is marginally selective for the C-2 adduct (e.g. TS9 vs. TS13; TS10 vs. TS14) whereas *s*-cis acrolein is not selective at all.

6. As a general conclusion, the conformation of acrolein (*s*-trans vs. *s*-cis) has greater implications on the activation barrier than its approach (endo vs. exo; an example of which is TS5 vs. TS6 compared to TS5 vs. TS7). Furthermore, all *s*-cis TSs are more stable (i.e. lower energy) than the corresponding *s*-trans TSs (e.g. TS2 vs. TS4); all endo TSs are more stable than the corresponding exo TSs (e.g. TS15 vs. TS16), with one exception (TS7 vs. TS8).

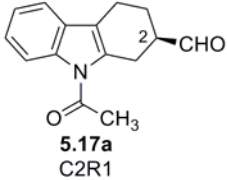
7.  $\Delta^\ddagger G$  is typically 10-15 kcal·mol<sup>-1</sup> higher than  $\Delta^\ddagger E$  and is typical for bimolecular reactions in which the entropy raises the free energy barrier relative to the electronic barrier alone.<sup>456</sup>

8. Considering  $\Delta^\ddagger G$ , the C-3 regioisomer is predicted to be in slight excess of C-2 (i.e. TS11 compared to TS15). However, further inspection of  $\Delta^\ddagger E$  and  $\Delta^\ddagger H$ , predict regioselectivities of ~6:1 (C-2:C-3) that are in accord with experimental observations presented in Chapter 4 (vide infra).

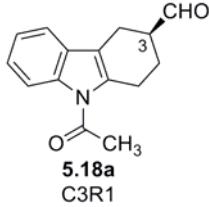
9. Acquisition of TS3 was denied despite many repeated computational attempts. However, based on the data presented in Tables 5.10 and 5.11 for methacrolein and crotonaldehyde, respectively, it may be reasonably assumed that the barrier for TS3 is higher than that for

TS11, and thus TS11 may be assumed to possess the lowest energy barrier for the C-2 adduct.

**Table 5.6:** Selected structural data and energies of TS structures of Diels-Alder reactions of *N*-Ac-IQDM and acrolein obtained at the DFT B3LYP 6-31G(d) level.<sup>a</sup>

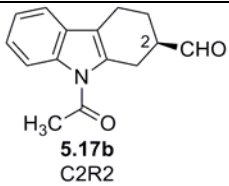
TS for DA Adduct	TSs	Bond distance (Å)	Dienophile	$\Delta^\ddagger E$ , <sup>c</sup> $\Delta^\ddagger H$ , <sup>d</sup> $\Delta^\ddagger G$ <sup>e</sup>
	IF <sup>b</sup>	C3 $\alpha$ -C3'	Approach	$E_{elec.} + ZPE$ <sup>f</sup>
		C2 $\alpha$ -C2'		$E_0 + H_{corr}$ <sup>g</sup>
				$E_0 + G_{corr}$ <sup>h</sup>
 <p>5.17a C2R1</p>	TS1	2.09094	<i>s</i> -trans, endo	<b>13.483</b> <sup>c</sup>
	-424.9	2.65019	top	<b>12.883</b> <sup>d</sup>
				<b>26.086</b> <sup>e</sup>
				-785.485494 <sup>f</sup>
				-785.468522 <sup>g</sup>
				-785.529466 <sup>h</sup>
	TS2	2.09970	<i>s</i> -trans, exo	<b>13.914</b>
	-433.2	2.62459	bottom	<b>13.315</b>
				<b>26.575</b>
				-785.484806
				-785.467834
				-785.528686
TS3	na	<i>s</i> -cis, endo	na	
na		top		
TS4	2.05982	<i>s</i> -cis, exo	<b>10.518</b>	
-401.6	2.80888	bottom	<b>9.906</b>	
			<b>23.227</b>	
			-785.487541	
			-785.470587	
			-785.531488	

**Table 5.6** (continued)

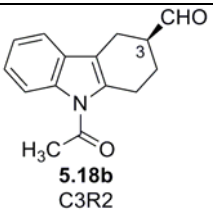
TS for DA Adduct	TSs	Bond distance (Å)	Dienophile	$\Delta^\ddagger E,^c \Delta^\ddagger H,^d \Delta^\ddagger G^e$
	IF <sup>b</sup>	C3 $\alpha$ -C2'	Approach	$E_{elec.} + ZPE^f$
		C2 $\alpha$ -C3'		$E_0 + H_{corr}^g$
				$E_0 + G_{corr}^h$
 <p><b>5.18a</b> C3R1</p>	TS5	2.56472	<i>s</i> -trans, endo	<b>14.639<sup>c</sup></b>
	-437.1	2.12036	top	<b>14.028<sup>d</sup></b>
				<b>27.477<sup>e</sup></b>
				-785.483652 <sup>f</sup>
				-785.466698 <sup>g</sup>
				-785.527249 <sup>h</sup>
	TS6	2.52746	<i>s</i> -trans, exo	<b>14.814</b>
	-442.5	2.13518	bottom	<b>14.235</b>
				<b>27.486</b>
				-785.483373
				-785.466368
				-785.527235
TS7	2.67924	<i>s</i> -cis, endo	<b>12.499</b>	
-407.3	2.10248	top	<b>11.847</b>	
			<b>25.457</b>	
			-785.484384	
			-785.467494	
			-785.527934	
TS8	2.70327	<i>s</i> -cis, exo	<b>11.258</b>	
-412.4	2.08080	bottom	<b>10.618</b>	
			<b>24.155</b>	
			-785.486363	
			-785.469453	
			-785.530009	



**Table 5.6** (continued)

TS for DA Adduct	TSs	Bond distance (Å)	Dienophile	$\Delta^\ddagger E$ , <sup>c</sup> $\Delta^\ddagger H$ , <sup>d</sup> $\Delta^\ddagger G$ <sup>e</sup>
	IF <sup>b</sup>	C3 $\alpha$ -C3' C2 $\alpha$ -C2'	Approach	$E_{elec.} + ZPE$ <sup>f</sup> $E_0 + H_{corr}$ <sup>g</sup> $E_0 + G_{corr}$ <sup>h</sup>
 <p><b>5.17b</b> C2R2</p>	TS9	2.08393	<i>s</i> -trans, endo	<b>14.083</b> <sup>c</sup>
	-432.8	2.68613	top	<b>13.545</b> <sup>d</sup>
				<b>26.609</b> <sup>e</sup>
				-785.483329 <sup>f</sup>
				-785.466286 <sup>g</sup>
				-785.527641 <sup>h</sup>
	TS10	2.08150	<i>s</i> -trans, exo	<b>14.497</b>
	-432.5	2.68116	bottom	<b>13.943</b>
				<b>26.979</b>
				-785.482669
				-785.465651
				-785.527050
TS11	2.08857	<i>s</i> -cis, endo	<b>10.012</b>	
-397.6	2.77886	top	<b>9.340</b>	
			<b>23.133</b>	
			-785.487140	
			-785.470307	
			-785.530647	
TS12	2.06209	<i>s</i> -cis, exo	<b>10.432</b>	
-406.0	2.82166	bottom	<b>9.818</b>	
			<b>23.211</b>	
			-785.486470	
			-785.469546	
			-785.530522	

**Table 5.6** (continued)

TS for DA Adduct	TSs	C3 $\alpha$ -C2'	Dienophile	$\Delta^\ddagger E,^c$ $\Delta^\ddagger H,^d$ $\Delta^\ddagger G^e$
	IF <sup>b</sup>	C2 $\alpha$ -C3'	Approach	$E_{elec.} + ZPE^f$ $E_0 + H_{corr}^g$ $E_0 + G_{corr}^h$
 <p><b>5.18b</b> C3R2</p>	TS13	2.58281	<i>s</i> -trans, endo	<b>14.012<sup>c</sup></b>
	-440.2	2.10354	top	<b>13.417<sup>d</sup></b>
				<b>26.685<sup>e</sup></b>
				-785.483442 <sup>f</sup>
				-785.466489 <sup>g</sup>
				-785.527519 <sup>h</sup>
	TS14	2.54983	<i>s</i> -trans, exo	<b>14.474</b>
	-442.3	2.11574	bottom	<b>13.872</b>
				<b>27.124</b>
				-785.482706
				-785.465765
				-785.526820
TS15	2.76527	<i>s</i> -cis, endo	<b>11.050</b>	
-404.6	2.06480	top	<b>10.425</b>	
			<b>23.099</b>	
			-785.485485	
			-785.468578	
			-785.530699	
TS16	2.73868	<i>s</i> -cis, exo	<b>11.111</b>	
-409.2	2.05902	bottom	<b>10.505</b>	
			<b>23.850</b>	
			-785.485389	
			-785.468452	
			-785.529503	

- a. Each TS calculation was carried out using the Synchronous Transit-Guided Quasi-Newton Method (QST2 or QST3, Ref. 317,318) using Gaussian 03 rev. B.04 or C.02 implemented on a desktop computer running Linux OS (Redhat). TS calculations times were typically 8-12 hours in duration. All structures reported here as TSs exhibit only one imaginary frequency. The imaginary vibrations were animated with Gaussview 3.09 or 4.1 to determine if they were in qualitative agreement with the bond-making/bond-breaking processes associated with the reaction of interest. In each case, intrinsic reaction coordinate (IRC, Ref. 313,314) calculations were performed to determine that the observed TS could be linked reasonably to the assumed reactant and product geometries.
- b. IF = imaginary frequency in reciprocal centimeters and are not scaled (Ref. 315).
- c.  $\Delta^\ddagger E$  ( $= \Delta^\ddagger E0$ ), d.  $\Delta^\ddagger H$ , e.  $\Delta^\ddagger G$  in kcal/mol.
- f. *Eelec.* + ZPE ( $= E0$ ), g.  $H = E0 + H_{\text{corr}}$ , h.  $G = E0 + G_{\text{corr}}$  in a.u. (1 a.u. = 627.5095 kcal/mol).

The most important observation from the VT NMR studies of **5.1** (S.R. White in this group) was the conformational preference for R1. The use of low temperatures employed by Wu as described in Chapter 4 would favor the R1 conformation and hence may justify the C-2 regioselectivity. The regioselective outcome is the *weighted* average of all TSs combined, each of which is described in Table 5.6.

A simple estimate of regioselectivity can be shown as the arithmetical difference between the free energy barrier for a C-2 adduct and a C-3 adduct obtained from representative transition states. First, one must identify the lowest activation barriers in this data set that furnishes the C-2-substituted and the C-3-substituted carbazoles. These are TS11 ( $\Delta^\ddagger G = 23.133 \text{ kcal}\cdot\text{mol}^{-1}$ ) and TS15 ( $\Delta^\ddagger G = 23.099 \text{ kcal}\cdot\text{mol}^{-1}$ ), respectively. This gives a difference of  $\sim 0.033 \text{ kcal}\cdot\text{mol}^{-1}$  (i.e.  $\Delta\Delta^\ddagger G = 32.63 \text{ cal}\cdot\text{mol}^{-1}$ ). The two products of the Diels-Alder reaction are kinetic. That is, the ratio of products is a function of the ratio of kinetic rate constants,  $k_{C3}/k_{C2}$ . Therefore, using the Eyring relationship, equation 5.3:

$$(5.3) \quad k = \kappa(k_b T/h) e^{(-\Delta^\ddagger G/RT)}$$

$$k_{C3}/k_{C2} = e^{(-\Delta\Delta^\ddagger G/RT)}$$

$$k_{C3}/k_{C2} = e^{[-32.63 \text{ cal/mol}/(1.98588 \text{ cal/K}\cdot\text{mol}) (298\text{K})]}$$

$$k_{C3}/k_{C2} = e^{-0.055}$$

Taking the absolute value of the exponent;

$$k_{C3}/k_{C2} = e^{|-0.055|}$$

$$k_{C3}/k_{C2} = e^{0.055}$$

$$k_{C3}/k_{C2} = 1.06$$

From these calculations, the C-3 regioisomer is predicted to be the major product as it has the lower  $\Delta^\ddagger G$ , although the selectivity is marginal. From the Eyring rate law, the calculated TS energies give selectivities of 1.06:1 (i.e.  $\sim 1:1$  for C-3:C-2) which do not agree with the experimental results from this lab. However, when one compares the  $\Delta^\ddagger E$  and  $\Delta^\ddagger H$  values for TS11 and TS15 and calculates the corresponding  $\Delta\Delta^\ddagger E = 1.039 \text{ kcal}\cdot\text{mol}^{-1}$  and  $\Delta\Delta^\ddagger H = 1.085 \text{ kcal}\cdot\text{mol}^{-1}$ , the C-2 regioisomer is predicted to be the major product, giving a regioselectivity of 5.79:1 and 6.26:1, respectively (i.e.  $\sim 6:1$  for C-2:C-3 using equation 5.3 and substituting  $\Delta\Delta^\ddagger E$  and/or  $\Delta\Delta^\ddagger H$  for  $\Delta\Delta^\ddagger G$ ). These data are in reasonable agreement with the experimental results of Diels-Alder reactions of *N*-Ac-IQDM with acrolein ( $\sim 3:1$  ratio for C-2:C-3). The reason(s) for the discrepancy between calculated and experimental results are not clear.

At this time, the qualitative differences between the energy barriers listed in Table 5.6 should be made obvious. The  $\Delta^\ddagger E$  data set provides the potential energy barrier and thus represents the minimum energy pathway (MEP) connecting the reactants to the products on the potential energy surface (PES),<sup>457-459</sup> also known as the hypersurface. The PES has  $3N-6$  degrees of freedom for an *N*-atom system ( $N > 3$  atoms).  $\Delta^\ddagger E$  is the electronic energy difference between reactant and transition state and is the most important contribution to  $\Delta^\ddagger G$  and is the most difficult to calculate accurately.<sup>460</sup> It is important to realize that no

thermodynamic corrections have been applied to  $\Delta^\ddagger E$ . The PES helps to define the scope of each elementary reaction and the MEP facilitates understanding the nature of a *transition state structure*, TSs, (not to be confused with the *transition state*, vide infra) and is just one representative of the population of molecules passing from reactants to products.<sup>461</sup> More specifically, the TSs is saddle point associated with particular molecular structure and is a stationary point on the energy surface,<sup>462</sup> where the first derivative of the energy function is zero with respect to all coordinates and one (and only one) negative second derivative of the energy<sup>463,464</sup> (i.e. a single negative eigenvalue of the Hessian matrix and is often referred to as the imaginary frequency for motion over the saddle point<sup>465</sup>). Finally,  $\Delta^\ddagger E$  differs  $\Delta^\ddagger H$  by  $RT$  (vide infra).<sup>466</sup>

On the other hand, the  $\Delta^\ddagger G$  data set represents the free energy surface and in effect, hovers above the PES, in which the *transition state* (also known as the "activated complex"), an ensemble of species that populate a range of energy levels in the vicinity of a saddle point on the PES, can be found.<sup>462,467</sup> It is the free energy of populations of molecules that almost always govern the kinetics and equilibria of reacting systems, not the potential energy of single molecules.<sup>467</sup> The TSs is a specific entity with a definite structure; the transition state is a thermodynamic concept in which a  $N$ -atom system is a surface with  $3N-7$  degrees of freedom.<sup>462</sup> The position of the TS is thought to be the at the maximum of the PES (electronic energy surface) but in actuality it should be the maximum of the Gibbs free energy surface ( $\Delta G$ ).<sup>468</sup> The contribution(s) to the free energy of activation ( $\Delta^\ddagger G$ ) from sources other than the potential energy difference ( $\Delta^\ddagger E$ ) must taken into consideration, including differences in entropy, thermal energy, zero point vibrational energy (ZPVE), and

the  $PV$  term.<sup>462</sup> Thus entropy plays a role and consequently the geometry of the TS will depend on temperature.<sup>469</sup> Variational TS theory<sup>470-472</sup> is one such approach that is used to address this issue.

The salient points are summarized here. The total internal thermal energy ( $E_{tot}$ ) is made up of the internal energy due to translation, rotational motion, vibrational motion and electronic motion, given by:

$$(5.4) \quad E_{tot} = E_t + E_r + E_v + E_e$$

The thermal corrections (not shown) applied to the Enthalpy and the Gibbs Free Energy and are given by:

$$(5.5) \quad H_{corr} = E_{tot} + k_B T \quad (= \text{thermal correction to enthalpy})$$

$$(5.6) \quad G_{corr} = H_{corr} - TS_{tot} \quad (= \text{thermal correction to Gibbs free energy})$$

Applying these corrections gives the electronic and thermal enthalpy ( $H$ ) and the electronic and thermal free energies ( $G$ ), equations 5.9 and 5.10, respectively. As well, the zero point vibrational energy (ZPVE) corrected electronic energy ( $E_0$ , equation 5.7) is shown:

$$(5.7) \quad E_0 = E_{elec} + \text{ZPVE} \quad (= \text{sum of electronic and zero point Energies})$$

$$(5.8) \quad E_{tot} = E_{transl} + E_{rot} + E_{vib} + E_0 \quad (= \text{sum of electronic and thermal Energies})$$

$$(5.9) \quad H = E_{tot} + RT \quad (= E_0 + H_{corr} = \text{sum of electronic and thermal Enthalpies})$$

$$(5.10) \quad G = H - TS \quad (= E_0 + G_{corr} = \text{sum of electronic and thermal free Energies})$$

Thus the energy barriers are calculated as:

$$(5.11) \quad \Delta^\ddagger E_0 = (E_{elec} + ZPVE)_{TS} - (E_{elec} + ZPVE)_{reactants} = \text{Activation energy}$$

$$(5.12) \quad \Delta^\ddagger H = (E_0 + H_{corr})_{TS} - (E_0 + H_{corr})_{reactants} = \text{Activation enthalpy}$$

$$(5.13) \quad \Delta^\ddagger G = (E_0 + G_{corr})_{TS} - (E_0 + G_{corr})_{reactants} = \text{Free energy of Activation}$$

Disagreement between theory and experiment can be justified by either by the theoretical approach or some intrinsic source of error of which there can be many. Firstly, one of the major assumptions is that of non-interacting particles and that the system under study behaves as an ideal gas. Some error can be expected from this assumption. Secondly, and related to aforementioned gas phase calculation scenario is that solvent effects are not explicitly included in the calculations for the present study. This has a pronounced effect on energy barriers where it has been shown that the inclusion of solvent effects can give results opposite of those acquired in the gas phase. This is dealt with more in depth in the discussion on Lewis acid catalyzed DA reaction of IQDMs (Section 5.3.5).

In this study of DA reactions with *N*-Ac IQDM and acrolein, the computational method has not provided a prediction of regioselectivity that is consistent with the experimentally observed result. Clearly some further computational effort in this area is required before reliable predictions of regioselectivity of D-A reactions of *N*-Ac-IQDM are possible. Although time constraints preclude the possibility of pursuing this issue further in the context of the present thesis, it is worth considering briefly various issues that might be addressed in future work. The methodology employed in this study has been employed very successfully in making predictions of reactivity and stereoselectivity in numerous Diels-Alder reactions in

both the gas and condensed phase, most notably by the Houk<sup>333,436</sup> and Paddon-Row groups.<sup>473</sup> The failure to give an accurate prediction in the present work suggests that consideration be given to the unique nature of the diene in this work.

The ground state calculations of **5.1a** and **5.1b**, R1 and R2, respectively, indicate a slight twisting about the amide group as well as the diene portion suggesting that there might be a small facial selectivity issue in DA reactions of *N*-Ac-IQDMs. Such subtle effects may play a role in the  $\Delta\Delta^\ddagger G$  between the two TSs that provide the C-2 adduct, which in this instance, is less than 0.1 kcal·mol<sup>-1</sup> (i.e. if one compares TS4 and TS11, TSs in which R1 and R2 are invoked, respectively, furnishing the C-2 adduct). Owing to this very small difference, it may be suggested that TS calculations be carried out using minimized structures that possess bond angles and dihedral angles that are "opposite" of the those minimized structures employed in the present study. Future efforts in this direction are recommended in the present case.



**Figure 5.9:** The transition state structures of TS11 and TS15.

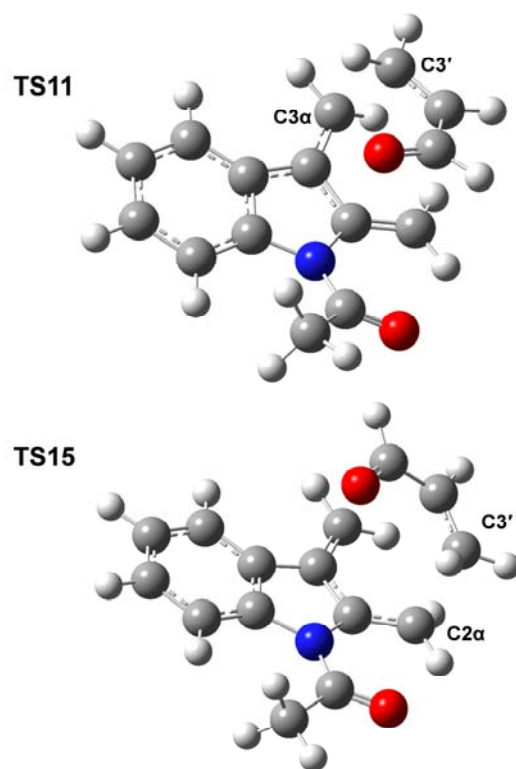


Figure 5.9 shows two TS structures from the aforementioned calculations, TS11 and TS15. In both cases advanced bond development occurs between C-3' of acrolein and either C-3 $\alpha$  (TS11) or C-2 $\alpha$  (TS15) of *N*-Ac-IQDM and thus are asynchronous. Examination of the vibrational mode corresponding to the imaginary frequencies (TS11 = -398 cm<sup>-1</sup>; TS15 = -405 cm<sup>-1</sup>) indicates this motion is principally between C-3 $\alpha$  and C-3' (TS11) and C-2 $\alpha$  and C-3' (TS15) and is another measure of asynchronous character. A further means to characterize asynchronicity is to measure the pyramidalization at each of the sp<sup>2</sup> carbon centers. This may be accomplished by summing all of the bond angles of the atom in question. In TS11, C-3 $\alpha$  is 351.8° and C-3' is 351.4° which is more advanced upon comparison to C-2 $\alpha$  at 359.3°

and C-2' at 359.8°. In TS15, C-2 $\alpha$  is 351.1° and C-3' is 351.0° and the other pair, C-3 $\alpha$  and C-2', display angles of 359.2° and 359.8°, respectively. Here the pyramidalization manifests principally at C-2 $\alpha$  and C-3'. Other sophisticated studies to further characterize transition states such as Wiberg bond indices<sup>474</sup> and/or NBO analysis<sup>475</sup> (which has shown to be a more reliable than Mulliken population analysis<sup>476</sup>), were not pursued.

Thus quantum chemical studies of Diels-Alder cycloadditions of *N*-Ac-IQDM with acrolein provides reasonably accurate data on structure and energies. Whereas  $\Delta^\ddagger G$  was found not to be predictive of regiochemistry, the calculated barriers  $\Delta^\ddagger E$  and  $\Delta^\ddagger H$  parallel experimental trends previously accomplished by others in this group and elsewhere. Evaluation of both  $\alpha$ - and  $\beta$ -substituted systems could now be pursued and are discussed below.

#### 5.3.4.2 Methacrolein and Crotonaldehyde

Table 5.7 shows the ground state energies of the reactants and products for cycloadditions of methacrolein and crotonaldehyde and display the same trends as found for acrolein:

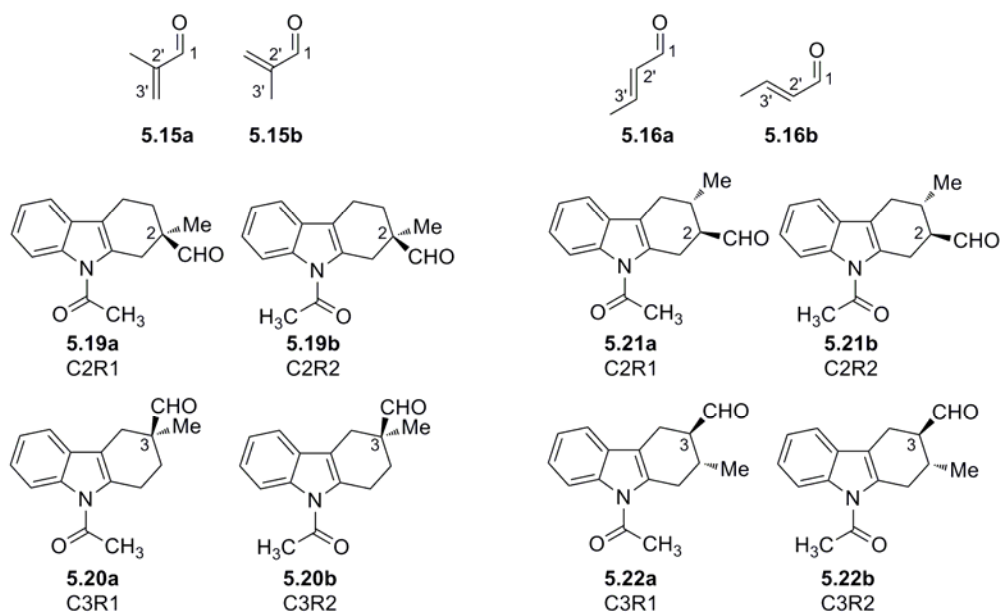
1. Dienophiles are more stable as their *s*-trans conformation.
2. Rotamer 2 adducts are more stable than rotamer 1 adducts.

The frontier molecular orbital (FMO) energies for methacrolein **5.15** and crotonaldehyde **5.16** are shown in Figures 5.10 and 5.11, respectively along with **5.1**. There are two possible interactions: HOMO<sub>diene</sub>-LUMO<sub>dienophile</sub> and HOMO<sub>dienophile</sub>-LUMO<sub>diene</sub>. Both methacrolein and crotonaldehyde are similar to acrolein in which the HOMO<sub>diene</sub>-LUMO<sub>dienophile</sub> indicates the reactivity of this cycloaddition is governed by this interaction owing to the smaller energy gap, should the reaction be FMO controlled. The HOMO-LUMO gap has also slightly

increased on comparison to the acrolein data set and is corroborated by the energetic data presented in Tables 5.10 and 5.11, should the reaction be FMO controlled.

Table 5.8 and Table 5.9 show the FMO energies and corresponding MO coefficients of **5.15** and **5.16**, respectively. Taken together and disregarding sterics for the moment, this would indicate that methacrolein and crotonaldehyde are similar to acrolein in that there would be negligible differences in the regioselectivity of DA reactions, if FMO interactions were the determining factor.

**Table 5.7:** The energies (a.u.) and relative energies ( $\text{kcal}\cdot\text{mol}^{-1}$ ) of methacrolein and crotonaldehyde and their corresponding Diels-Alder adducts obtained at the DFT B3LYP 6-31G(d) level.

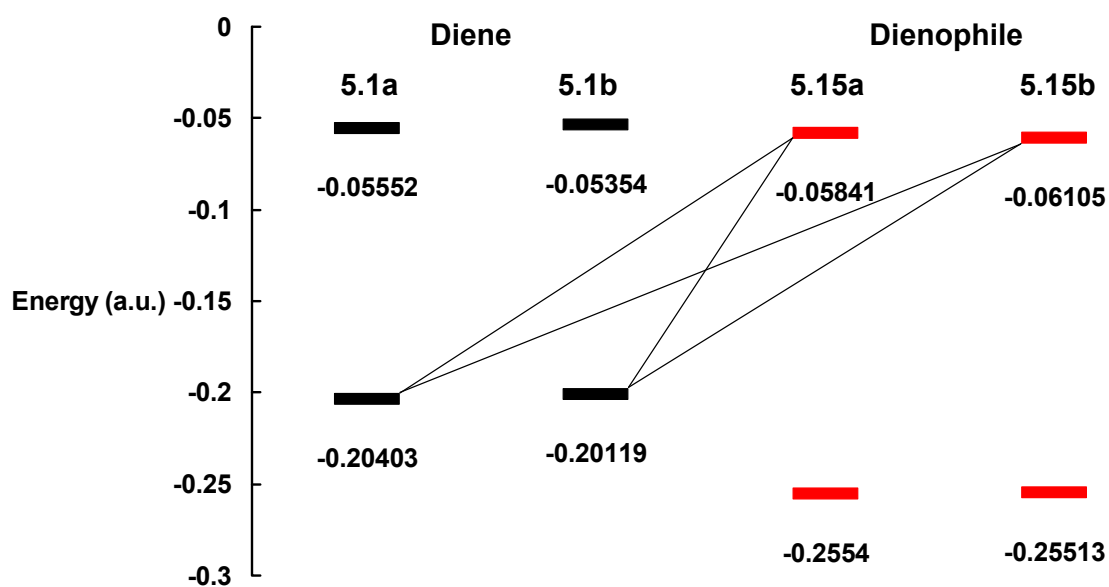


Entry	Structure	Energy $E,^a H,^b G^c$ (a.u.) <sup>d</sup>	Relative Energy (kcal·mol <sup>-1</sup> )	Structure	Energy $E,^a H,^b G^c$ (a.u.) <sup>d</sup>	Relative Energy (kcal·mol <sup>-1</sup> )
1	<b>5.15a</b>	-231.143442 <sup>a</sup>	0.44	<b>5.15b</b>	-231.139099 <sup>a</sup>	3.16
		-231.136818 <sup>b</sup>	0.37		-231.132365 <sup>b</sup>	3.16
		-231.172065 <sup>c</sup>	0.45		-231.167909 <sup>c</sup>	3.06
2	<b>5.16a</b>	-231.144138	0	<b>5.16b</b>	-231.141979	1.35
		-231.137402	0		-231.135250	1.35
		-231.172786	0		-231.170696	1.31
3	<b>5.19a</b>	-824.855790	1.48	<b>5.19b</b>	-824.857771	0.23
		-824.838140	1.53		-824.840191	0.24
		-824.900292	1.64		-824.902140	0.48
4	<b>5.20a</b>	-824.856483	1.04	<b>5.20b</b>	-824.858145	0
		-824.838858	1.08		-824.840573	0
		-824.900927	1.24		-824.902432	0.29
5	<b>5.21a</b>	-824.855945	1.38	<b>5.21b</b>	-824.857859	0.18
		-824.838126	1.54		-824.840146	0.27
		-824.901101	1.13		-824.902595	0.19
6	<b>5.22a</b>	-824.856349	1.13	<b>5.22b</b>	-824.858009	0.09
		-824.838560	1.26		-824.840287	0.18
		-824.901316	0.99		-824.902906	0

a., b., c. Energies are taken from minimized structures and are a) the electronic and zero point energies (i.e.  $E = E_{\text{elec}} + \text{ZPE} = E0$ ), b) the electronic, zero point and thermal enthalpies (i.e.  $H = E0 + H_{\text{corr}}$ ), c) the electronic, zero point and thermal free energies (i.e.  $G = E0 + G_{\text{corr}}$ ).

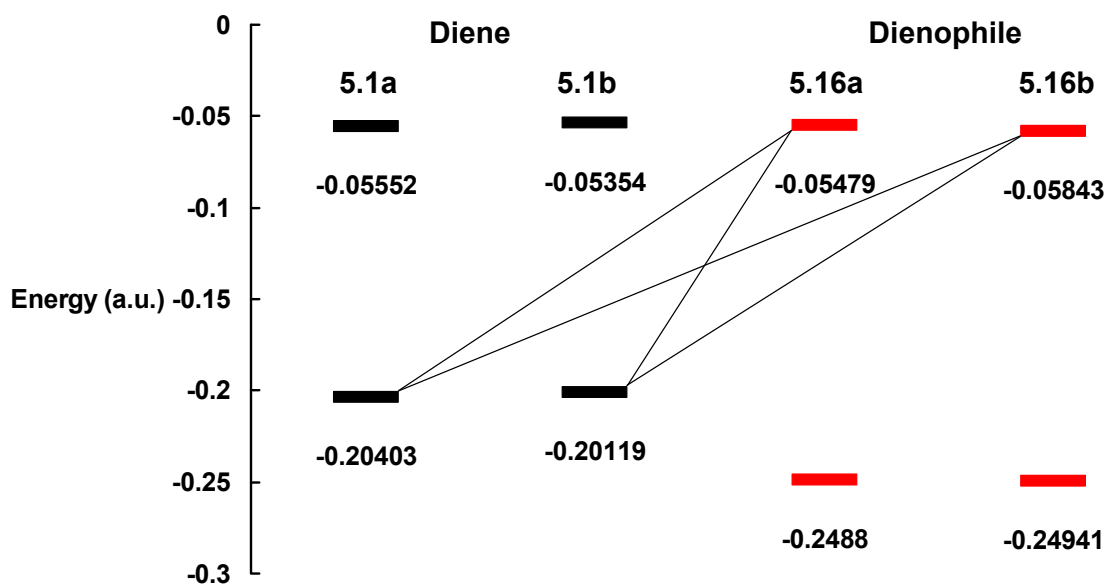
d. One atomic unit (a.u.) = 627.5095 kcal/mol.

**Figure 5.10:** Frontier molecular orbital energies (a.u) for the  $[4\pi_s+2\pi_s]$  cycloaddition of **5.1** with **5.15** calculated at the DFT B3LYP 6-31G(d) level. The four black solid lines indicate the four possible lowest energy HOMO-LUMO interactions of the HOMO of *N*-Ac-IQDM **5.1** (diene, black) with the LUMO of methacrolein **5.15** (dienophile, red).



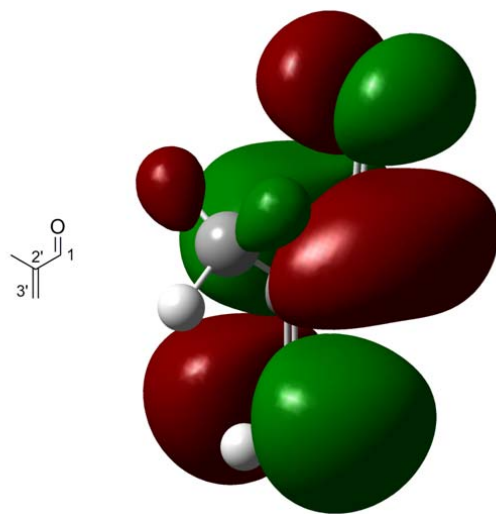
One atomic unit (a.u.) = 627.5095 kcal/mol.

**Figure 5.11:** Frontier molecular orbital energies (a.u) for the  $[4\pi_s+2\pi_s]$  cycloaddition of **5.1** with **5.16** calculated at the DFT B3LYP 6-31G(d) level. The four black solid lines indicate the four possible lowest energy HOMO-LUMO interactions of the HOMO of *N*-Ac-IQDM **5.1** (diene, black) with the LUMO of crotonaldehyde **5.16** (dienophile, red).



One atomic unit (a.u.) = 627.5095 kcal/mol.

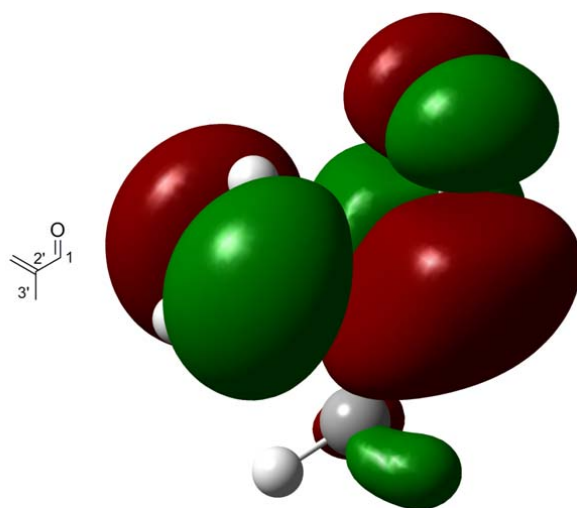
**Table 5.8:** FMO energy (a.u.) and orbital coefficients of the LUMO of methacrolein **5.15a** and **5.15b** obtained at the DFT B3LYP 6-31G(d) level.



**5.15a**

	Energy (a.u.)	Orbital	Coefficient
<b>LUMO</b>	-0.05841	C1 2p <sub>z</sub>	-0.35619
		C1 3p <sub>z</sub>	-0.33111
		C2' 2p <sub>z</sub>	-0.20650
		C2' 3p <sub>z</sub>	-0.26688
		C3' 2p <sub>z</sub>	0.36160
		C3' 3p <sub>z</sub>	0.43047

**Table 5.8** (continued)

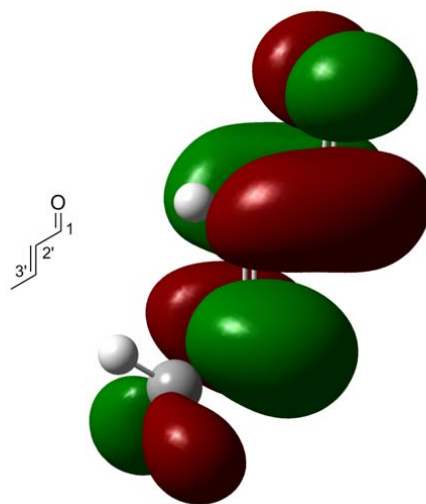


**5.15b**

	Energy (a.u.)	Orbital	Coefficient
<b>LUMO</b>	-0.06105	C1 2p <sub>z</sub>	-0.36376
		C1 3p <sub>z</sub>	-0.34793
		C2' 2p <sub>z</sub>	-0.19326
		C2' 3p <sub>z</sub>	-0.26085
		C3' 2p <sub>z</sub>	0.34078
		C3' 3p <sub>z</sub>	0.42962



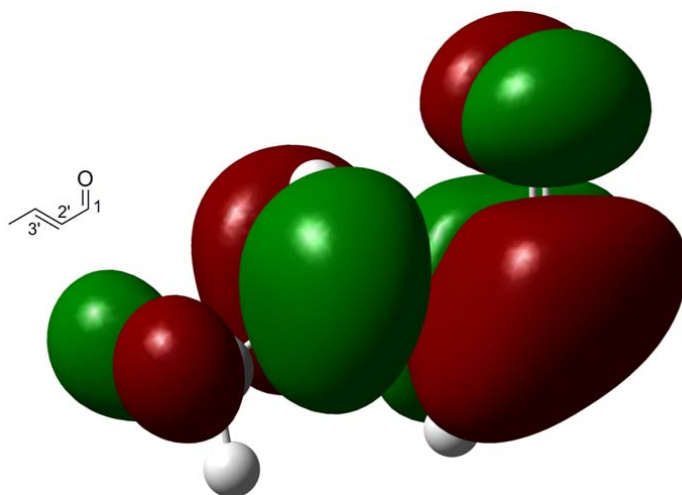
**Table 5.9:** FMO energy (a.u.) and orbital coefficients of the LUMO of crotonaldehyde **5.16a** and **5.16b** obtained at the DFT B3LYP 6-31G(d) level.



**5.16a**

	Energy (a.u.)	Orbital	Coefficient
<b>LUMO</b>	-0.05479	C1 2p <sub>z</sub>	-0.33810
		C1 3p <sub>z</sub>	-0.31455
		C2' 2p <sub>z</sub>	-0.19776
		C2' 3p <sub>z</sub>	-0.24853
		C3' 2p <sub>z</sub>	0.38941
		C3' 3p <sub>z</sub>	0.42400

**Table 5.9** (continued)



**5.16b**

	Energy (a.u.)	Orbital	Coefficient
<b>LUMO</b>	-0.05843	C1 2p <sub>z</sub>	-0.34484
		C1 3p <sub>z</sub>	-0.32729
		C2' 2p <sub>z</sub>	-0.18148
		C2' 3p <sub>z</sub>	-0.24729
		C3' 2p <sub>z</sub>	0.37562
		C3' 3p <sub>z</sub>	0.44083

TS calculations involving methacrolein and crotonaldehyde were carried out in a manner identical to that used for DA reactions of acrolein, the results of which are shown in Tables 5.10 and 5.11, respectively. Some general trends are observed upon inspection of the TS structures and their corresponding barriers ( $\Delta^\ddagger G$ ) and, in many respects, a similar pattern emerges to that of acrolein:

1. Inspection of all TSs reveals an asynchronous cycloaddition.
2. The *s*-cis TSs are more asynchronous than the corresponding *s*-trans TSs as shown by the larger difference in bond length between the two nascent bonds (e.g. TS17 vs. TS19; TS33 vs. TS35).
3. In all cases, a lower energy barrier is achieved by the *s*-cis conformer of the dienophile (e.g. TS18 vs. TS20), the higher energy conformations of these dienophiles.
4. All cycloadditions with methacrolein and crotonaldehyde possess larger energy barriers than the corresponding cycloadditions with acrolein with crotonaldehyde possessing the largest energy barriers of the three dienophiles (TS1 vs. TS17 and TS33). This reflects the effect of  $\beta$ -substitution of the dienophile in [4+2] cycloadditions.
5. The *s*-trans TSs for methacrolein are endoselective (e.g. TS17 vs. TS18). This is not the case with crotonaldehyde in which half of the *s*-trans TSs possess lower barriers than their exo counterparts (e.g. TS33 vs. TS34 compared with TS37 vs. TS38).
6. Of the TSs with methacrolein, lower barriers are observed in six instances of endo approach and two instances of exo approach of the eight cognate TS pairs (e.g. TS17 with TS18). With crotonaldehyde, lower energy barriers are observed with three endo approaches

and five exo approaches of the eight cognate TS pairs (e.g. TS33 with TS34). This is likely an indication of the steric contribution to the diastereofacial approach of the dienophile.

7. For methacrolein, both rotamer 1 and rotamer 2 furnish C-2 adducts with lower barriers than that for the corresponding C-3 adducts. This is somewhat true of crotonaldehyde with two exceptions (TS41 with TS45; TS42 with TS46). Upon comparison to acrolein, substitution in the  $\alpha$  position increases regioselectivity for the C-2 regioisomer and is true of methacrolein (vide infra).

8. As a general conclusion, the conformation of methacrolein and crotonaldehyde (*s*-trans vs. *s*-cis) has greater implications on the energy barrier than their approach (endo vs. exo) with two exceptions (TS17 and TS18 compared to TS17 and TS19; TS21 and TS22 compared to TS21 and TS23).

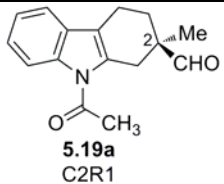
9. Considering  $\Delta^\ddagger G$ , the regioselectivity is predicted to be  $\sim 4.4:1$  (C-2:C-3) for methacrolein and  $\sim 2.3:1$  (C-2:C-3) for crotonaldehyde. Furthermore,  $\Delta^\ddagger E$  and  $\Delta^\ddagger H$  together predict regioselectivities of  $\sim 8.2\text{-}8.5:1$  (C-2:C-3) for methacrolein and  $\sim 2:1$  (C-2:C-3) for crotonaldehyde (vide infra).

Using the Eyring relationship (equation 5.3), the regioselectivity of these cycloadditions with methacrolein and crotonaldehyde can be illustrated. In the methacrolein data set (Table 5.10), the lowest activation barriers in this data set that furnishes the C-2-substituted and the C-3-substituted carbazoles are TS27 ( $\Delta^\ddagger G = 24.882 \text{ kcal}\cdot\text{mol}^{-1}$ ) and TS31 ( $\Delta^\ddagger G = 25.752 \text{ kcal}\cdot\text{mol}^{-1}$ ), respectively. This gives a difference of  $\sim 0.87 \text{ kcal}\cdot\text{mol}^{-1}$  ( $\Delta\Delta^\ddagger G = 870.4 \text{ cal}\cdot\text{mol}^{-1}$ ) furnishing  $k_{C2}/k_{C3} = \sim 4.35$ . In the crotonaldehyde data set (Table 5.11), the lowest

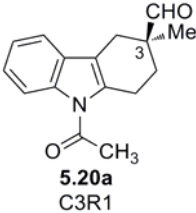
activation barriers in this data set that furnishes the C-2-substituted and the C-3-substituted carbazoles are TS43 ( $\Delta^\ddagger G = 27.918 \text{ kcal}\cdot\text{mol}^{-1}$ ) and TS48 ( $\Delta^\ddagger G = 28.407 \text{ kcal}\cdot\text{mol}^{-1}$ ), respectively. This gives a difference of  $\sim 0.49 \text{ kcal}\cdot\text{mol}^{-1}$  ( $\Delta\Delta^\ddagger G = 489.5 \text{ cal}\cdot\text{mol}^{-1}$ ) which provides  $k_{C2}/k_{C3} = \sim 2.29$ .

In summary, on comparison to the acrolein data set (Table 5.6), the  $\Delta\Delta^\ddagger G$  predicts that both  $\alpha$ -substitution (i.e. methacrolein) and  $\beta$ -substitution (i.e. crotonaldehyde) increases regioselectivity for the C-2 regioisomer. Furthermore, both the  $\Delta\Delta^\ddagger E$  and  $\Delta\Delta^\ddagger H$  data sets for methacrolein (calculations not shown) also predicts increased regioselectivity for the C-2 adduct. However, with crotonaldehyde, both the  $\Delta\Delta^\ddagger E$  and  $\Delta\Delta^\ddagger H$  data sets indicate that  $\beta$ -substitution mitigates C-2 regioselectivity.

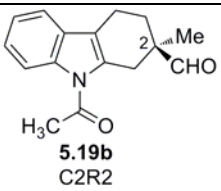
**Table 5.10:** Selected structural data and energies for TS structures of Diels-Alder reactions of *N*-Ac-IQDM and methacrolein obtained at the DFT B3LYP 6-31G(d) level.<sup>a</sup>

TS for DA Adduct	TSs	Bond distance (Å)	Dienophile	$\Delta^\ddagger E$ , <sup>c</sup> $\Delta^\ddagger H$ , <sup>d</sup> $\Delta^\ddagger G$ <sup>e</sup>
	IF <sup>b</sup>	C3 $\alpha$ -C3'	Approach	$E_{elec.} + ZPE$ <sup>f</sup>
		C2 $\alpha$ -C2'		$E_0 + H_{corr}$ <sup>g</sup>
				$E_0 + G_{corr}$ <sup>h</sup>
 <p><b>5.19a</b> C2R1</p>	TS17	2.05861	<i>s</i> -trans, endo	<b>14.482<sup>c</sup></b>
	-423.7	2.78531	top	<b>14.122<sup>d</sup></b>
				<b>27.099<sup>e</sup></b>
				-824.777028 <sup>f</sup>
				-824.758348 <sup>g</sup>
				-824.823324 <sup>h</sup>
	TS18	2.06554	<i>s</i> -trans, exo	<b>15.979</b>
	-427.9	2.74443	bottom	<b>15.519</b>
				<b>29.074</b>
				-824.774643
				-824.756122
				-824.820176
TS19	2.06405	<i>s</i> -cis, endo	<b>12.738</b>	
-394.6	2.94936	top	<b>12.235</b>	
			<b>25.782</b>	
			-824.775464	
			-824.756902	
			-824.821267	
TS20	2.04280	<i>s</i> -cis, exo	<b>12.053</b>	
-403.6	2.94590	bottom	<b>11.542</b>	
			<b>25.072</b>	
			-824.776556	
			-824.758007	
			-824.822399	

**Table 5.10** (continued)

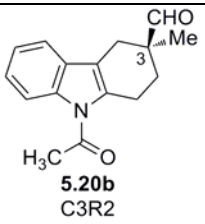
TS for DA Adduct	TSs	Bond distance (Å)	Dienophile	$\Delta^\ddagger E,^c \Delta^\ddagger H,^d \Delta^\ddagger G^e$
	IF <sup>b</sup>	C3 $\alpha$ -C2' C2 $\alpha$ -C3'	Approach	$E_{elec.} + ZPE^f$ $E_0 + H_{corr}^g$ $E_0 + G_{corr}^h$
 <p><b>5.20a</b> C3R1</p>	TS21	2.68560	<i>s</i> -trans, endo	<b>15.942<sup>c</sup></b>
	-432.5	2.07672	top	<b>15.589<sup>d</sup></b>
				<b>28.698<sup>e</sup></b>
				-824.774702 <sup>f</sup>
				-824.756009 <sup>g</sup>
				-824.820776 <sup>h</sup>
	TS22	2.64290	<i>s</i> -trans, exo	<b>17.353</b>
	-438.6	2.08656	bottom	<b>16.874</b>
				<b>30.584</b>
				-824.772454
				-824.753962
				-824.817771
TS23	2.79176	<i>s</i> -cis, endo	<b>14.245</b>	
-403.9	2.07563	top	<b>13.715</b>	
			<b>27.511</b>	
			-824.773063	
			-824.754544	
			-824.818511	
TS24	2.83572	<i>s</i> -cis, exo	<b>13.211</b>	
-406.8	2.04589	bottom	<b>12.656</b>	
			<b>26.492</b>	
			-824.774711	
			-824.756231	
			-824.820135	

**Table 5.10** (continued)

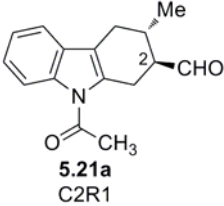
TS for DA Adduct	TSs IF <sup>b</sup>	Bond distance (Å) C3 $\alpha$ -C3' C2 $\alpha$ -C2'	Dienophile Approach	$\Delta^\ddagger E$ , <sup>c</sup> $\Delta^\ddagger H$ , <sup>d</sup> $\Delta^\ddagger G$ <sup>e</sup> $E_{elec.} + ZPE$ <sup>f</sup> $E_0 + H_{corr}$ <sup>g</sup> $E_0 + G_{corr}$ <sup>h</sup>
 <p><b>5.19b</b> C2R2</p>	TS25	2.05309	<i>s</i> -trans, endo	<b>15.122<sup>c</sup></b>
	-423.8	2.82516	top	<b>14.773<sup>d</sup></b>
				<b>27.818<sup>e</sup></b>
				-824.774800 <sup>f</sup>
				-824.756128 <sup>g</sup>
				-824.821187 <sup>h</sup>
	TS26	2.05144	<i>s</i> -trans, exo	<b>16.472</b>
	-432.7	2.79854	bottom	<b>16.084</b>
				<b>29.236</b>
				-824.772649
				-824.754039
				-824.818927
TS27	2.07431	<i>s</i> -cis, endo	<b>11.473</b>	
-393.8	2.89587	top	<b>10.934</b>	
			<b>24.882</b>	
			-824.776273	
			-824.757794	
			-824.821710	
TS28	2.04402	<i>s</i> -cis, exo	<b>12.026</b>	
-400.4	2.96208	bottom	<b>11.529</b>	
			<b>25.064</b>	
			-824.775391	
			-824.756846	
			-824.821420	



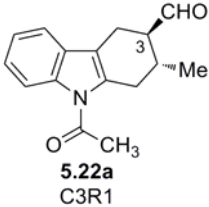
**Table 5.10** (continued)

TS for DA Adduct	TSS	Bond distance (Å)	Dienophile	$\Delta^\ddagger E, {}^c \Delta^\ddagger H, {}^d \Delta^\ddagger G^e$
	IF <sup>b</sup>	C3 $\alpha$ -C2'	Approach	$E_{elec.} + ZPE^f$
		C2 $\alpha$ -C3		$E_0 + H_{corr}^g$
				$E_0 + G_{corr}^h$
 <p>5.20b C3R2</p>	TS29	2.70887	<i>s</i> -trans, endo	<b>15.483<sup>c</sup></b>
	-434.4	2.05751	top	<b>15.051<sup>d</sup></b>
				<b>28.493<sup>e</sup></b>
				-824.774226 <sup>f</sup>
				-824.755686 <sup>g</sup>
				-824.820112 <sup>h</sup>
	TS30	2.69042	<i>s</i> -trans, exo	<b>16.737</b>
	-435.3	2.06099	bottom	<b>16.265</b>
				<b>29.859</b>
				-824.772227
				-824.753751
				-824.817934
TS31	2.90925	<i>s</i> -cis, endo	<b>12.715</b>	
-398.5	2.04129	top	<b>12.199</b>	
			<b>25.752</b>	
			-824.774293	
			-824.755778	
			-824.820323	
TS32	2.91043	<i>s</i> -cis, exo	<b>12.834</b>	
-406.6	2.01775	bottom	<b>12.304</b>	
			<b>25.956</b>	
			-824.774103	
			-824.755610	
			-824.819998	

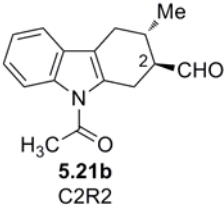
**Table 5.11:** Selected structural data and energies for TS structures of Diels-Alder reactions of *N*-Ac-IQDM and crotonaldehyde obtained at the DFT B3LYP 6-31G(d) level.<sup>a</sup>

TS for DA Adduct	TSs IF <sup>b</sup>	Bond distance (Å) C3 $\alpha$ -C3' C2 $\alpha$ -C2'	Dienophile Approach	$\Delta^\ddagger E$ , <sup>c</sup> $\Delta^\ddagger H$ , <sup>d</sup> $\Delta^\ddagger G$ <sup>e</sup> $E_{elec.} + ZPE$ <sup>f</sup> $E_0 + H_{corr}$ <sup>g</sup> $E_0 + G_{corr}$ <sup>h</sup>
 <p>5.21a C2R1</p>	TS33	2.12278	<i>s</i> -trans, endo	<b>18.523<sup>c</sup></b>
	-442.8	2.54088	top	<b>17.952<sup>d</sup></b>
				<b>31.462<sup>e</sup></b>
				-824.771285 <sup>f</sup>
				-824.752829 <sup>g</sup>
				-824.817092 <sup>h</sup>
	TS34	2.11241	<i>s</i> -trans, exo	<b>18.682</b>
	-451.1	2.54807	bottom	<b>18.124</b>
				<b>31.837</b>
				-824.771031
				-824.752554
				-824.816495
TS35	2.06174	<i>s</i> -cis, endo	<b>16.003</b>	
-418.3	2.74661	top	<b>15.414</b>	
			<b>29.203</b>	
			-824.773142	
			-824.754721	
			-824.818602	
TS36	2.03365	<i>s</i> -cis, exo	<b>14.873</b>	
-417.7	2.75720	bottom	<b>14.288</b>	
			<b>28.075</b>	
			-824.774943	
			-824.756515	
			-824.820399	

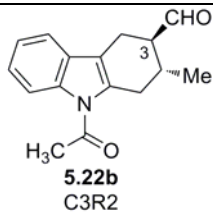
**Table 5.11** (continued)

TS for DA Adduct	TSs	Bond distance (Å)	Dienophile	$\Delta^\ddagger E, {}^c \Delta^\ddagger H, {}^d \Delta^\ddagger G^e$
	IF <sup>b</sup>	C3 $\alpha$ -C2' C2 $\alpha$ -C3	Approach	$E_{elec.} + ZPE^f$ $E_0 + H_{corr}^g$ $E_0 + G_{corr}^h$
 <p><b>5.22a</b> C3R1</p>	TS37	2.44143	<i>s</i> -trans, endo	<b>19.509<sup>c</sup></b>
	-450.0	2.17611	top	<b>18.928<sup>d</sup></b>
				<b>32.804<sup>e</sup></b>
				-824.769713 <sup>f</sup>
				-824.751273 <sup>g</sup>
				-824.814954 <sup>h</sup>
	TS38	2.45462	<i>s</i> -trans, exo	<b>19.230</b>
	-458.7	2.15754	bottom	<b>18.651</b>
				<b>32.515</b>
				-824.770158
				-824.751715
				-824.815414
TS39	2.61592	<i>s</i> -cis, endo	<b>17.063</b>	
-424.0	2.09837	top	<b>16.443</b>	
			<b>30.444</b>	
			-824.771452	
			-824.753081	
			-824.816624	
TS40	2.65285	<i>s</i> -cis, exo	<b>15.267</b>	
-430.1	2.06500	bottom	<b>14.655</b>	
			<b>28.731</b>	
			-824.774314	
			-824.755931	
			-824.819354	

**Table 5.11** (continued)

TS for DA Adduct	TSs IF <sup>b</sup>	Bond distance (Å) C3 $\alpha$ -C3' C2 $\alpha$ -C2'	Dienophile Approach	$\Delta^\ddagger E$ , <sup>c</sup> $\Delta^\ddagger H$ , <sup>d</sup> $\Delta^\ddagger G$ <sup>e</sup> $E_{elec.} + ZPE$ <sup>f</sup> $E_0 + H_{corr}$ <sup>g</sup> $E_0 + G_{corr}$ <sup>h</sup>
 <p><b>5.21b</b> C2R2</p>	TS41	2.11049	<i>s</i> -trans, endo	<b>19.199<sup>c</sup></b>
	-442.1	2.58799	top	<b>18.679<sup>d</sup></b>
				<b>32.127<sup>e</sup></b>
				-824.768999 <sup>f</sup>
				-824.750488 <sup>g</sup>
				-824.815041 <sup>h</sup>
	TS42	2.09493	<i>s</i> -trans, exo	<b>19.288</b>
	-448.9	2.59616	bottom	<b>18.772</b>
				<b>32.173</b>
				-824.768857
				-824.750340
				-824.814968
TS43	2.06402	<i>s</i> -cis, endo	<b>14.591</b>	
-416.6	2.75499	top	<b>13.992</b>	
			<b>27.918</b>	
			-824.774183	
			-824.755805	
			-824.819659	
TS44	2.03681	<i>s</i> -cis, exo	<b>14.793</b>	
-421.6	2.77330	bottom	<b>14.194</b>	
			<b>27.982</b>	
			-824.773862	
			-824.755483	
			-824.819557	

**Table 5.11** (continued)

TS for DA Adduct	TSs	Bond distance (Å)	Dienophile	$\Delta^\ddagger E, {}^c \Delta^\ddagger H, {}^d \Delta^\ddagger G^e$
	IF <sup>b</sup>	C3 $\alpha$ -C2' C2 $\alpha$ -C3'	Approach	$E_{elec.} + ZPE^f$ $E_0 + H_{corr}^g$ $E_0 + G_{corr}^h$
 <p>5.22b C3R2</p>	TS45	2.46461	<i>s</i> -trans, endo	<b>18.949<sup>c</sup></b>
	-454.7	2.15415	top	<b>18.380<sup>d</sup></b>
				<b>32.092<sup>e</sup></b>
				-824.769397 <sup>f</sup>
				-824.750964 <sup>g</sup>
				-824.815097 <sup>h</sup>
	TS46	2.49935	<i>s</i> -trans, exo	<b>18.680</b>
	-460.5	2.11764	bottom	<b>18.092</b>
				<b>31.950</b>
				-824.769826
				-824.751423
				-824.815323
TS47	2.73912	<i>s</i> -cis, endo	<b>15.543</b>	
-424.3	2.03921	top	<b>14.917</b>	
			<b>28.692</b>	
			-824.772666	
			-824.754332	
			-824.818425	
TS48	2.69132	<i>s</i> -cis, exo	<b>15.014</b>	
-427.4	2.03472	bottom	<b>14.408</b>	
			<b>28.407</b>	
			-824.773510	
			-824.755142	
			-824.818879	

a. Each TS calculation was carried out using the Synchronous Transit-Guided Quasi-Newton Method (QST2 or QST3, Ref. 317,318) using Gaussian 03 rev. B.04 or C.02 implemented on a desktop computer running Linux OS (Redhat). TS calculations times were typically 8-12 hours in duration. All structures reported here as TSs exhibit only one imaginary frequency. The imaginary vibrations were animated with Gaussview 3.09 or 4.1 to determine if they were in qualitative agreement with the bond-making/bond-breaking processes associated with the reaction of interest. In each case, intrinsic reaction coordinate (IRC, Ref. 313,314) calculations were performed to determine that the observed TS could be linked reasonably to the assumed reactant and product geometries.

b. IF = imaginary frequency in reciprocal centimeters and are not scaled (Ref. 315).

c.  $\Delta_{\ddagger}E$  ( $= \Delta_{\ddagger}E0$ ), d.  $\Delta_{\ddagger}H$ , e.  $\Delta_{\ddagger}G$  in kcal/mol.

f.  $E_{elec.} + ZPE$  ( $= E0$ ), g.  $H = E0 + H_{corr}$ , h.  $G = E0 + G_{corr}$  in a.u. (1 a.u. = 627.5095 kcal/mol).

**Figure 5.12:** The transition state structures of a) TS27 and TS31; b) TS43 and TS48.

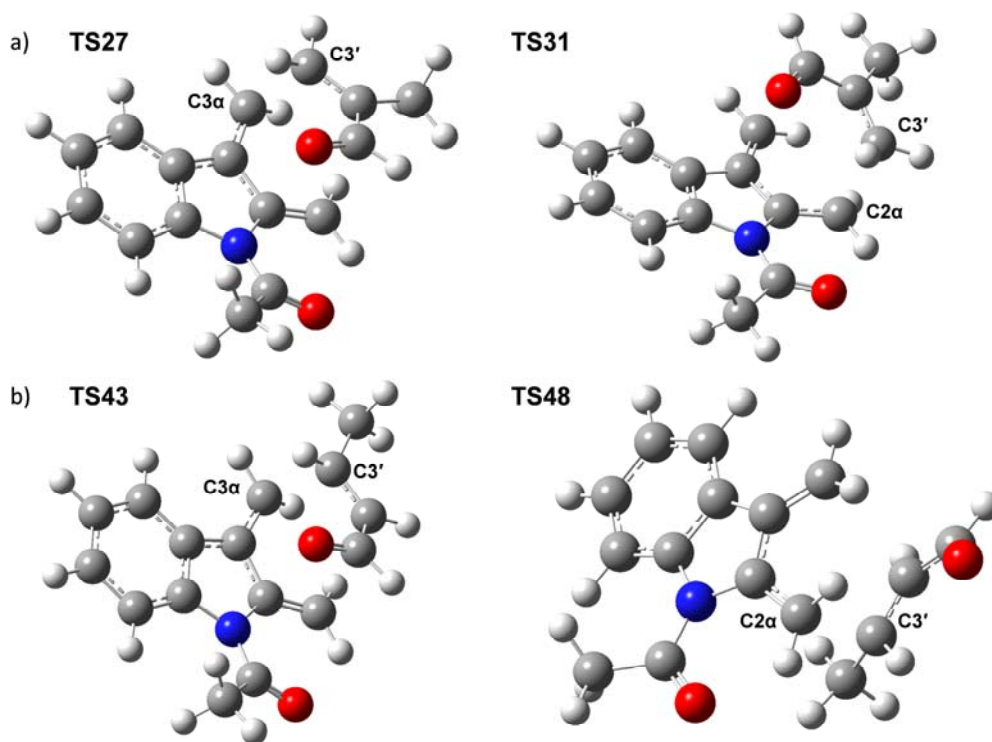


Figure 5.12 shows the relevant TS structures obtained from the methacrolein data set (TS27 and TS31) and the crotonaldehyde data set (TS43 and TS48). Akin to acrolein, advanced bond development occurs between C-3' of the dienophile and C-3 $\alpha$  (TS27; TS43) or C-2 $\alpha$  (TS31; TS48) of *N*-Ac-IQDM, consistent with asynchronicity. Asynchronicity was further

supported upon examination of the vibrational mode corresponding to the imaginary frequencies (TS27 =  $-394\text{ cm}^{-1}$ ; TS31 =  $-399\text{ cm}^{-1}$ ; TS43 =  $-417\text{ cm}^{-1}$ ; TS48 =  $-427\text{ cm}^{-1}$ ). This revealed that the principle motion is between C-3 $\alpha$  and C-3' (TS27; TS43) or C-2 $\alpha$  and C-3' (TS31; TS48).

In analogous fashion to that of acrolein, pyramidalization is evident at the relevant reacting loci: TS27 shows C-3 $\alpha$  =  $351.4^\circ$ , C-3' =  $351.3^\circ$  and is advanced over that of C2 $\alpha$  =  $359.5^\circ$ , C-2' =  $359.8^\circ$ ; TS31 shows C-2 $\alpha$  =  $350.5^\circ$ , C-3' =  $350.8^\circ$  and is advanced over that of C3 $\alpha$  =  $359.5^\circ$ , C-2' =  $359.8^\circ$ ; TS43 shows C-3 $\alpha$  =  $350.2^\circ$ , C-3' =  $349.3^\circ$  and is advanced over that of C2 $\alpha$  =  $359.2^\circ$ , C-2' =  $359.7^\circ$ ; TS48 shows C-2 $\alpha$  =  $351.2^\circ$ , C-3' =  $348.9^\circ$  and is advanced over that of C3 $\alpha$  =  $358.5^\circ$ , C-2' =  $359.4^\circ$ .

Thus far, this investigation into the chemistry of *N*-Ac IQDM has revealed important structural and energetic data and has reproduced experimental trends reasonably well. In the next section, the effect of Lewis acid catalysis on cycloadditions of *N*-Ac IQDM is discussed.

### 5.3.5 Theoretical Investigation of Lewis acid catalyzed Diels-Alder Reactions of the *N*-Acetyl-Indole-2,3-Quinodimethanes

The effect of Lewis acids on Diels-Alder cycloadditions is well known.<sup>394</sup> Studies by Wu revealed a 3.5:1 selectivity for BF<sub>3</sub>-catalyzed cycloadditions of acrolein and *N*-Ac-IQDM (Chapter 4). Although the regioselectivity is only marginally enhanced over that of the non-catalyzed reactions, it was felt that investigation into conditions that use Lewis acids would be initiated with boron-type Lewis acids for two reasons. Firstly, there is no precedent in this laboratory of computational efforts towards Lewis acid-catalyzed reactions. Hence, these initial efforts are exploratory and using one of the simplest Lewis acids would be an appropriate ruler to assess these types of calculations. Secondly, owing to the low atomic masses of boron and fluorine there is a substantially reduced computational cost upon comparison to using transition metal catalysts, making this an attractive choice for initial computational study. Computations in which SnCl<sub>4</sub> was used were not accommodated by the 6-31G(d) basis set and consequently these studies were abandoned.

This section focuses on two different projects. Firstly, calculations of BF<sub>3</sub> complexes of the three dienophiles **5.7**, **5.15** and **5.16** were accomplished. The corresponding cycloadditions of BF<sub>3</sub>-acrolein with *N*-Ac-IQDM are then presented and discussed. Secondly, computations on the aluminum and titanium-oxazolidinone catalyzed cycloadditions would be investigated. As discussed in Chapter 4, regioselectivity could be controlled, affording either the C-2 or C-3 regioisomer in excess of the other by using either TiCl<sub>4</sub> or Et<sub>2</sub>AlCl.



**Table 5.12:** The energies (a.u.) and relative energies (kcal·mol<sup>-1</sup>) of BF<sub>3</sub>-complexed acrolein, methacrolein and crotonaldehyde and their corresponding Diels-Alder adducts obtained at the DFT B3LYP 6-31G(d) level.

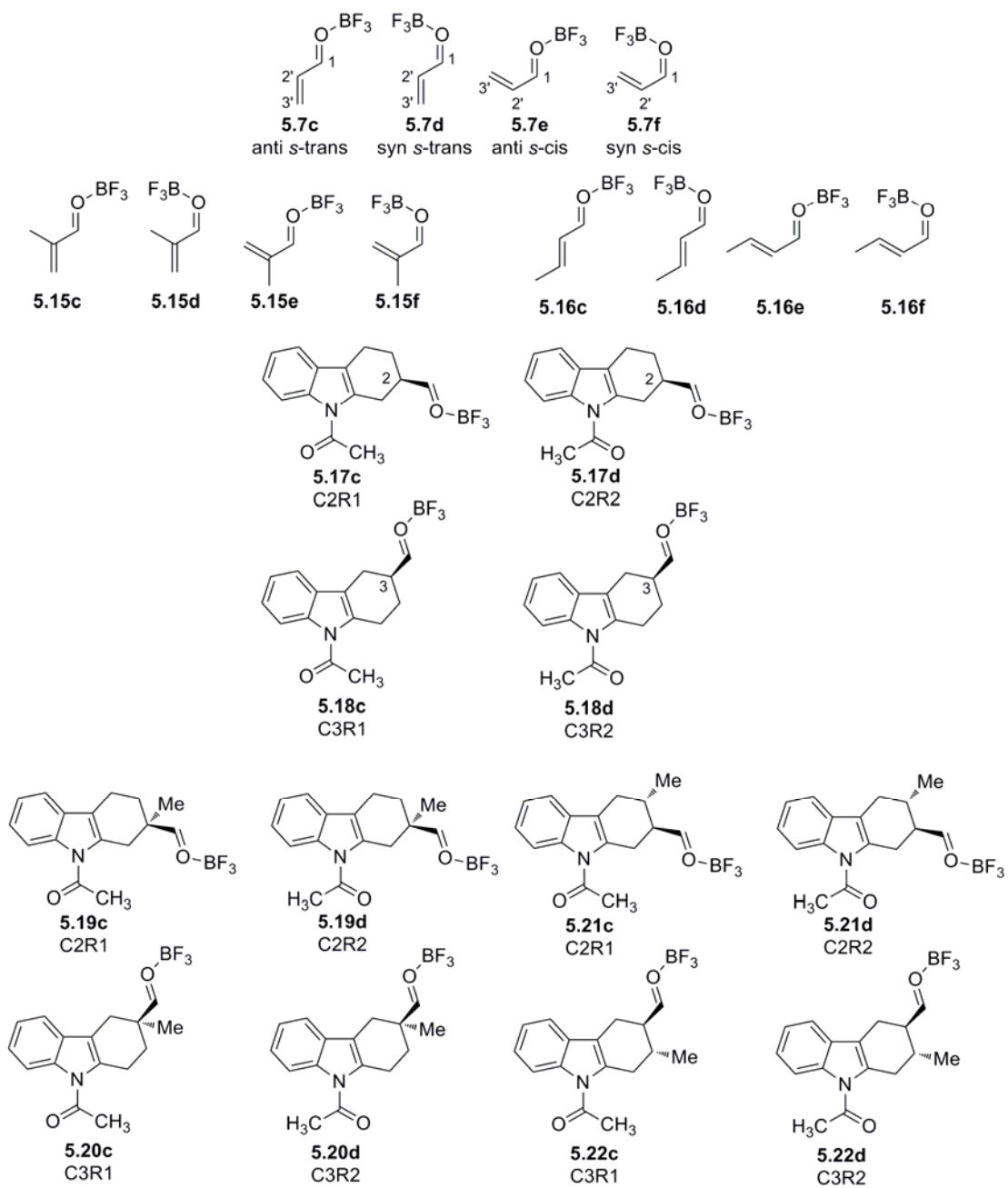


**Table 5.12** (continued)

Entry	Structure	Energy $E,^a H,^b G^c$ (a.u.) <sup>d</sup>	Relative Energy (kcal·mol <sup>-1</sup> )	Structure	Energy $E,^a H,^b G^c$ (a.u.) <sup>d</sup>	Relative Energy (kcal·mol <sup>-1</sup> )
1	<b>5.7c</b>	-516.407710 <sup>a</sup>	0	<b>5.7d</b>	-516.405064 <sup>a</sup>	1.66
		-516.398296 <sup>b</sup>	0		-516.395559 <sup>b</sup>	1.72
		-516.441760 <sup>c</sup>	0		-516.439215 <sup>c</sup>	1.59
2	<b>5.7e</b>	-516.404897	1.77	<b>5.7f</b>	-516.398948	5.49
		-516.395452	1.78		-516.389524	5.50
		-516.439120	1.66		-516.432532	5.79
3	<b>5.15c</b>	-555.701360	1.81	<b>5.15d</b>	-555.694399	6.18
		-555.690517	1.79		-555.683375	6.28
		-555.737499	1.84		-555.730557	6.19
4	<b>5.15e</b>	-555.696668	4.75	<b>5.15f</b>	-555.689758	9.09
		-555.685682	4.83		-555.678754	9.18
		-555.733212	4.53		-555.725676	9.25
5	<b>5.16c</b>	-555.704240	0	<b>5.16d</b>	-555.701638	1.63
		-555.693383	0		-555.690697	1.69
		-555.740424	0		-555.738126	1.44
6	<b>5.16e</b>	-555.701873	1.49	<b>5.16f</b>	-555.696383	4.93
		-555.690961	1.52		-555.685592	4.89
		-555.738271	1.35		-555.731828	5.39
7	<b>5.17c</b>	-1110.125499 (eq.) <sup>e</sup>	2.33	<b>5.17d</b>	-1110.128751 (eq.) <sup>e</sup>	0.29
		-1110.104733 (eq.)	2.51		-1110.108076 (eq.)	0.42
		-1110.176640 (eq.)	2.10		-1110.179933 (eq.)	0.04
		-1110.125325 (ax.) <sup>f</sup>	2.44		-1110.129218 (ax.) <sup>f</sup>	0
		-1110.104721 (ax.)	2.52		-1110.108739 (ax.)	0
		-1110.175918 (ax.)	3.01		-1110.179699 (ax.)	0.18
8	<b>5.18c</b>	-1110.126553 (eq.) <sup>e</sup>	1.67	<b>5.18d</b>	-1110.128993 (eq.) <sup>e</sup>	0.14

		-1110.105759 (eq.)	1.87		-1110.108355 (eq.)	0.24
		-1110.177935 (eq.)	1.29		-1110.179989 (eq.)	0
		-1110.128060 (ax.) <sup>f</sup>	0.73		-1110.128369 (ax.) <sup>f</sup>	0.53
		-1110.107916 (ax.)	0.52		-1110.107883 (ax.)	0.54
		-1110.176497 (ax.)	2.19		-1110.179030 (ax.)	0.60
9	<b>5.19c</b>	-1149.411359	2.59	<b>5.19d</b>	-1149.414466	0.64
		-1149.389235	2.59		-1149.392437	0.58
		-1149.463543	2.78		-1149.466582	0.88
10	<b>5.20c</b>	-1149.412630	1.79	<b>5.20d</b>	-1149.415145	0.22
		-1149.390471	1.82		-1149.393082	0.18
		-1149.464935	1.91		-1149.467200	0.49
11	<b>5.21c</b>	-1149.412042	2.16	<b>5.21d</b>	-1149.415208	0.18
		-1149.389790	2.24		-1149.393134	0.14
		-1149.465426	1.60		-1149.467284	0.44
12	<b>5.22c</b>	-1149.413058	1.52	<b>5.22d</b>	-1149.415488	0
		-1149.390784	1.62		-1149.393364	0
		-1149.466271	1.07		-1149.467980	0

a., b., c. Energies are taken from minimized structures and are a) the electronic and zero point energies (i.e.  $E = E_{elec} + ZPE = E0$ ), b) the electronic, zero point and thermal enthalpies (i.e.  $H = E0 + H_{corr}$ ), c) the electronic, zero point and thermal free energies (i.e.  $G = E0 + G_{corr}$ ).

d. One atomic unit (a.u.) = 627.5095 kcal/mol.

e, f. The abbreviations eq. and ax. refer to the cyclohexene ring conformation in which the CHO group is in an equatorial and axial orientation, respectively.

### 5.3.5.1 BF<sub>3</sub>-catalyzed Diels-Alder cycloadditions with Acrolein

Table 5.12 shows the energy data of the BF<sub>3</sub>-complexed dienophiles acrolein, methacrolein and crotonaldehyde and their corresponding cycloadducts. The anti *s*-trans conformers **5.7c**, **5.15c** and **5.16c** are the lowest energy forms in their respective data sets. Of interest are the anti *s*-cis conformers **5.15e** and **5.16e** which are lower in energy than the syn *s*-trans

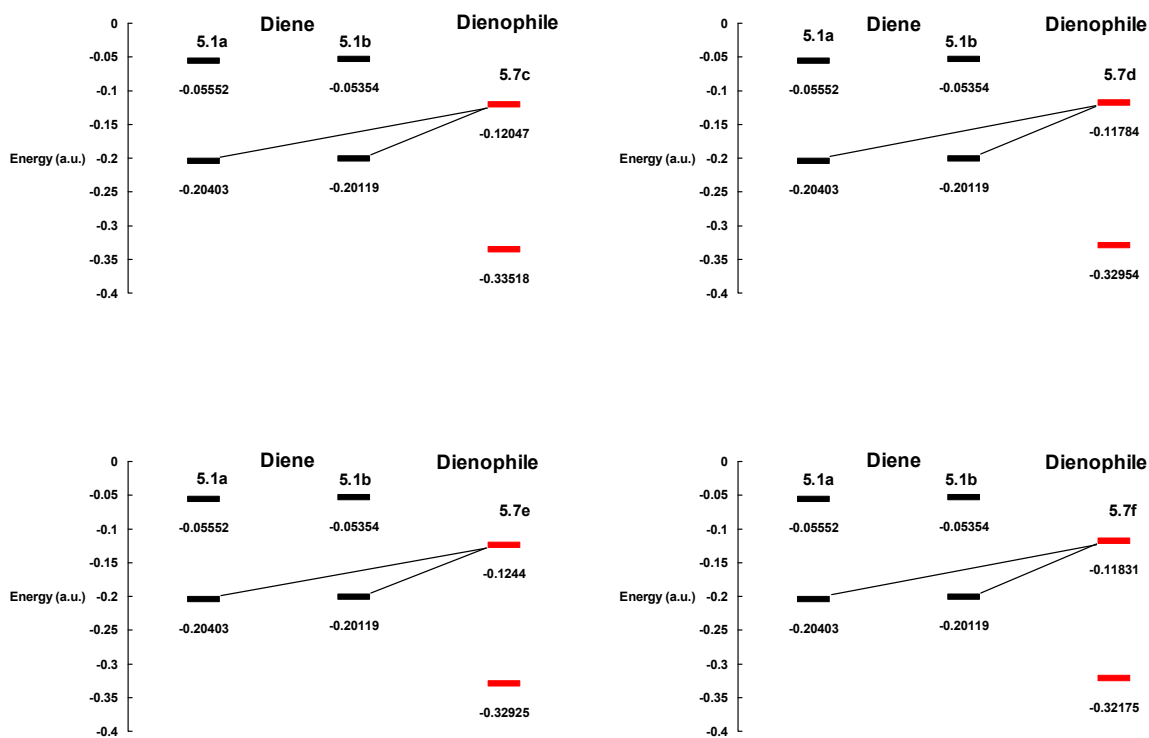
conformers **5.15d** and **5.16d**, respectively, reflecting the contribution of allylic interactions to the ground state energies. As well, rotamer 2 adducts are more stable than the rotamer 1 adducts in all instances.

The FMO energies of *N*-Ac-IQDM and BF<sub>3</sub>-complexed acrolein are shown in Figure 5.13. As in the cases with acrolein, methacrolein and crotonaldehyde, the lowest energy interaction is that of the HOMO of **5.1** with the LUMO of **5.7c**, **5.7d**, **5.7e** and **5.7f** (HOMO<sub>diene</sub>-LUMO<sub>dienophile</sub>). The most important observation is that the LUMO energies are lowered considerably from ~0.065 a.u. to ~0.12 a.u. upon Lewis acid complexation (cf. Figure 5.13 to Figure 5.8). Accordingly, this should give lower activation barriers than the non-catalyzed versions, thus increasing the rate of reaction if these reactions are FMO controlled.

Table 5.13 shows the FMO energies and corresponding MO coefficients of **5.7c**, **5.7d**, **5.7e** and **5.7f**. The largest coefficients reside on C-1. The coefficients have increased at C-1, decreased at C-2 and are virtually unchanged at C-3 upon comparison to the values presented in Table 5.5. The relative difference in magnitude between the eigenvectors has increased between C-2 and C-3 (cf. Table 5.5). Hence, the difference between the eigenvectors at C-2 and C-3 should attribute to increased asynchronicity and thus regioselectivity, owing to the “big-big” FMO interactions. As well, stereoselectivity (endo:exo) should also increase due to the increase of the C-1 eigenvector (i.e. the carbonyl carbon is more polarized). Consequently, stronger secondary orbital interactions with the diene should exist, thus increasing endoselectivity. However, as previously stated, FMO theory does not provide a rationalization for the regioselectivity observed in DA reactions of IQDMs and thus there would be negligible differences in the regioselectivity of these DA reactions, despite the

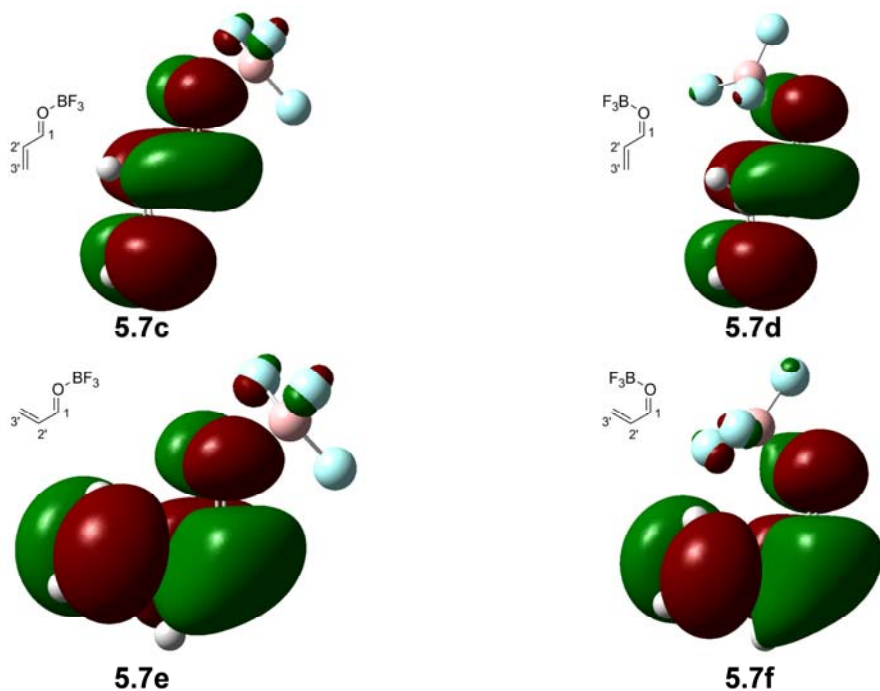
marked effect of Lewis acids. Many theoretical studies have attempted to explain the effect of Lewis acids on Diels-Alder reactions with respect to regio- and stereoselectivity. The following discussion focuses on transition state calculations of  $\text{BF}_3$ -catalyzed cycloadditions of acrolein and *N*-Ac-IQDM.

**Figure 5.13:** Frontier molecular orbital energies (a.u.) for the  $[4\pi_s-2\pi_s]$  cycloaddition of **5.1** with **5.7c**, **5.7d**, **5.7e**, and **5.7f** calculated at the DFT B3LYP 6-31G(d) level. In each case, the black solid lines indicate the lowest possible energy interaction of the HOMO of *N*-Ac-IQDM **5.1** (diene, black) with the LUMO of  $\text{BF}_3$ -complexed acrolein **5.7** (dienophile, red).



One atomic unit (a.u.) = 627.5095 kcal/mol.

**Table 5.13:** FMO energies (a.u.) and orbital coefficients of the LUMO of BF<sub>3</sub>-complexed acrolein **5.7c**, **5.7d**, **5.7e** and **5.7f** obtained at the DFT B3LYP 6-31G(d) level.



	<b>5.7c</b>	<b>5.7d</b>	<b>5.7e</b>	<b>5.7f</b>	
<b>Energy (a.u.)</b>	-0.12047	-0.11784	-0.12440	-0.11831	
<b>LUMO</b>					
	<b>Orbital</b>	<b>Coefficient</b>			
	C1 2p <sub>z</sub>	-0.39198	-0.40099	-0.39467	0.39720
	C1 3p <sub>z</sub>	-0.34617	-0.35640	-0.35396	0.35662
	C2' 2p <sub>z</sub>	-0.16124	-0.15153	-0.14935	0.12202
	C2' 3p <sub>z</sub>	-0.19118	-0.17792	-0.19077	0.16929
	C3' 2p <sub>z</sub>	0.37813	0.37547	0.36597	-0.34533
	C3' 3p <sub>z</sub>	0.40801	0.40145	0.41423	-0.36953

Transition state calculations were undertaken on BF<sub>3</sub>-catalyzed reactions of acrolein and *N*-Ac-IQDM, the results of which are shown in Table 5.14. There are thirty-two possible reaction channels producing four products (two when one does not take into consideration rotation of the amide carbonyl) and TS calculations were attempted on all thirty-two channels. Of these, twenty-two transition state structures were obtained. Despite several attempts, there were ten reaction channels that did not converge. For many of these, non-convergence could be attributed to steric issues. The corresponding reactions of methacrolein and crotonaldehyde were not pursued owing to time constraints.

Inspection of structural and energetic data ( $\Delta^\ddagger G$ ) from Table 5.14 reveals the following trends:

1. The BF<sub>3</sub>-catalyzed DA reactions with acrolein are *more* asynchronous than the corresponding uncatalyzed DA reactions with acrolein (Table 5.5) with  $\Delta d > 1.0 \text{ \AA}$  in one case (TS78). This trend has been reported by others for catalyzed DA reactions with other dienes.<sup>334,395,449,477</sup>
2. On comparison to the uncatalyzed DA reactions, the  $\Delta^\ddagger G$  for the BF<sub>3</sub>-catalyzed DA reactions of acrolein are significantly reduced. These observations have also been reported by others.<sup>334,449,477</sup> Examination of the  $\Delta^\ddagger E$  data set reveals that, in some cases, this decrease is by an order of magnitude (e.g. TS1 vs. TS51).
3. The *s*-trans TSs are endoselective *regardless* of the coordination of BF<sub>3</sub>.
4. The lowest energy barriers for each of the four data sets found in Table 5.14 are with the *s*-cis conformation (**5.7e**, **5.7f**) and exo approach (TS56, TS62, TS70) and endo approach

(TS77). Salvatella and coworkers reported that the endo *s*-cis was the most stable TS found in studies of BF<sub>3</sub>-acrolein and butadiene.<sup>334</sup>

5. Rotamer 1 (**5.1a**) furnishes C-2 adducts with lower energy barriers than the corresponding C-3 adducts (e.g. TS50 compared to TS58). On the other hand, rotamer 2 (**5.1b**) furnishes C-3 adducts with lower activation energies than the corresponding C-2 adducts (e.g. TS65 compared to TS73).

6. Rotamer 1 (**5.1a**) furnishes C-2 adducts with lower barriers than rotamer 2 (**5.1b**) does (e.g. TS50 compared to TS66). A corollary to this is that rotamer 2 furnishes C-3 adducts with lower barriers than rotamer 1 (e.g. TS57 compared to TS73).

7. All *s*-cis TSs are more stable (i.e. lower energy) than the corresponding *s*-trans TSs with one exception (TS51 compared to TS55); all endo TSs are more stable than the corresponding exo TSs with one exception (TS55 compared to TS56).

8. From the twenty-two available data sets, the  $\Delta^\ddagger G$  predicts the C-2 adduct to be the major product at ~8.7:1 (C-2:C-3) predicting a higher regioselectivity than the uncatalyzed reaction and is in general agreement with experimental results from this lab with acrolein and other dienophiles. Furthermore, the  $\Delta^\ddagger E$  and  $\Delta^\ddagger H$  data sets predict ~3:1 regioselectivity (C-2:C-3).

There are two barrierless reactions TS56 and TS77 (i.e. negative  $\Delta^\ddagger E$  of -2.25 and -1.59 kcal·mol<sup>-1</sup>, respectively). The corresponding  $\Delta^\ddagger G$  are 11.525 (TS56) and 12.803 kcal·mol<sup>-1</sup> (TS77). These two cases, TS56 and TS77, in which both the  $\Delta^\ddagger E$  and  $\Delta^\ddagger H$  are negative (i.e. barrierless) and the  $\Delta^\ddagger G$  is positive have also been observed by others and almost always involves gas phase calculations and, in some these instances, Lewis acid catalysts have been employed.<sup>332,333,478</sup>

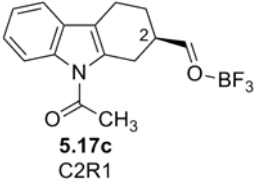


Bickelhaupt remarked that the first step in a reaction is the exothermic formation of a "reactant complex", the occurrence of which is a typical feature of gas phase calculations and, upon solvation, the complexation becomes less important and may disappear altogether in the condensed phase.<sup>478</sup> Although the TSs are higher in energy than the corresponding reactant complexes, they may be below the reactants and thus appear as negative activation energies. However, negative activation barriers do not imply a "barrierless" reaction. The reaction is also governed by a statistical or entropic "bottleneck" as one goes from the separate unbound starting materials to the tightly bound transition state. This "bottleneck" is associated with the decrease in the number of available quantum states (translational, rotational, and vibrational) on going from the reactants to transition state. Upon solvation, these barriers become positive. The effect of differential solvation of the reactant(s) and the transition state can induce a negative activation energy to become a positive one. Furthermore, one may also observe a reversal of activation energies of two competing reactions, such that the selectivity for one reaction over another in the gas phase may be reversed upon solvation. Indeed, this phenomena has been shown by Evanseck and coworkers study of DA reactions employing the bis(oxazoline) Cu(II) catalyst with an achiral *N*-acryloxazolidinone.<sup>332</sup> Houk and coworkers study of DA reactions employing Evans' chiral *N*-acyloxazolidinone auxiliary catalyzed by Me<sub>2</sub>AlCl has also shown negative  $\Delta^\ddagger E$  values and positive  $\Delta^\ddagger G$  values.<sup>333</sup> Inspection of TS56 and TS77 follow these trends outlined above.

The lowest activation barriers in this data set that furnishes the C-2-substituted and the C-3-substituted carbazoles are TS56 ( $\Delta^\ddagger G = 11.525 \text{ kcal}\cdot\text{mol}^{-1}$ ) and TS77 ( $\Delta^\ddagger G = 12.803$

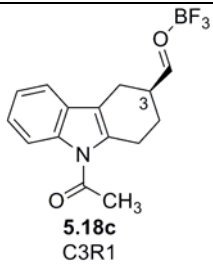
kcal·mol<sup>-1</sup>), respectively. This gives a difference of ~1.28 kcal·mol<sup>-1</sup> (i.e.  $\Delta\Delta^\ddagger G = 1277.6$  cal·mol<sup>-1</sup>), which gives  $k_{C2}/k_{C3} = \sim 8.66$ . The  $\Delta^\ddagger E$  and  $\Delta^\ddagger H$  values for TS56 and TS77 provide the corresponding  $\Delta\Delta^\ddagger E = 0.65$  kcal·mol<sup>-1</sup> and  $\Delta\Delta^\ddagger H = 0.68$  kcal·mol<sup>-1</sup> and predicts the C-2 regioisomer to be the major product with a regioselectivity of 2.9:1 and 3.1:1, respectively (~3:1).

**Table 5.14:** Selected structural data and energies of TS structures of Diels-Alder reactions of *N*-Ac-IQDM and BF<sub>3</sub>-complexed acrolein obtained at the DFT B3LYP 6-31G(d) level.<sup>a</sup>

TS for DA Adduct	TSs	Bond distance (Å)	Dienophile	$\Delta^\ddagger E,^c \Delta^\ddagger H,^d \Delta^\ddagger G^c$
	IF <sup>b</sup>	C3 $\alpha$ -C3' C2 $\alpha$ -C2'	Approach	$E_{elec.} + ZPE^f$ $E_0 + H_{corr}^g$ $E_0 + G_{corr}^h$
 <p>5.17c C2R1</p>	TS49	na	anti, <i>s</i> -trans	na
	na		endo, top	
	TS50	2.09470	anti, <i>s</i> -trans	<b>4.505<sup>c</sup></b>
	-357.9	2.99961	exo, bottom	<b>3.721<sup>d</sup></b>
				<b>18.704<sup>e</sup></b>
				-1110.057196 <sup>f</sup>
				-1110.036401 <sup>g</sup>
				-1110.106398 <sup>h</sup>
	TS51	2.17682	syn, <i>s</i> -trans	<b>1.311</b>
	-321.0	2.87847	endo, top	<b>0.494</b>
				<b>15.515</b>
				-1110.059639
			-1110.038806	
			-1110.108935	
TS52	2.17333	syn, <i>s</i> -trans	<b>2.259</b>	
-319.6	2.93978	exo, bottom	<b>1.519</b>	
			<b>16.098</b>	
			-1110.058128	
			-1110.037173	
			-1110.108005	
TS53	na		anti, <i>s</i> -cis	na
na			endo, top	

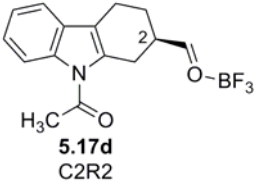
TS54	2.16795	anti, <i>s</i> -cis	<b>1.111</b>
-296.8	3.13825	exo, bottom	<b>0.513</b>
			<b>14.525</b>
			-1110.059791
			-1110.038670
			-1110.110417
TS55	2.22125	syn, <i>s</i> -cis	<b>2.489</b>
-271.2	3.13553	endo, top	<b>1.806</b>
			<b>16.727</b>
			-1110.051645
			-1110.030681
			-1110.100320
TS56	2.22334	syn, <i>s</i> -cis	<b>-2.249</b>
-235.9	3.06832	exo, bottom	<b>-2.946</b>
			<b>11.525</b>
			-1110.059198
			-1110.038254
			-1110.108609

**Table 5.14** (continued)

TS for DA Adduct	TSs	Bond distance (Å)	Dienophile	$\Delta^\ddagger E,^c \Delta^\ddagger H,^d \Delta^\ddagger G^e$
	IF <sup>b</sup>	C3 $\alpha$ -C2' C2 $\alpha$ -C3'	Approach	$E_{elec.} + ZPE^f$ $E_0 + H_{corr}^g$ $E_0 + G_{corr}^h$
 <p><b>5.18c</b> C3R1</p>	TS57	2.88618	anti, <i>s</i> -trans	<b>2.738<sup>c</sup></b>
	-335.5	2.12602	endo, top	<b>1.995<sup>d</sup></b>
				<b>17.091<sup>e</sup></b>
				-1110.060011 <sup>f</sup>
				-1110.039152 <sup>g</sup>
				-1110.108968 <sup>h</sup>
	TS58	2.93877	anti, <i>s</i> -trans	<b>6.640</b>
	-346.3	2.08586	exo, bottom	<b>6.027</b>
				<b>20.189</b>
				-1110.053793
			-1110.032727	
			-1110.104031	
TS59	2.92763	syn, <i>s</i> -trans	<b>3.534</b>	
-328.3	2.13096	endo, top	<b>2.816</b>	
			<b>17.449</b>	
			-1110.056097	
			-1110.035107	
			-1110.105852	
TS60	2.84768	syn, <i>s</i> -trans	<b>5.249</b>	
-337.1	2.13339	exo, bottom	<b>4.575</b>	
			<b>18.894</b>	
			-1110.053364	
			-1110.032304	
			-1110.103550	
TS61	na	na	anti, <i>s</i> -cis	na

na		endo, top	
TS62	3.11913	anti, <i>s</i> -cis	<b>1.276</b>
-293.7	2.15177	exo, bottom	<b>0.675</b>
			<b>14.759</b>
			-1110.059528
			-1110.038411
			-1110.110044
TS63	na	syn, <i>s</i> -cis	na
na		endo, top	
TS64	na	syn, <i>s</i> -cis	na
na		exo, bottom	

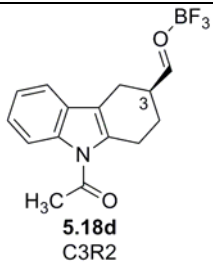
**Table 5.14** (continued)

TS for DA Adduct	TSs	Bond distance (Å)	Dienophile	$\Delta^\ddagger E,^c \Delta^\ddagger H,^d \Delta^\ddagger G^e$
	IF <sup>b</sup>	C3 $\alpha$ -C3' C2 $\alpha$ -C2'	Approach	$E_{elec.} + ZPE^f$ $E_0 + H_{corr}^g$ $E_0 + G_{corr}^h$
 <p><b>5.17d</b> C2R2</p>	TS65	2.14835	anti, <i>s</i> -trans	<b>3.342<sup>c</sup></b>
	-332.4	3.01128	endo, top	<b>2.726<sup>d</sup></b>
				<b>17.655<sup>e</sup></b>
				-1110.057841 <sup>f</sup>
				-1110.036805 <sup>g</sup>
				-1110.107078 <sup>h</sup>
	TS66	2.08856	anti, <i>s</i> -trans	<b>7.107</b>
	-354.5	3.00433	exo, bottom	<b>6.659</b>
				<b>19.457</b>
				-1110.051841
			-1110.030536	
			-1110.104206	
TS67	2.13714	syn, <i>s</i> -trans	<b>3.736</b>	
-337.1	3.01904	endo, top	<b>3.097</b>	
			<b>17.122</b>	
			-1110.054567	
			-1110.033477	
			-1110.105382	
TS68	2.13741	syn, <i>s</i> -trans	<b>5.634</b>	
-330.9	3.08747	exo, bottom	<b>5.081</b>	
			<b>18.476</b>	
			-1110.051542	
			-1110.030315	
			-1110.103225	
TS69	na	na	anti, <i>s</i> -cis	na

na		endo, top	
TS70	2.16621	anti, <i>s</i> -cis	<b>1.288</b>
-297.4	3.13972	exo, bottom	<b>0.698</b>
			<b>14.577</b>
			-1110.058301
			-1110.037192
			-1110.109343
TS71	na	syn, <i>s</i> -cis	na
na		endo, top	
TS72	na	syn, <i>s</i> -cis	na
na		exo, bottom	



**Table 5.14** (continued)

TS for DA Adduct	TSs	Bond distance (Å)	Dienophile	$\Delta^\ddagger E$ , <sup>c</sup> $\Delta^\ddagger H$ , <sup>d</sup> $\Delta^\ddagger G$ <sup>e</sup>
	IF <sup>b</sup>	C3 $\alpha$ -C2' C2 $\alpha$ -C3'	Approach	$E_{elec.} + ZPE$ <sup>f</sup> $E_0 + H_{corr}$ <sup>g</sup> $E_0 + G_{corr}$ <sup>h</sup>
	TS73	2.89042	anti, <i>s</i> -trans	<b>0.895</b> <sup>c</sup>
	-331.1	2.12068	endo, top	<b>0.133</b> <sup>d</sup>
				<b>15.113</b> <sup>e</sup>
				-1110.061740 <sup>f</sup>
				-1110.040937 <sup>g</sup>
				-1110.111129 <sup>h</sup>
	TS74	3.01387	anti, <i>s</i> -trans	<b>4.976</b>
	-343.1	2.06254	exo, bottom	<b>4.361</b>
				<b>18.539</b>
				-1110.055238
			-1110.034199	
			-1110.105670	
TS75	2.94974	syn, <i>s</i> -trans	<b>1.950</b>	
-324.6	2.11523	endo, top	<b>1.246</b>	
			<b>15.843</b>	
			-1110.057413	
			-1110.036426	
			-1110.107420	
TS76	3.00073	syn, <i>s</i> -trans	<b>3.301</b>	
-320.9	2.10742	exo, bottom	<b>2.667</b>	
			<b>16.740</b>	
			-1110.055260	
			-1110.034162	
			-1110.105991	
TS77	3.15310	anti, <i>s</i> -cis	<b>-1.599</b>	

-288.9	2.18823	endo, top	<b>-2.269</b>
			<b>12.803</b>
			-1110.062903
			-1110.041921
			-1110.112170
TS78	3.21361	anti, <i>s</i> -cis	<b>0.219</b>
-289.0	2.12716	exo, bottom	<b>-0.371</b>
			<b>13.677</b>
			-1110.060005
			-1110.038896
			-1110.110777
TS79	na	syn, <i>s</i> -cis	na
na		endo, top	
TS80	na	syn, <i>s</i> -cis	na
na		exo, bottom	

a. Each TS calculation was carried out using the Synchronous Transit-Guided Quasi-Newton Method (QST2 or QST3, Ref. 317,318) using Gaussian 03 rev. B.04 or C.02 implemented on a desktop computer running Linux OS (Redhat). TS calculations times were typically 12-24 hours in duration. All structures reported here as TSs exhibit only one imaginary frequency. The imaginary vibrations were animated with Gaussview 3.09 or 4.1 to determine if they were in qualitative agreement with the bond-making/bond-breaking processes associated with the reaction of interest. In each case, intrinsic reaction coordinate (IRC, Ref. 313,314) calculations were performed to determine that the observed TS could be linked reasonably to the assumed reactant and product geometries.

b. IF = imaginary frequency in reciprocal centimeters and are not scaled (Ref. 315).

c.  $\Delta^\ddagger E$  (=  $\Delta^\ddagger E0$ ), d.  $\Delta^\ddagger H$ , e.  $\Delta^\ddagger G$  in kcal/mol.

f. *Eelec.* + ZPE (= *E0*), g. *H* = *E0* + *Hcorr*, h. *G* = *E0* + *Gcorr* in a.u. (1 a.u. = 627.5095 kcal/mol).

Experimentally, the regioselectivity of the uncatalyzed reaction is 3:1 in favour of the C-2 regioisomer, whereas the theoretical analysis predicts a nearly equal yield of C-2 and C-3 products. In the BF<sub>3</sub>-catalyzed process, the regioselectivity observed experimentally is 3.5:1 in favour of the C-2 isomer whereas the theoretical analysis predicts a 8.7:1 ratio of C-2 to C-3 regioisomers. It is feasible that, in solution, the Lewis acid is complexing with the amide carbonyl of **5.1** and it is these conditions that are representative of what is occurring in

solution as shown in Scheme 5.4. Owing to time constraints, transition state calculations of the scenarios presented in Scheme 5.4 were not pursued but will be the focus of follow up computational studies in the near future. Finally, the  $\Delta\Delta^\ddagger E$  and  $\Delta\Delta^\ddagger H$  data sets (calculations not shown) indicate decreased regioselectivity upon comparison to the acrolein data set.

**Scheme 5.4:** Possible  $\text{BF}_3$  complexes of *N*-Ac IQDM and subsequent cycloadditions.

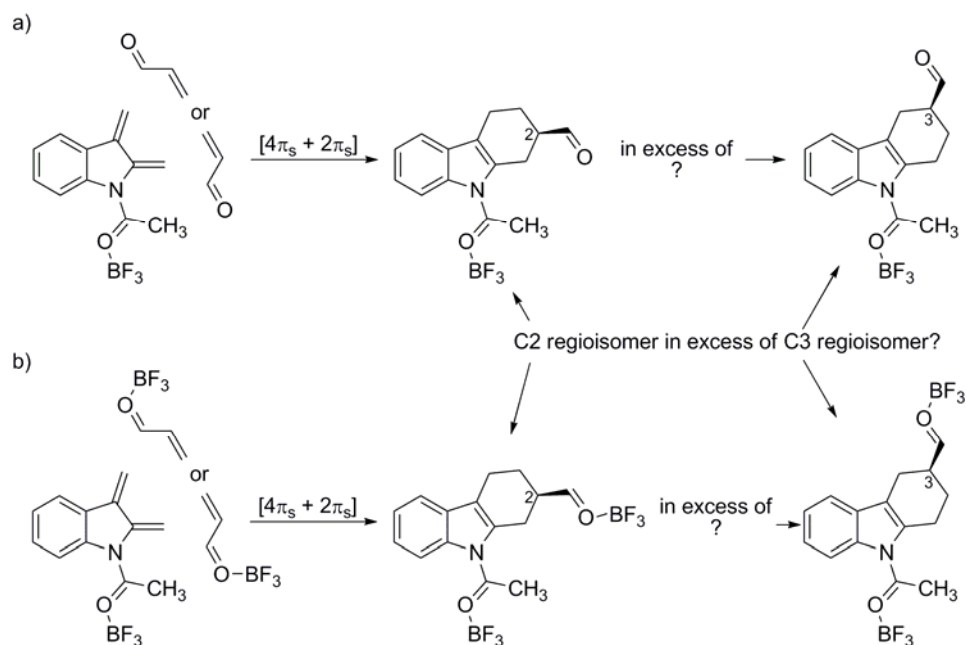


**Figure 5.14:** The transition state structures of TS56 and TS77.

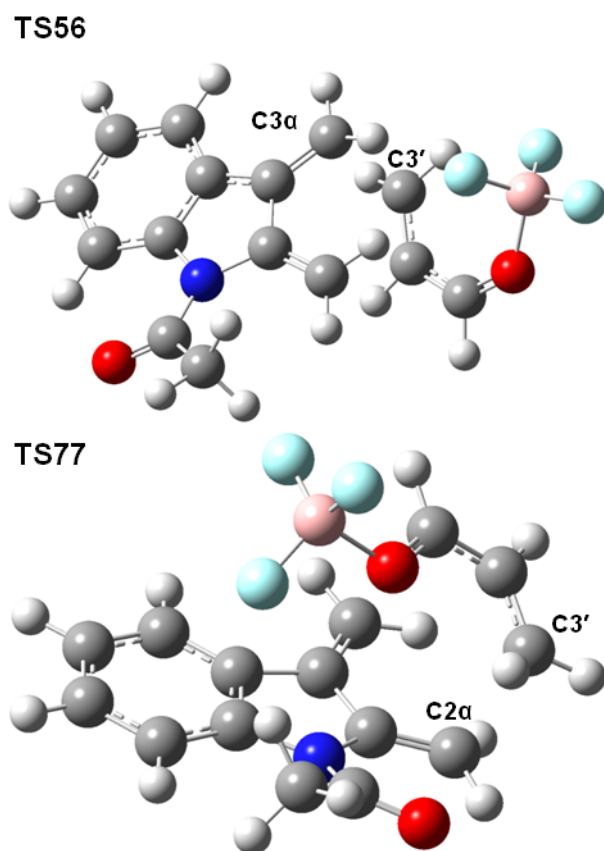
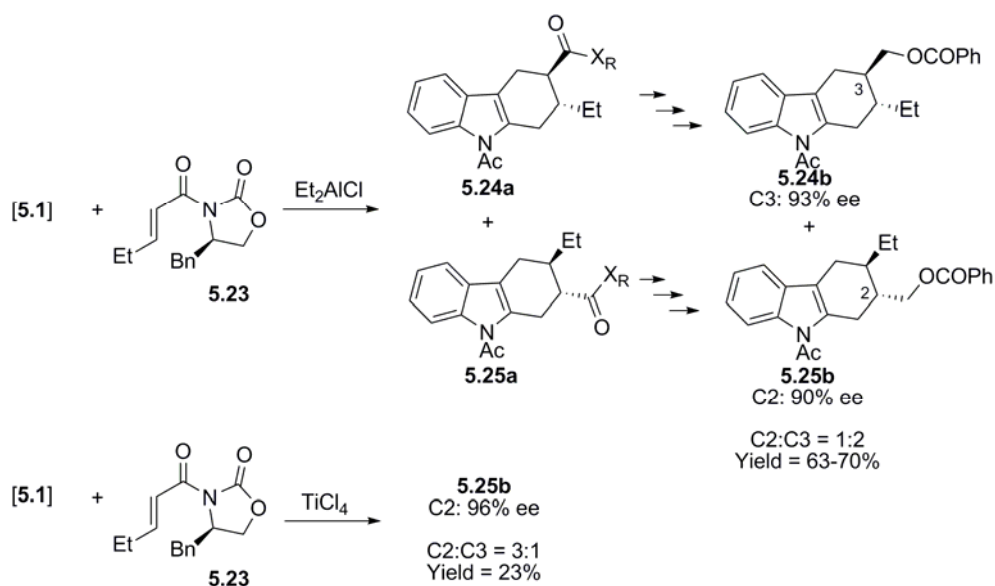


Figure 5.14 shows the TS structures for TS56 and TS77. Asynchronicity manifests as advanced bond development between C-3' and C-3 $\alpha$  (TS56) or C-3' and C-2 $\alpha$  (TS77) and is corroborated by vibrational mode corresponding to the imaginary frequencies (TS56 = -236  $\text{cm}^{-1}$ ; TS77 = -289  $\text{cm}^{-1}$ ) in which the principle motion is between C-3' and C-3 $\alpha$  (TS56) or C-3' and C-2 $\alpha$  (TS77). Further examination gives the following pyramidalization data: TS56 shows C-3 $\alpha$  = 356.1 $^\circ$ , C-3' = 354.6 $^\circ$  and is advanced over that of C2 $\alpha$  = 359.9 $^\circ$ , C-2' = 359.9 $^\circ$ ; TS77 shows C-2 $\alpha$  = 353.9 $^\circ$ , C-3' = 354.4 $^\circ$  and is advanced over that of C3 $\alpha$  = 359.9 $^\circ$ , C-2' = 359.9 $^\circ$ .

### 5.3.5.2 Diels-Alder cycloadditions of Aluminum and Tin acroyloxazolidinones

Wu's studies employing chiral aluminum and titanium (*R,E*)-4-benzyl-3-(pent-2-enoyl)oxazolidin-2-one **5.23**<sup>386</sup> revealed either the C-2 or C-3 regioisomer could be produced in excess of the other and was attributed to either a possible FMO or charge controlled reaction, respectively (Scheme 5.5). These types of issues can be potentially explored by computational studies.

**Scheme 5.5:** Wu's stereoselective Diels-Alder reactions of *N*-Ac-IQDM using **5.23**.



Before this investigation began it was imperative that the correct metal-oxazolidinone structures used in TS calculations were consistent with structures obtained from structural elucidation studies on Evans' auxiliary-metal chelates.<sup>479-481</sup> More recently, Houk and coworkers have computationally examined Diels-Alder reactions involving the oxazolidinone-containing dienophile with  $\text{Me}_2\text{AlCl}$  catalyst **5.26** (Figure 5.15).<sup>333</sup> Furthermore, it was felt that molecular modeling studies would be initiated in this laboratory

using the achiral acrylates **5.27** and **5.28** as this would reduce computational costs considerably. Then, time permitting, studies would be pursued with the chiral 3-pent-2-enoyloxazolidin-2-ones **5.23**.

**Figure 5.15:** Achiral aluminum and titanium oxazolidinones.

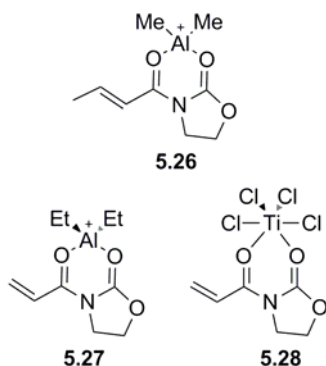
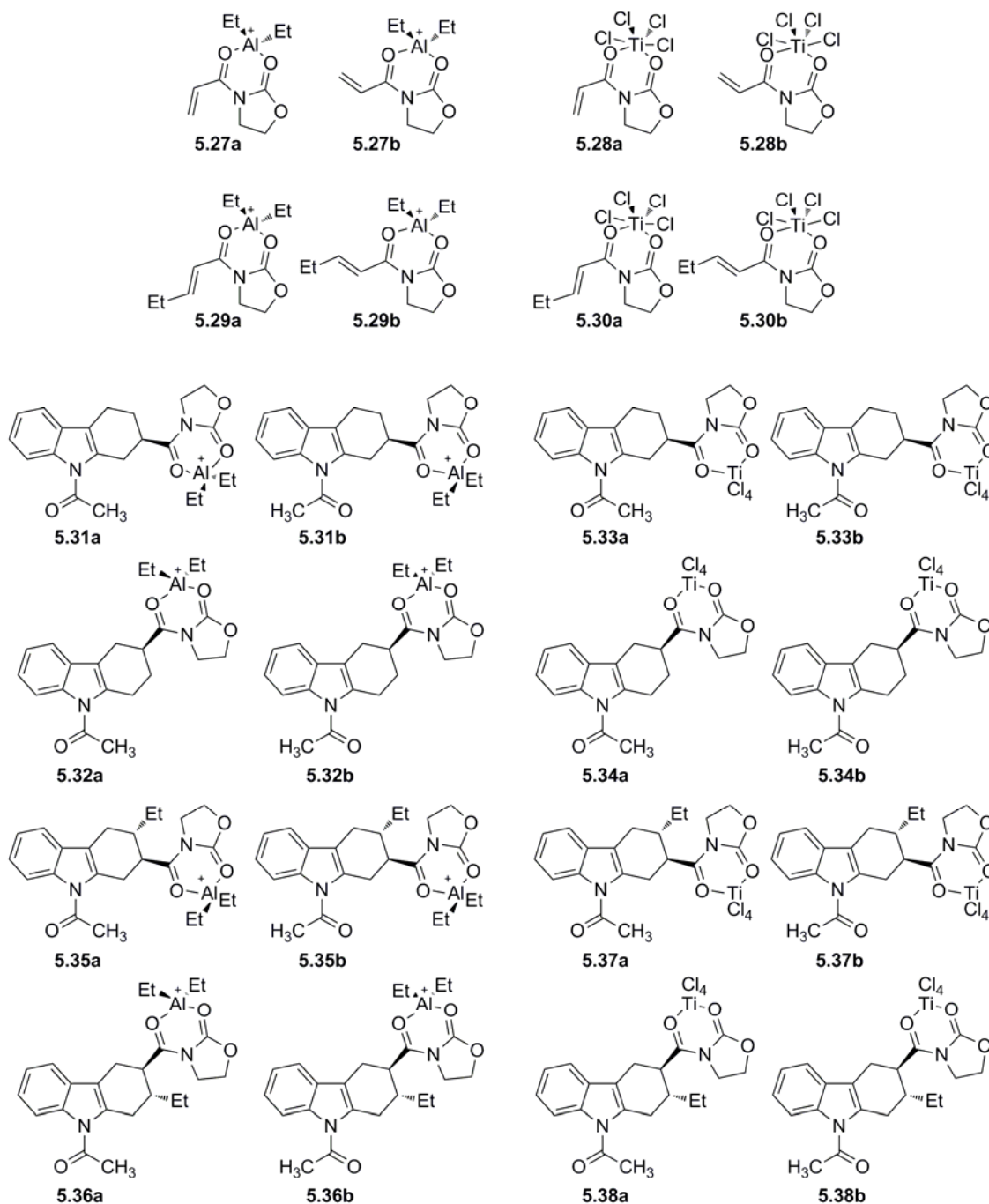


Table 5.15 shows the relevant energy data of aluminum and titanium *N*-acyloxazolidinone **5.27** and **5.28**, respectively and their corresponding adducts. All dienophiles (**5.27**, **5.28**, **5.29**, **5.30**) are more stable in their *s*-cis conformation ("b" series). Rotamer 2 cycloadducts ("b" series) are more stable than the corresponding rotamer 1 cycloadducts ("a" series) in all instances.

**Table 5.15:** The energies (a.u.) and relative energies ( $\text{kcal}\cdot\text{mol}^{-1}$ ) of aluminum and titanium *N*-acyloxazolidinones and their corresponding Diels-Alder adducts obtained at the DFT B3LYP 6-31G(d) level.



**Table 5.15** (continued)

Entry	Structure	Energy $E,^a H,^b G^c$ (a.u.) <sup>d</sup>	Relative Energy (kcal·mol <sup>-1</sup> )	Structure	Energy $E,^a H,^b G^c$ (a.u.) <sup>d</sup>	Relative Energy (kcal·mol <sup>-1</sup> )
1	<b>5.27a</b>	-913.749587 <sup>a</sup>	4.977	<b>5.27b</b>	-913.757518 <sup>a</sup>	0
		-913.730771 <sup>b</sup>	4.765		-913.738365 <sup>b</sup>	0
		-913.797164 <sup>c</sup>	6.158		-913.806977 <sup>c</sup>	0
2	<b>5.28a</b>	-3203.622048	4.191	<b>5.28b</b>	-3203.628727	0
		-3203.603546	4.149		-3203.610159	0
		-3203.670100	4.345		-3203.677024	0
3	<b>5.29a</b>	-992.334377	5.855	<b>5.29b</b>	-992.343708	0
		-992.312604	5.792		-992.321834	0
		-992.386597	6.038		-992.396219	0
4	<b>5.30a</b>	-3282.201767	5.253	<b>5.30b</b>	-3282.210138	0
		-3282.180334	5.216		-3282.188646	0
		-3282.254426	5.356		-3282.262962	0
5	<b>5.31a</b>	-1507.476461	5.896	<b>5.31b</b>	-1507.485857	0
		-1507.446138	6.022		-1507.455735	0
		-1507.540123	5.580		-1507.549016	0
6	<b>5.32a</b>	-1507.472521	8.368	<b>5.32b</b>	-1507.478570	4.573
		-1507.442425	8.352		-1507.448572	4.495
		-1507.535528	8.464		-1507.541240	4.879
7	<b>5.33a</b>	-3797.351550	1.453	<b>5.33b</b>	-3797.353866	0
		-3797.321522	1.635		-3797.324127	0
		-3797.415732	0.914		-3797.417188	0
8	<b>5.34a</b>	-3797.344838	5.665	<b>5.34b</b>	-3797.347438	4.034
		-3797.315076	5.679		-3797.317718	4.022
		-3797.408316	5.567		-3797.411196	3.760



9	<b>5.35a</b>	-1586.047217	5.511	<b>5.35b</b>	-1586.055999	0
		-1586.013928	5.559		-1586.022788	0
		-1586.114579	5.669		-1586.123613	0
10	<b>5.36a</b>	-1586.041760	8.935	<b>5.36b</b>	-1586.047974	5.036
		-1586.008767	8.798		-1586.015048	4.857
		-1586.107692	9.991		-1586.113935	6.073
11	<b>5.37a</b>	na	na	<b>5.37b</b>	-3875.923242	0
		na	na		-3875.890451	0
		na	na		-3875.990363	0
12	<b>5.38a</b>	-3875.915162	5.070	<b>5.38b</b>	-3875.917746	3.449
		-3875.882539	4.965		-3875.885200	3.295
		-3875.981482	5.573		-3875.984097	3.932

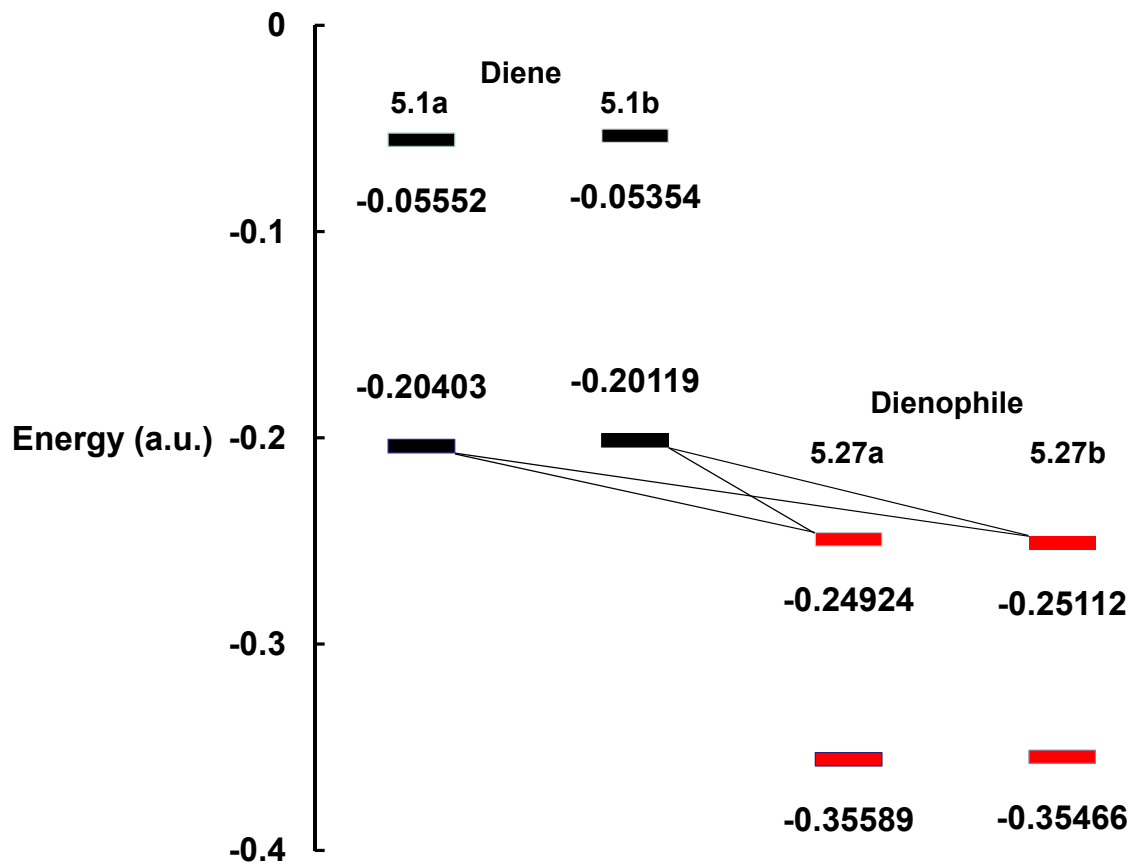
a., b., c. Energies are taken from minimized structures and are a) the electronic and zero point energies (i.e.  $E = E_{elec} + ZPE = E0$ ), b) the electronic, zero point and thermal enthalpies (i.e.  $H = E0 + H_{corr}$ ), c) the electronic, zero point and thermal free energies (i.e.  $G = E0 + G_{corr}$ ).

d. One atomic unit (a.u.) = 627.5095 kcal/mol.

The FMO energies of *N*-Ac-IQDM and of aluminum and titanium *N*-acyloxazolidinone **5.27** and **5.28**, are shown in Figures 5.16 and 5.17, respectively. The lowest energy interaction is that of the HOMO of **5.1** with the LUMO of **5.27** and **5.28** (HOMO<sub>diene</sub>-LUMO<sub>dienophile</sub>). An important observation is that the LUMO energies of **5.27** are lowered considerably from  $\sim -0.065$  a.u. observed for acrolein to  $\sim -0.25$  a.u. and is lower in energy than the HOMO of **5.1**, demonstrating the powerful Lewis acid effect of Et<sub>2</sub>AlCl. With **5.28**, the LUMO is lowered to that observed previously with BF<sub>3</sub> (cf. Figure 5.16 to Figure 5.8 and Figure 5.13). Consequently, a lowering of the activation barrier would occur as compared to the non-catalyzed versions, thus increasing the rate of reaction if FMO interactions are important.

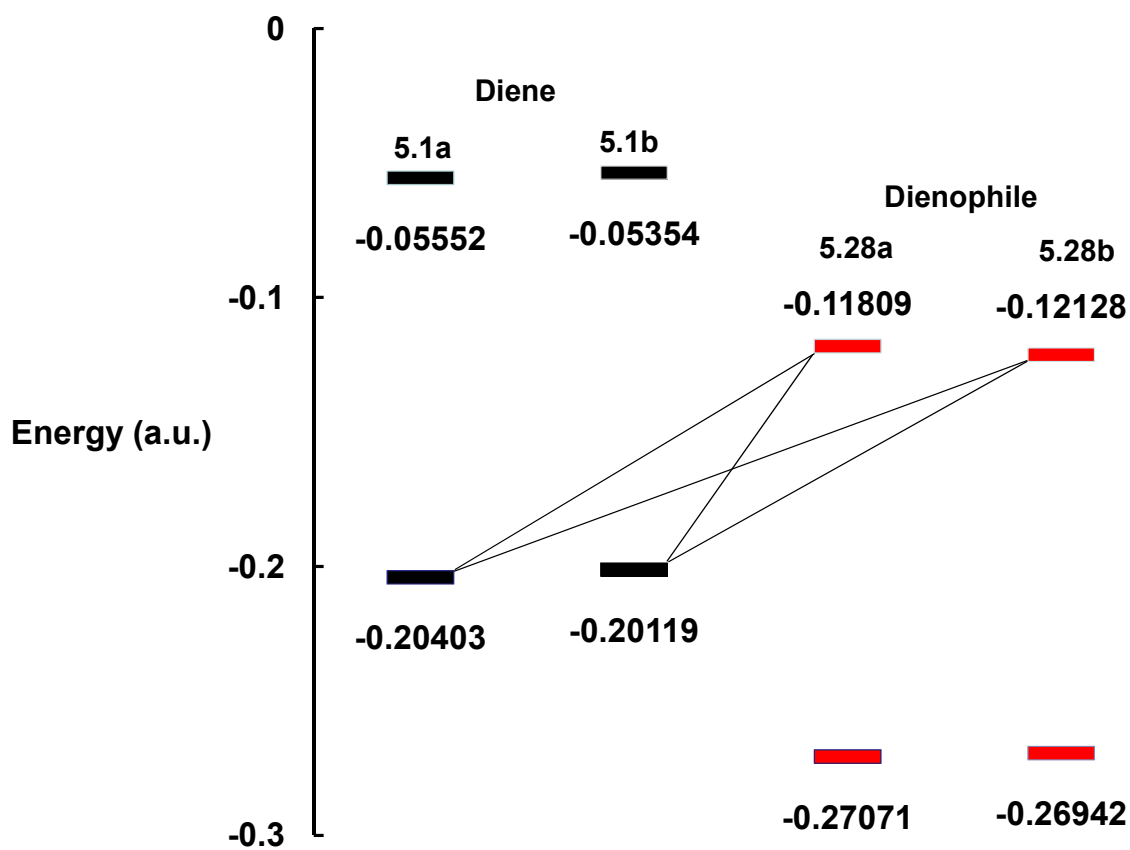
Tables 5.16 and 5.17 shows the FMO energies and corresponding MO coefficients of **5.27** and **5.28**, respectively. The largest coefficients reside on C-1. The coefficients have increased at C-1 (exception **5.28b**) and decreased at C-2 and C-3 upon comparison to the values presented in Table 5.5. Stereoselectivity (endo:exo) and regioselectivity may increase owing to the bulky auxiliary but can only be determined by a thorough in depth theoretical study. The following discussion focuses on transition state calculations of aluminum and titanium *N*-acyloxazolidinone-catalyzed cycloadditions with *N*-Ac-IQDM.

**Figure 5.16:** Frontier molecular orbital energies (a.u.) for the  $[4\pi_s + 2\pi_s]$  cycloaddition of **5.1** with **5.27** calculated at the DFT B3LYP 6-31 G(d) level. The four black lines indicate the four possible lowest energy HOMO-LUMO interactions of the HOMO of *N*-Ac IQDM **5.1** (diene, black) with the LUMO of **5.27** (dienophile, red).



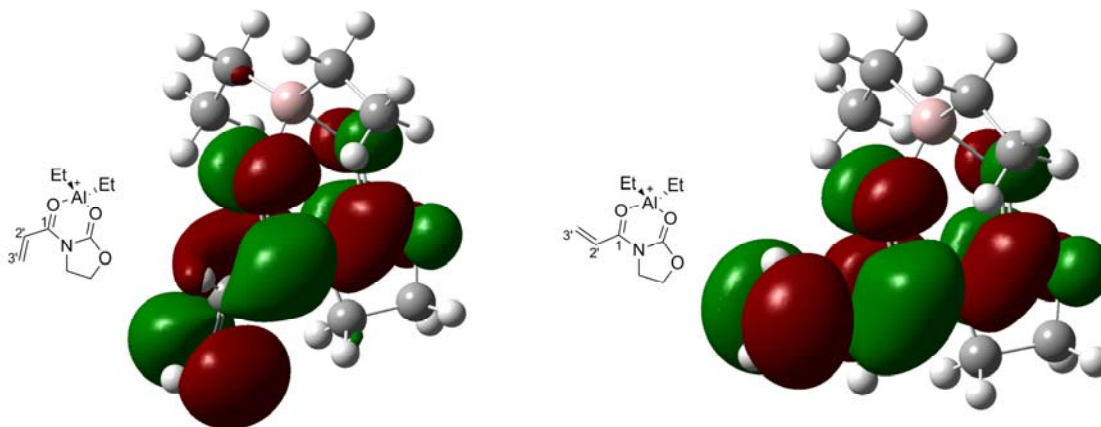
One atomic unit (a.u.) = 627.5095 kcal/mol.

**Figure 5.17:** Frontier molecular orbital energies (a.u.) for the  $[4\pi_s + 2\pi_s]$  cycloaddition of **5.1** with **5.28** calculated at the DFT B3LYP 6-31 G(d) level. The four black lines indicate the four possible lowest energy HOMO-LUMO interactions of the HOMO of *N*-Ac IQDM **5.1** (diene, black) with the LUMO of **5.28** (dienophile, red).



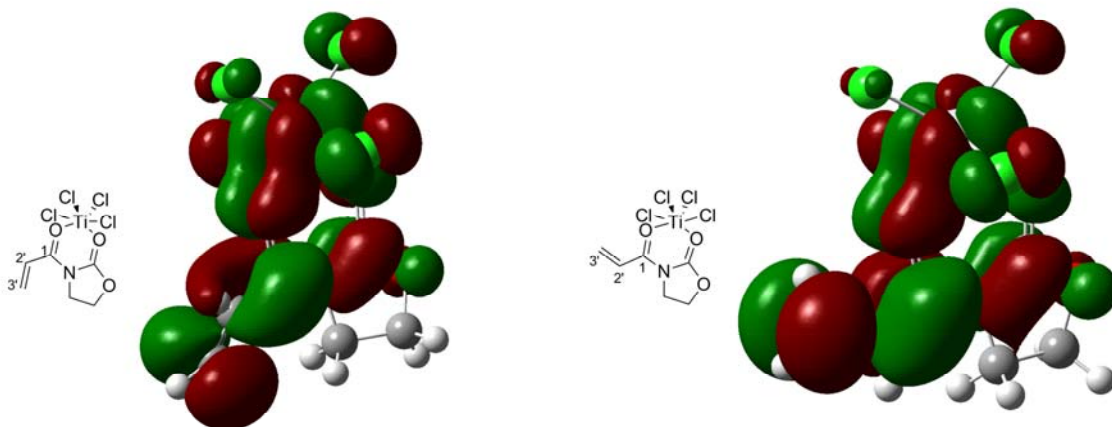
One atomic unit (a.u.) = 627.5095 kcal/mol.

**Table 5.16:** FMO energy (a.u.) and orbital coefficients of the LUMO of **5.27a** and **5.27b** obtained at the DFT B3LYP 6-31G(d) level.



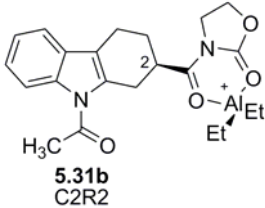
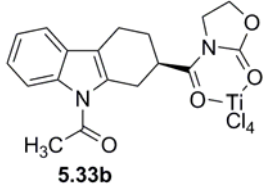
	<b>5.27a</b>	<b>5.27b</b>		
<b>Energy (a.u.)</b>	-0.24924	-0.25112		
<b>LUMO</b>				
	<b>Orbital</b>	<b>Coefficient</b>	<b>Orbital</b>	<b>Coefficient</b>
	C1 2p <sub>y</sub>	0.30483	C1 2p <sub>z</sub>	0.39499
	C1 2p <sub>z</sub>	-0.28420	C1 3p <sub>z</sub>	0.32165
	C1 3p <sub>y</sub>	0.26417	C2' 2p <sub>z</sub>	0.10543
	C1 3p <sub>z</sub>	-0.22253	C2' 3p <sub>z</sub>	0.14401
	C2' 2p <sub>y</sub>	0.08412	C3' 2p <sub>z</sub>	-0.33979
	C2' 3p <sub>y</sub>	0.11499	C3' 3p <sub>z</sub>	-0.36451
	C3' 2p <sub>x</sub>	-0.16115		
	C3' 2p <sub>y</sub>	-0.22918		
	C3' 2p <sub>z</sub>	0.15745		
	C3' 3p <sub>x</sub>	-0.15433		
	C3' 3p <sub>y</sub>	-0.25817		
	C3' 3p <sub>z</sub>	0.14645		

**Table 5.17:** FMO energy (a.u.) and orbital coefficients of the LUMO of **5.28a** and **5.28b** obtained at the DFT B3LYP 6-31G(d) level.



	<b>5.28a</b>	<b>5.28b</b>		
<b>Energy (a.u.)</b>	-0.11809	-0.12128		
<b>LUMO</b>				
	<b>Orbital</b>	<b>Coefficient</b>	<b>Orbital</b>	<b>Coefficient</b>
	C1 2p <sub>z</sub>	-0.29649	C1 2p <sub>z</sub>	-0.32624
	C1 3p <sub>z</sub>	-0.24840	C1 3p <sub>z</sub>	-0.27017
	C2' 2p <sub>z</sub>	-0.07996	C2' 2p <sub>z</sub>	-0.12758
	C2' 3p <sub>z</sub>	-0.13269	C2' 3p <sub>z</sub>	-0.17755
	C3' 2p <sub>x</sub>	-0.16106	C3' 2p <sub>z</sub>	0.30238
	C3' 2p <sub>y</sub>	-0.08334	C3' 3p <sub>z</sub>	0.34700
	C3' 2p <sub>z</sub>	0.15883		
	C3' 3p <sub>x</sub>	-0.16783		
	C3' 3p <sub>y</sub>	-0.12347		
	C3' 3p <sub>z</sub>	0.17864		

**Table 5.18:** Selected structural data and energies of TS structures of Diels-Alder reactions of *N*-Ac-IQDM **5.1** and **5.27** and **5.28** obtained at the DFT B3LYP 6-31G(d) level.

TS for DA Adduct	TSs	Bond distance (Å)	Dienophile	$\Delta^\ddagger E$ , <sup>c</sup> $\Delta^\ddagger H$ , <sup>d</sup> $\Delta^\ddagger G$ <sup>c</sup>
	IF <sup>b</sup>	C3 $\alpha$ -C3'	Approach	$E_{elec.} + ZPE$ <sup>f</sup>
		C2 $\alpha$ -C2'		$E_0 + H_{corr}$ <sup>g</sup>
				$E_0 + G_{corr}$ <sup>h</sup>
 <p><b>5.31b</b> C2R2</p>	TS81	2.22750	<i>s</i> -cis, exo	<b>-10.058<sup>c</sup></b>
	-256.4	3.11615	bottom	<b>-10.432<sup>d</sup></b>
				<b>4.009<sup>e</sup></b>
				-1507.429003 <sup>f</sup>
				-1507.397842 <sup>g</sup>
				-1507.494040 <sup>h</sup>
 <p><b>5.33b</b></p>	TS82	2.08618	<i>s</i> -cis, exo	<b>2.195</b>
	-352.1	3.00475	bottom	<b>1.846</b>
				<b>15.765</b>
				-3797.280686
				-3797.250070
				-3797.345526

a. Each TS calculation was carried out using the Synchronous Transit-Guided Quasi-Newton Method (QST2 or QST3, Ref. 317,318) using Gaussian 03 rev. B.04 or C.02 implemented on a desktop computer running Linux OS (Redhat). TS calculations times were typically 48-60 hours in duration. All structures reported here as TSs exhibit only one imaginary frequency. The imaginary vibrations were animated with Gaussview 3.09 or 4.1 to determine if they were in qualitative agreement with the bond-making/bond-breaking processes associated with the reaction of interest. In each case, intrinsic reaction coordinate (IRC, Ref. 313,314) calculations were performed to determine that the observed TS could be linked reasonably to the assumed reactant and product geometries.

b. IF = imaginary frequency in reciprocal centimeters and are not scaled (Ref. 315).

c.  $\Delta^\ddagger E$  ( $= \Delta^\ddagger E0$ ), d.  $\Delta^\ddagger H$ , e.  $\Delta^\ddagger G$  in kcal/mol.

f.  $E_{elec.} + ZPE$  ( $= E0$ ), g.  $H = E0 + H_{corr}$ , h.  $G = E0 + G_{corr}$  in a.u. (1 a.u. = 627.5095 kcal/mol).

Despite many repeated attempts, acquisition of only two TSs were obtained for the DA adducts listed in Table 5.15. This precludes any analysis and subsequent comparison of the reversal of regioselectivity provided by the aluminum and titanium catalysts as discussed in Chapter 4. The reasons no TSs were obtained for the C-3 adducts are not immediately clear.

No obvious steric clashes were observed during modeling efforts for TS calculations for the C-3 adducts and casual inspection of TS81 and TS82 with input files for the corresponding C-3 TS calculations confirms this. The C-2 adducts were obtained using the *s*-cis conformation (**5.27b**, **5.28b**) with an *exo* approach. This approach seemed appropriate for C-3 TSs and was pursued, yet modeling efforts were denied despite repeated attempts. Houk and coworkers' study of DA reactions of siloxydienes and silylated dienes with *N*-acyloxazolidinones catalyzed by Me<sub>2</sub>AlCl found that an *exo* approach with the dienophile in the *s*-cis conformation gave barriers that were completely consistent with the experimentally observed diastereoselectivity.<sup>333</sup> In that study, it was found that *exo* selectivity was due to the result of more severe reactant distortions, overwhelming the more favorable interaction energies in the *endo* TS. The notion that the activation barrier ( $\Delta^\ddagger E$ ) is the sum of distortion ( $\Delta^\ddagger E_d$ ) and interaction energies ( $\Delta^\ddagger E_i$ ) has been used to rationalize *endo* vs. *exo* selectivity<sup>332-335,478</sup> and has also been applied in rationalizing 1,3-dipolar cycloadditions.<sup>329-331</sup> Whether this type analysis can be applied to rationalize the reversal of regioselectivity with the catalysts **5.27** and **5.28** remains to be answered by future modeling experiments.

The experimental results obtained by J.Y.J. Wu from this laboratory provided the primary motivation for the computational work on Lewis acid catalyzed reactions employing **5.27** and **5.28** in efforts towards elucidating a cause for the reversal of selectivity. Despite insufficient data that would allow insight into the reversal of regioselectivity provided by **5.27** and **5.28**, others have shown that a reversal of stereoselectivity can be obtained simply by employing Et<sub>2</sub>AlCl or TiCl<sub>4</sub> ("stereodichotomy").<sup>482,483</sup> Currently, there is a paucity of information regarding the effect of different Lewis acids on regioselectivity.



The TS82 is more asynchronous ( $\Delta d = 0.91857 \text{ \AA}$ ) but it possesses higher barriers compared to that of the TS81 ( $\Delta d = 0.88865 \text{ \AA}$ ). Thus it would appear that one cannot predict relative energy barriers based on  $\Delta d$  data alone when comparing two different metal catalysts. This is further supported upon inspection of the analogous  $\text{BF}_3$ -catalyzed version (TS70) in which  $\Delta d = 0.97351 \text{ nm}$  and a  $\Delta^\ddagger G = 14.577 \text{ kcal}\cdot\text{mol}^{-1}$ . These reactions are not FMO controlled and thus rules out the argument of a closer HOMO-LUMO gap influencing energy barriers of **5.1** and **5.27** compared to that of **5.1** and **5.28** (c.f. Figures 5.16 and 5.17). Thus other factors are influencing the energy barriers of these cycloadditions.

**Figure 5.18:** The transition state structures of TS81 and TS82

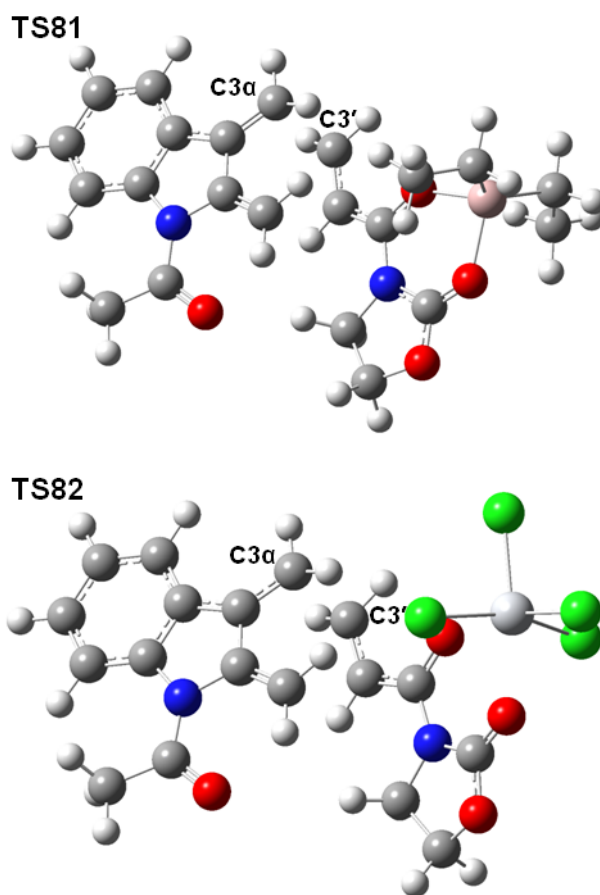


Figure 5.18 shows the TS structures for TS81 and TS82. Asynchronicity is observed as advanced bond development between C-3' and C-3 $\alpha$  and is further supported upon examination of the vibrational mode corresponding to the imaginary frequencies (TS81 = -256 cm<sup>-1</sup>; TS82 = -352 cm<sup>-1</sup>) in which the principle motion is between C-3' and C-3 $\alpha$ . The pyramidalization data is as follows: TS81 shows C-3 $\alpha$  = 354.4°, C-3' = 354.5° and is advanced over that of C2 $\alpha$  = 359.7°, C-2' = 359.9°; TS82 shows C-3 $\alpha$  = 352.9°, C-3' = 351.6° and is advanced over that of C2 $\alpha$  = 359.5°, C-2' = 359.9°.

## 5.4 Conclusion

A thorough in depth theoretical study of the *N*-acetyl indole-2,3-quinodimethanes (*N*-Ac IQDM) has been accomplished. Calculations at the DFT B3LYP 6-31 G(d) level of theory have provided insight into conformational populations of the *N*-Ac IQDM, its Diels-Alder cycloadducts and the associated energy barriers of corresponding transition state structures (TSs).

Good agreement was observed for the description of the rotamer populations and energy barriers for amide rotation of *N*-Ac IQDM. The potential energy surface and free energy surface was described through extensive TS calculations of DA reactions with acrolein in which  $\Delta\Delta^\ddagger G$  failed to predict the experimentally observed regioselectivity. Calculations that are not representative of experimental conditions (e.g. temperature issues, gas phase vs. solvent inclusion, etc.) may have implications on these results. However,  $\Delta\Delta^\ddagger E$  and  $\Delta\Delta^\ddagger H$  data sets was found to be predictive of the regioselectivity observed experimentally.

The  $\Delta\Delta^\ddagger G$  predicts that both  $\alpha$ -substitution (i.e. methacrolein) and  $\beta$ -substitution (i.e. crotonaldehyde) increases regioselectivity for the C-2 regioisomer. Furthermore, both the  $\Delta\Delta^\ddagger E$  and  $\Delta\Delta^\ddagger H$  data sets for methacrolein predicts increased regioselectivity for the C-2 adduct. However, with crotonaldehyde, both the  $\Delta\Delta^\ddagger E$  and  $\Delta\Delta^\ddagger H$  data sets indicate that  $\beta$ -substitution diminishes C-2 regioselectivity.

The  $\Delta\Delta^\ddagger G$  data set with  $\text{BF}_3$ -acrolein predicts increased regioselectivity over that of the non-catalyzed version as per experimental evidence; however, it is overestimated by the range of 2.5 to 9-fold and may be owing to  $\text{BF}_3$  complexation of *N*-Ac IQDM. The  $\Delta\Delta^\ddagger E$  and

$\Delta\Delta^\ddagger H$  data sets (calculations not shown) indicate decreased regioselectivity upon comparison to the acrolein data set.

Limited data obtained from transition state calculations of aluminum and titanium *N*-acyloxazolidinone-catalyzed cycloadditions with *N*-Ac-IQDM could not provide insight on the reversal of regioselectivity observed experimentally by J.Y.J Wu from this laboratory.

Future computational efforts will be directed towards calculations in which solvent effects and temperature corrections are to be included to address issues of selectivity and the accuracy of calculated energies in the context of experimental results.

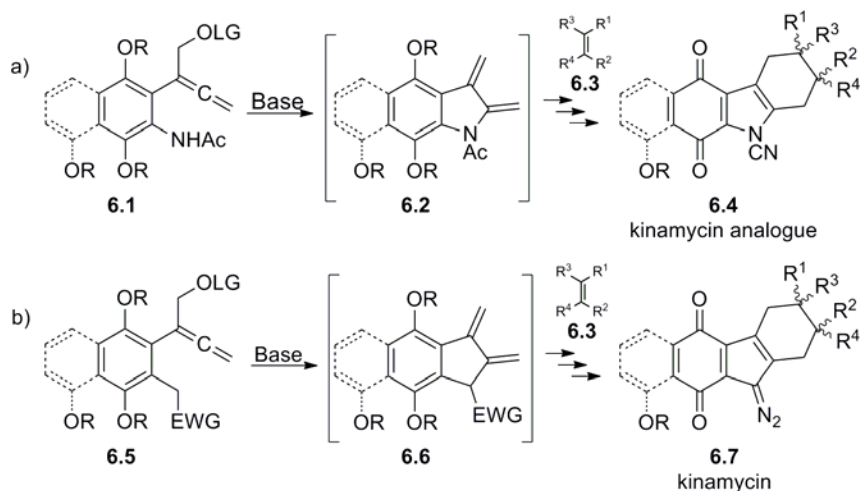
## Chapter 6

# Efforts towards the Synthesis of Substituted Tetrahydrofluorenes through Diels-Alder Reactions of 2,3-Dimethylene Indene Carboxylates and Malonates

### 6.1 Introduction

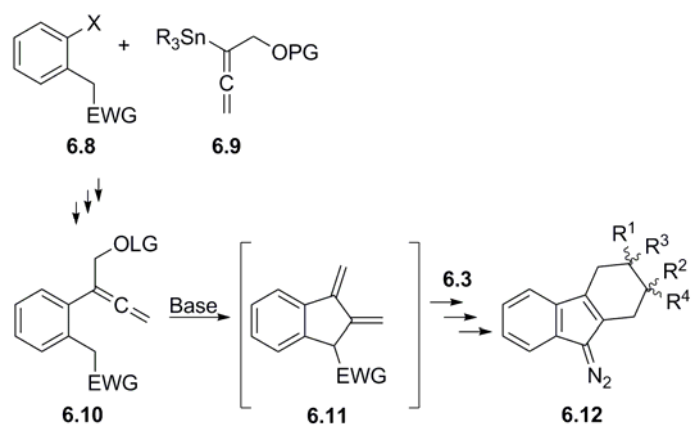
Chapter 4 illustrated the generation and use of *N*-acetyl-indole-2,3-quinodimethanes (*N*-Ac-IQDM) **6.2** in Diels-Alder cycloadditions to access carbazoloquinones **6.4** which in principle could furnish kinamycin analogues (Scheme 6.1a). This chapter presents synthetic efforts towards **6.6**, the bis-methylene carbocyclic analogues of the *N*-Ac-IQDM and their use in Diels-Alder reactions to generate substituted tetrahydrofluorenes and ultimately the kinamycins (Scheme 6.1b). The purpose of these studies is to provide an efficient route to **6.7** that parallels the potential IQDM route to the carbazole **6.4**.

**Scheme 6.1:** Access to a) carbazoloquinones **6.4** and b) fluorenequinones **6.7**.



A proposed synthetic plan is outlined in Scheme 6.2 illustrating the generation of **6.11** which could provide the diazofluorene **6.12**. The chemistry used to obtain **6.9** has already been discussed in Chapter 4. Hence efforts have focused on optimizing conditions for X (halogen, triflate, etc.), EWG (carboxylate, malonate, nitrile, etc.) and OLG (mesylate, acetoxy, carbonate, etc.) of **6.8** and **6.10** to provide the most expedient access to **6.12**.

**Scheme 6.2:** Generation of bis-methylene indene **6.11** and its use in Diels-Alder cycloadditions.

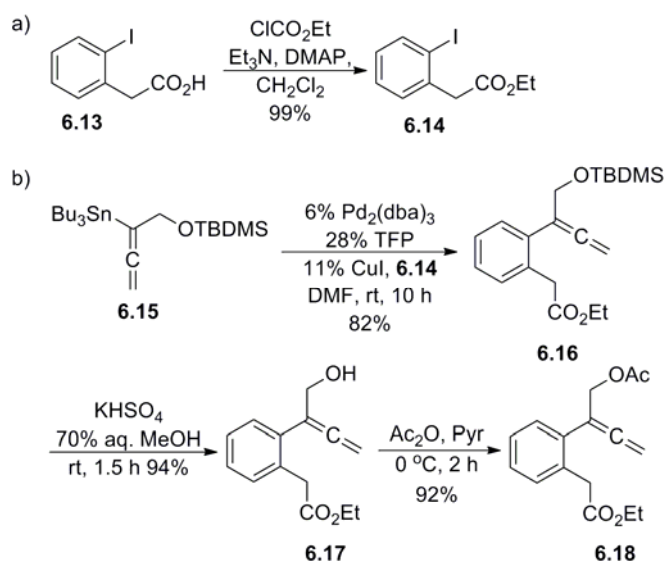


## 6.2 Synthesis

### 6.2.1 Ethyl 2-(2-(1-acetoxybuta-2,3-dien-2-yl)phenyl)acetate

Efforts towards **6.10** were initiated using the ethyl ester of 2-iodo-phenylacetic acid **6.14** produced from 2-iodophenylacetic acid **6.13** in 99% yield and was subsequently employed in a Stille cross-coupling to furnish **6.16** in 82% yield. Deprotection and acetylation provided **6.18** in 86% yield over two steps (Scheme 6.3).

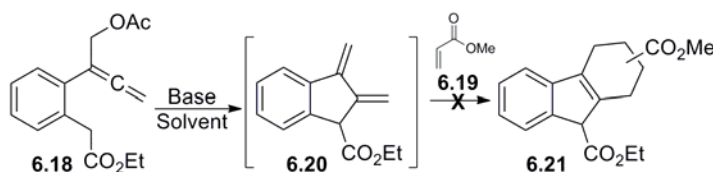
**Scheme 6.3:** Synthesis of **6.18**.



With sufficient amounts of **6.18** in hand, optimization of conditions suitable for Diels-Alder reactions was pursued. Reactions using methyl acrylate **6.19**, DBU, NaH or NaOtBu in either CH<sub>2</sub>Cl<sub>2</sub> or CH<sub>3</sub>CN were investigated (Table 6.1). Dichloromethane was explored first. Use of DBU in CH<sub>2</sub>Cl<sub>2</sub> returned starting material, whereas using NaH led to total decomposition of starting materials and products. Sodium *tert*-butoxide gave a complex mixture as indicated by analytical TLC, <sup>1</sup>H NMR and GCMS analysis. These attempts were repeated in acetonitrile in which the use of DBU did not provide the desired adduct **6.21**, but instead produced the eneyne **6.22** in 21% yield with a 27% recovery of the starting material (Pathway 1 Scheme 6.4). A separate fraction contained an inseparable mixture of what was thought to be **6.20**, **6.21** and/or **6.23** as inferred from GCMS data obtained from the crude residue that provided a *m/z* for molecular ions 214 and 300 (Pathway 2 Scheme 6.4). The <sup>1</sup>H NMR spectrum of this fraction provided two sets of what appeared to be overlapping

doublets centered at ~5.80 and ~5.40 ppm and is consistent with the olefinic protons of the diene moiety of either **6.20** and/or **6.23**. As well, multiplets observed between ~2.2 and ~3.2 ppm can be tentatively assigned to the methylene protons of the substituted cyclohexene ring of **6.21** and/or the  $\alpha$  and  $\beta$  carbons of the ester moiety of **6.23**.

**Table 6.1:** Attempted optimization of Diels-Alder reactions of **6.18** with **6.19**.



Entry	Solvent	Base (eq.) Temp./Time	Products (%)	Recovery of <b>6.18</b> (%)
1	CH <sub>2</sub> Cl <sub>2</sub> <sup>a</sup>	DBU (1.1) rt/31 h	trace <b>6.22</b> by <sup>1</sup> H NMR	98
		NaH (6.9) rt/44 h	nil	0
		NaOtBu (1.1) rt/4 h	<b>6.22</b> by <sup>1</sup> H NMR; complex mixture <sup>c</sup>	0
2	CH <sub>3</sub> CN <sup>b</sup>	DBU (2.2) rt/12 h	complex mixture: <b>6.22</b> (21); <b>6.20</b> , <b>6.21</b> and/or <b>6.23</b> (trace) <sup>d</sup>	27
		NaH (3.2) rt/2.5 h	<b>6.22</b> by <sup>1</sup> H NMR; complex mixture	0
		NaOtBu (1.1) rt/1.5	<b>6.22</b> by <sup>1</sup> H NMR; complex mixture	not isolated <sup>e</sup>

a. Using 1.1 equivalents of **6.19**.

b. Using 2 equivalents of **6.19**.

c.  $m/z$  = 228, 242, 286, 300, 314 obtained from GCMS analysis of the crude residue.

d. Inferred from  $m/z$  obtained from GCMS analysis.

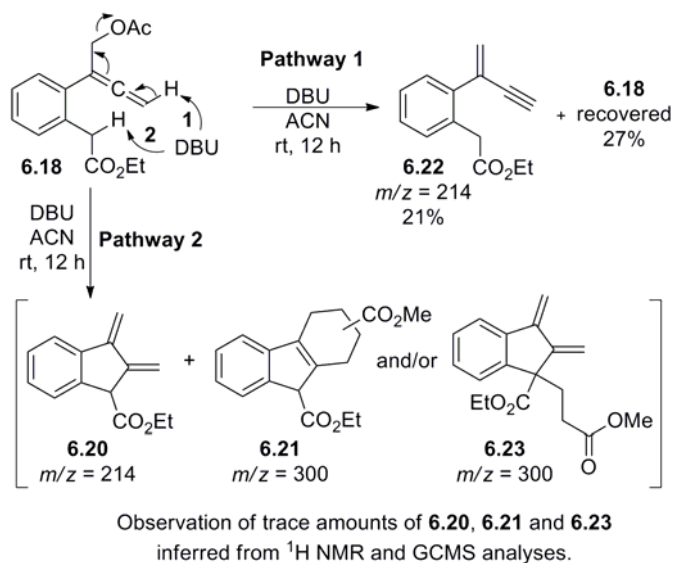
e. **6.18** observed in the proton NMR of the crude residue.

It was anticipated that stronger bases such as NaOtBu and/or NaH may provide the desired adduct; however, in practice both of these bases produced complex mixtures. Use of NaH



resulted in the complete consumption of **6.18**, generating small amounts of **6.22** as observed in the  $^1\text{H}$  NMR spectrum of the crude residue. Employing  $\text{NaOtBu}$  generated small amounts of **6.22** but also returned a large quantity of **6.18**. A quantitative workup was not pursued and further efforts of using **6.18** in cycloaddition reactions were abandoned.

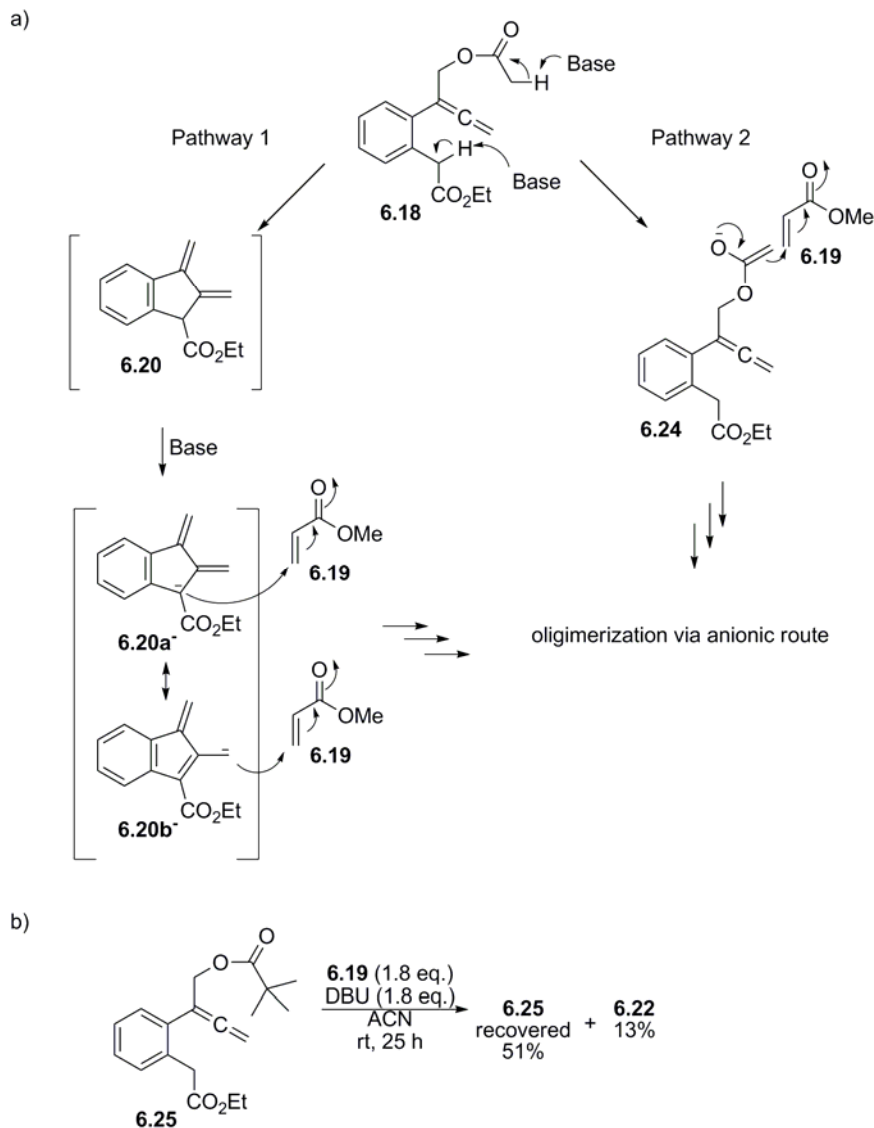
**Scheme 6.4:** Attempted Diels-Alder reactions of allenyl phenyl acetate **6.18**.



One possible route of decomposition is that the starting materials may be consumed by oligomerization via an anionic route (Scheme 6.5a). Deprotonation could occur at either the benzylic position or the acetoxy group of **6.18** generating the corresponding enolates which would then add to methyl acrylate, eventually leading to polymerization. Ketene generation was felt to be another possible route of decomposition; however, esters typically afford the corresponding enolates whereas ketenes are not generally considered. Hence, a control experiment was conceived in which the acetoxy group was replaced by the pivaloyl group to confirm or refute decomposition by pathway 2. Treatment of **6.25** with DBU in ACN

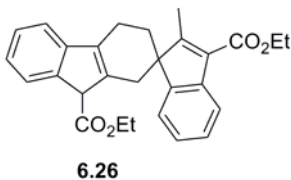
provided a 51% recovery of starting material and 13% yield of the eneyne (Scheme 6.5b) with little evidence of a cycloadduct appearing in the  $^1\text{H}$  NMR spectrum of the crude residue. Although the recovery of starting material had almost doubled in this instance, it is not clear that enolate generation contributed to the decomposition of **6.18** as its corresponding alcohol was never recovered from any of the experiments listed in Table 6.1. In any event, it was determined that **6.18** was not suitable as a diene precursor presumably owing to the low acidity of the benzylic protons and/or sluggish reactivity of the diene.

**Scheme 6.5:** a) Possible decomposition of **6.18** via oligomerization b) Attempted cycloadditions using pivalate **6.25**.



These initial studies provided some evidence for the generation of **6.20** despite the fact that cycloadducts could not be isolated in pure form or fully characterized. This would suggest that the cycloaddition process is not as facile as hoped and this is borne out by the fact that

the homodimer **6.26** (or an isomer thereof) was not observed at any point during these studies.



This is in contrast to the *N*-Ac IQDM which dimerizes readily as discussed in Chapter 4. As previously stated, a possible reason for the failure of the desired reactions to occur may be competing deprotonation pathways (i.e. Pathway 1 and 2, Scheme 6.4) which in turn may furnish a low concentration of **6.20**. Upon the formation of **6.20** it is reasonable to expect that in the presence of excess base, a second deprotonation event even more facile than the first occurs at the benzylic position of **6.20** and the resultant anion may subsequently add in a 1,4 addition to **6.19**, generating **6.23** rather than the producing the desired cycloadduct **6.21**. These concerns invited quantum chemical calculations that are the focus of discussion found later on in this chapter.

### 6.2.2 Diethyl 2-(2-(1-acetoxybuta-2,3-dien-2-yl)phenyl)malonate

It was decided that increasing the acidity of the benzylic protons while providing only a single such proton in the precursor might be helpful to achieve the desired process. This might be accomplished via a malonate or similar alternative. Efforts towards synthesis of the malonate **6.27** were envisioned as a deprotonation of **6.16** under basic conditions and quenching with a suitable carboxyalkylation reagent (Table 6.2). However, in practice it was found this was not as straightforward as initially envisioned. Carboxyalkylation reagents such

as diethyl carbonate (DEC), ethyl chloroformate (ECF) and methyl magnesium carbonate (MMC) were all utilized but none gave the desired malonate. Using NaH with either DEC or ECF returned starting material. Employing DBU and LDA with ECF also returned starting material. Using MMC in DMF gave a complex mixture in which the homodimer **6.26** (and fragments thereof) in varying amounts was observed from data obtained from GCMS analyses. Several different experiments were executed in which the reaction time and amounts of MMC were allowed to vary consistently producing the same profile of products. When the amount of NaH was increased to eight equivalents in DEC, a brown turbid mixture was produced within five minutes of its addition. The reaction was allowed to stir for fifty minutes and after workup and purification, three separate fractions were obtained containing **6.28**, **6.29** and **6.26** (Scheme 6.6). This experiment was repeated several times, consistently generating the same products. The desired malonate **6.27** was never isolated in any of these reactions.

**Scheme 6.6:** Attempts at carboxyalkylation of **6.16**.

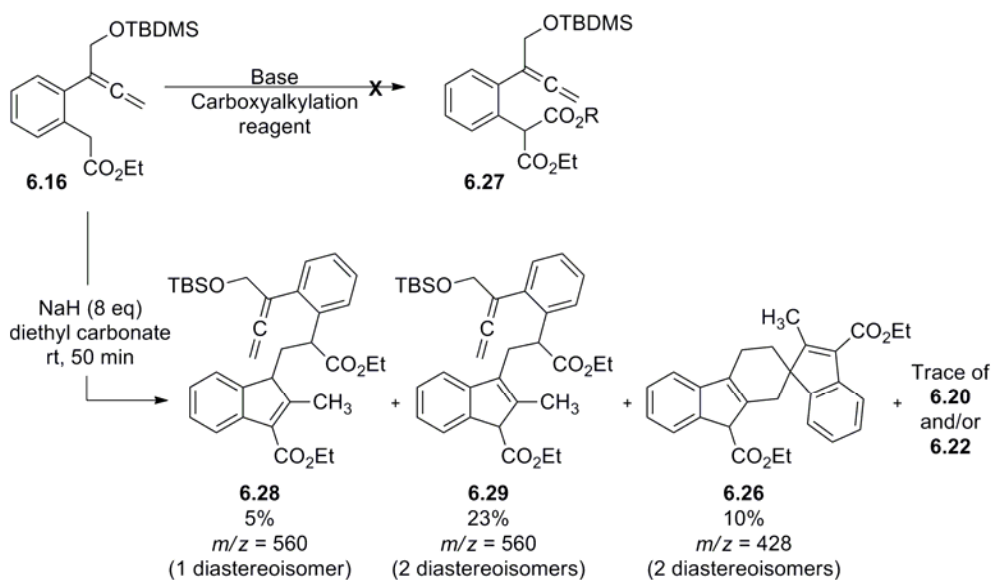
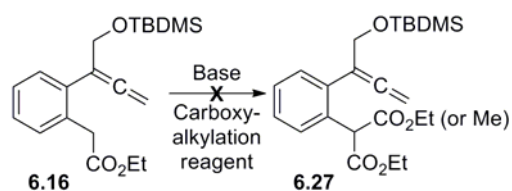


**Table 6.2:** Attempts at carboxyalkylation of **6.16**.



Entry	Solvent	Base (eq.)	Carboxy- alkylation Reagent (eq.)	Temp./ Time	Products (%)	Recovery of <b>6.16</b> (%)
1	DEC <sup>a</sup>	NaH (2.6)	DEC	rt/17 h	nil	95
2	DEC	NaH (8)	DEC	rt/50 min	complex mixture: <b>6.28</b> (5) <b>6.29</b> (23) <b>6.26</b> (10)	0
3	ECF <sup>b</sup>	NaH (5)	ECF	rt/39 h	nil	>100
4	THF	LDA (1)	ECF (2)	0°C→rt /25 min	nil	>100
5	ACN	DBU (4.9)	ECF (1.5)	rt/19 h	nil	>100
6	DMF	nil	MMC <sup>c</sup> (15-20)	120 °C/ 2-14 h	complex mixture: <b>6.26</b> <sup>d</sup>	0

a. DEC = Diethyl carbonate.

b. ECF = Ethyl chloroformate.

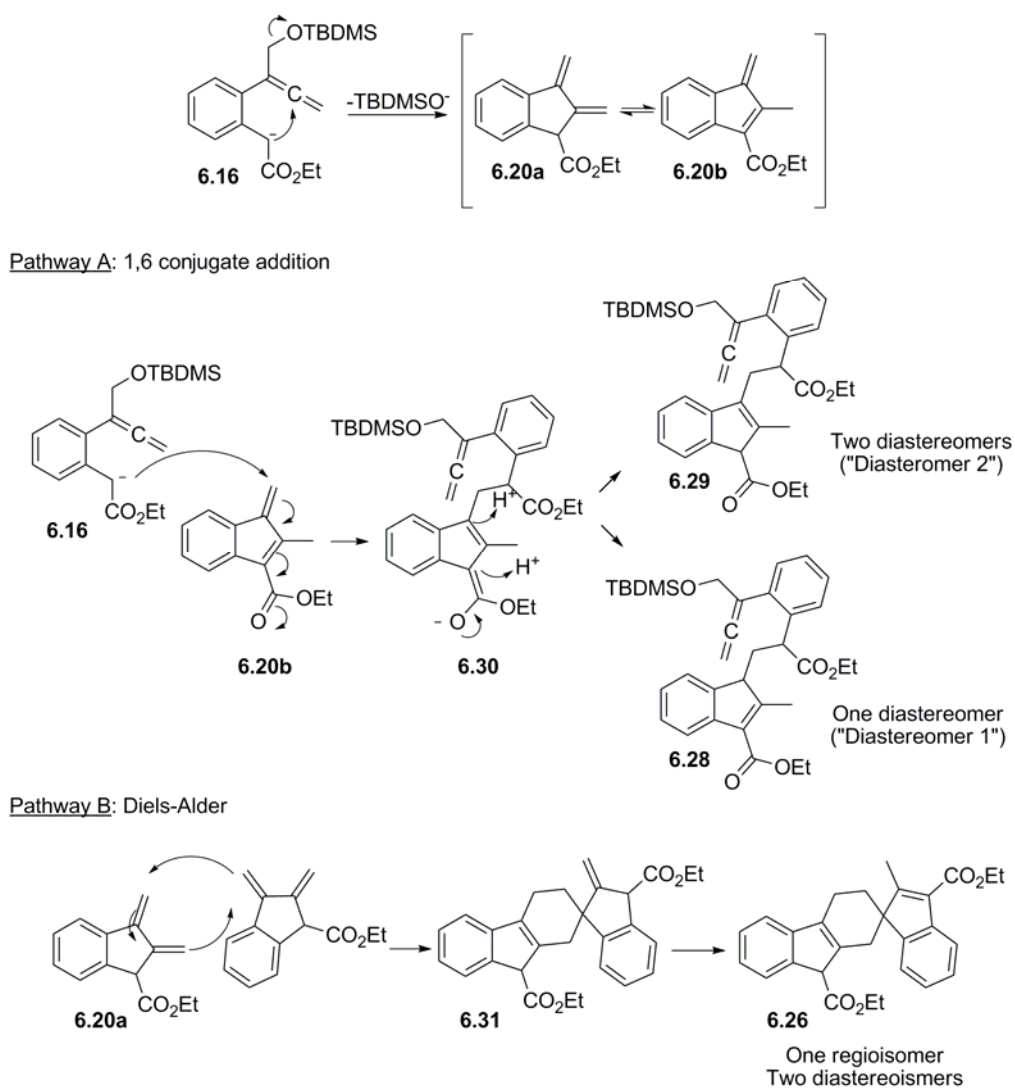
c. MMC = Methyl magnesium carbonate.

d. Inferred from *m/z* of 398, 400, 414, 428 obtained from GCMS analysis obtained from four different trials.

A pathway that might furnish these products is shown in Scheme 6.7. Deprotonation of **6.16** generates **6.20a** which is in equilibrium with **6.20b**, the incipient electrophile for **6.16** producing **6.30** in the process. Aqueous workup provides the products **6.28** and **6.29**. A

single diastereomer was observed for **6.28**, whereas two diastereomers of **6.29** were observed as an inseparable mixture. The Diels-Alder reaction of **6.20a** provides two diastereomers and/or regioisomers of the homodimer **6.26** as an inseparable mixture. Isolation and characterization of these three products provided confirmation that the diene **6.20** had been generated, but apparently not the malonate **6.27**. Clearly, a new direction towards synthesis of the malonate was in order.

**Scheme 6.7:** Possible mechanistic pathways furnishing **6.28**, **6.29** and **6.26**<sup>a</sup>.

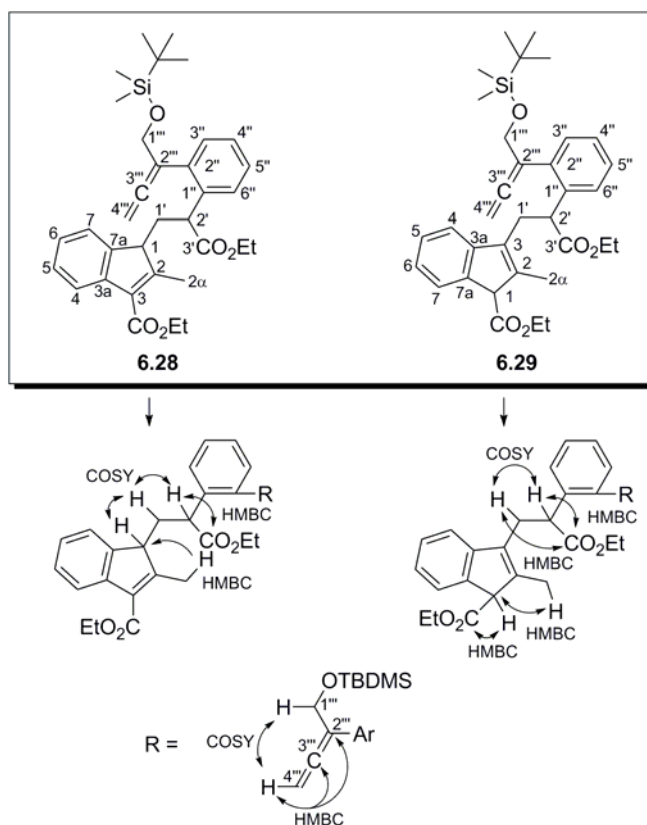


a. All of the spectroscopic data is consistent with the assignment of the structure as the mixture of diastereomers **6.26** except for the presence of four signals in the  $\delta$  164.6-165.4 range in the Carbon 13 NMR spectrum. If the structure **6.26** is correct, two of the Carbon 13 signals in that range must arise from unidentified impurities.

The structures of **6.28**, **6.29** and **6.26** were elucidated through standard spectroscopic means using 1D NMR ( $^1\text{H}$ ,  $^{13}\text{C}$ , JMOD) and 2D NMR (COSY, HMQC, HMBC) as well as LRMS obtained from GCMS analyses. The correlations permitted the assignment of the proposed structures of **6.28** and **6.29** and are shown in Figure 6.1. In particular, signals observed for **6.28** in which the COSY spectrum shows correlations for H-1' ( $\delta$  2.82-2.77/1.53-1.47) to H-1 ( $\delta$  3.43, dd) and to H-2' ( $\delta$  4.35). The HMBC spectrum shows correlations for H-2' to the ester carbonyl ( $\delta$  165.1) and correlations for H-2 $\alpha$  ( $\delta$  2.40) to C-1 ( $\delta$  52.6). This in contrast to **6.29** in which correlations are not observed in the COSY spectrum of H-1 ( $\delta$  4.12, 4.02) to H-1' and appears as singlets in the  $^1\text{H}$  NMR spectrum (overlapped by signals from the ester methylene moieties). As well, the HMBC spectrum show correlations of H-1 ( $\delta$  4.12, 4.02) to the ester carbonyl ( $\delta$  170.78, 170.75), a correlation of H-1' ( $\delta$  3.32-3.26, 2.93, 2.87) and H-2' ( $\delta$  4.40) to the ester carbonyl ( $\delta$  173.7, 173.6) and a correlation of H-2 $\alpha$  ( $\delta$  1.97, 1.74) to C-1 ( $\delta$  58.4, 58.3).



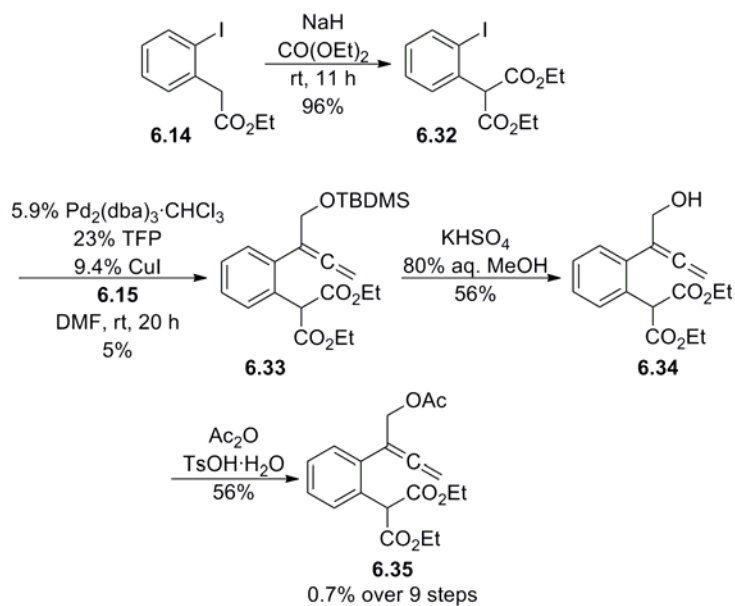
**Figure 6.1:** Selected 2D NMR correlations of **6.28** and **6.29**.

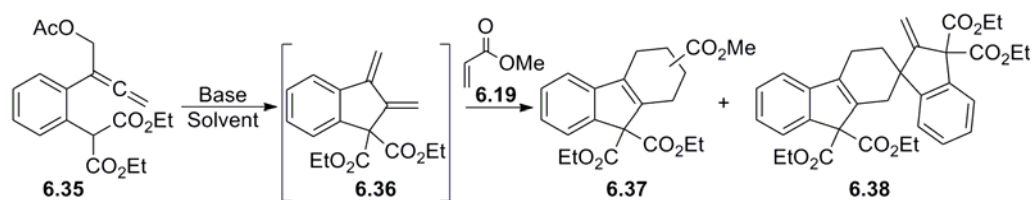


Generating the malonate **6.32** first followed by the Stille cross-coupling provided the desired target but this route was plagued by low yields and tedious purification (0.7% over nine steps, Scheme 6.8). In particular, purification of **6.33**, the product obtained from the cross-coupling reaction, consistently produced unreacted starting materials and unknown by-products that remained even after repeated chromatography. A small amount of **6.33** was eventually acquired for purposes of characterization. On one occasion, it was found that desilylation of an incompletely purified portion of **6.33** to afford its corresponding alcohol

was a sufficient means to adequately remove the unwanted impurities. However, this method was found to be irreproducible often leading to an inseparable mixture.

**Scheme 6.8:** Synthesis of malonate **6.35**.



**Table 6.3:** Diels-Alder cycloadditions of **6.35** with **6.19**.

Entry	Base (eq.) Solvent	Dienophile (eq.)	Temp./ Time	<b>6.35</b> (%)	<b>6.37</b> (%)	<b>6.38</b> (%)
1 <sup>a</sup>	K <sub>2</sub> CO <sub>3</sub> (1.1) DMF	<b>6.19</b> (1.2)	rt/9.5 h	nil <sup>b</sup>	nil	~50
2 <sup>a</sup>	DBU (1.1) CH <sub>2</sub> Cl <sub>2</sub>	<b>6.19</b> (1.1)	rt/9 h	nil <sup>b</sup>	nil <sup>c</sup>	~50
3	DBU (1.1) CH <sub>2</sub> Cl <sub>2</sub>	<b>6.19</b> (21)	rt/12 h	nil <sup>b</sup>	not isolated <sup>d</sup>	not isolated <sup>d</sup>
4	DBU (1.0) <sup>e</sup> CH <sub>2</sub> Cl <sub>2</sub>	<b>6.19</b> (21)	rt/15 h	nil <sup>b</sup>	not isolated <sup>f</sup>	not isolated <sup>f</sup>
5	DBU (2) <sup>e</sup> CH <sub>2</sub> Cl <sub>2</sub>	<b>6.40</b> (20)	rt/14.5 h		77 % of <b>6.41</b>	

a. **6.36** not isolated but is suggested by  $\delta$  5.28, 5.06 in proton NMR and  $m/z$  286 (M<sup>+</sup>) in GCMS of crude residue.

b. Trace amount observed by GCMS analysis only.

c. Trace of **6.37** not isolated but is suggested by  $m/z$  372 (M<sup>+</sup>) in GCMS of crude residue.

d. 1.5:1 ratio of **6.37**:**6.38** as observed by proton NMR.

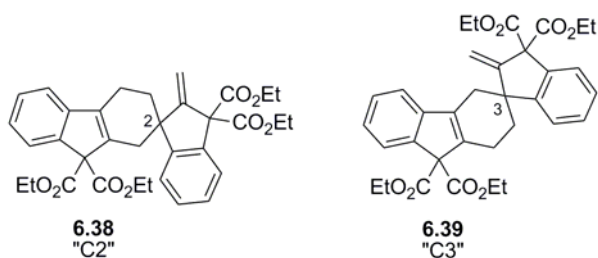
e. DBU in dichloromethane added via syringe over 2 h period.

f. 1.3:1 ratio of **6.37**:**6.38** as observed by proton NMR.

With a small amount of **6.35** in hand, exploratory efforts into Diels-Alder reactions could now be pursued using the approach described by Mukai.<sup>376</sup> This approach failed to generate **6.37** and instead produced the homodimer **6.38** (Entry 1, Table 6.3). All other attempts employed DBU in CH<sub>2</sub>Cl<sub>2</sub> (Entry 2-4, Table 6.3). Using one equivalent of DBU and one equivalent of **6.19** produced **6.38** in 45% but failed to generate the cycloadduct **6.37** (Entry

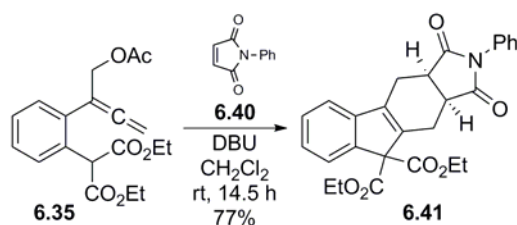
2). It was felt that the generation of **6.38** may be due in part to the work-up, particularly during rotary evaporation of the solvent at elevated temperatures. The experiment was repeated, increasing the number equivalents of methyl acrylate **6.19** to ~20 and the solvent was removed via a gentle stream of nitrogen. For the first time, a chemical shift observed at  $\delta$  3.69 appeared in the  $^1\text{H}$  NMR spectrum of the crude residue and was assigned to Me of the ester moiety of **6.37**. This provided initial evidence of a cycloadduct in an estimated 1.5:1 ratio of **6.37**:**6.38** from the  $^1\text{H}$  NMR spectrum (Entry 3). Adding DBU via syringe over a two hour period failed to increase the amount of **6.37** and provided essentially the same results (Entry 4). Furthermore, attempts at separating **6.37** from **6.38** proved futile. One possible route leading to the generation of the homodimer **6.38** is that DBU might be attacking methyl acrylate in a 1,4-conjugate addition which may go on to polymerize in situ. This would deplete the pool of dienophile available to react with diene **6.36**, leaving the diene to react with itself, consequently generating the dimer in the process. Although the structure assigned to the homodimer is shown to be **6.38**, further spectroscopic studies (i.e. H2BC) could not unequivocally assign its structure and it is possible that its regioisomer **6.39** may be an alternative. Future studies will attempt to confirm the structural assignment of the homodimer to **6.38** (C2 regioisomer) or **6.39** (C3 regioisomer).

**Figure 6.2**



Thus attention turned towards employing a suitable alternative dienophile for the purposes of obtaining a cycloadduct that could easily be resolved from **6.38** and in good amounts. *N*-phenylmaleimide **6.40** satisfied this criterion and provided the desired cycloadduct **6.41** in 77% yield which was easily separated from **6.38** (Scheme 6.9).

**Scheme 6.9:** Cycloaddition reaction of **6.35** with **6.40** to furnish **6.41**.



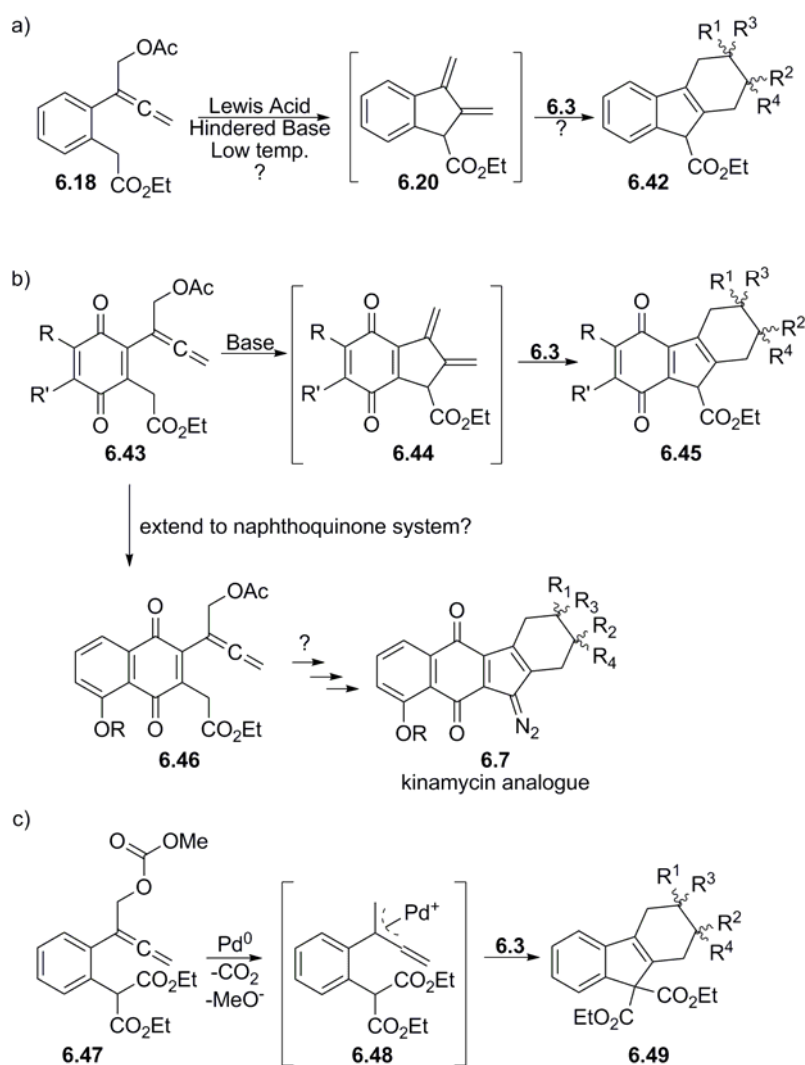
The procurement of **6.41** provided confirmation of the generation of **6.36** and thus the potential use of **6.35** in cycloaddition reactions. However, it appears that the utility of **6.35** might be limited by the need for the use of highly reactive dienophiles such as **6.40** at ambient conditions. Alternative strategies that would make use of **6.18** and/or **6.35** are discussed below.

### 6.2.3 Future synthetic efforts

The use of Lewis acids and an appropriate non-nucleophilic base at low temperatures that could make the use of the allenyl phenyl acetate **6.18** is one such avenue has not yet been explored which may avoid the need to use the malonate **6.35** (Scheme 6.10a). Another alternative is using the quinone **6.43**, which would permit facile deprotonation with a weak base and subsequent cyclization in situ. This then might be extended to the naphthoquinone

system **6.46** that could potentially furnish kinamycin analogues **6.7** (Scheme 6.10b). The malonate **6.35** might be amenable to other types chemistry that do not require acids or bases. This chemistry might be better pursued at elevated temperatures using palladium-catalyzed cycloadditions with carbonate **6.47** or a similar alternative (Scheme 6.10c).

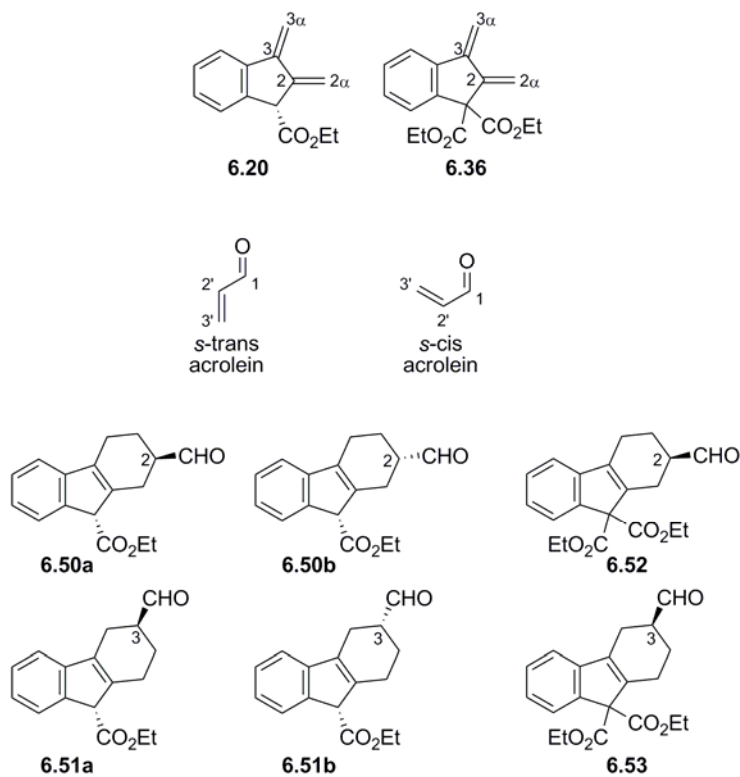
**Scheme 6.10:** Diels-Alder cycloadditions using alternative strategies.



### 6.3 Quantum chemical calculations

Theoretical calculations described here were pursued in an identical manner to those presented in Chapter 5. Table 6.4 shows the energies of **6.20** and **6.36** and their corresponding cycloadducts obtained with acrolein.

**Table 6.4:** The energies (a.u.) and relative energies ( $\text{kcal}\cdot\text{mol}^{-1}$ ) of carboxylate **6.20**, malonate **6.36** and acrolein and their corresponding Diels-Alder adducts calculated at the DFT B3LYP 6-31 G(d) level.



Entry	Structure	Energy $E,^a H,^b G^c$ (a.u.) <sup>d</sup>	Relative Energy (kcal·mol <sup>-1</sup> )	Structure	Energy $E,^a H,^b G^c$ (a.u.) <sup>d</sup>	Relative Energy (kcal·mol <sup>-1</sup> )
1	<b>6.20</b>	-692.105593 <sup>a</sup>	na	<b>6.36</b>	-959.220785 <sup>a</sup>	na
		-692.090055 <sup>b</sup>	na		-959.199234 <sup>b</sup>	na
		-692.148932 <sup>c</sup>	na		-959.272039 <sup>c</sup>	na
2	acrolein	-191.850315	0	acrolein	-191.847638	1.68
	( <i>s</i> -trans)	-191.845018	0	( <i>s</i> -cis)	-191.842339	1.68
		-191.876592	0		-191.874058	1.59
3	<b>6.50a</b>	-884.013465 (eq) <sup>e</sup>	0.71	<b>6.50b</b>	-884.013567 (eq) <sup>e</sup>	0.65
		-883.994386 (eq)	0.87		-883.994469 (eq)	0.82
		-884.061747 (eq)	0.09		-884.061896 (eq)	0
		-884.014077 (ax) <sup>f</sup>	0.33		-884.014292 (ax) <sup>f</sup>	0.19
		-883.995208 (ax)	0.36		-883.995418 (ax)	0.22
		-884.061607 (ax)	0.18		-884.061873 (ax)	0.01
4	<b>6.51a</b>	-884.013510 (eq)	0.68	<b>6.51b</b>	-884.013360 (eq)	0.78
		-883.994447 (eq)	0.83		-883.994293 (eq)	0.93
		-884.061621 (eq)	0.17		-884.061523 (eq)	0.23
		-884.013948 (ax)	0.41		-884.014600 (ax)	0
		-883.995113 (ax)	0.42		-883.995776 (ax)	0
		-884.061304 (ax)	0.37		-884.061676 (ax)	0.14
5	<b>6.52</b>	-1151.127598 (eq)	0.29	<b>6.53</b>	-1151.127510 (eq)	0.34
		-1151.102405 (eq)	0.44		-1151.102376 (eq)	0.46
		-1151.184095 (eq)	0		-1151.183638 (eq)	0.29
		-1151.128057 (ax)	0			
		-1151.103110 (ax)	0			
		-1151.183660 (ax)	0.27			

a., b., c. Energies are taken from minimized structures and are a) the electronic and zero point energies (i.e.  $E = E_{\text{elec}} + \text{ZPE} = E0$ ), b) the electronic, zero point and thermal enthalpies (i.e.  $H = E0 + H_{\text{corr}}$ ), c) the electronic, zero point and thermal free energies (i.e.  $G = E0 + G_{\text{corr}}$ ).

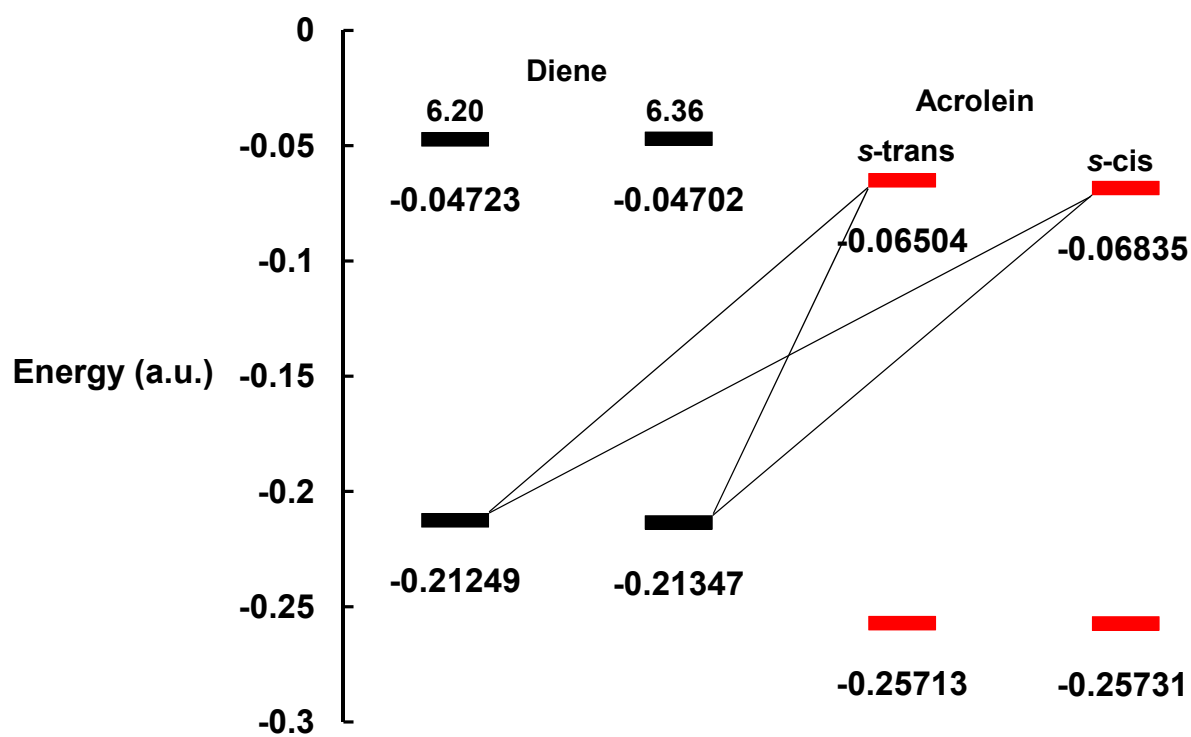


d. One atomic unit (a.u.) = 627.5095 kcal/mol.

e, f. The abbreviations eq. and ax. refer to the cyclohexene ring conformation in which the CHO group is in an equatorial and axial orientation, respectively.

Figure 6.3 illustrates the FMO energies of **6.20** and **6.35** and acrolein. If these reactions are FMO controlled, the HOMO<sub>diene</sub>-LUMO<sub>dienophile</sub> would indicate the reactivity of Diels-Alder cycloadditions of **6.20** and **6.36** are governed by these interactions due to the smaller energy gap.

**Figure 6.3:** Frontier molecular orbital energies (a.u.) for the  $[4\pi_s + 2\pi_s]$  cycloaddition of **6.20** and **6.36** with acrolein obtained the DFT B3LYP 6-31 G(d) level. The four black solid lines indicate the four possible lowest energy HOMO-LUMO interactions of the HOMO of **6.20** and **6.36** (diene, black) with the LUMO of acrolein (red).

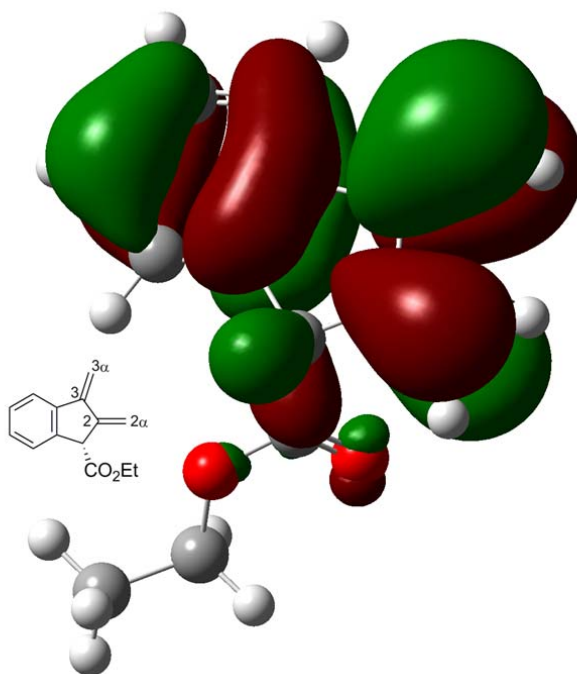


1 atomis unit (a.u.) = 627.5095 kcal/mol.

Table 6.5 and 6.6 show the FMO energies and corresponding coefficients of **6.20** and **6.36**, respectively. Unlike the *N*-Ac IQDM in which the terminal coefficients were essentially identical (see Chapter 5), the two dienes **6.20** and **6.36** have termini that are significantly different and thus would suggest that FMO interactions would be a determining factor in the regioselectivity of Diels-Alder cycloadditions. In the case of acrolein, inspection of the MO coefficients indicates that the C-2 cycloadducts would be the major regioisomer. Furthermore, the coefficients are markedly different at C-2 and C-3, especially in the case of the malonate **6.36**, such that secondary orbital interactions may also play a role in such cycloadditions.

Transition state calculations were undertaken in a manner identical to that described in Chapter 5 the results of which are shown in Tables 6.7 and 6.8 for **6.20** and **6.36**, respectively. These calculations were pursued in an effort to provide insight into structure, energy and regioselectivity.

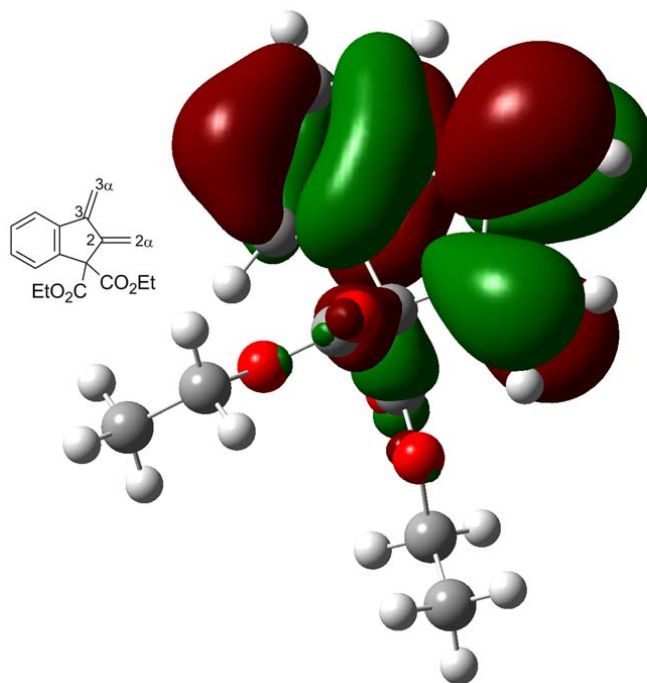
**Table 6.5:** FMO energy (a.u.) and orbital coefficients of the HOMO of **6.20** calculated at the DFT B3LYP 6-31 G(d) level.



**6.20**

	Energy (a.u.)	Orbital	Coefficient	Orbital	Coefficient
<b>HOMO</b>	-0.21249	C2 $\alpha$ 2p <sub>x</sub>	-0.06584	C3 2p <sub>z</sub>	0.20168
		C2 $\alpha$ 2p <sub>z</sub>	-0.22102	C3 3p <sub>x</sub>	0.04606
		C2 $\alpha$ 3p <sub>x</sub>	-0.04566	C3 3p <sub>z</sub>	0.12553
		C2 $\alpha$ 3p <sub>z</sub>	-0.17404	C3 $\alpha$ 2p <sub>x</sub>	0.10422
		C2 2p <sub>x</sub>	-0.04281	C3 $\alpha$ 2p <sub>y</sub>	-0.01656
		C2 2p <sub>z</sub>	-0.14155	C3 $\alpha$ 2p <sub>z</sub>	0.32964
		C2 3p <sub>x</sub>	-0.03079	C3 $\alpha$ 3p <sub>x</sub>	0.08489
		C2 3p <sub>z</sub>	-0.09299	C3 $\alpha$ 3p <sub>y</sub>	-0.01188
		C3 2p <sub>x</sub>	0.06114	C3 $\alpha$ 3p <sub>z</sub>	0.26957

**Table 6.6:** FMO energy (a.u.) and orbital coefficients of the HOMO of **6.36** calculated at the DFT B3LYP 6-31 G(d) level.



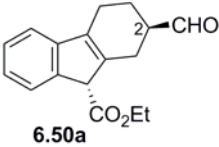
**6.36**

	Energy (a.u.)	Orbital	Coefficient	Orbital	Coefficient
<b>HOMO</b>	-0.21347	C2 $\alpha$ 2p <sub>y</sub>	-0.10319	C3 2p <sub>z</sub>	0.18760
		C2 $\alpha$ 2p <sub>z</sub>	-0.19429	C3 3p <sub>y</sub>	0.06443
		C2 $\alpha$ 3p <sub>y</sub>	-0.08129	C3 3p <sub>z</sub>	0.11579
		C2 $\alpha$ 3p <sub>z</sub>	-0.14913	C3 $\alpha$ 2p <sub>y</sub>	0.16426
		C2 2p <sub>z</sub>	-0.12688	C3 $\alpha$ 2p <sub>z</sub>	0.30344
		C2 3p <sub>z</sub>	-0.07546	C3 $\alpha$ 3p <sub>y</sub>	0.13491
		C3 2p <sub>y</sub>	0.09933	C3 $\alpha$ 3p <sub>z</sub>	0.24723

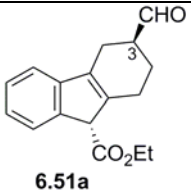
Consideration of transition state structures (TSs) and their corresponding energy barriers reveal important information on these systems. In many instances the data presented in Tables 6.7 and 6.8 reveal similar trends as for the *N*-Ac-IQDM (Table 5.6, Chapter 5):

1. Inspection of all TSs reveals an asynchronous cycloaddition.
2. In all cases, the *s*-cis TSs are more asynchronous than the corresponding *s*-trans TSs as evidenced by a larger  $\Delta d$ .
3. In all cases, a lower energy barrier is achieved with *s*-cis acrolein.
4. All *s*-trans TSs are endo selective for both the carboxylate **6.20** and the malonate **6.36** (e.g. TS83 vs. TS83).
5. Generally speaking, the conformation of acrolein (*s*-trans vs. *s*-cis) has greater impact on the energy barrier than its approach (endo vs. exo). For example, compare TS83 vs. TS84 to TS83 vs. TS85 (exception: TS103 vs. TS104 compared to TS103 vs. TS105). All *s*-cis TSs are more stable (lower in energy) than the corresponding *s*-trans (e.g. TS104 vs. TS106). All *s*-trans endo TSs are more stable (lower in energy) than the corresponding exo TSs.
6. For the carboxylate series, the TSs which possess the lowest  $\Delta^\ddagger G$  are TS85 and TS90 for the C-2 and C-3 adduct, respectively to give  $\Delta\Delta^\ddagger G = 2.43 \text{ kcal}\cdot\text{mol}^{-1}$  predicting 60:1 (C-2:C-3) and agrees with the qualitative interpretation that FMO arguments provide. Consideration of  $\Delta^\ddagger E$  and  $\Delta^\ddagger H$  predict C-2:C-3 of 51:1 and 46:1, respectively.
7. For the malonate series, the TSs which possess the lowest  $\Delta^\ddagger G$  are TS102 and TS106 for the C-2 and C-3 adduct, respectively to give  $\Delta\Delta^\ddagger G = 3.76 \text{ kcal}\cdot\text{mol}^{-1}$  predicting 576:1 (C-2:C-3) and agrees with the qualitative interpretation that FMO arguments provide. Consideration of  $\Delta^\ddagger E$  and  $\Delta^\ddagger H$  predict C-2:C-3 of 184:1 and 145:1, respectively.

**Table 6.7:** Selected structural data and energies of TS structures of Diels-Alder reactions of **6.20** and acrolein obtained at the DFT B3LYP 6-31 G(d) level.

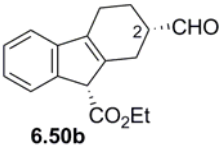
TS for DA Adduct	TSs	Bond distance (Å)	Dienophile	$\Delta^\ddagger E$ , <sup>c</sup> $\Delta^\ddagger H$ , <sup>d</sup> $\Delta^\ddagger G$ <sup>e</sup>
	IF <sup>a</sup>	C3 $\alpha$ -C3'	Approach	$E_{elec.} + ZPE$ <sup>f</sup>
		C2 $\alpha$ -C2'		$E_0 + H_{corr}$ <sup>g</sup>
				$E_0 + G_{corr}$ <sup>h</sup>
 <p><b>6.50a</b></p>	TS83	2.02647	<i>s</i> -trans, endo	<b>15.648<sup>c</sup></b>
	-436.3	2.70197	top	<b>15.024<sup>d</sup></b>
				<b>28.417<sup>e</sup></b>
				-883.930972 <sup>f</sup>
				-883.911131 <sup>g</sup>
				-883.980239 <sup>h</sup>
	TS84	2.03209	<i>s</i> -trans, exo	<b>15.389</b>
	-439.6	2.67471	bottom	<b>14.559</b>
				<b>29.419</b>
				-883.931384
				-883.911872
				-883.978641
TS85	2.04329	<i>s</i> -cis, endo	<b>11.064</b>	
-398.5	2.83630	top	<b>10.371</b>	
			<b>24.383</b>	
			-883.935599	
			-883.915866	
			-883.984134	
TS86	2.01785	<i>s</i> -cis, exo	<b>11.282</b>	
-415.7	2.78830	bottom	<b>10.579</b>	
			<b>24.679</b>	
			-883.935252	
			-883.915535	
			-883.983662	

**Table 6.7** (continued)

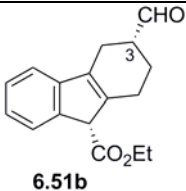
		C3 $\alpha$ -C2'		
		C2 $\alpha$ -C3'		
 <p><b>6.51a</b></p>	TS87	2.51714	<i>s</i> -trans, endo	<b>17.148<sup>c</sup></b>
	-472.5	2.08579	top	<b>16.522<sup>d</sup></b>
				<b>29.711<sup>e</sup></b>
				-883.928581 <sup>f</sup>
				-883.908744 <sup>g</sup>
				-883.978177 <sup>h</sup>
	TS88	2.44458	<i>s</i> -trans, exo	<b>17.801</b>
	-481.8	2.12152	bottom	<b>17.105</b>
				<b>30.902</b>
				-883.927541
				-883.907815
				-883.976279
TS89	2.73621	<i>s</i> -cis, endo	<b>13.694</b>	
-425.9	2.01586	top	<b>12.938</b>	
			<b>27.282</b>	
			-883.931409	
			-883.911776	
			-883.979514	
TS90	2.60591	<i>s</i> -cis, exo	<b>13.389</b>	
-455.3	2.04603	bottom	<b>12.631</b>	
			<b>26.810</b>	
			-883.931893	
			-883.912266	
			-883.980265	



**Table 6.7** (continued)

TS for DA Adduct	TSs	Bond distance (Å)	Dienophile	$\Delta^\ddagger E$ , <sup>c</sup> $\Delta^\ddagger H$ , <sup>d</sup> $\Delta^\ddagger G$ <sup>e</sup>
	IF <sup>a</sup>	C3 $\alpha$ -C3' C2 $\alpha$ -C2'	Approach	$E_{elec.} + ZPE$ <sup>f</sup> $E_0 + H_{corr}$ <sup>g</sup> $E_0 + G_{corr}$ <sup>h</sup>
	TS91	na	<i>s</i> -trans, endo	na
	na		bottom	
	TS92	2.02182	<i>s</i> -trans, exo	<b>16.114</b> <sup>c</sup>
	-438.4	2.69710	top	<b>15.514</b> <sup>d</sup> <b>28.984</b> <sup>e</sup> -883.930228 <sup>f</sup> -883.910350 <sup>g</sup> -883.979335 <sup>h</sup>
	TS93	na	<i>s</i> -cis, endo	na
	na		bottom	
	TS94	2.00416	<i>s</i> -cis, exo	<b>12.361</b>
	-406.8	2.86682	top	<b>11.726</b> <b>25.426</b> -883.933533 -883.913707 -883.982471

**Table 6.7** (continued)

		C3 $\alpha$ -C2'		
		C2 $\alpha$ -C3'		
 <p><b>6.51b</b></p>	TS95	na	<i>s</i> -trans, endo	na
	na		bottom	
	TS96	2.48998	<i>s</i> -trans, exo	<b>17.661<sup>c</sup></b>
	-475.9	2.09738	top	<b>17.007<sup>d</sup></b>
				<b>30.487<sup>e</sup></b>
				-883.927764 <sup>f</sup>
				-883.907971 <sup>g</sup>
				-883.976940 <sup>h</sup>
	TS97	na	<i>s</i> -cis, endo	na
	na		bottom	
TS98	2.65031	<i>s</i> -cis, exo	<b>14.429</b>	
-440.9	2.03914	top	<b>13.742</b>	
			<b>27.688</b>	
			-883.930237	
			-883.910494	
			-883.978867	

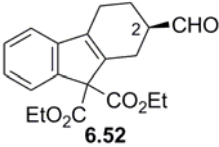
a. Each TS calculation was carried out using the Synchronous Transit-Guided Quasi-Newton Method (QST2 or QST3, Ref. 317,318) using Gaussian 03 rev. B.04 or C.02 implemented on a desktop computer running Linux OS (Redhat). TS calculations times were typically 8-12 hours in duration. All structures reported here as TSs exhibit only one imaginary frequency. The imaginary vibrations were animated with Gaussview 3.09 or 4.1 to determine if they were in qualitative agreement with the bond-making/bond-breaking processes associated with the reaction of interest. In each case, intrinsic reaction coordinate (IRC, Ref. 313,314) calculations were performed to determine that the observed TS could be linked reasonably to the assumed reactant and product geometries.

b. IF = imaginary frequency in reciprocal centimeters and are not scaled.

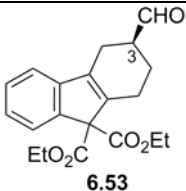
c.  $\Delta^\ddagger E$  (=  $\Delta^\ddagger E0$ ), d.  $\Delta^\ddagger H$ , e.  $\Delta^\ddagger G$  in kcal/mol.

f. *Eelec.* + ZPE (= *E0*), g. *H* = *E0* + *Hcorr*, h. *G* = *E0* + *Gcorr* in a.u. (1 a.u. = 627.5095 kcal/mol)

**Table 6.8:** Selected structural data and energies of TS structures of Diels-Alder reactions of **6.36** and acrolein obtained at the DFT B3LYP 6-31 G(d) level.

TS for DA Adduct	TSs	Bond distance (Å)	Dienophile	$\Delta^\ddagger E,^c \Delta^\ddagger H,^d \Delta^\ddagger G^e$
	IF <sup>a</sup>	C3 $\alpha$ -C3'	Approach	$E_{elec.} + ZPE^f$
		C2 $\alpha$ -C2'		$E_0 + H_{corr}^g$
				$E_0 + G_{corr}^h$
	TS99	2.02084	<i>s</i> -trans, endo	<b>14.123</b>
	-434.0	2.70487	top	<b>13.331</b>
				<b>27.729</b>
				-1151.048594
				-1151.023007
				-1151.104441
	TS100	2.03417	<i>s</i> -trans, exo	<b>15.090</b>
	-438.4	2.66176	bottom	<b>14.310</b>
				<b>28.854</b>
				-1151.047052
				-1151.021447
				-1151.102650
	TS101	2.03622	<i>s</i> -cis, endo	<b>12.673</b>
	-405.9	2.85606	top	<b>11.947</b>
				<b>26.478</b>
			-1151.048227	
			-1151.022535	
			-1151.103901	
TS102	2.00131	<i>s</i> -cis, exo	<b>12.251</b>	
-408.2	2.84920	bottom	<b>11.691</b>	
			<b>24.833</b>	
			-1151.048899	
			-1151.022942	
			-1151.106523	

**Table 6.8** (continued)

		C3 $\alpha$ -C2'		
		C2 $\alpha$ -C3'		
 <p><b>6.53</b></p>	TS103	2.46020	<i>s</i> -trans, endo	<b>16.405<sup>c</sup></b>
	-482.7	2.11316	top	<b>15.723<sup>d</sup></b>
				<b>29.744<sup>e</sup></b>
				-1151.044957 <sup>f</sup>
				-1151.019198 <sup>g</sup>
				-1151.101231 <sup>h</sup>
	TS104	2.47344	<i>s</i> -trans, exo	<b>18.373</b>
	-482.1	2.11336	bottom	<b>17.713</b>
				<b>31.487</b>
				-1151.041821
				-1151.016024
				-1151.098454
TS105	2.59412	<i>s</i> -cis, endo	<b>15.257</b>	
-453.3	2.05318	top	<b>14.488</b>	
			<b>28.819</b>	
			-1151.044110	
			-1151.018485	
			-1151.100171	
TS106	2.63180	<i>s</i> -cis, exo	<b>15.338</b>	
-449.2	2.04210	bottom	<b>14.635</b>	
			<b>28.594</b>	
			-1151.043980	
			-1151.018251	
			-1151.100529	

a. Each TS calculation was carried out using the Synchronous Transit-Guided Quasi-Newton Method (QST2 or QST3, Ref. 317,318) using Gaussian 03 rev. B.04 or C.02 implemented on a desktop computer running Linux OS (Redhat). TS calculations times were typically 8-12 hours in duration. All structures reported here as TSs exhibit only one imaginary frequency. The imaginary vibrations were animated with Gaussview 3.09 or 4.1 to determine if they were in qualitative agreement with the bond-making/bond-breaking processes associated with the reaction of interest. In each case, intrinsic reaction coordinate (IRC, Ref. 313,314) calculations were performed to determine that the observed TS could be linked reasonably to the assumed reactant and product geometries.

b. IF = imaginary frequency in reciprocal centimeters and are not scaled.

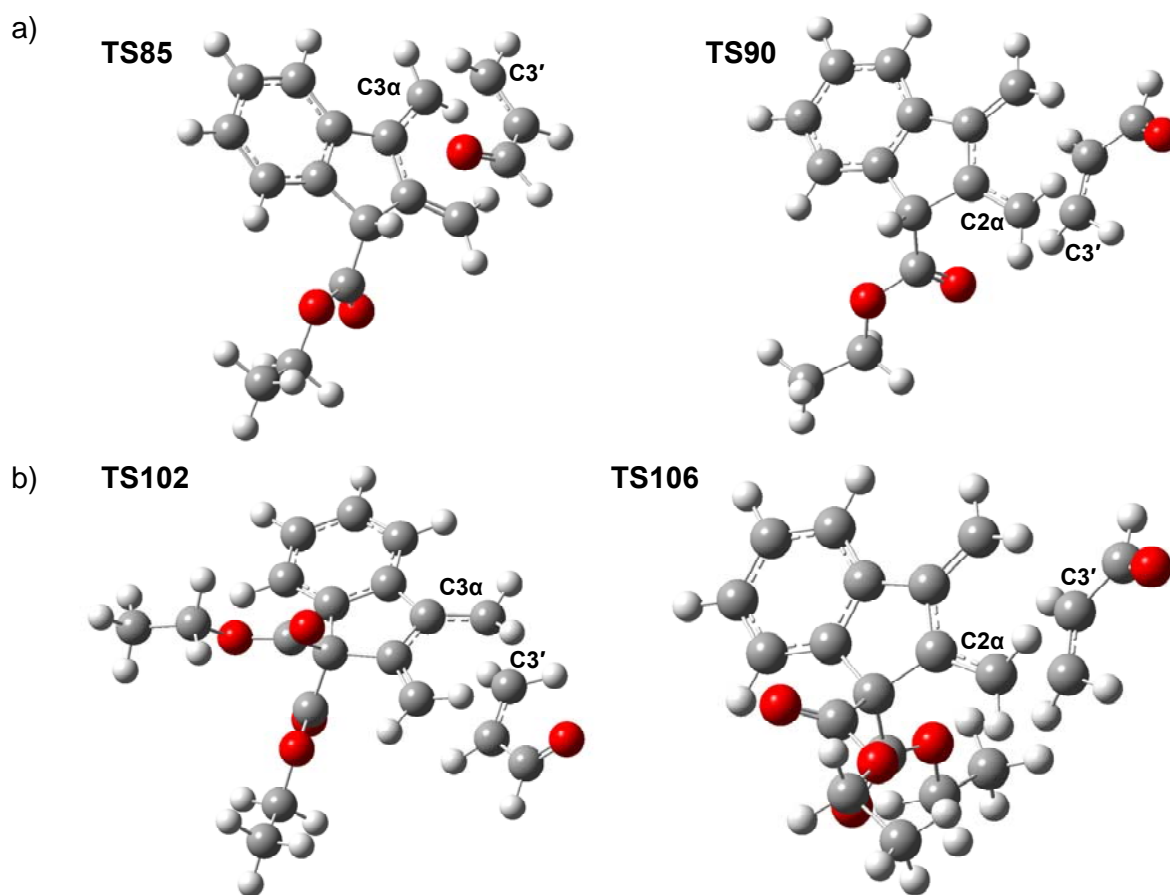
c.  $\Delta^\ddagger E$  ( $= \Delta^\ddagger E0$ ), d.  $\Delta^\ddagger H$ , e.  $\Delta^\ddagger G$  in kcal/mol.

f.  $E_{elec.} + ZPE$  ( $= E0$ ), g.  $H = E0 + H_{corr}$ , h.  $G = E0 + G_{corr}$  in a.u. (1 a.u. = 627.5095 kcal/mol).

Figure 6.4 shows the relevant TS structures obtained from the carboxylate data set (TS85 and TS90) and the malonate data set (TS102 and TS106). Advanced bond development occurs between C-3' of the dienophile and C-3 $\alpha$  (TS85; TS102) or C-2 $\alpha$  (TS90; TS106) of the corresponding diene, consistent with asynchronicity. Asynchronicity was further supported upon examination of the vibrational mode corresponding to the imaginary frequencies (TS85 = -399 cm<sup>-1</sup>; TS90 = -455 cm<sup>-1</sup>; TS102 = -408 cm<sup>-1</sup>; TS106 = -449 cm<sup>-1</sup>). This revealed that the principle motion is between C-3 $\alpha$  and C-3' (TS85; TS102) or C-2 $\alpha$  and C-3' (TS90; TS106).

Pyramidalization is evident at the relevant reacting loci: TS85 shows C-3 $\alpha$  = 350.9°, C-3' = 350.0° and is advanced over that of C2 $\alpha$  = 359.4°, C-2' = 359.9°; TS90 shows C-2 $\alpha$  = 352.2°, C-3' = 351.2° and is advanced over that of C3 $\alpha$  = 358.2°, C-2' = 359.1°; TS102 shows C-3 $\alpha$  = 350.9°, C-3' = 349.1° and is advanced over that of C2 $\alpha$  = 359.3°, C-2' = 359.9°; TS106 shows C-2 $\alpha$  = 351.1°, C-3' = 350.6° and is advanced over that of C3 $\alpha$  = 358.3°, C-2' = 359.3°.

**Figure 6.4:** The transition state structures of a) TS85 and TS90; b) TS102 and TS106.



## 6.4 Conclusion

This work described in this chapter has provided the foundation for future experimental studies of Diels-Alder reactions of 2,3-dimethylene carboxylates and malonates with suitable dienophiles as a potential synthetic strategy towards the kinamycin group of natural products. Additionally, quantum chemical calculations indicate that these reactions are expected to be highly regioselective. Future synthetic efforts will assess the accuracy of the computational predictions of regioselectivity.

## Chapter 7 Experimental

### 7.1 General Procedures

**Materials and Methods.** All reactions were carried out under an atmosphere of nitrogen and/or argon in flame-dried and/or oven-dried glassware with magnetic stirring unless otherwise stated. Where required, the purification of solvents and reagents was accomplished according to standard procedures.<sup>484</sup> All solvents were reagent grade unless otherwise stated. Dichloromethane and triethylamine were distilled from calcium hydride. DMSO was distilled from calcium hydride under high vacuum. Tetrahydrofuran and diethyl ether were distilled from sodium benzophenone ketyl. Anhydrous ethanol was prepared by reacting absolute ethanol with magnesium and iodine as described.<sup>484</sup> Dimethylformamide was pre-dried with calcium hydride and distilled under high vacuum from 3Å molecular sieves and stored over 3Å molecular sieves. Alternatively, selected solvents were procured from the M. Braun Solvent Purification System, Department of Chemistry, University of Waterloo. The maintenance of reactions at very low temperatures for extended periods of time was accomplished with the Flexi Cool Immersion Cooler (KINETICS Thermal systems) with the cooling coil immersed in an acetone or a methanol bath pre-cooled with dry ice.

All commercial reagents used were purchased from the Aldrich Chemical Co. or VWR Canada (EMD, BDH, Alfa Aesar and J.T. Baker) and were used as received unless otherwise stated. Reactions were monitored by analytical thin layer chromatography (TLC) with silica coated aluminum sheets (EMD TLC Silica gel 60 F<sub>254</sub>). Visualization was accomplished using UV light (254 nm) or basic KMnO<sub>4</sub> stain. Unless otherwise stated, purification of crude reaction products was carried out using flash silica gel chromatography (Silicycle SiliaFlash<sup>®</sup>

P60 40-63  $\mu\text{m}$ , 230-400 mesh) according to established procedures.<sup>485</sup> All reported yields refer to chromatographically and spectroscopically pure compounds unless otherwise stated.

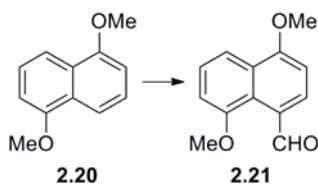
**Characterization Methods.** In some instances, compounds previously reported in the literature in which the characterization data was insufficient are reported here with a more complete characterization data set. Melting points were obtained on a MEL-TEMP<sup>®</sup> apparatus (Laboratory Devices Inc., Holliston MA, USA) and are uncorrected. <sup>1</sup>H NMR spectra were acquired on a Brüker AC300 (300 MHz), Brüker AVANCE300 (300 MHz) or Brüker AVANCE500 (500 MHz) spectrometer and are reported in parts per million (ppm) in either CD<sub>2</sub>Cl<sub>2</sub> or CDCl<sub>3</sub> using the solvent residual peak as the internal standard. For CDCl<sub>3</sub> this was 7.24 and 77.0 ppm for <sup>1</sup>H NMR and <sup>13</sup>C NMR, respectively. Data are reported as chemical shift in ppm, integrated intensity; peak multiplicities; coupling constants *J* (Hz) and assignment. The following abbreviations are used for reporting peak multiplicities: br = broad, w = weak, s = singlet, d = doublet, t = triplet, q = quartet, dd = doublet of doublets, dt = doublet of triplets, m = multiplet. <sup>13</sup>C NMR spectra were broadband decoupled and acquired on Brüker AC300 (75.5 MHz), Brüker AVANCE300 (75.5 MHz) or Brüker AVANCE500 (125.8 MHz) spectrometers and are reported in ppm in CD<sub>2</sub>Cl<sub>2</sub> or CDCl<sub>3</sub>, using the carbon signal of the deuterated solvent as the internal standard. <sup>15</sup>N NMR spectra were recorded on a Brüker AVANCE300 (30.4 MHz) and reported in ppm using external <sup>15</sup>N-formamide in DMSO-*d*<sub>6</sub> as the reference standard at 112.8056 ppm relative to NH<sub>3</sub> at 0 ppm. Samples were dissolved in CDCl<sub>3</sub> and transferred to a 5 mm NMR tube to which a 3 mm coaxial NMR tube was inserted containing DMSO-*d*<sub>6</sub> as the lock solvent. Infrared spectra (IR) were recorded on a Perkin Elmer Spectrum RX I FT-IR System



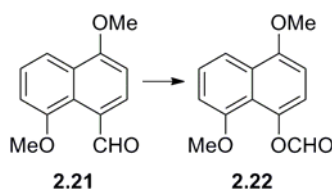






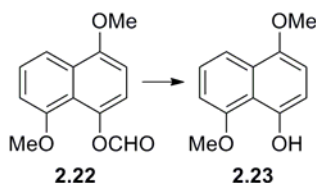


**4,8-Dimethoxy-1-naphthaldehyde (2.21).** Following a known procedure,<sup>200</sup> 1,5-dimethoxynaphthalene **2.20** (18.77 g, 0.0997 mol), toluene (20 mL) and DMF (12 mL, 0.155 mol) were mixed together and cooled to 0 °C. To this was added POCl<sub>3</sub> (12 mL, 0.129 mol) and stirring was continued for another hour. The mixture was then heated at 110 °C for two hours, cooled to room temperature and poured into 300 mL of 10% NaOH containing 100 mL ice. The mixture was then extracted with benzene three times. The extracts were pooled, washed twice with 1 M HCl, twice with water, once with brine, dried over Na<sub>2</sub>SO<sub>4</sub>, filtered and concentrated in vacuo to furnish 19.73 g (92%) of the title compound as a light orange solid that was of satisfactory purity for the next step. A small amount (0.1462 g) was purified by column chromatography (silica, 1:1 hexanes:ether) and recrystallized from ethanol to furnish fine white needles: mp 127-128 °C (lit. value<sup>200</sup> 125-126 °C); IR (KBr, cm<sup>-1</sup>)  $\nu_{\max}$  3073, 3025, 2971, 2908, 2838, 1663, 1587, 1517, 1465, 1412, 1330, 1270, 1225, 1064, 868, 828, 801, 765; <sup>1</sup>H NMR (300 MHz, CDCl<sub>3</sub>)  $\delta$  11.03 (1H, s, CHO), 8.05 (1H, d, *J* = 8.3 Hz, ArH), 7.93 (1H, dd, *J* = 0.7, 8.3 Hz, ArH), 7.42 (1H, dd, *J* = 7.9, 8.3 Hz, ArH), 7.01 (1H, d, *J* = 7.9 Hz, ArH), 6.87 (1H, d, *J* = 8.3 Hz, ArH), 4.03 (3H, s, OCH<sub>3</sub>), 3.99 (3H, s, OCH<sub>3</sub>); <sup>13</sup>C NMR (75.5 Hz, CDCl<sub>3</sub>)  $\delta$  194.6, 159.5, 156.4, 129.3, 127.7, 127.1, 125.8, 124.7, 115.3, 107.8, 103.9, 55.9, 55.6; MS *m/z* (rel. intensity) (EI) 216 (M<sup>+</sup>, 100), 215 (30), 201 (19), 185 (17), 173 (10), 143 (3), 115 (17), 102 (5); HRMS (EI) calc. for C<sub>13</sub>H<sub>12</sub>O<sub>3</sub>: 216.0786, found: 216.0783.



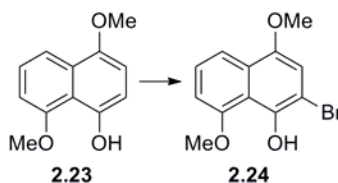
**4,8-Dimethoxynaphthalen-1-yl formate (2.22).** Following a published procedure,<sup>200</sup> to a solution of naphthaldehyde **2.21** (19.61 g, 0.0906 mol) in CH<sub>2</sub>Cl<sub>2</sub> (900 mL) was added *m*CPBA (39.3051 g at 75.7% assay, 0.172 mol). The solution was stirred vigorously at room temperature for 2 h 40 min. This solution was then poured into 10% Na<sub>2</sub>S<sub>2</sub>O<sub>3</sub> (700 mL) and stirred for 25 min. The aqueous layer was removed and water (900 mL) was added. The mixture was stirred for 5 min and the aqueous layer removed. This sequence was repeated once more. The solution was then transferred to a separatory funnel and washed with a 10% solution of Na<sub>2</sub>S<sub>2</sub>O<sub>3</sub> twice with water washings between and three washings with saturated NaHCO<sub>3</sub> solution with water washings between, brine once, dried over Na<sub>2</sub>SO<sub>4</sub>, filtered and the solvent evaporated in vacuo producing 19.44 g (92%) of the crude formate as a brown solid. The crude material was employed in the next step without further purification. A small portion (0.5874 g) was purified by column chromatography (silica, 2:1 hexanes:ether) to afford 0.2248 g of the title compound as fine colourless needles: mp 136 °C (lit. value<sup>489</sup> 137-138.5 °C); IR (NaCl, film, cm<sup>-1</sup>)  $\nu_{\max}$  2938, 1737, 1599, 1516, 1449, 1411, 1378, 1267, 1148, 1125, 1061, 846, 789, 746; <sup>1</sup>H NMR (300 MHz, CDCl<sub>3</sub>)  $\delta$  8.32 (1H, s, CHO), 7.88 (1H, dd, *J* = 0.7, 8.3 Hz, ArH), 7.39 (1H, dd, *J* = 8.0, 8.3 Hz, ArH), 7.03 (1H, d, *J* = 8.3 Hz, ArH), 6.89 (1H, d, *J* = 8.0 Hz, ArH), 6.75 (1H, d, *J* = 8.3 Hz, ArH), 3.97 (3H, s, ArOCH<sub>3</sub>), 3.89 (3H, s, ArOCH<sub>3</sub>); <sup>13</sup>C NMR (75.5 MHz, CDCl<sub>3</sub>)  $\delta$  160.9, 154.9, 153.7, 138.9, 128.3, 126.2, 119.2, 118.8, 115.0, 107.1, 103.7, 55.82, 55.78; MS *m/z* (rel. intensity) (EI) 232 (M<sup>+</sup>,

32), 204 (54), 189 (100), 174 (18), 161 (5), 146 (3), 118 (3), 102 (6); HRMS (EI) calc. for  $C_{13}H_{12}O_4$ : 232.0736, found: 232.0739.



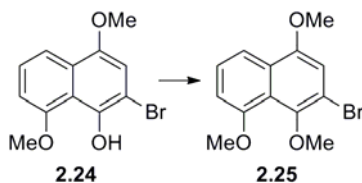
**4,8-Dimethoxynaphthalen-1-ol (2.23).** Following a known procedure,<sup>200</sup> the crude formate **2.22** (24.39 g, 0.105 mol) was dissolved in a 1:1 mixture of degassed MeOH/THF (750 mL) and stirred on ice at 0 °C. Potassium hydroxide (17.1858 g, 0.3063 mol) was dissolved in methanol (150 ml), extensively degassed, cooled to 0 °C and added to the formate solution that was then stirred for 1 h. The reaction was quenched with 5% aq. HCl (130 mL) to obtain a pH ~2, poured into water (3 L) and extracted three times with dichloromethane. The organic extracts were pooled, washed twice with water and dried over sodium sulfate, filtered through a sintered funnel and the solvent evaporated in vacuo to yield 20.60 g of a dark brown solid. The crude naphthenol was purified by flash column chromatography (silica,  $CHCl_3$ ) furnishing 13.6464 g (64%) of the title compound as a pale yellow solid: mp 153-154 °C (lit. value<sup>200</sup> 155-156 °C); IR (NaCl, film,  $cm^{-1}$ )  $\nu_{max}$  3419, 2942, 1631, 1514, 1446, 1412, 1288, 1071, 815, 752;  $^1H$  NMR (300 MHz,  $CDCl_3$ )  $\delta$  8.92 (1H, s, ArOH), 7.84 (1H, dd,  $J = 0.8, 8.3$  Hz, ArH), 7.32 (1H, dd,  $J = 7.9, 8.3$  Hz, ArH), 6.82 (1H, d,  $J = 7.9$  Hz, ArH), 6.77, 6.75 (2H, AB<sub>q</sub>,  $J = 8.5$  Hz, H2, H3), 4.03 (3H, s, ArOCH<sub>3</sub>), 3.92 (3H, s, ArOCH<sub>3</sub>);  $^{13}C$  NMR (75.5 MHz,  $CDCl_3$ )  $\delta$  155.9, 148.1, 147.9, 127.8, 125.1, 115.9, 115.5, 109.0, 106.3, 104.9, 56.1, 55.9; MS  $m/z$  (rel. intensity) (EI) 204 ( $M^+$ , 82), 189

(100), 174 (19), 161 (5), 146 (3), 131 (2), 118 (4), 102 (5); HRMS (EI) calc. for C<sub>12</sub>H<sub>12</sub>O<sub>3</sub>: 204.0786, found: 204.0780.



**2-Bromo-4,8-dimethoxynaphthalen-1-ol (2.24).** Following a published procedure,<sup>200</sup> a naphthenol solution **2.23** (12.1569 g, 0.0595 mol) in CCl<sub>4</sub> (600 mL) was stirred vigorously at room temperature. A separate flask was charged with bromine (9.7463 g, 0.0609 mol) dissolved in CCl<sub>4</sub> (100 mL) which was immediately transferred to a dropping funnel. The flask was rinsed with two separate washings of CCl<sub>4</sub> (25 mL each) and these rinses were added to the dropping funnel to ensure quantitative transfer of bromine. The bromine solution was then added drop-wise to the stirred solution of naphthenol over the course of 2 h, after which stirring continued for another hour at which time a 20% solution of Na<sub>2</sub>S<sub>2</sub>O<sub>3</sub> (800 mL) was added and stirred for 10 min. This solution was transferred to a separatory funnel and the aqueous and organic layers separated. The aqueous layer was extracted three times with CH<sub>2</sub>Cl<sub>2</sub> and the extracts were pooled, washed twice with a 10% solution of Na<sub>2</sub>S<sub>2</sub>O<sub>3</sub>, once with water, once with brine and dried over Na<sub>2</sub>SO<sub>4</sub>, filtered and concentrated under reduced pressure. The same workup procedure was also applied to the CCl<sub>4</sub> layer. The crude products were pooled together to give 16.7275 g (99%) of the title compound as a brown solid which was judged by <sup>1</sup>H NMR to be sufficiently pure for the following step. A small portion (0.1814 g) was purified by column chromatography (silica, 2:1 hexanes:ether) to afford

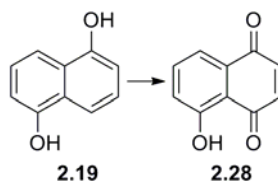
0.1519 g of a white solid as fine needles: mp 138-139 °C (lit. value<sup>200</sup> 141-142 °C); IR (NaCl, film, cm<sup>-1</sup>)  $\nu_{\max}$  3358, 1609, 1509, 1398, 1294, 1238, 1068, 872, 820, 798, 771, 750; <sup>1</sup>H NMR (300 MHz, CDCl<sub>3</sub>)  $\delta$  9.59 (1H, s, ArOH), 7.79 (1H, d, *J* = 8.3 Hz, ArH), 7.33 (1H, dd, *J* = 8.0, 8.3 Hz, ArH), 6.92 (1H, s, ArH), 6.86 (1H, d, *J* = 8.0 Hz, ArH), 4.03 (3H, s, ArOCH<sub>3</sub>), 3.90 (3H, s, ArOCH<sub>3</sub>); <sup>13</sup>C NMR (75.5 Hz, CDCl<sub>3</sub>)  $\delta$  155.1, 148.1, 144.4, 127.2, 125.6, 116.2, 115.6, 110.1, 106.1, 102.8, 56.4, 56.0; MS *m/z* (rel. intensity) (EI) 284 (M<sup>+</sup> for C<sub>12</sub>H<sub>11</sub><sup>81</sup>BrO<sub>3</sub>, 99), 282 (M<sup>+</sup> for C<sub>12</sub>H<sub>11</sub><sup>79</sup>BrO<sub>3</sub>, 100), 269 (83), 267 (85), 254 (5), 252 (6), 241 (4), 239 (5), 226 (2), 224 (2), 187 (7), 173 (9), 159 (3), 145 (10), 129 (4), 101 (3), 89 (3); HRMS (EI) calc. for C<sub>12</sub>H<sub>11</sub><sup>79</sup>BrO<sub>3</sub>: 281.9892, found: 281.9888.



**2-Bromo-1,4,8-trimethoxynaphthalene (2.25).** To a stirred solution of bromonaphthenol **2.24** (0.9064 g, 3.2 mmol) in acetone (100 mL) was added K<sub>2</sub>CO<sub>3</sub> (3.1869 g, 23.1 mmol) and dimethyl sulfate (1.8 mL, 19 mmol). The mixture was heated at reflux (60 °C oil bath) for 21 h. The solution was cooled to ambient temperature, filtered through Celite 545 and the solvent evaporated on a rotary evaporator. The residue was dissolved in ether (50 mL) and triethylamine (5 mL) and the solution was stirred for 25 min. The solution was then washed with 10% HCl twice, water once, brine once and dried over MgSO<sub>4</sub>, filtered and concentrated in vacuo to yield 1.1554 g of dark orange brown solid that was purified by column chromatography (silica, 12:1 hexanes:ethyl acetate) affording 0.8775 g (92%) of the title

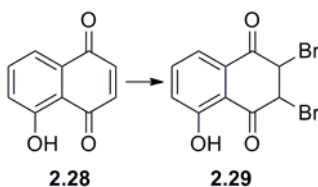


compound as a white solid: mp 81-82 °C (lit. value<sup>490</sup> 85-87 °C); IR (NaCl, film, cm<sup>-1</sup>)  $\nu_{\max}$  2934, 1576, 1508, 1450, 1413, 1337, 1326, 1267, 1071, 1006, 970, 874; <sup>1</sup>H NMR (300 MHz, CDCl<sub>3</sub>)  $\delta$  7.80 (1H, d,  $J$  = 8.3 Hz, ArH), 7.37 (1H, dd,  $J$  = 8.0, 8.3 Hz, ArH), 6.94 (1H, d,  $J$  = 8.0 Hz, ArH) overlapping with 6.93 (1H, s, ArH), 3.97 (3H, s, ArOCH<sub>3</sub>), 3.93 (3H, s, ArOCH<sub>3</sub>), 3.83 (3H, s, ArOCH<sub>3</sub>); <sup>13</sup>C NMR (75.5 MHz, CDCl<sub>3</sub>)  $\delta$  155.4, 151.7, 146.7, 128.1, 126.0, 121.2, 114.9, 114.1, 108.9, 107.9, 61.6, 56.4, 55.9; MS  $m/z$  (rel. intensity) (EI) 298 (M<sup>+</sup> for C<sub>13</sub>H<sub>13</sub><sup>81</sup>BrO<sub>3</sub>, 98), 296 (M<sup>+</sup> for C<sub>13</sub>H<sub>13</sub><sup>79</sup>BrO<sub>3</sub>, 100), 283 (23), 281 (24), 253 (4), 251 (3), 225 (3), 223 (4), 202 (57), 187 (32), 159 (11), 149 (4), 129 (8), 116 (6), 113 (4), 101 (4); HRMS (EI) for C<sub>13</sub>H<sub>13</sub><sup>79</sup>BrO<sub>3</sub>: 296.0048, found: 296.0058.

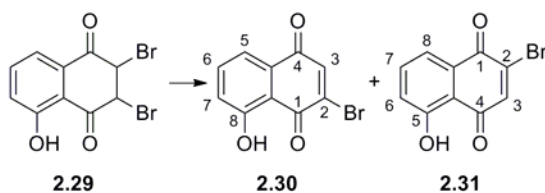


**5-Hydroxynaphthalene-1,4-dione (Juglone) (2.28).** Following a known procedure,<sup>213</sup> to a stirred solution of **2.19** (30.0553 g, 0.1876 mol) in acetonitrile (500 mL) was added CuCl (12.2495 g, 0.1237 mol). The mixture was stirred vigorously while a strong current of air was bubbled through for 15 h. The solution was then filtered through a Buchner funnel and the filter cake washed with acetonitrile. The crude product was concentrated under reduced pressure and was purified via Soxhlet extraction with *n*-heptane over 4.5 days after which the solution was filtered through a sintered funnel and evaporated in vacuo producing the title compound as an orange solid (12.06 g, 37%): mp 150-151 °C (lit. value<sup>213</sup> 154-161 °C); IR (NaCl, film, cm<sup>-1</sup>)  $\nu_{\max}$  1663, 1645, 1592, 1450, 1363, 1289, 1224, 1153, 1079, 857, 833,

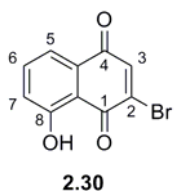
746, 697, 628;  $^1\text{H}$  NMR (300 MHz,  $\text{CDCl}_3$ )  $\delta$  11.89 (1H, s, ArOH), 7.65-7.58 (2H, m, ArH), 7.27 (1H, dd,  $J = 2.4, 7.2$  Hz, ArH), 6.93 (2H, s, H2, H3);  $^{13}\text{C}$  NMR (75.5 MHz,  $\text{CDCl}_3$ )  $\delta$  190.3, 184.2, 161.4, 139.5, 138.6, 136.5, 131.7, 124.5, 119.1, 114.9; MS  $m/z$  (rel. intensity) (EI) 174 ( $\text{M}^+$ , 100) 173 (22), 158 (3), 146 (8), 118 (18), 92 (9), 63 (6).



**2,3-Dibromo-5-hydroxy-2,3-dihydronaphthalene-1,4-dione (2.29).** Following a published procedure,<sup>214</sup> to a stirred solution of juglone **2.28** (0.4011 g, 2.30 mmol) in  $\text{CHCl}_3$  (5 mL) and 6 drops of acetic acid stirring at 0 °C was added slowly a solution of bromine (0.4045 g, 2.53 mmol) in  $\text{CHCl}_3$  (5 mL). The mixture was stirred for 2 h and then brought to room temperature. The solution was concentrated under reduced pressure to give the title compound as a black solid (0.7546 g, 98%):  $^1\text{H}$  NMR (300 MHz,  $\text{CDCl}_3$ )  $\delta$  11.40 (1H, s, ArOH), 7.72 (1H, dd,  $J = 7.4, 8.3$  Hz, ArH), 7.63 (1H, d,  $J = 7.4$  Hz, ArH), 7.34 (1H, d,  $J = 8.3$  Hz, ArH), 4.93, 4.90 (2H, AB<sub>q</sub>,  $J = 3.1$  Hz, H2, H3);  $^{13}\text{C}$  NMR (75.5 MHz,  $\text{CDCl}_3$ )  $\delta$  192.7, 185.7, 162.6, 140.0, 130.2, 125.4, 120.3, 112.9, 45.5, 45.4; MS  $m/z$  (rel. intensity) (EI) 336 ( $\text{M}^+$  for  $\text{C}_{12}\text{H}_6^{81,81}\text{Br}_2\text{O}_3$ , 24), 334 ( $\text{M}^+$  for  $\text{C}_{12}\text{H}_6^{79,81}\text{Br}_2\text{O}_3$ , 54), 332 ( $\text{M}^+$  for  $\text{C}_{12}\text{H}_6^{79,79}\text{Br}_2\text{O}_3$ , 36), 255 (93), 253 (100), 174 (42), 173 (20), 146 (15), 145 (11), 120 (11), 118 (16), 92 (13), 89 (9), 63 (12).

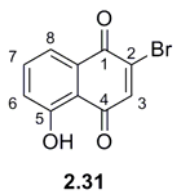


**2-Bromo-8-hydroxynaphthalene-1,4-dione (3-bromojuglone) (2.30); 2-bromo-5-hydroxynaphthalene-1,4-dione (2-bromojuglone) (2.31).** Following a modification of known procedures,<sup>203,207,215</sup> 2,3-Dibromo-5-hydroxy-2,3-dihydro-1,4-naphthalenedione **2.29** (0.5201 g, 1.56 mmol) was dissolved in ethanol (5 mL) and the solution was refluxed for 11 min. The solution was cooled to room temperature and concentrated under reduced pressure to give 0.4175 g of crude product containing the desired target 3-bromojuglone **2.30** in excess of the 2-bromojuglone **2.31** in ~3:1 ratio as well as trace of the vinyl ether **2.32**. The mixture was subjected to silica gel chromatography (20:1 then 10:1 hexanes:ethyl acetate) to give 0.1803 g (31%) of a mixture of the two regioisomers and a small amount of the vinyl ether. A portion of this mixture (0.117 g) was subjected to another round of silica gel chromatography (15:1 hexanes:ether) to afford a pure mixture of the two regioisomers as an orange residue (0.0504 g, 9%). Assignment of the two regioisomers, 3-bromojuglone (**2.30**) and 2-bromojuglone (**2.31**), was based on previous work in other laboratories<sup>214,215</sup> and in conjunction with <sup>1</sup>H, <sup>13</sup>C, JMOD and 2D (COSY, HMQC and HMBC)

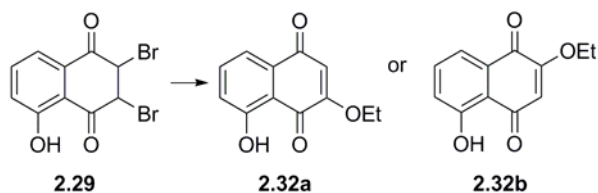


NMR analyses:

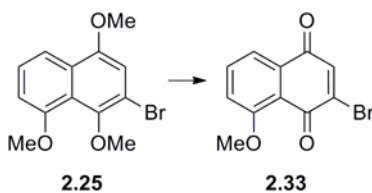
**2-Bromo-8-hydroxynaphthalene-1,4-dione (2.30).** <sup>1</sup>H NMR (300 MHz, CDCl<sub>3</sub>) δ 11.67 (1H, s, ArOH), 7.68-7.56 (2H, m, ArH), 7.44 (1H, s, H3), 7.25 (1H, d, *J* = 9.0 Hz, ArH); <sup>13</sup>C NMR (75.5 MHz, CDCl<sub>3</sub>) δ 182.8, 181.6, 162.0, 141.2, 139.3, 137.1, 131.5, 124.7, 119.9, 113.9.



**2-Bromo-5-hydroxynaphthalene-1,4-dione (2.31).**  $^1\text{H}$  NMR (300 MHz,  $\text{CDCl}_3$ )  $\delta$  11.73 (1H, s, ArOH), 7.70-7.58 (2H, m, ArH), 7.47 (1H, s, H3), 7.27 (1H, d,  $J = 8.3$  Hz, ArH);  $^{13}\text{C}$  NMR (75.5 MHz,  $\text{CDCl}_3$ )  $\delta$  187.4, 177.2, 161.7, 140.9, 140.2, 136.4, 130.6, 125.1, 120.9, 114.6.

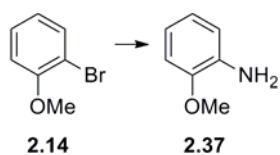


**2-Ethoxy-8-hydroxynaphthalene-1,4-dione (2.32).** The title compound (0.1814 g, 0.83 mmol, 7%) was obtained from 3.8432 g of **2.29** under conditions identical to those described above for the production of **2.30** and **2.31**:  $^1\text{H}$  NMR (300 MHz,  $\text{CDCl}_3$ )  $\delta$  11.75 (1H, s, ArOH), 7.62-7.56 (2H, m, ArH), 7.19 (1H, dd,  $J = 2.8, 6.8$  Hz, ArH), 6.09 (1H, s, H3), 4.07 (2H, q,  $J = 7.0$  Hz,  $\text{OCH}_2\text{CH}_3$ ), 1.51 (3H, t,  $J = 7.0$  Hz,  $\text{OCH}_2\text{CH}_3$ );  $^{13}\text{C}$  NMR (75.5 MHz,  $\text{CDCl}_3$ )  $\delta$  185.0, 184.1, 161.9, 159.3, 137.1, 131.9, 123.7, 118.8, 114.3, 110.7, 65.5, 13.9; MS  $m/z$  (rel. intensity) (EI) 218 ( $\text{M}^+$ , 100), 203 (5), 189 (9), 174 (65), 162 (15), 146 (10), 121 (16), 120 (14), 105 (12), 92 (6), 63 (5), 50 (3); HRMS (EI) calc. for  $\text{C}_{12}\text{H}_{10}\text{O}_4$ : 218.0579, found: 218.0572.

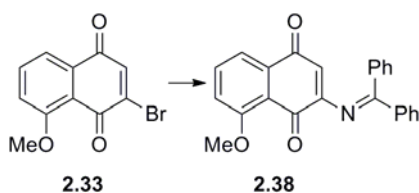


**2-Bromo-8-methoxynaphthalene-1,4-dione (2.33).** Following a known procedure,<sup>200</sup> to a stirred solution of 2-bromo-1,4,8-trimethoxynaphthalene **2.25** (2.4785 g, 8.3 mmol) in acetonitrile (250 mL) was added a solution (75 mL) of ceric ammonium nitrate (10.3866 g, 18.9 mmol) dissolved in water, via a dropping funnel over a 5 min period. The solution was allowed to stir for 10 min, diluted with water (500 mL) and extracted with CH<sub>2</sub>Cl<sub>2</sub>. The organic extracts were pooled, washed with water, a saturated solution of sodium bicarbonate, water, brine, dried over anhydrous sodium sulfate, filtered and the solvent evaporated under reduced pressure to afford the title compound as an orange solid (1.3669 g, 61%): mp 151-152 °C (lit. value<sup>200</sup> 154-155 °C); <sup>1</sup>H NMR (300 MHz, CDCl<sub>3</sub>) δ 7.70-7.67 (2H, m, ArH), 7.41 (1H, s, ArH), 7.32-7.26 (1H, m, ArH), 3.99 (3H, s, ArOCH<sub>3</sub>); <sup>13</sup>C NMR (75.5 MHz, CDCl<sub>3</sub>) δ 182.5, 176.1, 160.3, 142.6, 138.3, 135.5, 133.9, 119.4, 118.6, 118.1, 56.5; MS *m/z* (rel. intensity) (EI) 268 (M<sup>+</sup> for C<sub>11</sub>H<sub>7</sub><sup>81</sup>BrO<sub>3</sub>, 100), 266 (M<sup>+</sup> for C<sub>11</sub>H<sub>7</sub><sup>79</sup>BrO<sub>3</sub>, 99), 237 (6), 210 (3), 186 (32), 159 (36), 129 (34), 116 (18), 101 (16), 76 (17), 62 (11); HRMS (EI) for C<sub>11</sub>H<sub>7</sub><sup>79</sup>BrO<sub>3</sub>: 265.9579, found: 265.9578.



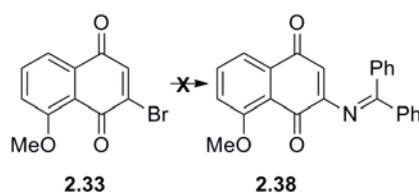


**2-Methoxyaniline (2.37).** The title compound was produced under similar conditions as described for **2.25**→**2.52**→**2.46**. The amounts used were 0.2121 g (1.13 mmol) of 2-bromoanisole, 0.2215 g (1.22 mmol) of benzophenone imine, 0.0023 g (0.44 mol%) of Pd<sub>2</sub>(dba)<sub>3</sub>, 0.0054 g (0.76 mol%) of (±)-BINAP, 0.1465 g (1.52 mmol) of NaOtBu in toluene (4 mL) to give 0.2310 g (73%) of a yellow oil after chromatography (silica, 10:1 hexanes:ethyl acetate). Subsequent hydrogenolysis using 0.3034 g of Pd/C (5%) and 0.6959 g (11.2 mmol) ammonium formate in 3.7 mL methanol furnished 0.0382 g (42%) of the title compound as a light brown oil after chromatography (silica, 10:1 than 3:1 hexanes:ethyl acetate): <sup>1</sup>H NMR (300 MHz, CDCl<sub>3</sub>) δ 6.81-6.69 (4H, m, ArH), 3.84 (3H, s, ArOCH<sub>3</sub>), 3.79 (2H, br s, ArNH<sub>2</sub>); <sup>13</sup>C NMR (75.5 MHz, CDCl<sub>3</sub>) δ 147.4, 135.7, 121.0, 118.7, 115.2, 110.4, 55.4; MS *m/z* (rel. intensity) (EI) 123 (M<sup>+</sup>, 100), 108 (45), 80 (14), 69 (6).



**2-((Diphenylmethylene)amino)-8-methoxynaphthalene-1,4-dione (2.38).** Following a known procedure,<sup>222</sup> a 25 mL two-neck flask was charged with Pd<sub>2</sub>(dba)<sub>3</sub> (0.0088 g, 9.61 μmol), (±)-BINAP (0.0372 g, 0.059 mmol) and toluene (2 mL). The mixture was degassed with two freeze-thaw cycles under high vacuum with argon purges. To the frozen mixture

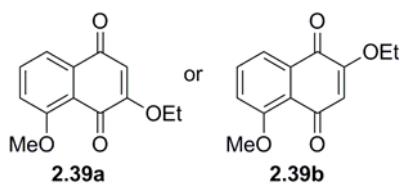
was added **2.33** (0.0518 g, 0.194 mmol), benzophenone imine (0.0435 mL, 0.260 mmol) and NaOtBu (0.0254 g, 0.264 mmol) under argon atmosphere and the mixture was subjected to another round of freeze-thawing under high vacuum and then heated to 85 °C for 6 h. The mixture was cooled to ambient temperature, filtered through a Celite 545 pad and the material was concentrated under reduced pressure to yield a dark brown residue that was purified using flash silica gel column chromatography (3:1 hexanes:ethyl acetate) furnishing the title compound as a yellow residue (0.0119 g, 17%): <sup>1</sup>H NMR (300 MHz, CDCl<sub>3</sub>) δ 7.69-7.57 (2H, m, ArH), 7.51-7.48 (4H, m, ArH), 7.43-7.32 (6H, m, ArH), 7.18 (1H, d, *J* = 8.1 Hz, ArH), 6.09 (1H, s, H3), 3.92 (3H, s, ArOCH<sub>3</sub>); <sup>13</sup>C NMR (75.5 MHz, CDCl<sub>3</sub>) δ 196.8, 183.2, 180.1, 160.0, 149.4, 137.6, 135.9, 135.7, 132.4, 130.1, 128.3, 119.0, 118.2, 116.2, 103.3, 56.4; MS *m/z* (rel. intensity) (EI) 366 (1), 308 (2), 280 (4), 234 (1), 203 (100), 186 (9), 176 (10), 158 (8), 147 (11), 135 (13), 130 (8), 105 (9), 76 (11).



**Synthetic efforts towards 2-((Diphenylmethylene)amino)-8-methoxynaphthalene-1,4-dione (2.38).** The following is a modification of a procedure described by Nakazumi and coworkers.<sup>223</sup> To a solution of the naphthoquinone **2.33** (0.0423 g, 0.158 mmol) in ethanol (5 mL) was added benzophenone imine (0.0265 mL, 0.159 mmol) and the solution was heated at 80 °C for 16 h. Potassium carbonate (0.0235 g, 0.170 mmol) suspended in ethanol (1 mL) was then added to the mixture and heating continued for another 5 h. The mixture was cooled



to room temperature and quenched with a saturated solution of  $\text{NH}_4\text{Cl}$  and extracted with  $\text{CH}_2\text{Cl}_2$ . The organic extracts were combined washed with water, brine, dried over  $\text{Na}_2\text{SO}_4$ , filtered and concentrated to dryness and the residue purified by flash silica gel chromatography (1:1 to 1:5 hexanes:ethyl acetate) to give the side product **2.39** as a light brown residue (0.0042 g, 11%): **2-Ethoxy-8-methoxynaphthalene-1,4-dione (2.39a)** or **2-**



**Ethoxy-5-methoxynaphthalene-1,4-dione (2.39b).**  $^1\text{H}$

NMR (300 MHz,  $\text{CDCl}_3$ )  $\delta$  7.78 (1H, d,  $J = 7.6$  Hz, ArH),

7.61 (1H, dd,  $J = 7.6, 8.3$  Hz, ArH), 7.28 (1H, d,  $J = 8.3$

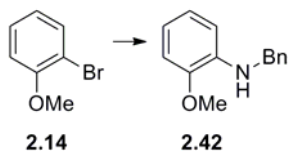
Hz, ArH), 6.04 (1H, s, H3), 4.03 (2H, q,  $J = 7.0$  Hz,  $\text{CH}_2\text{CH}_3$ ), 3.98 (3H, s,  $\text{ArOCH}_3$ ), 1.48

(3H, t,  $J = 7.0$  Hz,  $\text{CH}_2\text{CH}_3$ );  $^{13}\text{C}$  NMR (75.5 MHz,  $\text{CDCl}_3$ )  $\delta$  184.8, 180.5, 159.3, 157.7,

134.2, 133.5, 130.0, 119.6, 118.5, 112.4, 65.0, 56.6, 13.9; MS  $m/z$  (rel. intensity) (EI) 232

( $\text{M}^+$ , 90), 217 (62), 203 (52), 188 (53), 175 (74), 158 (40), 147 (41), 130 (32), 119 (45), 105

(100), 89 (35), 76 (52), 69 (25), 63 (19), 50 (9).

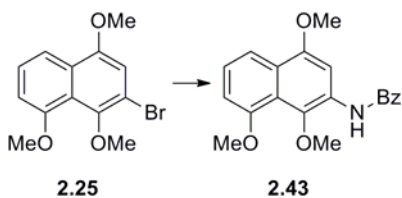


**N-Benzyl-2-methoxyaniline (2.42).** The following is a modification of a known procedure.<sup>491</sup> A 25 mL two-neck flask was charged with 2-bromoanisole (0.25 mL, 2.01 mmol), benzylamine (0.27 mL, 2.47 mmol),  $\text{KO}t\text{Bu}$  (0.3786 g, 3.37 mmol) and toluene (8 mL). The mixture was degassed with two freeze-thawing cycles under high vacuum with argon purges. To the frozen mixture was added (*S*)-BINAP (0.1077 g, 8.6 mol%) and  $\text{Pd}_2(\text{dba})_3 \cdot \text{CHCl}_3$  (0.069 g, 6.6 mol%) under argon atmosphere and the mixture was subjected

to another two rounds of freeze-thawing under high vacuum and then heated to 90 °C for 19.5 h. The mixture was cooled to room temperature, filtered through a bed of Celite 545 and the crude material concentrated in vacuo and purified by flash silica gel chromatography (15:1 hexanes:ethyl acetate) to give 0.3663 g (86%) of the title compound as a faint yellow oil: IR (NaCl, film,  $\text{cm}^{-1}$ )  $\nu_{\text{max}}$  3427, 3063, 3039, 3029, 2937, 2834, 1602, 1513, 1455, 1429, 1346, 1297, 1247, 1222, 1177, 1126, 1050, 1028, 737, 698;  $^1\text{H}$  NMR (300 MHz,  $\text{CDCl}_3$ )  $\delta$  7.40-7.26 (5H, m, ArH), 6.83-6.77 (2H, m, ArH), 6.68 (1H, dd,  $J = 7.6, 7.6$  Hz, ArH), 6.60 (1H, d,  $J = 7.8$  Hz, ArH), 4.66 (1H, br s, ArNH), 4.34 (2H, d,  $J = 5.7$  Hz, ArCH<sub>2</sub>NH), 3.84 (3H, s, ArOCH<sub>3</sub>);  $^{13}\text{C}$  NMR (300 MHz,  $\text{CDCl}_3$ )  $\delta$  146.7, 139.5, 138.1, 128.5, 127.5, 127.1, 121.2, 116.6, 110.0, 109.3, 55.3, 48.0; MS  $m/z$  (mass intensity) (EI) 213 ( $\text{M}^+$ , 100), 198 (24), 196 (4), 180 (3), 154 (1), 136 (7), 120 (7), 106 (4), 91 (49), 65 (7), 51 (2).

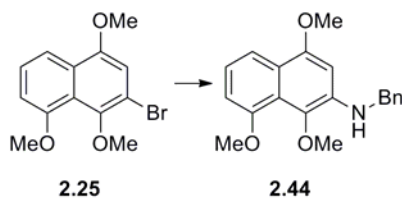
**Alternative procedure using CuI:** Following a known procedure,<sup>228</sup> a 25 mL two-neck flask was charged with  $\text{K}_3\text{PO}_4$  (0.8734 g, 3.98 mmol), *N,N*-diethylsalicylamide (0.0899 g, 0.45 mmol), CuI (0.0216 mg, 0.11 mmol), *o*-bromoanisole (0.250 mL, 1.95 mmol) and DMF (1 mL) and the mixture stirred for 3 min under nitrogen atmosphere. To this was added benzylamine (0.33 mL, 2.99 mmol) and DMF (1 mL) and the mixture was heated at 100 °C for 15 h at which time another 0.8 mL of DMF was added and heating was continued for 6 h. The mixture was cooled to ambient temperature and filtered through Celite 545. The filtrate was extracted with ethyl acetate, washed with water and dried over anhydrous  $\text{MgSO}_4$  and filtered through Celite 545. The crude product was concentrated in vacuo to give a brown oil which was purified by silica gel chromatography (15:1 then 5:1 hexanes:ethyl acetate) to

afford 0.1051 g of a light yellow oil as a 1:1 inseparable mixture of **2.14** and the title compound.

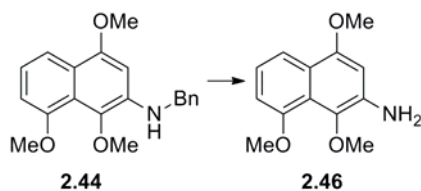


**N-(1,4,8-Trimethoxynaphthalen-2-yl)benzamide (2.43).** The title compound was produced under similar conditions as described for **2.14**→**2.17**. The amounts used were CuI (0.0132 g, 0.069 mmol), benzamide (0.103 g, 0.85 mmol), potassium carbonate (0.2024 g, 1.46 mmol), bromonaphthalene (0.2065 g, 0.695 mmol), ( $\pm$ )-*trans*-1,2-diaminocyclohexane (0.008 mL, 0.067 mmol), 4 Å molecular sieves (0.250 g) and 1,4-dioxane (1 mL) and refluxed at 110 °C for 23 h. The solution was then allowed to cool, diluted with ethyl acetate and filtered through a small plug of Celite 545 and the solvent evaporated in vacuo. The residue was purified by flash silica gel chromatography (12:1 hexanes:ethyl acetate) to afford 0.018 g (8%) of the title compound as a yellow solid: mp 139-140 °C; IR (NaCl, film,  $\text{cm}^{-1}$ )  $\nu_{\text{max}}$  3418, 2934, 2834, 1673, 1602, 1525, 1503, 1488, 1454, 1423, 1381, 1259, 1074;  $^1\text{H}$  NMR (300 MHz,  $\text{CDCl}_3$ )  $\delta$  8.96 (1H, br s, NH), 8.28 (1H, s, ArH), 7.91 (2H, m, ArH), 7.85 (1H, d,  $J = 8.4$  Hz, ArH), 7.58-7.49 (3H, m, ArH), 7.30 (1H, dd,  $J = 8.0, 8.2$  Hz, ArH), 6.90 (1H, d,  $J = 7.7$  Hz, ArH), 4.03 (3H, s,  $\text{ArOCH}_3$ ), 4.01 (3H, s,  $\text{ArOCH}_3$ ), 3.84 (3H, s,  $\text{ArOCH}_3$ );  $^{13}\text{C}$  NMR (75.5 MHz,  $\text{CDCl}_3$ )  $\delta$  165.3, 155.1, 151.9, 136.9, 135.1, 131.9, 129.1, 128.9, 127.0, 125.0, 124.4, 119.6, 115.0, 107.0, 99.0, 62.4, 56.1, 55.9; MS  $m/z$  (rel. intensity)

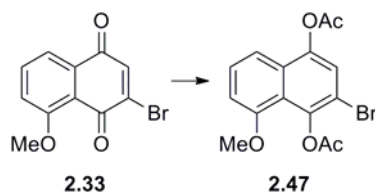
(EI) 337 ( $M^+$ , 100), 322 (100), 296 (6), 219 (4), 205 (5), 202 (5), 187 (4), 149 (5), 145 (3), 105 (74), 77 (16), 57 (4).



***N*-Benzyl-1,4,8-trimethoxynaphthalen-2-amine (2.44).** The title compound was produced under similar conditions as described for **2.24**→**2.42**. The amounts used were 0.1801 g (0.61 mmol) of the bromonaphthalene **2.25**, 0.080 mL (0.73 mmol) of benzylamine, 0.023 g (7.3 mol%) of  $\text{Pd}_2(\text{dba})_2 \cdot \text{CHCl}_3$ , 0.0361 g (9.6 mol%) of (*S*)-BINAP, 0.1006 g (0.89 mmol)  $\text{KO}t\text{Bu}$  in toluene (8 mL) to give 0.1612 g (82%) of a yellow oil after chromatography (silica, 4:1 hexanes:ethyl acetate) as the title compound as well as containing small amounts of **2.45** as an inseparable mixture:  $^1\text{H}$  NMR (300 MHz,  $\text{CDCl}_3$ )  $\delta$  7.72 (1H, dd,  $J = 0.6, 8.4$  Hz, *ArH*), 7.40-7.23 (5H, m, *ArH*), 7.08 (1H, dd,  $J = 7.6, 8.4$  Hz, *ArH*), 6.81 (1H, d,  $J = 7.6$  Hz, *ArH*), 6.46 (1H, s, *ArH*), 5.11 (1H, br s, *NH*), 4.49 (2H, s,  $\text{CH}_2\text{NH}$ ), 3.97 (3H, s,  $\text{ArOCH}_3$ ), 3.83 (3H, s,  $\text{ArOCH}_3$ ), 3.78 (3H, s,  $\text{ArOCH}_3$ );  $^{13}\text{C}$  NMR (75.5 MHz,  $\text{CDCl}_3$ )  $\delta$  154.2, 152.5, 139.8, 138.6, 133.3, 128.6, 127.2, 127.1, 121.1, 120.9, 120.8, 114.9, 106.8, 94.8, 61.1, 56.1, 55.6, 48.3; MS  $m/z$  (mass intensity) (EI) 323 ( $M^+$ , 49), 308 (100), 278 (11), 231 (2), 218 (11), 203 (9), 190 (4), 175 (2), 115 (2), 91 (13), 65 (1); HRMS (EI) calc. for  $\text{C}_{20}\text{H}_{21}\text{NO}_3$ : 323.1521, found: 323.1521.

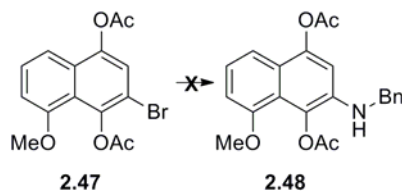


**1,4,8-Trimethoxynaphthalen-2-amine (2.46).** A solution of *N*-Benzyl naphthylamine **2.44** (0.0993 g, 0.31 mmol) dissolved in acetic acid (6 mL) was stirred briefly under nitrogen and Pd/C (10%, 0.092 g) was added. The mixture was then briefly purged with hydrogen and then allowed to stir for 4 h under an atmosphere of hydrogen using a balloon reservoir. The mixture was then filtered through Celite 545 and the solvent evaporated under reduced pressure. The crude material was purified by silica gel chromatography (3:1 hexanes:ethyl acetate) to afford 0.0185 g (26%) of a purple solid. Spectroscopic data matched that from other experiments producing **2.46** from **2.52**.



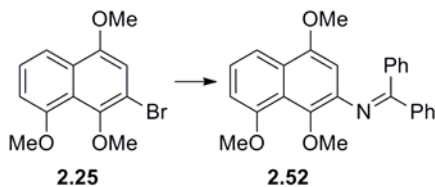
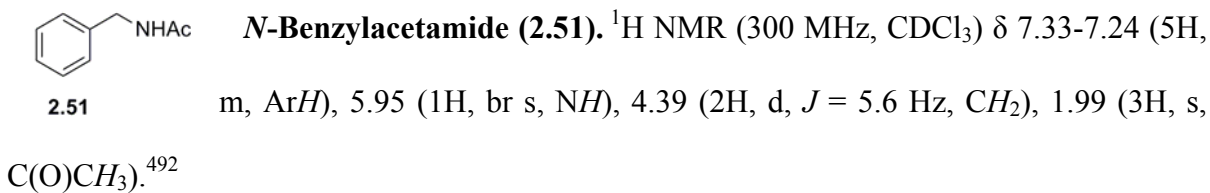
**2-Bromo-8-methoxynaphthalene-1,4-diy l diacetate (2.47).** A solution of the bromonaphthoquinone **2.33** (0.0993 g, 0.37 mmol), zinc powder (0.0535 g, 0.82 mmol), acetic anhydride (2 mL, 21.2 mmol) and triethylamine (0.14 mL, 1 mmol) was heated at 80 °C for 11 min, cooled and filtered through a bed of Celite 545. The filtrate was then poured into ice cold water (60 mL) and the mixture was extracted with chloroform three times. The chloroform extracts were pooled, washed with water, brine and dried over anhydrous sodium sulfate, filtered and concentrated in vacuo to afford the title compound as a tan colored solid

(0.1247 g, 95%): IR (NaCl, film,  $\text{cm}^{-1}$ )  $\nu_{\text{max}}$  3075, 2943, 2841, 1765, 1595, 1578, 1507, 1471, 1460, 1415, 1372, 1348, 1332, 1266, 1216, 1190, 1158, 1100, 1056, 1038, 1010, 930, 903, 811, 784, 749, 728, 682;  $^1\text{H}$  NMR (300 MHz,  $\text{CDCl}_3$ )  $\delta$  7.47 (1H, s, ArH), 7.41 (2H, m, ArH), 6.87 (1H, m ArH), 3.91 (3H, s,  $\text{ArOCH}_3$ ), 2.42 (3H, s,  $\text{OC(O)CH}_3$ ), 2.40 (3H, s,  $\text{OC(O)CH}_3$ );  $^{13}\text{C}$  NMR (75.5 MHz,  $\text{CDCl}_3$ )  $\delta$  168.8, 167.7, 154.9, 144.1, 141.7, 128.9, 127.5, 122.5, 120.6, 114.1, 112.9, 107.6, 56.3, 20.9, 20.7; MS  $m/z$  (rel. intensity) (EI) 354 ( $\text{M}^+$  for  $\text{C}_{15}\text{H}_{13}^{81}\text{BrO}_5$ , 17), 352 ( $\text{M}^+$  for  $\text{C}_{15}\text{H}_{13}^{79}\text{BrO}_5$ , 17), 312 (23), 310 (23), 270 (99), 268 (100), 255 (14), 253 (14), 231 (2), 188 (5), 173 (3), 129 (3), 102 (3), 76 (2); HRMS (EI) calc. for  $\text{C}_{15}\text{H}_{13}\text{BrO}_5$ : 351.9946, found 351.9940.



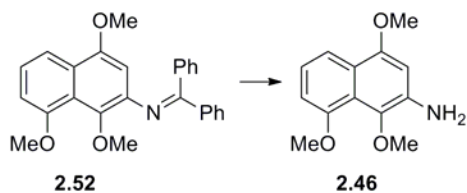
**Synthetic efforts towards 2-(Benzylamino)-8-methoxynaphthalene-1,4-diyl diacetate (2.48).** A 100 mL two-neck flask was charged with the bromonaphthalene **2.47** (0.0801 g, 0.23 mmol),  $\text{Pd}_2(\text{dba})_3 \cdot \text{CHCl}_3$  (0.0121 g, 0.023 mmol), (*S*)-BINAP (0.0196 g, 0.031 mmol) and toluene (6 mL) and was degassed with three freeze-thawing cycles with nitrogen purges. A separate 5 mL flask was charged with benzylamine (0.026 mL, 0.24 mmol) and potassium *tert*-butoxide (0.0258 g, 0.23 mmol) and purged with nitrogen for 10 min to which toluene (2 mL) was added and stirred. This solution was added to the naphthalene mixture with an additional 4 mL of toluene added and heated to 80 °C for 16 h. The mixture was cooled to ambient temperature and filtered through Celite 545 and the solvent was evaporated under

reduced pressure to give 0.0887 g of a brown oil that was purified by silica gel chromatography (3:1 hexanes:ethyl acetate) to give 0.0474 g of residue. Another round of chromatographic purification (silica, 2:1 hexanes:ethyl acetate) gave 0.0126 g of a clear residue as the side product **2.51**:



**N-(Diphenylmethylene)-1,4,8-trimethoxynaphthalen-2-amine (2.52).** Following a known procedure,<sup>222</sup> a 25 mL two-neck flask was charged with bromonaphthalene **2.25** (0.2023 g, 0.68 mmol), benzophenone imine (0.1642 g, 0.91 mmol), sodium *tert*-butoxide (0.0824 g, 0.86 mmol) and toluene (4 mL) under argon environment and the mixture was degassed with two freeze–thawing cycles under high vacuum with argon purges. To the frozen mixture was added  $\text{Pd}_2(\text{dba})_3$  (0.002 g, 0.64 mol%) and ( $\pm$ ) BINAP (0.0073 g, 1.7 mol%) and the mixture was freeze–thawed twice again and then heated at 85 °C for 14 h. The mixture was allowed to cool, diluted with ether, filtered through Celite 545 and concentrated in vacuo to yield a yellow oil that was purified using flash silica column chromatography (4:1 than 2:1 hexanes:ether) producing 0.2506 g (93%) of a bright yellow solid as the title compound: mp 160-162 °C; IR (NaCl, film,  $\text{cm}^{-1}$ )  $\nu_{\text{max}}$  3058, 2931, 2832, 1616, 1596, 1576,

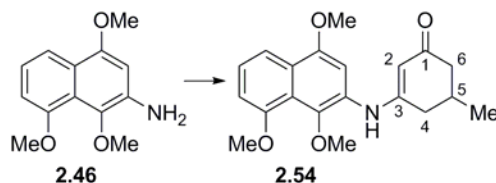
1507, 1447, 1412, 1364, 1337, 1316, 1290, 1264, 1202, 1076, 1017;  $^1\text{H}$  NMR (300 MHz,  $\text{CDCl}_3$ )  $\delta$  7.85 to 7.83 (2H, m, ArH), 7.70 (1H, dd,  $J = 0.6, 8.4$  Hz, ArH), 7.51 to 7.40 (3H, m, ArH), 7.27 to 7.17 (6H, m, ArH), 6.84 (1H, d,  $J = 7.6$  Hz, ArH), 6.17 (1H, s, ArH), 3.90 (3H, s,  $\text{ArOCH}_3$ ), 3.83 (3H, s,  $\text{ArOCH}_3$ ), 3.69 (3H, s,  $\text{ArOCH}_3$ );  $^{13}\text{C}$  NMR (75.5 MHz,  $\text{CDCl}_3$ )  $\delta$  168.6, 156.2, 151.1, 141.6, 139.5, 137.7, 136.7, 130.6, 129.4, 128.8, 128.5, 128.1, 127.8, 125.4, 123.7, 121.4, 114.7, 107.7, 101.1, 60.1, 56.7, 55.6; MS  $m/z$  (mass intensity) (EI) 397 ( $\text{M}^+$ , 84), 382 (100), 367 (11), 352 (15), 290 (3), 280 (2), 230 (2), 191 (3), 165 (18), 160 (3), 105 (2); HRMS (EI) calc. for  $\text{C}_{26}\text{H}_{23}\text{NO}_3$ : 397.1678, found: 397.1668.



**1,4,8-Trimethoxynaphthalen-2-amine (2.46).** Following a known procedure,<sup>222</sup> a mixture of the imine **2.52** (0.2506 g, 0.63 mmol), 5% palladium on carbon (0.1616 g, 12 mol%) and ammonium formate (0.6806 g, 10.9 mmol) in methanol (5 mL) was heated at reflux for 1 h 40 min. The mixture was cooled to room temperature and diluted ten-fold with dichloromethane. The mixture was filtered through a bed of Celite 545, washed once with 0.1 M NaOH, dried over sodium sulfate, filtered and concentrated in vacuo to give 0.2319 g of a light brown solid that was further purified by flash silica gel chromatography (1:12 hexanes:ether) to afford 0.1229 g (84%) of the title compound as a light tan solid: mp 118-119 °C (lit. value<sup>493</sup> 125 °C); IR (NaCl, film,  $\text{cm}^{-1}$ )  $\nu_{\text{max}}$  3482, 3368, 2960, 1623, 1603, 1512, 1448, 1421, 1388, 1341, 1258, 1211, 1163, 1070;  $^1\text{H}$  NMR (300 MHz,  $\text{CDCl}_3$ )  $\delta$  7.72 (1H,

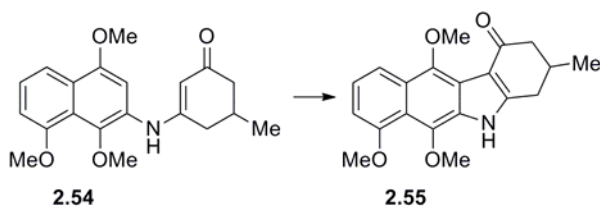


dd,  $J = 0.6, 8.3$  Hz, ArH), 7.11 (1H, dd,  $J = 7.8, 8.3$  Hz, ArH), 6.83 Hz (1H, d,  $J = 7.8$  Hz, ArH), 6.40 (1H, s, ArH), 3.98 (2H, br s, ArNH<sub>2</sub>) overlapping with 3.96 (3H, s, ArOCH<sub>3</sub>), 3.90 (3H, s, ArOCH<sub>3</sub>), 3.78 (3H, s, ArOCH<sub>3</sub>); <sup>13</sup>C NMR (75.5 MHz, CDCl<sub>3</sub>) δ 154.4, 152.2, 136.6, 133.6, 122.5, 121.7, 121.2, 114.9, 107.2, 97.8, 60.9, 56.1, 55.6; MS  $m/z$  (rel. intensity) (EI) 233 (M<sup>+</sup>, 74), 218 (100), 201 (8), 173 (13), 159 (3), 145 (6), 130 (3), 116 (5), 102 (3) 101 (2), 89 (2), 76 (2), 63 (1) 51 (1); HRMS (EI) calc. for C<sub>13</sub>H<sub>15</sub>NO<sub>3</sub>: 233.1052, found: 233.1059.



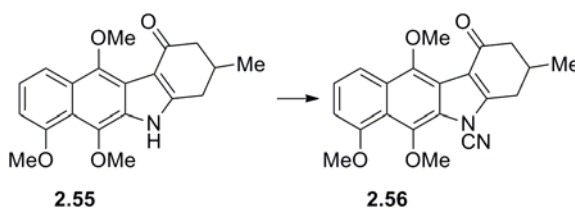
**5-Methyl-3-(1,4,8-trimethoxynaphthalen-2-ylamino)cyclohex-2-enone (2.54).** A mixture of naphthylamine **2.46** (0.0989 g, 0.42 mmol), 5-methylcyclohexane-1,3-dione (0.0547 g, 0.43 mmol), *p*-TsOH hydrate (0.0105 g, 0.055 mmol) in toluene (4 mL) was heated at reflux for 6 h. The solution was cooled and the solvent evaporated in vacuo. The residue was purified by flash silica gel chromatography (ethyl acetate) providing the title compound as a white solid (0.1245 g, 86%): mp 169-170 °C; IR (NaCl, film, cm<sup>-1</sup>)  $\nu_{\max}$  3226, 2954, 1581, 1529, 1502, 1450, 1417, 1378, 1338, 1262, 1142, 1075, 1016; <sup>1</sup>H NMR (300 MHz, CDCl<sub>3</sub>) δ 7.80 (1H, d,  $J = 8.4$  Hz, ArH), 7.31 (1H, dd,  $J = 7.7, 8.4$  Hz, ArH), 6.89 (1H, d,  $J = 7.7$  Hz, ArH), 6.83 (1H, s, ArH), 6.43 (1H, br s, NH), 5.71 (1H, s, H<sub>2</sub>), 3.96 (3H, s, ArOCH<sub>3</sub>), 3.91 (3H, s, ArOCH<sub>3</sub>), 3.72 (3H, s, ArOCH<sub>3</sub>), 2.49 to 2.29 (4H, m, H<sub>4</sub>, H<sub>6</sub>), 2.12 to 2.04 (1H, m, H<sub>5</sub>), 1.12 (3H, d,  $J = 5.4$  Hz, CHCH<sub>3</sub>); <sup>13</sup>C NMR (75.5 Hz, CDCl<sub>3</sub>) δ 198.1,

160.7, 155.4, 151.8, 141.1, 128.4, 126.1, 125.2, 120.4, 114.9, 107.4, 101.4, 99.9, 62.4, 56.1, 55.9, 44.9, 38.3, 29.3, 21.0; MS  $m/z$  (rel. intensity) (EI) 341 ( $M^+$ , 66), 326 (100), 310 (4), 294 (4), 278 (3), 240 (5), 217 (5), 204 (3), 189 (2), 141 (2), 120 (6), 103 (2), 69 (3), 57 (1); HRMS (EI) calc. for  $C_{20}H_{23}NO_4$ : 341.1627, found: 341.1628.



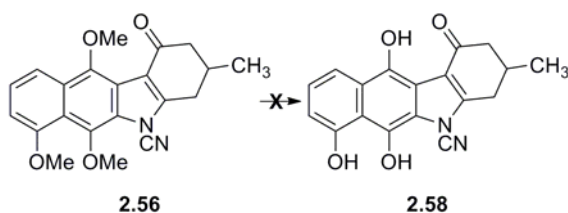
**6,7,11-Trimethoxy-3-methyl-3,4-dihydro-2H-benzo[*b*]carbazol-1(5H)-one (2.55).** From a modification of procedures described by Akermark,<sup>229</sup> a mixture of the anilino ketone **2.54** (0.0315 g, 0.09 mmol), palladium acetate (0.0425 g, 0.189 mmol) in glacial acetic acid (5 mL) was heated at 95 °C for 90 min. The mixture was cooled to ambient temperature, filtered through a small pad of Celite 545 and the residue concentrated under reduced pressure and purified by column chromatography (silica, 1:7 hexanes:ethyl acetate) to furnish 0.0151 g (51%) of a light brown solid as the title compound: m.p. > 260 °C decomposition; IR (NaCl, film,  $cm^{-1}$ )  $\nu_{max}$  3231, 3072, 2996, 2956, 2929, 2840, 1620, 1543, 1505, 1479, 1465, 1445, 1428, 1395, 1357, 1263, 1247, 1215, 1134, 1100, 1058, 1004;  $^1H$  NMR (500 MHz,  $CDCl_3$ )  $\delta$  9.15 (1H, br s, *NH*), 7.96 (1H, d,  $J = 8.7$  Hz, *ArH*), 7.27 (1H, dd,  $J = 7.5, 8.7$  Hz, *ArH*), 6.79 (1H, d,  $J = 7.5$  Hz, *ArH*), 4.03 (3H, s,  $ArOCH_3$ ), 4.00 (3H, s,  $ArOCH_3$ ), 3.99 (3H, s,  $ArOCH_3$ ), 3.05 (1H, dd,  $J = 4.3, 16.5$  Hz, *H4*), 2.69 to 2.63 (2H, m, *H2, H4*), 2.50 to 2.44 (1H, m, *H3*), 2.36 (1H, dd,  $J = 11.7, 15.8$  Hz, *H2*), 1.16 (3H, d,  $J = 6.5$  Hz,  $CHCH_3$ );  $^{13}C$  NMR (125.8 MHz,  $CDCl_3$ )  $\delta$  191.1, 155.5, 154.9, 145.4, 135.7, 130.7, 127.4, 123.2, 118.2,

117.0, 115.9, 112.6, 103.8, 63.7, 63.0, 55.9, 47.2, 32.2, 30.8, 21.2; MS  $m/z$  (rel. intensity) (EI) 339 ( $M^+$ , 66), 324 (100), 310 (4), 267 (5), 239 (3), 218 (6), 186 (7), 170 (9), 142 (13), 129 (41), 104 (33), 91 (10), 57 (5); HRMS (EI) calc. for  $C_{20}H_{21}NO_4$ : 339.1471, found: 339.1480.

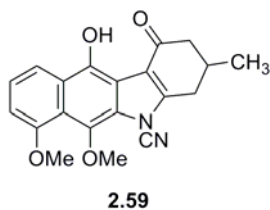


**6,7,11-Trimethoxy-3-methyl-1-oxo-3,4-dihydro-1H-benzo[b]carbazole-5(2H)-carbonitrile (2.56).** A solution of the carbazole **2.55** (0.0174 g, 0.051 mmol), phenyl cyanate<sup>230</sup> (0.040 mL, 0.37 mmol) and triethylamine (0.030 mL, 0.21 mmol) in dry DMSO (0.8 mL) was stirred at room temperature for 4 h after which another 2 drops of triethylamine (~0.012 g, 0.12 mmol) was added and stirring was continued overnight. The solution was then diluted with water (10 mL) and extracted with ethyl acetate three times and the organic extracts were pooled. The pooled extracts were washed three times with water, brine once and dried over  $Na_2SO_4$ , filtered and concentrated under reduced pressure to yield the title compound as a light tan solid (0.0186 g, 99%): mp 183-184 °C; IR (NaCl, film,  $cm^{-1}$ )  $\nu_{max}$  2930, 2841, 2244, 1752, 1680, 1613, 1570, 1508, 1452, 1408, 1391, 1356, 1342, 1266, 1099, 1066, 1044, 997, 967, 912, 882, 810, 761, 729;  $^1H$  NMR ( $CDCl_3$ , 300 MHz)  $\delta$  7.92 (1H, d,  $J = 8.6$  Hz, ArH), 7.39 (1H, dd,  $J = 7.6, 8.6$  Hz, ArH), 6.89 (1H, d,  $J = 7.6$  Hz, ArH), 4.024 (3H, s, ArOCH<sub>3</sub>), 4.019 (3H, s, ArOCH<sub>3</sub>), 3.95 (3H, s, ArOCH<sub>3</sub>), 3.23 (1H, dd,  $J = 4.2, 17.5$  Hz, H4), 2.81 to 2.71 (2H, m, H2, H4), 2.66 to 2.49 (1H, m, H3), 2.42 (1H, dd,  $J = 11.6, 15.5$

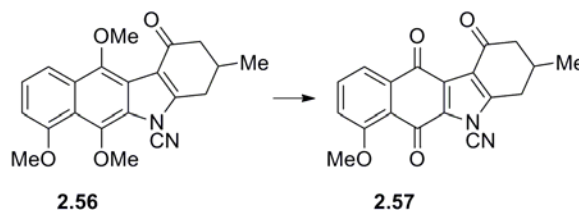
Hz, *H*2), 1.26 (3H, d, *J* = 6.3 Hz, CHCH<sub>3</sub>); <sup>13</sup>C NMR (75.5 MHz, CDCl<sub>3</sub>) δ 190.7, 155.9, 154.3, 146.2, 138.3, 129.6, 128.4, 125.4, 118.8, 117.3, 116.6, 115.7, 106.3, 105.7, 64.7, 64.1, 56.1, 47.1, 30.7, 30.2, 21.0; MS *m/z* (rel. intensity) (EI) 364 (M<sup>+</sup>, 99), 349 (100), 335 (4), 322 (2), 292 (3), 264 (3), 237 (3), 182 (4), 149 (2), 126 (3), 111 (1), 69 (11), 57 (1); HRMS (EI) calc. for C<sub>21</sub>H<sub>20</sub>N<sub>2</sub>O<sub>4</sub>: 364.1423, found: 364.1414.



**Synthetic efforts towards 6,7,11-Trihydroxy-3-methyl-1-oxo-3,4-dihydro-1H-benzo[*b*]carbazole-5(2*H*)-carbonitrile (2.58).** A 25 mL flask was charged with carbazole **2.56** (0.0116g, 0.032 mmol) and CH<sub>2</sub>Cl<sub>2</sub> (1.5 mL) and cooled to -78 °C. To this was added BCl<sub>3</sub> (0.2 mL, 0.2 mmol of a 1.0 M solution in heptane) and stirred for 30 min. The colour of the reaction mixture changed from light yellow to orange. The flask was allowed to come to room temperature over the period of an hour and the mixture became a dark brown-orange. The reaction was quenched with ice water and extracted with CH<sub>2</sub>Cl<sub>2</sub>. The pooled organic extracts were washed with water twice, brine once, and dried over Na<sub>2</sub>SO<sub>4</sub>, filtered and concentrated in vacuo to produce 0.0104 g of a green residue. The residue was purified by silica gel chromatography (3:1 hexanes:ethyl acetate, then 100% ethyl acetate) to give 0.0014 g (13%) of a light yellow solid as the side product **2.59**:

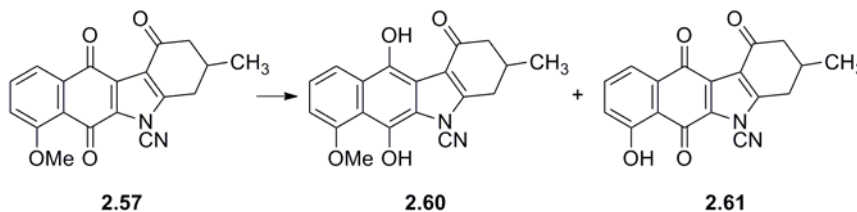


**11-Hydroxy-6,7-dimethoxy-3-methyl-1-oxo-3,4-dihydro-1H-benzo[*b*]carbazole-5(2*H*)-carbonitrile (2.59).** <sup>1</sup>H NMR (300 MHz, CDCl<sub>3</sub>) δ 10.75 (1H, s, *OH*), 7.97 (1H, d, *J* = 8.7 Hz, *ArH*), 7.34 (1H, dd, *J* = 7.7, 8.7 Hz, *ArH*), 6.91 (1H, d, *J* = 7.7 Hz, *ArH*), 4.03 (3H, s, *ArOCH*<sub>3</sub>), 3.99 (3H, s, *ArOCH*<sub>3</sub>), 3.21 (1H, dd, *J* = 4.2, 17.3 Hz, *H*<sub>4</sub>), 2.81-2.71 (2H, m *H*<sub>2</sub>, *H*<sub>4</sub>), 2.68-2.54 (1H, m, *H*<sub>3</sub>), 2.45 (1H, dd, *J* = 10.9, 16.3 Hz, *H*<sub>2</sub>), 1.26 (3H, d, *J* = 6.4 Hz, *CHCH*<sub>3</sub>); MS *m/z* (rel. intensity) (EI) 350 (99, *M*<sup>+</sup>), 335 (100), 308 (14), 280 (8), 264 (10), 238 (3), 207 (2), 175 (6), 167 (2), 149 (2), 105 (2), 77 (4), 57 (2).



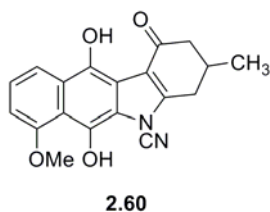
**7-Methoxy-3-methyl-1,6,11-trioxo-3,4,6,11-tetrahydro-1H-benzo[*b*]carbazole-5(2*H*)-carbonitrile (2.57).** Carbazole **2.56** (0.0122 g, 0.033 mmol) was dissolved in acetonitrile (1 mL) and the solution cooled to 0 °C. To this solution was added ceric ammonium nitrate (0.0475 g, 0.087 mmol) dissolved in distilled water (0.3 mL), in 0.04 mL aliquots over a 5 min period. The solution was then allowed to come to room temperature over a period of 10 minutes and water (20 mL) was added. This mixture was extracted with CH<sub>2</sub>Cl<sub>2</sub> four times and the extracts were pooled, washed with water, a saturated solution of NaHCO<sub>3</sub>, water, brine and dried over Na<sub>2</sub>SO<sub>4</sub>. The solution was then filtered and concentrated in vacuo to give the crude product as an orange solid which was purified chromatographically (silica, 2:5 then 1:5 hexanes:ethyl acetate) to afford the title compound as an orange solid (0.0106 g,

95%): mp > 240 °C decomposition; IR (CDCl<sub>3</sub>, cm<sup>-1</sup>)  $\nu_{\text{max}}$  3693, 2259, 1701, 1662, 1586, 1528, 1472, 1454, 1440, 1408, 1298, 1272, 1240, 1168, 1041, 1005, 929; <sup>1</sup>H NMR (300 MHz, CDCl<sub>3</sub>)  $\delta$  7.89 (1H, d,  $J$  = 7.7 Hz, ArH), 7.71 (1H, dd,  $J$  = 7.7, 8.4 Hz, ArH), 7.31 (1H, d,  $J$  = 8.4 Hz, ArH), 4.03 (3H, s, ArOCH<sub>3</sub>), 3.18 (1H, dd,  $J$  = 4.4, 17.3 Hz, H<sub>4</sub>), 2.77 to 2.66 (2H, m, H<sub>2</sub>, H<sub>4</sub>), 2.60 to 2.49 (1H, m, H<sub>3</sub>) 2.40 (1H, dd,  $J$  = 11.4, 15.7 Hz, H<sub>2</sub>), 1.24 (3H, d,  $J$  = 6.4 Hz, CHCH<sub>3</sub>); <sup>13</sup>C NMR (75.5 MHz, CDCl<sub>3</sub>)  $\delta$  190.0, 177.2, 174.0, 160.7, 152.7, 136.1, 136.0, 135.7, 124.1, 120.9, 120.5, 118.4, 118.0, 103.3, 56.6, 47.1, 30.3, 29.9, 20.9; MS  $m/z$  (rel. intensity) (EI) 334 (M<sup>+</sup>, 100), 321 (19), 307 (11), 292 (37), 279 (19), 264 (41), 237 (63), 221 (5), 206 (6), 178 (4), 151 (4), 105 (6), 76 (6), 51 (2); HRMS calc. for C<sub>19</sub>H<sub>14</sub>N<sub>2</sub>O<sub>4</sub>: 334.0954, found: 334.0951.



**Synthetic efforts towards 7-Hydroxy-3-methyl-1,6,11-trioxo-3,4,6,11-tetrahydro-1H-benzo[*b*]carbazole-5(2*H*)-carbonitrile (2.61).** A 25 mL flask was charged with 0.012 g (0.036 mmol) of carbazole **2.57** and CH<sub>2</sub>Cl<sub>2</sub> (3 mL) and the solution was cooled to -78 °C. To this solution was added BBr<sub>3</sub> (0.08 mL, 0.08 mmol of 1.0 M solution in CH<sub>2</sub>Cl<sub>2</sub>) and the mixture was stirred for 15 min. The reaction flask was removed from the CO<sub>2</sub>-acetone bath and allowed to warm to ~0 °C at which time the reaction was quenched with water (5 mL) and a saturated solution of sodium bicarbonate (1 mL). The mixture was extracted with

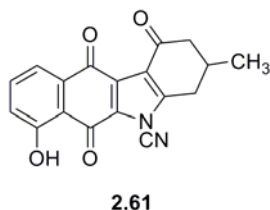
CH<sub>2</sub>Cl<sub>2</sub> three times and pooled. The pooled extracts were washed with water twice, brine once, dried over Na<sub>2</sub>SO<sub>4</sub>, filtered and the solvent evaporated on a rotary evaporator to give 0.0109 g of a yellow-green residue that was purified chromatographically (silica, 1:1 hexanes:ethyl acetate) to furnish 0.0024 g of a yellow-green residue (20%) as the side product **2.60** and 0.0012 g (10%) of the title compound **2.61** as a



yellow residue:

**6,11-Dihydroxy-7-methoxy-3-methyl-1-oxo-3,4-dihydro-1H-benzo[b]carbazole-5(2H)-carbonitrile (2.60):** IR (CDCl<sub>3</sub>, cm<sup>-1</sup>)

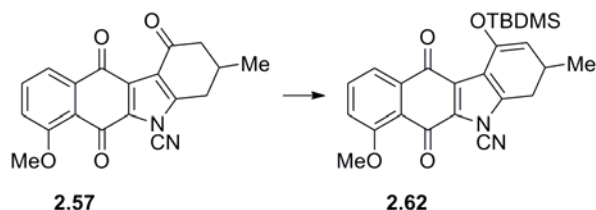
$\nu_{\max}$  3695, 3394, 2967, 2250, 1711, 1638, 1581, 1519, 1456, 1444, 1432, 1370, 1344, 1262, 1248, 1225, 1098, 1057, 1010; <sup>1</sup>H NMR (300 MHz, CDCl<sub>3</sub>)  $\delta$  10.40 (1H, s, OH), 9.19 (1H, s, OH), 7.87 (1H, d,  $J$  = 8.6 Hz, ArH), overlapping with solvent signal 7.27 (1H, dd,  $J$  = 7.7 Hz, ArH), 6.80 (1H, d,  $J$  = 7.7 Hz, ArH), 4.05 (3H, s, ArOCH<sub>3</sub>), 3.13 (1H, m H4), 2.78-2.55 (3H, m, H2, H3, H4), 2.44 (1H, dd,  $J$  = 11.6, 16.2 Hz, H2), 1.28 (3H, d,  $J$  = 6.2 Hz, CHCH<sub>3</sub>); MS  $m/z$  (rel. intensity) (EI) 336 (100, M<sup>+</sup>), 321 (75), 305 (5), 292 (5), 278 (9), 264 (4), 251 (3), 237 (5), 201 (3) 168 (4), 121(1), 71 (2).



**7-Hydroxy-3-methyl-1,6,11-trioxo-3,4,6,11-tetrahydro-1H-benzo[b]carbazole-5(2H)-carbonitrile (2.61):** IR (CDCl<sub>3</sub>, cm<sup>-1</sup>)

$\nu_{\max}$  3692, 2966, 2256, 1710, 1641, 1601, 1519, 1454, 1422, 1364, 1271, 1225, 1160, 1116, 1074; <sup>1</sup>H NMR (300 MHz, CDCl<sub>3</sub>)  $\delta$  11.56 (1H, s, OH), 7.76 (1H, dd,  $J$  = 1.0, 7.5 Hz, ArH), 7.65 (1H, dd,  $J$  = 7.5, 8.2 Hz, ArH), overlapping with solvent signal 7.27 (1H, dd,  $J$  = 1.0 Hz, ArH), 3.21 (1H, dd,  $J$  = 4.4, 17.6 Hz, H4), 2.79-2.69 (2H, m, H2, H4), 2.62-2.48 (1H, m, H3), 2.41 (1H, dd,  $J$  = 11.4, 15.7 Hz, H2), 1.25 (3H, d,  $J$  = 6.4

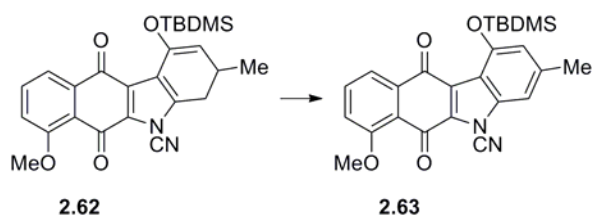
Hz, CHCH<sub>3</sub>); MS *m/z* (rel. intensity) (EI) 320 (72, M<sup>+</sup>), 305 (4), 278 (100), 253 (19), 250 (16), 194 (9), 167 (2), 139 (3), 120 (3), 92 (2), 82 (2), 63 (1).



**1-((*tert*-Butyldimethylsilyl)oxy)-7-methoxy-3-methyl-6,11-dioxo-6,11-dihydro-3*H*-benzo[*b*]carbazole-5(4*H*)-carbonitrile (2.62).** Following a procedure described by Mander and Sethi,<sup>494</sup> *N*-cyanocarbazoloquinone **2.57** (0.216 g, 0.65 mmol) was dissolved in dichloromethane (12 mL) and the solution was cooled to 0 °C. To this was added TBSOTf (0.24 mL, 1.05 mmol) and the mixture was stirred for 2 min. Triethylamine (0.25 mL, 1.79 mmol) was added and was stirring continued at room temperature for 1 h. Dichloromethane was then added and the reaction was quenched with an excess of an ice cold solution of saturated sodium bicarbonate. The organic phase was dried over sodium sulfate, evaporated in vacuo and purified by flash silica column chromatography (2:3 hexanes:ether) to afford 0.1025 g (35%) of the title compound as an orange solid: IR (CDCl<sub>3</sub>, cm<sup>-1</sup>)  $\nu_{\max}$  2961, 2932, 2860, 1679, 1652, 1619, 1586, 1509, 1471, 1439, 1418, 1365, 1339, 1279, 1253, 1235, 1186, 1165, 1141, 1026, 1012, 994, 974, 944; <sup>1</sup>H NMR (300 MHz, CDCl<sub>3</sub>)  $\delta$  7.83 (1H, d, *J* = 7.5 Hz, *ArH*), 7.65 (1H, dd, *J* = 7.5, 8.2 Hz, *ArH*), 7.26 overlapping with CHCl<sub>3</sub> peak (1H, d, *J* = 8.2 Hz, *ArH*), 4.96 (1H, d, *J* = 3.9 Hz, *H2*), 4.01 (3H, s, ArOCH<sub>3</sub>), 2.95 (1H, dd, *J* = 7.3, 16.1 Hz, *H4*), 2.88 to 2.76 (1H, m, *H3*), 2.55 (1H, dd, *J* = 9.6, 16.1 Hz, *H4*), 1.14 (3H, d, *J* = 6.8 Hz, CHCH<sub>3</sub>), 0.98 (9H, s, SiC(CH<sub>3</sub>)<sub>3</sub>), 0.21 (3H, s, Si(CH<sub>3</sub>)), 0.19 (3H, s, Si(CH<sub>3</sub>)); <sup>13</sup>C

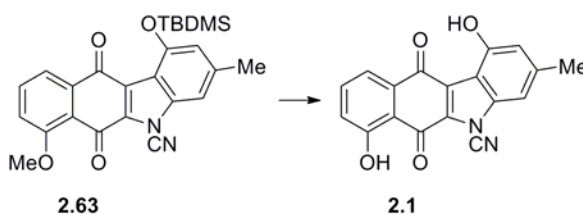


NMR (75.5 MHz, CDCl<sub>3</sub>)  $\delta$  177.7, 173.7, 160.5, 144.5, 141.9, 136.6, 135.2, 134.4, 123.4, 120.3, 119.9, 119.0, 117.5, 110.6, 104.2, 56.5, 29.3, 28.2, 26.0, 20.7, 18.7, -4.26, -4.31; MS *m/z* (rel. intensity) (EI) 448 (M<sup>+</sup>, 1), 433 (3), 391 (100), 364 (20), 349 (12), 320 (8), 319 (4), 292 (3), 279 (2), 262 (1), 174 (3), 149 (3), 111(1), 73 (5), 57 (3); HRMS (EI) calc. for C<sub>21</sub>H<sub>19</sub>O<sub>4</sub>N<sub>2</sub>Si (M<sup>+</sup> - *t*Bu): 391.1114, found: 391.1110.



**1-((*tert*-Butyldimethylsilyl)oxy)-7-methoxy-3-methyl-6,11-dioxo-6,11-dihydro-5H-benzo[*b*]carbazole-5-carbonitrile (2.63).** Silyl enol ether **2.62** (0.0051 g, 0.011 mmol) was dissolved in benzene (1 mL) and DDQ (0.003 g, 0.013 mmol) was added and stirring was continued for 3.5 h at room temperature. The reaction mixture was diluted with dichloromethane (10 mL), concentrated under reduced pressure and the residue purified by column chromatography (silica, 1:3 hexanes:ether) to yield a yellow solid (0.0045 g, 88%) as the title compound: IR (CDCl<sub>3</sub>, cm<sup>-1</sup>)  $\nu_{\max}$  2932, 2860, 1675, 1657, 1615, 1587, 1576, 1549, 1500, 1471, 1437, 1415, 1373, 1352, 1321, 1280, 1253, 1232, 1183, 1133, 1106, 1070, 1032, 1014; <sup>1</sup>H NMR (300 MHz, CDCl<sub>3</sub>)  $\delta$  7.89 (1H, d, *J* = 7.8 Hz, *ArH*), 7.69 (1H, dd, *J* = 7.8, 8.4 Hz, *ArH*), 7.29 (1H, d, *J* = 8.4 Hz, *ArH*), 7.12 (1H, s, *ArH*), 6.72 (1H, s, *ArH*), 4.03 (3H, s, ArOCH<sub>3</sub>), 2.47 (3H, s, ArCH<sub>3</sub>), 1.05 (9H, s, SiC(CH<sub>3</sub>)<sub>3</sub>), 0.32 (6H, s, Si(CH<sub>3</sub>)<sub>2</sub>); <sup>13</sup>C NMR (75.5 MHz, CDCl<sub>3</sub>)  $\delta$  177.5, 175.3, 160.4, 152.3, 142.0, 141.1, 136.5, 136.3, 135.7, 122.4,

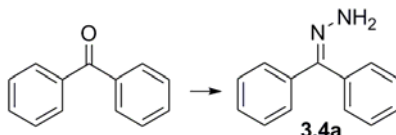
120.4, 118.9, 118.1, 117.5, 114.5, 105.0, 104.8, 56.5, 26.1, 22.1, 18.9, -3.8; MS  $m/z$  (rel. intensity) (EI) 431 (2), 405 (4), 389 (100), 374 (13), 362 (36), 346 (11), 334 (14), 332 (5), 304 (3), 288 (2), 261 (1), 181 (3), 173 (2), 152 (1), 97(1), 73 (1), 57 (2); HRMS (EI) calc. for  $C_{21}H_{17}O_4N_2Si$  ( $M^+ - tBu$ ): 389.0958, found: 389.0959.



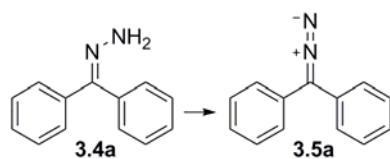
### **1,7-Dihydroxy-3-methyl-6,11-dioxo-6,11-dihydro-5H-benzo[*b*]carbazole-5-**

**carbonitrile (2.1).** *N*-Cyanocarbazoloquinone **2.63** (0.0748 g, 0.168 mmol) was dissolved in dichloromethane (7 mL) and the solution was cooled to  $-78\text{ }^{\circ}\text{C}$ . To this was added  $\text{BBr}_3$  (1.2 mL of a 1 M solution in  $\text{CH}_2\text{Cl}_2$ , 1.2 mmol) and the mixture was stirred for 40 min, allowed to come to room temperature over a 15 min period and then quenched with an ice cold solution of saturated sodium bicarbonate. The mixture was diluted with dichloromethane, washed with water, dried over  $\text{Na}_2\text{SO}_4$ , filtered and the solvent evaporated in vacuo. The crude material was purified by flash silica gel chromatography (1:1 then 2:3 hexanes:ether) to afford the target compound as a blackish-purple solid (0.0181 g, 34%): IR ( $\text{CDCl}_3$ ,  $\text{cm}^{-1}$ )  $\nu_{\text{max}}$  3692, 3208, 3123, 2927, 2247, 1627, 1593, 1553, 1455, 1430, 1408, 1300, 1250, 1219, 1184, 1164, 1089;  $^1\text{H}$  NMR (500 MHz,  $\text{CDCl}_3$ )  $\delta$  11.81 (1H, s, ArOH), 10.17 (1H, s, ArOH), 7.82 (1H, d,  $J = 7.5$  Hz, ArH), 7.67 (1H, dd,  $J = 7.5, 8.1$  Hz, ArH), 7.34 (1H, d,  $J = 8.1$  Hz, ArH), 7.01 (1H, s, ArH), 6.79 (1H, s, ArH), 2.49 (3H, s, ArCH<sub>3</sub>);  $^{13}\text{C}$  NMR (125.8 MHz,  $\text{CDCl}_3$ )  $\delta$  182.2, 179.4, 162.9, 153.1, 145.5, 140.8, 136.9, 133.2, 132.0, 126.8, 124.9, 121.4,

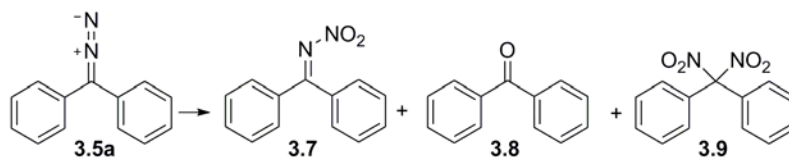
114.6, 113.7, 111.1, 104.4, 103.1, 22.5; MS  $m/z$  (rel. intensity) (EI) 318 ( $M^+$ , 100), 293 (6), 289 (3), 261 (2), 219 (3), 190 (3), 159 (3), 115 (1), 87 (2); HRMS (EI) calc. for  $C_{18}H_{10}N_2O_4$ : 318.0641, found: 318.0645.



**(Diphenylmethylenediamine) (3.4a).** Benzophenone (2.6839 g, 0.0147 mol) was dissolved in dry ethanol (60 mL, distilled from Mg/I<sub>2</sub>) under argon atmosphere. To this solution was added hydrazine monohydrate (1 mL, 0.0184 mol) and 4 drops of concentrated HCl. The solution was then refluxed at 85 °C for 72 h. The reaction mixture was cooled to room temperature and evaporated to dryness under reduced pressure. The residue was then taken up in CH<sub>2</sub>Cl<sub>2</sub>, washed sequentially with a saturated solution of sodium bicarbonate, water and brine and dried over Na<sub>2</sub>SO<sub>4</sub> and the solvent evaporated in vacuo to yield 2.8315 g (98%) of the title compound as a white solid as: mp = 98 °C (lit. value<sup>495</sup> 98 °C); IR (NaCl, film, cm<sup>-1</sup>)  $\nu_{\max}$  3421, 3273, 1582, 1559, 1491, 1442, 1334, 768, 695, 652; <sup>1</sup>H NMR (300 MHz, CDCl<sub>3</sub>)  $\delta$  7.52-7.44 (5H, m, ArH), 7.29-7.24 (5H, m, ArH), 5.41 (2H, br s, NH<sub>2</sub>); <sup>13</sup>C NMR (75.5 MHz, CDCl<sub>3</sub>)  $\delta$  149.2, 138.4, 132.9, 129.4, 128.9, 128.8, 128.1, 126.4; MS  $m/z$  (rel. intensity) (EI) 196 ( $M^+$ ,100), 195 (34), 180 (20), 165 (33), 152 (4), 139 (3), 119 (8), 93 (6), 77 (19), 51 (7); HRMS (EI) calc. for  $C_{13}H_{12}N_2$ : 196.1000, found: 196.0997.



**Diphenyldiazomethane (3.5a).** To a solution of benzophenone hydrazone (2.9939 g, 0.0153 mol) in petroleum ether 30-60 (30 mL) was added yellow mercuric oxide (3.7108 g, 0.0171 mol) and was vigorously shaken in the dark for 6 h. The mixture was then filtered and the solvent evaporated in vacuo to yield the title compound as a dark purple solid (2.9584 g, 99%): mp = 27-28 °C (lit. value<sup>496</sup> 29-30 °C); IR (NaCl, film,  $\text{cm}^{-1}$ )  $\nu_{\text{max}}$  2038;  $^1\text{H}$  NMR (300 MHz,  $\text{CDCl}_3$ )  $\delta$  7.41-7.36 (4H, m, ArH), 7.31-7.27 (4H, m, ArH), 7.20-7.15 (2H, m, ArH);  $^{13}\text{C}$  NMR (75.5 MHz,  $\text{CDCl}_3$ )  $\delta$  129.5, 129.1, 125.5, 125.1, 62.3; MS  $m/z$  (rel. intensity) (EI) 194 ( $\text{M}^+$ , 8) 166 (69), 165 (100), 139 (8), 115 (3), 105 (3), 82 (3), 63 (3), 51 (3); HRMS (EI) calc. for  $\text{C}_{13}\text{H}_{10}\text{N}_2$ : 194.0844, found: 194.0846.



***N*-(Diphenylmethylene)nitramide (3.7), Benzophenone (3.8), Dinitrodiphenylmethane (3.9).** Diphenyldiazomethane (0.7465 g, 3.84 mmol) was dissolved in a 50/50 (v/v) solution of benzene/cyclohexane (70 mL) that was extensively degassed under vacuum and purged with  $\text{N}_2$ . This solution was then purged continuously with a constant flow of nitric oxide for 2-2.5 h. NO was generated by the slow addition of separate degassed solutions of sodium nitrite (93.15 g in 250 mL aqueous solution) via a dropping funnel into L-ascorbic acid (118.8 g in 500 mL aqueous solution) using an in-house gas generating apparatus (Appendix

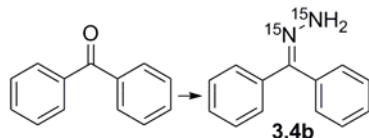
A). The reaction flask was vented to prevent pressure buildup. The reaction flask was then sealed 2-3 h after the entire addition of the NaNO<sub>2</sub> solution, and stirring continued overnight in the dark for another 12-14 h. The solution typically went from a deep purple to a lemon yellow color overnight. The crude reaction mixture was then concentrated under reduced pressure and the residue purified by silica gel column chromatography (5:1, 2:1 then 1:2 hexanes:dichloromethane) to afford three products as white solids: nitrimine 0.4698 g (54%), benzophenone 0.1484 g (21%), and dinitrodiphenylmethane 0.0818 g (8%).

***N*-(Diphenylmethylene)nitramide (3.7).** mp = 64 °C (lit. value<sup>274</sup> 67-69 °C); IR (NaCl, film, cm<sup>-1</sup>)  $\nu_{\max}$  3063, 2846, 1561, 1490, 1447, 1292, 970, 882, 783, 691; <sup>1</sup>H NMR (300 MHz, CDCl<sub>3</sub>)  $\delta$  7.65-7.33 (10 H, m, ArH); <sup>13</sup>C NMR (75.5 MHz, CDCl<sub>3</sub>)  $\delta$  171.5, 133.3, 133.2, 131.2, 131.1, 130.1, 128.7, 128.6, 127.8; MS *m/z* (rel. intensity) (EI) 226 (M<sup>+</sup>, 1), 180 (100), 165 (4), 152 (2), 103 (3), 77 (34), 51 (11); HRMS (EI) calc. for C<sub>13</sub>H<sub>10</sub>N<sub>2</sub>O<sub>2</sub>: 226.0742, found: 226.0741.

**Benzophenone (3.8).** <sup>1</sup>H NMR (300 MHz, CDCl<sub>3</sub>)  $\delta$  7.80-7.78 (4H, m, ArH), 7.60-7.55 (2H, m, ArH), 7.49-7.44 (4H, m, ArH); <sup>13</sup>C NMR (75.5 MHz, CDCl<sub>3</sub>)  $\delta$  196.7, 137.6, 132.4, 130.0, 128.2; MS *m/z* (rel. intensity) (EI) 182 (M<sup>+</sup>, 94), 152 (5), 105 (100), 77 (44), 51 (16); HRMS (EI) calc. for C<sub>13</sub>H<sub>10</sub>O: 182.0732, found: 182.0729.

**Dinitrodiphenylmethane (3.9).** mp = 75 °C (lit. value<sup>296</sup> 80.4 °C); IR (NaCl, film, cm<sup>-1</sup>)  $\nu_{\max}$  3069, 2892, 1585, 1563, 1496, 1450, 1319, 1227, 832, 800, 740, 693, 569; <sup>1</sup>H NMR (300 MHz, CDCl<sub>3</sub>)  $\delta$  7.58-7.52 (2H, m, ArH), 7.49-7.43 (4H, m, ArH), 7.40-7.36 (4H, m, ArH); <sup>1</sup>H NMR (300 MHz, CD<sub>2</sub>Cl<sub>2</sub>)  $\delta$  7.63-7.58 (2H, m, ArH), 7.53-7.48 (4H, m, ArH), 7.42-7.39 (4H, m, ArH); <sup>13</sup>C NMR (75.5 MHz, CDCl<sub>3</sub>)  $\delta$  131.6, 131.1, 129.8, 128.6, 126.7; <sup>13</sup>C

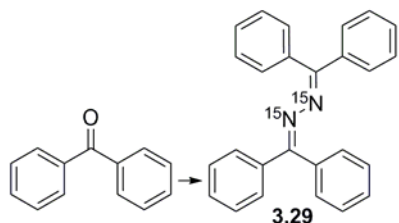
NMR (75.5 MHz, CD<sub>2</sub>Cl<sub>2</sub>) 132.1, 131.4, 130.2, 129.0, 127.5; MS *m/z* (rel. intensity) (EI) 212 (79), 182 (19), 165 (100), 152 (8), 105 (81), 77 (18), 51 (5); HRMS (EI) calc. for C<sub>13</sub>H<sub>10</sub>NO<sub>2</sub>: 212.0712, found: 212.0714.



**<sup>15</sup>N, <sup>15</sup>N'-(Diphenylmethylene)hydrazine (3.4b).** Benzophenone (2.7065 g, 0.0148 mol) was dissolved dry ethanol (60 mL distilled from Mg/I<sub>2</sub>) under argon atmosphere. To this solution was added doubly labeled <sup>15</sup>N hydrazine monohydrate (0.9 mL, 0.0185 mol) and 4 drops of concentrated HCl. The solution was then heated to 85 °C for 73 h during which a yellow color started to develop and deepen over time and was attributed to formation of the azine **3.29**. The reaction mixture cooled to room temperature and workup as previously stated yielded 2.862 g of an off-white solid. Flash silica gel chromatography (5:1 hexanes:ethyl acetate) afforded 1.1762 g of an off-white solid identified as the azine (44%) and 1.4859 g (51%) of the title compound as a white solid: IR (CDCl<sub>3</sub>, CaF<sub>2</sub>, cm<sup>-1</sup>)  $\nu_{\max}$  3412, 3083, 3063, 3027, 1608, 1584, 1552, 1495, 1444, 1331, 1267, 1164, 1074, 1048, 1023, 951; <sup>1</sup>H NMR (500 MHz, CDCl<sub>3</sub>)  $\delta$  7.53-7.43 (5H, m, ArH), 7.29-7.24 (5H, m, ArH), 5.42 (2H, d, <sup>1</sup>J<sub>NH</sub> = 77.3 Hz, =NNH<sub>2</sub>); <sup>13</sup>C NMR (125.8 MHz, CDCl<sub>3</sub>)  $\delta$  149.1 (d, <sup>1</sup>J<sub>CN</sub> = 6.3 Hz, C=NNH<sub>2</sub>) 138.4 (dd, J<sub>CN</sub> = 9.1 Hz, J<sub>CN</sub> = 2.4 Hz, ArC), 132.9 (dd, J<sub>CN</sub> = 2.3 Hz, J<sub>CN</sub> = 2.0 Hz, ArC), 129.4, 128.84, 128.76, 128.07, 128.03, 126.40, 126.38; <sup>15</sup>N NMR (30.4 MHz, CDCl<sub>3</sub>, DMSO-*d*<sub>6</sub> lock solvent)  $\delta$  320.4 (d, <sup>1</sup>J<sub>NN</sub> = 12.4 Hz), 106.2 (br m); MS *m/z* (rel. intensity) (EI) 198 (M<sup>+</sup>,

100), 197 (36), 181 (21), 165 (35), 152 (5), 139 (3), 121 (8), 120 (4), 94 (7), 77 (26), 51 (9);

HRMS (EI) calc. for  $C_{13}H_{12}^{15}N_2$ : 198.0941, found:



198.0941.

**$^{15}N,^{15}N'$ -1,2-bis(Diphenylmethylene)hydrazine (3.29).**

mp = 163-164 °C; IR ( $CDCl_3$ ,  $CaF_2$ ,  $cm^{-1}$ )  $\nu_{max}$  3085,

3063, 3027, 1550, 1490, 1445, 1323, 1300, 1179, 1075, 1029, 953;  $^1H$  NMR (500 MHz,

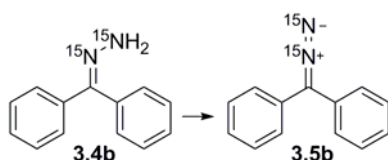
$CDCl_3$ )  $\delta$  7.49-7.24 (10H, m, ArH);  $^{13}C$  NMR (125.8 MHz,  $CDCl_3$ )  $\delta$  158.8 (dd,  $J_{NC} = 3.4$

Hz,  $J_{NC} = 3.4$  Hz, C=N) 138.2 (dd,  $J_{NC} = 5.4$ ,  $J_{NC} = 5.4$  Hz, ArC), 135.5, 129.5, 129.3,

128.63, 128.61, 127.9, 127.8;  $^{15}N$  NMR (30.4 MHz,  $CDCl_3$ , DMSO- $d_6$  lock solvent)  $\delta$

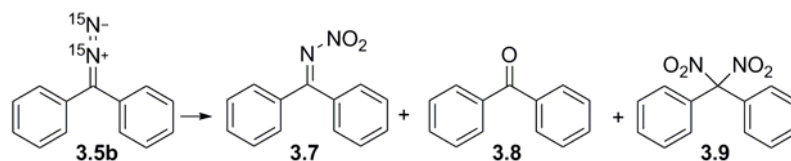
353.05; MS  $m/z$  (rel. intensity) (EI) 362 ( $M^+$ , 79), 285 (100), 258 (14), 207 (5), 181 (29), 165

(28), 105 (7), 77 (21), 51 (4); HRMS (EI) calc. for  $C_{26}H_{20}^{15}N_2$ : 362.1567, found: 362.1569.



**$^{15}N,^{15}N'$ -Diphenyldiazomethane (3.5b).** To a solution of  $^{15}N$  enriched benzophenone hydrazone (0.6135 g, 3.09 mmol) in petroleum ether 30-60 (30 mL) was added yellow mercuric oxide (1.2369 g, 5.71 mmol) and the mixture was vigorously shaken in the dark for 10.5 h. The mixture was then filtered and the solvent evaporated in vacuo to yield a dark purple solid (0.5539 g, 92%): IR ( $CDCl_3$ ,  $CaF_2$ ,  $cm^{-1}$ )  $\nu_{max}$  1978, ( $NaCl$ , film,  $cm^{-1}$ )  $\nu_{max}$  1973;  $^1H$  NMR (500 MHz,  $CDCl_3$ )  $\delta$  7.41-7.37 (4H, m, ArH), 7.31-7.29 (4H, m, ArH), 7.21-7.16 (2H, m, ArH);  $^{13}C$  NMR (125.8 MHz,  $CDCl_3$ )  $\delta$  129.5 (d,  $^2J_{NC} = 1.4$  Hz, ArC) 129.1,

125.6, 125.2, 62.3 (dd,  $^1J_{\text{NC}} = 23.7$  Hz,  $^2J_{\text{NC}} = 2.9$  Hz, C=N<sub>2</sub>);  $^{15}\text{N}$  NMR (30.4 MHz, CDCl<sub>3</sub>, DMSO-*d*<sub>6</sub> lock solvent)  $\delta$  439.9 (d,  $^1J_{\text{NN}} = 9.6$  Hz), 304.9 (d,  $^1J_{\text{NN}} = 9.6$  Hz); MS *m/z* (rel. intensity) (EI) 196 (M<sup>+</sup>, 8), 182 (3), 166 (68), 165 (100), 139 (8), 115 (3), 105 (3), 82 (6), 63 (3), 51 (3); HRMS (EI) calc. for C<sub>13</sub>H<sub>10</sub><sup>15</sup>N<sub>2</sub>: 196.0785, found: 196.0780.



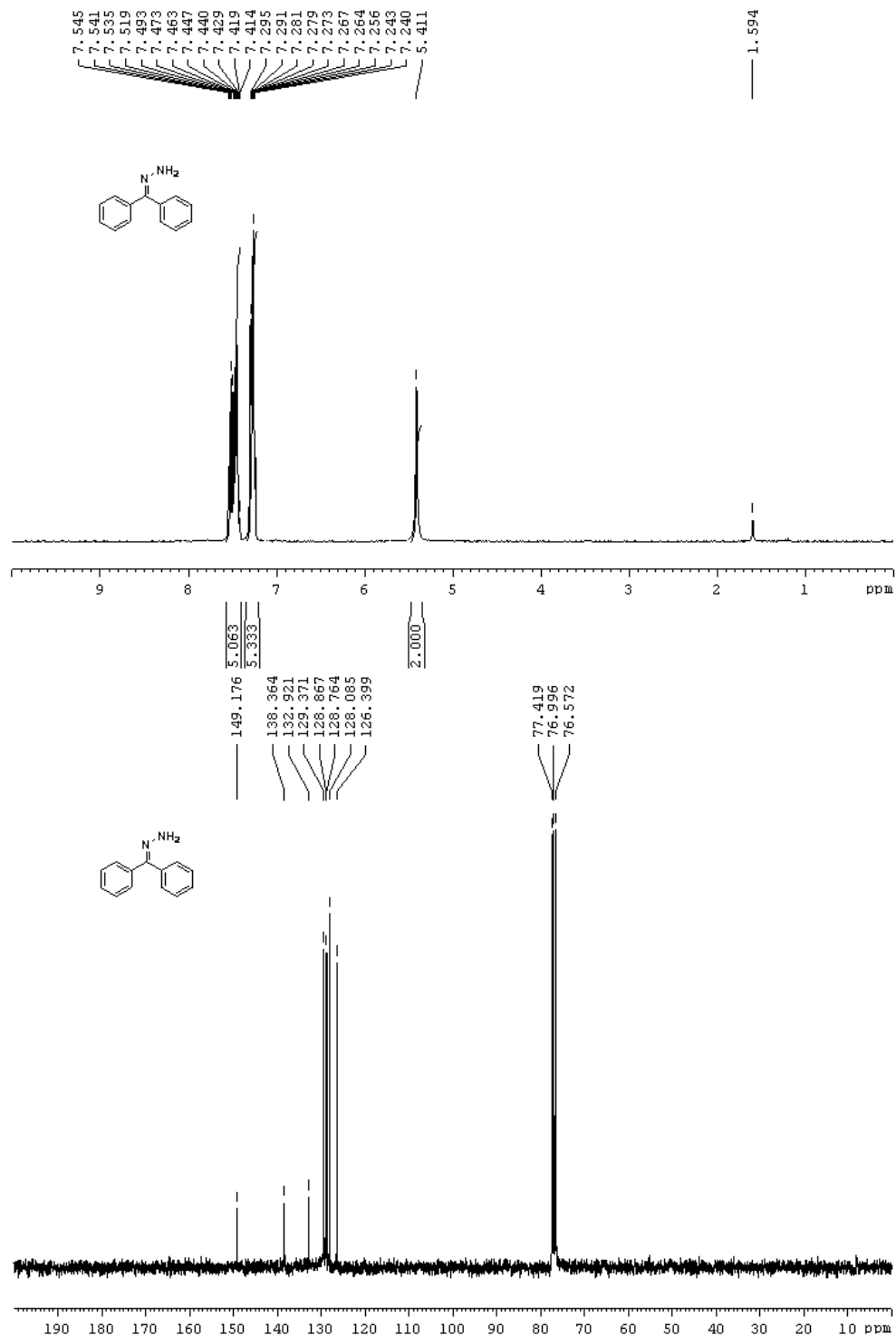
***N*-(Diphenylmethylene)nitramide (3.7), Benzophenone (3.8), Dinitrodiphenylmethane (3.9).**  $^{15}\text{N}$ -enriched diphenyldiazomethane (0.4049 g, 2.07 mmol) was dissolved in a degassed solution of a 50/50 (v/v) benzene/cyclohexane (70 mL). This solution was then purged continuously with a constant flow of nitric oxide for 2.5 h. NO was generated by the slow addition of separate degassed solutions of sodium nitrite (93.15 g in 250 mL aqueous solution) via a dropping funnel into L-ascorbic acid (118.8 g in 500 mL aqueous solution) using an in-house gas generating apparatus (Appendix A). The reaction flask was vented to prevent pressure buildup. The reaction flask was then sealed three hours after the entire addition of the sodium nitrite solution, and stirring continued overnight in the dark for another 14 h. The solution went from a deep purple to a yellow color overnight. The crude reaction mixture was then concentrated under reduced pressure and purified by silica gel column chromatography (5:1 then 2:1 hexanes:dichloromethane) to afford three products as white solids: nitrimine (0.2583 g, 55%), benzophenone (0.0675 g, 18%), and dinitrodiphenylmethane (0.027 g, 5%) which were equivalent to the corresponding products



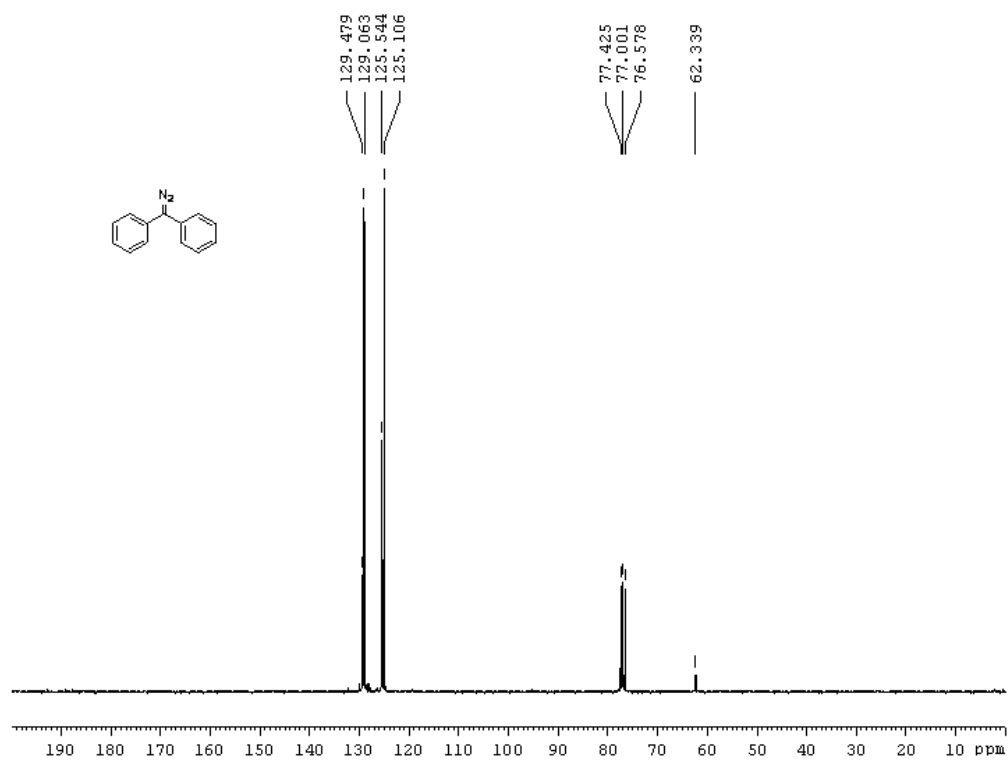
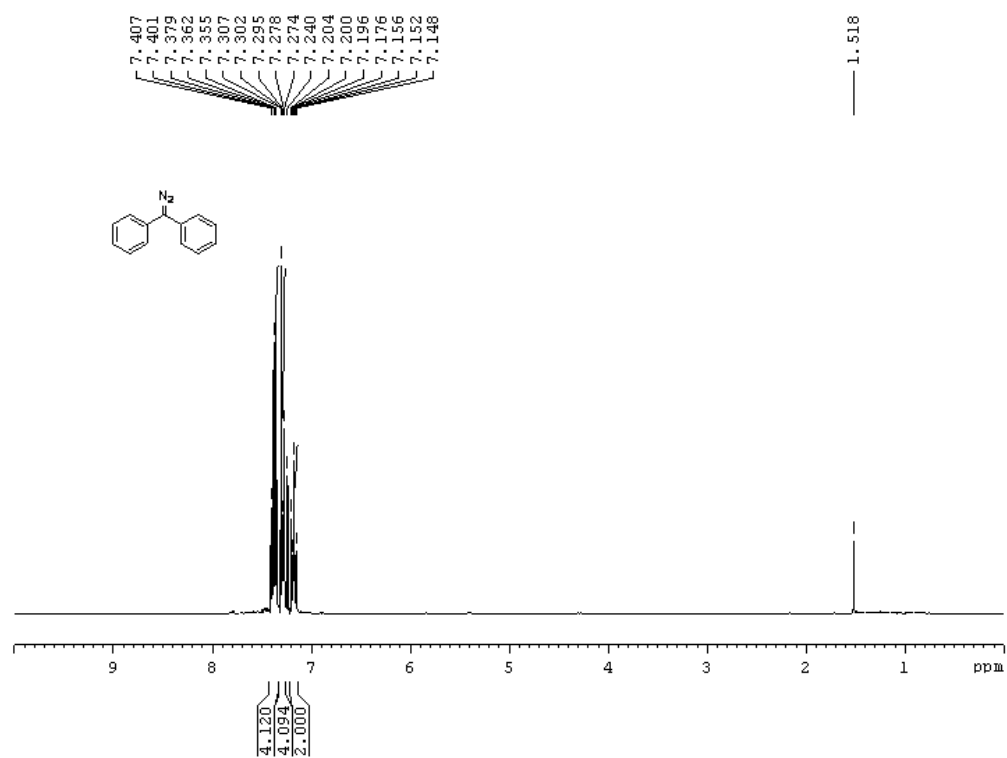
isolated from experiments employing **3.5a** by  $^1\text{H}$  NMR,  $^{13}\text{C}$  NMR and IR spectroscopy and MS spectrometry.

$^1\text{H}$ ,  $^{13}\text{C}$  and  $^{15}\text{N}$  NMR spectra

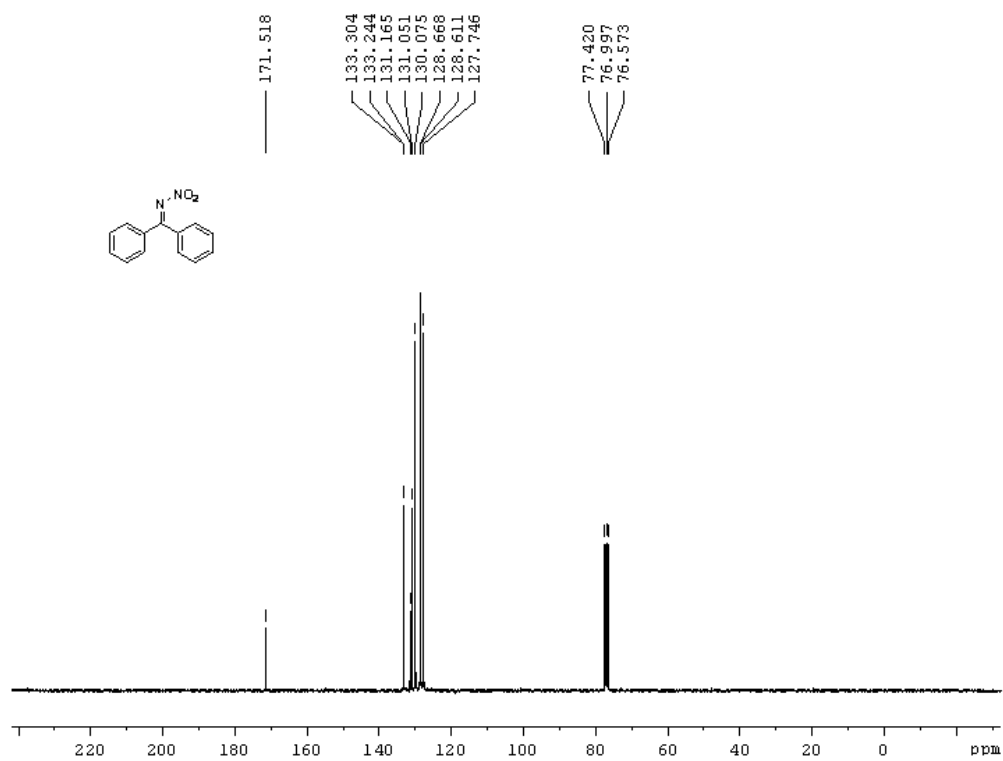
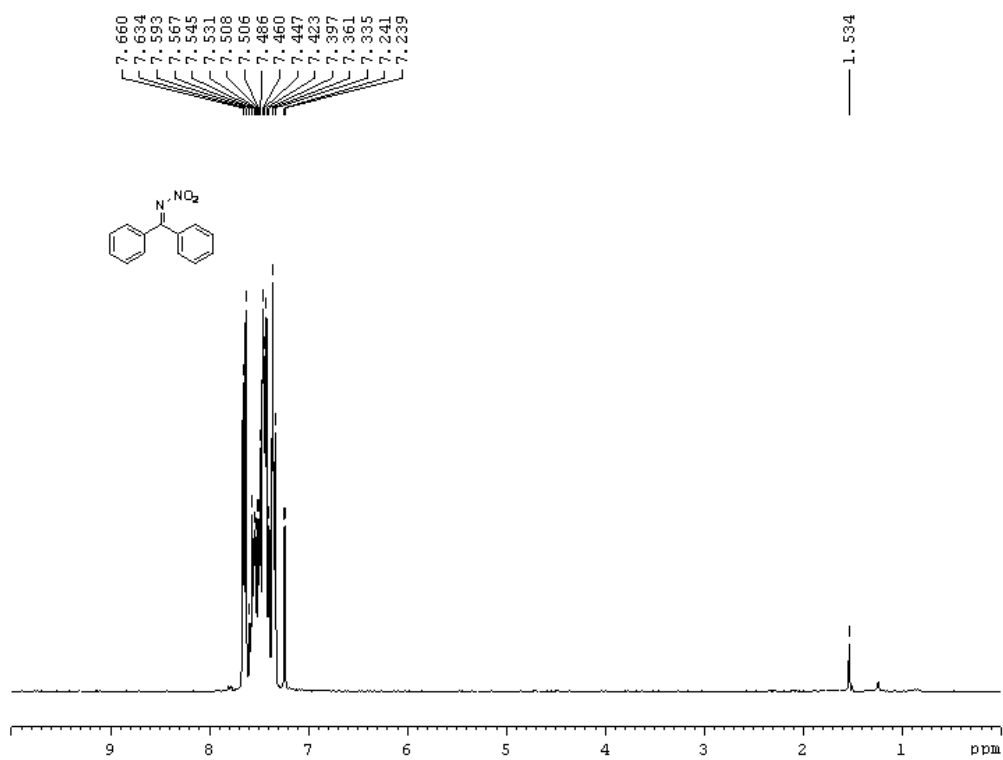
(Diphenylmethylene)hydrazine **3.4a** ( $^1\text{H}$  NMR 300 MHz;  $^{13}\text{C}$  NMR 75.5 MHz,  $\text{CDCl}_3$ ).



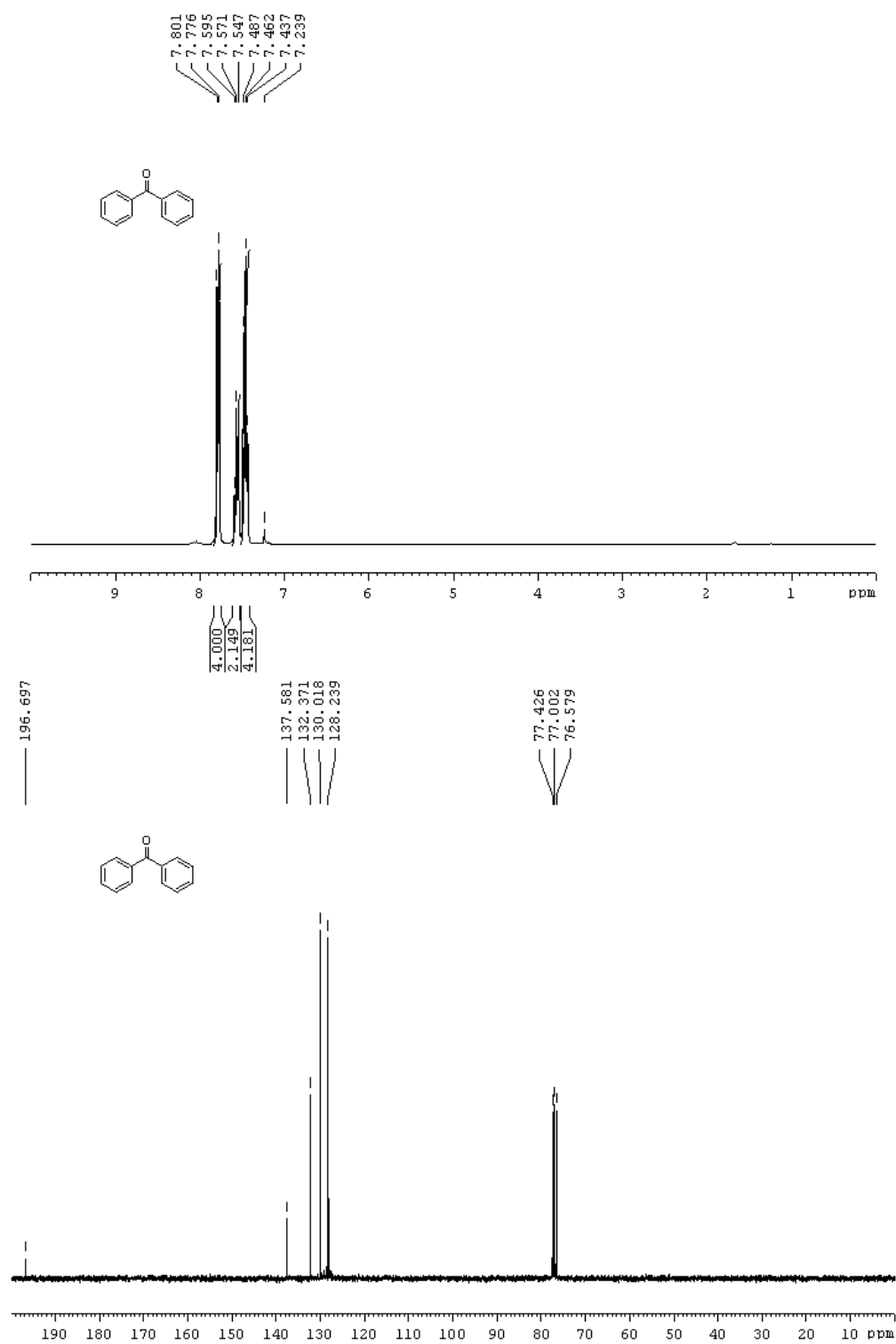
(Diazomethylene)dibenzene **3.5a** ( $^1\text{H}$  NMR 300 MHz;  $^{13}\text{C}$  NMR 75.5 MHz,  $\text{CDCl}_3$ ).



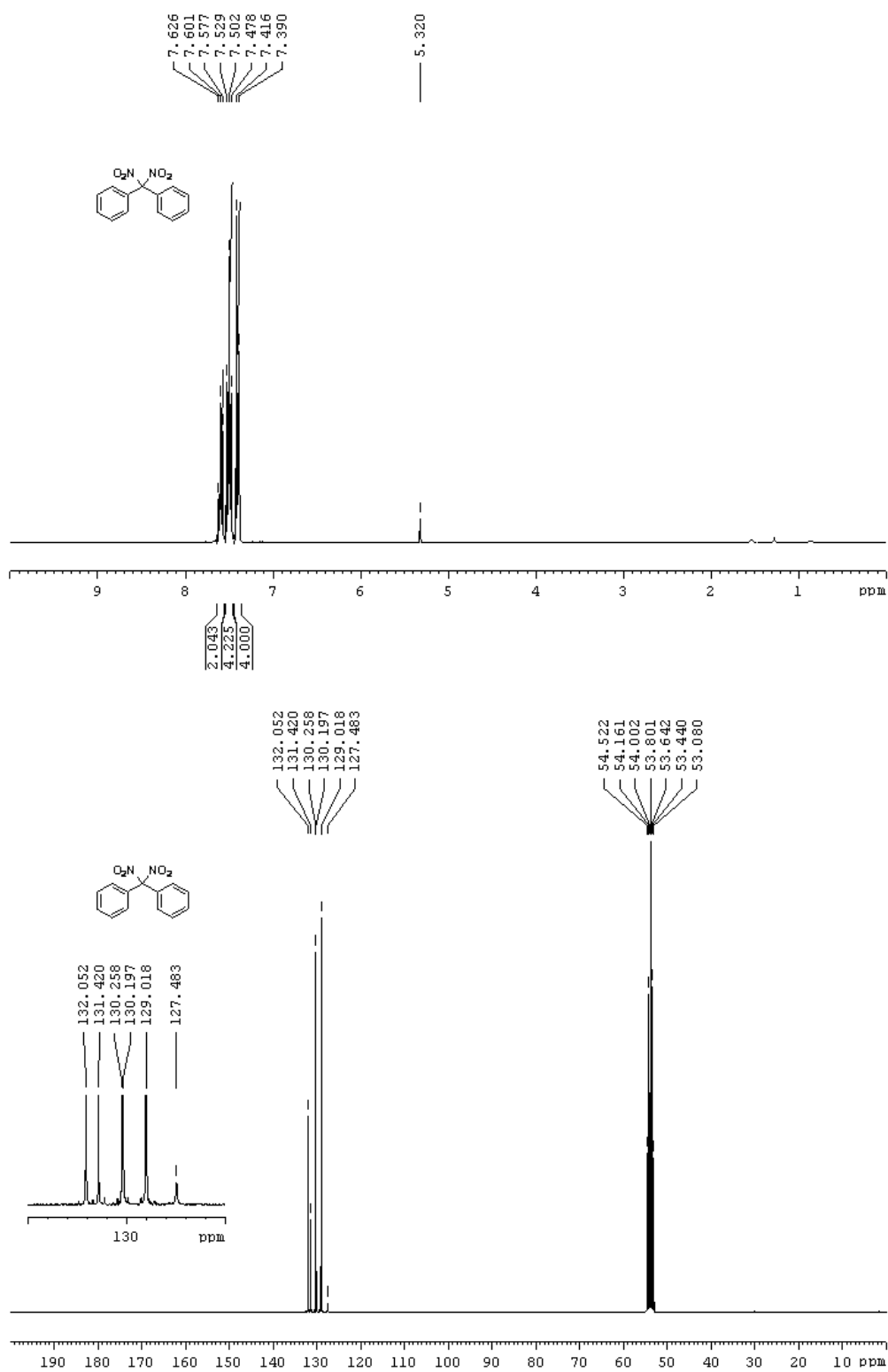
***N*-(Diphenylmethylene)nitramide 3.7** ( $^1\text{H}$  NMR 300 MHz;  $^{13}\text{C}$  NMR 75.5 MHz,  $\text{CDCl}_3$ ).



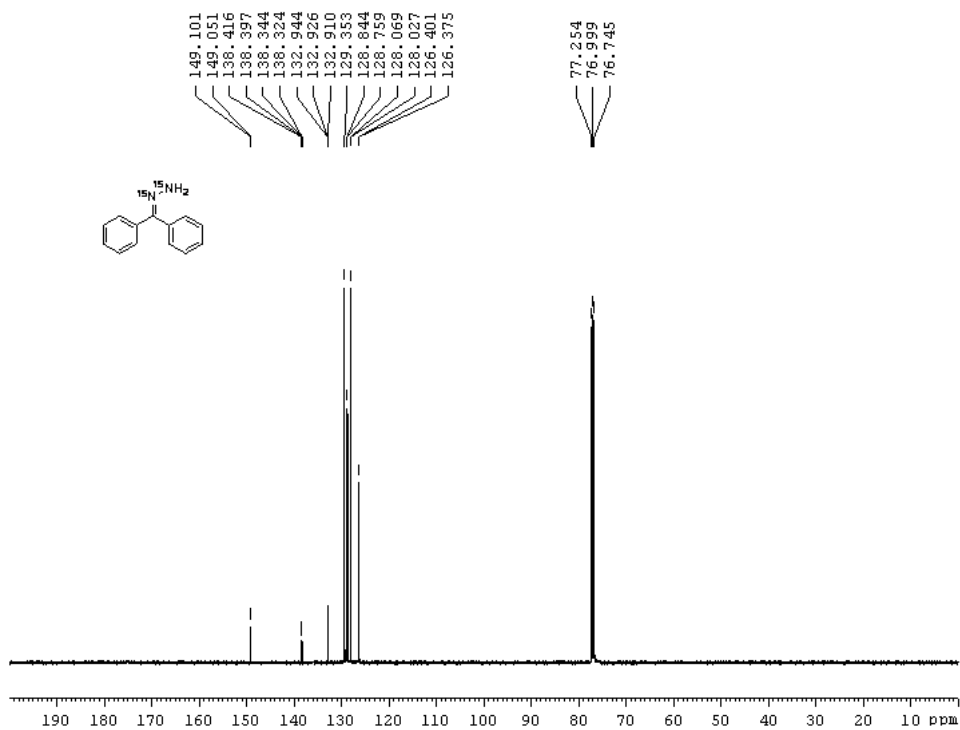
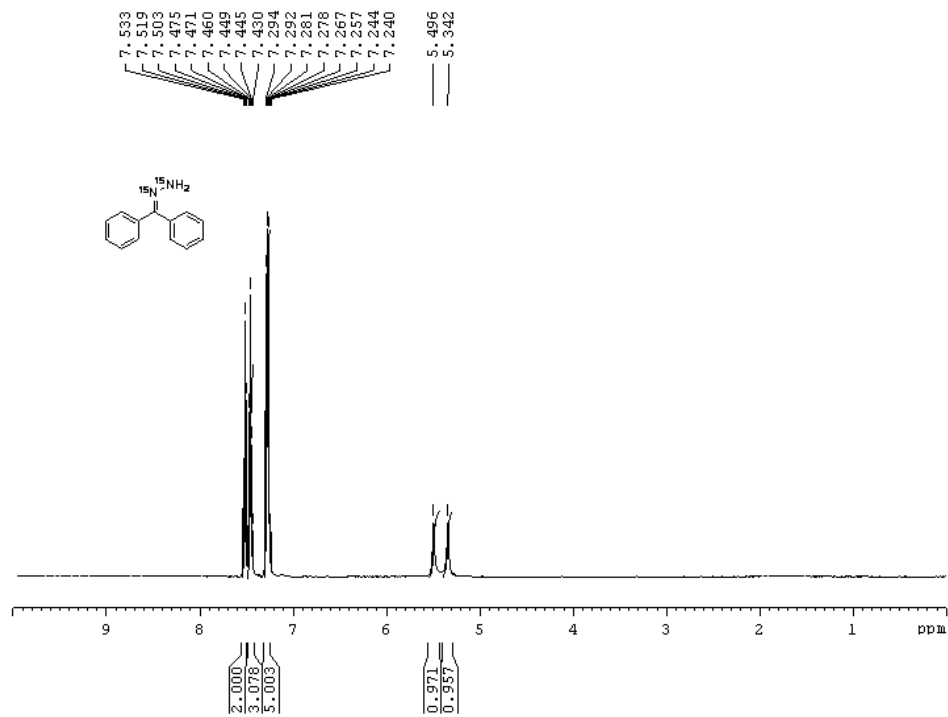
**Benzophenone 3.8** ( $^1\text{H}$  NMR 300 MHz;  $^{13}\text{C}$  NMR 75.5 MHz,  $\text{CDCl}_3$ ).

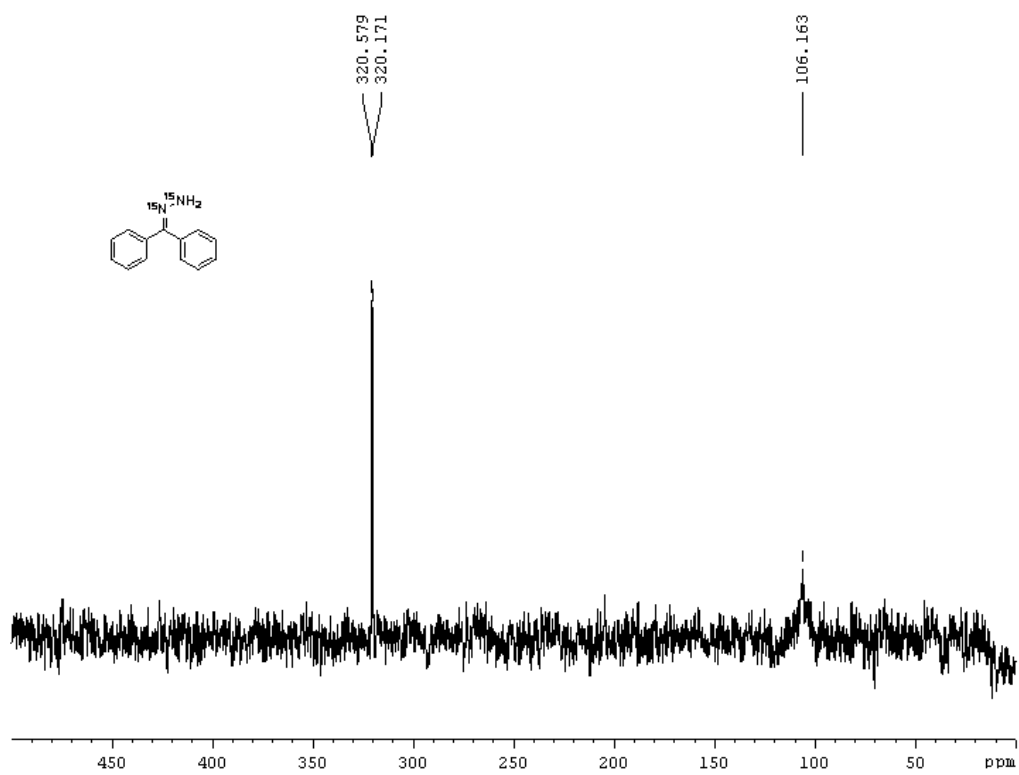


**Dinitrodiphenylmethane 3.9** ( $^1\text{H}$  NMR 300 MHz;  $^{13}\text{C}$  NMR 75.5 MHz,  $\text{CD}_2\text{Cl}_2$ ).



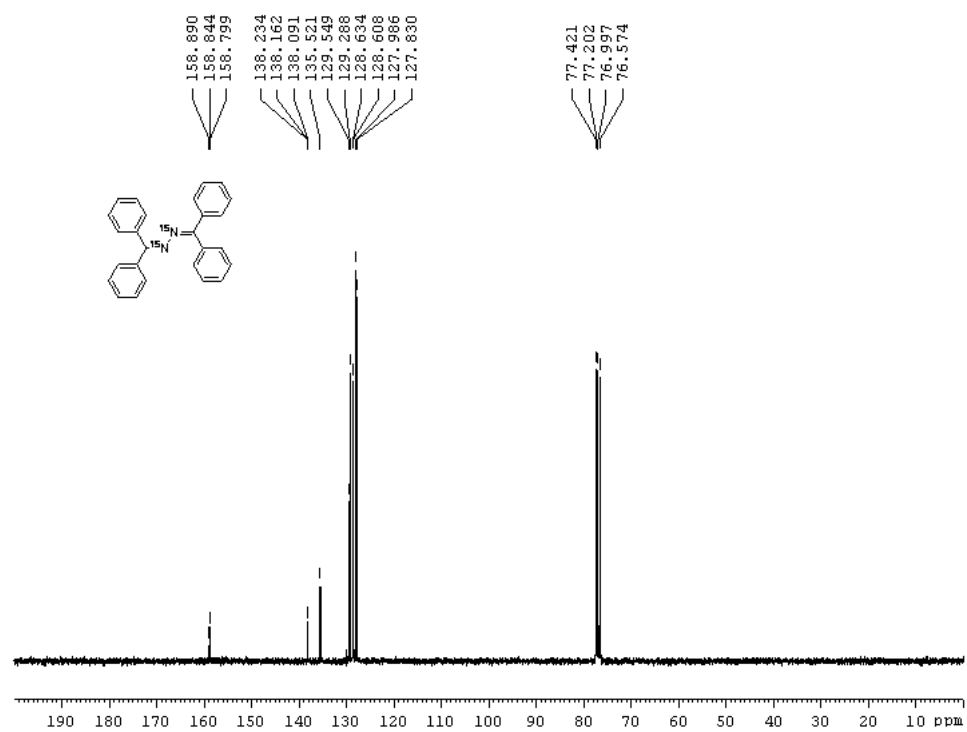
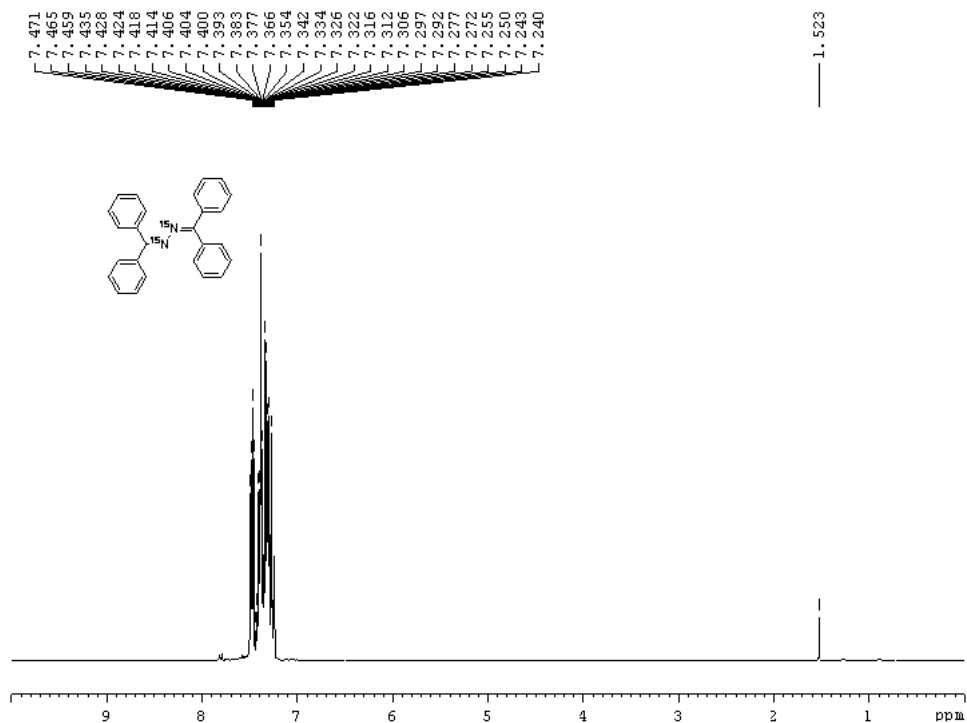
$^{15}\text{N}, ^{15}\text{N}'$ -(Diphenylmethylene)hydrazine **3.4b** ( $^1\text{H}$  NMR 500 MHz;  $^{13}\text{C}$  NMR 125.8 MHz,  $\text{CDCl}_3$ ;  $^{15}\text{N}$  30.4 MHz  $\text{CDCl}_3$ ,  $\text{DMSO-}d_6$  lock solvent).

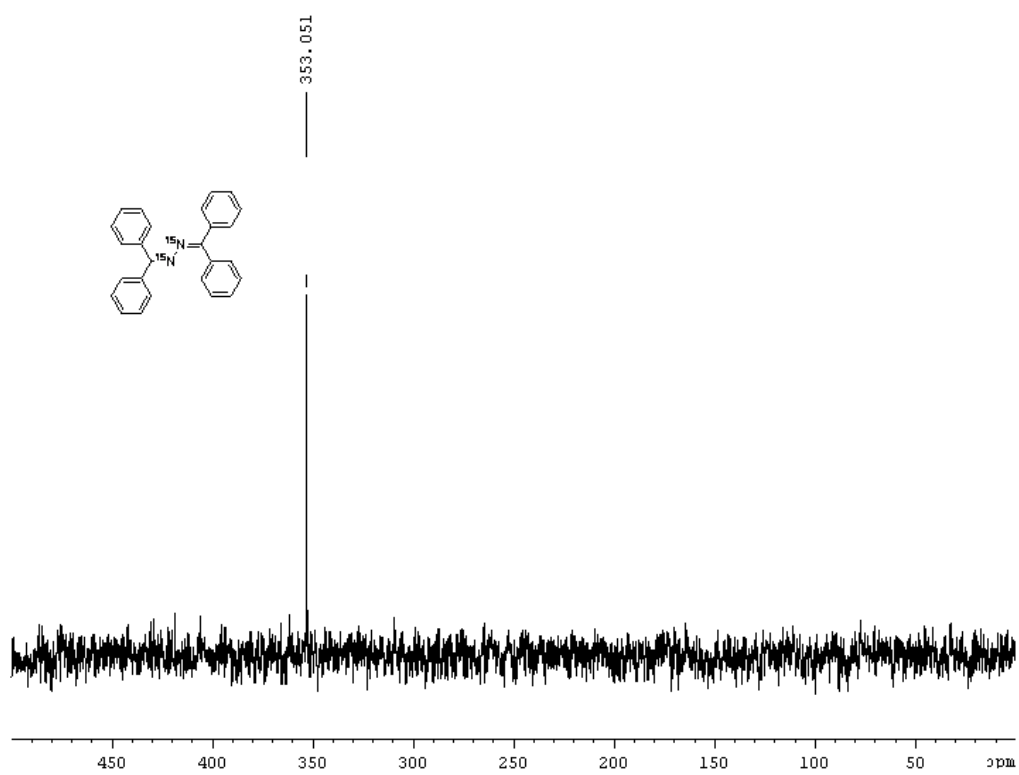




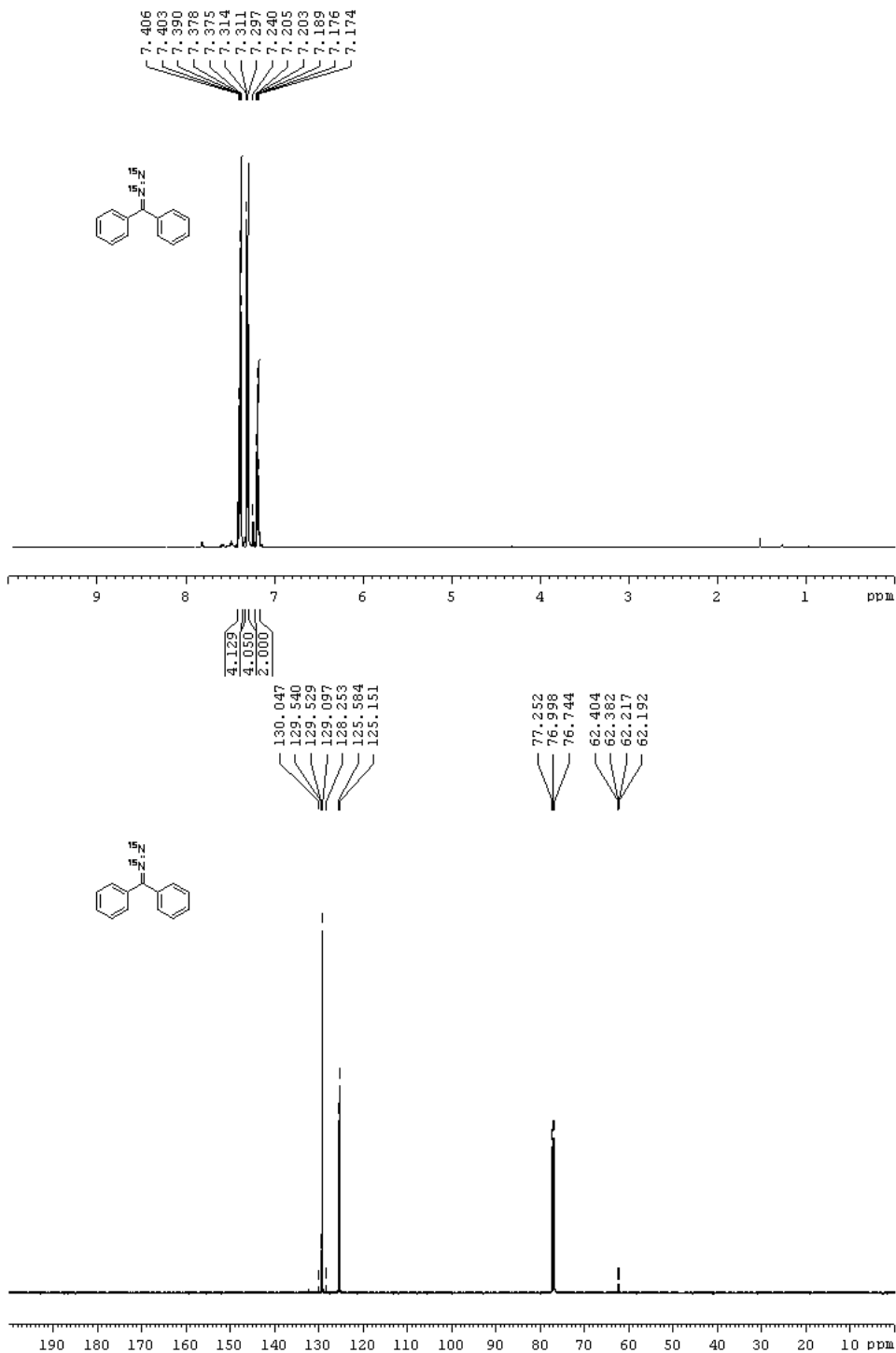


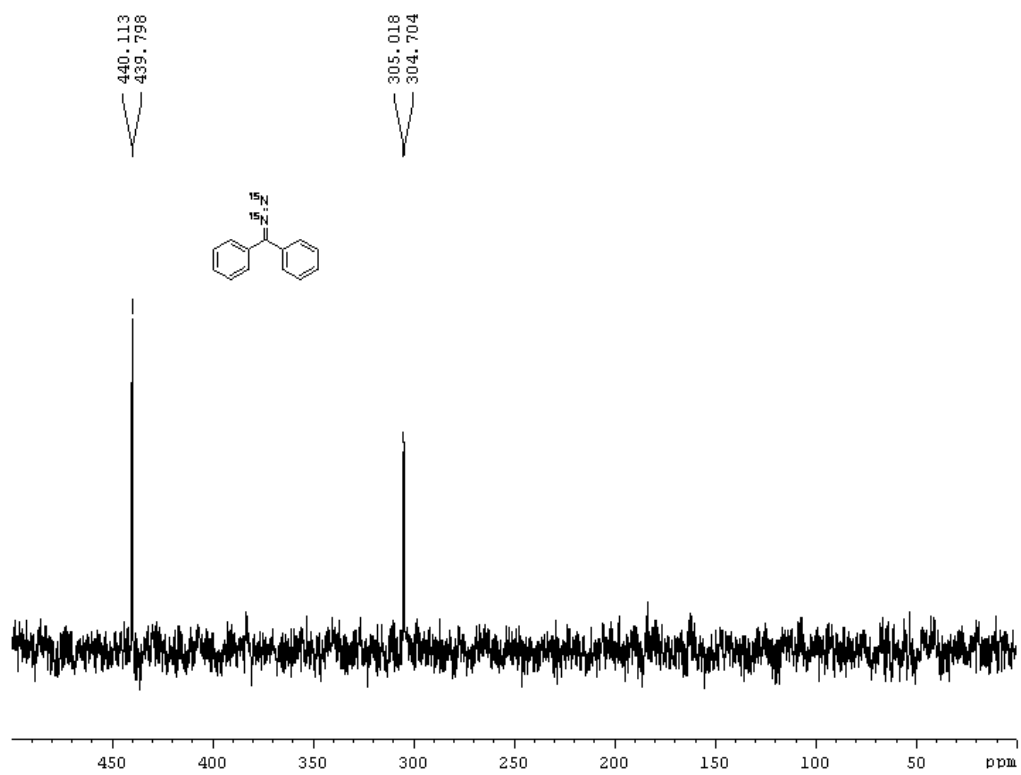
$^{15}\text{N}, ^{15}\text{N}'$ -1,2-bis(Diphenylmethylene)hydrazine **3.29** ( $^1\text{H}$  NMR 300 MHz;  $^{13}\text{C}$  NMR 75.5 MHz,  $\text{CDCl}_3$ ;  $^{15}\text{N}$  30.4 MHz  $\text{CDCl}_3$ ,  $\text{DMSO}-d_6$  lock solvent).

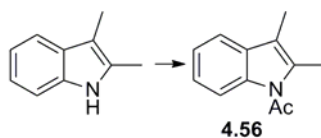




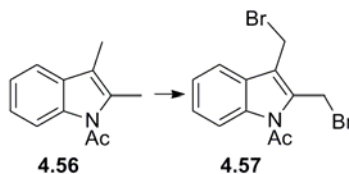
$^{15}\text{N}, ^{15}\text{N}'$ -(Diazomethylene)dibenzene **3.5b** ( $^1\text{H}$  NMR 500 MHz;  $^{13}\text{C}$  NMR 125.8 MHz,  $\text{CDCl}_3$ ;  $^{15}\text{N}$  30.4 MHz  $\text{CDCl}_3$ ,  $\text{DMSO-}d_6$  lock solvent).





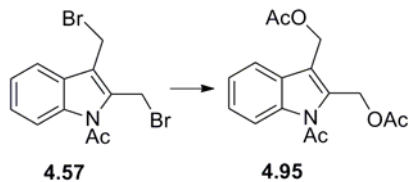


**1-(2,3-Dimethyl-1H-indol-1-yl)ethanone (4.56).** The following procedure is a modification of the procedure reported by Dave and Wharnoff.<sup>497</sup> To a stirred solution of *para*-toluenesulfonic acid hydrate (0.253 g, 1.33 mmol) in acetic anhydride (300 mL) was added 2,3-dimethylindole (22.9981 g, 0.158 mol) and then refluxed at 130 °C for 11 h. The residue was cooled and the excess acetic anhydride was evaporated either by vacuum distillation or on a rotary evaporator. The crude material was then applied to a bed of silica gel and target compound was purified eluting with 30:70 ether:pet ether to furnish the title compound as an off-white solid (23.33 g, 79%): mp 69-70 °C (lit. value<sup>497</sup> 68-70 °C); <sup>1</sup>H NMR (300 MHz, CDCl<sub>3</sub>) δ 7.96-7.93 (1H, m, ArH), 7.40-7.38 (1H, m, ArH), 7.25-7.22 (2H, m, ArH), 2.58 (3H, s, NC(O)CH<sub>3</sub>), 2.45 (3H, s, CH<sub>3</sub>), 2.13 (3H, s, CH<sub>3</sub>); <sup>13</sup>C NMR (75.5 MHz, CDCl<sub>3</sub>) δ 170.1, 135.6, 132.5, 131.2, 123.7, 122.8, 118.1, 115.4, 114.9, 27.5, 14.4, 8.7; MS *m/z* (rel. intensity) (EI) 187 (M<sup>+</sup>, 84), 145 (100), 144 (82), 130 (32), 115 (5), 77 (6), 51(2).



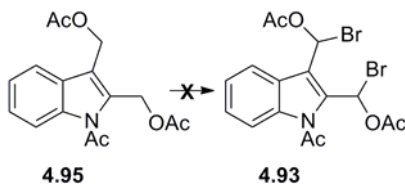
**1-(2,3-bis(Bromomethyl)-1H-indol-1-yl)ethanone (4.57).** The following procedure is a modification of the procedure described by Wu.<sup>386</sup> A solution of *N*-acetyl-2,3-dimethylindole **4.56** (4.0057 g, 21.4 mmol) and NBS (8.0067 g, 44.9 mmol) in CH<sub>2</sub>Cl<sub>2</sub> (350 mL) was heated

at reflux using a 250 W Brooder lamp for 100 min, cooled to ambient temperature and filtered through Celite 545. The solution was washed twice with water, once with brine, dried over Na<sub>2</sub>SO<sub>4</sub>, filtered and evaporated under reduced pressure to afford 7.3664 g (99%) of the title compound<sup>498</sup> as a white solid: <sup>1</sup>H NMR (300 MHz, CDCl<sub>3</sub>) δ 7.75 (1H, d, *J* = 8.2 Hz, Ar*H*), 7.68 (1H, d, *J* = 7.5 Hz, Ar*H*), 7.42-7.32 (2H, m, Ar*H*), 5.08 (2H, s, CH<sub>2</sub>Br), 4.69 (2H, s, CH<sub>2</sub>Br), 2.85 (3H, s, NC(O)CH<sub>3</sub>); <sup>13</sup>C NMR (75.5 MHz, CDCl<sub>3</sub>) δ 169.9, 135.8, 134.9, 127.8, 126.2, 123.6, 120.0, 119.7, 114.7, 27.5, 23.1, 21.1; MS *m/z* (rel. intensity) (EI) 347 (4, M<sup>+</sup> for C<sub>12</sub>H<sub>11</sub><sup>81</sup>Br<sub>2</sub>NO), 345 (9, M<sup>+</sup> for C<sub>12</sub>H<sub>11</sub><sup>81/79</sup>Br<sub>2</sub>NO), 343 (4, M<sup>+</sup> for C<sub>12</sub>H<sub>11</sub><sup>79</sup>Br<sub>2</sub>NO), 266 (28), 264 (28), 224 (46), 222 (47), 167 (16), 149 (36), 143 (100), 115 (13), 102 (4), 57 (4).

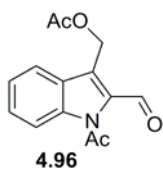


**(1-Acetyl-1*H*-indole-2,3-diyl)bis(methylene) diacetate (4.95).** Following a published procedure,<sup>401</sup> a round bottom flask was charged with acetic acid (20 mL), acetic anhydride (4 mL) and zinc oxide (0.5283 g, 6.49 mmol) and stirred for 10 min. Indole **4.57** (1.5384 g, 4.46 mmol) was added and the solution was stirred vigorously for 3.5 h at which point water (60 mL) was added and the mixture briefly stirred. The mixture was filtered and extracted with ether three times. The ethereal extracts were pooled and washed with a saturated solution of NaHCO<sub>3</sub> until bubbling ceased. CAUTION: abundant gas (CO<sub>2</sub>) evolution. The pooled extracts were dried over Na<sub>2</sub>SO<sub>4</sub>, filtered and the solvent evaporated in vacuo, producing a

yellow oil which was purified through a small plug (20 mL) of silica gel (2:1 hexanes:ethyl acetate) furnishing the target compound as a light tan-yellow solid (0.9614 g, 71%): mp 61-62 °C; IR (NaCl, film,  $\text{cm}^{-1}$ )  $\nu_{\text{max}}$  1740, 1461, 1373, 1306, 1234, 1142, 1023, 962, 750;  $^1\text{H}$  NMR (300 MHz,  $\text{CDCl}_3$ )  $\delta$  7.86 (1H, d,  $J = 8.2$  Hz, ArH), 7.68 (1H, d,  $J = 7.8$  Hz, ArH), 7.40-7.27 (2H, m, ArH), 5.56 (2H, s,  $\text{CH}_2\text{OAc}$ ), 5.36 (2H, s,  $\text{CH}_2\text{OAc}$ ), 2.79 (3H, s,  $\text{NC(O)CH}_3$ ), 2.05 (3H, s,  $\text{OC(O)CH}_3$ ), 2.03 (3H, s,  $\text{OC(O)CH}_3$ );  $^{13}\text{C}$  NMR (75.5 MHz,  $\text{CDCl}_3$ )  $\delta$  170.8, 170.4, 169.8, 135.8, 133.4, 128.6, 125.8, 123.5, 119.9, 119.1, 114.9, 57.0, 56.2, 27.1, 20.8; MS  $m/z$  (rel. intensity) (EI) 303 (41,  $\text{M}^+$ ), 278 (4), 261 (28), 243 (11), 224 (1), 202 (27), 201 (26), 173 (8), 159 (100), 145 (31), 142 (32), 130 (18), 115 (6), 84 (10), 77 (3), 51 (3).

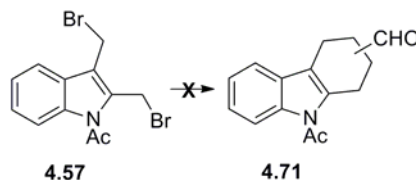


**Synthetic efforts towards (1-Acetyl-1H-indole-2,3-diyl)bis(bromomethylene) diacetate (4.93).** A solution of the bis-acetoxy indole **4.95** (1.0011 g, 3.3 mmol) in dry  $\text{CH}_2\text{Cl}_2$  (120 mL) and NBS (1.3495 g, 7.6 mmol) was heated at reflux using a 250 W Brooder lamp for 3 h generating a complex mixture. The solvent was evaporated under reduced pressure. The residue was dissolved in a small amount of  $\text{CH}_2\text{Cl}_2$  at which time gaseous fumes of acetic acid were generated. Purification by silica gel chromatography (3:1 hexanes:ethyl acetate) provided the side product **4.96** (0.1107 g, 13%) as a yellow oil:



**(1-Acetyl-2-formyl-1H-indol-3-yl)methyl acetate (4.96).**  $^1\text{H}$  NMR (300 MHz,  $\text{CDCl}_3$ )  $\delta$  10.46 (1H, s, CHO), 8.39 (1H, d,  $J = 7.6$  Hz, ArH), 7.76 (1H, d,  $J = 7.9$  Hz, ArH), 7.45-7.35 (2H, m, ArH), 5.76 (2H, s,  $\text{CH}_2\text{OAc}$ ),

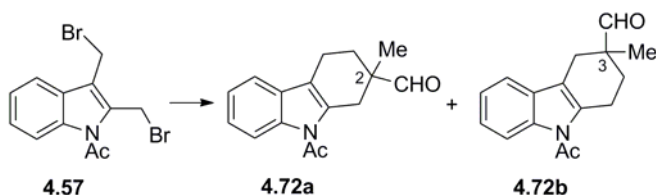
2.86 (3H, s,  $\text{NHCOCH}_3$ ), 2.08 (3H, s,  $\text{OCOCH}_3$ );  $^{13}\text{C}$  NMR (75.5 MHz,  $\text{CDCl}_3$ )  $\delta$  186.4, 170.5, 170.2, 142.5, 135.4, 126.4, 125.9, 124.9, 122.7, 120.6, 114.0, 56.1, 27.3, 20.7; MS  $m/z$  (rel. intensity) (EI) 259 ( $\text{M}^+$ , 20), 217 (45), 199 (14), 175 (100), 157 (42), 144 (19), 129 (55), 102 (11), 77 (6), 51 (2).



**Synthetic efforts towards increasing the yield of Diels-Alder adduct 4.71.** A solution of 2,3-bis(bromomethyl) indole **4.57** (0.1291 g, 0.37 mmol) in  $\text{CH}_2\text{Cl}_2$  (2 mL) was cooled to  $-78$  °C. To this was added a solution of TBAI (1.0438 g, 2.83 mmol) in  $\text{CH}_2\text{Cl}_2$  (2 mL), stirred for 5 min and then transferred to a  $-30$  °C bath. The temperature was permitted to rise to  $-23$  °C (approximately 20 min) at which time a white precipitate disappeared and the solution turned brown in colour. The solution was then re-cooled to  $-78$  °C. To this was added a separate solution of 1,3-propanedithiol (0.040 mL, 0.39 mmol) and 2,6-di-*tert*-butyl-4-methylpyridine (0.1432 g, 0.69 mmol) in  $\text{CH}_2\text{Cl}_2$  (0.5 mL) and the solution was stirred for 30 min. Then a solution of acrolein (0.055 mL at 90%,  $\sim 0.74$  mmol, filtered through a bed of  $\text{CaSO}_4$ ) in  $\text{CH}_2\text{Cl}_2$  (0.5 mL) was added to the reaction mixture which was then stirred for 7 min. To this was added  $\text{SnCl}_4$  (0.44 mL of a 1.0 M solution in  $\text{CH}_2\text{Cl}_2$ , 0.44 mmol) and

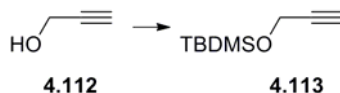


stirred for 18 h at -78 °C. The reaction mixture was quenched with a saturated solution of sodium bicarbonate at this temperature and permitted to come to ambient temperature at which time a portion of a saturated solution of NaS<sub>2</sub>O<sub>3</sub> was added. The mixture was extracted with ether three times and pooled. The extracts were washed once with a saturated solution of NaS<sub>2</sub>O<sub>3</sub>, water once, brine once and dried over Na<sub>2</sub>SO<sub>4</sub>, filtered and the solvent evaporated in vacuo to give 0.1439 g of a yellow-white residue that contained the known dimer **4.55** as the major constituent.

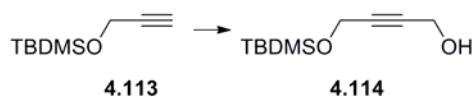


**Synthetic efforts towards increasing the yield of Diels-Alder adduct 4.72.** This experiment was executed under similar conditions as described above for **4.71**. The amounts of the reagents are given and are listed in the order in which they were employed: 2,3-bis(bromomethyl) indole (0.1322 g, 0.38 mmol), TBAI (1.0686 g, 2.89 mmol), Proton sponge® (0.1485 g, 0.69 mmol), methacrolein (0.06 mL, 0.73 mmol), SnCl<sub>4</sub> (0.42 mL of a 1.0 M solution in CH<sub>2</sub>Cl<sub>2</sub>, 0.42 mmol). Silica gel chromatography (3:1 hexanes:ethyl acetate) afforded 0.0553 g (57%) of an inseparable mixture of the two regioisomers as a yellow solid in a ratio of 21:1 for **4.72a**:**4.72b**. The ratio was obtained by integrating the aldehydic protons for each regioisomer. The remaining signals of the minor regioisomer were obscured. The following assignments apply to the C-2 regioisomer **4.72a**: <sup>1</sup>H NMR (500 MHz, CDCl<sub>3</sub>) δ 9.58 (1H, s, CHO), 7.91 (1H, d, *J* = 8.1 Hz, ArH), 7.43 (1H, d, *J* = 7.1 Hz, ArH), 7.34-7.26

(2H, m, ArH), 3.50 (1H, d,  $J = 17.7$  Hz, CH), 2.90 (1H, d,  $J = 17.7$  Hz, CH), 2.83 (3H, s, NHC(O)CH<sub>3</sub>), 2.75-2.69 (2H, m, CH), 2.16-2.13 (1H, m, CH), 1.83-1.79 (1H, m, CH), 1.25 (3H, s, CH<sub>3</sub>).



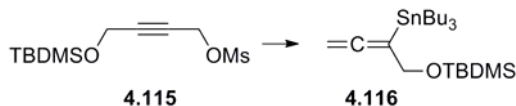
**tert-Butyldimethyl(prop-2-yn-1-yloxy)silane (4.113).** Following procedures described by Marshall and Palovich,<sup>405</sup> a stirred solution of propargyl alcohol (20 mL, 0.34 mol) and imidazole (36.09 g, 0.53 mol) in DMF (250 mL) was cooled to 0 °C and TBDMSCl (52.31 g, 0.35 mol) was added. Stirring was continued for 5 h. The reaction was quenched with water and the reaction mixture was extracted with ether three times. The ethereal extracts were pooled, washed with water twice, brine once, dried over MgSO<sub>4</sub>, filtered and concentrated in vacuo to yield 57.23 g (98%) of the title compound<sup>499</sup> as clear pale yellow oil: IR (NaCl film, cm<sup>-1</sup>)  $\nu_{\max}$  3314, 2931, 2860, 1473, 1369, 1257, 1099, 1005, 838, 779, 662; <sup>1</sup>H NMR (300 MHz, CDCl<sub>3</sub>)  $\delta$  4.29 (2H, d,  $J = 2.4$  Hz, TBDMSOCH<sub>2</sub>), 2.37 (1H, t,  $J = 2.4$ , C≡CH), 0.89 (9H, s, SiC(CH<sub>3</sub>)<sub>3</sub>), 0.10 (6H, s, Si(CH<sub>3</sub>)<sub>2</sub>); <sup>13</sup>C NMR (75.5 MHz, CDCl<sub>3</sub>)  $\delta$  82.4, 72.8, 51.5, 25.8, 18.3, -5.2; MS  $m/z$  (rel. intensity) (EI) 170 (M<sup>+</sup>, 4), 155 (3), 113 (100), 83 (63), 75 (13).



**4-((tert-Butyldimethylsilyl)oxy)but-2-yn-1-ol (4.114).** Following a published procedure,<sup>405</sup> a stirred solution of the silyl ether 4.113 (34.80 g, 0.204 mol) in THF (500 mL)

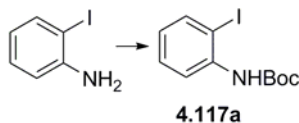


mesyl chloride (11 mL, 0.142 mol) were added and stirring continued for 40 min at 0 °C. The reaction mixture was then quenched with a saturated solution of sodium bicarbonate and extracted three times with CH<sub>2</sub>Cl<sub>2</sub>. The pooled extracts were washed with water, brine and dried over sodium sulfate, filtered and concentrated in vacuo to yield the title compound<sup>501</sup> as a gold oil (24.72 g, 91%): IR (NaCl, film, cm<sup>-1</sup>)  $\nu_{\max}$  3030, 2931, 2859, 1473, 1363, 1256, 1177, 1143, 1083, 942, 836, 716, 668; <sup>1</sup>H NMR (300 MHz, CDCl<sub>3</sub>)  $\delta$  4.86 (2H, t,  $J$  = 1.7 Hz, MsOCH<sub>2</sub>), 4.34 (2H, t,  $J$  = 1.7 Hz, SiOCH<sub>2</sub>), 3.09 (3H, s, SO<sub>2</sub>CH<sub>3</sub>), 0.87 (9H, s, SiC(CH<sub>3</sub>)<sub>3</sub>), 0.08 (6H, s, Si(CH<sub>3</sub>)<sub>2</sub>); <sup>13</sup>C NMR (75.5 MHz, CDCl<sub>3</sub>)  $\delta$  88.5, 76.7, 57.8, 51.4, 38.9, 25.7, 18.2, -5.3; MS  $m/z$  (rel. intensity) (EI) 221 (M<sup>+</sup> - *t*Bu, 1), 183 (3), 153 (100), 125 (3), 111 (2), 75 (23).



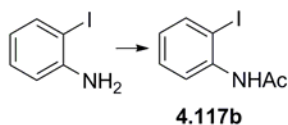
***tert*-Butyldimethyl((2-(tributylstannyl)buta-2,3-dien-1-yl)oxy)silane (4.116).** Following a published procedure,<sup>406</sup> a solution of diisopropylamine (9.0 mL, 0.064 mol) in THF (200 mL) was cooled to 0 °C to which *n*-BuLi (24.5 mL at 2.5 M, 0.061 mmol) was added and stirred for 30 min. Tributyltin hydride<sup>502</sup> (16.0 mL, 0.059 mmol) was added and stirring continued for another 30 min. The solution turned a lemon yellow color and the temperature was dropped to -78 °C. Then CuBr·SMe<sub>2</sub> (12.3143 g, 0.059 mmol), prepared by a modification of the methods described by Theis and Townsend<sup>503</sup> and Wuts,<sup>504</sup> was added in several portions over 15 min and stirred for a further 30 min in which the reaction solution developed a deep dark red colour. The mesylate **4.115** (8.1444 g, 0.029 mmol) was dissolved

in THF (10 mL) and cannulated into the tin-copper mixture. The solution was kept at -78 °C for 5 min and then the temperature was raised slowly to -20 °C over the course of 2 h. The solution developed a deep dark blackish-blue colour over this time. The reaction mixture was then poured into a 10% solution of NaCN (250 mL; or alternatively 19:1 NH<sub>4</sub>Cl:NH<sub>4</sub>OH and stirred until deep blue) and stirred vigorously. The black precipitates were allowed to settle, and the mixture was filtered through glass wool twice and ether (200 mL) was added. The organic phase was washed with water, brine, dried over Na<sub>2</sub>SO<sub>4</sub> and evaporated to dryness. The residue was purified by flash chromatography (100% hexanes) to yield 7.9752 g (58%) of the known allenylstannane<sup>406</sup> as clear colorless oil: IR (NaCl, film, cm<sup>-1</sup>)  $\nu_{\max}$  2929, 2856, 1930, 1464, 1361, 1255, 1081, 1049, 838, 802, 777, 668; <sup>1</sup>H NMR (300 MHz, CDCl<sub>3</sub>)  $\delta$  4.33-4.26 (2H, m, SiOCH<sub>2</sub>), 4.22-4.15 (2H, m, C=CH<sub>2</sub>), 1.55-0.85 (27H, m, (C<sub>4</sub>H<sub>9</sub>)<sub>3</sub>) overlapping with 0.89 (9H, s, SiC(CH<sub>3</sub>)<sub>3</sub>), 0.05 (6H, s, Si(CH<sub>3</sub>)<sub>2</sub>); <sup>13</sup>C NMR (75.5 MHz, CDCl<sub>3</sub>)  $\delta$  202.9, 94.3, 66.5, 64.1, 28.9, 27.3, 26.0, 18.5, 13.7, 10.4, -5.3; MS *m/z* (rel. intensity) (EI) 417 (for C<sub>18</sub>H<sub>37</sub>OSi<sup>120</sup>Sn = M<sup>+</sup> - Bu, 100), 415 (for C<sub>18</sub>H<sub>37</sub>OSi<sup>118</sup>Sn = M<sup>+</sup> - Bu, 74), 365 (67), 363 (58), 291 (29), 289 (23), 235 (33), 233 (26), 179 (28), 177 (26), 121 (6), 96 (4), 75 (39), 57 (5).



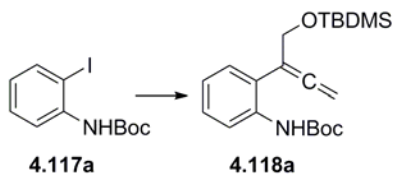
***tert*-Butyl (2-iodophenyl)carbamate (4.117a).** Following procedures described by Lamba and Tour,<sup>407</sup> 2-iodoaniline (5.5451 g, 0.025 mol) was added to a suspension of NaH (0.7051 g, 0.029 mol, previously washed three times with dry hexane) in THF (300 mL). The mixture

was heated at reflux at 80 °C for 50 min. The mixture was cooled to room temperature, di-*tert*-butyl dicarbonate (6.9471 g, 0.032 mol) was added and the reaction mixture was stirred for 35 min. A second portion of NaH was added (0.6451 g, 0.027 mol) and the solution was brought back to reflux for 9 h. The solution was cooled, quenched with water and extracted three times with ether and the extracts were pooled. The combined ethereal extracts were washed once with a saturated solution of NH<sub>4</sub>Cl, a saturated solution of NaHCO<sub>3</sub>, brine, dried over Na<sub>2</sub>SO<sub>4</sub>, filtered and the solvent evaporated in vacuo to give an amorphous brown oil. The oil was purified by silica gel chromatography (20:1 hexanes:ether) to afford 6.2953 g (78%) of the title compound<sup>505</sup> as a light yellow oil: IR (NaCl, film, cm<sup>-1</sup>)  $\nu_{\max}$  3395, 2979, 2931, 1737, 1588, 1573, 1517, 1454, 1432, 1392, 1368, 1298, 1279, 1247, 1223, 1155, 1120, 1061, 1042, 1024, 1011, 898, 830, 768, 749, 650; <sup>1</sup>H NMR (300 MHz, CDCl<sub>3</sub>)  $\delta$  8.03 (1H, d,  $J$  = 7.9 Hz, ArH6), 7.72 (1H, d,  $J$  = 7.7 Hz, ArH3), 7.29 (1H, dd,  $J$  = 7.7, 7.9 Hz, ArH5), 6.79 (1H, br s, NH) overlapping with 6.74 (1H, t,  $J$  = 7.7 Hz, ArH4), 1.51 (9H, s, OC(CH<sub>3</sub>)<sub>3</sub>); <sup>13</sup>C NMR (75.5 MHz, CDCl<sub>3</sub>)  $\delta$  152.5, 138.8, 129.1, 124.6, 120.1, 88.7, 80.9, 28.3, 27.9; MS  $m/z$  (rel. intensity) (EI) 319 (M<sup>+</sup>, 56), 263 (79), 245 (9), 219 (100), 136 (24), 119 (4), 91 (14), 90 (11), 57 (94).



***N*-(2-Iodophenyl)acetamide (4.117b).** Following procedures described by Sarvari and Sharghi,<sup>408</sup> 2-iodoaniline (4.9905 g, 0.022 mol) was added to a stirred suspension of zinc oxide (0.9394 g, 0.012 mol) in acetic anhydride (2.4 mL). The mixture was stirred for 45

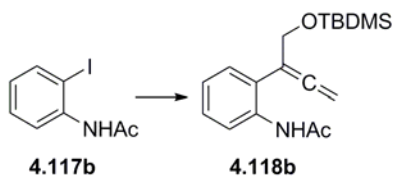
min. CAUTION: the flask becomes extremely hot as the acetic anhydride is consumed. Dichloromethane (5 mL) was added to the reaction mixture and stirring was continued for 15 min longer after which an additional portion of dichloromethane was added (5 mL). The solution was filtered, washed with a saturated solution of NaHCO<sub>3</sub>, water, brine, dried over Na<sub>2</sub>SO<sub>4</sub>, filtered and the solvent was evaporated under reduced pressure. The crude product was purified by silica gel chromatography (3:1 hexanes:ethyl acetate) to afford 5.3331 g (91%) of the title compound as a white solid: mp 106-107 °C (lit. value<sup>506</sup> 109-111 °C); IR (NaCl, film, cm<sup>-1</sup>)  $\nu_{\max}$  3273, 1659, 1582, 1575, 1532, 1464, 1532, 1464, 1433, 1369, 1294, 1016, 751; <sup>1</sup>H NMR (300 MHz, CDCl<sub>3</sub>)  $\delta$  8.18 (1H, br d, *J* = 7.7 Hz, Ar*H*6), 7.76 (1H, d, *J* = 7.9 Hz, Ar*H*3), 7.39 (1H, br s, NH) overlapping with 7.32 (1H, td, *J* = 7.7, 1.0 Hz, Ar*H*5), 6.83 (1H, dd, *J* = 7.7, 7.9 Hz, Ar*H*4), 2.22 (3H, s, NHC(O)CH<sub>3</sub>); <sup>13</sup>C NMR (75.5 MHz, CDCl<sub>3</sub>)  $\delta$  168.2, 138.7, 138.2, 129.3, 125.9, 122.1, 89.9, 24.8; MS *m/z* (rel. intensity) (EI) 261 (M<sup>+</sup>, 42), 219 (100), 134 (88), 92 (30), 65 (11); HRMS (EI) calc. for C<sub>8</sub>H<sub>8</sub>INO: 260.9651, found: 260.9655.



***tert*-Butyl (2-(1-((*tert*-butyldimethylsilyl)oxy)buta-2,3-dien-2-yl)phenyl)carbamate (4.118a).** From a modification of the procedure described by Mukai and Takahashi,<sup>406</sup> a flame dried round bottom flask was charged with the iodoaniline **4.117a** (2.1154 g, 6.63 mmol), allenylstannane **4.116** (3.4756 g, 7.34 mmol) and DMF (40 mL). This solution was

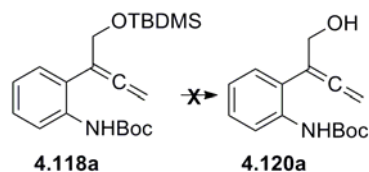
degassed twice under high vacuum using freeze-thaw conditions with argon purges. While the reaction mixture was still frozen, tri-(2-furyl)-phosphine (0.3749 g, 1.62 mmol), Pd<sub>2</sub>(dba)<sub>3</sub>·CHCl<sub>3</sub> (0.2111 g, 0.2 mmol), and CuI (0.1313 g, 0.69 mmol) were added under an argon atmosphere and degassed twice more and then stirred at room temperature for 16 h. The reaction was quenched with 10% NH<sub>4</sub>OH and extracted three times with ether and pooled. The pooled extracts were washed with water twice, brine once, dried over Na<sub>2</sub>SO<sub>4</sub>, filtered and the solvent evaporated in vacuo. The crude product was purified by flash chromatography (20:1 hexanes:ether) to afford 1.277 g (51%) of the allenylaniline<sup>406</sup> as a light yellow oil: IR (NaCl, film, cm<sup>-1</sup>)  $\nu_{\max}$  3426, 3339, 2930, 2858, 1954, 1732, 1585, 1520, 1449, 1392, 1367, 1300, 1238, 1159, 1048, 1024, 1007, 940, 902, 839, 777, 754, 670; <sup>1</sup>H NMR (300 MHz, CDCl<sub>3</sub>)  $\delta$  7.99 (1H, d,  $J$  = 7.9 Hz, ArH6), 7.53 (1H, br s, NH), 7.23 (1H, td,  $J$  = 7.9, 1.0 Hz, ArH5), 7.16 (1H, dd,  $J$  = 1.0, 7.7 Hz, ArH3), 6.98 (1H, ddd,  $J$  = 1.0, 7.7, 7.9 Hz, ArH4), 4.96 (2H, t,  $J$  = 2.3 Hz, C=CH<sub>2</sub>), 4.37 (2H, t,  $J$  = 2.3 Hz, SiOCH<sub>2</sub>), 1.49 (9H, s, OC(CH<sub>3</sub>)<sub>3</sub>), 0.87 (9H, s, SiC(CH<sub>3</sub>)<sub>3</sub>), 0.04 (6H, s, Si(CH<sub>3</sub>)<sub>2</sub>); <sup>13</sup>C NMR (75.5 MHz, CDCl<sub>3</sub>)  $\delta$  207.4, 153.1, 136.6, 128.8, 128.3, 124.9, 122.7, 120.2, 101.9, 80.1, 76.7, 65.4, 28.4, 25.9, 18.4, -5.4; MS  $m/z$  (rel. intensity) (CI, NH<sub>4</sub><sup>+</sup>) 393 (M<sup>+</sup> + 18, 19), 376 (M<sup>+</sup> + 1, 100), 337 (10), 320 (28), 274 (8), 233 (14), 218 (2), 159 (3), 144 (3), 90 (3).



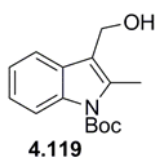


***N*-(2-(1-((*tert*-Butyldimethylsilyl)oxy)buta-2,3-dien-2-yl)phenyl)acetamide (4.118b).** In a similar fashion to the procedure described above for **4.118a**, a round bottom flask was charged with *N*-(2-iodophenyl)acetamide **4.117b** (1.2097 g, 4.63 mmol), allenylstannane **4.116** (1.8856 g, 3.98 mmol) and DMF (35 mL) under an argon atmosphere. This solution was degassed twice under high vacuum using freeze-thaw conditions with argon purges. While the reaction mixture was still frozen, tri-(2-furyl)-phosphine (0.2106 g, 0.91 mmol), Pd<sub>2</sub>(dba)<sub>3</sub> (0.1099 g, 0.12 mmol), and CuI (0.0764 g, 0.4 mmol) were added under an argon atmosphere. The mixture was degassed twice more and stirred at room temperature for 20 h. The reaction was quenched with 10% NH<sub>4</sub>OH and extracted three times with ether and pooled. The pooled extracts were washed with water twice, brine once, dried over Na<sub>2</sub>SO<sub>4</sub>, filtered and the solvent evaporated in vacuo. The crude product was purified by flash chromatography (5:1 then 3.5:1 hexanes:ethyl acetate) to afford 1.0451 g (83%) of the title compound as an orange oil: IR (NaCl, film, cm<sup>-1</sup>)  $\nu_{\max}$  3301, 3060, 2930, 1953, 1682, 1583, 1520, 1368, 1298, 1076, 833, 756; <sup>1</sup>H NMR (300 MHz, CDCl<sub>3</sub>)  $\delta$  8.35 (1H, br s, *NH*), 8.14 (1H, d, *J* = 8.2 Hz, *ArH*), 7.28-7.19 (2H, m, *ArH*), 7.05 (1H, t, *J* = 7.4 Hz, *ArH*), 4.97 (2H, m, C=CH<sub>2</sub>), 4.41 (2H, m, SiOCH<sub>2</sub>), 2.14 (3H, s, COCH<sub>3</sub>), 0.85 (9H, s, SiC(CH<sub>3</sub>)<sub>3</sub>), 0.03 (6H, s, Si(CH<sub>3</sub>)<sub>2</sub>); <sup>13</sup>C NMR (75.5 MHz, CDCl<sub>3</sub>)  $\delta$  207.9, 168.1, 135.9, 128.8, 128.3, 125.6, 124.0, 122.0, 101.9, 76.7, 65.7, 25.8, 24.7, 18.4, -5.3; MS *m/z* (rel. intensity) (EI) 317 (M<sup>+</sup>, 3), 302

(4), 274 (31), 260 (100), 242 (4), 230 (5), 218 (14), 200 (9), 186 (11), 168 (9), 143 (58), 115 (11), 75 (34), 73 (45); HRMS (EI) calc. for C<sub>18</sub>H<sub>27</sub>NO<sub>2</sub>Si: 317.1811, found: 317.1801.



**Synthetic efforts towards *tert*-Butyl (2-(1-hydroxybuta-2,3-dien-2-yl)phenyl)carbamate (4.120a).** Following a known procedure,<sup>376</sup> glacial acetic acid (0.14 mL, 2.43 mmol) was added to a solution of the allenylaniline **4.118a** (1.1739 g, 3.13 mmol) in THF (20 mL) and cooled to 0 °C. Then TBAF (9.8 mL of a 1.0 M solution, 9.8 mmol) was added and stirring was continued at 0 °C for 4 h. The reaction was quenched with a saturated solution of NH<sub>4</sub>Cl and extracted three times with ethyl acetate. The extracts were pooled, washed with water twice, brine once, dried over Na<sub>2</sub>SO<sub>4</sub>, filtered and the solvent evaporated on a rotary evaporator to give 0.9283 g of the crude product as a gold oil. Purification by silica gel chromatography (10:1 then 3:1 hexanes:ethyl acetate) afforded 0.7006 g (86%) of the side product **4.119**<sup>406</sup> as a pale yellow-green oil:



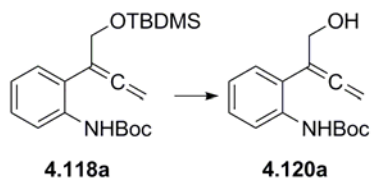
***tert*-Butyl 3-(hydroxymethyl)-2-methyl-1*H*-indole-1-carboxylate**

**(4.119).** <sup>1</sup>H NMR (300 MHz, CDCl<sub>3</sub>); δ 8.10 (1H, d, *J* = 7.8 Hz, Ar*H*), 7.57

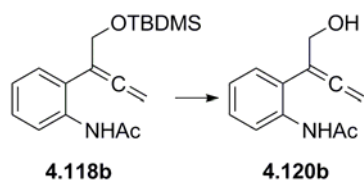
(1H, d, *J* = 7.5 Hz, Ar*H*), 7.23 (2H, m, Ar*H*), 4.73 (2H, s, OCH<sub>2</sub>), 2.58 (3H,

s, CCH<sub>3</sub>), 2.04 (1H, br s, OH), 1.69 (9H, s, OC(CH<sub>3</sub>)<sub>3</sub>); <sup>13</sup>C NMR (75.5 MHz, CDCl<sub>3</sub>) δ 150.6, 135.6, 135.4, 128.9, 123.5, 122.6, 117.9, 117.5, 115.3, 83.7, 55.1, 28.1, 13.7; MS *m/z*

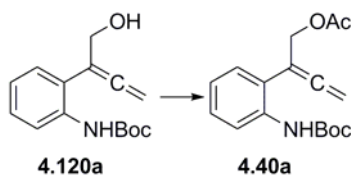
(rel. intensity) (EI) 261 ( $M^+$ , 50), 205 (100), 188 (14), 161 (28), 144 (50), 130 (9), 84 (11), 57 (49).



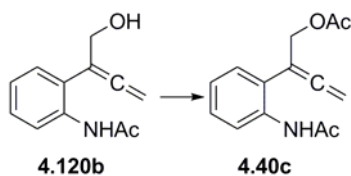
**tert-Butyl (2-(1-hydroxybuta-2,3-dien-2-yl)phenyl)carbamate (4.120a).** The following procedure is a modification of that described by Perumal and coworkers.<sup>409</sup> To a stirred solution of the allenylaniline **4.118a** (0.6668 g, 1.78 mmol) in 75% methanol (8 mL) was added  $KHSO_4$  (0.2052 g, 1.51 mmol) and stirred vigorously for 7 h to which water (5 mL) was added and the methanol evaporated under reduced pressure. The mixture was then extracted with ethyl acetate twice and pooled. The pooled extracts were washed with water twice, dried over  $Na_2SO_4$ , filtered and the solvent evaporated in vacuo to give 0.4847 g of the crude product as a gold oil which was purified by column chromatography (silica, 10:1 then 3:1 hexanes:ethyl acetate) to afford the title compound as a colorless oil (0.3575g, 77%): IR (NaCl, film,  $cm^{-1}$ )  $\nu_{max}$  3418, 2979, 2932, 2876, 1950, 1729, 1584, 1520, 1450, 1393, 1368, 1303, 1245, 1159, 1047, 1025, 850, 756;  $^1H$  NMR (300 MHz,  $CDCl_3$ )  $\delta$  7.91 (1H, d,  $J = 8.2$  Hz, ArH), 7.22 (3H, m, ArH, NH), 7.04 (1H, dd,  $J = 7.4, 7.6$  Hz, ArH), 5.08 (2H, s,  $C=CH_2$ ), 4.38 (2H, dd,  $J = 3.0$  Hz, 6.1 Hz,  $HOCH_2$ ), 2.13 (1H, t,  $J = 6.1$  Hz, OH), 1.49 (9H, s,  $OC(CH_3)_3$ );  $^{13}C$  NMR (75.5 MHz,  $CDCl_3$ )  $\delta$  206.4, 153.2, 136.2, 128.6, 128.2, 124.5, 123.5, 121.3, 102.4, 80.5, 77.1, 63.6, 28.4; MS  $m/z$  (rel. intensity) (EI) 261 ( $M^+$ , 1), 243 (3), 205 (3), 187 (8), 160 (94), 143 (51), 130 (44), 117 (11), 77 (6), 57 (100).



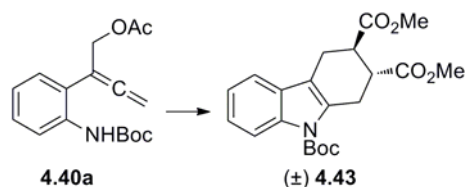
***N*-(2-(1-Hydroxybuta-2,3-dien-2-yl)phenyl)acetamide (4.120b).** In a similar fashion to the procedure described for **4.120a**, KHSO<sub>4</sub> (0.2939 g, 2.16 mmol) was added to a stirred solution of the allenylacetanilide **4.118b** (0.5960 g, 1.88 mmol) in 75% methanol (12 mL) and stirred vigorously for 10 h to which water (5 mL) was added and the methanol evaporated under reduced pressure. The mixture was then extracted with ethyl acetate three times and the extracts were pooled. The pooled extracts were washed with water twice, brine once, dried over Na<sub>2</sub>SO<sub>4</sub>, filtered and the solvent evaporated under reduced pressure to give 0.3436 g of the crude product as a yellow oil which was purified by column chromatography (silica, 1:4 hexanes:ethyl acetate) to afford the title compound as a light yellow oil (0.2537 g, 67%): IR (NaCl, film, cm<sup>-1</sup>)  $\nu_{\max}$  3271, 3059, 2933, 2875, 1949, 1668, 1583, 1532, 1448, 1371, 1307, 1012, 852, 761; <sup>1</sup>H NMR (300 MHz, CDCl<sub>3</sub>)  $\delta$  8.75 (1H, br s, *NH*), 7.95 (1H, d, *J* = 7.5 Hz, *ArH*), 7.24-7.18 (2H, m, *ArH*), 7.05 (1H, dd, *J* = 7.4, 7.5 Hz, *ArH*), 4.93 (2H, s, C=CH<sub>2</sub>), 4.33 (2H, s, HOCH<sub>2</sub>), 3.93 (1H, br s, *OH*), 2.04 (3H, s, C(O)CH<sub>3</sub>); <sup>13</sup>C NMR (75.5 MHz, CDCl<sub>3</sub>)  $\delta$  208.2, 169.1, 135.6, 128.7, 128.2, 126.5, 124.6, 122.7, 102.2, 76.6, 63.9, 24.1; MS *m/z* (rel. intensity) (EI) 203 (M<sup>+</sup>, 6), 185 (6), 172 (3), 160 (100), 143 (96), 130 (50), 117 (37), 115 (15), 103 (9), 77 (11), 51 (3); HRMS (EI) calc. for C<sub>12</sub>H<sub>13</sub>NO<sub>2</sub>: 203.0946, found: 203.0939.



**2-(2-((*tert*-Butoxycarbonyl)amino)phenyl)buta-2,3-dien-1-yl acetate (4.40a).** Following a published procedure,<sup>376</sup> a solution of the alcohol **4.120a** (0.7521 g, 2.88 mmol) in pyridine (8.5 mL) was cooled to 0 °C to which acetic anhydride (1.4 mL, 14.81 mmol) was added and stirring continued for 3 h. The reaction was quenched with a saturated solution of ammonium chloride and extracted with ethyl acetate. The organic layer was washed with water and dried over Na<sub>2</sub>SO<sub>4</sub>, filtered and the solvent evaporated on a rotary evaporator to give 0.4007 g of a pale yellow oil that was purified chromatographically (silica, 4:1 hexanes:ethyl acetate) furnishing 0.3757 g (97%) of the title compound<sup>376</sup> as a colorless oil: IR (NaCl, film, cm<sup>-1</sup>)  $\nu_{\max}$  3426, 2979, 1952, 1732, 1585, 1520, 1451, 1368, 1299, 1231, 1159, 1048, 1025; <sup>1</sup>H NMR (300 MHz, CDCl<sub>3</sub>)  $\delta$  7.99 (1H, d,  $J = 7.9$  Hz, ArH), 7.25 (1H, ddd,  $J = 1.0, 7.5, 7.9$  Hz, ArH), 7.18 (1H, dd  $J = 1.0, 7.5$ , ArH) overlapping with 7.14 (1H, br s, NH), 7.01 (1H, td,  $J = 7.5, 0.8$  Hz, ArH), 5.05 (2H, t,  $J = 2.6$  Hz, C=CH<sub>2</sub>), 4.78 (2H, t,  $J = 2.6$  Hz, OCH<sub>2</sub>) 2.06 (3H, s, COCH<sub>3</sub>), 1.50 (9H, s, OC(CH<sub>3</sub>)<sub>3</sub>); <sup>13</sup>C NMR (75.5 MHz, CDCl<sub>3</sub>)  $\delta$  207.6, 170.5, 152.9, 136.3, 128.7, 128.4, 123.3, 123.0, 120.4, 98.1, 80.3, 77.9, 64.5, 28.3, 20.8; MS  $m/z$  (rel. intensity) (CI, NH<sub>4</sub><sup>+</sup>) 321 (M<sup>+</sup> + 18, 90), 304 (M<sup>+</sup> + 1, 9), 265 (100), 248 (4), 202 (6), 143 (6).

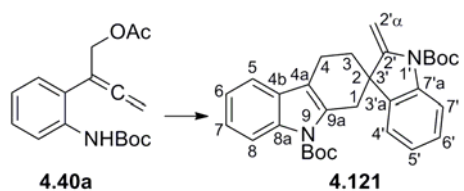


**2-(2-Acetamidophenyl)buta-2,3-dien-1-yl acetate 4.40c.** In a similar fashion to the procedure described for **4.40a**, acetic anhydride (0.7 mL, 7.4 mmol) was added to a solution of the alcohol **4.120b** (0.2470 g 1.22 mmol) in pyridine (3.75 mL, 46.4 mmol) at 0 °C and stirred for 1 h. The solution was then quenched with 5 mL of a saturated solution of NH<sub>4</sub>Cl and extracted with ethyl acetate twice and the extracts were pooled. The pooled extracts were washed with a saturated solution of NH<sub>4</sub>Cl, water, brine and dried over Na<sub>2</sub>SO<sub>4</sub>, filtered and the solvent evaporated under reduced pressure to give 0.2762 g of a gold oil that was purified by silica gel chromatography (1:2 hexanes:ethyl acetate) to afford 0.2502 g (84%) of the title compound as a light yellow oil: IR (NaCl, film, cm<sup>-1</sup>)  $\nu_{\max}$  3335, 3058, 1954, 1739, 1693, 1584, 1526, 1450, 1376, 1297, 1233, 1027, 761; <sup>1</sup>H NMR (300 MHz, CDCl<sub>3</sub>)  $\delta$  8.27 (1H, d,  $J$  = 7.9 Hz, ArH) overlapping with 8.23 (1H, br s, NH), 7.29-7.24 (1H, m, ArH), 7.15 (1H, d,  $J$  = 7.4 Hz, ArH), 7.03 (1H, t,  $J$  = 7.4 Hz, ArH), 5.01 (2H, t,  $J$  = 3.4 Hz, C=CH<sub>2</sub>), 4.66 (2H, t,  $J$  = 3.4 Hz, OCH<sub>2</sub>), 2.19 (3H, s, OCOCH<sub>3</sub>), 2.08 (3H, s, NHCOCH<sub>3</sub>); <sup>13</sup>C NMR (75.5 MHz, CDCl<sub>3</sub>)  $\delta$  206.1, 171.2, 168.7, 136.2, 128.9, 128.8, 123.8, 123.1, 121.3, 98.8, 78.4, 63.3, 24.5, 20.8; MS  $m/z$  (rel. intensity) (EI) 245 (M<sup>+</sup>, 2), 202 (20), 185 (9), 160 (19), 143 (100), 142 (73), 132 (9), 130 (14), 115 (14), 77 (5); HRMS (EI) calc. for C<sub>14</sub>H<sub>15</sub>NO<sub>3</sub>: 245.1052, found: 245.1053.



**9-tert-Butyl 2,3-dimethyl 3,4-dihydro-1H-carbazole-2,3,9(2H)-tricarboxylate (4.43).**

Following a published procedure,<sup>376</sup> K<sub>2</sub>CO<sub>3</sub> (0.0704 g, 0.51 mmol) was added to a stirred solution of the allenylaniline **4.40a** (0.1463 g, 0.48 mmol) and dimethyl fumarate (0.0699 g, 0.48 mmol) in DMF (2 mL) at 0 °C. The solution was allowed to come to room temperature and stirred for 20 h at which time the reaction appeared complete by TLC. The reaction was then quenched with a saturated solution of ammonium chloride and extracted with ether three times. The ethereal extracts were pooled, washed with water twice, brine once and dried over Na<sub>2</sub>SO<sub>4</sub> and the residue purified by silica gel chromatography (5:1 hexanes:ethyl acetate) to give 0.1868 g (100%) of the title compound<sup>376</sup> as a white solid: <sup>1</sup>H NMR (300 MHz, CDCl<sub>3</sub>) δ 8.06 (1H, d, *J* = 8.0 Hz, Ar*H*), 7.35 (1H, d, *J* = 7.3 Hz, Ar*H*), 7.27-7.17 (2H, m, Ar*H*), 3.74 (3H, s, CO<sub>2</sub>CH<sub>3</sub>), 3.73 (3H, s, CO<sub>2</sub>CH<sub>3</sub>), 3.58-3.51 (1H, dd, *J* = 3.4, 16.8 Hz), 3.18-3.08 (4H, m), 2.83-2.73 (1H, m), 1.65 (9H, s, CO<sub>2</sub>C(CH<sub>3</sub>)<sub>3</sub>); <sup>13</sup>C NMR (75.5 MHz, CDCl<sub>3</sub>) δ 174.9, 174.6, 154.4, 135.2, 132.7, 128.3, 124.0, 122.7, 117.6, 115.6, 114.3, 83.9, 52.1, 52.1, 42.5, 41.2, 28.3, 28.1, 23.8.



**Di-tert-butyl 2'-methylene-3,4-dihydrospiro[carbazole-2,3'-indoline]-1',9(1*H*)-dicarbonylate (4.121).** To a stirring solution of the *N*-Boc protected allenyl aniline **4.40a** (0.37 g, 1.22 mmol) in DMF (5 mL) was added  $K_2CO_3$  (0.1755 g, 1.27 mmol) and stirred for 17 h at which time the reaction was quenched with a saturated solution of  $NH_4Cl$ . The solution was extracted three times with diethyl ether and the extracts were pooled. The pooled extracts were washed with water twice, once with brine, dried over  $Na_2SO_4$ , filtered and the solvent evaporated under reduced pressure to produce 0.3018 g of a light yellow solid. The crude residue was purified by flash silica gel chromatography (10:1 hexanes:ether) furnishing 0.2903 g (98%) of the title compound as a clear colorless oil:  $^1H$  NMR (500 MHz,  $CDCl_3$ )  $\delta$  8.17 (1H, d,  $J = 7.9$  Hz, Ar*H*8), 7.84 (1H, d,  $J = 8.2$  Hz, Ar*H*7'), 7.47 (1H, dd,  $J = 1.0, 7.3$  Hz, Ar*H*5), 7.31 (1H, ddd,  $J = 1.0, 7.4, 7.9$  Hz, Ar*H*7') overlapping with 7.27 (1H, ddd,  $J = 1.2, 7.3, 7.4$  Hz, Ar*H*6), 7.21 (1H, ddd,  $J = 1.4, 7.5, 8.2$  Hz, Ar*H*6'), 6.96 (1H, dd,  $J = 1.4, 7.5$  Hz, Ar*H*4'), 6.91 (1H, td,  $J = 7.5, 0.8$  Hz, Ar*H*5'), 5.72 (1H, d,  $J = 1.3$  Hz, *H*2' $\alpha$ ), 4.67 (1H, d,  $J = 1.3$  Hz, *H*2' $\alpha$ ), 3.40, 3.32 (2H, AB<sub>q</sub>,  $J = 18.5$  Hz, *H*1a, *H*1b), 2.91 (1H, ddd,  $J = 4.9, 5.1, 16.9$  Hz, *H*4a), 2.80-2.74 (1H, m, *H*4b), 1.94 (2H, m, *H*3a, *H*3b), 1.66 (9H, s,  $OC(CH_3)_3$ ), 1.65 (9H, s,  $OC(CH_3)_3$ );  $^{13}C$  NMR (125.5 MHz,  $CDCl_3$ )  $\delta$  153.9 (C2'), 151.7 (carbonyl carbon), 150.5 (carbonyl carbon), 140.9 (C7'a), 136.3 (C3'a), 136.1 (C8a), 134.2 (C9a), 128.9 (C4b), 127.8 (C6'), 123.8 (C7), 123.3 (C5'), 123.1 (C4'), 122.6 (C6), 117.9 (C5), 116.2 (C4a), 115.54 (C7'), 115.48 (C8), 93.4 (C2' $\alpha$ ), 83.7 (quat. C of *t*-Bu), 82.6 (quat.



C of *t*-Bu), 46.9 (C2/3'), 38.1 (C1), 35.2 (C3), 28.3 (methyl carbons of *t*-Bu), 28.2 (methyl carbons of *t*-Bu), 17.9 (C4).

COSY (500 MHz, CDCl<sub>3</sub>):

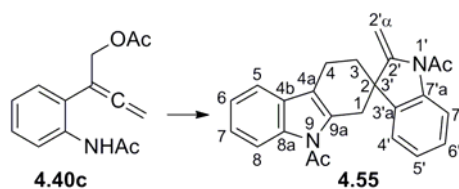
Entry	Proton ( $\delta$ )	Correlation
1	H1a (3.40)	H1b
2	H1b (3.32)	H1a
3	H2' $\alpha$ a (5.72)	H2 $\alpha$ b
4	H2' $\alpha$ b (4.67)	H2 $\alpha$ a
5	H3a (1.94)	H3b, H4a, H4b
6	H3b (1.94)	H3a, H4a, H4b
7	H4a (2.91)	H3a, H3b, H4b
8	H4b (2.80-2.74)	H3a, H3b, H4a
9	H5 (7.47)	H6, H7 (v. wk.)
10	H6 (7.27)	H5, H7, H8 (v. wk.)
11	H7 (7.31)	H5 (v. wk.), H6, H8
12	H8 (8.17)	H6 (v. wk.), H7
13	H4' (6.96)	H5'
14	H5' (6.91)	H4', H6'
15	H6' (7.21)	H5', H7'
16	H7' (7.84)	H6'

HMQC (500 MHz, CDCl<sub>3</sub>):

Entry	Proton	Correlation: <sup>13</sup> C-Chemical Shift in ppm (Assignment)
1	H1	38.1 (C1)
2	H2'α	93.4 (C2'α)
3	H3	35.2 (C3)
4	H4	17.9 (C4)
5	H5	117.9 (C5)
6	H6	122.6 (C6)
7	H7	123.8 (C7)
8	H8	115.48 (C8)
9	H4'	123.1 (C4')
10	H5'	123.3 (C5')
11	H6'	127.8 (C6')
12	H7'	115.54 (C7')
13	Methyl H's	28.3 (Methyl C's)
14	Methyl H's	28.2 (Methyl C's)

HMBC (500 MHz, CDCl<sub>3</sub>):

Entry	Proton	Correlation: <sup>13</sup> C-Chemical Shift in ppm (Assignment)
1	H1	153.9 (C2'), 46.9 (C2/C3'), 35.2 (C3), 136.3 (C3'a), 17.9 (C4, v. wk.), 116.2 (C4a), 134.2 (C9a)
2	H2'α	153.9 (C2'), 46.9 (C2/C3'), 35.2 (C3)
3	H3	38.1 (C1), 153.9 (C2'), 46.9 (C2/C3'), 136.3 (C3'a), 17.9 (C4), 116.2 (C4a)
4	H4	46.9 (C2/C3'), 35.2 (C3), 116.2 (C4a), 134.2 (C9a)
5	H5	116.2 (C4a), 128.9 (C4b, v. wk.), 123.8 (C7), 136.1 (C8a)
6	H6	128.9 (C4b), 115.48 (C8)
7	H7	117.9 (C5), 136.1 (C8a)
8	H8	128.9 (C4b), 122.6 (C6), 136.1 (C8a, v. wk.)
9	H4'	46.9 (C2/C3'), 127.8 (C6'), 140.9 (C7'a)
10	H5'	136.3 (C3'a), 127.8 (C6', v. wk.), 115.54 (C7')
11	H6'	123.1 (C4'), 115.54 (C7', v. wk.), 140.9 (C7'a)
12	H7'	136.3 (C3'a), 123.3 (C5'), 140.9 (C7'a, v. wk.)



**1,1'-(2'-Methylene-3,4-dihydrospiro[carbazole-2,3'-indolin]-1',9(1*H*)-diyl)diethanone (4.55).** To a stirring solution of the allenyl acetanilide **4.40c** (0.2475 g, 1.01 mmol) in DMF (4 mL) was added 0.1445 g  $K_2CO_3$  (1.05 mmol). The mixture was stirred for 24 h at which time the reaction was quenched with 2 mL of a saturated solution of  $NH_4Cl$ . The solution was extracted three times with diethyl ether and the extracts were pooled. The pooled extracts were washed three times with water, once with brine, dried over  $Na_2SO_4$ , filtered and the solvent evaporated under reduced pressure to afford 0.1458 g (78%) of the title compound<sup>382</sup> as a white solid: IR (NaCl, film,  $cm^{-1}$ )  $\nu_{max}$  2918, 1698, 1674, 1599, 1477, 1462, 1371, 1347, 1310, 1288, 1221, 1204, 1032, 910, 732;  $^1H$  NMR (300 MHz,  $CD_2Cl_2$ )  $\delta$  8.01-7.98 (2H, m, Ar*H*), 7.51 (1H, d,  $J = 7.8$  Hz, Ar*H*), 7.36-7.21 (3H, m, Ar*H*), 7.09-6.99 (2H, m, Ar*H*), 5.11 (1H, d,  $J = 1.1$  Hz, *H2* $\alpha$ ), 4.82 (1H, d,  $J = 1.1$  Hz, *H2* $\alpha$ ), 3.48, 3.38 (2H, AB<sub>q</sub>,  $J = 18.0$  Hz, *H1*), 2.91-2.78 (2H, m, *H4*), 2.71 (3H, s,  $NC(O)CH_3$ ), 2.50 (3H, s,  $NC(O)CH_3$ ), 1.98-1.94 (2H, m, *H3*);  $^1H$  NMR (600 MHz,  $CDCl_3$ )  $\delta$  8.04 (1H, d,  $J = 8.2$  Hz, Ar*H7'*), 7.98 (1H, d,  $J = 8.1$  Hz, Ar*H8*), 7.52 (1H, dd,  $J = 1.2, 7.8$  Hz, Ar*H5*), 7.37 (1H, ddd,  $J = 1.2, 7.4, 8.1$  Hz, Ar*H7*), 7.33 (1H, ddd,  $J = 1.0, 7.4, 7.8$  Hz, Ar*H6*), 7.27 (1H, d,  $J = 1.8, 7.1, 8.2$  Hz, Ar*H6'*), 7.07 (1H, dd,  $J = 1.8, 7.5$  Hz, Ar*H4'*), 7.04 (1H, ddd,  $J = 0.9, 7.1, 7.5$  Hz, Ar*H5'*), 5.14 (1H, d,  $J = 2.4$  Hz, *H2* $\alpha$ ), 4.85 (1H, d,  $J = 2.4$  Hz, *H2* $\alpha$ ), 3.52, 3.43 (2H, AB<sub>q</sub>,  $J = 18.0$  Hz, *H1*), 2.91-2.80 (2H, m, *H4*), 2.77 (3H, s,  $NC(O)CH_3$ ), 2.55 (3H, s,  $NC(O)CH_3$ ), 2.01-1.93 (2H, m, *H3*);  $^{13}C$  NMR (75.5 MHz,  $CD_2Cl_2$ )  $\delta$  170.1, 169.71, 155.3,

141.9, 137.2, 136.6, 134.6, 129.9, 128.2, 124.6, 124.5, 123.4, 122.9, 118.6, 117.9, 116.9, 115.5, 96.6, 47.9, 37.0, 33.7, 27.6, 25.7, 18.5;  $^{13}\text{C}$  NMR (150.9 MHz,  $\text{CDCl}_3$ )  $\delta$  169.8 (carbonyl carbon), 169.5 (carbonyl carbon), 154.9 (C2'), 141.4 (C7'a), 136.6 (C3'a), 136.1 (C8a), 134.5 (C9a), 129.6 (C4b), 128.1 (C6'), 124.5 (C5'), 124.3 (C7), 123.2 (C6), 122.6 (C4'), 118.4 (C5), 117.6 (C4a), 116.9 (C7'), 115.0 (C8), 96.6 (C2' $\alpha$ ), 47.5 (C2/C3'), 36.7 (C1), 33.4 (C3), 27.4 (methyl carbon), 25.6 (methyl carbon), 18.2 (C4); MS  $m/z$  (rel. intensity) (EI) 370 ( $\text{M}^+$ , 71), 328 (31), 327 (33), 313 (9), 286 (16), 285 (44), 269 (9), 256 (4), 241 (3), 185 (9), 144 (14), 143 (100), 115 (4), 102 (1), 77 (1); HRMS (EI) calc. for  $\text{C}_{24}\text{H}_{22}\text{N}_2\text{O}_2$ : 370.1681, found: 370.1672.

COSY (600 MHz,  $\text{CDCl}_3$ ):

Entry	Proton ( $\delta$ )	Correlation
1	H1a (3.52)	H1b
2	H1b (3.43)	H1a
3	H2' $\alpha$ a (5.14)	H2 $\alpha$ b
4	H2' $\alpha$ b (4.85)	H2 $\alpha$ a
5	H3a (2.01-1.93)	H3b, H4a, H4b
6	H3b (2.01-1.93)	H3a, H4a, H4b
7	H4a (2.91-2.80)	H3a, H3b, H4b
8	H4b (2.91-2.80)	H3a, H3b, H4a
9	H5 (7.52)	H6, H7 (v. wk.)
10	H6 (7.33)	H5, H7, H8 (v. wk.)
11	H7 (7.37)	H5 (v. wk.), H6, H8
12	H8 (7.98)	H6 (v. wk.), H7
13	H4' (7.07)	H5', H6' (v. wk.)

14	H5' (7.04)	H4', H6'
15	H6' (7.27)	H4' (v. wk.), H5', H7'
16	H7' (8.04)	H6'

---

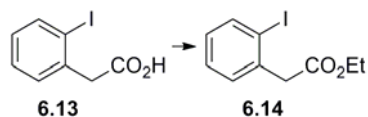
HMQC (600 MHz, CDCl<sub>3</sub>):

Entry	Proton	Correlation: <sup>13</sup> C-Chemical Shift in ppm (Assignment)
1	H1	36.7 (C1)
2	H2'α	96.6 (C2'α)
3	H3	33.4 (C3)
4	H4	18.2 (C4)
5	H5	118.4 (C5)
6	H6	123.2 (C6)
7	H7	124.3 (C7)
8	H8	115.0 (C8)
9	H4'	122.6 (C4')
10	H5'	124.5 (C5')
11	H6'	128.1 (C6')
12	H7'	116.9 (C7')

---

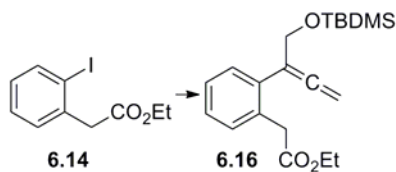
HMBC (600 MHz, CDCl<sub>3</sub>):

Entry	Proton	Correlation: <sup>13</sup> C-Chemical Shift in ppm (Assignment)
1	H1	154.9 (C2'), 47.5 (C2/C3'), 33.4 (C3), 136.6 (C3'a), 117.6 (C4a), 136.1 (C8a), 134.5 (C9a)
2	H2'α	154.9 (C2'), 47.5 (C2/C3'), 33.4 (C3, v. wk.)
3	H3	36.7 (C1), 154.9 (C2'), 47.5 (C2/C3'), 136.6 (C3'a), 18.2 (C4), 117.6 (C4a)
4	H4	47.5 (C2/C3'), 33.4 (C3), 117.6 (C4a), 134.5 (C9a)
5	H5	117.6 (C4a), 129.6 (C4b, v. wk.), 124.3 (C7), 115.0 (C8, v. wk.), 136.1 (C8a)
6	H6	129.6 (C4b), 118.4 (C5), 124.3 (C7, wk.), 115.0 (C8), 136.1 (C8a)
7	H7	129.6 (C4b), 118.4 (C5), 115.0 (C8), 136.1 (C8a)
8	H8	129.6 (C4b), 118.4 (C5, v. wk.), 123.2 (C6), 136.1 (C8a, v. wk.)
9	H4'	47.5 (C2/C3', v. wk), 136.6 (C3'a), 128.1 (C6'), 116.9 (C7'), 141.4 (C7'a)
10	H5'	47.5 (C2/C3', v. wk.), 136.6 (C3'a), 122.6 (C4', v. wk.), 128.1 (C6'), 116.9 (C7'), 141.4 (C7'a)
11	H6'	136.6 (C3'a, v. wk.), 122.6 (C4'), 124.5 (C5', v. wk.), 116.9 (C7', v. wk.), 141.4 (C7'a)
12	H7'	136.6 (C3'a), 124.5 (C5'), 141.4 (C7'a)



**Ethyl 2-(2-iodophenyl)acetate (6.14).** Following procedures described by Kim and coworkers,<sup>507</sup> ethyl chloroformate (4 mL, 0.0418 mol) and DMAP (0.5113 g, 4.18 mmol) was added to a stirred solution of 2-iodophenylacetic acid (10.7408 g, 0.0402 mol) and triethylamine (6.3 mL, 0.045 mol) in dichloromethane (130 mL) at 0 °C. Stirring was continued for 1 h at 0 °C. The reaction solution was diluted with dichloromethane (250 mL), washed twice with a saturated solution of NaHCO<sub>3</sub>, once with 0.1 M HCl, once with brine, dried over Na<sub>2</sub>SO<sub>4</sub>, filtered and the solvent evaporated under reduced pressure. The residue was purified chromatographically (silica, 7:1 hexanes:ethyl acetate) to give 11.4857 g (99%) of the title compound<sup>508</sup> as a white solid: IR (NaCl, film, cm<sup>-1</sup>)  $\nu_{\max}$  2981, 1736, 1587, 1564, 1466, 1438, 1367, 1338, 1216, 1158, 1014; <sup>1</sup>H NMR (300 MHz, CDCl<sub>3</sub>)  $\delta$  7.83 (1H, d,  $J$  = 8.2 Hz, ArH), 7.33-7.24 (2H, m, ArH), 6.96-6.91 (1H, m, ArH), 4.17 (2H, q,  $J$  = 7.1 Hz, OCH<sub>2</sub>CH<sub>3</sub>), 3.77 (2H, s, ArCH<sub>2</sub>), 1.26 (3H, t,  $J$  = 7.1 Hz, CH<sub>2</sub>CH<sub>3</sub>); <sup>13</sup>C NMR (75.5 MHz, CDCl<sub>3</sub>)  $\delta$  170.5, 139.5, 137.9, 130.6, 128.8, 128.4, 100.9, 61.0, 46.3, 14.2; MS  $m/z$  (rel. intensity) (EI) 290 (M<sup>+</sup>, 11), 245 (4), 217 (100), 163 (79), 135 (92), 107 (8), 90 (46), 89 (23), 63 (8); HRMS (EI) calc. for C<sub>10</sub>H<sub>11</sub>IO<sub>2</sub>: 289.9804, found: 289.9795.

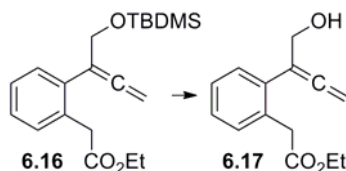




**Ethyl 2-(2-(1-((*tert*-butyldimethylsilyloxy)buta-2,3-dien-2-yl)phenyl)acetate (6.16).**

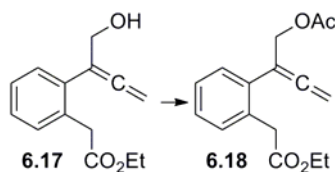
Following a modification of procedures published by Mukai and Takahashi,<sup>406</sup> a round bottom flask was charged with the ethyl 2-(2-iodophenyl)acetate **6.14** (4.6585 g, 16.1 mmol), allenylstannane **6.15** (8.3944 g, 17.7 mmol) and DMF (100 mL) under argon environment. This mixture was degassed twice under high vacuum using freeze-thaw conditions with argon purges. While the reaction mixture was still frozen, tri-(2-furyl)-phosphine (1.0316 g, 4.44 mmol), Pd<sub>2</sub>(dba)<sub>3</sub>·CHCl<sub>3</sub> (0.5137 g, 0.99 mmol), and CuI (0.3249 g, 1.7 mmol) were added under argon atmosphere. The reaction mixture was then degassed twice more using freeze-thaw conditions and then stirred at room temperature for 10 h. The reaction mixture was quenched with 10% NH<sub>4</sub>OH and extracted three times with ether and pooled. The pooled extracts were washed with water twice, brine once, dried over Na<sub>2</sub>SO<sub>4</sub>, filtered and the solvent evaporated on a rotary evaporator. The crude product was purified by flash chromatography (15:1 hexanes:ether) to afford 4.5485 g (82%) of the title compound as a pale yellow oil: IR (NaCl, film, cm<sup>-1</sup>) ν<sub>max</sub> 3063, 2956, 2930, 2896, 2857, 1957, 1740, 1472, 1464, 1368, 1333, 1253, 1208, 1156, 1080, 1033, 839, 777; <sup>1</sup>H NMR (300 MHz, CDCl<sub>3</sub>) δ 7.31-7.21 (4H, m, ArH), 4.89 (2H, t, *J* = 3.0 Hz, OCH<sub>2</sub>), 4.35 (2H, t, *J* = 3.0 Hz, C=CH<sub>2</sub>), 4.12 (2H, q, *J* = 7.1 Hz, OCH<sub>2</sub>CH<sub>3</sub>), 3.73 (2H, s, C(O)CH<sub>2</sub>), 1.22 (3H, t, *J* = 7.1 Hz, OCH<sub>2</sub>CH<sub>3</sub>), 0.86 (9H, s, SiC(CH<sub>3</sub>)<sub>3</sub>), 0.02 (6H, s, Si(CH<sub>3</sub>)<sub>2</sub>); <sup>13</sup>C NMR (75.5 MHz, CDCl<sub>3</sub>) δ 206.4, 171.7, 135.2, 132.9, 130.6, 128.8, 127.5, 127.1, 103.9, 77.1, 64.7, 60.6, 39.1, 25.8,

18.3, 14.2, -5.4; MS  $m/z$  (rel. intensity) (EI) 346 ( $M^+$ , 11), 331 (3), 301 (14), 289 (100), 273 (8), 243 (72), 215 (58), 197 (43), 169 (18), 141 (41), 115 (13), 84 (41), 75 (47), 51 (10); HRMS (EI) calc. for  $C_{20}H_{30}O_3Si$ : 346.1964, found: 346.1956.

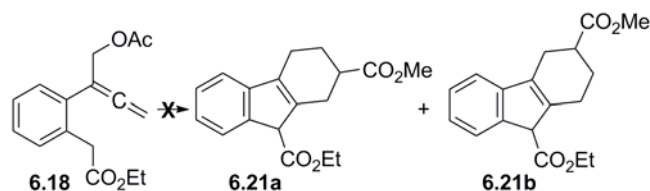


**Ethyl 2-(2-(1-hydroxybuta-2,3-dien-2-yl)phenyl)acetate (6.17).** Following a modification of procedures described by Perumal and coworkers<sup>409</sup>,  $KHSO_4$  (0.7523 g, 5.53 mmol) was added to a solution of the silyl protected alcohol **6.16** (1.4943 g, 4.31 mmol) in 70% methanol (18 mL) and stirred at room temperature for 85 min. The methanol was then evaporated under reduced pressure. Water was added and the mixture was extracted with ethyl acetate three times. The pooled organic extracts were dried over  $Na_2SO_4$ , filtered and evaporated under reduced pressure. The residue was purified chromatographically (silica, 4:1 hexanes:ethyl acetate) to afford the title compound as a clear, colorless oil (0.9447 g, 94%): IR (NaCl, film,  $cm^{-1}$ )  $\nu_{max}$  3435, 3062, 2982, 2936, 2873, 1952, 1732, 1490, 1452, 1416, 1393, 1369, 1336, 1252, 1211, 1158, 1098, 1074, 1030, 852, 763;  $^1H$  NMR (300 MHz,  $CDCl_3$ )  $\delta$  7.32-7.24 (4H, m, ArH), 4.95 (2H, t,  $J = 2.6$  Hz,  $C=CH_2$ ), 4.38 (2H, t,  $J = 2.6$  Hz,  $CH_2OH$ ), 4.13 (2H, q,  $J = 7.1$  Hz,  $OCH_2CH_3$ ), 3.76 (2H, s,  $ArCH_2C(O)$ ), 2.42 (1H, t,  $J = 5.8$  Hz, OH), 1.24 (3H, t,  $J = 7.1$  Hz,  $OCH_2CH_3$ );  $^{13}C$  NMR (75.5 MHz,  $CDCl_3$ )  $\delta$  205.3, 172.4, 134.6, 132.9, 130.9, 128.3, 127.8, 127.6, 103.9, 77.6, 63.9, 61.0, 39.0, 14.1; MS  $m/z$  (rel.

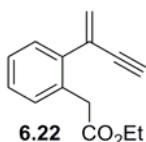
intensity) (EI) 232 ( $M^+$ , 88), 214 (51), 202 (68), 173 (24), 159 (43), 141 (64), 129 (100), 128 (89), 115 (47), 84 (42), 77 (8); HRMS (EI) calc. for  $C_{14}H_{16}O_3$ : 232.1099, found: 232.1094.



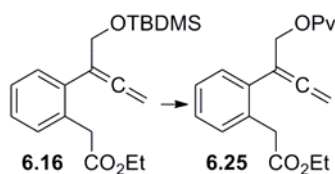
**Ethyl 2-(2-(1-acetoxybuta-2,3-dien-2-yl)phenyl)acetate (6.18).** Following procedures described by Mukai and coworkers,<sup>376</sup> alcohol **6.17** (0.8840 g, 3.81 mmol) was dissolved in pyridine (12 mL) and cooled to 0 °C. Acetic anhydride (3 mL, 31.74 mmol) was then added and stirred for 2 h. The reaction solution was then quenched with a saturated solution of ammonium chloride, extracted three times with ethyl acetate and the extracts were pooled. The pooled extracts were washed with water, brine and dried over  $Na_2SO_4$ , filtered and evaporated under reduced pressure. The residue was purified by silica gel chromatography (5:1 hexanes:ethyl acetate) to afford 0.9561 g (92%) of the title compound as a clear colorless oil: IR (NaCl, film,  $cm^{-1}$ )  $\nu_{max}$  3063, 2983, 2939, 1955, 1732, 1491, 1448, 1431, 1377, 1335, 1226, 1158, 1098, 1060, 1029, 961, 927, 858, 765;  $^1H$  NMR (300 MHz,  $CDCl_3$ )  $\delta$  7.28-7.24 (4H, m, ArH), 4.95 (2H, t,  $J = 2.6$  Hz,  $C=CH_2$ ), 4.79 (2H, t,  $J = 2.6$  Hz,  $CH_2OAc$ ), 4.12 (2H, q,  $J = 7.1$  Hz,  $OCH_2CH_3$ ), 3.74 (2H, s,  $ArCH_2C(O)$ ), 2.03 (3H, s,  $C(O)CH_3$ ), 1.23 (3H, t,  $J = 7.1$  Hz,  $OCH_2CH_3$ );  $^{13}C$  NMR (75.5 MHz,  $CDCl_3$ )  $\delta$  207.1, 171.5, 170.5, 134.3, 133.1, 130.9, 128.5, 127.9, 127.4, 99.9, 77.4, 64.8, 60.7, 39.0, 20.9, 14.2; MS  $m/z$  (rel. intensity) (EI) 274 ( $M^+$ , 5), 232 (100), 214 (3), 186 (25), 158 (76), 141 (34), 115 (27), 102 (4), 84 (23), 77 (3); HRMS (EI) calc. for  $C_{16}H_{18}O_4$ : 274.1205, found: 274.1196.



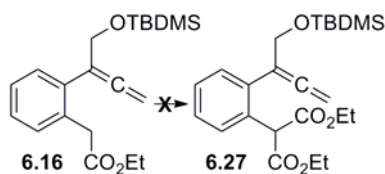
Synthetic efforts towards 9-Ethyl 2-methyl 2,3,4,9-tetrahydro-1*H*-fluorene-2,9-dicarboxylate (**6.21a**) and 9-Ethyl 3-methyl 2,3,4,9-tetrahydro-1*H*-fluorene-3,9-dicarboxylate (**6.21b**). To a stirring solution of the allenyl arene **6.18** (0.0501 g, 0.18 mmol) and methyl acrylate (0.034 mL, 0.38 mmol) in acetonitrile (1.2 mL) was added DBU (0.06 mL, 0.4 mmol) and stirred for 12 h at which point the solution was quenched with a saturated solution of ammonium chloride (2 mL). The mixture was then extracted three times with ethyl acetate and pooled. The pooled extracts were washed once with water, once with brine, dried over sodium sulfate, filtered and the solvent removed under reduced pressure to give 0.0473 g of a yellow residue. The crude residue was purified by flash chromatography to return 0.0137 g (27%) of **6.18**, 0.037 g of residue assumed to contain **6.20**, **6.21**, **6.23** and 0.0081 g (21%) of the enyne **6.22** as a clear colourless film:



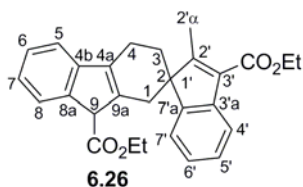
**Ethyl 2-(2-(but-1-en-3-yn-2-yl)phenyl)acetate (6.22).**  $^1\text{H}$  NMR (300 MHz,  $\text{CDCl}_3$ )  $\delta$  7.29-7.24 (4H, m, ArH), 5.87 (1H, s, C=CH), 5.57 (1H, s, C=CH), 4.12 (2H, q,  $J = 7.1$  Hz,  $\text{OCH}_2\text{CH}_3$ ), 3.81 (2H, s,  $\text{ArCH}_2\text{C(O)}$ ), 3.04 (1H, s,  $\text{C}\equiv\text{CH}$ ), 1.22 (3H, t,  $J = 7.1$  Hz,  $\text{OCH}_2\text{CH}_3$ );  $^{13}\text{C}$  NMR (75.5 MHz,  $\text{CDCl}_3$ )  $\delta$  ; 171.6, 139.1, 131.7, 130.7, 129.9, 129.1, 128.3, 127.9, 127.4, 83.3, 78.9, 60.8, 38.8, 14.2; MS  $m/z$  (rel. intensity) (EI) 214 ( $\text{M}^+$ , 58), 185 (9), 170 (23), 157 (51), 141 (100), 139(41), 129 (11), 115 (86), 89 (8), 75 (3), 63 (9), 51 (4).



**2-(2-(2-Ethoxy-2-oxoethyl)phenyl)buta-2,3-dien-1-yl pivalate (6.25).** To a solution of the silyl protected alcohol **6.16** (1.6878 g, 4.87 mmol) in 70% methanol (19 mL) was added  $\text{KHSO}_4$  (0.7264 g, 5.33 mmol) and stirred at room temperature for 2 h. The rest of the procedure follows that as for **6.17**. The residue (1.2113 g) was then purified chromatographically (silica, 3:1 hexanes:ethyl acetate) to afford the allenyl alcohol **6.17** as a yellow oil (0.2770 g, 24%). The allenyl alcohol (0.2764 g, 1.19 mmol) was then dissolved in pyridine (6 mL) and stirred at 0 °C to which pivaloyl chloride (0.22 mL, 1.79 mmol) was added and stirring continued for another 2 h. The rest of the procedure follows that as for **6.18** producing 0.3125 g the crude residue as a dark gold oil. Chromatographic purification (silica, 3:1 hexanes:ethyl acetate) afforded the title compound as a clear, pale yellow oil (0.2006 g, 53%): IR (NaCl, film,  $\text{cm}^{-1}$ )  $\nu_{\text{max}}$  2979, 1956, 1733, 1480, 1460, 1430, 1397, 1368, 1335, 1280, 1250, 1209, 1148, 1033, 958, 856, 763;  $^1\text{H}$  NMR (300 MHz,  $\text{CDCl}_3$ )  $\delta$  7.29-7.24 (4H, m, ArH), 4.94 (2H, t,  $J = 3.0$  Hz,  $\text{C}=\text{CH}_2$ ), 4.78 (2H, t,  $J = 3.0$  Hz,  $\text{CH}_2\text{OPv}$ ), 4.12 (2H, q,  $J = 7.1$  Hz,  $\text{OCH}_2\text{CH}_3$ ), 3.74, (2H, s,  $\text{ArCH}_2\text{C}(\text{O})$ ), 1.24 (3H, t,  $J = 7.1$  Hz,  $\text{OCH}_2\text{CH}_3$ );  $^{13}\text{C}$  NMR (75.5 MHz,  $\text{CDCl}_3$ )  $\delta$  206.6, 177.9, 171.6, 134.2, 133.0, 130.8, 128.6, 127.8, 127.3, 100.2, 77.7, 64.2, 60.7, 39.1, 38.7, 27.2, 14.2; MS  $m/z$  (rel. intensity) (EI) 316 ( $\text{M}^+$ , 8), 291 (2), 271 (3), 259 (2), 232 (39), 215 (9), 186 (16), 158 (49), 141 (28), 115 (18), 85 (16), 75 (2), 57 (100); HRMS (EI) calc. for  $\text{C}_{19}\text{H}_{24}\text{O}_4$ : 316.1675, found: 316.1685.



**Synthetic efforts towards Diethyl 2-(2-(1-((*tert*-butyldimethylsilyl)oxy)buta-2,3-dien-2-yl)phenyl)malonate (6.27).** To a stirring solution of silyl protected alcohol **6.16** (0.2966 g, 0.86 mmol) in diethyl carbonate (5 mL) was added NaH (0.1624 g, 6.77 mmol, previously washed twice with dry hexane) and stirred at room temperature for 50 min. The reaction mixture was quenched with a saturated solution of NH<sub>4</sub>Cl and extracted with ethyl acetate. The organic layers were pooled, washed with water, brine, dried over Na<sub>2</sub>SO<sub>4</sub> filtered and the solvent removed under reduced pressure to give a gold oil (0.2304 g). Chromatographic purification (silica, 10:1 hexanes:ethyl acetate) provided the side products **6.26** (0.0186 g, 10%), **6.28** (0.0128 g, 5%) and **6.29** (0.0561 g, 23%):



**Diethyl 2'-methyl-1,3,4,9-tetrahydrospiro[fluorene-2,1'-indene]-3',9-dicarboxylate (6.26).** Two diastereomers: <sup>1</sup>H NMR (500 MHz, CDCl<sub>3</sub>) δ 7.89 (2H, d, *J* = 7.7 Hz, *ArH*), 7.58-7.56 (2H, m, *ArH*), 7.49 (2H, d, *J* = 7.6 Hz, *ArH*), 7.29-7.24 (2H, m, *ArH*), 7.21-7.18 (2H, m, *ArH*), 7.13-7.08 (4H, m, *ArH*), 7.06-7.01 (2H, m, *ArH*), 4.43-4.38 (4H, m, OCH<sub>2</sub>CH<sub>3</sub>) overlapping with 4.40 (1H, s, *H*<sub>9</sub>), 4.34 (1H, s, *H*<sub>9</sub>) overlapping with 4.34-4.16 (4H, m, OCH<sub>2</sub>CH<sub>3</sub>), 2.91-2.83 (4H, m, *H*<sub>1</sub>, *H*<sub>4</sub>), 2.67-2.62 (2H, m, *H*<sub>4</sub>), 2.38 (3H, s, *H*<sub>2α'</sub>), 2.36 (3H, s, *H*<sub>2α'</sub>), 2.31-2.23 (2H, m, *H*<sub>1</sub>), 2.21-2.14 (2H, m, *H*<sub>3</sub>), 1.46-1.42 (6H, m, OCH<sub>2</sub>CH<sub>3</sub>), 1.38-1.37 (2H, m, *H*<sub>3</sub>) overlapping with 1.34 (3H, t, *J* = 7.1 Hz, OCH<sub>2</sub>CH<sub>3</sub>), 1.31 (3H, t, *J* = 7.1 Hz, OCH<sub>2</sub>CH<sub>3</sub>); <sup>13</sup>C NMR (125.5 MHz, CDCl<sub>3</sub>) δ 170.84 (ester carbonyl), 170.77 (ester

carbonyl), 165.40 (ester carbonyl), 165.38 (ester carbonyl), 165.0 (ester carbonyl), 164.6 (ester carbonyl), 150.1, 150.0, 144.9, 144.8, 140.9, 140.7, 139.8, 139.6, 138.6, 138.5, 137.7, 137.6, 127.9, 127.7, 127.6, 127.1, 127.0, 125.22, 125.16, 125.0, 123.6, 123.4, 123.3, 122.5, 122.1, 121.9, 118.3, 118.1, 61.3 (ester methylene), 61.2 (ester methylene), 60.3 (ester methylene), 57.1 (C9), 56.3 (C9), 53.1 (C2/C1'), 29.3 (C3), 28.8 (C3), 27.6 (C1), 27.5 (C1), 22.8 (C4), 22.7 (C4), 14.4 (ester methyl), 14.33 (ester methyl), 14.31 (ester methyl), 13.1 (C2' $\alpha$ ), 12.9 (C2' $\alpha$ ), (Two of the signals in the  $\delta$  164.6-165.4 range are suspected to arise from unidentified impurities); MS *m/z* (rel. intensity) (EI) 428 (M<sup>+</sup>, 33), 382 (10), 354 (7), 309 (3), 265 (9), 239 (2), 214 (100), 185 (21), 141 (39), 115 (9), 91 (1), 63 (1).

COSY (500 MHz, CDCl<sub>3</sub>):

Entry	Proton	Correlation
1	H1a	H1b, H3 (wk.)
2	H1b	H1a, H3 (wk.)
3	H3a	H3b, H4a, H4b, H1(wk.)
4	H3b	H3a, H4a, H4b, H1 (wk.)
3	H4a	H4b, H3a, H3b
4	H4b	H4a, H3a, H3b
5	Ester CH <sub>2</sub> ( $\delta$ 4.43-4.38)	Ester CH <sub>3</sub> ( $\delta$ 1.46-1.42)
6	Ester CH <sub>2</sub> ( $\delta$ 4.34-4.16)	Ester CH <sub>3</sub> ( $\delta$ 1.34, 1.31)
7	Ester CH <sub>3</sub> ( $\delta$ 1.46-1.42)	Ester CH <sub>2</sub> ( $\delta$ 4.43-4.38)
8	Ester CH <sub>3</sub> ( $\delta$ 1.34, 1.31)	Ester CH <sub>2</sub> ( $\delta$ 4.34-4.16)

HMQC (500 MHz, CDCl<sub>3</sub>):

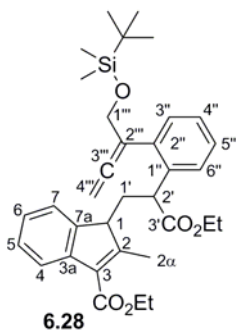
Entry	Proton	Correlation: <sup>13</sup> C-Chemical Shift in ppm (Assignment)
1	H1	27.6 (C1), 27.5 (C1)
2	H2'α	13.1 (C2'α), 12.9 (C2'α)
3	H3	29.3 (C3), 28.8 (C3)
4	H4	22.8 (C4), 22.7 (C4)
5	H9	57.1 (C9), 56.3 (C9)
6	Ester CH <sub>2</sub>	61.3 (ester methylene), 61.2 (ester methylene), 60.3 (ester methylene)
7	Ester CH <sub>3</sub>	14.4 (ester methyl), 14.33 (ester methyl), 14.31 (ester methyl)

HMBC (500 MHz, CDCl<sub>3</sub>):

Entry	Proton	Correlation: <sup>13</sup> C-Chemical Shift in ppm (Assignment)
1	H1	13.1 (C2'α), 12.9 (C2'α), 29.3 (C3), 28.8 (C3)
2 <sup>a</sup>	H2'α	165.40 (ester carbonyl), 165.38 (ester carbonyl), 165.0 (ester carbonyl), 164.6 (ester carbonyl), 53.1 (C2/C1')
3	H9	165.40 (ester carbonyl), 165.38 (ester carbonyl), 165.0 (ester carbonyl), 164.6 (ester carbonyl)
4	Ester CH <sub>2</sub> (δ 4.43-4.38)	165.40 (ester carbonyl), 165.38 (ester carbonyl), 165.0 (ester carbonyl), 164.6 (ester carbonyl), 14.4 (ester methyl), 14.33 (ester methyl), 14.31 (ester methyl)
5	Ester CH <sub>3</sub> (δ 1.46-1.42)	60.3 (ester methylene)
6	Ester CH <sub>3</sub> (δ 1.34, 1.31)	61.3 (ester methylene), 61.2 (ester methylene)

a. Since the apparent ester carbonyl signals at 164.6-165.4 ppm are closely spaced, it is unclear which of these correlates with H2'α.





6.28

**Ethyl 1-(2-(2-(1-(tert-butyl)dimethylsilyloxy)buta-2,3-dien-2-yl)phenyl)-3-ethoxy-3-oxopropyl)-2-methyl-1H-indene-3-carboxylate (6.28).**  $^1\text{H}$  NMR (500 MHz,  $\text{CDCl}_3$ )  $\delta$  7.88 (1H, d,  $J = 7.7$  Hz, ArH), 7.53 (1H, d,  $J = 7.8$  Hz, ArH), 7.47 (1H, d,  $J = 7.4$  Hz, ArH), 7.30-7.24 (2H, m, ArH), 7.22-7.17 (3H, m, ArH), 4.63 (1H, td,  $J$

= 10.8, 3.1 Hz, C=CH), 4.36 (2H, q,  $J = 7.1$  Hz,  $\text{OCH}_2\text{CH}_3$ ) overlapping with 4.35 (1H,  $H2'$ ), 4.29-4.23 (2H, m,  $\text{SiOCH}_2$ ), 4.12 (1H, td,  $J = 10.8, 3.1$  Hz, C=CH), 4.05-3.98 (2H, m,  $\text{OCH}_2\text{CH}_3$ ), 3.43 (1H, dd,  $J = 3.8, 9.4$  Hz,  $H1$ ), 2.82-2.77 (1H, m,  $H1'$ ), 2.40 (3H, s,  $H2\alpha$ ), 1.53-1.47 (1H, m,  $H1'$ ), 1.40 (3H, t,  $J = 7.1$  Hz,  $\text{OCH}_2\text{CH}_3$ ), 1.15 (3H, t,  $J = 7.1$  Hz,  $\text{OCH}_2\text{CH}_3$ ), 0.85 (9H, s,  $\text{SiC}(\text{CH}_3)_3$ ), -0.02 (3H, s,  $\text{Si}(\text{CH}_3)_3$ ), -0.03 (3H, s,  $\text{Si}(\text{CH}_3)_3$ );  $^{13}\text{C}$  NMR (125.5 MHz,  $\text{CDCl}_3$ )  $\delta$  205.9 (=C=), 173.8 (ester carbonyl), 165.1 (ester carbonyl), 161.3, 144.5, 141.8, 137.7 ( $\text{C}1''$ ), 134.9, 129.7, 128.5, 127.9, 127.2, 126.9, 124.6, 123.6, 122.0, 103.2 ( $\text{C}2'''$ ), 76.8 ( $\text{C}4'''$ ), 65.0 ( $\text{C}1'''$ ), 60.8 (ester methylene), 60.1 (ester methylene), 52.6 ( $\text{C}1$ ), 44.8 ( $\text{C}2'$ ), 35.7 ( $\text{C}1'$ ), 25.9 ( $t$ -Bu), 18.4 (quat. C of  $t$ -Bu), 15.3 ( $\text{C}2\alpha$ ), 14.4 (ester methyl), 14.1 (ester methyl), -5.38 (TBDMS methyl), -5.45 (TBDMS methyl); MS  $m/z$  (rel. intensity) (EI) 560 ( $\text{M}^+$ , 3), 503 (100), 457 (3), 429 (3), 383 (3), 355 (11), 313 (5), 289 (23), 243 (7), 215 (13), 169 (21), 141 (32), 103 (11), 73 (28).

COSY (500 MHz, CDCl<sub>3</sub>):

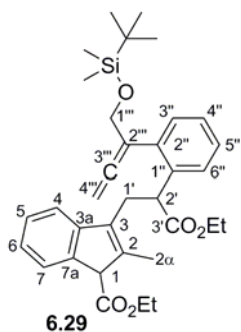
Entry	Proton ( $\delta$ )	Correlation
1	H1 (3.43)	H1'a, H1'b
2	H1'a (2.82-2.77)	H1, H1'b, H2'
3	H1'b (1.53-1.47)	H1, H1'a, H2' (wk.)
4	H1''' (4.29-4.23)	H4'''a, H4'''b
5	H2' (4.35)	H1'a, H1'b
6	H4'''a (4.63)	H1''', H4'''b
7	H4'''b (4.12)	H1''', H4'''a
8	Ester CH <sub>2</sub> ( $\delta$ 4.36)	Ester CH <sub>3</sub> ( $\delta$ 1.40)
9	Ester CH <sub>2</sub> ( $\delta$ 4.05-3.98)	Ester CH <sub>3</sub> ( $\delta$ 1.15)
10	Ester CH <sub>3</sub> ( $\delta$ 1.40)	Ester CH <sub>2</sub> ( $\delta$ 4.36)
11	Ester CH <sub>3</sub> ( $\delta$ 1.15)	Ester CH <sub>2</sub> ( $\delta$ 4.05-3.98)

HMQC (500 MHz, CDCl<sub>3</sub>):

Entry	Proton	Correlation: <sup>13</sup> C-Chemical Shift in ppm (Assignment)
1	H1	52.6 (C1)
2	H1'a	35.7 (C1')
3	H1'b	35.7 (C1')
4	H1'''	65.0 (C1''')
5	H2'	44.8 (C2')
6	H2 $\alpha$	15.3 (C2 $\alpha$ )
7	H4'''a	76.8 (C4''')
8	H4'''b	76.8 (C4''')
9	Ester CH <sub>2</sub> ( $\delta$ 4.36)	60.1
10	Ester CH <sub>2</sub> ( $\delta$ 4.05-3.98)	60.8
10	Ester CH <sub>3</sub> ( $\delta$ 1.40)	14.4
11	Ester CH <sub>3</sub> ( $\delta$ 1.15)	14.1
12	ArH ( $\delta$ 7.88)	122.0
13	ArH ( $\delta$ 7.53)	127.2
14	ArH ( $\delta$ 7.47)	123.6

HMBC (500 MHz, CDCl<sub>3</sub>):

Entry	Proton	Correlation: <sup>13</sup> C-Chemical Shift in ppm (Assignment)
1	H2'	165.1 (ester carbonyl), 137.7 (C1'', wk.)
2	H2 $\alpha$	52.6 (C1), 128.5, 141.8 (wk.), 161.3
3	H4'''a	103.2 (C2''')
4	H4'''b	103.2 (C2''', wk.), 65.0 (C1''', wk.)
5	Ester CH <sub>2</sub> ( $\delta$ 4.36)	165.1 (ester carbonyl), 1.40 (ester CH <sub>3</sub> ) or 1.15 (ester CH <sub>3</sub> )
6	Ester CH <sub>2</sub> ( $\delta$ 4.05-3.98)	173.8 (ester carbonyl), 1.40 (ester CH <sub>3</sub> , wk.) or 1.15 (ester CH <sub>3</sub> , wk.)
7	Ester CH <sub>3</sub> ( $\delta$ 1.40)	60.1 (ester CH <sub>2</sub> )
8	Ester CH <sub>3</sub> ( $\delta$ 1.15)	60.8 (ester CH <sub>2</sub> )
9	ArH ( $\delta$ 7.88)	144.5, 124.6
10	ArH ( $\delta$ 7.53)	134.9, 127.2 or 126.9, 44.8 (C2', wk.)
11	ArH ( $\delta$ 7.47)	141.8, 127.2 or 126.9, 52.6 (C1, wk.)



**Ethyl 3-(2-(2-(1-(*tert*-butyldimethylsilyloxy)buta-2,3-dien-2-yl)phenyl)-3-ethoxy-3-oxopropyl)-2-methyl-1*H*-indene-1-carboxylate (6.29).** Two diastereomers:  $^1\text{H}$  NMR (500 MHz,  $\text{CDCl}_3$ )  $\delta$  7.67-7.65 (2H, m, *ArH*), 7.44-7.41 (2H, m, *ArH*), 7.32-7.27 (6H, m, *ArH*), 7.24-7.20 (4H, m, *ArH*), 7.16-7.11 (2H, m, *ArH*), 4.79 (1H, td,  $J = 10.8, 3.2$  Hz,  $\text{C}=\text{CH}$ ), 4.69 (1 H, td,  $J = 10.5, 3.1$  Hz,  $\text{C}=\text{CH}$ ), 4.57 (1H, td,  $J = 10.8, 3.2$  Hz,  $\text{C}=\text{CH}$ ), 4.40 (1H, dd,  $J = 6.3, 9.0$  Hz,  $H_{2'}$ ), 4.32-4.25 (2H, m,  $\text{SiOCH}_2$ ) overlapping with (1H, m,  $H_{2'}$ ), 4.22 (1 H, td,  $J = 10.5, 3.1$  Hz,  $\text{C}=\text{CH}$ ), 4.19-4.01 (8H, m,  $\text{OCH}_2\text{CH}_3$ ) overlapping with 4.12 (1H, s,  $H_1$ ) overlapping with 4.02 (1H, s,  $H_1$ ) overlapping with (2H, m,  $\text{SiOCH}_2$ ), 3.32-3.26 (2H, m,  $H_{1'}$ ), 2.93 (1H, dd,  $J = 7.7, 13.8$  Hz,  $H_{1'}$ ), 2.87 (1H, dd,  $J = 6.3, 13.8$  Hz,  $H_{1'}$ ), 1.97 (3H, s,  $H_{2\alpha}$ ), 1.74 (3H, s,  $H_{2\alpha}$ ), 1.23 (3H, t,  $J = 7.1$  Hz,  $\text{OCH}_2\text{CH}_3$ ), 1.19 (3H, t,  $J = 7.1$  Hz,  $\text{OCH}_2\text{CH}_3$ ), 1.12 (3H, t,  $J = 7.1$  Hz,  $\text{OCH}_2\text{CH}_3$ ), 1.07 (3H, t,  $J = 7.1$  Hz,  $\text{OCH}_2\text{CH}_3$ ), 0.84 (9H, s,  $\text{SiC}(\text{CH}_3)_3$ ), 0.83 (9H, s,  $\text{SiC}(\text{CH}_3)_3$ ), -0.033 (3H, s,  $\text{Si}(\text{CH}_3)$ ), -0.046 (3H, s,  $\text{Si}(\text{CH}_3)$ ), -0.055 (3H, s,  $\text{Si}(\text{CH}_3)$ ), -0.064 (3H, s,  $\text{Si}(\text{CH}_3)$ );  $^{13}\text{C}$  NMR (125.5 MHz,  $\text{CDCl}_3$ )  $\delta$  206.0 ( $=\text{C}=\text{O}$ ), 205.9 ( $=\text{C}=\text{O}$ ), 173.7 (ester carbonyl), 173.6 (ester carbonyl), 170.78 (ester carbonyl alpha to C1), 170.75 (ester carbonyl alpha to C1), 145.7, 145.6, 140.5, 140.3, 138.96, 138.92, 137.2, 137.1, 136.5, 136.2, 135.7, 135.4, 129.9, 129.8, 127.82, 127.77, 127.6, 127.49, 127.43, 126.9, 124.53, 124.47, 123.09, 123.05, 118.8, 118.6, 104.2 ( $\text{C}_{2''}$ ), 103.9 ( $\text{C}_{2''}$ ), 76.8 ( $\text{C}_{4''}$ ), 76.3 ( $\text{C}_{4''}$ ), 64.92 ( $\text{C}_{1''}$ ), 64.87 ( $\text{C}_{1''}$ ), 60.89 (ester methylene), 60.86 (ester methylene), 60.79 (ester methylene), 60.65 (ester methylene), 58.4 (C1), 58.3 (C1), 45.6 ( $\text{C}_{2'}$ ), 45.5 ( $\text{C}_{2'}$ ), 30.60 ( $\text{C}_{1'}$ ), 30.57 ( $\text{C}_{1'}$ ), 25.8 (*t*-Bu), 18.4 (quat. C of *t*-Bu), 14.19 (ester methyl), 14.17 (ester methyl), 14.01 (ester methyl), 13.97 (ester methyl), 13.2

(C2 $\alpha$ ), 12.8 (C2 $\alpha$ ), -5.39 (TBDMS methyl), -5.43 (TBDMS methyl), -5.46 (TBDMS methyl);  
 MS *m/z* (rel. intensity) (EI) 560 (M<sup>+</sup>, 4), 503 (100), 457 (2), 429 (2), 383 (3), 355 (9), 313  
 (4), 289 (22), 281 (14), 243 (6), 215 (12), 169 (18), 141 (28), 103 (9), 73 (24).

COSY (500 MHz, CDCl<sub>3</sub>):

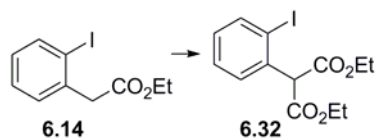
Entry	Proton	Correlation
1	H1'a	H1'b, H2'
2	H1'b	H1'a, H2'
3	H2'	H1'a, H1'b
4	H4'''a	H4'''b
5	H4'''b	H4'''a
6	Ester CH <sub>2</sub>	Ester CH <sub>3</sub>
7	Ester CH <sub>3</sub>	Ester CH <sub>2</sub>

HMQC (500 MHz, CDCl<sub>3</sub>):

Entry	Proton	Correlation: <sup>13</sup> C-Chemical Shift in ppm (Assignment)
1	H1	58.4 (C1), 58.3 (C1)
2	H1'	30.60 (C1'), 30.57 (C1')
3	H1'''	64.92 (C1'''), 64.87 (C1''')
4	H2'	45.6 (C2'), 45.5 (C2')
5	H2' $\alpha$	13.2 (C2 $\alpha$ ), 12.8 (C2 $\alpha$ )
6	H4'''	76.8 (C4'''), 76.3 (C4''')
7	Ester CH <sub>2</sub>	60.89, 60.86, 60.79, 60.65
8	Ester CH <sub>3</sub>	14.19, 14.17, 14.01, 13.97

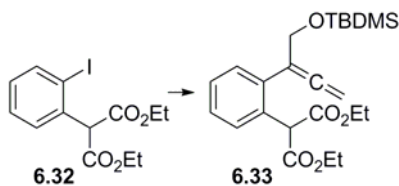
HMBC (500 MHz, CDCl<sub>3</sub>):

Entry	Proton	Correlation: <sup>13</sup> C-Chemical Shift in ppm (Assignment)
1	H1	170.78 (ester carbonyl alpha to C1), 170.75 (ester carbonyl alpha to C1)
2	H1'	173.7 (ester carbonyl alpha to C2'), 173.6 (ester carbonyl alpha to C2'), 145.7, 145.6, 45.6 (C2'), 45.5 (C2')
3	H2'	173.7 (ester carbonyl alpha to C2'), 173.6 (ester carbonyl alpha to C2'), 30.60 (C1'), 30.57 (C1')
4	H2 $\alpha$	58.4 (C1), 58.3 (C1)
5	H4'''	206.0 (=C=, wk.), 205.9 (=C=, wk.), 104.2 (C2'''), 103.9 (C2''')
6	ArH ( $\delta$ 7.67-7.65)	135.7, 135.4, 126.9, 45.6 (C2'), 45.5 (C2')
7	ArH ( $\delta$ 7.44-7.41)	145.7, 145.6, 58.4 (C1, wk.), 58.3 (C1, wk.)
8	ArH ( $\delta$ 7.16-7.11)	118.8, 118.6, 140.5 (wk.), 140.3 (wk.)



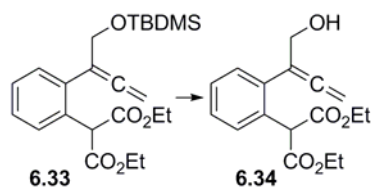
**Diethyl 2-(2-iodophenyl)malonate (6.32).** From procedures described by Larock and coworkers,<sup>508</sup> NaH (0.4769 g, 19.9 mmol, previously washed three times with dry hexane) was added to a solution of (2-iodophenyl)acetate **6.14** (1.4535g, 5 mmol) in diethyl carbonate (30 mL) and stirred at room temperature for 15 h. The reaction was quenched with a saturated solution of NH<sub>4</sub>Cl and extracted three times with dichloromethane. The organic extracts were pooled and dried over sodium sulfate, filtered and concentrated in vacuo to afford 1.3251 g of a gold oil. Purification by flash silica chromatography (6:1 hexanes:ethyl acetate) gave 1.2073 g (67%) of the title compound<sup>508</sup> as a pale yellow oil: IR (NaCl, film, cm<sup>-1</sup>)  $\nu_{\max}$  2982, 1735, 1468, 1368, 1305, 1260, 1219, 1148, 1031, 745; <sup>1</sup>H NMR (300 MHz, CDCl<sub>3</sub>)  $\delta$  7.85 (1H, dd,  $J = 1.0, 7.9$  Hz, ArH), 7.45 (1H, dd,  $J = 1.6, 7.8$  Hz, ArH), 7.35 (1H, dd,  $J = 1.0, 7.9$  Hz, ArH), 6.99 (1H, dd,  $J = 1.6, 7.8$  Hz, ArH), 5.10 (1H, s, CH), 4.16-4.28 (4H, m, OCH<sub>2</sub>CH<sub>3</sub>), 1.26 (6H, t,  $J = 7.1$  Hz, CH<sub>2</sub>CH<sub>3</sub>); <sup>13</sup>C NMR (75.5 MHz, CDCl<sub>3</sub>)  $\delta$  167.8, 139.6, 136.4, 129.8, 129.7, 128.6, 101.7, 62.2, 62.0, 14.1; MS  $m/z$  (rel. intensity) (EI) 362 (M<sup>+</sup>, 10), 317 (6), 289 (20), 261 (4), 235 (100), 207 (39), 179 (36), 162 (45), 134 (68), 89 (25), 78 (23), 63 (7); HRMS (EI) calc. for C<sub>13</sub>H<sub>15</sub>IO<sub>4</sub>: 362.0015, found: 362.0009.





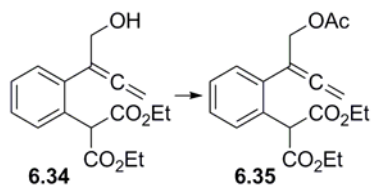
**Diethyl 2-(2-(1-((tert-butyldimethylsilyloxy)buta-2,3-dien-2-yl)phenyl)malonate (6.33).** From a modification of the procedure described by Mukai and Takahashi,<sup>406</sup> a flame dried round bottom flask was charged with the malonate **6.32** (1.0637 g, 2.94 mmol), stannylallene **6.15** (1.4930 g, 3.15 mmol) and DMF (30 mL). This solution was degassed twice under high vacuum using freeze-thaw conditions with argon purges. While still frozen, tri-(2-furyl)-phosphine (0.157 g, 0.68 mmol), Pd<sub>2</sub>(dba)<sub>3</sub>·CHCl<sub>3</sub> (0.0894 g, 0.17 mmol), and CuI (0.0528 g, 0.277 mmol) were added under argon atmosphere. The reaction mixture was degassed twice more and stirred at room temperature for 20 h at which time the mixture was quenched with 10% NH<sub>4</sub>OH and extracted three times with ether. The ethereal extracts were pooled, washed with water twice, brine once, dried over Na<sub>2</sub>SO<sub>4</sub>, filtered and the solvent evaporated in vacuo to provide the crude product as a dark gold oil (2.2954 g). Purification of the target compound by flash silica chromatography (10:1 hexanes:ethyl acetate) provided the title compound (0.9458 g, 77%) as a yellow oil contaminated with small amounts of the malonate **6.32** and the ligand. Another round of flash silica chromatography (12:1 hexanes:ethyl acetate) provided the title compound (0.0563 g, 5%) as a colourless oil: IR (NaCl, film, cm<sup>-1</sup>)  $\nu_{\max}$  2956, 2931, 2857, 1957, 1756, 1736, 1464, 1446, 1368, 1302, 1256, 1214, 1145, 1078, 1034, 839, 777; <sup>1</sup>H NMR (300 MHz, CDCl<sub>3</sub>)  $\delta$  7.52-7.49 (1H, m, ArH), 7.31-7.28 (3H, m, ArH), 5.14 (1H, s, CH), 4.89 (2H, t, *J* = 3.0 Hz, C=CH<sub>2</sub>), 4.35 (2H, t, *J* = 3.0 Hz, CH<sub>2</sub>OSi), 4.12-4.23 (4H, m, OCH<sub>2</sub>CH<sub>3</sub>), 1.22 (6H, t, *J* = 7.1 Hz, OCH<sub>2</sub>CH<sub>3</sub>), 0.86

(9H, s, SiC(CH<sub>3</sub>)<sub>3</sub>), 0.02 (6H, s, Si(CH<sub>3</sub>)<sub>2</sub>); <sup>13</sup>C NMR (75.5 MHz, CDCl<sub>3</sub>) δ 206.3, 168.5, 135.5, 131.6, 129.3, 128.9, 127.8, 127.7, 103.5, 77.3, 64.8, 61.6, 54.3, 25.8, 18.4, 14.0, -5.4; MS *m/z* (rel. intensity) (EI) 418 (M<sup>+</sup>, 8), 373 (11), 361 (100), 315 (26), 289 (48), 271 (8), 259 (28), 243 (36), 231 (9), 213 (31), 199 (8), 185 (17), 169 (13), 141 (28), 115 (8), 73 (36).



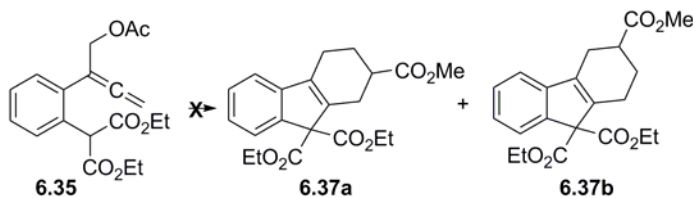
**Diethyl 2-(2-(1-hydroxybuta-2,3-dien-2-yl)phenyl)malonate (6.34).** To a solution of the silyl protected alcohol **6.33** (1.4708 g, 3.51 mmol) in 80% methanol (15 mL) was added KHSO<sub>4</sub> (0.5457 g, 4.01 mmol) and stirred at room temperature for 33 h. The rest of the procedure follows that as for **6.17**. The crude product was obtained as a yellow oil (1.1385 g) and was purified chromatographically (silica, 3:1 then 1:1 hexanes:ethyl acetate) to afford the title compound (0.5974 g, 56%) as a pale yellow oil: IR (NaCl, film, cm<sup>-1</sup>)  $\nu_{\max}$  3519, 3065, 2984, 2939, 2874, 1954, 1732, 1490, 1465, 1448, 1392, 1369, 1303, 1217, 1151, 1097, 1032, 861, 764, 719, 655; <sup>1</sup>H NMR (300 MHz, CDCl<sub>3</sub>) δ 7.54-7.50 (1H, m, ArH), 7.34-7.26 (3H, m, ArH), 5.16 (1H, s, CH), 4.97 (2H, t, *J* = 3.0 Hz, C=CH<sub>2</sub>), 4.34 (2H, br s, CH<sub>2</sub>OH), 4.27-4.14 (4H, m, OCH<sub>2</sub>CH<sub>3</sub>), 1.92 (1H, br s, OH), 1.24 (6H, t, *J* = 7.1 Hz, OCH<sub>2</sub>CH<sub>3</sub>); <sup>13</sup>C NMR (75.5 MHz, CDCl<sub>3</sub>) δ 205.4, 168.5, 135.0, 131.8, 129.5, 128.6, 128.3, 128.0, 103.5, 78.0, 64.3, 61.8, 54.3, 14.0; MS *m/z* (rel. intensity) (EI) 304 (M<sup>+</sup>, 77), 286 (24), 274 (58), 273 (25), 262 (10), 246 (12), 231 (19), 228 (21), 214 (26), 213 (79), 199 (37), 185 (100), 173 (22), 157

(55), 141 (45), 129 (99), 128 (65), 115 (50), 102 (6), 91 (9), 77 (10), 63 (4), 51 (4); HRMS (EI) calc. for C<sub>17</sub>H<sub>20</sub>O<sub>5</sub>: 304.1311, found: 304.1322.

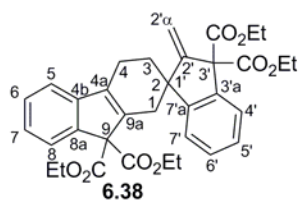


**Diethyl 2-(2-(1-acetoxybuta-2,3-dien-2-yl)phenyl)malonate (6.35).** TsOH·H<sub>2</sub>O (0.0028 g) was added to a stirring solution of the allenyl alcohol **6.34** (0.0462 g, 0.15 mmol) dissolved in acetic anhydride (2 mL). The solution was stirred at room temperature for 24 h. The reaction was quenched with water and CH<sub>2</sub>Cl<sub>2</sub> (4 mL) was added. The organic layer was washed with water containing one drop of a saturated solution of NaHCO<sub>3</sub>, a saturated solution of NH<sub>4</sub>Cl, brine, dried over Na<sub>2</sub>SO<sub>4</sub>, filtered and the solvent evaporated under reduced pressure. The residue (0.0514 g) was purified by silica gel chromatography (3:1 hexanes:ethyl acetate) to afford the title compound (0.0294 g, 56%) as a clear colourless oil: IR (NaCl, film, cm<sup>-1</sup>) ν<sub>max</sub> 2984, 2940, 2907, 1956, 1732, 1491, 1448, 1369, 1302, 1225, 1149, 1096, 1031, 974, 862, 767, 720; <sup>1</sup>H NMR (300 MHz, CDCl<sub>3</sub>) δ 7.53-7.50 (1H, m, ArH), 7.33-7.28 (3H, m, ArH), 5.14 (1H, s, CH), 4.94 (2H, t, *J* = 2.6 Hz, C=CH<sub>2</sub>), 4.78 (2H, t, *J* = 2.6 Hz, CH<sub>2</sub>OH), 4.24-4.13 (4H, m, OCH<sub>2</sub>CH<sub>3</sub>), 1.99 (3H, s, C(O)CH<sub>3</sub>), 1.24 (6H, t, *J* = 7.1 Hz, OCH<sub>2</sub>CH<sub>3</sub>); <sup>13</sup>C NMR (75.5 MHz, CDCl<sub>3</sub>) δ 207.2, 170.5, 168.4, 134.8, 131.8, 129.5, 128.6, 128.14, 128.07, 99.2, 77.4, 65.2, 61.7, 54.3, 20.8, 14.0; MS *m/z* (rel. intensity) (EI) 346 (M<sup>+</sup>, 7), 304 (100), 289 (13), 286 (19), 263 (4), 258 (25), 245 (5), 231 (31), 230

(94), 213 (46), 201 (24), 185 (85), 169 (9), 157 (77), 141 (30), 129 (36), 115 (26), 91 (3), 77 (4), 51 (1); HRMS (EI) calc. for C<sub>19</sub>H<sub>22</sub>O<sub>6</sub>: 346.1416, found: 346.1418.



**Synthetic efforts towards 9,9-Diethyl 2-methyl-3,4-dihydro-1*H*-fluorene-2,9,9(2*H*)-tricarboxylate (6.37a) and 9,9-Diethyl 3-methyl-3,4-dihydro-1*H*-fluorene-3,9,9(2*H*)-tricarboxylate (6.37b).** Malonate **6.35** (0.005 g, 0.0014 mmol) and methyl acrylate (0.0015-0.033 mL, 0.0017-0.37 mmol) were typically dissolved in ethyl acetate or CH<sub>2</sub>Cl<sub>2</sub> (0.5-2.0 mL). The appropriate base was then added as described in Table 6.3. Reactions were quenched with a saturated solution of NH<sub>4</sub>Cl and extracted with either ethyl acetate or CH<sub>2</sub>Cl<sub>2</sub>. The organic extracts were washed with water, brine and dried over Na<sub>2</sub>SO<sub>4</sub>, filtered and the solvent removed in vacuo. The crude residue contained variable amounts of the target **6.37** and **6.38** (Entries 3 and 4, Table 6.3). Flash silica gel chromatography (4:1 hexanes: ethyl acetate) provided a fraction containing the homodimer **6.38** (0.006 g, Entries 1 and 2, Table 6.3): **Tetraethyl 2'-methylene-3,4-dihydrospiro[fluorene-2,1'-indene]-3',3',9,9(1*H*,2'*H*)-tetracarboxylate (6.38).**



<sup>1</sup>H NMR (500 MHz, CDCl<sub>3</sub>) δ 7.68 (1H, d, *J* = 7.4 Hz, Ar*H*), 7.58-7.56 (1H, m, Ar*H*), 7.40 (1H, dd, *J* = 6.8, 7.5 Hz, Ar*H*), 7.37-7.26 (4H, m, Ar*H*), 7.21-7.19 (1H, m, Ar*H*), 5.65 (1H, s, C=CH, *H*2'*α*), 5.51 (1H, s, C=CH, *H*2'*α*), 4.26-4.15 (8H, m, OCH<sub>2</sub>CH<sub>3</sub>), 2.95, 2.91 (2H, AB<sub>q</sub>, *J* =

18.5 Hz, *H1*), 2.72-2.66 (2H, m, *H4*), 1.97-1.94 (2H, m, *H3*), 1.34-1.23 (9H, m, OCH<sub>2</sub>CH<sub>3</sub>), 1.16 (3H, t, *J* = 7.1 Hz, OCH<sub>2</sub>CH<sub>3</sub>); <sup>13</sup>C NMR (125.5 MHz, CDCl<sub>3</sub>) δ 169.7 (ester carbonyl), 169.6 (ester carbonyl), 168.12 (ester carbonyl), 168.05 (ester carbonyl), 154.1 (C2'), 150.1, 144.3, 140.61, 140.56, 137.9, 137.1, 129.1, 128.6, 127.4, 126.5, 125.8, 124.9, 123.6, 118.6, 113.4 (C2 $\alpha$ ), 71.0 (C9), 69.1 (C3'), 62.0 (ester methylene), 61.91 (ester methylene), 61.88 (ester methylene), 61.80 (ester methylene), 49.6 (C2/C1'), 36.4 (C1), 35.1 (C3), 20.3 (C4), 14.04 (ester methyl), 13.97 (ester methyl), 13.85 (ester methyl); MS *m/z* (rel. intensity) (EI) 572 (M<sup>+</sup>, 1), 499 (2), 452 (1), 372 (9), 346 (3), 312 (8), 286 (58), 273 (10), 252 (14), 231 (9), 214 (44), 213 (100), 185 (74), 168 (18), 157 (18), 149 (11), 141 (21), 129 (28), 128 (14), 115 (13), 83 (9), 57 (8); HRMS (EI) calc. for C<sub>34</sub>H<sub>36</sub>O<sub>8</sub>: 572.2410, found: 572.2401.

COSY (500 MHz, CDCl<sub>3</sub>):

Entry	Proton ( $\delta$ )	Correlation
1	H3 (5.65)	H4
2	H4 (5.51)	H3

HMQC (500 MHz, CDCl<sub>3</sub>):

Entry	Proton	Correlation: <sup>13</sup> C-Chemical Shift in ppm (Assignment)
1	H1	36.4 (C1)
2	H2' $\alpha$	113.4 (C2' $\alpha$ )
3	H3	35.1 (C3)
4	H4	20.3 (C4)
5	ArH (7.68)	124.9
6	ArH (7.58-7.56)	126.5

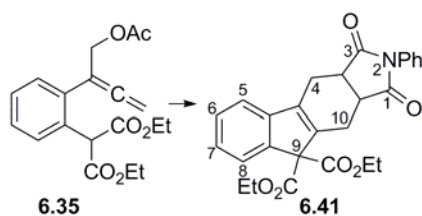
7	ArH (7.40)	128.6
8	ArH (7.37-7.26)	118.6, 125.8, 127.4, 129.1
9	ArH (7.21-7.19)	123.6
10	Ester CH <sub>2</sub>	61.80, 61.88, 61.91, 62.0
11	Ester CH <sub>3</sub>	13.85, 13.97, 14.04

---

HMBC (500 MHz, CDCl<sub>3</sub>):

Entry	Proton	Correlation: <sup>13</sup> C-Chemical Shift in ppm (Assignment)
1	H1	35.1 (C3, wk.), 49.6 (C2/C1'), 137.9, 140.61 or 140.56, 150.1, 154.1 (C2')
2	H2'αa	49.6 (C2/C1'), 69.1 (C3'), 154.1 (C2')
3	H2'αb	49.6 (C2/C1'), 69.1 (C3')
4	H3	20.3 (C4), 36.4 (C1), 49.6 (C2/C1'), 140.61 or 140.56, 150.1, 154.1 (C2')
5	H4	35.1 (C3, v. wk.), 49.6 (C2/C1', v. wk.), 137.9 (v. wk.), 140.61 or 140.56 (v. wk.)
6	ArH (7.68)	128.6, 144.3
7	ArH (7.58-7.56)	129.1, 150.1 (wk.)
8	ArH (7.40)	118.6 (v. wk.), 124.9, 140.61 or 140.56 (v. wk.), 144.3
9	ArH (7.21-7.19)	127.4, 137.1

---



**Diethyl 1,3-dioxo-2-phenyl-2,3,3a,4,10,10a-hexahydroindeno[1,2-*f*]isoindole-9,9(1*H*)-dicarboxylate (6.41).** To stirring solution of the malonate **6.35** (0.007g, 0.02 mmol) and *N*-phenylmaleimide (0.0717 g, 0.4 mmol) in CH<sub>2</sub>Cl<sub>2</sub> (0.5 mL) was added DBU (0.006 mL dissolved in 1 mL CH<sub>2</sub>Cl<sub>2</sub>) via syringe pump over a 2 h period. The reaction solution was stirred for 15.5 h and then quenched with a saturated solution of NH<sub>4</sub>Cl (2 mL). Water and CH<sub>2</sub>Cl<sub>2</sub> were added to the mixture and the mixture was washed with a saturated solution of NH<sub>4</sub>Cl, brine, dried over Na<sub>2</sub>SO<sub>4</sub> and filtered. The solvent was evaporated under reduced pressure to give a purple solid (0.0747 g). Two rounds of flash silica gel chromatography (4:1, 2:1 then 1:1 hexanes:ethyl acetate) provided the title compound (0.0071 g, 77%) as a white solid: <sup>1</sup>H NMR (300 MHz, CDCl<sub>3</sub>) δ 7.64-7.62 (1H, m, *ArH*), 7.41-7.21 (5H, m, *ArH*), 7.17-7.15 (2H, m, *ArH*), 4.22 (2H, q, *J* = 7.1 Hz, OCH<sub>2</sub>CH<sub>3</sub>), 4.11 (2H, q, *J* = 7.1 Hz, OCH<sub>2</sub>CH<sub>3</sub>), 3.53-3.45 (2H, m, *H*3a, *H*10a), 3.32-3.26 (2H, m, *H*4, *H*10), 2.93-2.71 (2H, m, *H*4, *H*10), 1.27 (3H, t, *J* = 7.1 Hz, OCH<sub>2</sub>CH<sub>3</sub>), 1.19 (3H, t, *J* = 7.1 Hz, OCH<sub>2</sub>CH<sub>3</sub>); <sup>13</sup>C NMR (75.5 MHz, CDCl<sub>3</sub>) δ 178.5 (maleimide carbonyl), 178.4 (maleimide carbonyl), 167.4 (ester carbonyl), 167.1 (ester carbonyl), 143.0, 140.1, 139.9, 137.5, 131.9, 129.0, 128.7, 128.5, 126.5, 126.4, 125.3, 118.7, 70.6 (*C*9), 62.4 (ester methylene), 62.2 (ester methylene), 39.5 (*C*3a or *C*10a), 38.9 (*C*3a or *C*10a), 23.9 (*C*4 or *C*10), 21.5 (*C*4 or *C*10), 14.0 (ester methyl), 13.9 (ester methyl); MS *m/z* (rel. intensity) (EI) 459 (*M*<sup>+</sup>, 100), 413 (6), 385 (81), 369 (11), 357 (9), 341 (88), 340 (38), 312 (2), 238 (24), 219 (3), 209 (9), 193 (21), 181 (7), 166 (22),

165 (76), 152 (3), 140 (3), 120 (2), 77 (2), 57 (1); HRMS (EI) calc. for  $C_{27}H_{25}NO_6$ :  
459.1682, found: 459.1688.



## Appendices

### Appendix A Nitric oxide gas generating apparatus



## Appendix B X-ray crystallographic data for *N*- (diphenylmethylene)nitramide 3.7

Figures of all X-ray crystal structures were generated using Mercury 2.2 or 2.3.

**Table B:** X-ray crystal structure of *N*-(diphenylmethylene)nitramide 3.7.

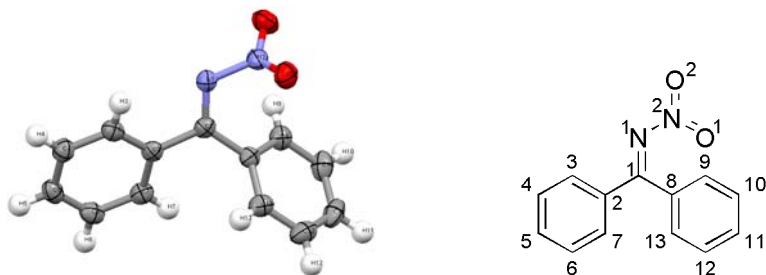


**Table B1:** Crystal data and structure refinement for 3.7.

Empirical formula	C <sub>13</sub> H <sub>10</sub> N <sub>2</sub> O <sub>2</sub>
Formula weight	226.23 g/mol
Temperature	180(2) K
Wavelength	0.71073 Å
Crystal system, space group	Triclinic, <i>P</i> -1
Unit cell dimensions	$a = 8.4915(14)\text{Å}$ , $b = 9.2184(15)\text{Å}$ , $c = 9.3932(15)\text{Å}$ $\alpha = 93.643(3)^\circ$ , $\beta = 116.436(3)^\circ$ , $\gamma = 111.577(3)^\circ$
Volume	589.01(17) Å <sup>3</sup>
Z, Calculated density	2, 1.276 g/cm <sup>3</sup>
Absorption coefficient	0.088 mm <sup>-1</sup>
F(000)	236
Crystal size	0.30 x 0.28 x 0.25 mm
Theta range for data collection	2.47 to 26.00 °
Limiting indices	-8 ≤ h ≤ 10, -11 ≤ k ≤ 11, -11 ≤ l ≤ 11
Reflections collected / unique	3907 / 2297 [R <sub>int</sub> = 0.0444]
Completeness to theta = 26.00	98.5 %
Absorption correction	None

Refinement method	Full-matrix least-squares on F <sup>2</sup>
Data / restraints / parameters	2297 / 0 / 156
Goodness-of-fit on F <sup>2</sup>	1.535
Final R indices [I>2σ(I)]	R1 = 0.0601, wR2 = 0.1322
R indices (all data)	R1 = 0.0661, wR2 = 0.1344
Extinction coefficient	0.040(7)
Largest diff. peak and hole	0.316 and -0.274 e Å <sup>-3</sup>

**Table B2:** Atomic coordinates (x 10<sup>4</sup>) and equivalent isotropic displacement parameters (Å<sup>2</sup> x 10<sup>3</sup>) for **3.7**.

	x	y	z	U <sub>eq</sub>
O(1)	726(3)	3841(2)	2021(2)	49(1)
O(2)	2011(3)	1680(2)	1265(2)	52(1)
N(1)	95(3)	2902(2)	4010(2)	36(1)
N(2)	-390(3)	2771(2)	2308(2)	38(1)
C(1)	1609(3)	2650(2)	4936(2)	31(1)
C(2)	2189(3)	2914(2)	6732(2)	31(1)
C(3)	1548(3)	3825(3)	7412(3)	36(1)
C(4)	1972(3)	3979(3)	9049(3)	40(1)
C(5)	3076(3)	3239(3)	10036(3)	40(1)
C(6)	3753(3)	2366(3)	9389(3)	40(1)
C(7)	3321(3)	2195(3)	7745(3)	36(1)
C(8)	2716(3)	2091(2)	4336(2)	31(1)
C(9)	1736(4)	672(3)	3035(3)	38(1)
C(10)	2796(4)	172(3)	2497(3)	47(1)
C(11)	4827(4)	1100(3)	3226(3)	50(1)
C(12)	5803(4)	2503(3)	4514(3)	48(1)

C(13)	4777(3)	2995(3)	5089(3)	39(1)
-------	---------	---------	---------	-------

---

**Table B3:** Hydrogen coordinates ( $\times 10^4$ ) and equivalent isotropic displacement parameters ( $\text{\AA}^2 \times 10^3$ ) for **3.7**.

---

	x	y	z	$U_{\text{eq}}$
H(3)	821	4339	6751	43
H(4)	1516	4580	9493	48
H(5)	3361	3336	11146	48
H(6)	4514	1883	10067	48
H(7)	3787	1596	7312	43
H(9)	355	55	2523	45
H(10)	2139	-798	1637	56
H(11)	5540	773	2842	59
H(12)	7180	3128	5004	58
H(13)	5458	3938	5986	47

---

**Table B4:** Bond lengths [ $\text{\AA}$ ] and angles [ $^\circ$ ] for **3.7**.

---

O(1)-N(2)	1.232(3)
O(2)-N(2)	1.234(2)
N(1)-C(1)	1.309(3)
N(1)-N(2)	1.447(2)
C(1)-C(8)	1.502(3)
C(1)-C(2)	1.506(3)
C(2)-C(3)	1.409(3)

C(2)-C(7)	1.415(3)
C(3)-C(4)	1.399(3)
C(4)-C(5)	1.407(3)
C(5)-C(6)	1.391(3)
C(6)-C(7)	1.402(3)
C(8)-C(9)	1.410(3)
C(8)-C(13)	1.417(3)
C(9)-C(10)	1.400(3)
C(10)-C(11)	1.401(4)
C(11)-C(12)	1.394(4)
C(12)-C(13)	1.391(3)
C(1)-N(1)-N(2)	115.40(17)
O(1)-N(2)-O(2)	125.87(19)
O(1)-N(2)-N(1)	118.00(18)
O(2)-N(2)-N(1)	115.62(18)
N(1)-C(1)-C(8)	125.44(18)
N(1)-C(1)-C(2)	114.78(18)
C(8)-C(1)-C(2)	119.75(18)
C(3)-C(2)-C(7)	119.06(19)
C(3)-C(2)-C(1)	120.55(19)
C(7)-C(2)-C(1)	120.35(19)
C(4)-C(3)-C(2)	120.6(2)
C(3)-C(4)-C(5)	119.7(2)
C(6)-C(5)-C(4)	120.2(2)
C(5)-C(6)-C(7)	120.5(2)
C(6)-C(7)-C(2)	119.9(2)
C(9)-C(8)-C(13)	119.2(2)
C(9)-C(8)-C(1)	121.01(19)

C(13)-C(8)-C(1)	119.77(18)
C(10)-C(9)-C(8)	120.1(2)
C(9)-C(10)-C(11)	120.0(2)
C(12)-C(11)-C(10)	120.1(2)
C(13)-C(12)-C(11)	120.6(2)
C(12)-C(13)-C(8)	120.0(2)

---

## Appendix C X-ray crystallographic data for Dinitrodiphenylmethane 3.9

### 3.9

**Table C:** X-ray crystal structure of Dinitrodiphenylmethane 3.9.

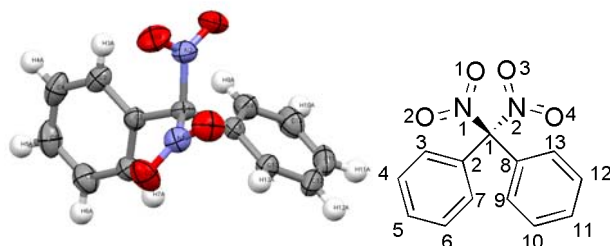


**Table C1:** Crystal data and structure refinement for 3.9.

Empirical formula	C <sub>13</sub> H <sub>10</sub> N <sub>2</sub> O <sub>4</sub>
Formula weight	258.23 g/mol
Temperature	200(2) K
Wavelength	0.71073 Å
Crystal system, space group	Monoclinic, P2 <sub>1</sub> /c
Unit cell dimensions	a = 8.364(3) Å, b = 11.722(4) Å, c = 12.753(4) Å β = 102.019(7) °
Volume	1222.8(7) Å <sup>3</sup>
Z, Calculated density	4, 1.403 g/cm <sup>3</sup>
Absorption coefficient	0.106 mm <sup>-1</sup>
F(000)	536
Crystal size	0.24 x 0.14 x 0.02 mm
Theta range for data collection	3.04 to 30.00 deg.
Limiting indices	-11 ≤ h ≤ 10, -16 ≤ k ≤ 16, -17 ≤ l ≤ 17
Reflections collected / unique	12052 / 3555 [R(int) = 0.0400]
Completeness to theta = 30.00	99.6 %
Absorption correction	Empirical
Max. and min. transmission	0.9979 and 0.9749
Refinement method	Full-matrix least-squares on F <sup>2</sup>
Data / restraints / parameters	3555 / 0 / 174
Goodness-of-fit on F <sup>2</sup>	1.114
Final R indices [I > 2σ(I)]	R1 = 0.0492, wR2 = 0.0770
R indices (all data)	R1 = 0.0896, wR2 = 0.0914
Extinction coefficient	0.0107(11)
Largest diff. peak and hole	0.182 and -0.191 e.Å <sup>-3</sup>

**Table C2:** Atomic coordinates ( $\times 10^4$ ) and equivalent isotropic displacement parameters ( $\text{\AA}^2 \times 10^3$ ) for **3.9**.

	x	y	z	U(eq)
O(1)	11353(2)	4668(1)	1420(1)	60(1)
O(2)	12737(2)	3377(1)	796(1)	63(1)
O(3)	12487(2)	3778(1)	3428(1)	62(1)
O(4)	10093(2)	3168(1)	3538(1)	68(1)
N(1)	11798(2)	3684(1)	1341(1)	43(1)
N(2)	11186(2)	3312(1)	3064(1)	45(1)
C(1)	10996(2)	2770(1)	1939(1)	34(1)
C(2)	11934(2)	1656(1)	2051(1)	35(1)
C(3)	12839(2)	1256(2)	3016(1)	45(1)
C(4)	13614(2)	205(2)	3053(2)	56(1)
C(5)	13508(2)	-437(2)	2143(2)	58(1)
C(6)	12616(2)	-40(2)	1187(2)	55(1)
C(7)	11820(2)	991(2)	1140(1)	45(1)
C(8)	9226(2)	2635(1)	1385(1)	35(1)
C(9)	8297(2)	1835(2)	1800(1)	46(1)
C(10)	6689(2)	1652(2)	1317(2)	56(1)
C(11)	6002(2)	2236(2)	395(2)	59(1)
C(12)	6921(2)	2998(2)	-37(1)	55(1)
C(13)	8525(2)	3213(1)	459(1)	43(1)

**Table C3:** Hydrogen coordinates ( $\times 10^4$ ) and equivalent isotropic displacement parameters ( $\text{\AA}^2 \times 10^3$ ) for **3.9**.

	x	y	z	U(eq)
H(3A)	12929	1699	3649	54
H(4A)	14223	-73	3717	67
H(5A)	14050	-1152	2174	69
H(6A)	12547	-480	554	66
H(7A)	11187	1251	476	54
H(9A)	8776	1413	2422	56
H(10A)	6052	1122	1617	67
H(11A)	4891	2110	61	71
H(12A)	6453	3383	-683	66
H(13A)	9146	3758	162	52



**Table C4:** Bond lengths [Å] and angles [°] for **3.9**.

---

O(1)-N(1)	1.2223(17)
O(2)-N(1)	1.2077(16)
O(3)-N(2)	1.2193(17)
O(4)-N(2)	1.2085(17)
N(1)-C(1)	1.5461(19)
N(2)-C(1)	1.5467(18)
C(1)-C(8)	1.509(2)
C(1)-C(2)	1.515(2)
C(2)-C(3)	1.385(2)
C(2)-C(7)	1.386(2)
C(3)-C(4)	1.388(2)
C(4)-C(5)	1.370(3)
C(5)-C(6)	1.371(2)
C(6)-C(7)	1.375(2)
C(8)-C(13)	1.382(2)
C(8)-C(9)	1.391(2)
C(9)-C(10)	1.375(2)
C(10)-C(11)	1.378(3)
C(11)-C(12)	1.367(3)
C(12)-C(13)	1.382(2)
O(2)-N(1)-O(1)	125.05(14)
O(2)-N(1)-C(1)	118.58(13)
O(1)-N(1)-C(1)	116.26(13)
O(4)-N(2)-O(3)	125.44(14)
O(4)-N(2)-C(1)	117.65(14)
O(3)-N(2)-C(1)	116.67(13)
C(8)-C(1)-C(2)	113.09(12)
C(8)-C(1)-N(1)	109.03(11)
C(2)-C(1)-N(1)	111.96(11)
C(8)-C(1)-N(2)	112.26(11)
C(2)-C(1)-N(2)	108.35(11)
N(1)-C(1)-N(2)	101.60(12)
C(3)-C(2)-C(7)	118.93(15)
C(3)-C(2)-C(1)	123.53(14)
C(7)-C(2)-C(1)	117.49(13)
C(2)-C(3)-C(4)	119.72(16)
C(5)-C(4)-C(3)	120.71(16)
C(4)-C(5)-C(6)	119.62(18)
C(5)-C(6)-C(7)	120.39(17)
C(6)-C(7)-C(2)	120.62(16)
C(13)-C(8)-C(9)	118.97(15)

C(13)-C(8)-C(1)	123.28(14)
C(9)-C(8)-C(1)	117.63(13)
C(10)-C(9)-C(8)	120.44(16)
C(9)-C(10)-C(11)	120.00(18)
C(12)-C(11)-C(10)	119.94(17)
C(11)-C(12)-C(13)	120.57(17)
C(12)-C(13)-C(8)	120.02(16)

---

## Appendix D X-ray crystallographic data for 1,1'-(2'-methylene-3,4-dihydrospiro[carbazole-2,3'-indolin]-1',9(1*H*)-diyl)diethanone 4.55

**Table D:** X-ray crystal structure of 1,1'-(2'-methylene-3,4-dihydrospiro[carbazole-2,3'-indolin]-1',9(1*H*)-diyl)diethanone **4.55**.

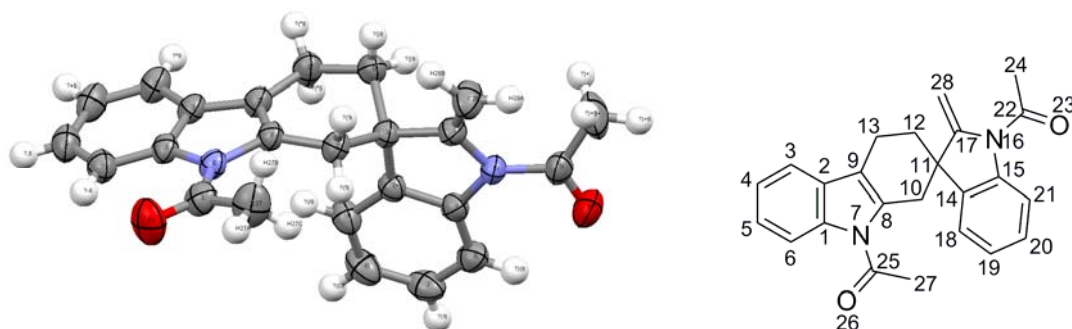


**Table D1:** Crystal data and structure refinement for **4.55**.

Empirical formula	C <sub>24</sub> H <sub>22</sub> N <sub>2</sub> O <sub>2</sub>
Formula weight	370.44
Temperature	296(2) K
Wavelength	0.71073 Å
Crystal system, space group	Triclinic, <i>P</i> -1
Unit cell dimensions	$a = 8.8698(8)$ Å, $b = 9.6311(9)$ Å, $c = 11.2047(10)$ Å $\alpha = 95.155(2)^\circ$ , $\beta = 98.9750(10)^\circ$ , $\gamma = 97.266(2)^\circ$
Volume	931.98(15) Å <sup>3</sup>
Z, Calculated density	2, 1.320 g/cm <sup>3</sup>
Absorption coefficient	0.085 mm <sup>-1</sup>
F(000)	392
Crystal size	0.24 x 0.12 x 0.08 mm
Theta range for data collection	3.40 to 26.00 °
Limiting indices	-10 ≤ h ≤ 9, -11 ≤ k ≤ 11, -13 ≤ l ≤ 13

Reflections collected / unique	5929 / 3619 [R(int) = 0.0204]
Completeness to theta = 26.00	98.9 %
Absorption correction	Empirical
Max. and min. transmission	0.9933 and 0.9800
Refinement method	Full-matrix least-squares on F <sup>2</sup>
Data / restraints / parameters	3619 / 0 / 260
Goodness-of-fit on F <sup>2</sup>	1.122
Final R indices [I>2σ(I)]	R1 = 0.0489, wR2 = 0.0971
R indices (all data)	R1 = 0.0781, wR2 = 0.1081
Extinction coefficient	0.0152(17)
Largest diff. peak and hole	0.187 and -0.174 e.Å <sup>-3</sup>

**Table D2:** Atomic coordinates ( $\times 10^4$ ) and equivalent isotropic displacement parameters ( $\text{\AA}^2 \times 10^3$ ) for **4.55**.

	x	y	z	U (eq)
C(1)	2078(2)	4672(2)	-268(2)	42(1)
C(2)	2736(2)	3818(2)	548(2)	43(1)
C(3)	2228(3)	2374(2)	422(2)	52(1)
C(4)	1048(3)	1822(2)	-523(2)	58(1)
C(5)	386(3)	2688(3)	-1321(2)	59(1)
C(6)	892(2)	4118(2)	-1213(2)	52(1)
N(7)	2811(2)	6070(2)	85(1)	42(1)
C(8)	3889(2)	6053(2)	1175(2)	40(1)
C(9)	3869(2)	4713(2)	1443(2)	44(1)
C(10)	4793(2)	7311(2)	1980(2)	43(1)
C(11)	5217(2)	6931(2)	3290(2)	40(1)
C(12)	5893(2)	5528(2)	3270(2)	47(1)
C(13)	4755(3)	4301(2)	2574(2)	52(1)
C(14)	3869(2)	6923(2)	3970(2)	40(1)
C(15)	4284(2)	7801(2)	5060(2)	40(1)
N(16)	5862(2)	8422(2)	5184(1)	42(1)
C(17)	6391(2)	8087(2)	4060(2)	44(1)
C(18)	2390(2)	6198(2)	3662(2)	50(1)
C(19)	1343(3)	6355(3)	4445(2)	60(1)
C(20)	1784(3)	7214(3)	5535(2)	58(1)
C(21)	3251(3)	7964(2)	5848(2)	51(1)
C(22)	6713(3)	9077(2)	6275(2)	52(1)
O(23)	6076(2)	9426(2)	7119(1)	68(1)
C(24)	8428(3)	9316(4)	6419(2)	89(1)

C(25)	2535(3)	7183(2)	-608(2)	52(1)
O(26)	1520(2)	6995(2)	-1487(2)	78(1)
C(27)	3535(3)	8565(3)	-275(2)	73(1)
C(28)	7645(3)	8691(3)	3715(3)	64(1)

U(eq) is defined as one third of the trace of the orthogonalized Uij tensor.

**Table D3:** Hydrogen coordinates ( $\times 10^4$ ) and equivalent isotropic displacement parameters ( $\text{\AA}^2 \times 10^3$ ) for **4.55**.

	x	y	z	U(eq)
H(3A)	2671	1798	960	62
H(4A)	693	861	-627	69
H(5A)	-417	2296	-1942	70
H(6A)	452	4689	-1755	62
H(10A)	4185	8080	1982	52
H(10B)	5726	7616	1668	52
H(12A)	6813	5629	2899	57
H(12B)	6193	5324	4099	57
H(13A)	5310	3535	2358	63
H(13B)	4040	3964	3092	63
H(18A)	2100	5609	2936	60
H(19A)	342	5881	4238	72
H(20A)	1081	7289	6065	70
H(21A)	3534	8561	6570	61
H(24A)	8852	9784	7216	133
H(24B)	8735	9891	5818	133
H(24C)	8801	8427	6317	133
H(27A)	3206	9212	-832	109
H(27B)	4585	8446	-316	109
H(27C)	3461	8928	536	109
H(28A)	8360(30)	9420(30)	4200(30)	96
H(28B)	7830(30)	8360(30)	2810(30)	96

**Table D4:** Bond lengths [ $\text{\AA}$ ] and angles [ $^\circ$ ] for **4.55**.

C(1)-C(6)	1.386(3)
C(1)-C(2)	1.394(3)
C(1)-N(7)	1.412(3)
C(2)-C(3)	1.395(3)
C(2)-C(9)	1.439(3)
C(3)-C(4)	1.383(3)
C(4)-C(5)	1.391(3)
C(5)-C(6)	1.382(3)
N(7)-C(25)	1.403(3)
N(7)-C(8)	1.431(2)

C(8)-C(9)	1.350(3)
C(8)-C(10)	1.502(3)
C(9)-C(13)	1.496(3)
C(10)-C(11)	1.546(3)
C(11)-C(14)	1.514(3)
C(11)-C(17)	1.524(3)
C(11)-C(12)	1.546(3)
C(12)-C(13)	1.521(3)
C(14)-C(18)	1.383(3)
C(14)-C(15)	1.392(3)
C(15)-C(21)	1.382(3)
C(15)-N(16)	1.431(2)
N(16)-C(22)	1.384(3)
N(16)-C(17)	1.435(2)
C(17)-C(28)	1.317(3)
C(18)-C(19)	1.386(3)
C(19)-C(20)	1.384(3)
C(20)-C(21)	1.383(3)
C(22)-O(23)	1.219(3)
C(22)-C(24)	1.490(3)
C(25)-O(26)	1.210(3)
C(25)-C(27)	1.485(3)

C(6)-C(1)-C(2)	121.2(2)
C(6)-C(1)-N(7)	130.80(19)
C(2)-C(1)-N(7)	107.99(17)
C(1)-C(2)-C(3)	120.6(2)
C(1)-C(2)-C(9)	107.54(18)
C(3)-C(2)-C(9)	131.8(2)
C(4)-C(3)-C(2)	118.1(2)
C(3)-C(4)-C(5)	120.7(2)
C(6)-C(5)-C(4)	121.6(2)
C(5)-C(6)-C(1)	117.7(2)
C(25)-N(7)-C(1)	123.05(17)
C(25)-N(7)-C(8)	129.77(18)
C(1)-N(7)-C(8)	107.04(16)
C(9)-C(8)-N(7)	108.94(18)
C(9)-C(8)-C(10)	124.05(18)
N(7)-C(8)-C(10)	126.74(17)
C(8)-C(9)-C(2)	108.41(18)
C(8)-C(9)-C(13)	124.08(19)
C(2)-C(9)-C(13)	127.11(18)
C(8)-C(10)-C(11)	110.05(16)
C(14)-C(11)-C(17)	101.65(15)
C(14)-C(11)-C(12)	112.89(17)
C(17)-C(11)-C(12)	109.21(16)
C(14)-C(11)-C(10)	111.87(16)
C(17)-C(11)-C(10)	110.84(16)
C(12)-C(11)-C(10)	110.09(16)
C(13)-C(12)-C(11)	112.45(17)
C(9)-C(13)-C(12)	111.76(18)

C(18)-C(14)-C(15)	119.55(19)
C(18)-C(14)-C(11)	129.92(19)
C(15)-C(14)-C(11)	110.53(17)
C(21)-C(15)-C(14)	121.5(2)
C(21)-C(15)-N(16)	129.14(19)
C(14)-C(15)-N(16)	109.40(17)
C(22)-N(16)-C(15)	122.95(17)
C(22)-N(16)-C(17)	128.27(18)
C(15)-N(16)-C(17)	108.37(16)
C(28)-C(17)-N(16)	126.8(2)
C(28)-C(17)-C(11)	124.9(2)
N(16)-C(17)-C(11)	108.32(16)
C(14)-C(18)-C(19)	119.5(2)
C(20)-C(19)-C(18)	120.2(2)
C(21)-C(20)-C(19)	121.1(2)
C(15)-C(21)-C(20)	118.2(2)
O(23)-C(22)-N(16)	120.7(2)
O(23)-C(22)-C(24)	120.1(2)
N(16)-C(22)-C(24)	119.1(2)
O(26)-C(25)-N(7)	119.7(2)
O(26)-C(25)-C(27)	120.9(2)
N(7)-C(25)-C(27)	119.3(2)

---

## References

- (1) Mann, J. *Secondary metabolism*; 2nd ed.; Clarendon Press; Oxford University Press: Oxford [Oxfordshire], New York, 1987; pp 1-374.
- (2) Mann, J. *Natural products: their chemistry and biological significance*; 1st ed.; Longman Scientific & Technical; Wiley: Harlow, Essex, England, New York, 1994; pp 1-455.
- (3) Bhat, S. V.; Nagasampagi, B. A.; Sivakumar, M. *Chemistry of Natural Products*; Springer; Narosa: Berlin, New York, New Delhi, 2005; pp 1-840.
- (4) Gould, S. J.; Hong, S. T.; Carney, J. R. *J. Antibiot.* **1998**, *51*, 50-57.
- (5) Kieser, T.; Bibb, M.; Buttner, M.; Chater, K.; Hopwood, D. *Practical Streptomyces Genetics*; 2nd ed.; John Innes Foundation: Norwich, England, 2000; pp 1-613.
- (6) Bartz, Q. R.; Elder, C. C.; Frohardt, R. P.; Fusari, S. A.; Haskell, T. H.; Johannessen, D. W.; Ryder, A. *Nature* **1954**, *173*, 72-73.
- (7) Fusari, S. A.; Haskell, T. H.; Frohardt, R. P.; Bartz, Q. R. *J. Am. Chem. Soc.* **1954**, *76*, 2881-2883.
- (8) Fusari, S. A.; Frohardt, R. P.; Ryder, A.; Haskell, T. H.; Johannessen, D. W.; Elder, C. C.; Bartz, Q. R. *J. Am. Chem. Soc.* **1954**, *76*, 2878-2881.
- (9) Dion, H. W.; Fusari, S. A.; Jakubowski, Z. L.; Zora, J. G.; Bartz, Q. R. *J. Am. Chem. Soc.* **1956**, *78*, 3075-3077.
- (10) Rao, K. V.; Brooks, S. C., Jr.; Kugelman, M.; Romano, A. A. *Antibiotics Annual* **1959**, *7*, 943-949.
- (11) Kameyama, T.; Takahashi, A.; Matsumoto, H.; Kurasawa, S.; Hamada, M.; Okami, Y.; Ishizuka, M.; Takeuchi, T. *J. Antibiot.* **1988**, *41*, 1561-1567.
- (12) Takahashi, A.; Nakamura, H.; Ikeda, D.; Naganawa, H.; Kameyama, T.; Kurasawa, S.; Okami, Y.; Takeuchi, T.; Iitaka, Y. *J. Antibiot.* **1988**, *41*, 1568-1574.
- (13) Nishimura, M.; Nakada, H.; Nakajima, H.; Hori, Y.; Ezaki, M.; Goto, T.; Okuhara, M. *J. Antibiot.* **1989**, *42*, 542-548.
- (14) Nishimura, M.; Nakada, H.; Takase, S.; Katayama, A.; Goto, T.; Tanaka, H.; Hashimoto, M. *J. Antibiot.* **1989**, *42*, 549-552.
- (15) Lee, M. D.; Fantini, A. A.; Kuck, N. A.; Greenstein, M.; Testa, R. T.; Borders, D. B. *J. Antibiot.* **1987**, *40*, 1657-1663.



- (16) De Voe, S. E.; Rigler, N. E.; Shay, A. J.; Martin, J. H.; Boyd, T. C.; Backus, E. J.; Mowat, J. H.; Bohonos, N. *Antibiotics Annual* **1956**, 730-735.
- (17) Patterson, E. L.; Johnson, B. L.; DeVoe, S. E.; Bohonos, N. *Antimicrob. Agents Chemother.* **1965**, 5, 115-118.
- (18) Singh, P. D.; Johnson, J. H.; Aklonis, C. A.; O'Sullivan, J. J. *J. Antibiot.* **1986**, 39, 1054-1058.
- (19) Bergy, M. E.; Pyke, T. R. U.S. Patent 3350269, 1967.
- (20) McGuire, J. N.; Wilson, S. R.; Rinehart, K. L. *J. Antibiot.* **1995**, 48, 516-519.
- (21) Gomi, S.; Ohuchi, S.; Sasaki, T.; Itoh, J.; Sezaki, M. *J. Antibiot.* **1987**, 40, 740-749.
- (22) Fukuda, D. S.; Mynderse, J. S.; Baker, P. J.; Berry, D. M.; Boeck, L. D.; Yao, R. C.; Mertz, F. P.; Nakatsukasa, W. M.; Mabe, J.; Ott, J.; Counter, F. T.; Ensminger, P. W.; Allen, N. E.; Alborn Jr., W. E.; Hobbs Jr., J. N. *J. Antibiot.* **1990**, 43, 623-633.
- (23) Imae, K.; Nihei, Y.; Oka, M.; Yamasaki, T.; Konishi, M.; Oki, T. *J. Antibiot.* **1993**, 46, 1031-1033.
- (24) Nihei, Y.; Hasegawa, M.; Suzuki, K.; Yamamoto, S.; Hanada, M.; Furumai, T.; Fukagawa, Y.; Oki, T. *J. Antibiot.* **1993**, 46, 900-907.
- (25) Ito, S.; Matsuya, T.; Omura, S.; Otani, M.; Nakagawa, A. *J. Antibiot.* **1970**, 23, 315-317.
- (26) Hata, T.; Omura, S.; Iwai, Y.; Nakagawa, A.; Otani, M. *J. Antibiot.* **1971**, 24, 353-359.
- (27) Omura, S.; Nakagawa, A.; Yamada, H.; Hata, T.; Furusaki, A.; Watanabe, T. *Chem. Pharm. Bull.* **1971**, 19, 2428-2430.
- (28) Furusaki, A.; Watanabe, T.; Hata, T.; Omura, S.; Nakagawa, A.; Matsui, M. *Isr. J. Chem.* **1972**, 10, 173-187.
- (29) Omura, S.; Nakagawa, A.; Yamada, H.; Hata, T.; Furusaki, A.; Watanabe, T. *Chem. Pharm. Bull. (Tokyo)* **1973**, 21, 931-940.
- (30) Gould, S. J.; Tamayo, N.; Melville, C. R.; Cone, M. C. *J. Am. Chem. Soc.* **1994**, 116, 2207-2208.
- (31) Mithani, S.; Weeratunga, G.; Taylor, N. J.; Dmitrienko, G. I. *J. Am. Chem. Soc.* **1994**, 116, 2209-2210.

- (32) Gould, S. J. *Chem. Rev.* **1997**, *97*, 2499-2510.
- (33) Proteau, P. J.; Li, Y. F.; Chen, J.; Williamson, R. T.; Gould, S. J.; Laufer, R. S.; Dmitrienko, G. I. *J. Am. Chem. Soc.* **2000**, *122*, 8325-8326.
- (34) He, H.; Ding, W. D.; Bernan, V. S.; Richardson, A. D.; Ireland, C. M.; Greenstein, M.; Ellestad, G. A.; Carter, G. T. *J Am Chem Soc* **2001**, *123*, 5362-5363.
- (35) Sato, Y.; Geckle, M.; Gould, S. J. *Tetrahedron Lett.* **1985**, *26*, 4019-4022.
- (36) Regitz, M.; Maas, G. *Diazo compounds: Properties and Synthesis*; Academic Press: Orlando, 1986; pp 96.
- (37) Laufer, R. S.; Dmitrienko, G. I. *J. Am. Chem. Soc.* **2002**, *124*, 1854-1855.
- (38) Liu, W.; Buck, M.; Chen, N.; Shang, M.; Taylor, N. J.; Asoud, J.; Wu, X.; Hasinoff, B. B.; Dmitrienko, G. I. *Org. Lett.* **2007**, *9*, 2915-2918.
- (39) Seaton, P. J.; Gould, S. J. *J. Am. Chem. Soc.* **1987**, *109*, 5282-5284.
- (40) Shinya, K.; Furihata, K.; Teshima, Y.; Hayakawa, Y.; Seto, H. *Tetrahedron Lett.* **1992**, *33*, 7025-7028.
- (41) Gould, S. J.; Melville, C. R.; Cone, M. C.; Chen, J.; Carney, J. R. *J. Org. Chem.* **1997**, *62*, 320-324.
- (42) Cone, M. C.; Melville, C. R.; Gore, M. P.; Gould, S. J. *J. Org. Chem.* **1993**, *58*, 1058-1061.
- (43) Gould, S. J.; Melville, C. R. *Bioorg. Med. Chem. Lett.* **1995**, *5*, 51-54.
- (44) Aoyama, T.; Zhao, W. J.; Kojima, F.; Muraoka, Y.; Naganawa, H.; Takeuchi, T.; Aoyagi, T. *J. Antibiot.* **1993**, *46*, 1471-1474.
- (45) Carney, J. R.; Hong, S. T.; Gould, S. J. *Tetrahedron Lett.* **1997**, *38*, 3139-3142.
- (46) Akiyama, T.; Harada, S.; Kojima, F.; Takahashi, Y.; Imada, C.; Okami, Y.; Muraoka, Y.; Aoyagi, T.; Takeuchi, T. *J. Antibiot.* **1998**, *51*, 553-559.
- (47) Akiyama, T.; Nakamura, K. T.; Takahashi, Y.; Naganawa, H.; Muraoka, Y.; Aoyagi, T.; Takeuchi, T. *J. Antibiot.* **1998**, *51*, 586-588.

- (48) Schneider, K.; Nicholson, G.; Strobele, M.; Baur, S.; Niehaus, J.; Fiedler, H. P.; Sussmuth, R. D. *J. Antibiot.* **2006**, *59*, 105-109.
- (49) Baur, S.; Niehaus, J.; Karagouni, A. D.; Katsifas, E. A.; Chalkou, K.; Meintanis, C.; Jones, A. L.; Goodfellow, M.; Ward, A. C.; Beil, W.; Schneider, K.; Sussmuth, R. D.; Fiedler, H. P. *J. Antibiot.* **2006**, *59*, 293-297.
- (50) Volkmann, C.; Rossner, E.; Metzler, M.; Zahner, H.; Zeeck, A. *Liebigs Ann.* **1995**, 1169-1172.
- (51) Meselhy, M. R.; Kadota, S.; Tsubono, K.; Kusai, A.; Hattori, M.; Namba, T. *Tetrahedron Lett.* **1994**, *35*, 583-586.
- (52) Isshiki, K. N.; Sawa, T. T.; Naganawa, H. S.; Matsuda, N. K.; Hattori, S. K.; Hamada, M. S.; Takeuchi, T. M.; Oosono, M. H.; Ishizuka, M. S.; Yang, Z. Z.; Zhu, B. Q.; Xu, W. S. *J. Antibiot.* **1989**, *42*, 467-469.
- (53) Smitka, T. A.; Bonjouklian, R.; Perun, T. J.; Hunt, A. H.; Foster, R. S.; Mynderse, J. S.; Yao, R. C. *J. Antibiot.* **1992**, *45*, 581-583.
- (54) Nicolaou, K. C.; Li, H. M.; Nold, A. L.; Pappo, D.; Lenzen, A. *J. Am. Chem. Soc.* **2007**, *129*, 10356-10357.
- (55) Seaton, P. J.; Gould, S. J. *J. Antibiot.* **1989**, *42*, 189-197.
- (56) Chen, N. Synthesis and Chemistry of Kinamycins and Related Antibiotics. Ph.D. thesis, University of Waterloo, Waterloo, Canada, 2010.
- (57) Seaton, P. J.; Gould, S. J. *J. Am. Chem. Soc.* **1988**, *110*, 5912-5914.
- (58) Ajisaka, K.; Takeshima, H.; Omura, S. *J. Chem. Soc., Chem. Commun.* **1976**, 571-572.
- (59) Dmitrienko, G. I.; Nielsen, K. E.; Steingart, C.; Ming, N. S.; Willson, J. M.; Weeratunga, G. *Tetrahedron Lett.* **1990**, *31*, 3681-3684.
- (60) Echavarren, A. M.; Tamayo, N.; Paredes, M. C. *Tetrahedron Lett.* **1993**, *34*, 4713-4716.
- (61) Hauser, F. M.; Zhou, M. T. *J. Org. Chem.* **1996**, *61*, 5722-5722.
- (62) Gould, S. J.; Chen, J.; Cone, M. C.; Gore, M. P.; Melville, C. R.; Tamayo, N. *J. Org. Chem.* **1996**, *61*, 5720-5721.
- (63) Duthaler, R. O.; Forster, H. G.; Roberts, J. D. *J. Am. Chem. Soc.* **1978**, *100*, 4974-4979.

- (64) Cone, M. C.; Seaton, P. J.; Halley, K. A.; Gould, S. J. *J. Antibiot.* **1989**, *42*, 179-188.
- (65) Sato, Y.; Gould, S. J. *Tetrahedron Lett.* **1985**, *26*, 4023-4026.
- (66) Sato, Y.; Gould, S. J. *J. Am. Chem. Soc.* **1986**, *108*, 4625-4631.
- (67) Liu, W. C.; Parker, W. L.; Slusarchyk, D. S.; Greenwood, G. L.; Graham, S. F.; Meyers, E. J. *J. Antibiot.* **1970**, *23*, 437-441.
- (68) Gore, M. P.; Gould, S. J.; Weller, D. D. *J. Org. Chem.* **1992**, *57*, 2774-2783.
- (69) Cone, M. C.; Hassan, A. M.; Gore, M. P.; Gould, S. J.; Borders, D. B.; Alluri, M. R. *J. Org. Chem.* **1994**, *59*, 1923-1924.
- (70) Fendrich, G.; Zimmermann, W.; Gruner, J.; Auden, J. A. L. Feb 22 1989, CH Appl. 87/3, 196, Aug 20 1987, Eur. Pat. Appl. EP 304, 400 (CI.C07D221/18), 1989.
- (71) Gould, S. J.; OHare, T.; Seaton, P.; Soodsma, J.; Tang, Z. W. *Biorg. Med. Chem.* **1996**, *4*, 987-994.
- (72) Larue, T. A. *Lloydia* **1977**, *40*, 307-321.
- (73) Walton, K.; Coombs, M. M.; Catterall, F. S.; Walker, R.; Ioannides, C. *Carcinogenesis* **1997**, *18*, 1603-1608.
- (74) Lancaster, J. R. *Nitric oxide: Principles and Actions*; Academic Press: San Diego, 1996; pp 1-355.
- (75) Weeratunga, G.; Prasad, G. K. B.; Dilley, J.; Taylor, N. J.; Dmitrienko, G. I. *Tetrahedron Lett.* **1990**, *31*, 5713-5716.
- (76) Kobayashi, K.; Takeuchi, H.; Seko, S.; Suginome, H. *Helv. Chim. Acta* **1991**, *74*, 1091-1094.
- (77) Tamayo, N.; Echavarren, A. M.; Paredes, M. C. *J. Org. Chem.* **1991**, *56*, 6488-6491.
- (78) O'Sullivan, P. J.; Moreno, R.; Murphy, W. S. *Tetrahedron Lett.* **1992**, *33*, 535-538.
- (79) Saa, J. M.; Marti, C.; Garciaraso, A. *J. Org. Chem.* **1992**, *57*, 589-594.
- (80) Estevez, J. C.; Estevez, R. J.; Castedo, L. *Tetrahedron Lett.* **1993**, *34*, 6479-6480.
- (81) Knolker, H. J.; O'Sullivan, N. *Tetrahedron Lett.* **1994**, *35*, 1695-1698.

- (82) Rajeswaran, W. G.; Srinivasan, P. C. *Synthesis* **1994**, 270-272.
- (83) Knolker, H. J.; O'Sullivan, N. *Tetrahedron* **1994**, *50*, 10893-10908.
- (84) Knolker, H. J.; Reddy, K. R. *Chem. Rev.* **2002**, *102*, 4303-4427.
- (85) Knolker, H. J. *Curr. Org. Synth.* **2004**, *1*, 309-331.
- (86) Knolker, H. J. Occurrence, Biological Activity, and Convergent Organometallic Synthesis of Carbazole Alkaloids. In *Current Topics in Chemistry: Natural Products Synthesis II: Targets, Methods, Concepts*; Mulzer, J., Ed.; Springer-Verlag: Berlin, Heidelberg, 2005; Vol. 244, pp 115-148.
- (87) Knolker, H.-J.; Reddy, K. R. Chemistry and Biology of Carbazole Alkaloids. In *The Alkaloids. Chemistry and Biology*; Cordell, G. A., Ed.; Academic Press: San Diego, 2008; Vol. 65, pp 1-430.
- (88) Gallagher, P. T. Product Class 15: Carbazoles. In *Science of Synthesis; Houben-Weyl Methods of Molecular Transformations*; 5th ed.; Thieme: Stuttgart, New York, 2001; Vol. 10, pp 693-744.
- (89) Fukui, K. *Theory of Orientation and Stereoselection*; Springer-Verlag: Berlin, New York, 1975; pp 1-134.
- (90) Fleming, I. *Frontier Orbitals and Organic Chemical Reactions*; Wiley: London, New York, 1976; pp 1-249.
- (91) Murphy, W. S.; O'Sullivan, P. J. *Tetrahedron Lett.* **1992**, *33*, 531-534.
- (92) Mithani, S. Synthetic Studies related to Reductively Activated Antitumour Antibiotics. Ph.D. Thesis, University of Waterloo, Waterloo, Canada, 1996.
- (93) Echavarren, A. M.; Tamayo, N.; deFrutos, O.; Garcia, A. *Tetrahedron* **1997**, *53*, 16835-16846.
- (94) Castedo, L.; Estevez, R. J.; Saa, J. M.; Suau, R. *J. Heterocycl. Chem.* **1982**, *19*, 1469-1472.
- (95) Castedo, L.; Suau, R.; Mourino, A. *Tetrahedron Lett.* **1976**, 501-502.
- (96) Hauser, F. M.; Rhee, R. P. *J. Org. Chem.* **1978**, *43*, 178-180.
- (97) Birman, V. B.; Zhao, Z. F.; Guo, L. *Org. Lett.* **2007**, *9*, 1223-1225.

- (98) Lei, X. G.; Porco, J. A. *J. Am. Chem. Soc.* **2006**, *128*, 14790-14791.
- (99) Kitani, Y.; Morita, A.; Kumamoto, T.; Ishikawa, T. *Helv. Chim. Acta* **2002**, *85*, 1186-1195.
- (100) Kumamoto, T.; Kitani, Y.; Tsuchiya, H.; Yamaguchi, K.; Seki, H.; Ishikawa, T. *Tetrahedron* **2007**, *63*, 5189-5199.
- (101) Chen, N.; Carriere, M. B.; Laufer, R. S.; Taylor, N. J.; Dmitrienko, G. I. *Org. Lett.* **2008**, *10*, 381-384.
- (102) Caron, M.; Sharpless, K. B. *J. Org. Chem.* **1985**, *50*, 1557-1560.
- (103) Woo, C. M.; Lu, L.; Gholap, S. L.; Smith, D. R.; Herzon, S. B. *J. Am. Chem. Soc.* **2010**, *132*, 2540-2541.
- (104) Moore, H. W. *Science* **1977**, *197*, 527-532.
- (105) Tomasz, M. *Chem. Biol.* **1995**, *2*, 575-579.
- (106) Rajski, S. R.; Williams, R. M. *Chem. Rev.* **1998**, *98*, 2723-2795.
- (107) Teng, S. P.; Woodson, S. A.; Crothers, D. M. *Biochemistry* **1989**, *28*, 3901-3907.
- (108) Millard, J. T.; Weidner, M. F.; Raucher, S.; Hopkins, P. B. *J. Am. Chem. Soc.* **1990**, *112*, 3637-3641.
- (109) Borowyborowski, H.; Lipman, R.; Tomasz, M. *Biochemistry* **1990**, *29*, 2999-3006.
- (110) Li, V. S.; Kohn, H. *J. Am. Chem. Soc.* **1991**, *113*, 275-283.
- (111) Kumar, S.; Lipman, R.; Tomasz, M. *Biochemistry* **1992**, *31*, 1399-1407.
- (112) Arya, D. P.; Jebaratnam, D. J. *J. Org. Chem.* **1995**, *60*, 3268-3269.
- (113) Yamamoto, K.; Kawanishi, S. *Chem. Res. Toxicol.* **1992**, *5*, 440-446.
- (114) Maiya, B. G.; Ramana, C. V.; Arounaguirri, S.; Nagarajan, M. *Bioorg. Med. Chem. Lett.* **1997**, *7*, 2141-2144.
- (115) Eppley, H. J.; Sato, S. M.; Ellington, A. D.; Zaleski, J. M. *Chem. Commun.* **1999**, 2405-2406.
- (116) Kato, T.; Kojima, K.; Hiramoto, K.; Kikugawa, K. *Mutat. Res.* **1992**, *268*, 105-114.

- (117) Hung, M. H.; Stock, L. M. *J. Org. Chem.* **1982**, *47*, 448-453.
- (118) Gannett, P. M.; Powell, J. H.; Rao, R.; Shi, X. L.; Lawson, T.; Kolar, C.; Toth, B. *Chem. Res. Toxicol.* **1999**, *12*, 297-304.
- (119) Patai, S. *The Chemistry of diazonium and diazo groups*; J. Wiley: Chichester [Eng.], New York, 1978; Vol. 1 and 2; pp 1-1069.
- (120) Myers, A. G. *Tetrahedron Lett.* **1987**, *28*, 4493-4496.
- (121) Goldberg, I. H. *Acc. Chem. Res.* **1991**, *24*, 191-198.
- (122) Sugiyama, H.; Fujiwara, T.; Saito, I. *Tetrahedron Lett.* **1994**, *35*, 8825-8828.
- (123) Murphy, J. A.; Griffiths, J. *Nat. Prod. Rep.* **1993**, *10*, 551-564.
- (124) Feldman, K. S.; Eastman, K. J. *J. Am. Chem. Soc.* **2005**, *127*, 15344-15345.
- (125) Feldman, K. S.; Eastman, K. J. *J. Am. Chem. Soc.* **2006**, *128*, 12562-12573.
- (126) Zeng, W.; Ballard, T. E.; Tkachenko, A. G.; Burns, V. A.; Feldheim, D. L.; Melander, C. *Bioorg. Med. Chem. Lett.* **2006**, *16*, 5148-5151.
- (127) Ballard, T. E.; Melander, C. *Tetrahedron Letters* **2008**, *49*, 3157-3161.
- (128) Taatjes, D. J.; Gaudiano, G.; Resing, K.; Koch, T. H. *J. Med. Chem.* **1996**, *39*, 4135-4138.
- (129) Fenick, D. J.; Taatjes, D. J.; Koch, T. H. *J. Med. Chem.* **1997**, *40*, 2452-2461.
- (130) Heinecke, C. L.; Melander, C. *Tetrahedron Lett.* **2010**, *51*, 1455-1458.
- (131) Khdour, O.; Skibo, E. B. *Org. Biomol. Chem.* **2009**, *7*, 2140-2154.
- (132) Hasinoff, B. B.; Wu, X.; Yalowich, J. C.; Goodfellow, V.; Laufer, R. S.; Adedayo, O.; Dmitrienko, G. I. *Anti-Cancer Drugs* **2006**, *17*, 825-837.
- (133) O'Hara, K. A.; Wu, X.; Patel, D.; Liang, H.; Yalowich, J. C.; Chen, N.; Goodfellow, V.; Adedayo, O.; Dmitrienko, G. I.; Hasinoff, B. B. *Free Radical Biology and Medicine* **2007**, *43*, 1132-1144.
- (134) O'Hara, K. A.; Dmitrienko, G. I.; Hasinoff, B. B. *Chem. Biol. Interact.* **2010**, *184*, 396-402.

- (135) Shvedov, V. I.; Kurilo, G. N.; Grinev, A. N. *Khim. Geterotsikl.* **1972**, 1079.
- (136) Kametani, T.; Suzuki, T.; Takahash.K; Fukumoto, K. *Tetrahedron* **1974**, 30, 2207-2210.
- (137) Forrester, A. R.; Ingram, A. S.; John, I. L.; Thomson, R. H. *J. Chem. Soc., Perkin Trans. I* **1975**, 1115-1120.
- (138) Watanabe, M.; Snieckus, V. *J. Am. Chem. Soc.* **1980**, 102, 1457-1460.
- (139) Kano, S.; Sugino, E.; Shibuya, S.; Hibino, S. *J. Org. Chem.* **1981**, 46, 2979-2981.
- (140) Saulnier, M. G.; Gribble, G. W. *Tetrahedron Lett.* **1983**, 24, 5435-5438.
- (141) Gribble, G. W.; Saulnier, M. G. *J. Chem. Soc., Chem. Commun.* **1984**, 168-169.
- (142) Gribble, G. W.; Keavy, D. J.; Davis, D. A.; Saulnier, M. G.; Pelcman, B.; Barden, T. C.; Sibi, M. P.; Olson, E. R.; Belbruno, J. J. *J. Org. Chem.* **1992**, 57, 5878-5891.
- (143) Gribble, G. W.; Saulnier, M. G.; Obazanutaitis, J. A.; Ketcha, D. M. *J. Org. Chem.* **1992**, 57, 5891-5899.
- (144) Fraser, H. L.; Gribble, G. W. *Can. J. Chem.* **2001**, 79, 1515-1521.
- (145) Liu, Y. B.; Gribble, G. W. *Tetrahedron Lett.* **2001**, 42, 2949-2951.
- (146) Moody, C. J. *J. Chem. Soc., Chem. Commun.* **1984**, 925-926.
- (147) Moody, C. J. *J. Chem. Soc., Perkin Trans. I* **1985**, 2505-2508.
- (148) Liebeskind, L. S.; Iyer, S.; Jewell, C. F. *J. Org. Chem.* **1986**, 51, 3065-3067.
- (149) Sha, C. K.; Chuang, K. S.; Wey, S. J. *J. Chem. Soc., Perkin Trans. I* **1987**, 977-980.
- (150) Griffith, W. P.; Ley, S. V.; Whitcombe, G. P.; White, A. D. *J. Chem. Soc., Chem. Commun.* **1987**, 1625-1627.
- (151) Kreher, R. P.; Dyker, G. Z. *Naturforsch., B: Chem. Sci.* **1987**, 42, 473-477.
- (152) Bergman, J.; Pelcman, B. *Tetrahedron* **1988**, 44, 5215-5228.
- (153) Pindur, U.; Erfanianabdoust, H. *Liebigs Ann. Chem.* **1988**, 803-805.



- (154) Pindur, U.; Haber, M.; Erfanianabdoust, H. *Heterocycles* **1992**, *34*, 781-790.
- (155) Drager, M.; Haber, M.; Erfanianabdoust, H.; Pindur, U.; Sattler, K. *Monatsh. Chem.* **1993**, *124*, 559-576.
- (156) Bittner, S.; Krief, P.; Massil, T. *Synthesis* **1991**, 215-216.
- (157) Kobayashi, K.; Takeuchi, H.; Seko, S.; Kanno, Y.; Kujime, S.; Suginome, H. *Helv. Chim. Acta* **1993**, *76*, 2942-2950.
- (158) Vanbroeck, P. I.; Vandoren, P. E.; Toppet, S. M.; Hoornaert, G. J. *J. Chem. Soc., Perkin Trans. 1* **1992**, 415-419.
- (159) Molina, P.; Alajarin, M.; Vidal, A.; Sanchezandrada, P. *J. Org. Chem.* **1992**, *57*, 929-939.
- (160) Brown, R. F. C.; Coulston, K. J.; Eastwood, F. W.; Moffat, M. R. *Tetrahedron* **1992**, *48*, 7763-7774.
- (161) Boese, R.; Van Sickle, A. P.; Vollhardt, K. P. C. *Synthesis* **1994**, 1374-1382.
- (162) Kucklander, U.; Pitzler, H.; Kuna, K. *Arch. Pharm.* **1994**, *327*, 137-142.
- (163) Asche, C.; Frank, W.; Albert, A.; Kucklaender, U. *Biorg. Med. Chem.* **2005**, *13*, 819-837.
- (164) Boogaard, A. T.; Pandit, U. K.; Koomen, G. J. *Tetrahedron* **1994**, *50*, 4811-4828.
- (165) Akermark, B.; Oslob, J. D.; Heuschert, U. *Tetrahedron Lett.* **1995**, *36*, 1325-1326.
- (166) Hagelin, H.; Oslob, J. D.; Akermark, B. *Chem. Eur. J.* **1999**, *5*, 2413-2416.
- (167) Markgraf, J. H.; Patterson, D. E. *J. Heterocycl. Chem.* **1996**, *33*, 109-111.
- (168) Luo, Y. L.; Chou, T. C.; Cheng, C. C. *J. Heterocycl. Chem.* **1996**, *33*, 113-117.
- (169) Martarello, L.; Joseph, D.; Kirsch, G. *Heterocycles* **1996**, *43*, 367-379.
- (170) Shi, C. S.; Wang, K. K. *J. Org. Chem.* **1998**, *63*, 3517-3520.
- (171) Kobayashi, K.; Taki, T.; Kawakita, M.; Uchida, M.; Morikawa, O.; Konishi, H. *Heterocycles* **1999**, *51*, 349-354.
- (172) Black, D. S.; Craig, D. C.; Santoso, M. *Tetrahedron Lett.* **1999**, *40*, 6653-6656.

- (173) Schmittel, M.; Rodriguez, D.; Steffen, J. P. *Angew. Chem. Int. Ed.* **2000**, *39*, 2152-2155.
- (174) Cruces, J.; Estevez, J. C.; Castedo, L.; Estevez, R. J. *Tetrahedron Lett.* **2001**, *42*, 4825-4827.
- (175) Barcia, J. C.; Cruces, J.; Estevez, J. C.; Estevez, R. J.; Castedo, L. *Tetrahedron Lett.* **2002**, *43*, 5141-5144.
- (176) Cruces, J.; Martinez, E.; Treus, M.; Martinez, L. A.; Estevez, J. C.; Estevez, R. J.; Castedo, L. *Tetrahedron* **2002**, *58*, 3015-3019.
- (177) Fernandez, M.; Barcia, C.; Estevez, J. C.; Estevez, R. J.; Castedo, L. *Synlett* **2004**, 267-270.
- (178) Otero, J. M.; Barcia, J. C.; Estevez, J. C.; Estevez, R. J. *Tetrahedron: Asymmetry* **2005**, *16*, 11-14.
- (179) Barcia, J. C.; Otero, J. M.; Estevez, J. C.; Estevez, R. J. *Synlett* **2007**, 1399-1402.
- (180) Miki, Y.; Tsuzaki, Y.; Matsukida, H. *Heterocycles* **2002**, *57*, 1645-1651.
- (181) Mal, D.; Senapati, B. K.; Pahari, P. *Synlett* **2005**, 994-996.
- (182) Mal, D.; Senapati, B. K.; Pahari, P. *Tetrahedron* **2007**, *63*, 3768-3781.
- (183) Pedersen, J. M.; Bowman, W. R.; Elsegood, M. R. J.; Fletcher, A. J.; Lovell, P. J. *J. Org. Chem.* **2005**, *70*, 10615-10618.
- (184) Mohammed, F. K. *Egypt. J. Chem.* **2006**, *49*, 139-147.
- (185) Hu, H. Y.; Liu, Y.; Ye, M.; Xu, J. H. *Synlett* **2006**, 1913-1917.
- (186) Liegault, B.; Lee, D.; Huestis, M. P.; Stuart, D. R.; Fagnou, K. *J. Org. Chem.* **2008**, *73*, 5022-5028.
- (187) Pindur, U.; Haber, M.; Sattler, K. *Pharm. Unserer Zeit* **1992**, *21*, 21-36.
- (188) Pindur, U.; Haber, M.; Sattler, K. *J. Chem. Educ.* **1993**, *70*, 263-272.
- (189) Buchwald, S. L.; Fugami, K.; Hiyama, T.; Kosugi, M.; Miura, M.; Miyaura, N.; Muci, A. R.; Nomura, M.; Shirakawa, E.; Tamao, K. *Cross-coupling reactions: A Practical Guide*.

In *Topics in Current Chemistry*; Miyaura, N., Ed.; Springer-Verlag: Berlin, 2002; Vol. 219, pp 1-248.

(190) Meijere, A. d.; Diederich, F. *Metal-catalyzed cross-coupling reactions*; 2nd ed. ed.; Wiley-VCH: Weinheim, 2004; Vol. 1 and 2; pp 1-916.

(191) Negishi, E.-i.; Meijere, A. d. *Handbook of organopalladium chemistry for organic synthesis*; Wiley-Interscience: New York, 2002; Vol. 1 and 2; pp 1-3350.

(192) Tsuji, J. *Palladium reagents and catalysts: new perspectives for the 21st century*; Wiley: Hoboken, NJ, 2004; pp 1-670.

(193) Metal catalysed carbon-carbon bond-forming reactions. In *Catalysts for fine chemical synthesis*; Roberts, S. M., Xiao, J., Whittall, J., Pickett, T. E., Eds.; Wiley: Chichester, 2004; Vol. 3, pp 1-268.

(194) Lee, S.; Jorgensen, M.; Hartwig, J. F. *Org. Lett.* **2001**, *3*, 2729-2732.

(195) Klapars, A.; Antilla, J. C.; Huang, X. H.; Buchwald, S. L. *J. Am. Chem. Soc.* **2001**, *123*, 7727-7729.

(196) Kauffman, G. B.; Fang, L. Y. *Inorg. Synth.* **1983**, *22*, 101-103.

(197) Altman, R.; Buchwald, S. L. Massachusetts Institute of Technology, Cambridge MA, USA. Personal communication, 2006.

(198) Tran, L. T. Synthesis of the Benzo[b]fluorene ring system of the Kinamycin-antitumor antibiotics. M.Sc. Thesis, University of Waterloo, Waterloo, Canada, 1998.

(199) Laufer, R. Synthesis of Compounds Related to the Kinamycin Antibiotics. Ph.D. Thesis, University of Waterloo, Waterloo, Canada, 2002.

(200) Hannan, R. L.; Barber, R. B.; Rapoport, H. *J. Org. Chem.* **1979**, *44*, 2153-2158.

(201) Franck, R. W.; Gupta, R. B. *J. Org. Chem.* **1985**, *50*, 4632-4635.

(202) Bolchi, C.; Catalano, P.; Fumagalli, L.; Gobbi, M.; Pallavicini, M.; Pedretti, A.; Villa, L.; Vistoli, G.; Valoti, E. *Biorg. Med. Chem.* **2004**, *12*, 4937-4951.

(203) Thomson, R. H. *J. Org. Chem.* **1948**, *13*, 377-383.

(204) Heinzman, S. W.; Grunwell, J. R. *Tetrahedron Lett.* **1980**, *21*, 4305-4308.

(205) Jung, M. E.; Hagenah, J. A. *J. Org. Chem.* **1983**, *48*, 5359-5361.

- (206) Grunwell, J. R.; Karipides, A.; Wigal, C. T.; Heinzman, S. W.; Parlow, J.; Surso, J. A.; Clayton, L.; Fleitz, F. J.; Daffner, M.; Stevens, J. E. *J. Org. Chem.* **1991**, *56*, 91-95.
- (207) Takeya, T.; Kajiyama, M.; Nakamura, C.; Tobinaga, S. *Chem. Pharm. Bull. (Tokyo)* **1999**, *47*, 209-219.
- (208) Liebeskind, L. S.; Riesinger, S. W. *J. Org. Chem.* **1993**, *58*, 408-413.
- (209) Dawood, K. M. *Tetrahedron* **2007**, *63*, 9642-9651.
- (210) Fukuyama, Y.; Kiriya, Y.; Kodama, M. *Tetrahedron Lett.* **1993**, *34*, 7637-7638.
- (211) Romanov, V. S.; Moroz, A. A.; Shvartsberg, M. S. *B. Acad. Sci. USSR Ch.* **1985**, *34*, 772-775.
- (212) Romanov, V. S.; Ivanchikova, I. D.; Moroz, A. A.; Shvartsberg, M. S. *Russ. Chem. Bull.* **2005**, *54*, 1686-1689.
- (213) Tietze, L. F.; Guntner, C.; Gericke, K. M.; Schuberth, I.; Bunkoczi, G. *Eur. J. Org. Chem.* **2005**, 2459-2467.
- (214) Brimble, M. A.; Brenstrum, T. J. *J. Chem. Soc., Perkin Trans. 1* **2001**, 1612-1623.
- (215) Tietze, L. F.; Gericke, K. M.; Singidi, R. R.; Schuberth, I. *Org. Biomol. Chem.* **2007**, *5*, 1191-1200.
- (216) Wheeler, A. S.; Scott, J. W. *J. Am. Chem. Soc.* **1919**, *41*, 833-841.
- (217) Shen, Q. L.; Hartwig, J. F. *J. Am. Chem. Soc.* **2006**, *128*, 10028-10029.
- (218) Surry, D. S.; Buchwald, S. L. *J. Am. Chem. Soc.* **2007**, *129*, 10354-10355.
- (219) Kim, J.; Chang, S. *Chem. Commun.* **2008**, 3052-3054.
- (220) Xia, N.; Taillefer, M. *Angew. Chem. Int. Ed.* **2009**, *48*, 337-339.
- (221) Vo, G. D.; Hartwig, J. F. *J. Am. Chem. Soc.* **2009**, *131*, 11049-11061.
- (222) Wolfe, J. P.; Ahman, J.; Sadighi, J. P.; Singer, R. A.; Buchwald, S. L. *Tetrahedron Lett.* **1997**, *38*, 6367-6370.
- (223) Nakazumi, H.; Kondo, K.; Kitao, T. *Synthesis* **1982**, 878-879.

- (224) Matsuoka, M.; Hamano, K.; Kitao, T.; Takagi, K. *Synthesis* **1984**, 953-955.
- (225) Tandon, V. K.; Yadav, D. B.; Singh, R. V.; Chaturvedi, A. K.; Shukla, P. K. *Bioorg. Med. Chem. Lett.* **2005**, *15*, 5324-5328.
- (226) Arnone, A.; Merlini, L.; Nasini, G.; De Pava, O. V. *Synth. Commun.* **2007**, *37*, 2569-2577.
- (227) Bolognesi, M. L.; Lizzi, F.; Perozzo, R.; Brun, R.; Cavalli, A. *Bioorg. Med. Chem. Lett.* **2008**, *18*, 2272-2276.
- (228) Kwong, F. Y.; Buchwald, S. L. *Org. Lett.* **2003**, *5*, 793-796.
- (229) Akermark, B.; Ebersson, L.; Jonsson, E.; Pettersson, E. *J. Org. Chem.* **1975**, *40*, 1365-1367.
- (230) Murray, R. E.; Zweifel, G. *Synthesis* **1980**, 150-151.
- (231) Overman, L. E.; Poon, D. J. *Angew. Chem. Int. Ed.* **1997**, *36*, 518-521.
- (232) Cabri, W.; Candiani, I.; Bedeschi, A.; Penco, S.; Santi, R. *J. Org. Chem.* **1992**, *57*, 1481-1486.
- (233) Goodwin, S.; Smith, A. F.; Horning, E. C. *J. Am. Chem. Soc.* **1959**, *81*, 1903-1908.
- (234) Juret, P.; Tanguy, A.; Girard, A.; Letalaer, J. Y.; Abbatucci, J. S.; Datxuong, N.; Lepecq, J. B.; Paoletti, C. *Eur. J. Cancer* **1978**, *14*, 205-206.
- (235) Paoletti, C.; Lepecq, J. B.; Datxuong, N.; Juret, P.; Garnier, H.; Amiel, J. L.; Rouesse, J. *Recent Results Cancer Res.* **1980**, *74*, 107-123.
- (236) Juret, P.; Heron, J. F.; Couette, J. E.; Delozier, T.; Letalaer, J. Y. *Cancer Treat. Rep.* **1982**, *66*, 1909-1916.
- (237) Dodion, P.; Rozenzweig, M.; Nicaise, C.; Piccart, M.; Cumps, E.; Crespeigne, N.; Kisner, D.; Kenis, Y. *Eur. J. Cancer Clin. Oncol.* **1982**, *18*, 519-522.
- (238) Clarysse, A.; Brugarolas, A.; Siegenthaler, P.; Abele, R.; Cavalli, F.; Dejager, R.; Renard, G.; Rozenzweig, M.; Hansen, H. H. *Eur. J. Cancer Clin. Oncol.* **1984**, *20*, 243-247.
- (239) Auclair, C.; Pierre, A.; Voisin, E.; Pepin, O.; Cros, S.; Colas, C.; Saucier, J. M.; Verschuere, B.; Gros, P.; Paoletti, C. *Cancer Res.* **1987**, *47*, 6254-6261.

- (240) Gribble, G. W. Synthesis and Antitumor Activity of the Ellipticine Alkaloids and Related Compounds. In *The Alkaloids*; Brossi, A., Ed.; Academic Press: New York, 1990; Vol. 39, pp 239-352.
- (241) Kansal, V. K.; Potier, P. *Tetrahedron* **1986**, *42*, 2389-2408.
- (242) Bates, A. D.; Maxwell, A. *Biochemistry* **2007**, *46*, 7929-7941.
- (243) Bush, J. A.; Long, B. H.; Catino, J. J.; Bradner, W. T. *J. Antibiot.* **1987**, *40*, 668-678.
- (244) Yamashita, Y.; Fujii, N.; Murakata, C.; Ashizawa, T.; Okabe, M.; Nakano, H. *Biochemistry* **1992**, *31*, 12069-12075.
- (245) Tamaoki, T.; Nomoto, H.; Takahashi, I.; Kato, Y.; Morimoto, M.; Tomita, F. *Biochem. Biophys. Res. Commun.* **1986**, *135*, 397-402.
- (246) Omura, S.; Sasaki, Y.; Iwai, Y.; Takeshima, H. *J. Antibiot.* **1995**, *48*, 535-548.
- (247) Osada, H.; Koshino, H.; Kudo, T.; Onose, R.; Isono, K. *J. Antibiot.* **1992**, *45*, 189-194.
- (248) Kojiri, K.; Kondo, H.; Yoshinari, T.; Arakawa, H.; Nakajima, S.; Satoh, F.; Kawamura, K.; Okura, A.; Suda, H.; Okanishi, M. *J. Antibiot.* **1991**, *44*, 723-728.
- (249) Rickards, R. W.; Rothschild, J. M.; Willis, A. C.; de Chazal, N. M.; Kirk, J.; Kirk, K.; Saliba, K. J.; Smith, G. D. *Tetrahedron* **1999**, *55*, 13513-13520.
- (250) Wu, G. Y.; Fang, Y. Z.; Yang, S.; Lupton, J. R.; Turner, N. D. *J. Nutr.* **2004**, *134*, 489-492.
- (251) *The Merck index: An encyclopedia of chemicals and drugs*; 9th ed.; Merck: Rahway, N.J., U.S.A., 1976; pp 4309.
- (252) Anslyn, E. V.; Dougherty, D. A. *Modern Physical Organic Chemistry*; University Science: Sausalito, Calif., 2006; pp 828.
- (253) Szabo, A.; Ostlund, N. S. *Modern Quantum Chemistry: Introduction to Advanced Electronic Structure Theory*; 1st. ed.; McGraw-Hill: New York, 1989; pp 127.
- (254) Ignarro, L. J. *Nitric oxide: Biology and Pathobiology*; Academic: San Diego, Calif.; London, 2000; pp 1-1003.
- (255) Cooper, C. E. *BBA-Bioenergetics* **1999**, *1411*, 215-216.

- (256) Murphy, K. P.; Travers, P.; Walport, M.; Janeway, C. *Janeway's Immunobiology*; 7th ed.; Garland Science: New York, 2008; pp 1-887.
- (257) Spiro, S. *FEMS Microbiol. Rev.* **2007**, *31*, 193-211.
- (258) Kurtz, D. M. *J. Chem. Soc., Dalton* **2007**, 4115-4121.
- (259) De Voe, S. E.; Rigler, N. E.; Shay, A. J.; Martin, J. H.; Boyd, T. C.; Backus, E. J.; Mowat, J. H.; Bohonos, N. *Antibiot. Annu.* **1956**, 730-735.
- (260) Patterson, E. L.; Johnson, B. L.; DeVoe, S. E.; Bohonos, N. *Antimicrob. Agents Chemother. (Bethesda)* **1965**, *5*, 115-118.
- (261) Rao, K. V.; Brooks, S. C., Jr.; Kugelman, M.; Romano, A. A. *Antibiot. Annu.* **1959**, *7*, 943-949.
- (262) Lee, M. D.; Fantini, A. A.; Kuck, N. A.; Greenstein, M.; Testa, R. T.; Borders, D. B. *J. Antibiot.* **1987**, *40*, 1657-1663.
- (263) Kameyama, T.; Takahashi, A.; Matsumoto, H.; Kurasawa, S.; Hamada, M.; Okami, Y.; Ishizuka, M.; Takeuchi, T. *J. Antibiot.* **1988**, *41*, 1561-1567.
- (264) Takahashi, A.; Nakamura, H.; Ikeda, D.; Naganawa, H.; Kameyama, T.; Kurasawa, S.; Okami, Y.; Takeuchi, T.; Iitaka, Y. *J. Antibiot.* **1988**, *41*, 1568-1574.
- (265) Nishimura, M.; Nakada, H.; Nakajima, H.; Hori, Y.; Ezaki, M.; Goto, T.; Okuhara, M. *J. Antibiot.* **1989**, *42*, 542-548.
- (266) Nishimura, M.; Nakada, H.; Takase, S.; Katayama, A.; Goto, T.; Tanaka, H.; Hashimoto, M. *J. Antibiot.* **1989**, *42*, 549-552.
- (267) Singh, P. D.; Johnson, J. H.; Aklonis, C. A.; O'Sullivan, J. *J. Antibiot.* **1986**, *39*, 1054-1058.
- (268) Imae, K.; Nihei, Y.; Oka, M.; Yamasaki, T.; Konishi, M.; Oki, T. *J. Antibiot.* **1993**, *46*, 1031-1033.
- (269) Nihei, Y.; Hasegawa, M.; Suzuki, K.; Yamamoto, S.; Hanada, M.; Furumai, T.; Fukagawa, Y.; Oki, T. *J. Antibiot.* **1993**, *46*, 900-907.
- (270) McGuire, J. N.; Wilson, S. R.; Rinehart, K. L. *J. Antibiot.* **1995**, *48*, 516-519.
- (271) Gomi, S.; Ohuchi, S.; Sasaki, T.; Itoh, J.; Sezaki, M. *J. Antibiot.* **1987**, *40*, 740-749.

- (272) Fukuda, D. S.; Mynderse, J. S.; Baker, P. J.; Berry, D. M.; Boeck, L. D.; Yao, R. C.; Mertz, F. P.; Nakatsukasa, W. M.; Mabe, J.; Ott, J.; et al. *J. Antibiot.* **1990**, *43*, 623-633.
- (273) Kirmse, W. *Naturwissenschaften* **1959**, *46*, 379-379.
- (274) Horner, L.; Hockenberger, L.; Kirmse, W. *Chem. Ber. Recl.* **1961**, *94*, 290-297.
- (275) Chapman, O. L.; Heckert, D. C. *Chem. Comm.* **1966**, 242-&.
- (276) Zhao, Y. L.; Bartberger, M. D.; Goto, K.; Shimada, K.; Kawashima, T.; Houk, K. N. *J. Am. Chem. Soc.* **2005**, *127*, 7964-7965.
- (277) Smith, L. I.; Howard, K. L. *Organic Syntheses* **1944**, *24*, 53-55.
- (278) Walton, J. C.; Park, J. S. B. *J. Chem. Soc., Perkin Trans. 2* **1997**, 2585-2588.
- (279) Griess, J. P. *Philos. Trans. R. Soc. Lond.* **1864**, *154*, 667.
- (280) Griess, J. P. *Ber. Deutsch. Chem. Ges.* **1879**, *12*, 426.
- (281) Green, L. C.; Wagner, D. A.; Glogowski, J.; Skipper, P. L.; Wishnok, J. S.; Tannenbaum, S. R. *Anal. Biochem.* **1982**, *126*, 131-138.
- (282) Nordenson, S.; Hvoslef, J. *Acta Crystallogr. B* **1981**, *37*, 373-378.
- (283) Nordenson, S. *Acta Crystallogr. B* **1981**, *37*, 1543-1547.
- (284) Bujak, M.; Ejsmont, K.; Kyziol, J.; Daszkiewicz, Z.; Zaleski, J. *Acta Crystallogr. C* **1998**, *54*, 1945-1948.
- (285) Daszkiewicz, Z.; Kyziol, J. B.; Zaleski, J. *J. Mol. Struct.* **1999**, *513*, 69-77.
- (286) Zaleski, J.; Daszkiewicz, Z.; Kyziol, J. B. *Acta Crystallogr. C* **2001**, *57*, 754-757.
- (287) Kyziol, J. B.; Broda, M. A.; Zaleski, J.; Daszkiewicz, Z. *J. Mol. Struct.* **2002**, *605*, 157-169.
- (288) Vasiliev, A. D.; Astachov, A. M.; Molokeev, M. S.; Kruglyakova, L. A.; Stepanov, R. S. *Acta Crystallogr. C* **2003**, *59*, O499-O501.
- (289) Bracuti, A. J. *J. Chem. Crystallogr.* **2004**, *34*, 135-140.
- (290) Zaleski, J.; Spaleniak, G.; Kyzio, J. B. *Acta Crystallogr. C* **2004**, *60*, O627-O629.



- (291) Yu, H. B.; Zhang, B. N.; Fang, J. X. *Acta Crystallogr. E* **2007**, *63*, O4242-U2681.
- (292) Apreyan, R. A.; Karapetyan, H. A.; Petrosyan, A. M. *J. Mol. Struct.* **2008**, *874*, 187-193.
- (293) Hu, Z. Q.; Yang, X. D.; An, G. W.; Yang, Z.; Xu, L. Z. *Acta Crystallogr. E* **2008**, *64*, O121-U3567.
- (294) Cameron, T. S.; Cordes, R. E.; Morris, D. G.; Murray, A. M. *J. Chem. Soc., Perkin Trans. 2* **1979**, 300-303.
- (295) Nordenson, S. *Acta Crystallogr. B* **1981**, *37*, 1774-1776.
- (296) Olah, G. A.; Prakash, G. K. S.; Arvanaghi, M.; Krishnamurthy, V. V.; Narang, S. C. *J. Am. Chem. Soc.* **1984**, *106*, 2378-2380.
- (297) Levy, G. C.; Lichter, R. L.; Nelson, G. L. *Carbon-13 nuclear magnetic resonance spectroscopy*; 2nd ed.; Wiley: New York, 1980; pp 7.
- (298) Padwa, A. *1,3-dipolar cycloaddition chemistry*; Wiley: New York, 1984; pp 1-1521.
- (299) Levy, G. C.; Lichter, R. L. *Nitrogen-15 nuclear magnetic resonance spectroscopy*; Wiley: New York, 1979; pp 109.
- (300) Levy, G. C.; Lichter, R. L. *Nitrogen-15 nuclear magnetic resonance spectroscopy*; Wiley: New York, 1979; pp 119-129.
- (301) Marek, R.; Lycka, A. *Curr. Org. Chem.* **2002**, *6*, 35-66.
- (302) Buchanan, G. W.; Dawson, B. A. *Can. J. Chem.* **1978**, *56*, 2200-2204.
- (303) Buchanan, G. W.; Dawson, B. A. *Org. Magn. Resonance* **1980**, *13*, 293-298.
- (304) Levy, G. C.; Lichter, R. L.; Nelson, G. L. *Carbon-13 nuclear magnetic resonance spectroscopy*; 2nd ed.; Wiley: New York, 1980; pp 163.
- (305) Lichter, R. L.; Dorman, D. E.; Wasylishen, R. *J. Am. Chem. Soc.* **1974**, *96*, 930-932.
- (306) Albright, T. A.; Freeman, W. J. *Org. Magn. Resonance* **1977**, *9*, 75-79.
- (307) Levy, G. C.; Lichter, R. L. *Nitrogen-15 nuclear magnetic resonance spectroscopy*; Wiley: New York, 1979; pp 96.

(308) Levy, G. C.; Lichter, R. L. *Nitrogen-15 nuclear magnetic resonance spectroscopy*; Wiley: New York, 1979; pp 28-142.

(309) *Gaussian 03, Revision C.02*, Frisch, M. J. T., G. W.; Schlegel, H. B.; Scuseria, G. E.; Robb, M. A.; Cheeseman, J. R.; Montgomery, Jr., J. A.; Vreven, T.; Kudin, K. N.; Burant, J. C.; Millam, J. M.; Iyengar, S. S.; Tomasi, J.; Barone, V.; Mennucci, B.; Cossi, M.; Scalmani, G.; Rega, N.; Petersson, G. A.; Nakatsuji, H.; Hada, M.; Ehara, M.; Toyota, K.; Fukuda, R.; Hasegawa, J.; Ishida, M.; Nakajima, T.; Honda, Y.; Kitao, O.; Nakai, H.; Klene, M.; Li, X.; Knox, J. E.; Hratchian, H. P.; Cross, J. B.; Bakken, V.; Adamo, C.; Jaramillo, J.; Gomperts, R.; Stratmann, R. E.; Yazyev, O.; Austin, A. J.; Cammi, R.; Pomelli, C.; Ochterski, J. W.; Ayala, P. Y.; Morokuma, K.; Voth, G. A.; Salvador, P.; Dannenberg, J. J.; Zakrzewski, V. G.; Dapprich, S.; Daniels, A. D.; Strain, M. C.; Farkas, O.; Malick, D. K.; Rabuck, A. D.; Raghavachari, K.; Foresman, J. B.; Ortiz, J. V.; Cui, Q.; Baboul, A. G.; Clifford, S.; Cioslowski, J.; Stefanov, B. B.; Liu, G.; Liashenko, A.; Piskorz, P.; Komaromi, I.; Martin, R. L.; Fox, D. J.; Keith, T.; Al-Laham, M. A.; Peng, C. Y.; Nanayakkara, A.; Challacombe, M.; Gill, P. M. W.; Johnson, B.; Chen, W.; Wong, M. W.; Gonzalez, C.; and Pople, J. A.; Gaussian, Inc., Wallingford CT, 2004.

(310) Becke, A. D. *J. Chem. Phys.* **1993**, *98*, 5648-5652.

(311) Lee, C. T.; Yang, W. T.; Parr, R. G. *Phys. Rev. B* **1988**, *37*, 785-789.

(312) *Encyclopedia of Computational Chemistry*; Schleyer, P. v. R., Ed.; John Wiley: New York, 1998; pp 1-3580.

(313) Fukui, K. *Acc. Chem. Res.* **1981**, *14*, 363-368.

(314) Dykstra, C. E. *Theory and applications of computational chemistry: the first forty years*; Elsevier: Amsterdam, Boston, 2005; pp 195-249.

(315) Curtiss, L. A.; Raghavachari, K.; Redfern, P. C.; Pople, J. A. *Chem. Phys. Lett.* **1997**, *270*, 419-426.

(316) Sustmann, R. *Pure Appl. Chem.* **1974**, *40*, 569-593.

(317) Peng, C. Y.; Schlegel, H. B. *Isr. J. Chem.* **1993**, *33*, 449-454.

(318) Peng, C. Y.; Ayala, P. Y.; Schlegel, H. B.; Frisch, M. J. *J. Comput. Chem.* **1996**, *17*, 49-56.

(319) Houk, K. N. *Acc. Chem. Res.* **1975**, *8*, 361-369.

(320) Fukui, K. *Acc. Chem. Res.* **1971**, *4*, 57-64.

- (321) Salem, L. *J. Am. Chem. Soc.* **1968**, *90*, 543-552.
- (322) Salem, L. *J. Am. Chem. Soc.* **1968**, *90*, 553-566.
- (323) Houk, K. N.; Sims, J.; Watts, C. R.; Luskus, L. J. *J. Am. Chem. Soc.* **1973**, *95*, 7301-7315.
- (324) Huisgen, R. *Angew. Chem. Int. Ed.* **1963**, *2*, 565, 633.
- (325) Huisgen, R.; Grashey, R.; Sauer, J. *The Chemistry of Alkenes*; Interscience: London, 1964; pp 739.
- (326) Huisgen, R. *J. Org. Chem.* **1968**, *33*, 2291-2297.
- (327) Houk, K. N. *J. Am. Chem. Soc.* **1972**, *94*, 8953-8955.
- (328) Houk, K. N.; Sims, J.; Duke, R. E.; Strozier, R. W.; George, J. K. *J. Am. Chem. Soc.* **1973**, *95*, 7287-7301.
- (329) Ess, D. H.; Houk, K. N. *J. Am. Chem. Soc.* **2007**, *129*, 10646-10647.
- (330) Ess, D. H.; Houk, K. N. *J. Am. Chem. Soc.* **2008**, *130*, 10187-10198.
- (331) Ess, D. H.; Jones, G. O.; Houk, K. N. *Org. Lett.* **2008**, *10*, 1633-1636.
- (332) DeChancie, J.; Acevedo, O.; Evanseck, J. D. *J. Am. Chem. Soc.* **2004**, *126*, 6043-6047.
- (333) Lam, Y. H.; Cheong, P. H. Y.; Mata, J. M. B.; Stanway, S. J.; Gouverneur, V.; Houk, K. N. *J. Am. Chem. Soc.* **2009**, *131*, 1947-1957.
- (334) Garcia, J. I.; Martinez-Merino, V.; Mayoral, J. A.; Salvatella, L. *J. Am. Chem. Soc.* **1998**, *120*, 2415-2420.
- (335) Sbai, A.; Branchadell, V.; Ortuno, R. M.; Oliva, A. *J. Org. Chem.* **1997**, *62*, 3049-3054.
- (336) Houk, K. N.; Gandour, R. W.; Strozier, R. W.; Rondan, N. G.; Paquette, L. A. *J. Am. Chem. Soc.* **1979**, *101*, 6797-6802.
- (337) Froese, R. D. J.; Coxon, J. M.; West, S. C.; Morokuma, K. *J. Org. Chem.* **1997**, *62*, 6991-6996.
- (338) Nagase, S.; Morokuma, K. *J. Am. Chem. Soc.* **1978**, *100*, 1666-1672.

- (339) Wang, X. H.; Weitz, E. *J. Organomet. Chem.* **2004**, *689*, 2354-2360.
- (340) Joo, H.; Kraka, E.; Quapp, W.; Cremer, D. *Mol. Phys.* **2007**, *105*, 2697-2717.
- (341) Finkelstein, H. *Ber. Deutsch. Chem. Ges.* **1910**, *43*, 1528-1532.
- (342) Cava, M. P.; Napier, D. R. *J. Am. Chem. Soc.* **1957**, *79*, 1701-1705.
- (343) Cava, M. P.; Deana, A. A.; Muth, K. *J. Am. Chem. Soc.* **1959**, *81*, 6458-6460.
- (344) Oppolzer, W. *Synthesis* **1978**, 793-802.
- (345) Charlton, J. L.; Alauddin, M. M. *Tetrahedron* **1987**, *43*, 2873-2889.
- (346) Segura, J. L.; Martin, N. *Chem. Rev.* **1999**, *99*, 3199-3246.
- (347) Kitagaki, S.; Ohdachi, K.; Katoh, K.; Mukai, C. *Org. Lett.* **2006**, *8*, 95-98.
- (348) Kitagaki, S.; Katoh, K.; Ohdachi, K.; Takahashi, Y.; Shibata, D.; Mukai, C. *J. Org. Chem.* **2006**, *71*, 6908-6914.
- (349) Plieninger, H.; Weinerth, K.; Muller, W. *Chem. Ber. Recl.* **1964**, *97*, 667-681.
- (350) Gallagher, T.; Magnus, P. *Tetrahedron* **1981**, *37*, 3889-3897.
- (351) Gallagher, T.; Magnus, P.; Huffman, J. C. *J. Am. Chem. Soc.* **1982**, *104*, 1140-1141.
- (352) Gallagher, T.; Magnus, P. *J. Am. Chem. Soc.* **1983**, *105*, 2086-2087.
- (353) Magnus, P.; Gallagher, T.; Brown, P.; Huffman, J. C. *J. Am. Chem. Soc.* **1984**, *106*, 2105-2114.
- (354) Magnus, P. D.; Exon, C.; Sear, N. L. *Tetrahedron* **1983**, *39*, 3725-3729.
- (355) Magnus, P. D.; Sear, N. L. *Tetrahedron* **1984**, *40*, 2795-2797.
- (356) Cardwell, K.; Hewitt, B.; Ladlow, M.; Magnus, P. *J. Am. Chem. Soc.* **1988**, *110*, 2242-2248.
- (357) Kutney, J. P.; Fuller, G. B. *Heterocycles* **1975**, *3*, 197-204.
- (358) Kuehne, M. E.; Frasier, D. A.; Spitzer, T. D. *J. Org. Chem.* **1991**, *56*, 2696-2700.

- (359) Angle, S. R.; Fevig, J. M.; Knight, S. D.; Marquis, R. W.; Overman, L. E. *J. Am. Chem. Soc.* **1993**, *115*, 3966-3976.
- (360) Kuehne, M. E.; Xu, F.; Brook, C. S. *J. Org. Chem.* **1994**, *59*, 7803-7806.
- (361) Sole, D.; Bonjoch, J.; GarciaRubio, S.; Surliol, R.; Bosch, J. *Tetrahedron Lett.* **1996**, *37*, 5213-5216.
- (362) Sole, D.; Bonjoch, J.; Bosch, J. *J. Org. Chem.* **1996**, *61*, 4194-4195.
- (363) Martin, S. F.; Clark, C. W.; Ito, M.; Mortimore, M. *J. Am. Chem. Soc.* **1996**, *118*, 9804-9805.
- (364) Bonjoch, J.; Sole, D.; GarciaRubio, S.; Bosch, J. *J. Am. Chem. Soc.* **1997**, *119*, 7230-7240.
- (365) Ito, M.; Clark, C. W.; Mortimore, M.; Goh, J. B.; Martin, S. F. *J. Am. Chem. Soc.* **2001**, *123*, 8003-8010.
- (366) Dadson, B. A.; Harley, J. *J. Chem. Soc., Chem. Commun.* **1969**, 665-&.
- (367) Legseir, B.; Henin, J.; Massiot, G.; Vercauteren, J. *Tetrahedron Lett.* **1987**, *28*, 3573-3576.
- (368) Gracia, J.; Bonjoch, J.; Casamitjana, N.; Amat, M.; Bosch, J. *J. Chem. Soc., Chem. Commun.* **1991**, 614-615.
- (369) Ishikawa, H.; Boger, D. L. *J. Synth. Org. Chem Jpn.* **2009**, *67*, 123-133.
- (370) Magnus, P.; Cairns, P. M. *J. Am. Chem. Soc.* **1986**, *108*, 217-221.
- (371) Ishikawa, H.; Colby, D. A.; Seto, S.; Va, P.; Tam, A.; Kakei, H.; Rayl, T. J.; Hwang, I.; Boger, D. L. *J. Am. Chem. Soc.* **2009**, *131*, 4904-4916.
- (372) Exon, C.; Gallagher, T.; Magnus, P. *J. Am. Chem. Soc.* **1983**, *105*, 4739-4749.
- (373) Chou, T. S. *Rev. Heteroatom Chem.* **1993**, *8*, 65-104.
- (374) Collier, S. J.; Storr, R. C. Heterocyclic *ortho*-Quinodimethanes. In *Progress in Heterocyclic Chemistry*; Gribble, G. W., Gilchrist, T. L., Eds.; Pergamon: New York, 1998; Vol. 10, pp 25-48.
- (375) Pindur, U.; Erfanianabdoust, H. *Chem. Rev.* **1989**, *89*, 1681-1689.

- (376) Kuroda, N.; Takahashi, Y.; Yoshinaga, K.; Mukai, C. *Org. Lett.* **2006**, *8*, 1843-1845.
- (377) Inagaki, F.; Mizutani, M.; Kuroda, N.; Mukai, C. *J. Org. Chem.* **2009**, *74*, 6402-6405.
- (378) Fuwa, H.; Sasaki, M. *Chem. Commun.* **2007**, 2876-2878.
- (379) Fuwa, H.; Tako, T.; Ebine, M.; Sasaki, M. *Chem. Lett.* **2008**, *37*, 904-905.
- (380) Marinelli, E. R. *Tetrahedron Lett.* **1982**, *23*, 2745-2748.
- (381) Vice, S. F. New Approaches to the Synthetic Elaboration of 2,3-Dialkylindoles. Ph.D. Thesis, University of Waterloo, Waterloo, Canada, 1984.
- (382) Vice, S. F.; Carvalho, H. N. d.; Taylor, N. G.; Dmitrienko, G. I. *Tetrahedron Lett.* **1989**, *30*, 7289-7292.
- (383) Carvalho, H. N. d. Studies on the Chemistry of Indole-2,3-Quinodimethanes and Stable Analogs. M.Sc. Thesis, University of Waterloo, Waterloo, Canada, 1985.
- (384) Jakiwczyk, O. M. Approaches to Regioselective Construction of Substituted Tetrahydrocarbazoles. M.Sc. Thesis, University of Waterloo, Waterloo, Canada, 1992.
- (385) White, S. R. Strategies for the Design and Synthesis of Squalene Epoxidase Inhibitors. M.Sc. Thesis, University of Waterloo, Waterloo, Canada, 1994.
- (386) Wu, J. Y. J. Control of the Regiochemistry and Stereochemistry of Intermolecular Diels-Alder Reaction of Indole-2,3-Quinodimethanes. M.Sc. Thesis, University of Waterloo, Waterloo, Canada, 2002.
- (387) Carvalho, H. N. d.; Dmitrienko, G. I.; Nielsen, K. E. *Tetrahedron* **1990**, *46*, 5523-5532.
- (388) Jakiwczyk, O. M.; Nielsen, K. E.; deCarvalho, H. N.; Dmitrienko, G. I. *Tetrahedron Lett.* **1997**, *38*, 6541-6544.
- (389) Jung, M. E.; McCombs, C. A. *Tetrahedron Lett.* **1976**, 2935-2938.
- (390) Woodward, R. B.; Hoffmann, R. *The conservation of orbital symmetry*; Verlag Chemie: Weinheim/Bergstr., 1970; pp 1-177.
- (391) Houk, K. N. *J. Am. Chem. Soc.* **1973**, *95*, 4092-4094.
- (392) Sauer, J.; Sustmann, R. *Angew. Chem. Int. Ed.* **1980**, *19*, 779-807.

- (393) Fringuelli, F.; Taticchi, A. *The Diels Alder reaction: Selected Practical Methods*; Wiley: Chichester; New York, 2002; pp 1-340.
- (394) Yates, P.; Eaton, P. *J. Am. Chem. Soc.* **1960**, *82*, 4436-4437.
- (395) Houk, K. N.; Strozier, R. W. *J. Am. Chem. Soc.* **1973**, *95*, 4094-4096.
- (396) Corey, E. J.; Loh, T. P. *J. Am. Chem. Soc.* **1991**, *113*, 8966-8967.
- (397) Hawkins, J. M.; Loren, S. *J. Am. Chem. Soc.* **1991**, *113*, 7794-7795.
- (398) Hawkins, J. M.; Loren, S.; Nambu, M. *J. Am. Chem. Soc.* **1994**, *116*, 1657-1660.
- (399) Ahrendt, K. A.; Borths, C. J.; MacMillan, D. W. C. *J. Am. Chem. Soc.* **2000**, *122*, 4243-4244.
- (400) Evans, D. A.; Chapman, K. T.; Bisaha, J. *J. Am. Chem. Soc.* **1984**, *106*, 4261-4263.
- (401) Gurudutt, K. N.; Ravindranath, B.; Srinivas, P. *Tetrahedron* **1982**, *38*, 1843-1846.
- (402) Fieser, L. F.; Fieser, M. *Reagents for organic synthesis*; Wiley: New York, 1972; Vol. 3; pp 22.
- (403) Mishra, S.; Singh, V.; Jain, A.; Verma, K. K. *Analyst* **2000**, *125*, 459-464.
- (404) Fieser, M.; Danheiser, R. L.; Roush, W., R. *Reagents for organic synthesis*; Wiley: New York, 1981; Vol. 9; pp 141.
- (405) Marshall, J. A.; Palovich, M. R. *J. Org. Chem.* **1997**, *62*, 6001-6005.
- (406) Mukai, C.; Takahashi, Y. *Org. Lett.* **2005**, *7*, 5793-5796.
- (407) Lamba, J. J. S.; Tour, J. M. *J. Am. Chem. Soc.* **1994**, *116*, 11723-11736.
- (408) Sarvari, M. H.; Sharghi, H. *Tetrahedron* **2005**, *61*, 10903-10907.
- (409) Arumugam, P.; Karthikeyan, G.; Perumal, P. T. *Chem. Lett.* **2004**, *33*, 1146-1147.
- (410) Dias, L. C. *J. Brazil. Chem. Soc.* **1997**, *8*, 289-332.
- (411) Corey, E. J. *Angew. Chem. Int. Ed.* **2002**, *41*, 1650-1667.
- (412) Ishihara, K.; Kurihara, H.; Matsumoto, M.; Yamamoto, H. *J. Am. Chem. Soc.* **1998**, *120*, 6920-6930.

- (413) Ryu, D. H.; Lee, T. W.; Corey, E. J. *J. Am. Chem. Soc.* **2002**, *124*, 9992-9993.
- (414) Corey, E. J.; Shibata, T.; Lee, T. W. *J. Am. Chem. Soc.* **2002**, *124*, 3808-3809.
- (415) Ryu, D. H.; Corey, E. J. *J. Am. Chem. Soc.* **2003**, *125*, 6388-6390.
- (416) Ryu, D. H.; Zhou, G.; Corey, E. J. *J. Am. Chem. Soc.* **2004**, *126*, 4800-4802.
- (417) Haber, M.; Pindur, U. *Tetrahedron* **1991**, *47*, 1925-1936.
- (418) Pindur, U.; Haber, M. *J. Prakt. Chem. Chem. Ztg.* **1993**, *335*, 12-16.
- (419) Pindur, U.; Haber, M. *Heterocycles* **1991**, *32*, 1463-1470.
- (420) Di Valentin, C.; Freccero, M.; Sarzi-Amade, M.; Zanaletti, R. *Tetrahedron* **2000**, *56*, 2547-2559.
- (421) Manoharan, M.; De Proft, F.; Geerlings, P. *J. Org. Chem.* **2000**, *65*, 7971-7976.
- (422) Tamilmani, V.; Daul, C. A.; Robles, J. L.; Bochet, C. G.; Venuvanalingam, P. *Chem. Phys. Lett.* **2005**, *406*, 355-359.
- (423) Corminboeuf, C.; Heine, T.; Weber, J. *Org. Lett.* **2003**, *5*, 1127-1130.
- (424) Tsoleridis, C. A.; Dimtsas, J.; Hatzimimikou, D.; Stephanidou-Stephanatou, J. *Tetrahedron* **2006**, *62*, 4232-4242.
- (425) Jursic, B.; Zdravkovski, Z. *J. Chem. Soc., Perkin Trans. 2* **1995**, 1223-1226.
- (426) Jursic, B. S. *J. Org. Chem.* **1995**, *60*, 4721-4724.
- (427) Goldstein, E.; Beno, B.; Houk, K. N. *J. Am. Chem. Soc.* **1996**, *118*, 6036-6043.
- (428) Wiest, O.; Houk, K. N. *Top. Curr. Chem.* **1996**, *183*, 1-24.
- (429) Froese, R. D. J.; Humbel, S.; Svensson, M.; Morokuma, K. *J. Phys. Chem. A* **1997**, *101*, 227-233.
- (430) Wiest, O.; Montiel, D. C.; Houk, K. N. *J. Phys. Chem. A* **1997**, *101*, 8378-8388.
- (431) Salvatella, L.; Ruiz-Lopez, M. F. *J. Am. Chem. Soc.* **1999**, *121*, 10772-10780.
- (432) Kong, S.; Evanseck, J. D. *J. Am. Chem. Soc.* **2000**, *122*, 10418-10427.



- (433) Paddon-Row, M. N.; Moran, D.; Jones, G. A.; Sherburn, M. S. *J. Org. Chem.* **2005**, *70*, 10841-10853.
- (434) Cayzer, T. N.; Paddon-Row, M. N.; Moran, D.; Payne, A. D.; Sherburn, M. S.; Turner, P. *J. Org. Chem.* **2005**, *70*, 5561-5570.
- (435) Alves, C. N.; Carneiro, A. S.; Andres, J.; Domingo, L. R. *Tetrahedron* **2006**, *62*, 5502-5509.
- (436) Paddon-Row, M. N.; Anderson, C. D.; Houk, K. N. *J. Org. Chem.* **2009**, *74*, 861-868.
- (437) Hohenberg, P.; Kohn, W. *Phys. Rev. B* **1964**, *136*, B864-871.
- (438) Schleyer, P. v. R. *Encyclopedia of computational chemistry*; John Wiley: New York, 1998; pp 3580.
- (439) Lambert, J. B.; Shurvell, H. F.; Lightner, D.; Cooks, R. G. *Organic structural spectroscopy*; Prentice Hall: Upper Saddle River, N.J., 1998; pp 96.
- (440) Alston, P. V.; Ottenbrite, R. M.; Shillady, D. D. *J. Org. Chem.* **1973**, *38*, 4075-4077.
- (441) Foresman, J. B.; Frisch, A.; Gaussian Inc. *Exploring chemistry with electronic structure methods*; 2nd ed.; Gaussian, Inc.: Pittsburgh, PA, 1996; pp 97-102.
- (442) Cramer, C. J. *Essentials of computational chemistry: theories and models*; 2nd ed.; J. Wiley: Hoboken, N.J., 2004; pp 166-175.
- (443) Jensen, F. *Introduction to computational chemistry*; 2nd ed.; John Wiley & Sons: Hoboken, NJ, 2007; pp 192-204.
- (444) Anslyn, E. V.; Dougherty, D. A. *Modern Physical Organic Chemistry*; University Science: Sausalito, Calif., 2006; pp 823.
- (445) Jorgensen, W. L.; Lim, D. C.; Blake, J. F. *J. Am. Chem. Soc.* **1993**, *115*, 2936-2942.
- (446) Froese, R. D. J.; Organ, M. G.; Goddard, J. D.; Stack, T. D. P.; Trost, B. M. *J. Am. Chem. Soc.* **1995**, *117*, 10931-10938.
- (447) Ruiz-Lopez, M. F.; Assfeld, X.; Garcia, J. I.; Mayoral, J. A.; Salvatella, L. *J. Am. Chem. Soc.* **1993**, *115*, 8780-8787.
- (448) Blake, J. F.; Lim, D.; Jorgensen, W. L. *J. Org. Chem.* **1994**, *59*, 803-805.

- (449) Garcia, J. I.; Mayoral, J. A.; Salvatella, L. *Tetrahedron* **1997**, *53*, 6057-6064.
- (450) Alder, K.; Schumacher, M. *Liebigs Ann. Chem.* **1951**, *571*, 87-107.
- (451) Houk, K. N. *Tetrahedron Lett.* **1970**, 2621-2624.
- (452) Alston, P. V.; Ottenbrite, R. M.; Cohen, T. *J. Org. Chem.* **1978**, *43*, 1864-1867.
- (453) Berson, J. A.; Mueller, W. A.; Hamlet, Z. *J. Am. Chem. Soc.* **1962**, *84*, 297-304.
- (454) Woodward, R. B.; Baer, H. *J. Am. Chem. Soc.* **1944**, *66*, 645-649.
- (455) Kahn, S. D.; Pau, C. F.; Overman, L. E.; Hehre, W. J. *J. Am. Chem. Soc.* **1986**, *108*, 7381-7396.
- (456) Jensen, F. *Introduction to computational chemistry*; 2nd ed.; John Wiley & Sons: Hoboken, NJ, 2007; pp 435.
- (457) Cramer, C. J. *Essentials of computational chemistry: theories and models*; 2nd ed.; J. Wiley: Hoboken, N.J., 2004; pp 111.
- (458) Jensen, F. *Introduction to computational chemistry*; 2nd ed.; John Wiley & Sons: Hoboken, NJ, 2007; pp 461.
- (459) Smith, I. W. M. *Chem. Soc. Rev.* **2008**, *37*, 812-826.
- (460) Jensen, F. *Introduction to computational chemistry*; 2nd ed.; John Wiley & Sons: Hoboken, NJ, 2007; pp 433, 437.
- (461) Cramer, C. J. *Essentials of computational chemistry: theories and models*; 2nd ed.; J. Wiley: Hoboken, N.J., 2004; pp 522-523.
- (462) Williams, I. H. *Chem. Soc. Rev.* **1993**, *22*, 277-283.
- (463) Cramer, C. J. *Essentials of computational chemistry: theories and models*; 2nd ed.; J. Wiley: Hoboken, N.J., 2004; pp 45-46, 185, 337-338.
- (464) Jensen, F. *Introduction to computational chemistry*; 2nd ed.; John Wiley & Sons: Hoboken, NJ, 2007; pp 432-433.
- (465) Leach, A. R. *Molecular modelling: principles and applications*; Longman: Harlow, England, 1996; pp 240.

- (466) Foresman, J. B.; Frisch, A.; Gaussian Inc. *Exploring chemistry with electronic structure methods*; 2nd ed.; Gaussian, Inc.: Pittsburgh, PA, 1996; pp 166.
- (467) Cramer, C. J. *Essentials of computational chemistry: theories and models*; 2nd ed.; J. Wiley: Hoboken, N.J., 2004; pp 523.
- (468) Jensen, F. *Introduction to computational chemistry*; 2nd ed.; John Wiley & Sons: Hoboken, NJ, 2007; pp 438.
- (469) Doubleday, C.; Mciver, J.; Page, M.; Zielinski, T. *J. Am. Chem. Soc.* **1985**, *107*, 5800-5801.
- (470) Truhlar, D. G.; Garrett, B. C. *Acc. Chem. Res.* **1980**, *13*, 440-448.
- (471) Truhlar, D. G.; Gordon, M. S. *Science* **1990**, *249*, 491-498.
- (472) Truhlar, D. G.; Garrett, B. C.; Klippenstein, S. J. *J. Phys. Chem.* **1996**, *100*, 12771-12800.
- (473) Paddon-Row, M. N.; Kwan, L. C. H.; Willis, A. C.; Sherburn, M. S. *Angew. Chem. Int. Ed.* **2008**, *47*, 7013-7017.
- (474) Wiberg, K. B. *Tetrahedron* **1968**, *24*, 1083-1096.
- (475) Reed, A. E.; Curtiss, L. A.; Weinhold, F. *Chem. Rev.* **1988**, *88*, 899-926.
- (476) Reed, A. E.; Weinstock, R. B.; Weinhold, F. *J. Chem. Phys.* **1985**, *83*, 735-746.
- (477) Birney, D. M.; Houk, K. N. *J. Am. Chem. Soc.* **1990**, *112*, 4127-4133.
- (478) Bickelhaupt, F. M. *J. Comput. Chem.* **1999**, *20*, 114-128.
- (479) Castellino, S. *J. Org. Chem.* **1990**, *55*, 5197-5200.
- (480) Castellino, S.; Dwight, W. J. *J. Am. Chem. Soc.* **1993**, *115*, 2986-2987.
- (481) Cozzi, P. G.; Solari, E.; Floriani, C.; ChiesiVilla, A.; Rizzoli, C. *Chem. Ber.* **1996**, *129*, 1361-1368.
- (482) Poll, T.; Helmchen, G.; Bauer, B. *Tetrahedron Lett.* **1984**, *25*, 2191-2194.
- (483) Poll, T.; Metter, J. O.; Helmchen, G. *Angew. Chem. Int. Ed.* **1985**, *24*, 112-114.

- (484) Armarego, W. L. F.; Perrin, D. D. *Purification of laboratory chemicals*; 4th ed.; Butterworth-Heinemann; Elsevier Science: Oxford, Boston, 1996; pp 1-529.
- (485) Still, W. C.; Kahn, M.; Mitra, A. *J. Org. Chem.* **1978**, *43*, 2923-2925.
- (486) Grimmel, H. W.; Guenther, A.; Morgan, J. F. *J. Am. Chem. Soc.* **1946**, *68*, 539-542.
- (487) Buuhoi, N. P.; Lavit, D. *J. Org. Chem.* **1955**, *20*, 1191-1196.
- (488) Cakmak, O.; Demirtas, I.; Balaydin, H. T. *Tetrahedron* **2002**, *58*, 5603-5609.
- (489) Tanoue, Y.; Terada, A.; Matsumoto, Y. *Bull. Chem. Soc. Jpn.* **1989**, *62*, 2736-2738.
- (490) Williams, W.; Sun, X.; Jebaratnam, D. *J. Org. Chem.* **1997**, *62*, 4364-4369.
- (491) Wolfe, J. P.; Wagaw, S.; Buchwald, S. L. *J. Am. Chem. Soc.* **1996**, *118*, 7215-7216.
- (492) Wille, U.; Heugert, G.; Jargstorff, C. *J. Org. Chem.* **2008**, *73*, 1413-1421.
- (493) Malesani, G.; Ferlin, M. G. *J. Heterocycl. Chem.* **1987**, *24*, 513-517.
- (494) Mander, L. N.; Sethi, S. P. *Tetrahedron Lett.* **1984**, *25*, 5953-5956.
- (495) Baltzly, R.; Mehta, N. B.; Grivsky, E. M.; Brooks, R. E.; Steinberg, A. M.; Russell, P. B. *J. Org. Chem.* **1961**, *26*, 3669-3676.
- (496) Javed, M. I.; Brewer, M. *Org. Lett.* **2007**, *9*, 1789-1792.
- (497) Dave, V.; Warnhoff, E. W. *Can. J. Chem.* **1971**, *49*, 1911-1920.
- (498) Vice, S. F.; Copeland, C. R.; Forsey, S. P.; Dmitrienko, G. I. *Tetrahedron Lett.* **1985**, *26*, 5253-5256.
- (499) Logue, M. W.; Teng, K. *J. Org. Chem.* **1982**, *47*, 2549-2553.
- (500) Najdi, S. D.; Olmstead, M. M.; Schore, N. E. *J. Organomet. Chem.* **1992**, *431*, 335-358.
- (501) Kitamura, T.; Sato, Y.; Mori, M. *Adv. Synth. Catal.* **2002**, *344*, 678-693.
- (502) Szammer, J.; Otvos, L. *Chem. Ind.* **1988**, 764-764.
- (503) Theis, A. B.; Townsend, C. A. *Synth. Commun.* **1981**, *11*, 157-166.

- (504) Wuts, P. G. M. *Synth. Commun.* **1981**, *11*, 139-140.
- (505) Kelly, T. A.; McNeil, D. W. *Tetrahedron Lett.* **1994**, *35*, 9003-9006.
- (506) Larock, R. C.; Yum, E. K.; Refvik, M. D. *J. Org. Chem.* **1998**, *63*, 7652-7662.
- (507) Kim, S.; Lee, J. I.; Kim, Y. C. *J. Org. Chem.* **1985**, *50*, 560-565.
- (508) Zhang, D. H.; Yum, E. K.; Liu, Z. J.; Larock, R. C. *Org. Lett.* **2005**, *7*, 4963-4966.